AD NUMBER

AD921578

NEW LIMITATION CHANGE

TO

Approved for public release, distribution unlimited

FROM

Distribution authorized to U.S. Gov't. agencies only; Test and Evaluation; 28 AUG 1974. Other requests shall be referred to Air Force Flight Dynamics Lab., Wright-Patterson AFB, OH 45433.

AUTHORITY

AFFDL ltr, 28 Nov 1979

AFFDL-TR-74-17

AD921578

# ADVANCED METALLIC AIR VEHICLE STRUCTURE PROGRAM

# PHASE II - DETAIL DESIGN AND ANALYSIS SUMMARY REPORT - TECHNICAL


C. E. HART, ET AL.

**GENERAL DYNAMICS**
*Convair Aerospace Division*
*Fort Worth Operation*


TECHNICAL REPORT AFFDL-TR-74-17

January 1974



Distribution limited to U.S. Government Agencies only. Reason: Test and Evaluation. Other requests for this document must be referred to Air Force Flight Dynamics Laboratory/FBA, Wright-Patterson Air Force Base, Ohio 45433.


Air Force Flight Dynamics Laboratory
Air Force Systems Command
Wright-Patterson Air Force Base, Ohio 45433

## NOTICES



AIR FORCE/56780/22 July 1974 — 300

# ADVANCED METALLIC AIR VEHICLE STRUCTURE PROGRAM

# PHASE II - DETAIL DESIGN AND ANALYSIS SUMMARY REPORT - TECHNICAL

## FOREWORD

This report presents the results of Phase II - Detail Design and Analysis of a wing carrythrough structure for an advanced metallic moveable wing aircraft. The efforts reported herein were sponsored by the Air Force Flight Dynamics Laboratory (AFFDL) under joint management and technical direction of AFFDL and the Air Force Materials Laboratory, Wright-Patterson Air Force Base, Ohio.

This work was performed under contract F33615-73-C-3001 "Advanced Metallic Air Vehicle Structure" (AMAVS) as part of the Advanced Metallic Structures, Advanced Development Programs (AMS ADP), Program Element Number 63211F, Project Number 486U. John C. Frishett, Major, USAF, is the ADP Manager while Mr. Frank D. Boensch is the Project Engineer for the AMAVS Program.

Phase Ia of this program has been previously reported in AFFDL-TR-73-4, Volume I, Parts 1 and 2, and Volume II.

Principal Convair contributors to this report were:

| | |
|---|---|
| C. E. Hart | - Program Manager |
| R. C. Bissell | - Deputy Program Manager |
| D. L. Duncan | - Non-Destructive Inspection |
| E. K. Hensley | - Design and Structures |
| J. W. Jennings | - Information Transfer |
| J. L. McDaniel | - Manufacturing Engineering |
| Dr. H. I. McHenry | - Fracture and Fatigue Analysis |
| R. E. Miller | - Stress Analysis |
| W. O. Sunafrank | - Manufacturing Engineering |
| J. M. Shults | - Materials Engineering |
| A. F. Stern | - Structural Design |
| W. M. Walker | - Test Coordination |

This work was performed during the period 1 February 1973 to 9 November 1973. It was submitted by the authors in January 1974.

This technical report has been reviewed and is approved for publication.

Frank D. Boensch
Project Engineer

John C. Frishett, Major, USAF
Program Manager
AMS Program Office
Structures Division

# ABSTRACT

This report covers the design, analysis, manufacturing and testing done during Phase II, Detail Design, of the Advanced Metallic Air Vehicle Structure (AMAVS) program. The objectives of Phase II were to complete the detail design work for two configurations of a wing carrythrough structure for a movable-wing aircraft, to complete materials and component testing in support of the two configurations, to select one of the configurations for manufacture in Phase III and to continue design and manufacture of a fixture for full-scale testing of the carrythrough structure.

Additional trade studies and design optimization studies were conducted in the early part of Phase II for the two configurations selected in Phase Ib: Fail Safe Integral Lug (FSIL) and "No-Box" Box (NBB). An updated baseline data package was received during Phase II and the configurations were revised to meet the modified baseline requirements.

Material testing and component testing were completed. Beta annealed 6Al-4V and Beta C titanium and 10Ni steel (HY180) were used in these tests.

Some detail design work remains on the full-scale test fixture but manufacturing has started. Manufacture of the simulated fuselage structure has also begun.

The NBB configuration which utilizes the outstanding fracture toughness and good crack growth characteristics of 10Ni steel has been selected for manufacture in Phase III.

# TABLE OF CONTENTS

TABLE OF CONTENTS (Continued)

TABLE OF CONTENTS (Continued)

TABLE OF CONTENTS (Continued)

# LIST OF ILLUSTRATIONS

LIST OF ILLUSTRATIONS
(Continued)

## LIST OF ILLUSTRATIONS
(Continued)

LIST OF ILLUSTRATIONS
(Continued)

## LIST OF ILLUSTRATIONS
(Continued)

LIST OF ILLUSTRATIONS
(Continued)

# LIST OF ILLUSTRATIONS
(Continued)

LIST OF ILLUSTRATIONS
(Continued)

## LIST OF ILLUSTRATIONS
(Continued)

## LIST OF ILLUSTRATIONS
(Continued)

## LIST OF ILLUSTRATIONS
(Continued)

## LIST OF ILLUSTRATIONS
(Continued)

## LIST OF ILLUSTRATIONS
(Continued)

## LIST OF ILLUSTRATIONS
(Continued)

LIST OF ILLUSTRATIONS
(Continued)

## LIST OF ILLUSTRATIONS
(Continued)

## LIST OF TABLES

LIST OF TABLES (Continued)

LIST OF TABLES (Continued)

# SECTION 1

# INTRODUCTION

This report summarizes the design, analysis and test activities of Phase II, Detail Design, for the Advanced Metallic Air Vehicle Structure (AMAVS) Program. The work done in the first portion of Phase II is presented in the Second Interim Technical Report, AFFDL-TR-73-77. Data presented in the Second Interim Report will not be repeated in this report unless it is required for a clear presentation of subsequent data. This work was performed under contract to the AFFDL by the Convair Aerospace Division of General Dynamics at Fort Worth, Texas.

The two configurations chosen for detail design were refined through additional trade studies and further study. The two configurations are designated as:

- Fail Safe Integral Lug (FSIL)
- "No-Box" Box (NBB)

Updated baseline data was received during the course of Phase II and both wing carry through structure configurations and the test fixture requirements were revised in accordance with the new data. Revised loads and interface geometry requirements were based on the elimination of the wing intrusion, new load conditions, revised gross weight and revised fairing support requirements. The design and analysis of both configurations were completed using updated data.

The Development Test Program consisting of Material Testing, Component Testing, NDI Development and Manufacturing Development was completed. Two of the three new materials were retained in the final configurations. These materials are beta annealed 6Al-4V titanium and 10 Ni steel (HY 180). Beta C titanium was dropped from both configurations.

Critical features of both configurations were evaluated in the Group II component tests. Additional problems were identified and solved in the brazing development program. Manufacturing capabilities were demonstrated for both configurations.

The design and manufacture of the full scale test fixture were continued. Manufacture of the simulated fuselage was started. Orders were placed for long-lead time materials needed for Phase III.

A design review was held to review the drawings and test results for both configurations. The NBB was selected for manufacture in Phase III.

# SECTION 2

# TECHNICAL DISCIPLINES PROGRESS

## 2.1 STRUCTURAL DESIGN

The two wing carrythrough structure configurations selected for detail design during Phase II are described in this section and are identified as follows:

"No-Box" Box (NBB)

This configuration utilizes the superior fracture resistance and weldability characteristics of 10 Nickel steel to achieve damage tolerance and fabrication reliability.

Fail-Safe Integral Lug (FSIL)

This configuration is characterized by brazing of titanium plates into a symmetrical three-element lower plate with integral pivot lugs.

Both configurations achieved the program objectives with respect to weight, cost and structural integrity.

### 2.1.1 "No-Box" Box

The objectives of the original "No-Box" Box configuration was to achieve a cost and weight efficient structure by use of the following major design approaches:

1. Direct and distinct load carrying member arrangement
2. Safe life concept
3. Minimal redundant internal structure
4. Simplified assembly and detail construction
5. Reduced number of fasteners.

This objective was pursued throughout Phase I and established the basic configuration. The pivot lugs were designed to direct the major portion of the load to the forward and aft bulkhead cap members. 10 Nickel steel (HY 180) was selected as the principal structural material for its excellent toughness. The weight penalty due to the marginal strength/density ratio of the 10 Nickel steel had to be overcome by the design concepts. Internal structure was limited to that needed to react loads at direction changes in the upper cover, the centerline fuel tank divider rib and structure for local interface load reactions. Machining time was minimized by using weldments to reduce the volume of metal removed and contour machining was confined to local areas of the bulkhead upper caps. The contour portion of the upper cover was confined to a single aluminum bonded panel. The reduced internal structure and direct load paths minimized the number of fasteners required.

The Phase II design effort was concentrated on improving the implementation of these design objectives. However, certain compromises were required due to baseline load changes imposed midway through this phase. These will be discussed in detail in the following paragraphs.

### 2.1.1.1 Lower Plate Assembly

The original version of this configuration did not include a lower plate at $Z_F0$. The lugs were attached to the outboard caps of the forward and aft bulkheads. Shear and fuel pressure loads were carried by the lower contour panels. Late in Phase I, concern about relative deflections of the lug and lower panels resulted in a study to incorporate a full plate at $Z_F0$. Landing gear interface requirements also made this desirable. The highly loaded lug splice requirements were also of some concern. These considerations finally evolved into the configuration shown on Dwg. No. X7224170, Figure 2-1.

The lower plate assembly consists of a single 10 Nickel steel plate from pivot lug to pivot lug. A cut-out in the center leaves only rails inboard of the $X_F84$ rib. The area between the $X_F84$ and the closure rib is pocketed on the under side. The outboard aft longeron attachment provisions are machined in the basic plate. Three beta processed 6Al-4V titanium bonded sandwich panels are installed between $X_F$ 84 and $X_F84$. These panels react shear, fuel pressure and the axial load not carried by the 10 Nickel steel rails. A machined aluminum (7050) beam is bolted to the under side of the steel plate at $X_F95$ to provide compression stability for negative loads. Machined 10 Nickel steel reinforcing plates are installed on the pivot lugs to provide additional reaction for pivot pin loads and meet the baseline lug thickness requirements. All fasteners through the 10 Nickel steel element are H11 steel Taper-loks.

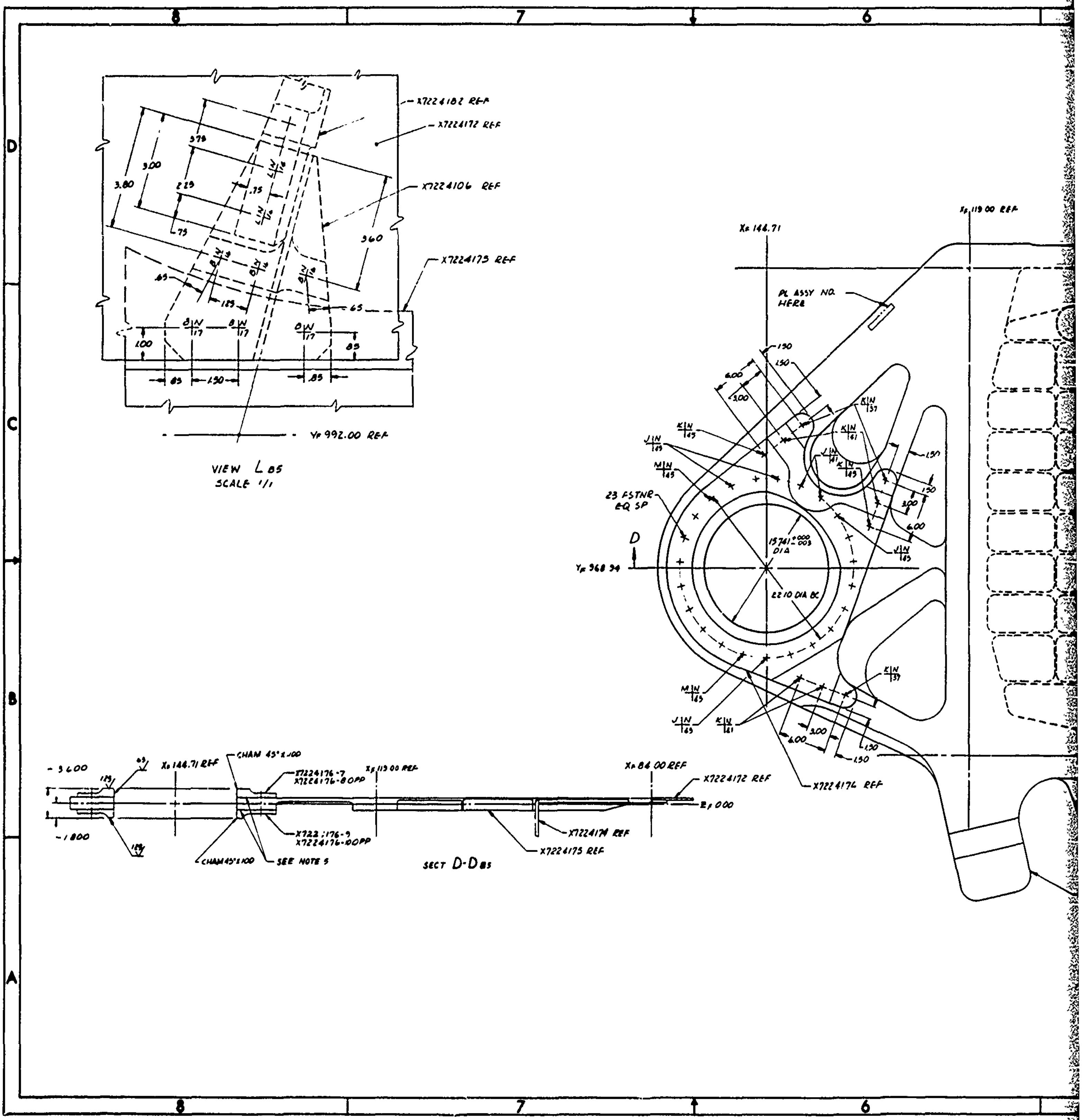

X7224182 REF
X7224172 REF
X7224106 REF
X7224175 REF
YF 992.00 REF
VIEW L B5
SCALE 1/1
XF 144.71
XF 119.00 REF
PL ASSY NO. HERE
23 FSTNR EQ SP
YF 968.54
2.210 DIA BC
X7224174 REF
XF 144.71 REF
CHAM 45° x .100
X7224176-7
X7224176-8 OPP
X7224176-9
X7224176-10 OPP
SEE NOTE 5
XF 84.00 REF
X7224172 REF
X7224174 REF
X7224175 REF
SECT D-D B5

| 6 | 5 | 4 | 3 |
|---|---|---|---|

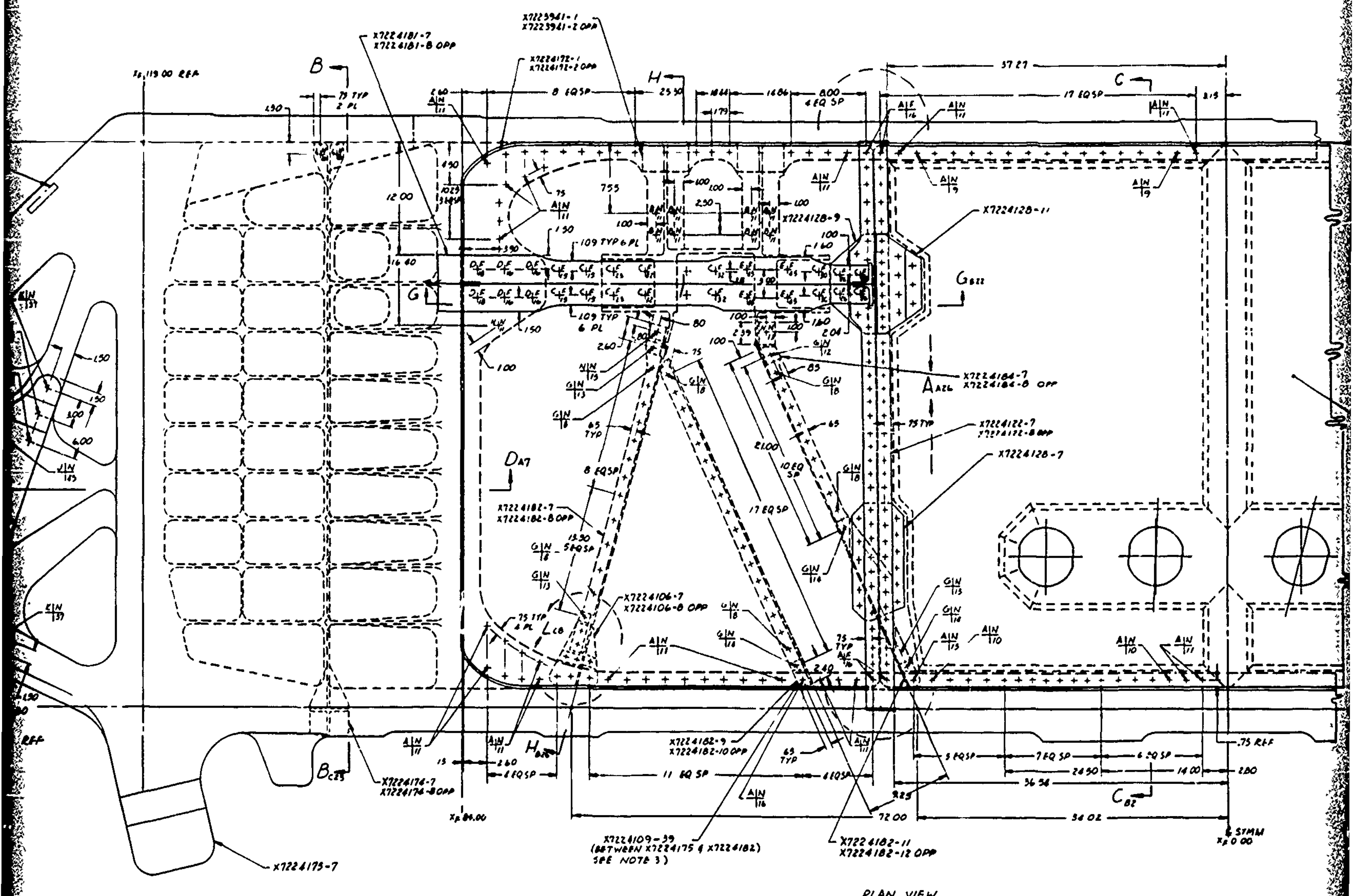


PLAN VIEW
-1 ASSY

| F33615-73C-3001 | | X7224170 | 1 |
|---|---|---|---|

| 6 | 5 | 4 | 3 |
|---|---|---|---|

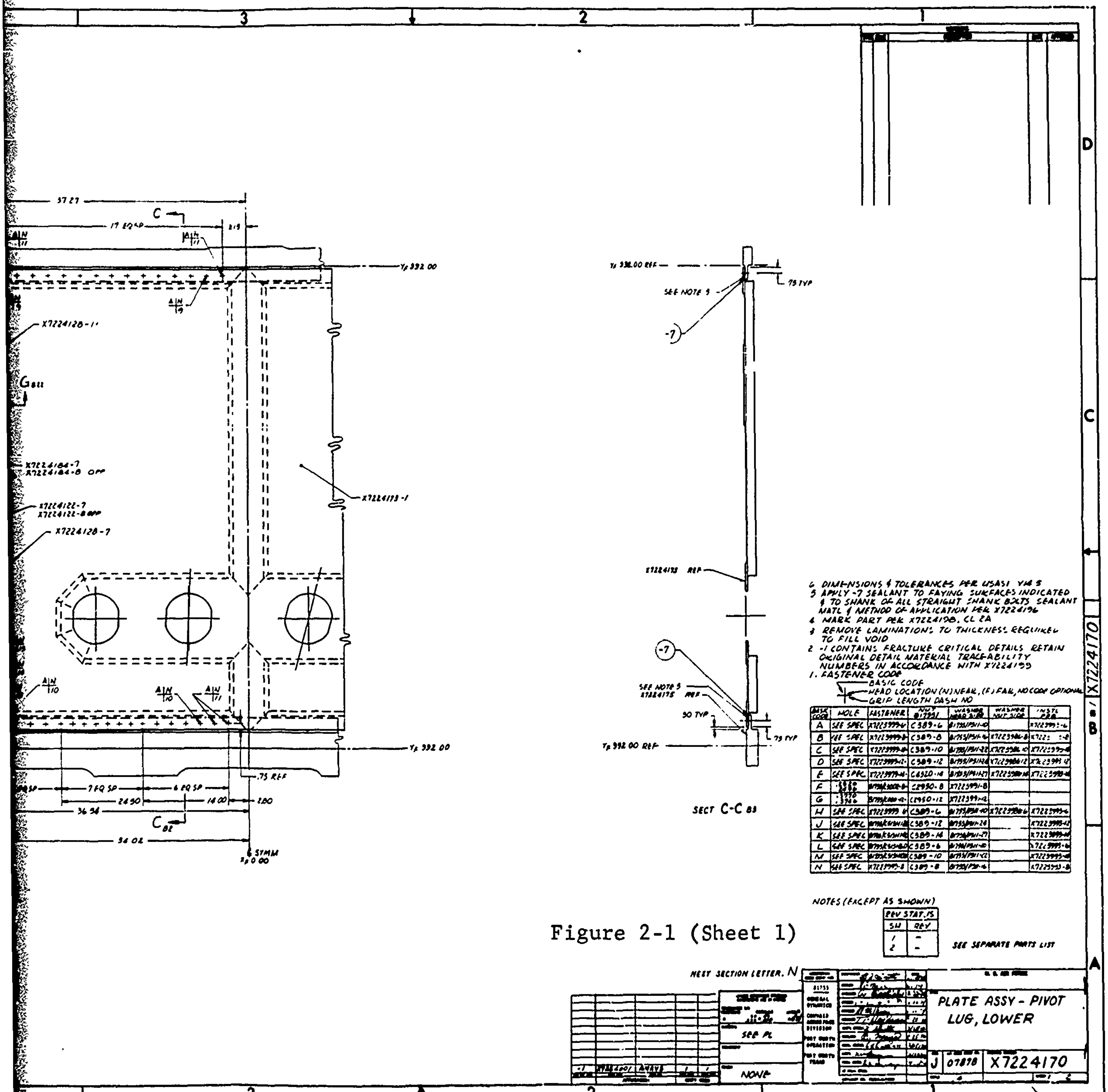


Figure 2-1 (Sheet 1)



3

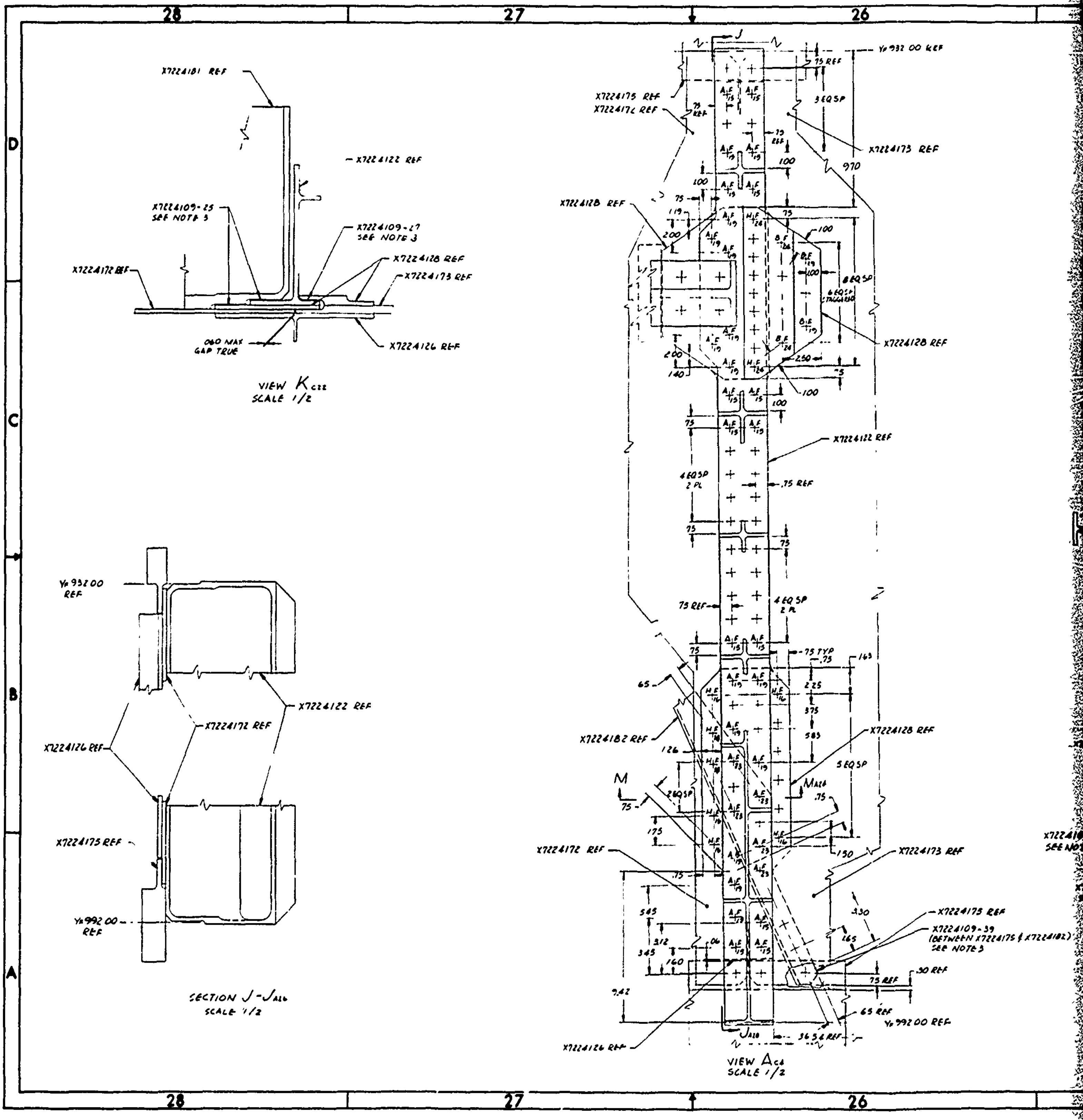
28
27
26
D
C
B
A
X7224181 REF
X7224122 REF
X7224109-25 SEE NOTE 3
X7224109-27 SEE NOTE 3
X7224128 REF
X7224172 REF
X7224173 REF
.060 MAX GAP TRUE
X7224126 REF
VIEW K C22
SCALE 1/2
Y=932.00 REF
X7224122 REF
X7224172 REF
X7224126 REF
X7224175 REF
Y=992.00 REF
SECTION J-J A16
SCALE 1/2
Y=932.00 REF
X7224175 REF
X7224176 REF
X7224173 REF
X7224128 REF
X7224128 REF
X7224122 REF
.75 REF
4 EQ SP 2 PL
4 EQ SP 2 PL
5 EQ SP
8 EQ SP
6 EQ SP STAGGERED
X7224182 REF
X7224128 REF
5 EQ SP
X7224172 REF
X7224173 REF
X7224175 REF
X7224109-39 (BETWEEN X7224175 & X7224182) SEE NOTE 3
.30 REF
.75 REF
.65 REF
Y=992.00 REF
.3654 REF
X7224126 REF
VIEW A C4
SCALE 1/2

| 25 | 24 | 23 |
|---|---|---|

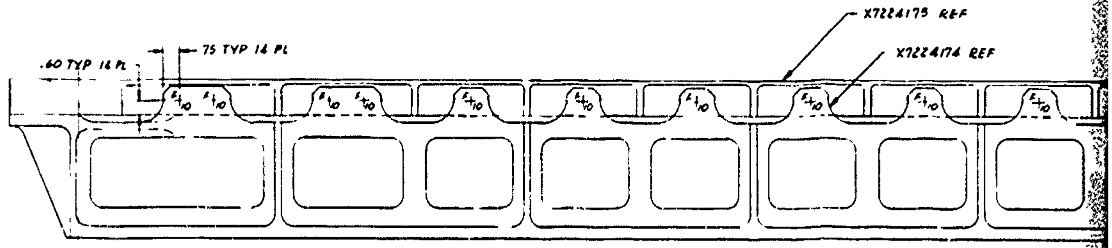


Y= 992.00 REF

SECTION B-B85
SCALE 1/2
ROTATED 90° CLOCKWISE

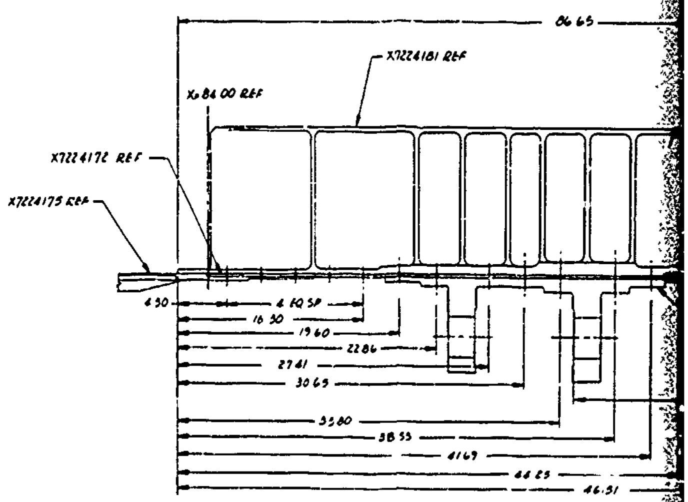


SECTION G-G

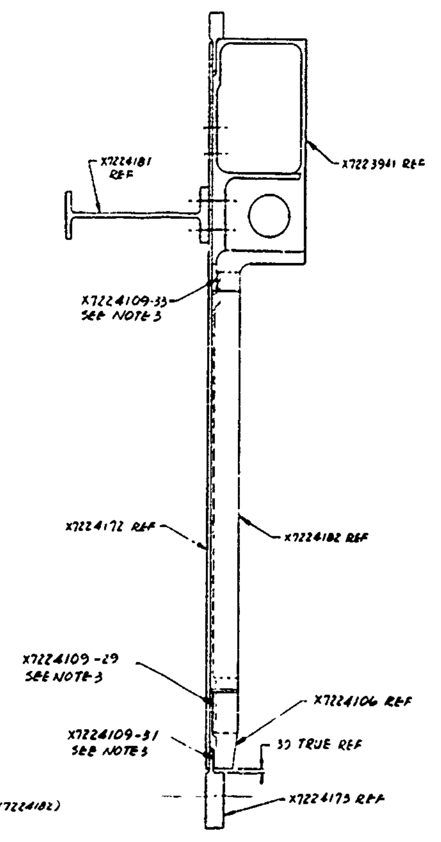


SECTION H-H85

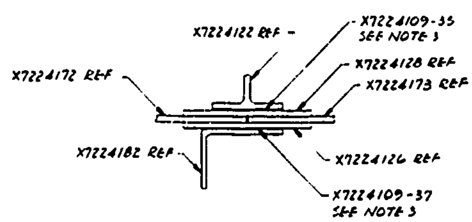


SECTION M-M
SCALE 1/2

| CONTRACT NO. | | DWG NO. | |
|---|---|---|---|
| F33615-73 C-3001 | | X7224170 | 2 |

| 25 | 24 | 23 |
|---|---|---|

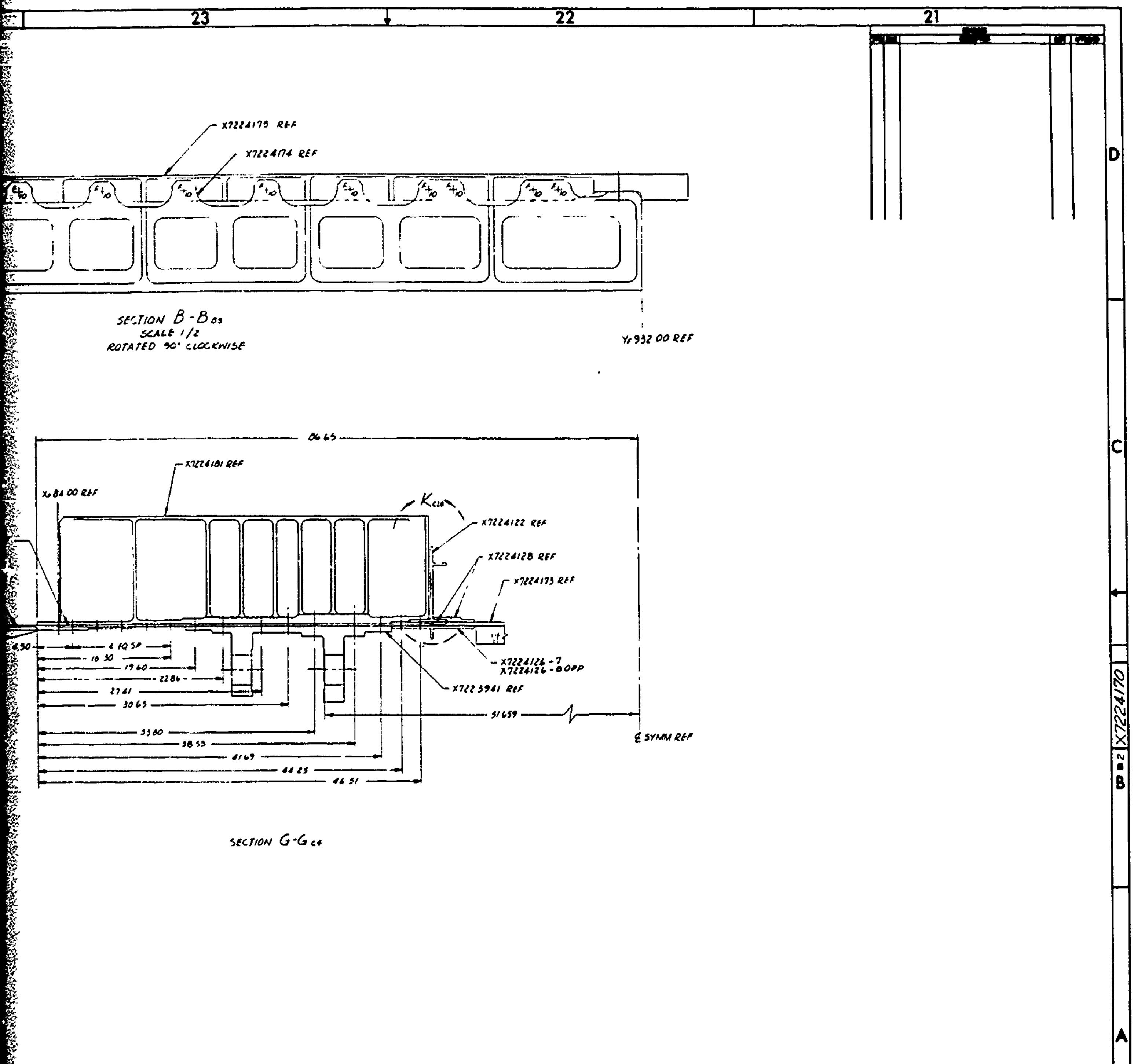


Figure 2-1 (Sheet 2)



3

### 2.1.1.2 $Y_F$ 932 Bulkhead

The forward bulkhead ($Y_F$ 932) Dwg. No. X7224080, Figure 2-2, consists of six major elements. The L/R outboard sections are integrally machined from weldments of 10 Nickel steel plate and bar. The lower flange of the weldment extends inboard to the centerline. The upper flange extends inboard to $X_F$32. A machined 10 Nickel steel Tee section is mechanically spliced at these points to complete the upper flange. The lower flanges are spliced with a short 10 Nickel steel angle. The lower flange is attached to the lower plate with taper-loks which also pick up the lower fairing support angles. The intermediate bulkhead web area is a beta processed 6Al-4V titanium sandwich extending from approximately $X_F$84 to $X_F$39. This area is primarily designed to react shear & fuel pressure loads and local axial loads near the top and bottom edges. Locally high shear loads are also introduced by the forward end of the MLG drag load fitting. This panel was originally proposed to be an aluminum bonded sandwich. However, the local high load introduction areas required excessive thicknesses resulting in inefficient splice arrangements.

The inboard web area from $X_F$39 to $X_F$39 is a 2024 aluminum alloy bonded panel. The fuel pressure loading over the large flat panel makes this arrangement efficient.

### 2.1.1.3 $Y_F$ 992 Bulkhead

The configuration of this bulkhead is essentially the same as the $Y_F$ 932 bulkhead. The outboard webs, lower flange and upper cap is 10 Nickel steel. The main difference is that the bolted-on web is a one-piece beta processed 6Al-4V titanium bonded panel. Aluminum alloy was also originally considered for this panel. However, increased loads imposed during this phase made the titanium more efficient. An additional consideration in the selection of titanium was the more severe fatigue spectrum in the lower aft center area which would limit the allowable operating stress in the aluminum and thus penalize the steel lower plate rails.

The general configuration of the bulkhead was established by the interface requirements: i.e., $X_F$ 119 and $X_F$ 103 shear web attachments, the entrance access provisions and the MLG trunnions, actuator bracket and side load fitting provisions. The bulkhead (Dwg. No. X7224060) is shown in Figure 2-3.

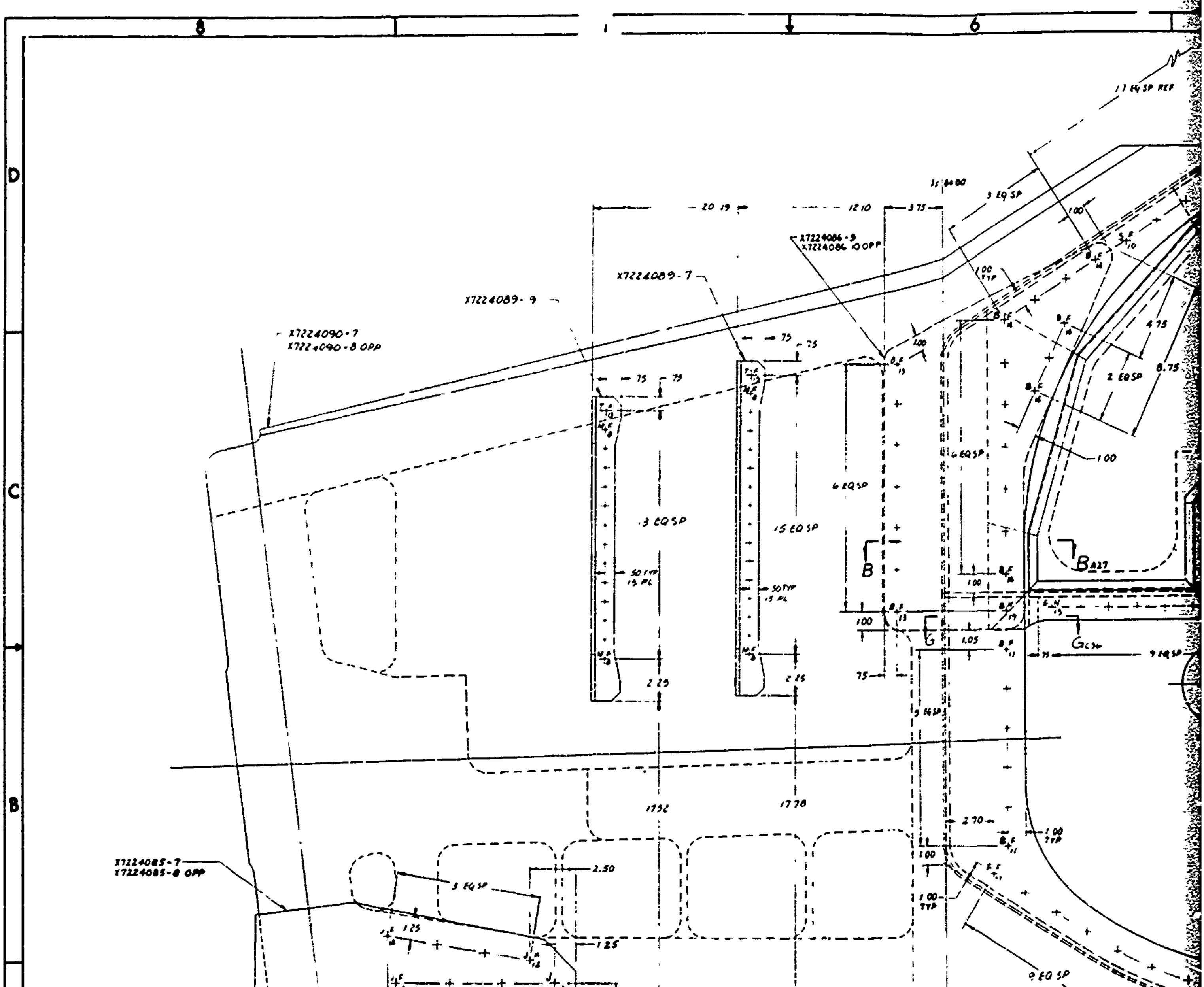

X7224090-7
X7224090-8 OPP
X7224089-9
X7224089-7
X7224086-9
X7224086-10 OPP
20.19
12.10
3.75
3 EQ SP
13 EQ SP
15 EQ SP
6 EQ SP
2 EQ SP
9 EQ SP
5 EQ SP
.50 TYP
15 PL
2.25
17.52
17.70
2.50
1.25
2.30
2.70
1.00 TYP
X7224085-7
X7224085-8 OPP
X7224050-7
X7224050-8 OPP
X7224170 REF
X7224162 REF
X 119.00 REF
X 122.55
X 122.80
10.00
10.45
4.75
8.75
1.05
B
G
A

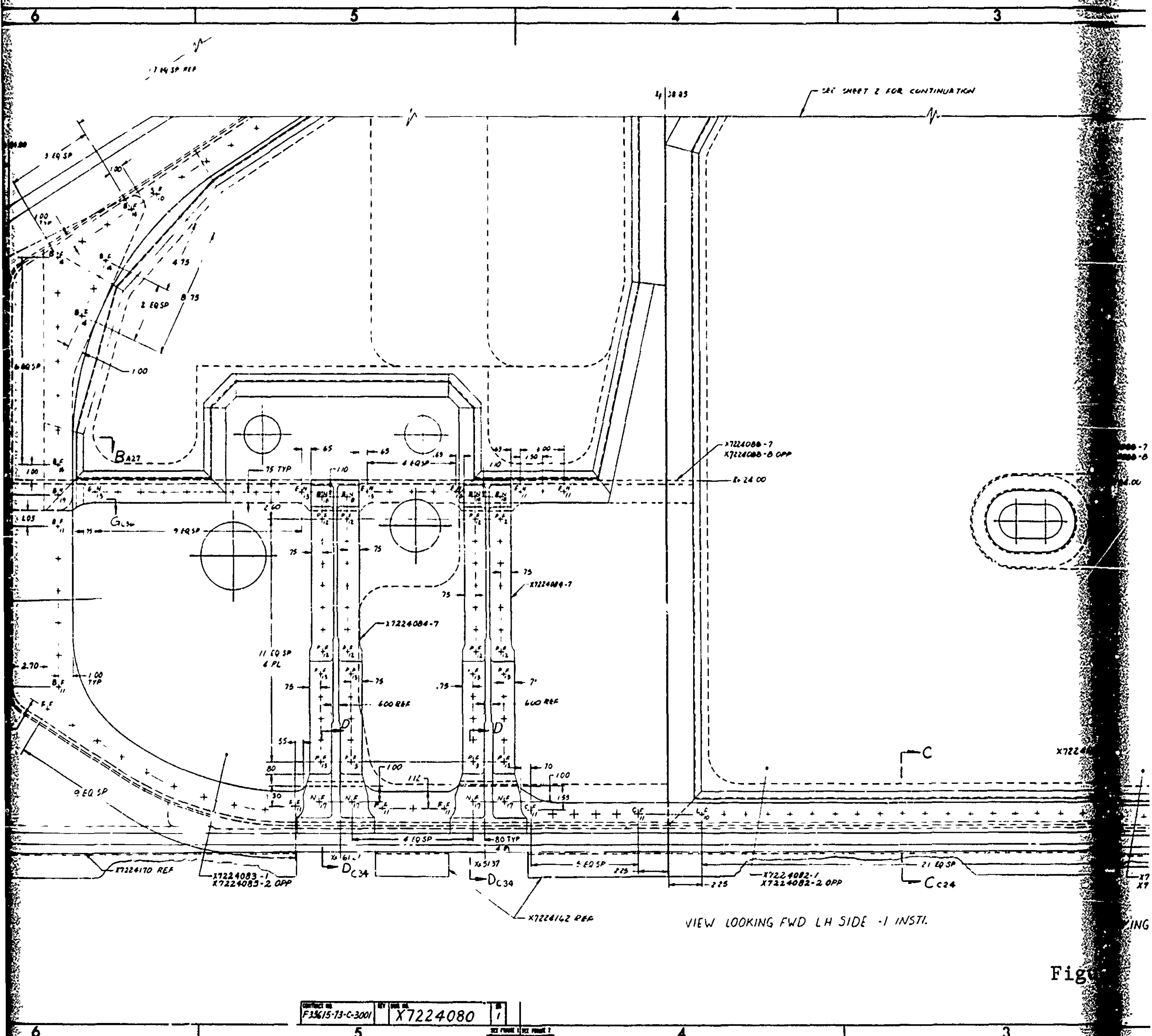
SEE SHEET 2 FOR CONTINUATION
X7224088-7
X7224088-8 OPP
X7224084-7
X7224170 REF
X7224083-1
X7224083-2 OPP
X7224162 REF
X7224082-1
X7224082-2 OPP
VIEW LOOKING FWD LH SIDE -1 INSTL.
F33615-73-C-3001
X7224080
6
5
4
3

Fig

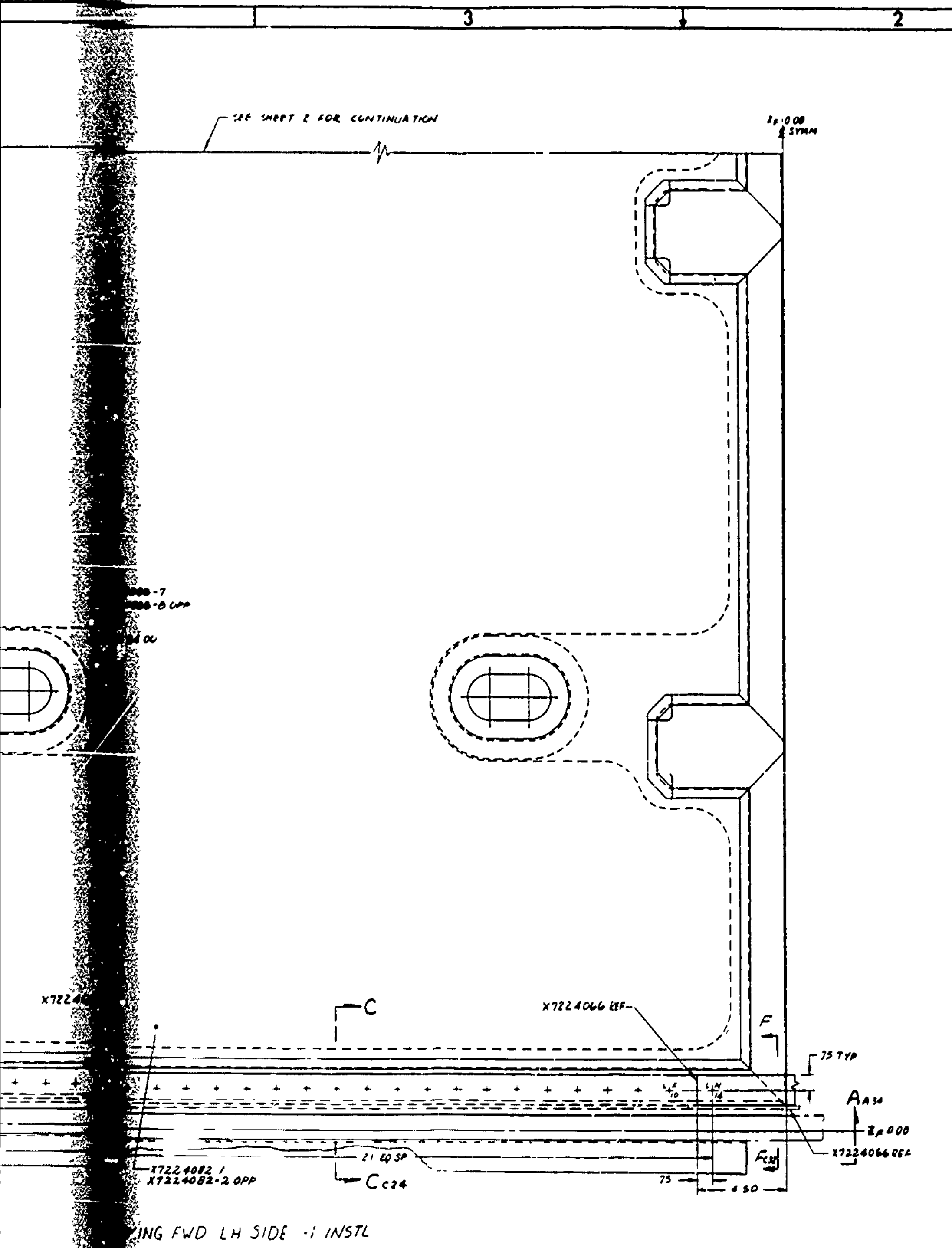


8 PENETRANT INSPECT -9 PER 81755/FPS-1064 ZONE C
7 ALL FASTENER HOLES THRU X7224162 SHALL BE STRAIGHT HOLES .030 LARGER IN DIA THAN THE MAX FASTENER DIA PENETRATING THE PART
6 REMOVE LAMINATIONS TO THICKNESS REQUIRED TO FILL VOID
5 APPLY -7 SEALANT TO FAYING SURFACES INDICATED AND TO SHANK OF ALL STRAIGHT SHANK BOLTS SEALANT MATL ¢ METHOD OF APPLICATION PER X7224196
4 MARK PARTS PER X7224198 CL 2A
3 -1 CONTAINS FRACTURE CRITICAL DETAILS RETAIN ORIGINAL DETAIL MATERIAL TRACEABILITY NUMBERS IN ACCORDANCE WITH X7224199
2 DIMENSIONS ¢ TOLERANCES PER USASI Y14.5
1 FASTENER CODE

BASIC CODE
HEAD LOCATION (N) NEAR; (F) FAR NO CODE OPTIONAL
GRIP LENGTH DASH NO

Δ - NOT LUBRICATED　　○ INDICATES GRIP FOR G, J, K ¢ L FASTENERS

| BASIC CODE | HOLE DIA | FASTENER | NUT | WASHER HEAD SIDE | WASHER NUT SIDE | TORQUE IN - LB | INSTL SPEC |
|---|---|---|---|---|---|---|---|
| A | .6275 .6241 | X7223996-10- | 81755/C077-10 | X7223992-10 | X7223994-10 | 100-2000Δ | NONE |
| B | .3770 .3746 | X72233966- | 81755/C077-6 | X7223992-6 | X7223994-6 | 160-390Δ | NONE |
| C | SEE SPEC | X7223993-6- | 81755/C389-6 | 81755/PS11-10 | NONE | SEE SPEC | X7223993-6 |
| D | .3770 .3746 | X7223980-12- | 81755/C2950-12 | X7223991-12 | NONE | 160-390Δ | NONE |
| E | .3770 .3746 | 81755/K020-12- | 81755/C2950-12 | X7223991-12 | X7223989-12 | 160-390Δ | NONE |
| F | SEE SPEC | X7223999-8- | 81755/C389-8 | 81755/PS11-16 | NONE | SEE SPEC | X7223993-8 |
| G | SEE SPEC | 81755/K5I3H8-○○ | 81755/C389-8 | 81755/PS11-17 | NONE | SEE SPEC | X7223993-8 |
| H | .6275 .6241 | 81755/K4550-10- | 81755/C077-10 | X7223992-10 | X7223994-10 | 100-2000Δ | NONE |
| J | SEE SPEC | 81755/K5I3H10-○○ | 81755/C389-10 | 81755/PS11-22 | NONE | SEE SPEC | X7223993-10 |
| K | SEE SPEC | 81755/K5I3H12-○○ | 81755/C389-12 | 81755/PS11-24 | NONE | SEE SPEC | X7223993-12 |
| L | SEE SPEC | 81755/K5I3H6-○○ | 81755/C389-6 | 81755/PS11-10 | NONE | SEE SPEC | X7223993-6 |
| M | .2520 .2496 | 81755/K020-8 | 81755/C2950-8 | X7223991-8 | NONE | 30-60Δ | NONE |
| N | SEE SPEC | X7223999-8- | 81755/K389-8 | 81755/PS11-16 | X7223986-8 | SEE SPEC | X7223993-8 |
| P | SEE SPEC | X7223999-6- | 81755/K389-6 | 81755/PS11-10 | X7223986-6 | SEE SPEC | X7223993-6 |
| R | SEE SPEC | X7223979-12- | 81755/K4520-12 | 81755/PS11-25 | X7223986-12 | SEE SPEC | X7223993-12 |
| S | .5026 .4996 | X7223996-8 | 81755/K077-8 | X7223992-8 | X7223994-8 | 480-1100Δ | NONE |
| T | .3770 .3746 | 81755/K4550-6 | 81755/K077-6 | X7223992-6 | X7223994-6 | 160-390Δ | NONE |
| U | SEE SPEC | X7223979-8- | 81755/K4520-8 | 81755/PS11-16 | X7223986-8 | SEE SPEC | X7223993-8 |

NOTES (EXCEPT AS SHOWN)

NEXT SECTION LETTER: J

| REV STATUS | |
|---|---|
| SH | REV |
| 1 | - |
| 2 | - |
| 3 | - |

SEE SEPARATE PARTS LIST

U. S. AIR FORCE

GENERAL DYNAMICS
CONVAIR AEROSPACE DIVISION
FORT WORTH OPERATION
FORT WORTH TEXAS

SEE PL

BULKHEAD INSTL - $Y_F$ 932.00

J　01818　X7224080

X7224080

Figure 2-2 (Sheet 1)

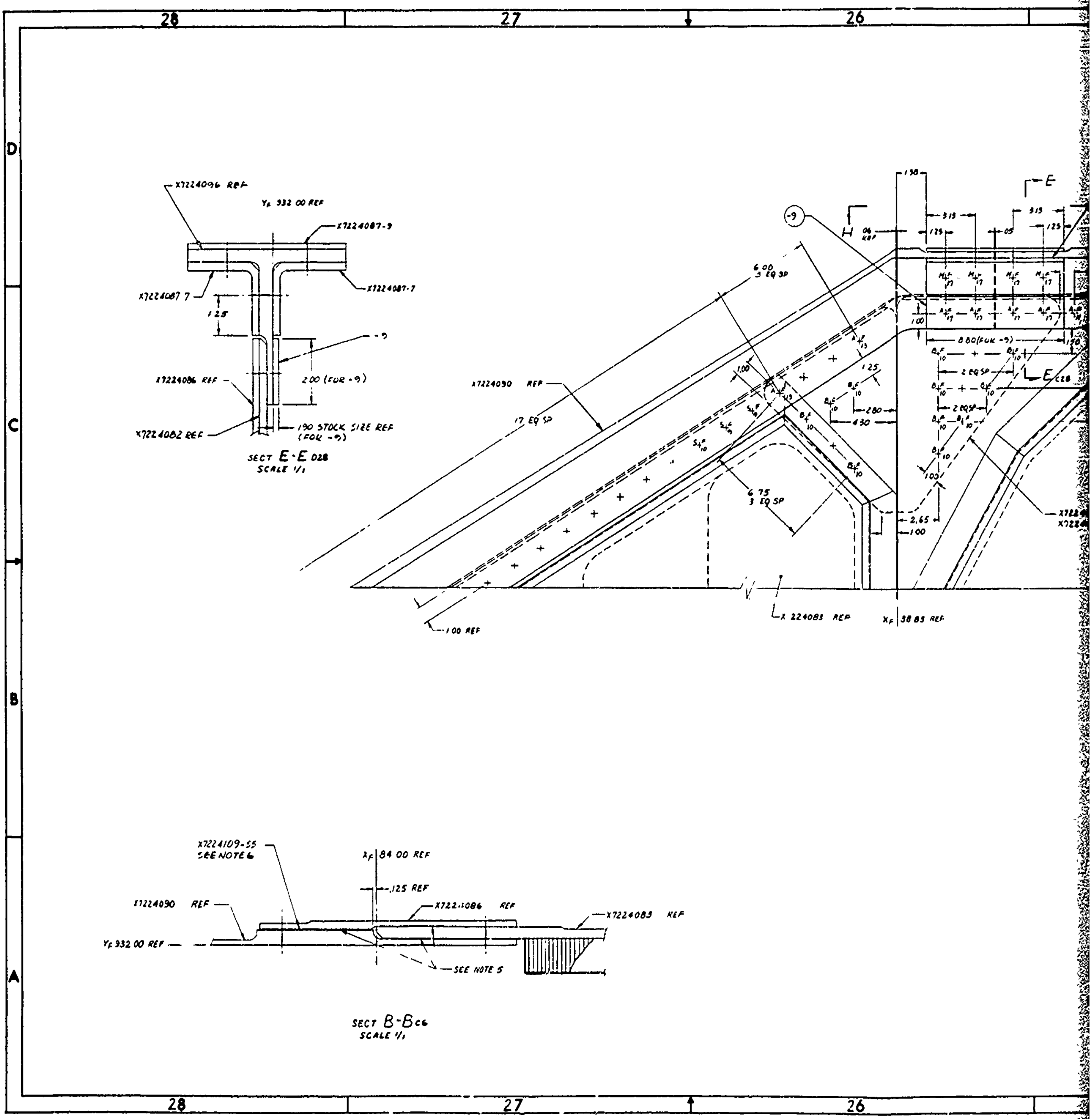

28
27
26
D
C
B
A
X7224096 REF
YF 932 00 REF
X7224087-9
X7224087 7
X7224087-7
125
-9
X7224086 REF
200 (FOR -9)
X7224082 REF
190 STOCK SIZE REF (FOR -9)
SECT E-E D28
SCALE 1/1
X7224090 REF
17 EQ SP
6 00
3 EQ SP
6 75
3 EQ SP
1 00 REF
X 224083 REF
XF 38 83 REF
880 (FOR -9)
2 EQ SP
280
430
2.65
100
X7224109-55
SEE NOTE 6
XF 84 00 REF
.125 REF
X7224090 REF
X7224086 REF
X7224083 REF
YF 932 00 REF
SEE NOTE 5
SECT B-B C6
SCALE 1/1

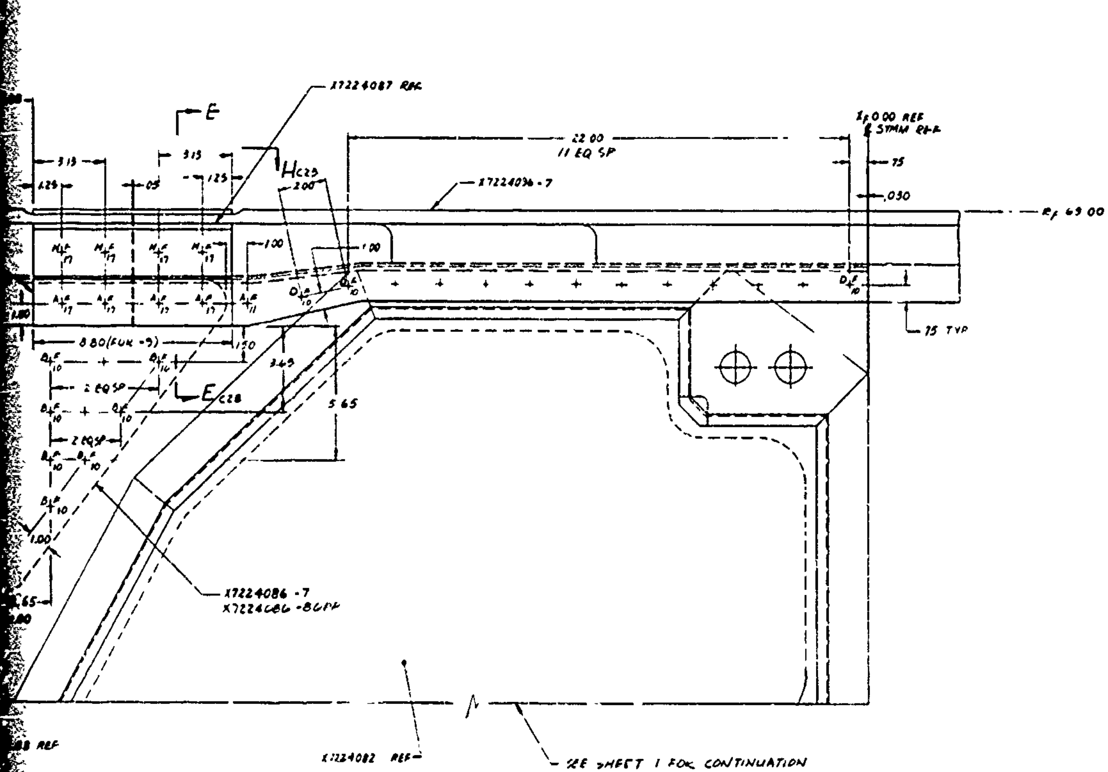


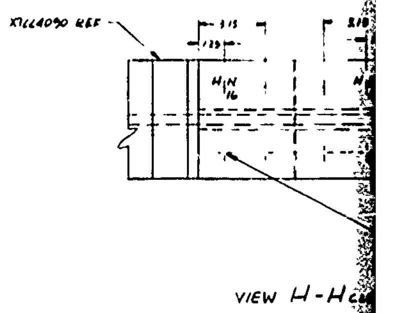


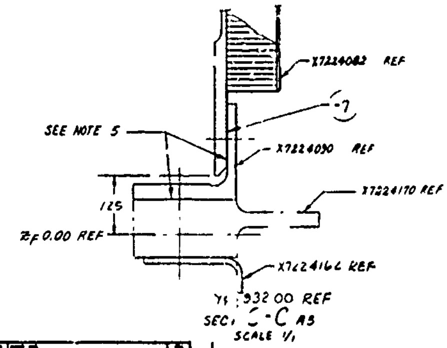


CONTRACT NO. F33615-73 C3001 | DWG NO. X7224080 | SH 2

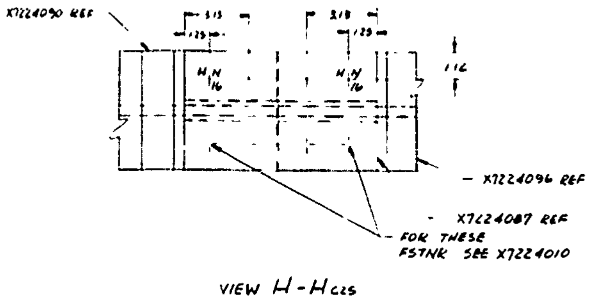



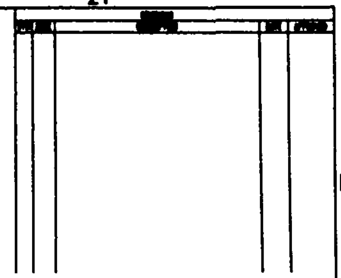

Figure 2-2 (Sheet 2)

U.S. AIR FORCE

GENERAL DYNAMICS

CONVAIR AEROSPACE DIVISION

FORT WORTH OPERATION

FORT WORTH TEXAS

BULKHEAD INSTL-
$Y_F$ 932.00

J 07878 X7224080

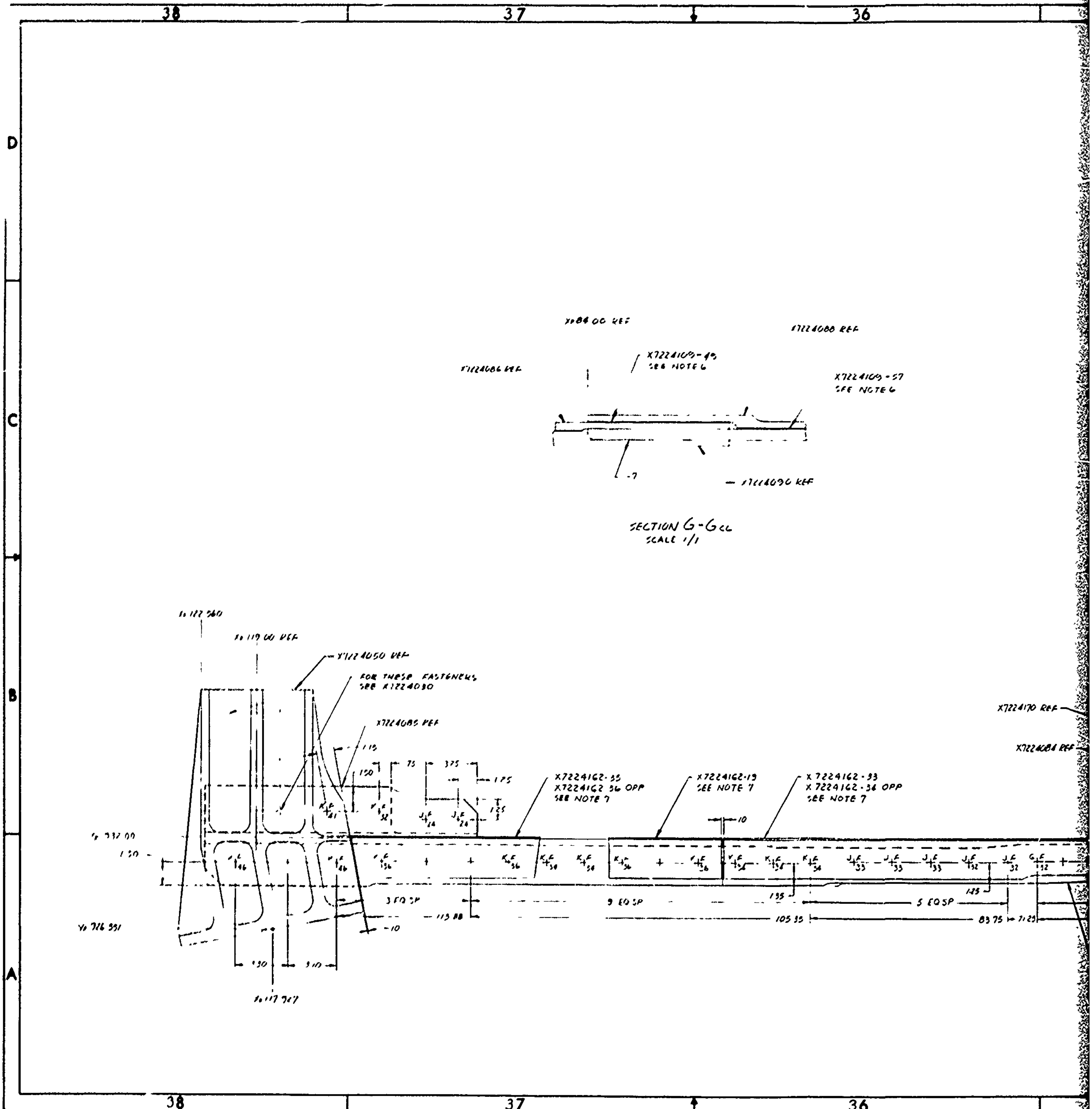

38
37
36
D
C
B
A
X7224088 REF
X7224109-49
SEE NOTE 6
X7224086 REF
X7224109-57
SEE NOTE 6
-7
X7224090 REF
SECTION G-G
SCALE 1/1
X7224050 REF
FOR THESE FASTENERS
SEE X7224030
X7224085 REF
X7224170 REF
X7224084 REF
X7224162-35
X7224162-36 OPP
SEE NOTE 7
X7224162-19
SEE NOTE 7
X 7224162-33
X 7224162-34 OPP
SEE NOTE 7
3 EQ SP
9 EQ SP
5 EQ SP
105.35
83.75

35 34 33

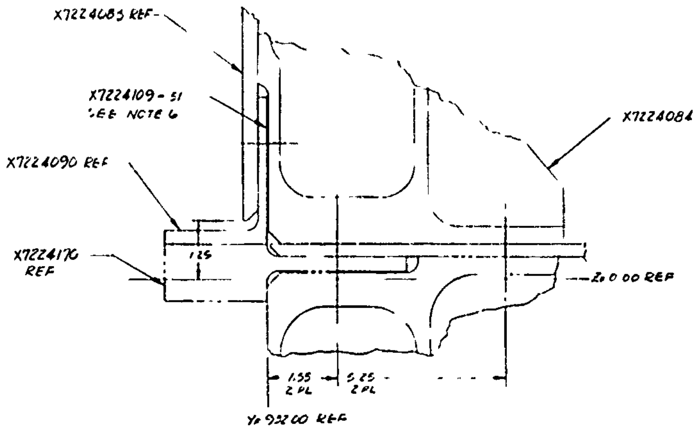


SECTION D-D A5
SCALE 1/1

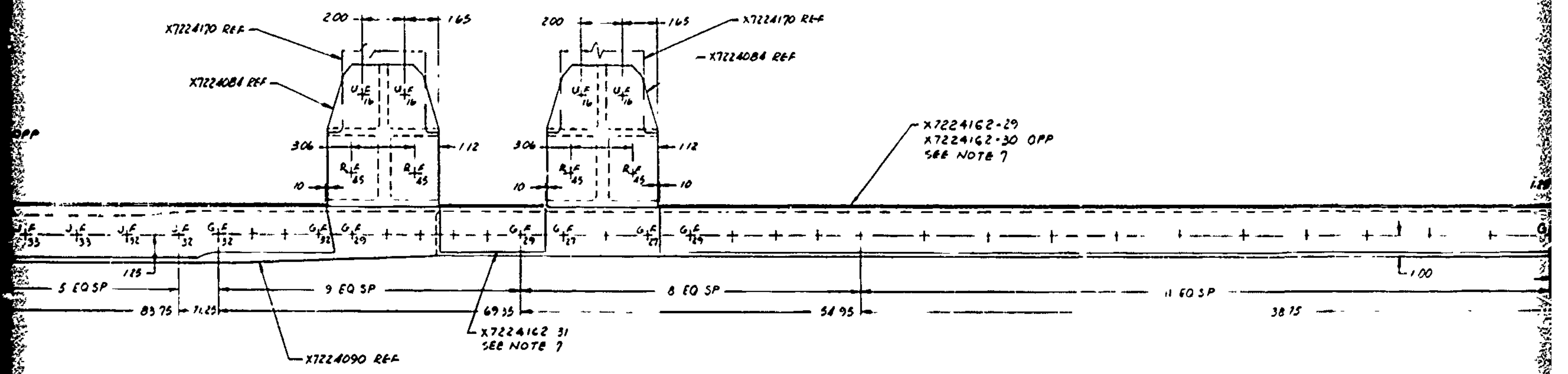


VIEW A-A A2

F33615 73 C 3001 | X7224080 | 3

35 34 33

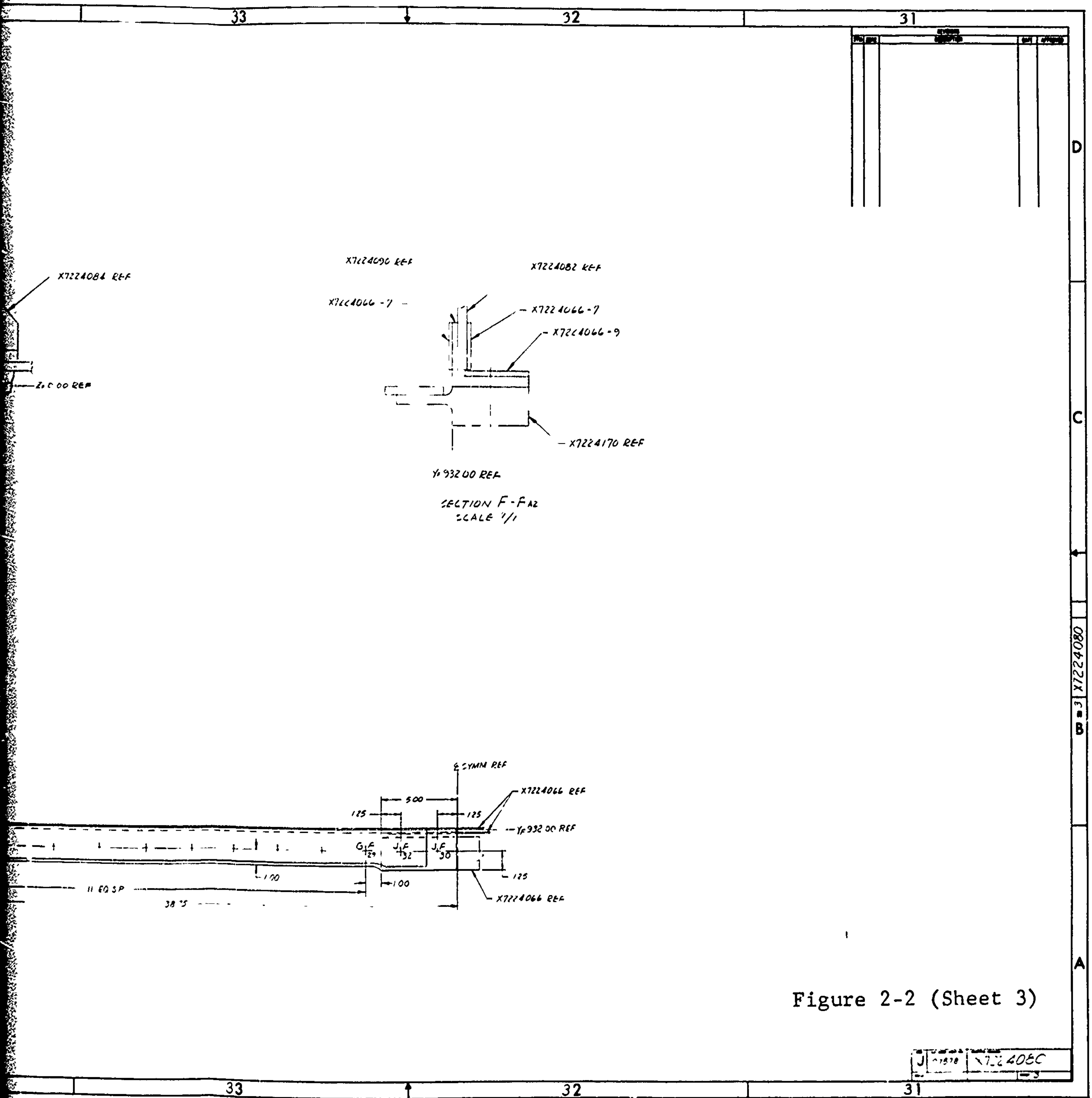


Figure 2-2 (Sheet 3)

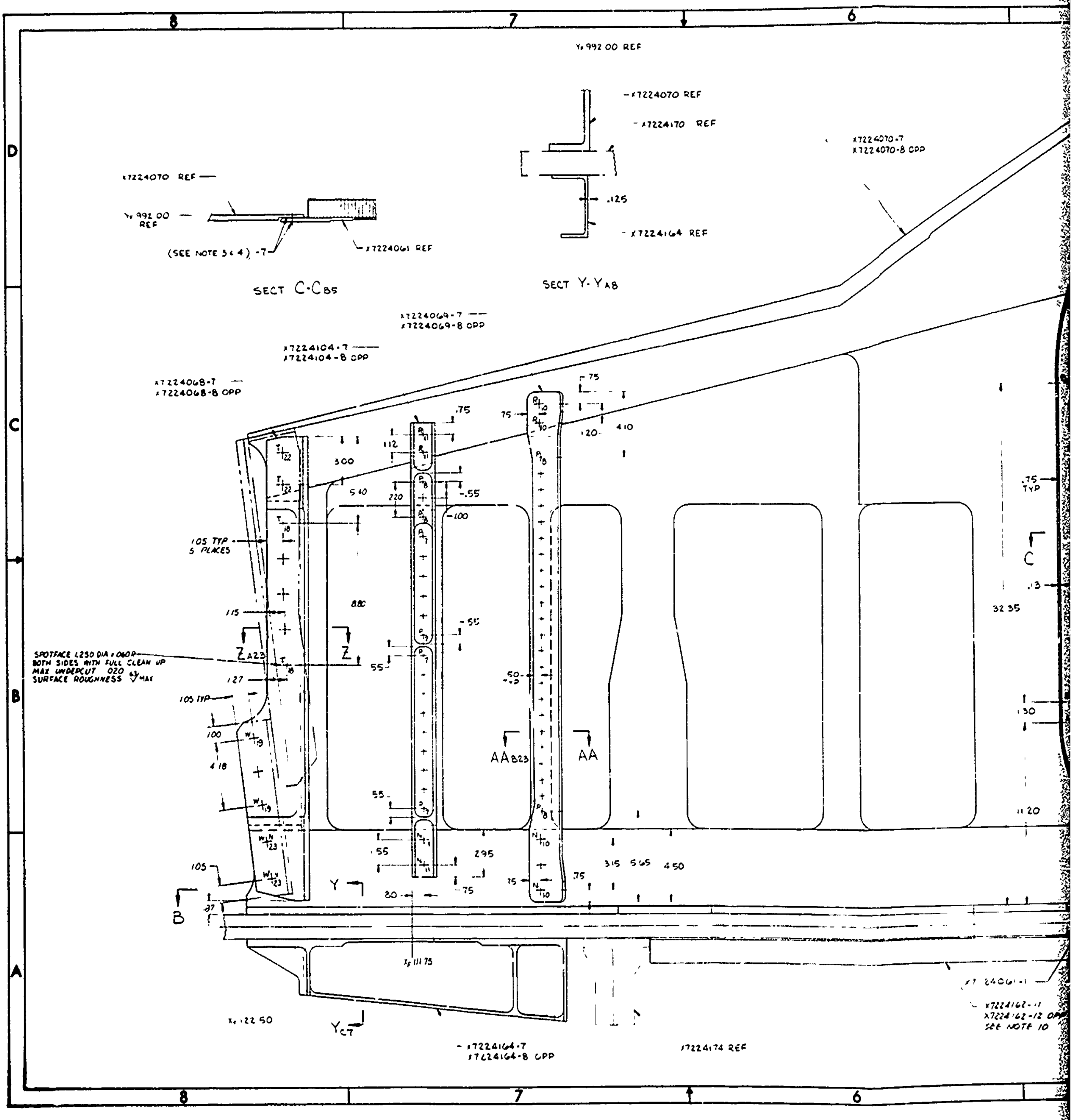

YF 992.00 REF
X7224070 REF
X7224170 REF
X7224070-7
X7224070-8 OPP
X7224070 REF
YF 992.00 REF
(SEE NOTE 3 & 4) -7
X7224061 REF
.125
X7224164 REF
SECT C-C B5
SECT Y-Y A8
X7224069-7
X7224069-8 OPP
X7224104-7
X7224104-8 OPP
X7224068-7
X7224068-8 OPP
105 TYP
5 PLACES
SPOTFACE L250 DIA x.060R
BOTH SIDES WITH FULL CLEAN UP
MAX UNDERCUT .020
SURFACE ROUGHNESS 63 MAX
Z A23
Z
AA B23
AA
C
32.35
B
Y
XF 111.75
XF 122.50
Y C7
X7224164-7
X7224164-8 OPP
X7224174 REF
X7224162-11
X7224162-12 OPP
SEE NOTE 10

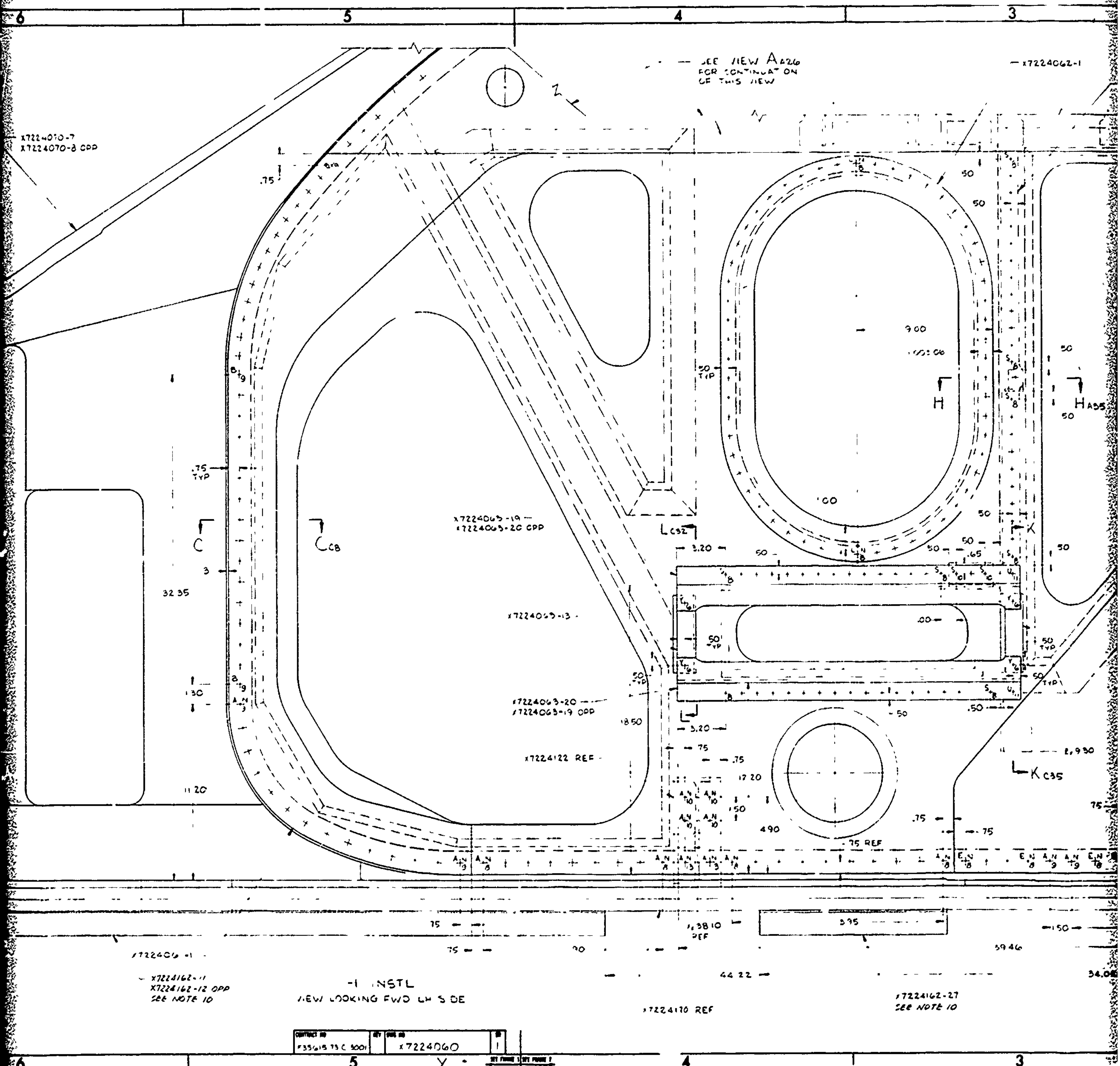
SEE VIEW A A26 FOR CONTINUATION OF THIS VIEW
X7224062-1
X7224070-7
X7224070-8 OPP
X7224063-19
X7224063-20 OPP
X7224063-13
X7224063-20
X7224063-19 OPP
X7224122 REF
X7224062-1
X7224162-11
X7224162-12 OPP
SEE NOTE 10
X7224130 REF
X7224162-27
SEE NOTE 10
-1 INSTL
VIEW LOOKING FWD LH SIDE
F33615 73 C 5001
X7224060

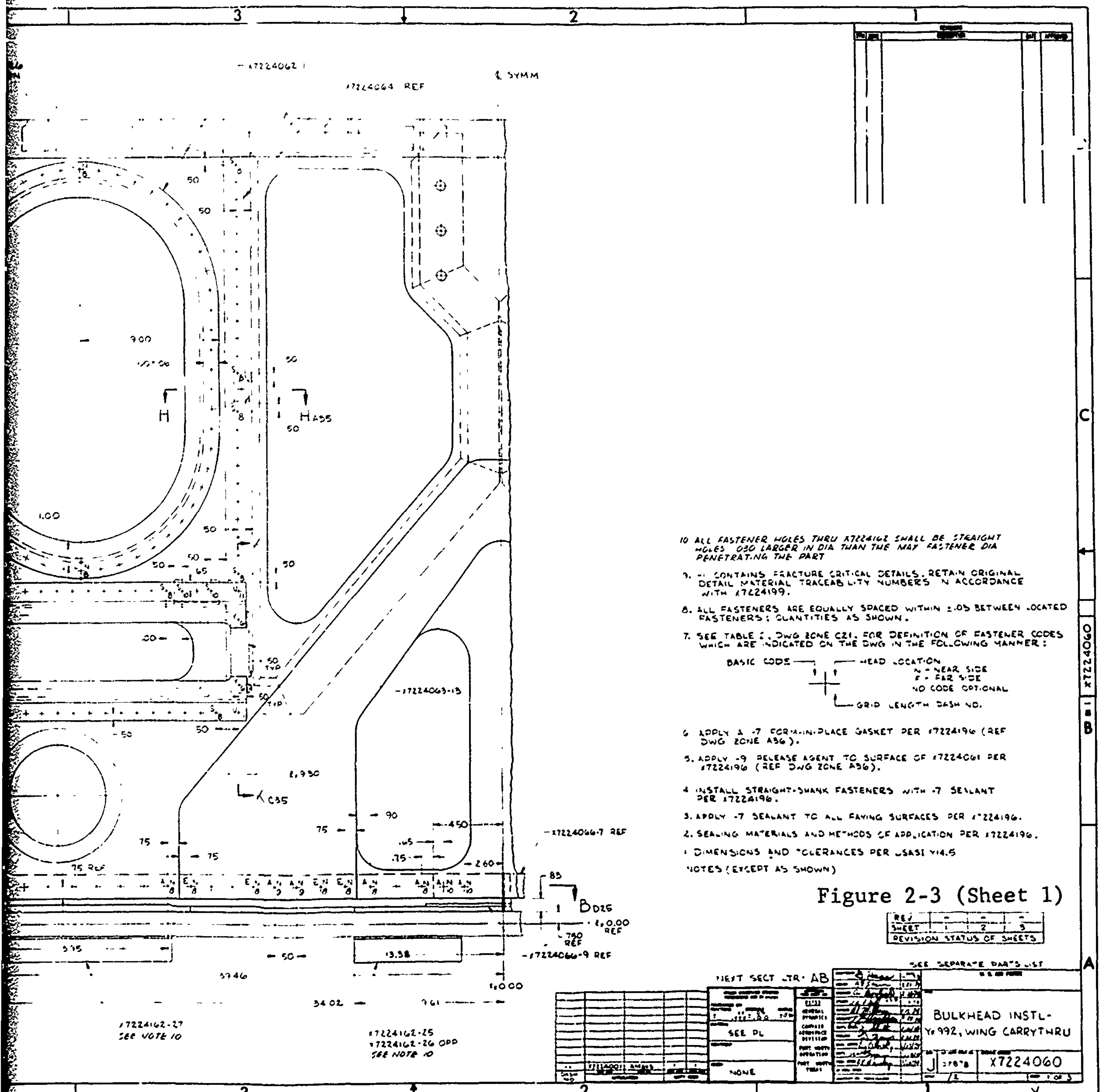


Figure 2-3 (Sheet 1)

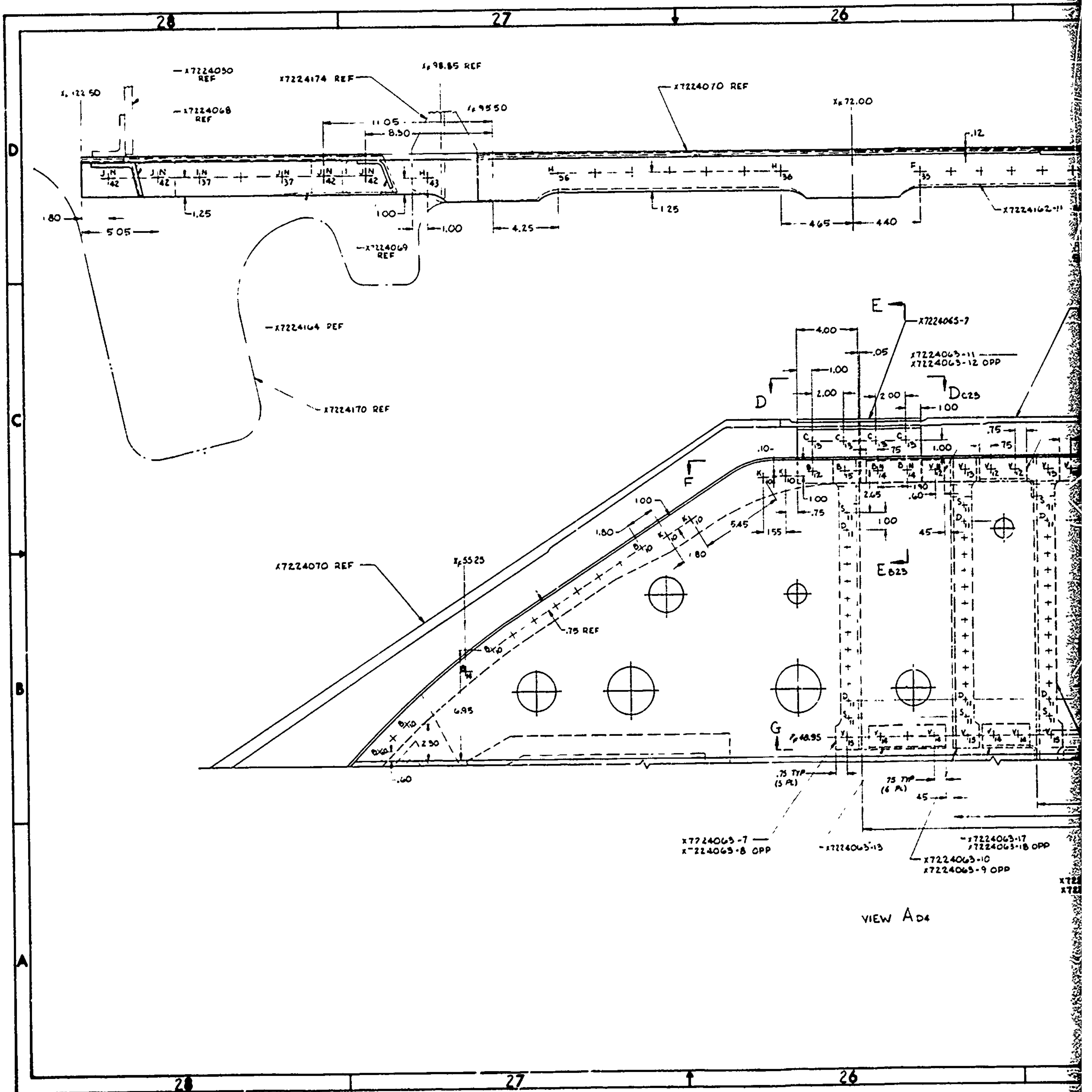

X7224050 REF
X7224068 REF
X7224174 REF
X7224070 REF
X7224069 REF
X7224164 REF
X7224170 REF
X7224162-11
X7224065-7
X7224063-11
X7224063-12 OPP
X7224063-7
X7224063-8 OPP
X7224063-13
X7224063-17
X7224063-18 OPP
X7224063-10
X7224063-9 OPP
.75 REF
.75 TYP (5 PL)
.75 TYP (6 PL)
VIEW A D4

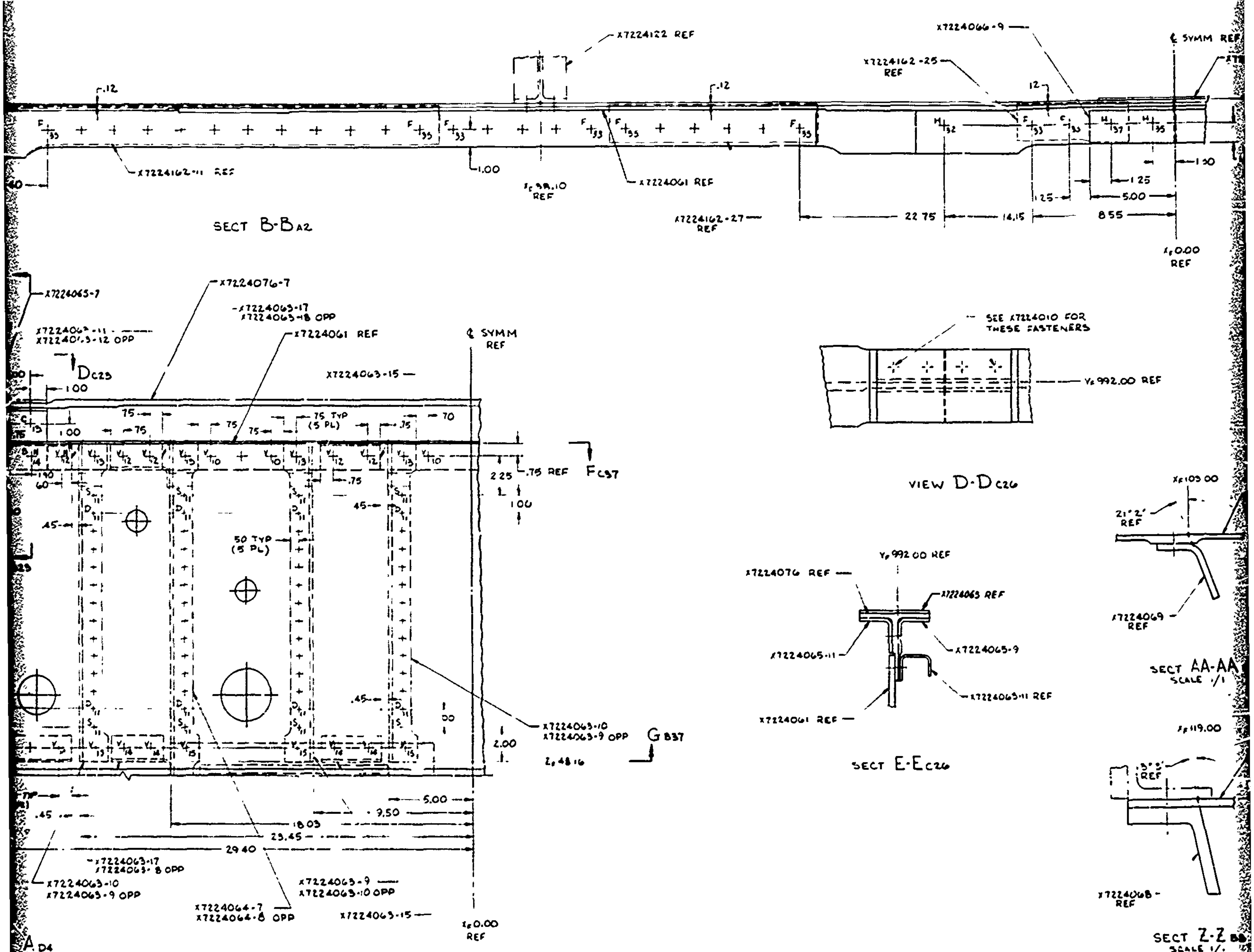


| 25 | 24 | 23 |
|---|---|---|

F33615-73-C-5001 | X7224060 | 2

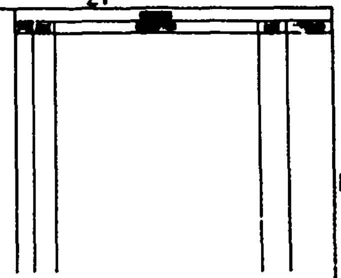


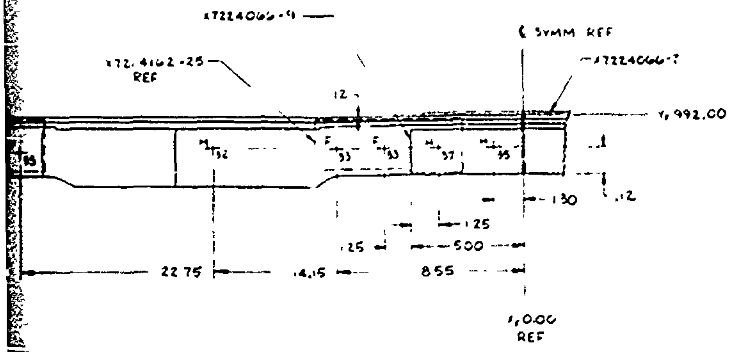


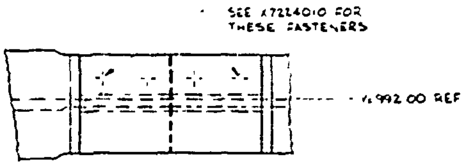


VIEW D-D C26

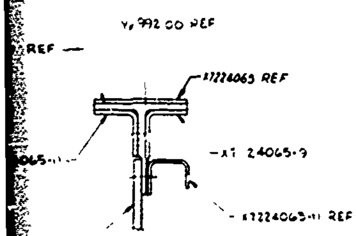


SECT F-E C26

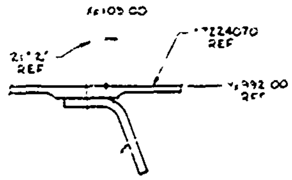


SECT AA-AA B7
SCALE 1/1

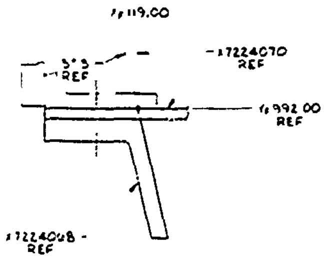


SECT Z-Z B8
SCALE 1/1

| TABLE I FASTENER CODES (SEE NOTE 7) | | | | | | | |
|---|---|---|---|---|---|---|---|
| BASIC CODE | HOLE DIA | FASTENER | NUT | WASHER (UNDER BOLT) | WASHER (UNDER NUT) | INSTL SPEC | TORQUE (IN-LB) |
| A | SEE SPEC | X7223999-6- | 81755/C389-6 | 81755/P511-10 | NONE | X7223993-6 | SEE SPEC |
| B | .3770/.3746 | X7223996-6- | 81755/C077-6 | X7223992-6 | X7223994-6 | NONE | 160-390 Δ |
| C | .5025/.4996 | 81755/CA550-8- | 81755/C077-8 | X7223992-8 | X7223994-8 | NONE | 480-1100 Δ |
| D | .2520/.2496 | 81755/C020-8- | 81755/C2950-8 | X7223991-8 | X7223989-8 | NONE | 30-60 Δ |
| E | SEE SPEC | X7223985-6- | 81755/C389-6 | NONE | NONE | X7223983-6 | SEE SPEC |
| F | SEE SPEC | 81755/C513H8- | 81755/C389-8 | 81755/P511-17 | NONE | X7223993-8 | SEE SPEC |
| G | .3145/.3121 | X7223996-5- | 81755/C077-5 | X7223992-5 | X7223994-5 | NONE | 100-225 Δ |
| H | SEE SPEC | 81755/C513H10- | 81755/C389-10 | 81755/P511-22 | NONE | X7223993-10 | SEE SPEC |
| J | SEE SPEC | 81755/C513H12- | 81755/C389-12 | 81755/P511-24 | NONE | X7223993-12 | SEE SPEC |
| K | .5025/.4996 | X7223996-8- | 81755/C077-8 | X7223992-8 | X7223994-8 | NONE | 480-1100 Δ |
| L | .2819/.2811 | X7223996- | NAS1474C4 | X7223992-4 | NONE | NONE | 50-100 Δ |
| M | .2520/.2496 | X7223955-4 | 81755/C906-4 | X7223988-4 | X7223987-4 | NONE | 00-110 Ⅱ |
| N | SEE SPEC | 81755/C513H6- | 81755/C389-6 | 81755/P511-10 | NONE | X7223993-6 | SEE SPEC |
| P | .2520/.2496 | 81755/C3002-8- | 81755/C2950-8 | X7223991-8 | NONE | NONE | 50-100 Δ |
| R | .3770/.3746 | 81755/C3002-12- | 81755/C2950-12 | X7223991-12 | NONE | NONE | 160-390 Δ |
| S | .2520/.2496 | X7223980-8- | 81755/C2950-8 | X7223991-8 | X7223989-8 | NONE | 50-100 Δ |
| T | .6275/.6241 | X7223996-10- | 81755/C077-10 | X7223992-10 | X7223994-10 | NONE | 1100-2400 Δ |
| U | .3145/.3121 | X7223980-10- | 81755/C2950-10 | X7223991-10 | X7223989-10 | NONE | 60-140 Δ |
| V | .3770/.3746 | X7223980-12- | 81755/C2950-12 | X7223991-12 | X7223989-12 | NONE | 140-380 Δ |
| W | SEE SPEC | X7223999-10- | 81755/C389-10 | 81755/P511-22 | X7223986-10 | X7223993-10 | SEE SPEC |
| Y | .2520/.2496 | 81755/C020-8- | 81755/C2950-8 | X7223991-8 | NONE | NONE | 30-60 Δ |
| | | | | | | | |

Δ - NOT LUBRICATED
Ⅱ - APPLY MIL T-5544 THREAD COMPOUND TO FAYING SURFACES OF NUT SIDE WASHER, BOLT THREADS AND NUT THREADS.

Figure 2-3 (Sheet 2)

BULKHEAD INSTL-
Y₀ 992, WING CARRYTHRU

J | 07878 | X7224060

23 22 21

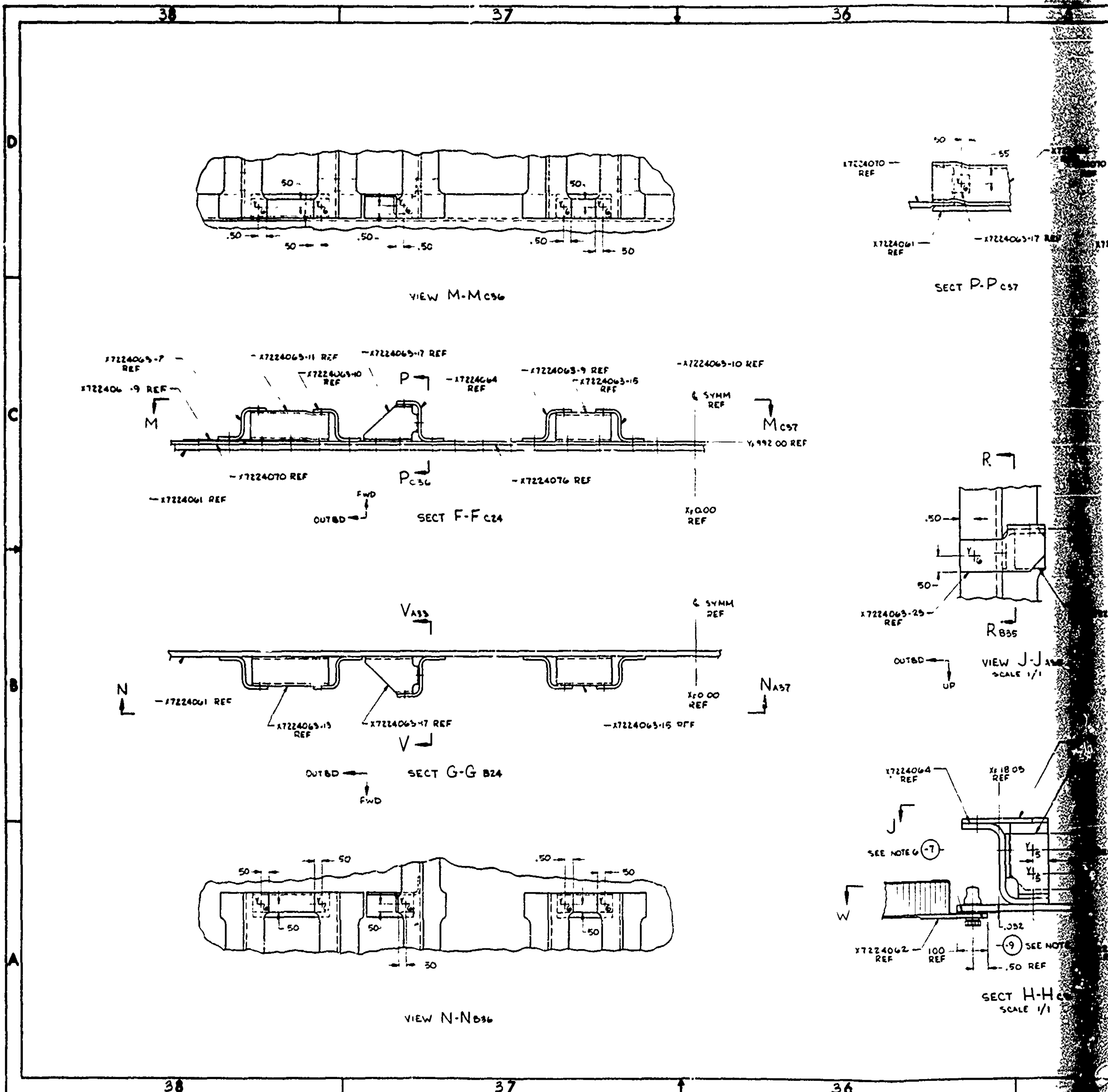

38
37
36
D
C
B
A
VIEW M-M C36
X7224070 REF
X7224061 REF
-X7224063-17 REF
SECT P-P C57
X7224063-7 REF
X722406 -9 REF
-X7224063-11 REF
-X7224063-17 REF
-X7224063-10 REF
P
-X7224064 REF
-X7224063-9 REF
-X7224063-15 REF
-X7224063-10 REF
℄ SYMM REF
M
M C57
Y1 992.00 REF
-X7224070 REF
P C36
-X7224076 REF
-X7224061 REF
FWD
OUTBD
SECT F-F C24
X1 0.00 REF
R
R B35
X7224063-29 REF
OUTBD
UP
VIEW J-J
SCALE 1/1
V A33
℄ SYMM REF
N
-X7224061 REF
X1 0.00 REF
N A37
X7224063-13 REF
-X7224063-17 REF
-X7224063-15 REF
V
OUTBD
FWD
SECT G-G B24
X7224064 REF
X1 18.05 REF
J
SEE NOTE 6 (-7)
W
X7224062 REF
.100 REF
.50 REF
(-9) SEE NOTE
.032
VIEW N-N B36
SECT H-H
SCALE 1/1

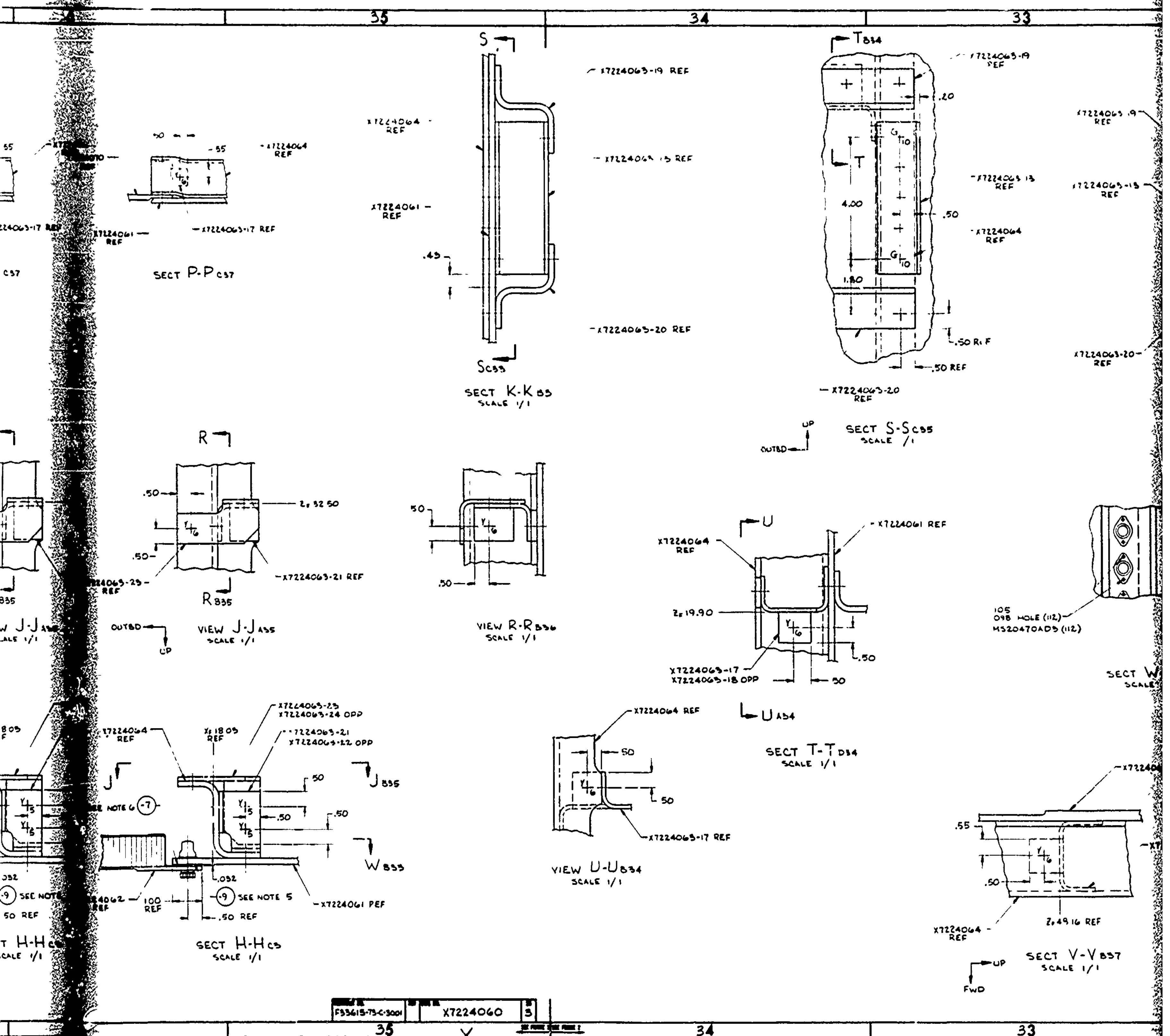

35
34
33
SECT P-P C37
SCALE 1/1
X7224064 REF
X7224063-17 REF
X7224061 REF
SECT K-K B35
SCALE 1/1
X7224063-19 REF
X7224063-15 REF
X7224063-20 REF
X7224064 REF
X7224061 REF
.45
SECT S-S C35
SCALE 1/1
X7224063-19 REF
X7224063-15 REF
X7224064 REF
X7224063-20 REF
4.00
1.80
.20
.50
.50 REF
UP
OUTBD
VIEW J-J A35
SCALE 1/1
Z 32.50
X7224063-21 REF
VIEW R-R B36
SCALE 1/1
SECT T-T D34
SCALE 1/1
X7224064 REF
X7224061 REF
Z 19.90
X7224063-17
X7224063-18 OPP
.50
105
098 HOLE (112)
MS20470AD5 (112)
SECT H-H C5
SCALE 1/1
X 18.05 REF
X7224063-25
X7224063-24 OPP
X7224063-21
X7224063-22 OPP
SEE NOTE 6
SEE NOTE 5
.032
100 REF
.50 REF
X7224061 REF
VIEW U-U B34
SCALE 1/1
X7224064 REF
X7224063-17 REF
SECT V-V B37
SCALE 1/1
.55
.50
Z 49.16 REF
X7224064 REF
UP
FWD
F33615-73-C-3001
X7224060

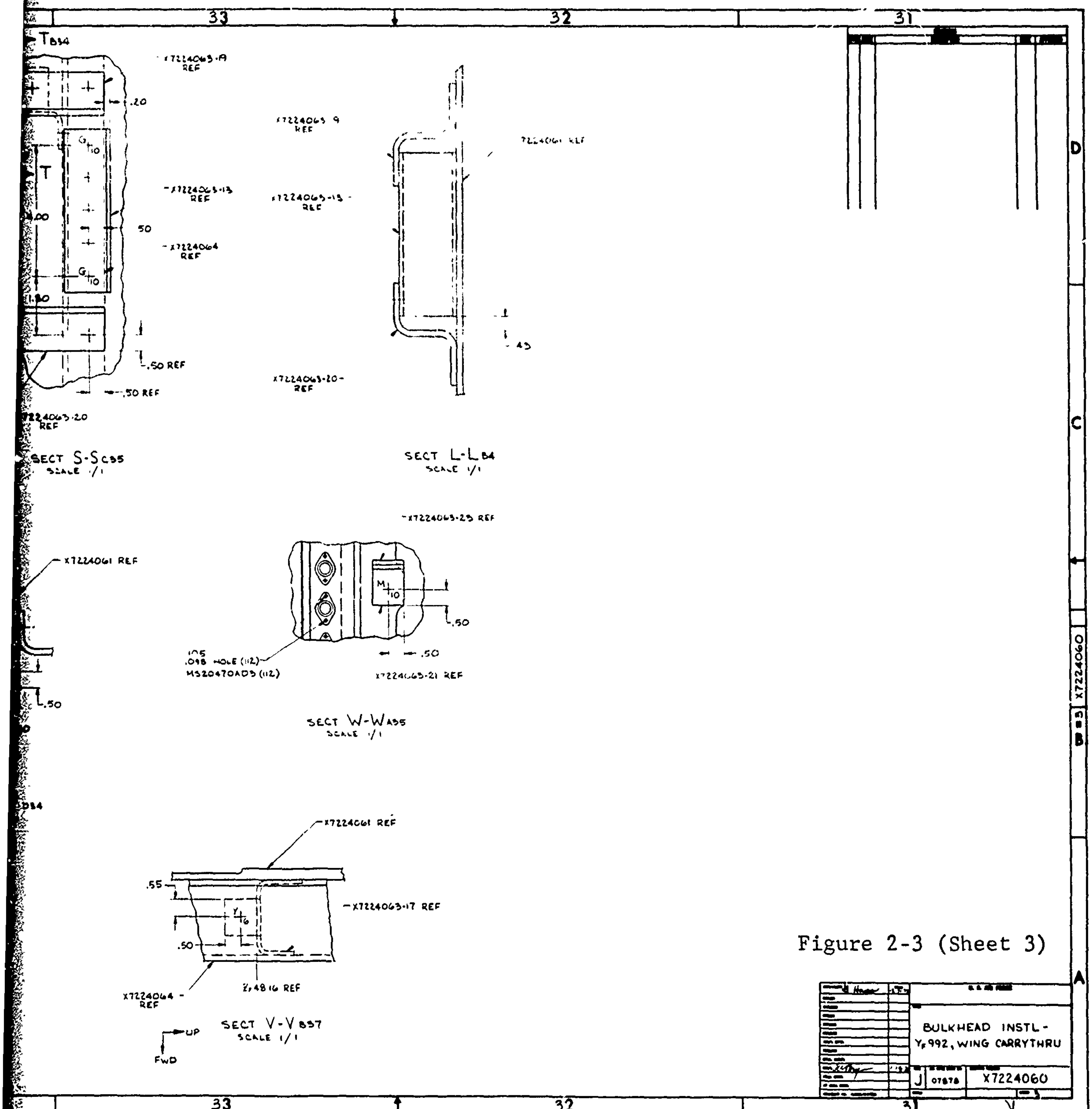


Figure 2-3 (Sheet 3)

#### 2.1.1.4 Upper Cover and Pivot Lugs

The upper cover, Drawing X7224010, Figure 2-4, is segmented into five components as it generally follows the air vehicle upper contour. The pivot lug and section outboard of $X_F84$ are integrally machined from a 10 Nickel steel plate that has been formed to accomodate the directional change required at the closure rib. This component transfers the majority of the axial load into the bulkhead caps by means of a single-shear bolted splice. The remaining axial load is transferred into aluminum sandwich panels which form the upper cover inboard of $X_F84$. These panels also react shear and fuel pressure loads. The left and right hand panels between $X_F39$ and $X_F84$ are contoured and partially form the external fuselage boundary. The outboard edge of these panels breaks below contour and forms an attach area for an aerodynamic fairing at the fuselage contour that extends outboard to approximately $X_F$ 123. The panel inboard of $X_F39$ is not contoured, but functions as the lower surface of the routing tunnel.

#### 2.1.1.5 Centerline Rib

The centerline rib (Figure 2-5, Drawing X7224110) is an aluminum sandwich panel which divides the left and right hand fuel tanks and distributes the loads introduced by the interface structure. This panel utilizes slug type edge members with integral attaching flanges at $Y_F$ 932 and $Y_F$ 992 bulkheads. Separate bolt-on attach angles are required at the upper and lower plates. Reinforcing beams are required to react and distribute the local concentration of loads introduced by the weapons launcher and the MLG side load fitting. These beams, two per side, are machined from 7050 Aluminum and are located at approximately $Z_F26$ and $Z_F44$.

#### 2.1.1.6 Inboard Intermediate Rib

The inboard rib at $X_F39$ (Figure 2-6, Drawing X7224120) is an aluminum sandwich panel with bolt-on aluminum tee flanges for attaching and splicing the upper and lower covers and the bulkhead webs at $Y_F$ 932 and 992. This rib distributes the loads resulting from the directional change in the upper cover and loads introduced by the MLG drag fitting back-up beam located at $Y_F$ 947. An access opening is provided in the middle of the panel to allow entry to the outboard section of the box structure during fabrication, service maintenance, and inspection. Fuel flow and venting are also adequately provided.

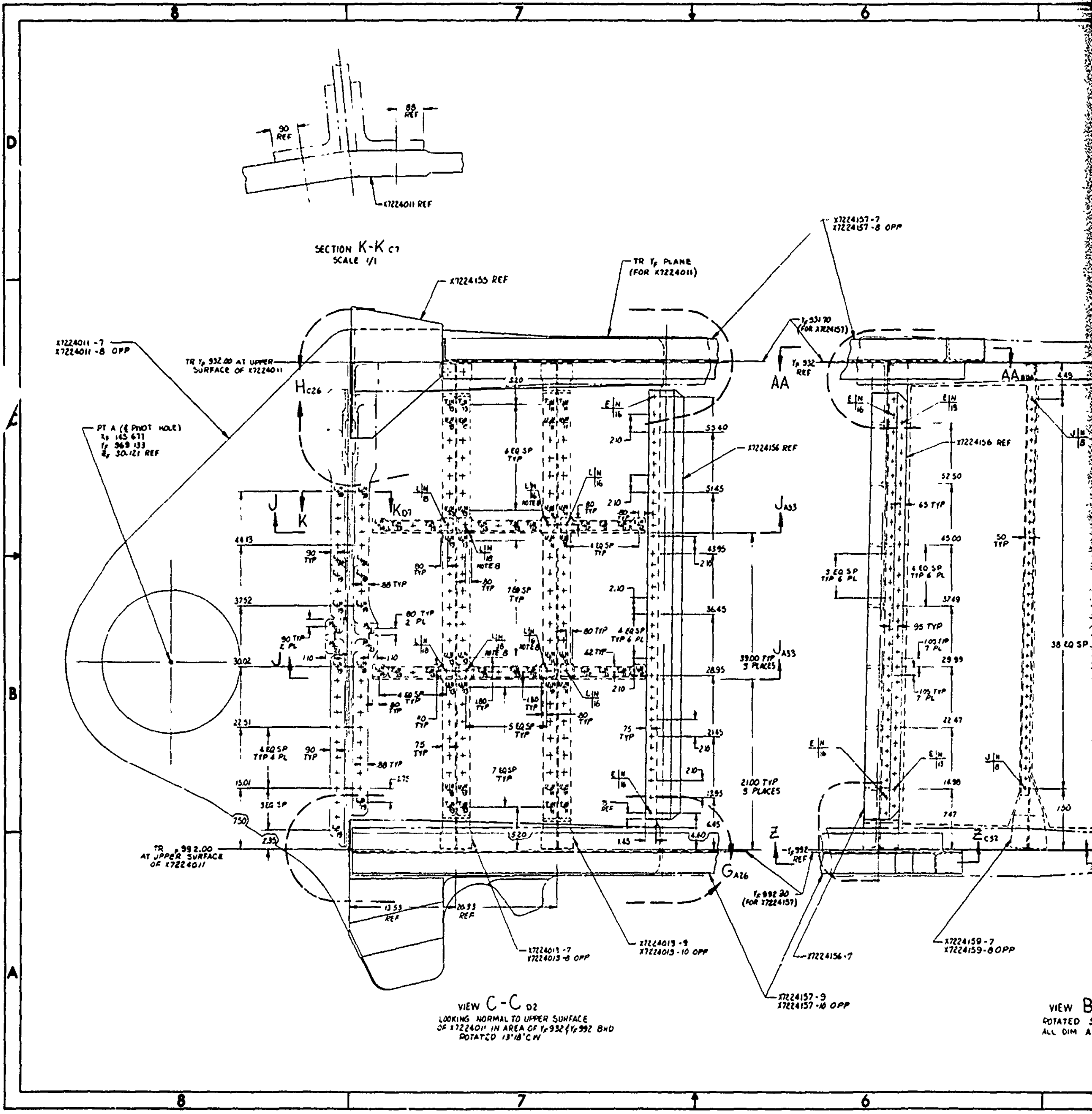

8
7
6
D
C
B
A
SECTION K-K C7
SCALE 1/1
X7224011 REF
X7224155 REF
TR Yp PLANE (FOR X7224011)
X7224157-7
X7224157-8 OPP
X7224011-7
X7224011-8 OPP
TR Yp 932.00 AT UPPER SURFACE OF X7224011
PT A (℄ PIVOT HOLE)
X7224156 REF
X7224156-7
TR Yp 992.00 AT UPPER SURFACE OF X7224011
X7224013-7
X7224013-8 OPP
X7224013-9
X7224013-10 OPP
X7224157-9
X7224157-10 OPP
X7224159-7
X7224159-8 OPP
VIEW C-C D2
LOOKING NORMAL TO UPPER SURFACE
OF X7224011 IN AREA OF Yp 932 & Yp 992 BHD
ROTATED 13°18' CW

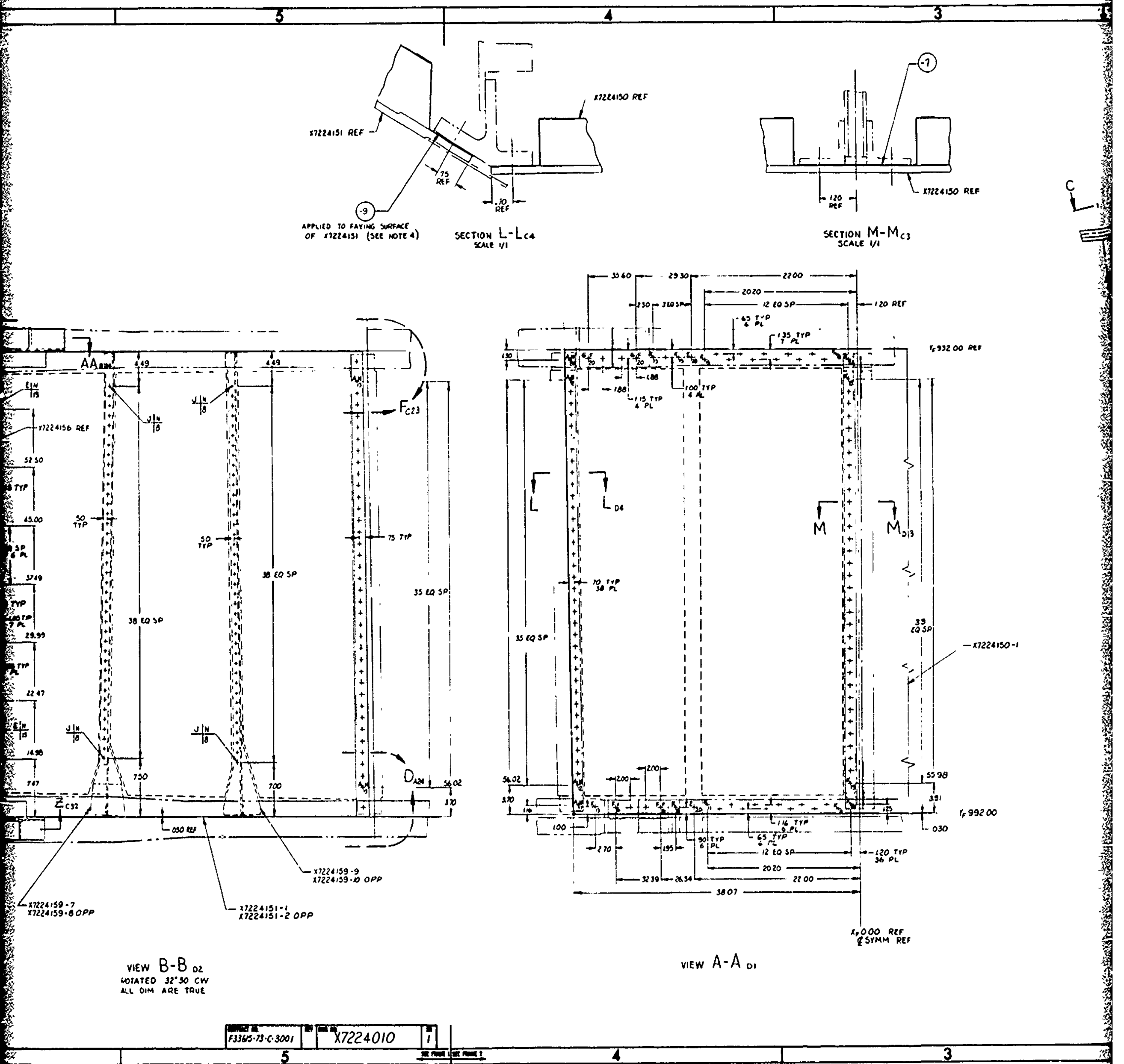

X7224151 REF
X7224150 REF
APPLIED TO FAYING SURFACE OF X7224151 (SEE NOTE 4)
SECTION L-L C4
SCALE 1/1
SECTION M-M C3
SCALE 1/1
X7224156 REF
X7224150-1
X7224159-9
X7224159-10 OPP
X7224159-7
X7224159-8 OPP
X7224151-1
X7224151-2 OPP
VIEW B-B D2
ROTATED 32°30 CW
ALL DIM ARE TRUE
VIEW A-A D1
F33615-73-C-3001
X7224010

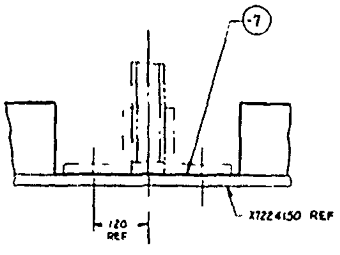


SECTION M-M C3
SCALE 1/1

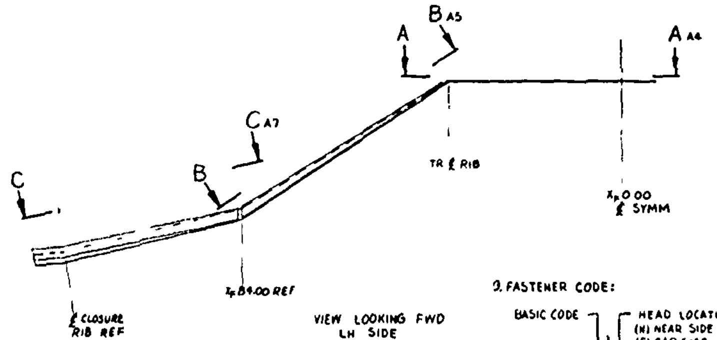


VIEW LOOKING FWD
LH SIDE
SCALE 1/10

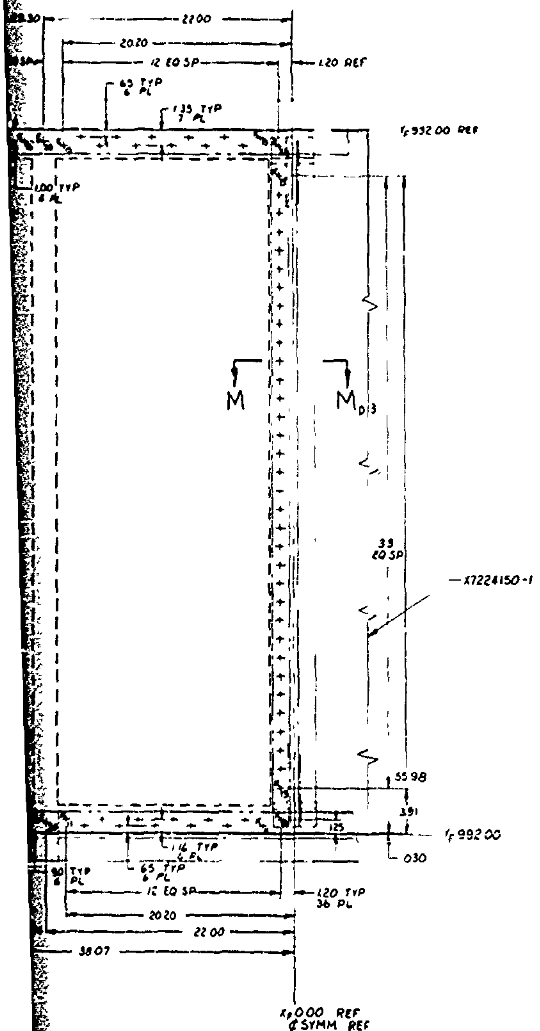


VIEW A-A D1

9. FASTENER CODE:

BASIC CODE — HEAD LOCATION
(N) NEAR SIDE
(F) FAR SIDE
NO CODE = LOCATION OPTIONAL
GRIP LENGTH DASH NO

| BASIC CODE | HOLE DIA | 100°CSK DIA | FASTENER | NUT 81755/ | WASHER UNDER HD | WASHER UNDER NUT | TORQUE PER 81755/MD16 |
|---|---|---|---|---|---|---|---|
| A | .3770 .3746 | .762 | 81755/C4551-6- | C077 6 | NONE | X7223994 6 | -6 B |
| B | 1.0025 .9991 | NONE | 81755/C4550 16- | C077 16 | X7223992-16 | X7223994-16 | -16 B |
| C | .2507 .2485 | NONE | 81755/C3002-8- | C2950-8 | X7223991-8 | NONE | -4 A |
| D | 1.0025 .9991 | NONE | X7223996-16- | C077-16 | X7223992-16 | X7223994 16 | -16 B |
| E | .3770 .3746 | NONE | 81755/C4550-6- | C077 6 | X7223992-6 | X7223994-6 | -6 B |
| F | .5025 .4996 | NONE | 81755/C4550-8- | C077 8 | X7223992 8 | X7223994-8 | -8 B |
| G | .6275 .6241 | NONE | 81755/C4550 10- | C077-10 | X7223992-10 | X7223994-10 | -10 B |
| H | .7525 .7491 | NONE | 81755/C4550 12 | C077 12 | X7223992 12 | X7223994 12 | -12 B |
| J | .2507 .2485 | .399 | 81755/C3001-8- | C2950-8 | NONE | NONE | -4 A |
| K | .3757 .3735 | NONE | 81755/C3002-12 | C2950 12 | X7223991-12 | NONE | -6 A |
| L | .5025 .4996 | NONE | X7223996-8- | C077-8 | X7223992-8 | X7223994-8 | -8 B |
| M | .5650 .5617 | NONE | X7223996-9- | C077-9 | X7223992-9 | X7223994-9 | -9 B |
| N | .6275 .6241 | NONE | X7223996-10- | C077-10 | X7223992-10 | X7223994 10 | -10 B |
| P | .7525 .7491 | NONE | X7223996-12- | C077 12 | X7223992-12 | X7223994 12 | -12 B |
| R | .5025 .4996 | 1.017 | X7223981-8- | C077-8 | NONE | X7223994-8 | -8 B |
| S | .3132 .3110 | .479 | 81755/C3001-10- | C2950 10 | NONE | NONE | -5A |
| T | .3770 .3746 | NONE | X7223980 12- | C2950-12 | X7223991-12 | X7223989 12 | -6A |
| U | .3770 .3746 | NONE | 81755/C020-12- | C2950-12 | X7223991 12 | X7223989 12 | -6A |
| | | | | | | | |
| | | | | | | | |
| | | | | | | | |
| | | | | | | | |

8. SPOTFACE NOTED HOLES 1.000 DIA x .062 R FAR SIDE WITH FULL CLEAN UP, MAX UNDERCUT .015, SURFACE ROUGHNESS 125/ MAX
7. FOR CONTOUR SEE MASTER DIMENSIONS DATA PACKAGE 43999/560101.01.
6. ALL FASTENERS TO BE INSTALLED NORMAL TO NEAR SURFACE
5. SURFACE ROUGHNESS OF ALL FASTENER HOLES SHALL NOT EXCEED 125/.
4. CLEAN NOTED FAYING SURFACES AND APPLY -9 MOLDED SHIM PER 81755/FPS-1071 CLASS II TYPE II.
3. SEALING MATERIALS AND METHODS OF APPLICATIONS PER X7224196.
2. APPLY -7 GENERAL SEALANT TO ALL FAYING SURFACES AND TO SHANK OF ALL FASTENERS.
1. DIMENSIONS AND TOLERANCES PER USASI Y14.5

NOTES (EXCEPT AS SHOWN)

| REV STATUS | |
|---|---|
| SH | REV |
| 1 | — |
| 2 | — |
| 3 | — |

Figure 2-4 (Sheet 1)

SEE SEPARATE PARTS LIST

NEXT SECTION LETTER: AC

SEE PL

NONE

GENERAL DYNAMICS
CONVAIR AEROSPACE DIVISION
FORT WORTH OPERATION
FORT WORTH TEXAS

U. S. AIR FORCE

COVER INSTL, UPPER-
Yf 932 TO Yf 992

J 07878 X7224010

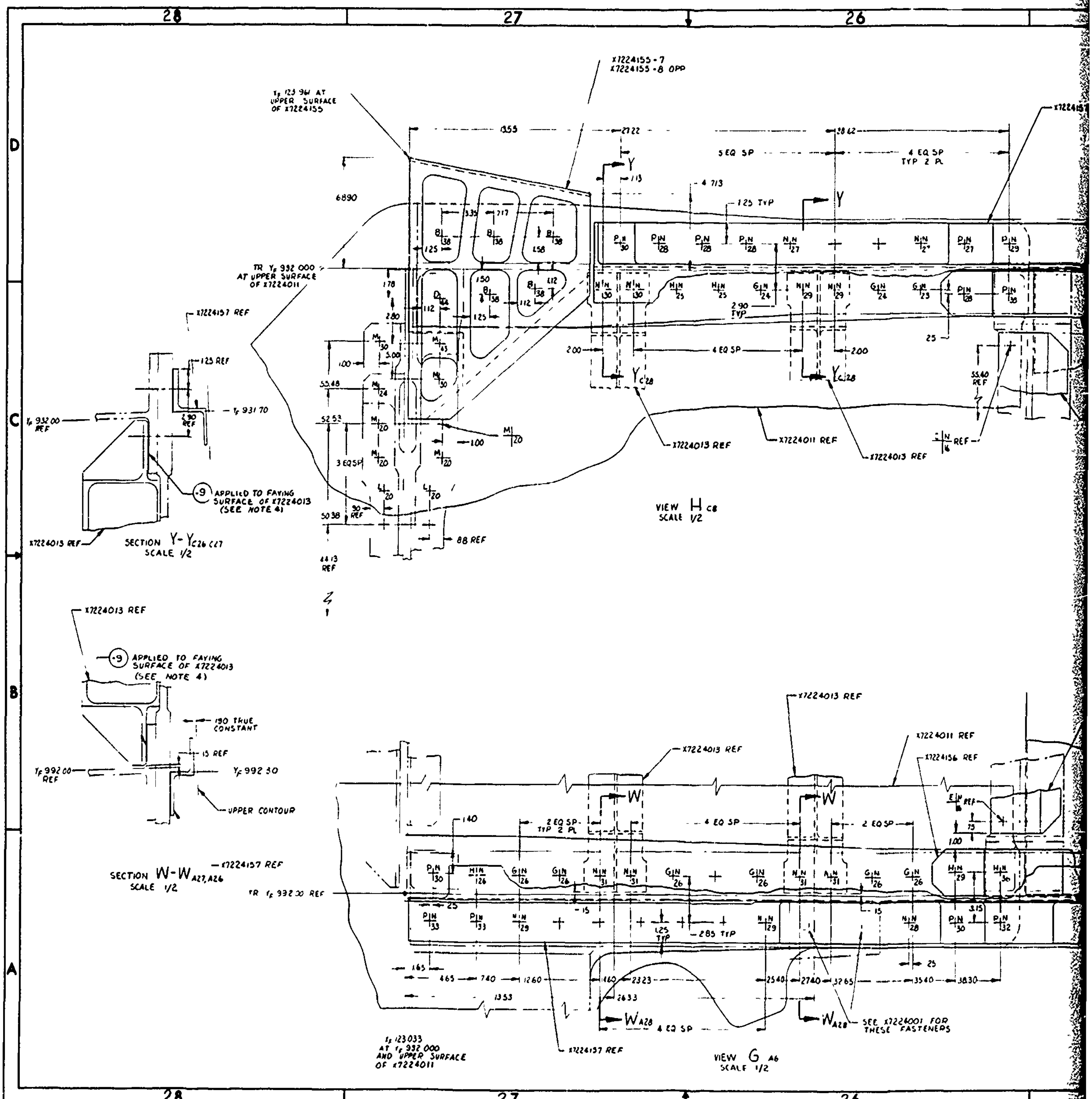

SECTION Y-Y C26 C27
SCALE 1/2
VIEW H C8
SCALE 1/2
SECTION W-W A27,A26
SCALE 1/2
VIEW G A6
SCALE 1/2
X7224155-7
X7224155-8 OPP
APPLIED TO FAYING SURFACE OF X7224013 (SEE NOTE 4)
X7224013 REF
X7224011 REF
X7224157 REF
X7224156 REF
UPPER CONTOUR
SEE X7224001 FOR THESE FASTENERS

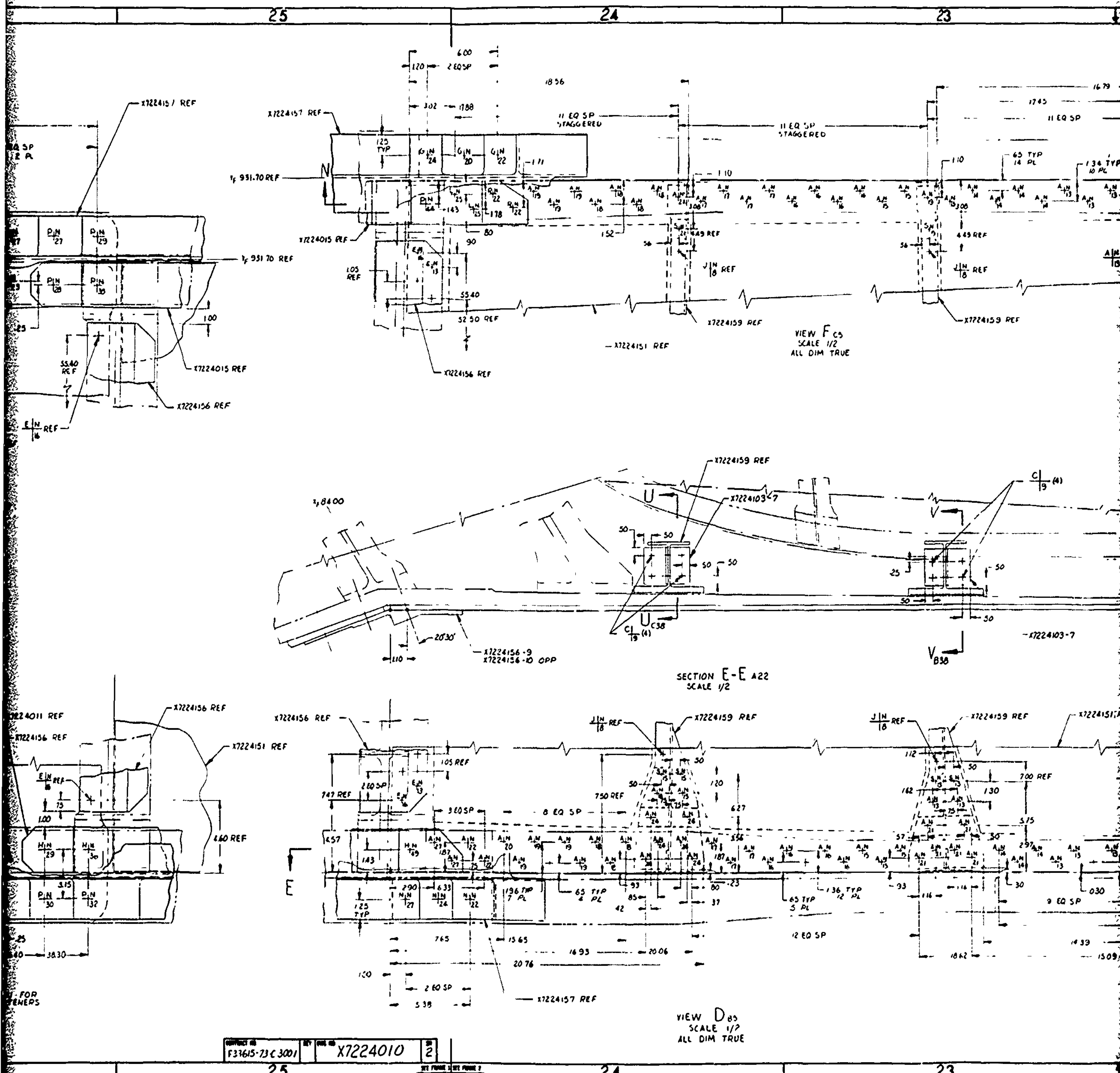
25
24
23
X7224157 REF
X7224015 REF
X7224156 REF
X7224159 REF
X7224151 REF
11 EQ SP STAGGERED
VIEW F C5
SCALE 1/2
ALL DIM TRUE
X7224103-7
X7224156-9
X7224156-10 OPP
SECTION E-E A22
SCALE 1/2
X7224011 REF
VIEW D B5
SCALE 1/2
ALL DIM TRUE
F33615-73C 3001
X7224010
2

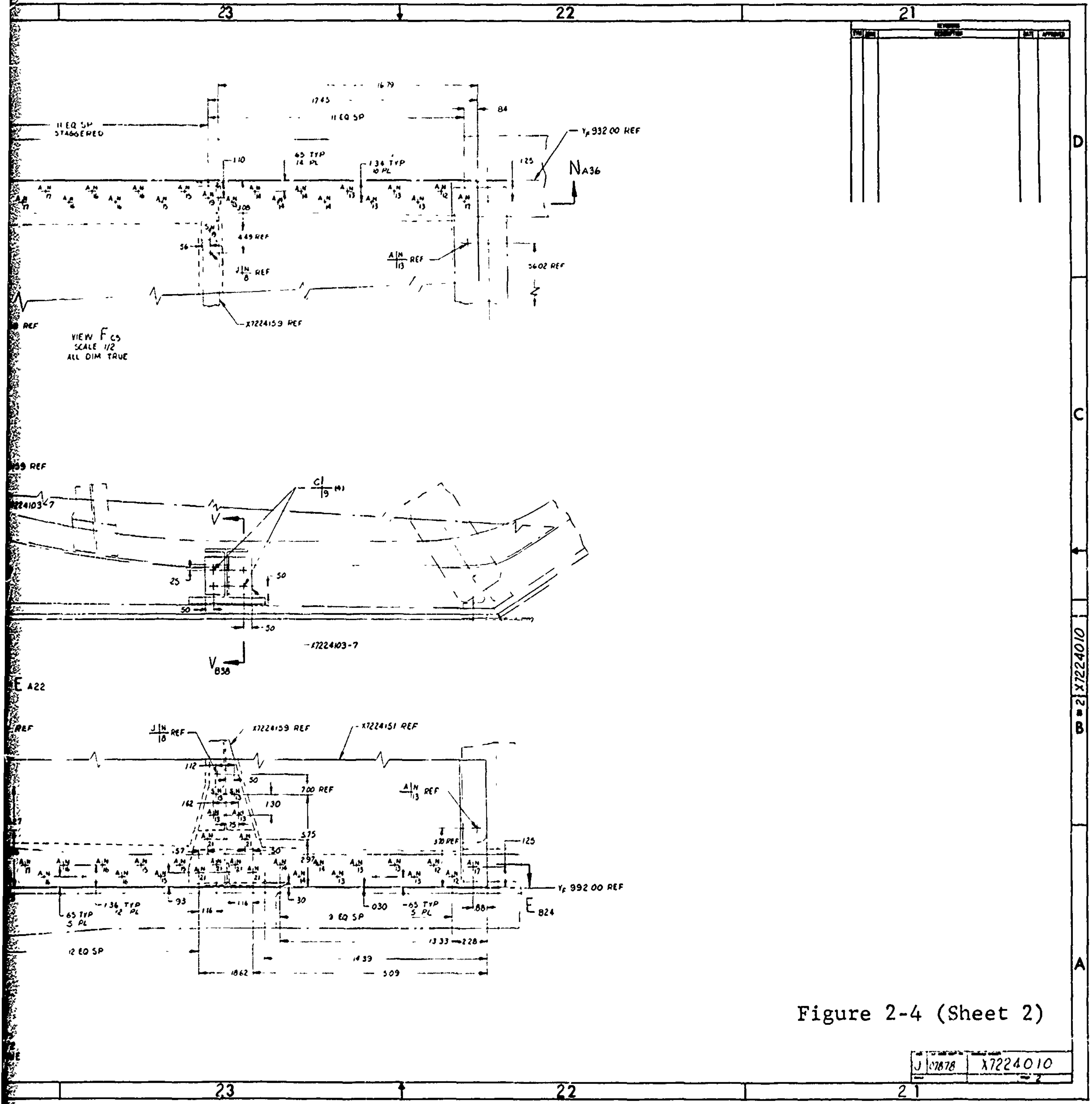


Figure 2-4 (Sheet 2)

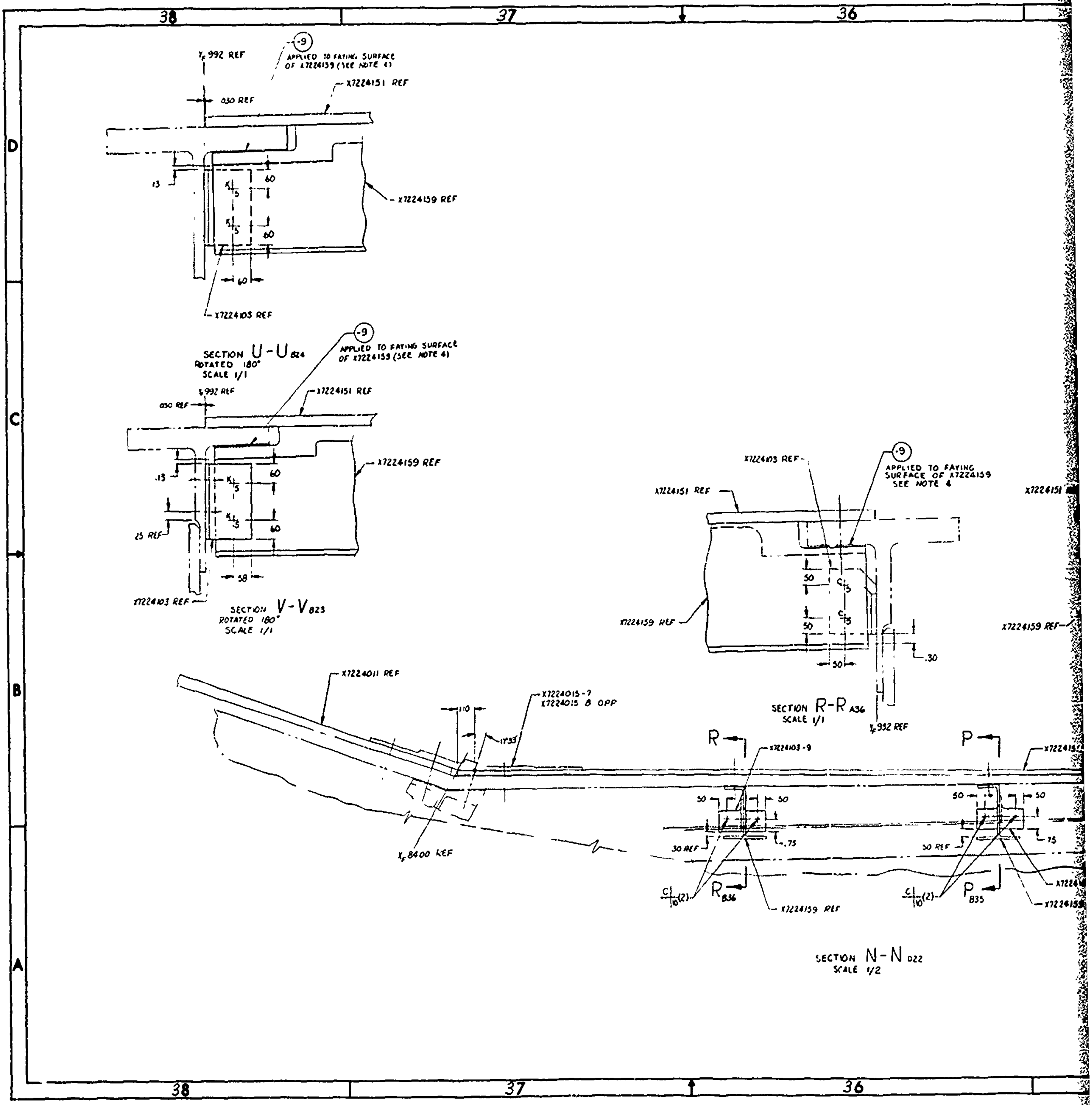

38
37
36
D
C
B
A
-9
APPLIED TO FAYING SURFACE OF X7224159 (SEE NOTE 4)
X7224151 REF
X7224159 REF
X7224103 REF
SECTION U-U B24
ROTATED 180°
SCALE 1/1
SECTION V-V B23
ROTATED 180°
SCALE 1/1
APPLIED TO FAYING SURFACE OF X7224159 SEE NOTE 4
SECTION R-R A36
SCALE 1/1
X7224011 REF
X7224015-7
X7224015 8 OPP
X7224103-9
X7224159 REF
SECTION N-N D22
SCALE 1/2

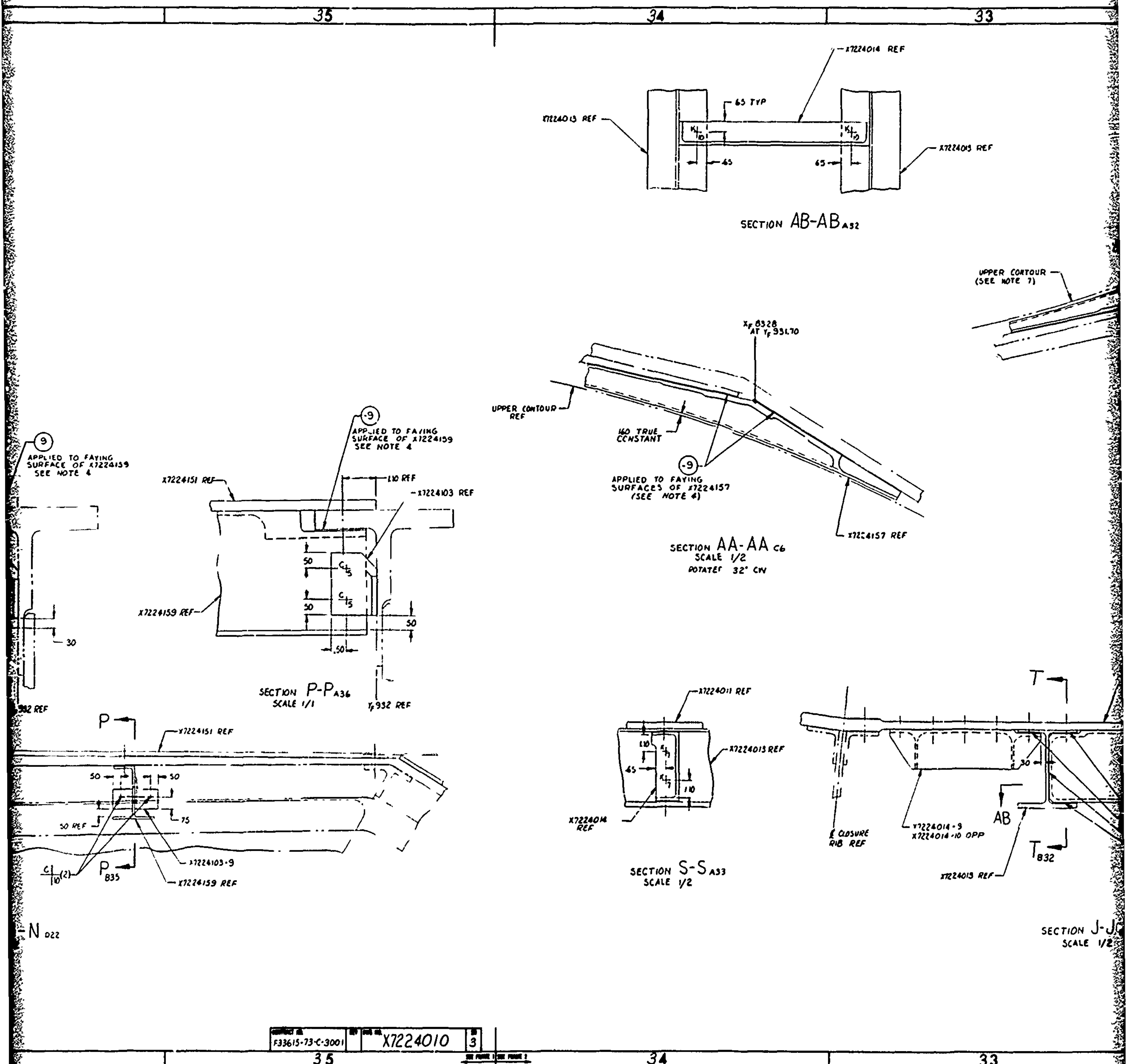
35
34
33
X7224014 REF
.65 TYP
X7224013 REF
X7224013 REF
.65
.65
SECTION AB-AB A32
UPPER CONTOUR
(SEE NOTE 7)
$X_F$ 8328
AT $Y_F$ 931.70
UPPER CONTOUR REF
.160 TRUE CONSTANT
9
APPLIED TO FAYING SURFACES OF X7224157 (SEE NOTE 4)
X7224157 REF
SECTION AA-AA C6
SCALE 1/2
ROTATED 32° CW
9
APPLIED TO FAYING SURFACE OF X7224159 SEE NOTE 4
9
APPLIED TO FAYING SURFACE OF X7224159 SEE NOTE 4
X7224151 REF
1.10 REF
X7224103 REF
X7224159 REF
.50
.50
.50
.50
.30
SECTION P-P A36
SCALE 1/1
$Y_F$ 932 REF
932 REF
P
X7224151 REF
.50
.50
.50 REF
.75
X7224103-9
X7224159 REF
P B35
X7224011 REF
X7224013 REF
1.10
.65
1.10
X7224014 REF
SECTION S-S A33
SCALE 1/2
T
.30
AB
℄ CLOSURE RIB REF
X7224014-9
X7224014-10 OPP
X7224013 REF
T B32
SECTION J-J
SCALE 1/2
N D22
F33615-73-C-3001
X7224010
3
35
34
33

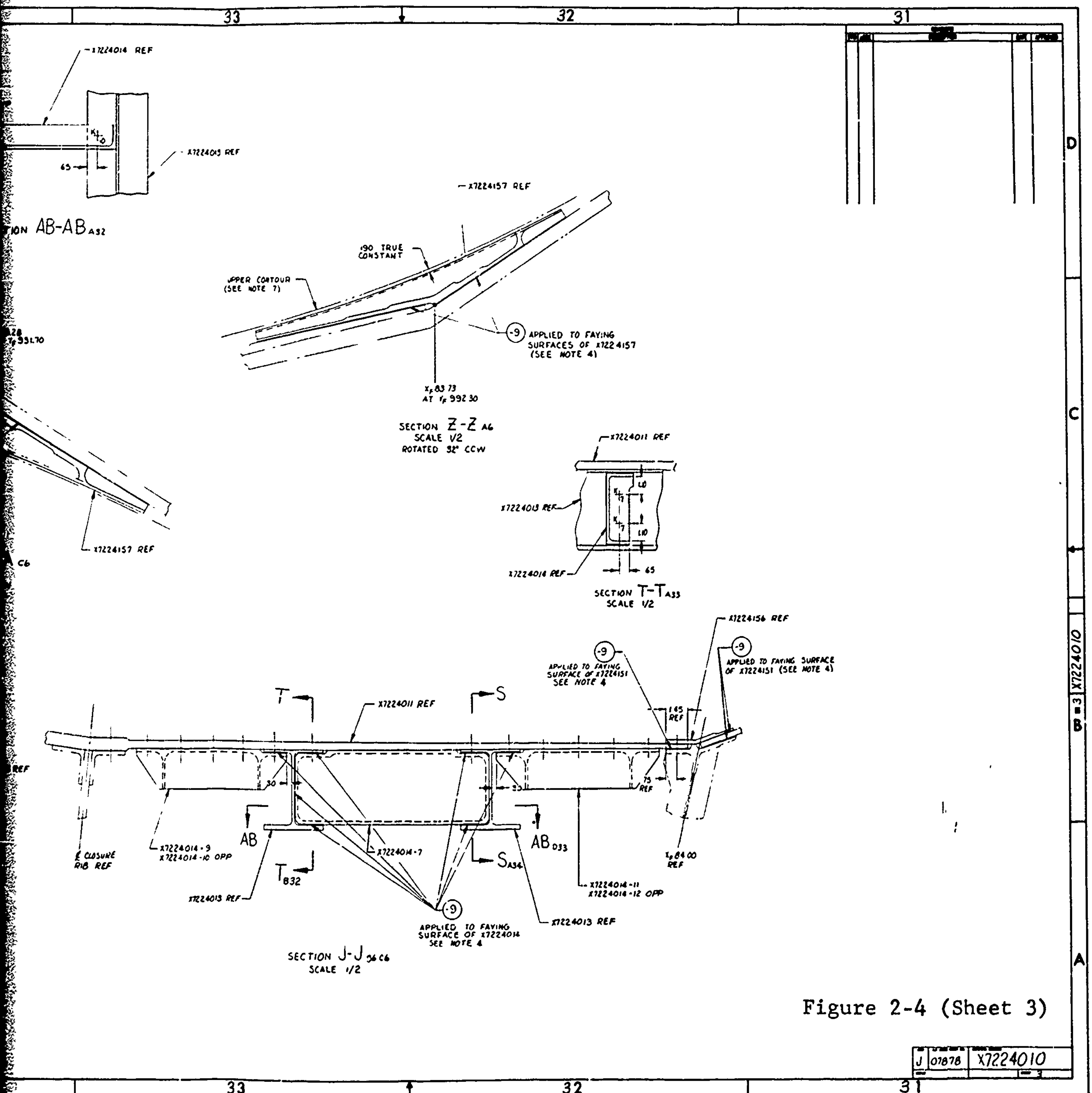


Figure 2-4 (Sheet 3)

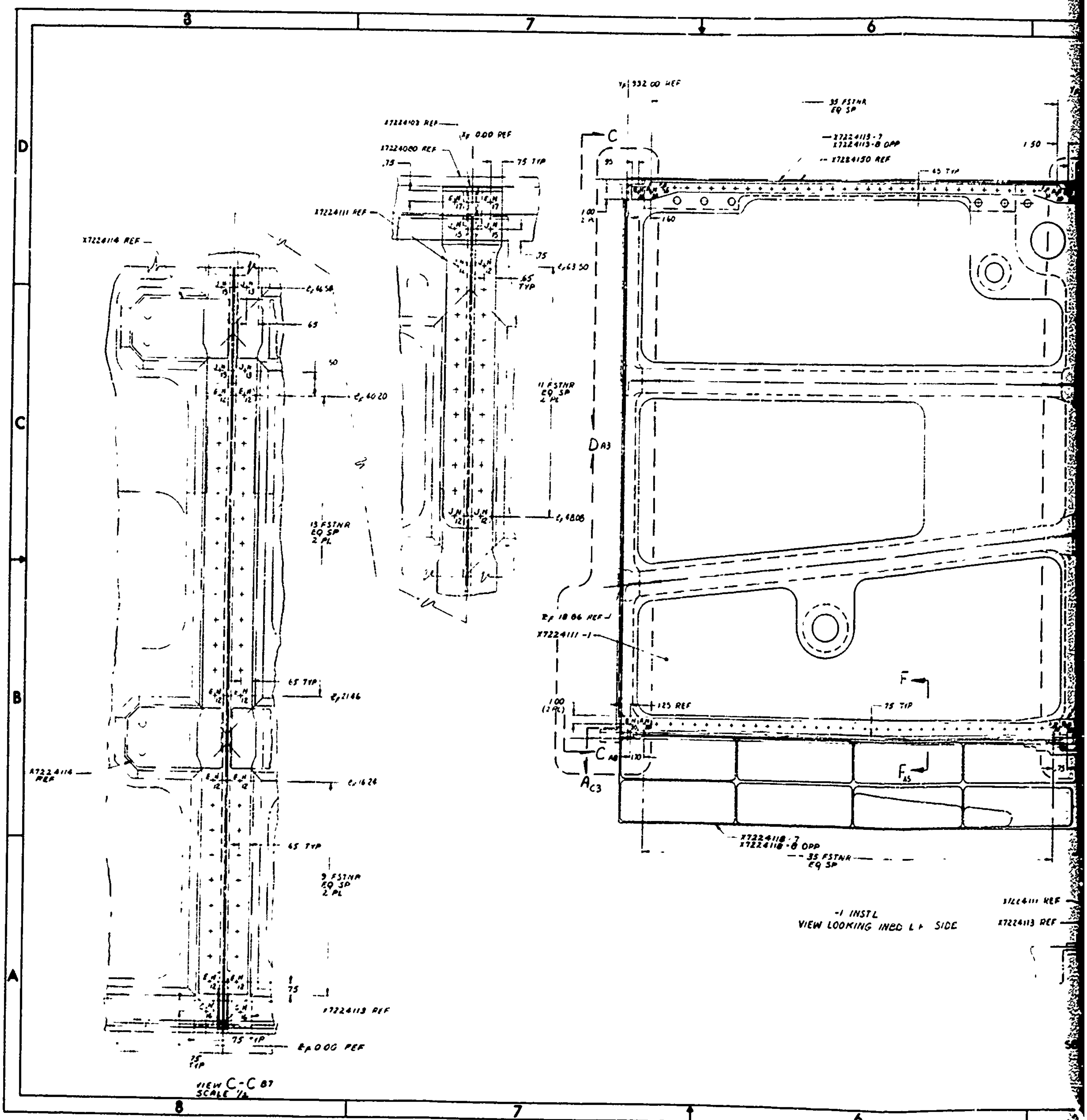

8
7
6
D
C
B
A
X7224111 REF
X7224114 REF
13 FSTNR
EQ SP
2 PL
9 FSTNR
EQ SP
2 PL
11 FSTNR
EQ SP
4 PL
.65 TYP
.75 TYP
X7224113 REF
35 FSTNR
EQ SP
X7224150 REF
X7224111 -1
.125 REF
X7224118 -7
X7224118 -8 OPP
-1 INSTL
VIEW LOOKING INBD LH SIDE
VIEW C-C B7
SCALE 1/2

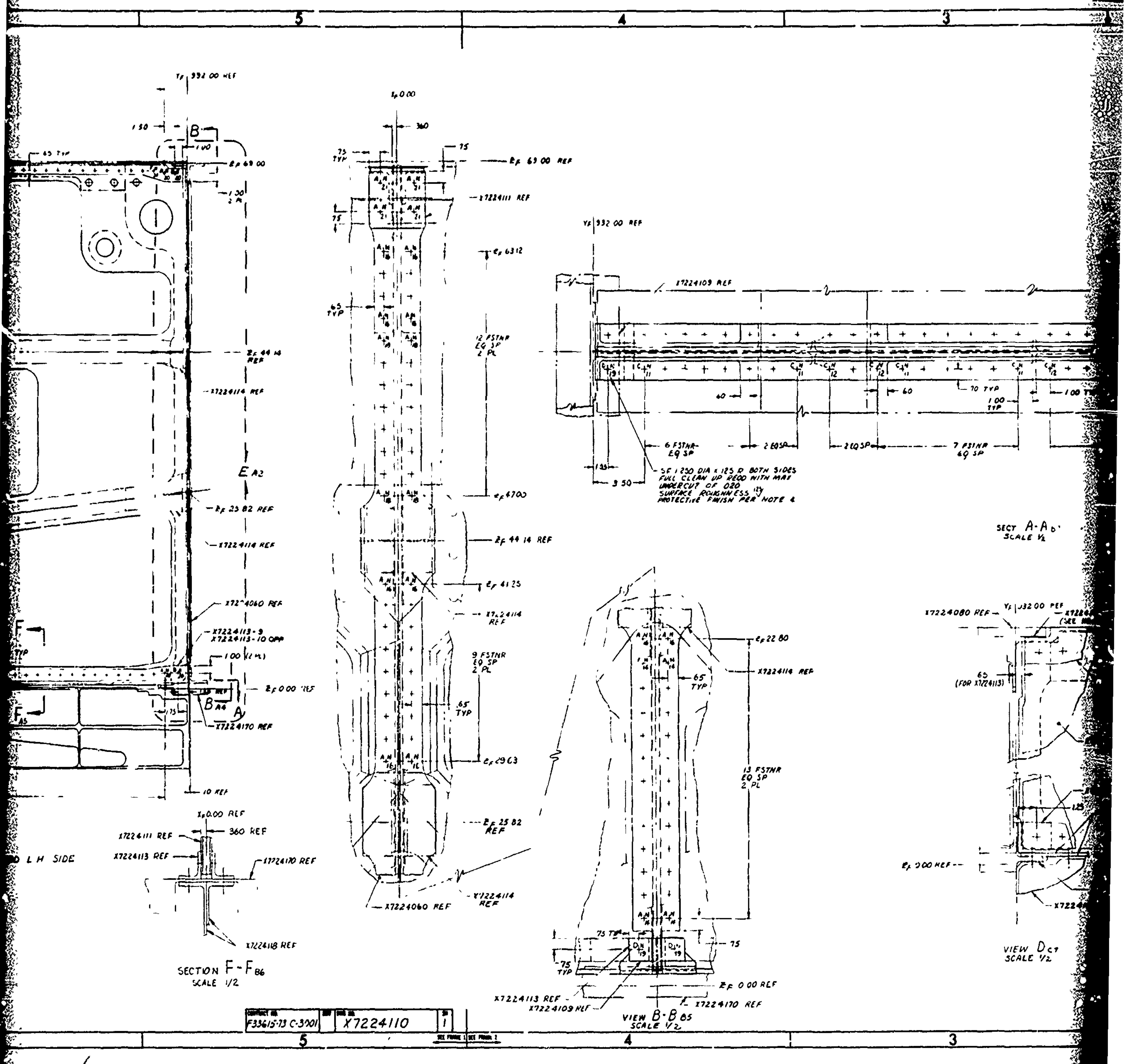
SECTION F-F B6
SCALE 1/2
VIEW B-B B5
SCALE 1/2
SECT A-A D
SCALE 1/2
VIEW D C7
SCALE 1/2
L H SIDE
X7224110
F33615-73 C-3001
SF 1.250 DIA x .125 R BOTH SIDES
FULL CLEAN UP REQD WITH MAX
UNDERCUT OF .020
SURFACE ROUGHNESS 125
PROTECTIVE FINISH PER NOTE 4
X7224109 REF
X7224111 REF
X7224113 REF
X7224114 REF
X7224170 REF
X7224060 REF
X7224080 REF
X7224118 REF
X7224113-9
X7224113-10 OPP
12 FSTNR EQ SP 2 PL
9 FSTNR EQ SP 2 PL
13 FSTNR EQ SP 2 PL
6 FSTNR EQ SP
7 FSTNR EQ SP
5
4
3

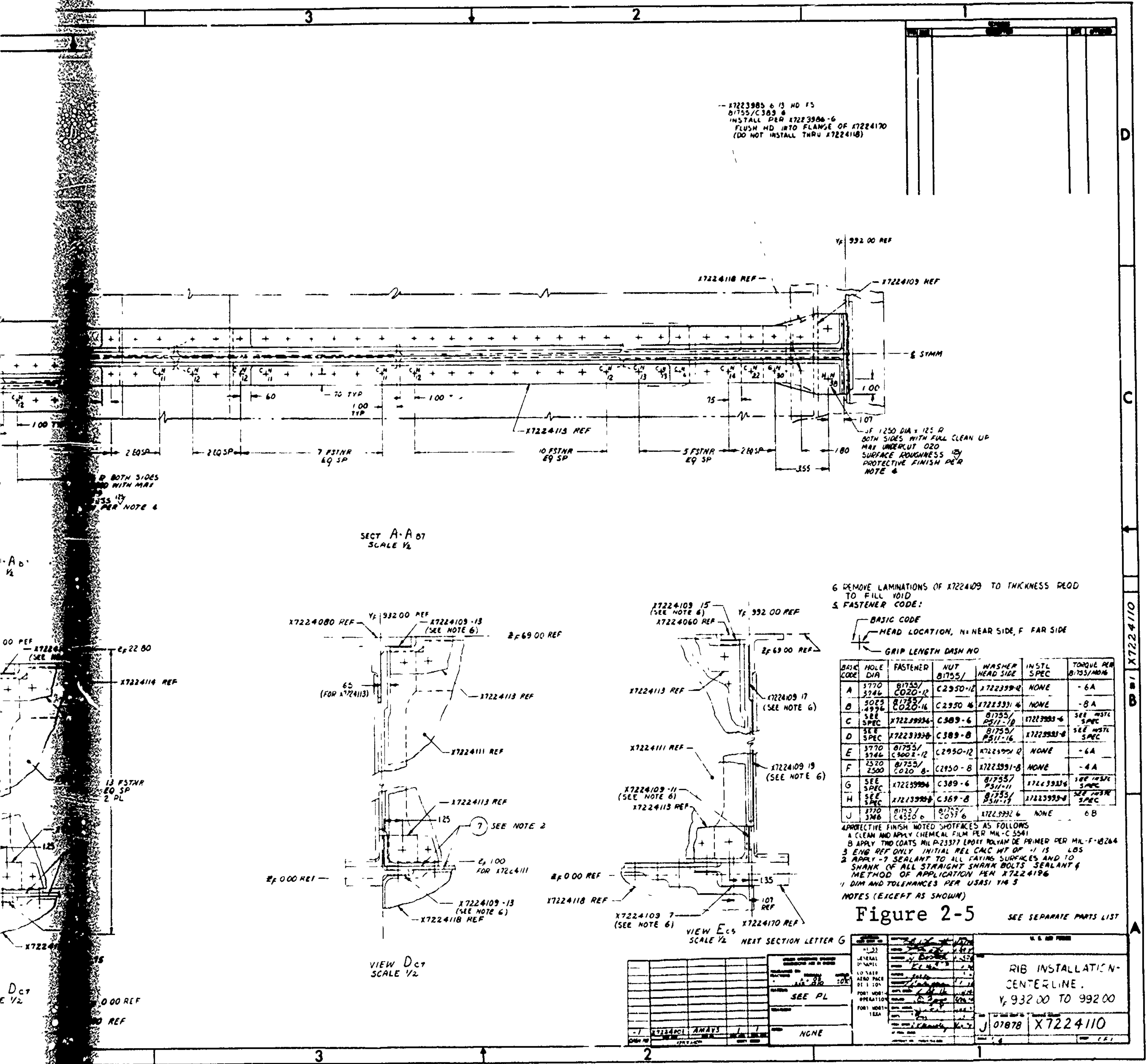


6 REMOVE LAMINATIONS OF X7224109 TO THICKNESS REQD TO FILL VOID

5 FASTENER CODE:

BASIC CODE — HEAD LOCATION, N = NEAR SIDE, F FAR SIDE — GRIP LENGTH DASH NO

| BASIC CODE | HOLE DIA | FASTENER | NUT 81755/ | WASHER HEAD SIDE | INSTL SPEC | TORQUE PER 81755/M016 |
|---|---|---|---|---|---|---|
| A | .3770 .3746 | 81755/ C020-12 | C2950-12 | X7223991-12 | NONE | -6A |
| B | .5025 .4996 | 81755/ C020-16 | C2950-16 | X7223991-16 | NONE | -8A |
| C | SEE SPEC | X72239936- | C389-6 | 81755/ P511-10 | X7223993-6 | SEE INSTL SPEC |
| D | SEE SPEC | X72239938 | C389-8 | 81755/ P511-16 | X7223993-8 | SEE INSTL SPEC |
| E | .3770 .3746 | 81755/ C3002-12 | C2950-12 | X7223991-12 | NONE | -6A |
| F | .2520 .2500 | 81755/ C020-8- | C2950-8 | X7223991-8 | NONE | -4A |
| G | SEE SPEC | X72239936 | C389-6 | 81755/ P511-11 | X7223993-6 | SEE INSTL SPEC |
| H | SEE SPEC | X72239938 | C389-8 | 81755/ P511-17 | X7223993-8 | SEE INSTL SPEC |
| J | .3770 .3746 | 81755/ C4550-6 | 81755/ C077-6 | X7223992-6 | NONE | 6B |

4 PROTECTIVE FINISH NOTED SPOTFACES AS FOLLOWS
A CLEAN AND APPLY CHEMICAL FILM PER MIL-C-5541
B APPLY TWO COATS MIL-P-23377 EPOXY POLYAMIDE PRIMER PER MIL-F-18264

3 ENG REF ONLY INITIAL REL CALC WT OF -1 IS LBS

2 APPLY -7 SEALANT TO ALL FAYING SURFACES AND TO SHANK OF ALL STRAIGHT SHANK BOLTS. SEALANT & METHOD OF APPLICATION PER X7224196

1 DIM AND TOLERANCES PER USASI Y14.5

NOTES (EXCEPT AS SHOWN)

Figure 2-5

SEE SEPARATE PARTS LIST

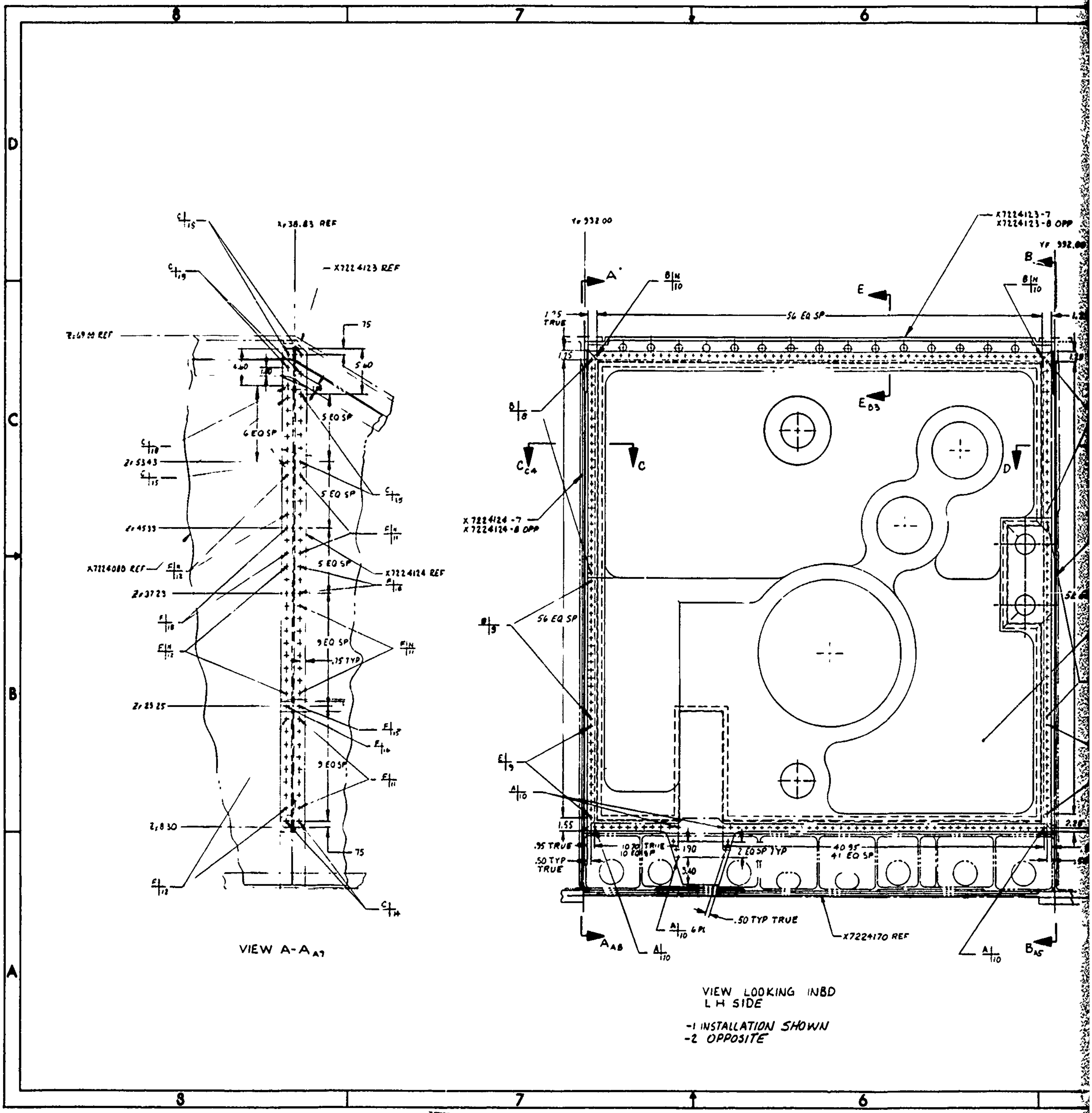
X7224123 REF
X7224080 REF
X7224124 REF
5 EQ SP
6 EQ SP
9 EQ SP
.75 TYP
VIEW A-A
X7224123-7
X7224123-8 OPP
56 EQ SP
X7224124-7
X7224124-8 OPP
.95 TRUE
.50 TYP TRUE
1.55
41 EQ SP
.50 TYP TRUE
X7224170 REF
VIEW LOOKING INBD
L H SIDE
-1 INSTALLATION SHOWN
-2 OPPOSITE

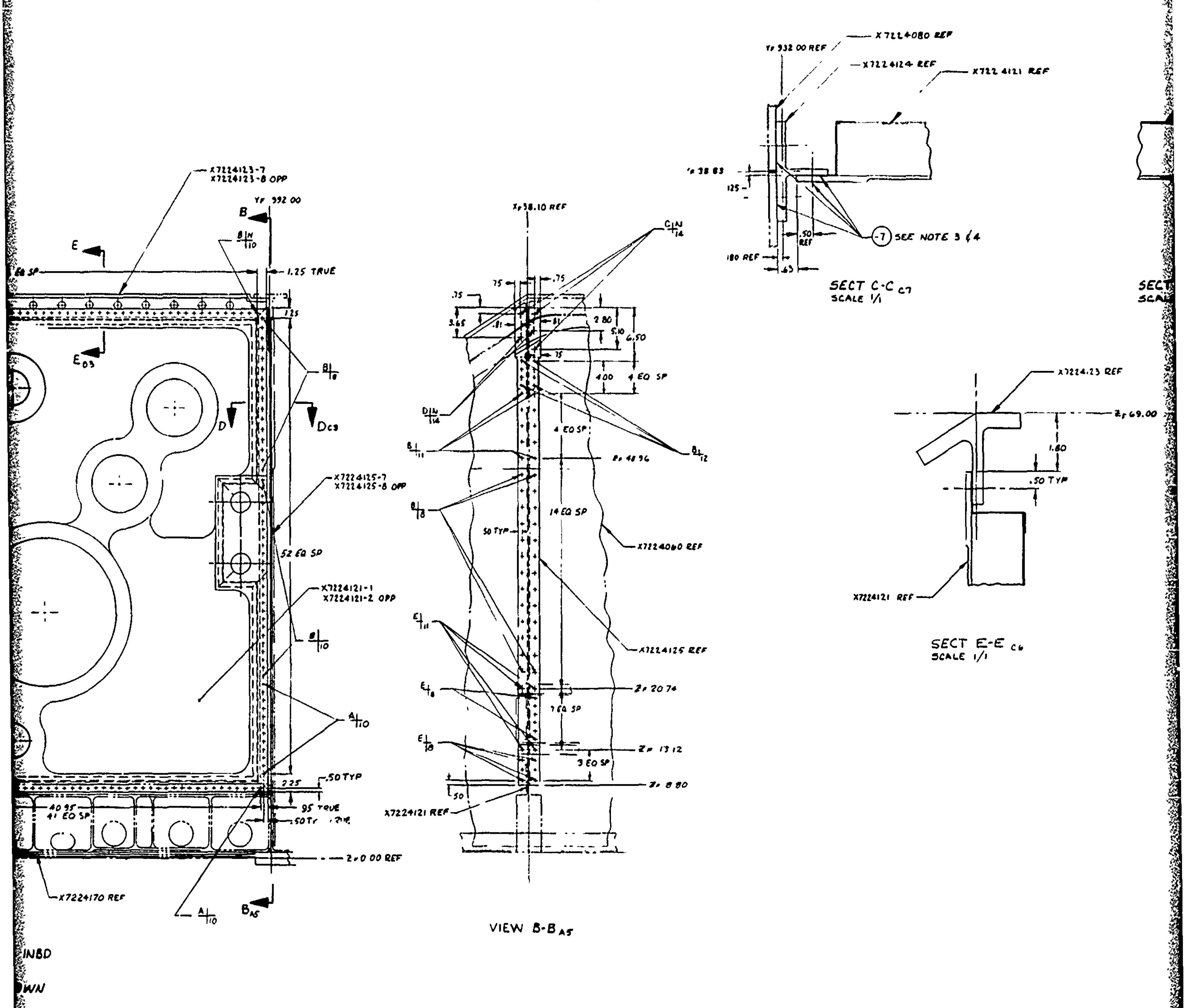


F33615-73-C-3001 X7224120

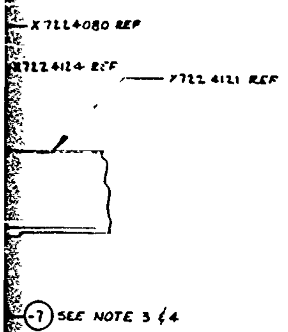


C-C C7
1/1

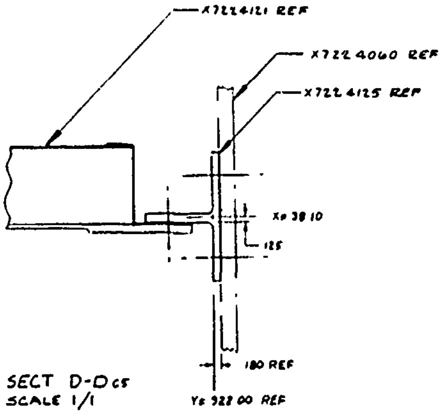


SECT D-D C5
SCALE 1/1

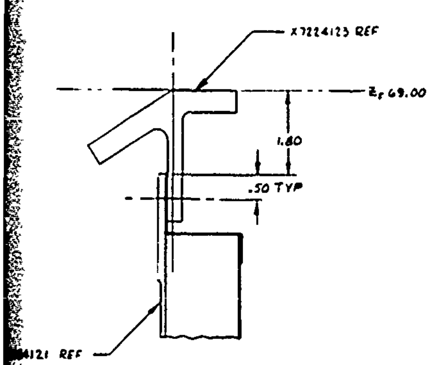


SECT E-E C6
SCALE 1/1

5 FASTENER CODE·

BASIC CODE
HEAD LOCATION (N) NEAR SIDE, (F) FAR SIDE, NO CODE OPTIONAL
GRIP

**FASTENER CODES**

| BASIC CODE | HOLE DIA | FASTENER | NUT | WASHER (UNDER BOLT HEAD) | WASHER (UNDER NUT) | TORQUE PER |
|---|---|---|---|---|---|---|
| A | .2520/.2496 | 81755/C3002-8 | 81755/C2950-8 | X7223991-8 | X7223989-8 | 81755/M016-4A |
| B | .2520/.2496 | 81755/C020-8 | 81755/C2950-8 | X7223991-8 | X7223989-8 | 81755/M016-4A |
| C | .3770/.3746 | X7223996-6 | 81755/C077-6 | X7223992-6 | X7223994-6 | 81755/M016-6B |
| D | .5025/.4996 | X7223996-8 | 81755/C077-8 | X7223992-8 | X7223994-8 | 81755/M016 8B |
| E | .2520/.2496 | X7223980-8 | 81755/C2950 8 | X7223991-8 | X7223989-8 | 81755/M016-4A |
| F | .3770/.3746 | X7223980-12 | 81755/C2950-12 | X7223991-12 | X7223989 12 | 81755/M016 6A |
| | | | | | | |
| | | | | | | |
| | | | | | | |

4 INSTALL ALL FASTENERS WITH -7 SEALANT PER X7224196

3. APPLY -7 SEALANT TO ALL FAYING SURFACES PER X7224196

2 ALL MACHINE SURFACES 125/

1. DIMENSIONS AND TOLERANCES PER USASI Y14.5

NOTES (EXCEPT AS SHOWN)

Figure 2-6

SEE SEPARATE PARTS LIST

NEXT SECT LTR. F

SEE PL

NONE

GENERAL DYNAMICS
CONVAIR AEROSPACE DIVISION
FORT WORTH OPERATION

RIB INSTL - XF 39, WING CARRY THRU

J 07878 X7224120

### 2.1.1.7 Outboard Intermediate Rib

The outboard rib at $X_F84$ (Figure 2-7, Drawing X7224130) is integrally machined from 7050 aluminum plate. This monolithic type construction was selected to efficiently distribute the torsional shear loads introduced by the pivot lugs, and to distribute the high concentrated reaction loads from the wing sweep actuator inboard attach bracket. This rib also supports the inboard end of the pivot lugs and splices them to the upper and lower cover sandwich panels. The kick load due to the directional change of the upper cover is also reacted by this rib. The outboard end of the $Y_F$ 947 beam is also supported by this rib. Provisions are made for access to the outboard area and for fuel flow and venting.

### 2.1.1.8 Outboard Closure Rib

The outboard closure rib (Figure 2-8, Drawing X7224030) has been redesigned from an integrally machined 10 Nickel steel weldment into a beta annealed 6AL-4V titanium web reinforced with aluminum stiffeners and attached by titanium angle sections. Separate bolt-on titanium fittings are utilized to react and distribute the high concentrated load introduced by the wing sweep actuator bracket. The closure rib is designed to resist the torsional shear loads introduced by the pivot lugs and to distribute the wing sweep actuator bracket kick loads. Although 10 Nickel steel was originally selected due to its superior fracture toughness, the beta annealed titanium provides sufficient safe crack growth capabilities at lower weight and reduced cost.

### 2.1.2 Fail-Safe Integral Lug Configuration

The fail-safe removable lug configuration of Phase Ib has been renamed to reflect the integral lug concept now employed for the lower plate. The objective of this configuration was to achieve a reliable fail-safe design with a minimum quantity of fasteners piercing the critical lower plate. In addition to minimizing fasteners, brazing functions as a crack arrestor to effectively increase the number of elements for additional fail-safe capability.

Other design changes incorporated during Phase II, in addition to the integral pivot lug, include the following:

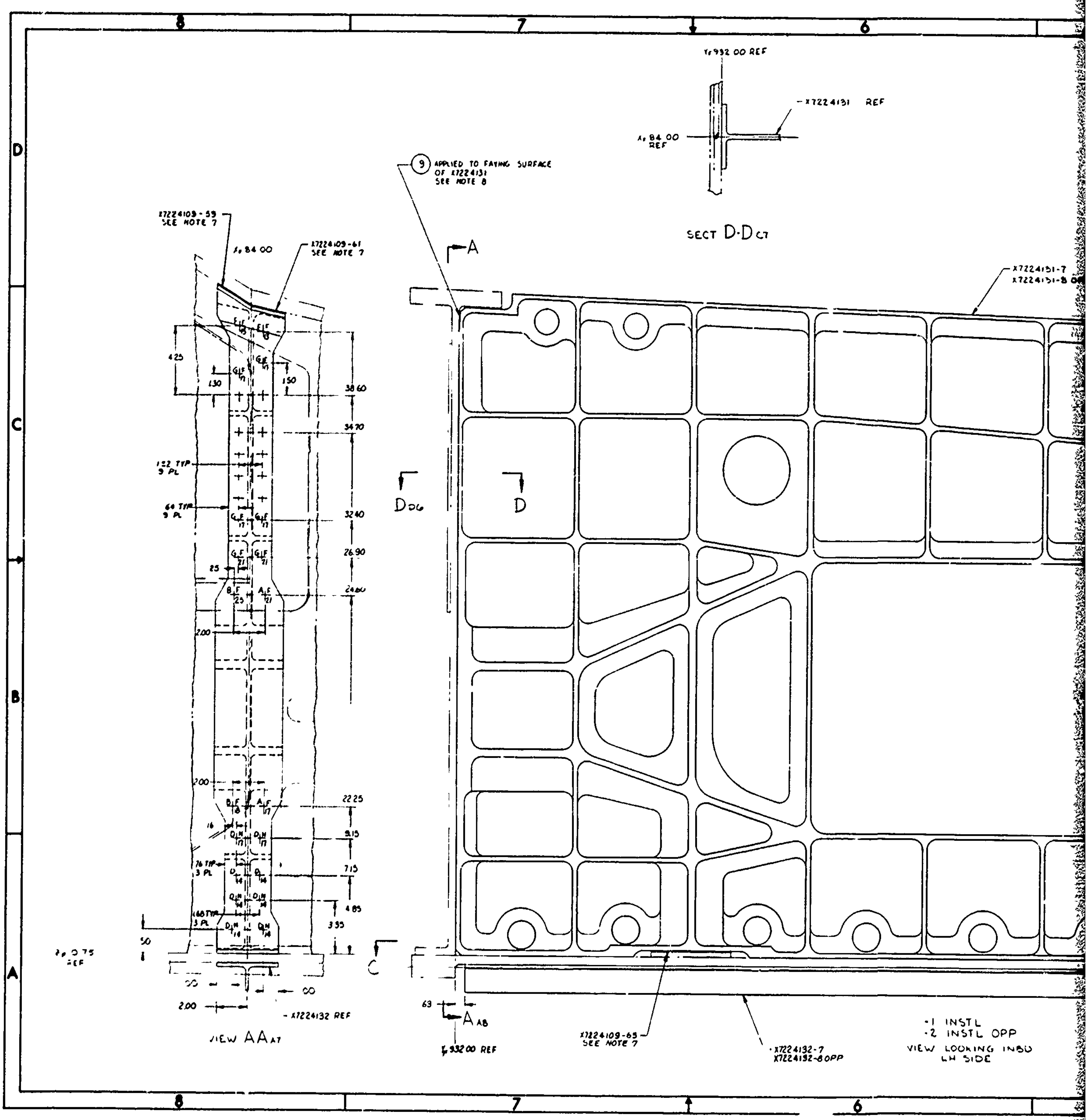

SECT D-D C7
VIEW AA A7
APPLIED TO FAYING SURFACE OF X7224131 SEE NOTE 8
X7224131 REF
X7224109-59 SEE NOTE 7
X7224109-61 SEE NOTE 7
X7224151-7
X7224132 REF
X7224109-65 SEE NOTE 7
X7224132-7
X7224132-8 OPP
-1 INSTL
-2 INSTL OPP
VIEW LOOKING INBD LH SIDE

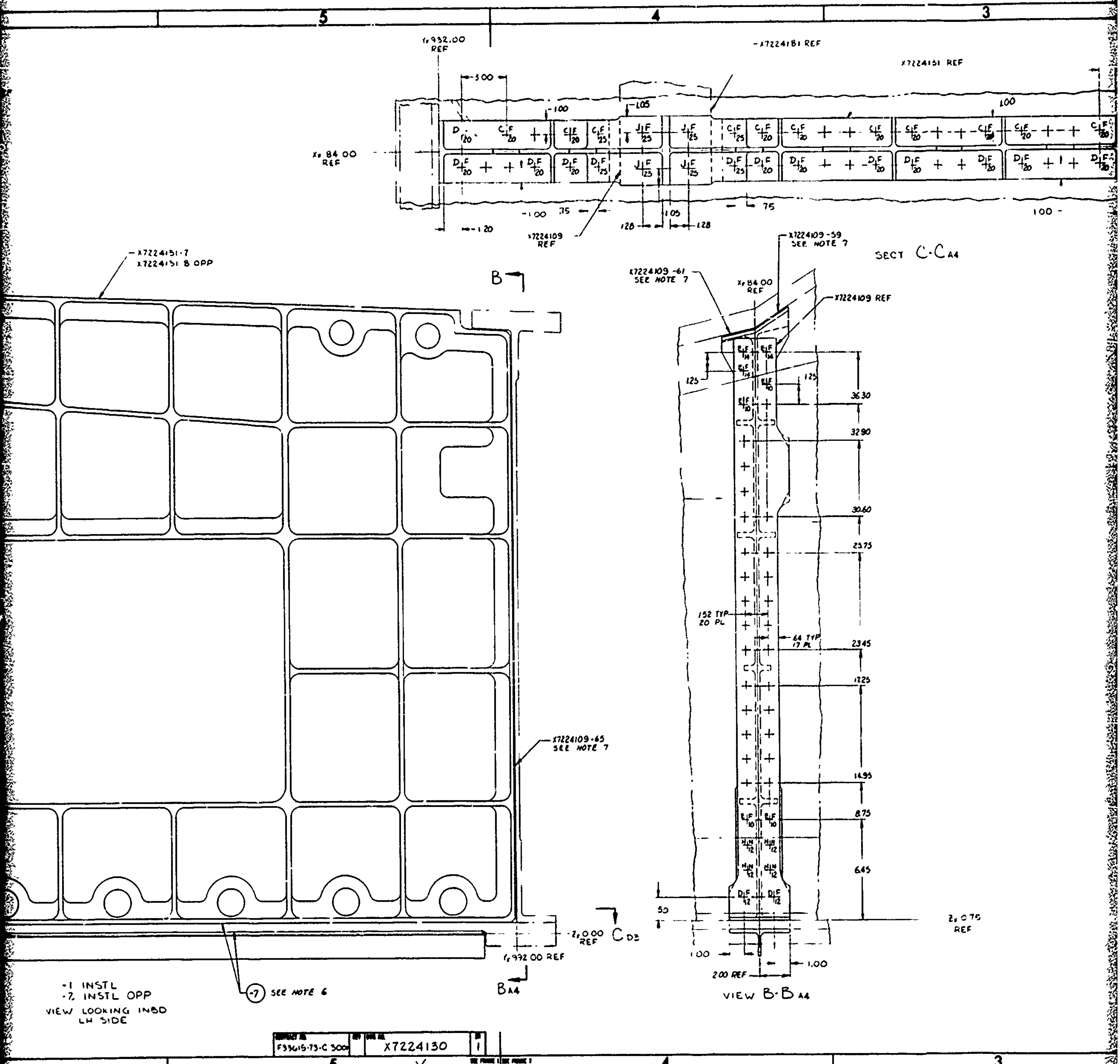
5
4
3
$Y_F$ 932.00 REF
X7224181 REF
X7224151 REF
$X_F$ 84.00 REF
X7224109 REF
X7224151-7
X7224151 8 OPP
B
X7224109-59 SEE NOTE 7
SECT C-C A4
X7224109-61 SEE NOTE 7
$X_F$ 84.00 REF
X7224109 REF
152 TYP 20 PL
.64 TYP 17 PL
X7224109-65 SEE NOTE 7
$Z_F$ 0.00 REF
C D3
$Y_F$ 932.00 REF
B A4
$Z_F$ 0.75 REF
200 REF
VIEW B-B A4
-1 INSTL
-2 INSTL OPP
VIEW LOOKING INBD LH SIDE
7 SEE NOTE 6
F33615-73-C 3001
X7224130

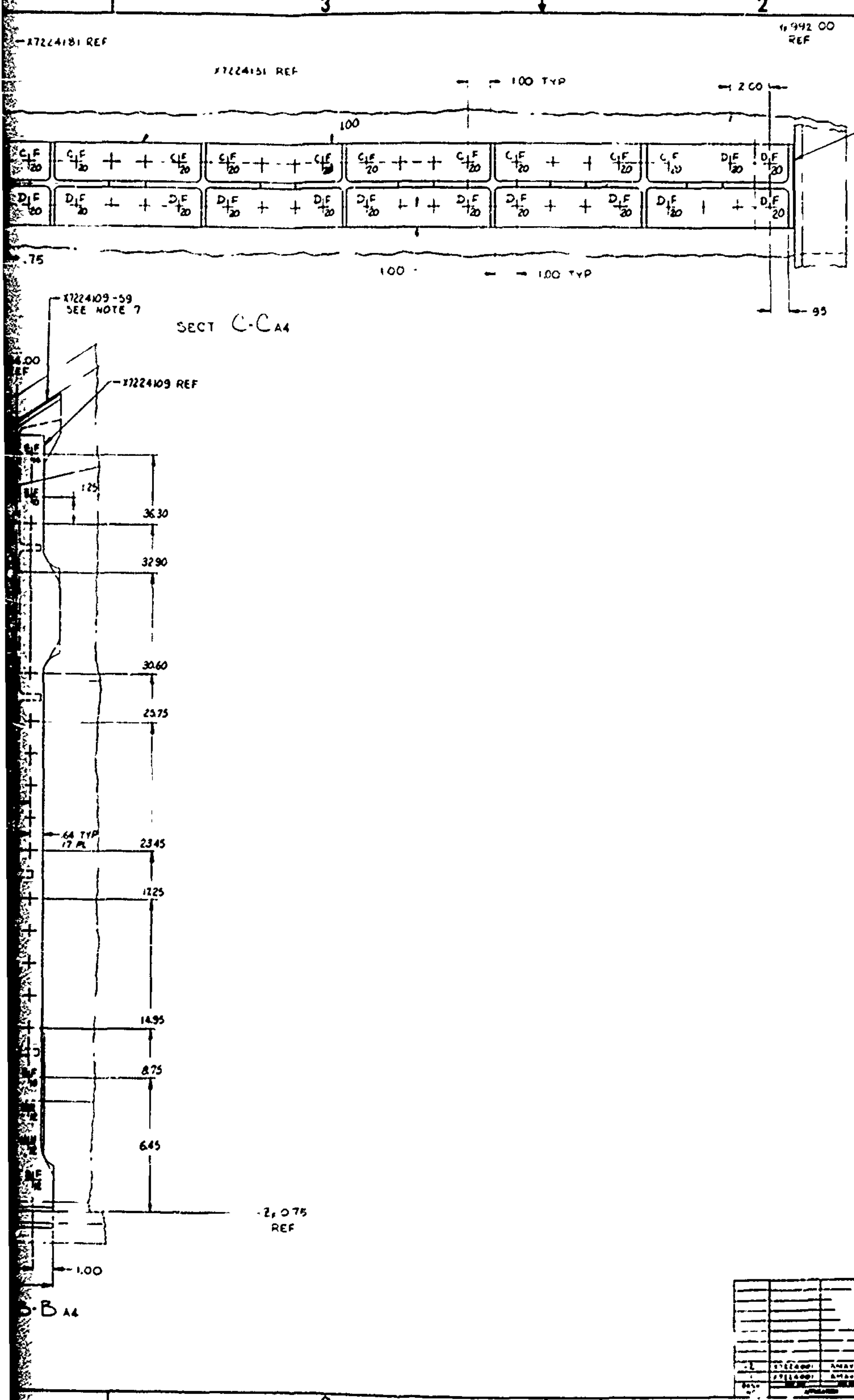


8 CLEAN FAYING SURFACE OF X7224131 AND APPLY -9 MOLDED SHIM PER 81755/FPS-1071 CLASS II, TYPE II

7 REMOVE LAMINATIONS FROM X7224109 SHIM AS REQD TO FILL GAP.

6. APPLY -7 SEALANT TO ALL FAYING SURFACES PER X7224196.

5. INSTALL STRAIGHT-SHANK FASTENERS WITH -7 SEALANT PER X7224196.

4. SEALING MATERIALS AND METHODS OF APPLICATION PER X7224196.

3. ALL FASTENERS ARE EQUALLY SPACED BETWEEN LOCATED FASTENERS; QUANTITIES AS SHOWN.

2. FASTENER CODE:

BASIC CODE — HEAD LOCATION (N) NEAR SIDE (F) FAR SIDE — GRIP LENGTH DASH NO

| BASIC CODE | HOLE DIA | FASTENER | NUT 81755/ | WASHER UNDER HD | WASHER UNDER NUT | INSTL SPEC | TORQUE PER |
|---|---|---|---|---|---|---|---|
| A | 3025 4996 | 81755/ C4550-8- | C077-8 | X7223992 8 | NONE | NONE | 81755/ M016-8B |
| B | 3025 4996 | X7223096 8- | C077-8 | X7223992-8 | X7223994-8 | NONE | 81755/ M016-8B |
| C | SEE SPEC | X7223999 8- | C389-8 | 81755/ P511-16 | NONE | X7223993-8 | SEE SPEC |
| D | SEE SPEC | 81755/ C513H8-AD | C389-8 | 81755/ P511-16 | NONE | X7223993 8 | SEE SPEC |
| E | 3770 3746 | 81755/ C3002-12- | C2550-12 | X7223991-12 | NONE | NONE | 81755/ M016 6A |
| F | 3770 3746 | 81755/ C4550-6- | C077-6 | X7223992 6 | NONE | NONE | 81755/ M016-6B |
| G | 3770 3746 | X7223996-6 | C077-6 | X7223992-6 | X7223994 6 | NONE | 81755/ M016-6B |
| H | SEE SPEC | 81755/ C513H6 AD | C389-6 | 81755/ P511 10 | NONE | X7223993-6 | SEE SPEC |
| J | SEE SPEC | X7223999 10- | C389-10 | 81755/ P511-22 | NONE | X7223993 10 | SEE SPEC |

▲ INDICATES GRIP DASH NO FOR D AND H FASTENERS

1. DIMENSIONS AND TOLERANCES PER USASI Y14.5 NOTES (EXCEPT AS SHOWN)

Figure 2-7

SEE SEPARATE PARTS LIST

NEXT SECTION LETTER: E

SEE PL

RIB INSTL - 4.5 WING CARRYTHRU

X7224130

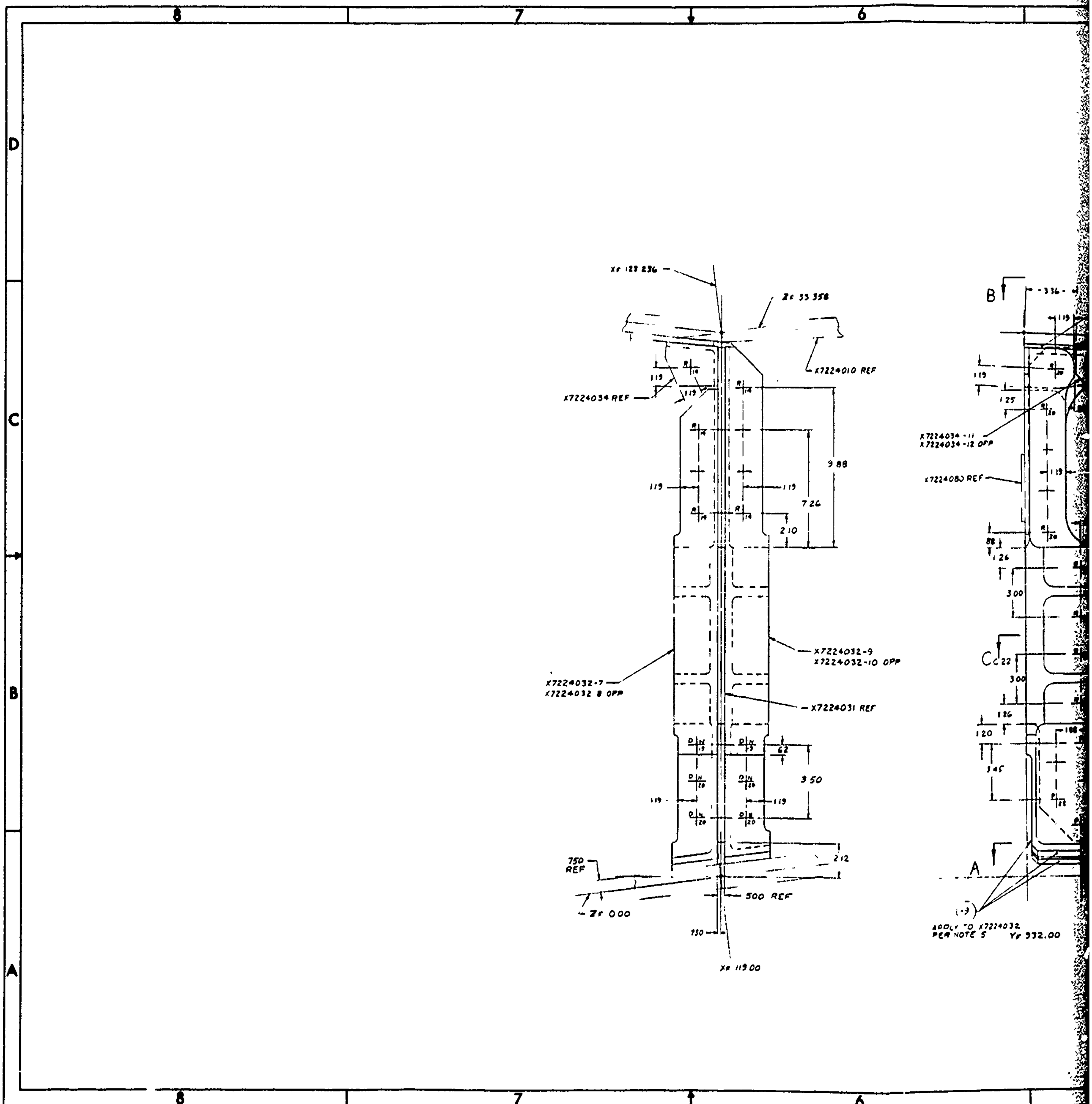

8
7
6
D
C
B
A
X7224010 REF
X7224034 REF
119
9.88
7.26
2.10
X7224032-9
X7224032-10 OPP
X7224032-7
X7224032 8 OPP
X7224031 REF
62
3.50
212
750 REF
500 REF
X= 119.00
B
C
A
119
125
X7224034-11
X7224034-12 OPP
X7224080 REF
300
120
APPLY TO X7224032 PER NOTE 5
Y= 332.00

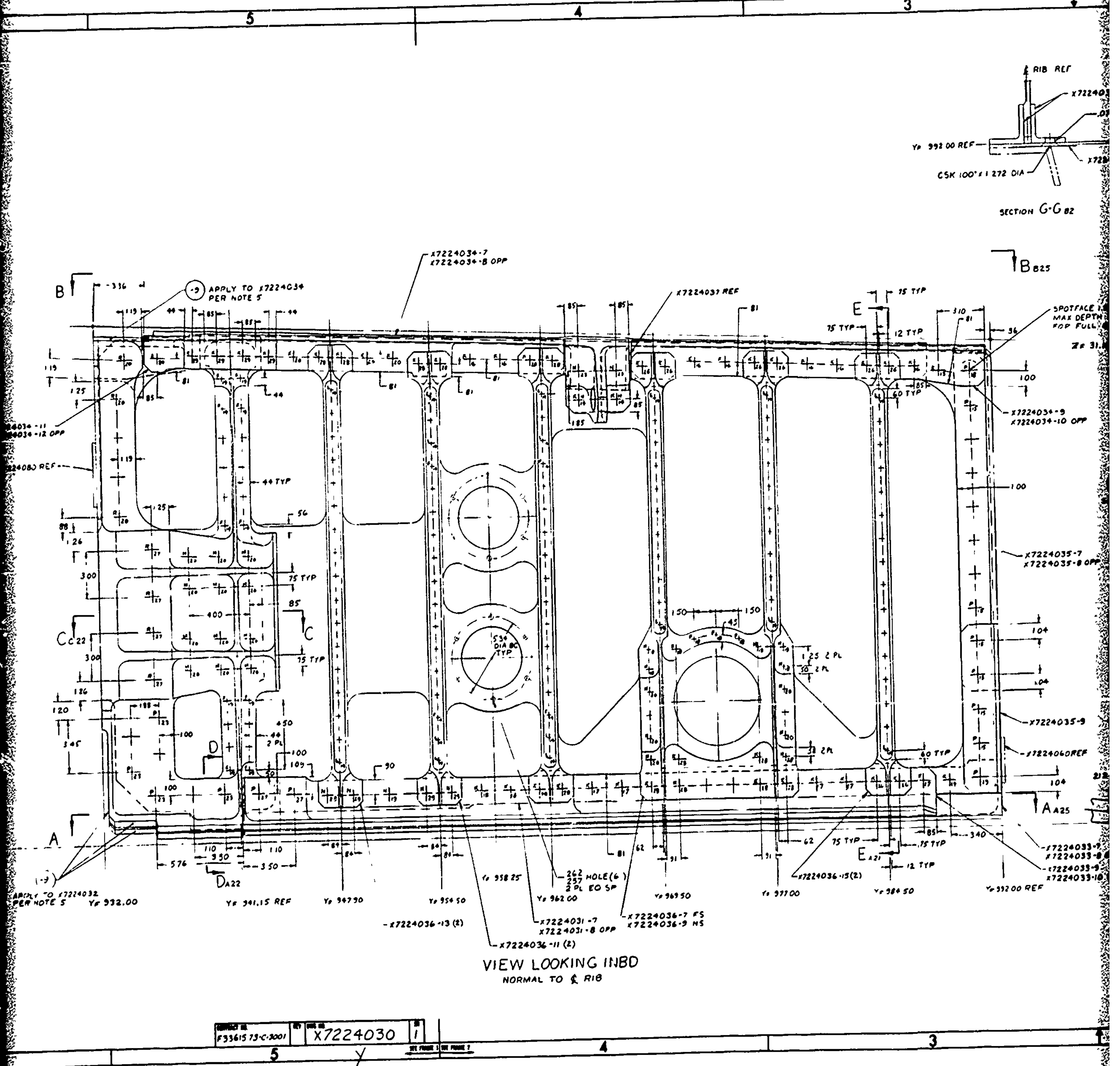
RIB REF
Y₀ 992.00 REF
CSK 100° × 1.272 DIA
SECTION G-G B2
X7224034-7
X7224034-8 OPP
APPLY TO X7224034
PER NOTE 5
X7224037 REF
X7224034-9
X7224034-10 OPP
X7224035-7
X7224035-8 OPP
X7224035-9
X7224060 REF
X7224033-9
X7224033-10
X7224036-15 (2)
APPLY TO X7224032
PER NOTE 5
Y₀ 932.00
Y₀ 941.15 REF
Y₀ 947.90
Y₀ 954.50
Y₀ 958.25
Y₀ 962.00
Y₀ 969.50
Y₀ 977.00
Y₀ 984.50
Y₀ 992.00 REF
.262 .257 HOLE (6) 2 PL EQ SP
X7224036-13 (2)
X7224031-7
X7224031-8 OPP
X7224036-7 FS
X7224036-9 NS
X7224036-11 (2)
VIEW LOOKING INBD
NORMAL TO ℄ RIB
F33615 73-C-3001
X7224030
1

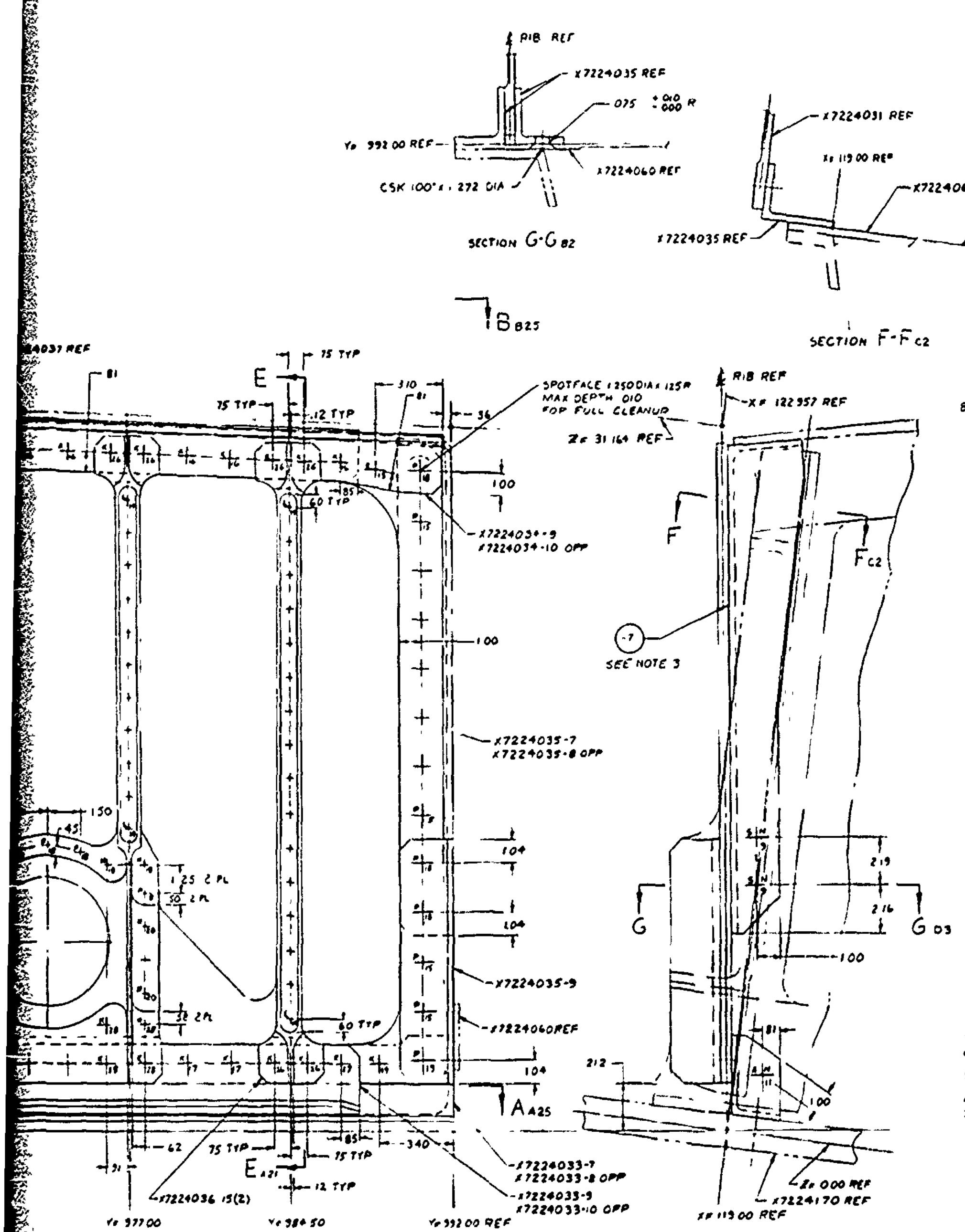


8 FASTENER CODE:

- BASIC CODE
- HEAD LOCATION, (N) NEAR, (F) FAR, NO CODE OPTIONAL
- GRIP LENGTH DASH NO

| BASIC CODE | NOM DIA REF | HOLE DIA | BOLT OR PIN | NUT | WASHER, HEAD SIDE | WASHER NUT SIDE | TORQUE | INSTL SPEC |
|---|---|---|---|---|---|---|---|---|
| A | 1/2 | SEE SPEC | X7223999-8 | 81755/C389-8 | 81755/PSH-16 | X7223986-8 | SEE SPEC | X7223993-8 |
| B | 9/16 | SEE SPEC | X7223999-9 | 81755/C389-9 | 81755/PSH-19 | X7223986-9 | SEE SPEC | X7223993-9 |
| C | 5/8 | SEE SPEC | X7223999-10 | 81755/C389-10 | 81755/PSH-22 | X7223986-10 | SEE SPEC | X7223993-10 |
| D | 3/4 | SEE SPEC | X7223999-12 | 81755/C389-12 | 81755/PSH-24 | X7223986-12 | SEE SPEC | X7223993-12 |
| E | 7/8 | SEE SPEC | X7223999-14 | 81755/C389-14 | 81755/PSH-27 | X7223986-14 | SEE SPEC | X7223993-14 |
| F | 1/4 | .2502 .2496 | X7223985-8 | 81755/C2950-8 | X7223991-8 | X7223989-8 | 81755/MO16.4A | NONE |
| | | | | | | | | |
| H | 3/8 | .3770 .3746 | X7223980-12 | 81755/C2950-12 | X7223991-12 | X7223989-12 | 81755/MO16.6A | NONE |
| | | | | | | | | |
| K | 1/2 | .5025 .4996 | X7223980-16 | 81755/C2950-16 | X7223991-16 | X7223989-16 | 81755/MO16.8A | NONE |
| L | 1/4 | .2502 .2495 | 81755/K010-8 | 81755/K2950-8 | X7223991-8 | X7223989-8 | 81755/MO16.4A | NONE |
| M | 1/2 | .5025 .4996 | X7223996-8 | 81755/C077-8 | X7223992-8 | X7223994-8 | 81755/MO16.8B | NONE |
| N | 9/16 | .5650 .5617 | X7223996-9 | 81755/C077-9 | X7223992-9 | X7223994-9 | 81755/MO16.9B | NONE |
| P | 5/8 | .6275 .6241 | X7223996-10 | 81755/C077-10 | X7223992-10 | X7223994-10 | 81755/MO16.10B | NONE |
| R | 3/4 | .7525 .7491 | X7223996-12 | 81755/C077-12 | X7223992-12 | X7223994-12 | 81755/MO16.12B | NONE |
| S | 5/8 | .6275 .6241 | X7223981-10 | 81755/K077-10 | NONE | X7223994-10 | 81755/MO16.10B | NONE |

7 -1 SHOWN -2 OPP
6 -1/-2 CONTAIN FRACTURE CRITICAL DETAILS. RETAIN ORIGINAL DETAIL MATERIAL TRACEABILITY NUMBERS IN ACCORDANCE WITH X7224199
5 CLEAN SURFACE OF NOTED PARTS AND APPLY -9 MOLDED SHIM PER 81755/FPS 1071 CLASS II TYPE II TO FILL VOID
4 ALL MACHINE SURFACES 125
3 APPLY -7 SEALANT TO ALL FAYING SURFACES AND SHANKS OF STRAIGHT SHANK FASTENERS, METHOD OF APPLICATION PER X7224196
2 ALL FASTENERS EQUALLY SPACED BETWEEN END LOCATED FASTENERS, QUANTITIES AS SHOWN
1 DIMENSIONS & TOLERANCES PER USASI Y14.5
NOTES (EXCEPT AS SHOWN)

Figure 2-8 (Sheet 1)

| REV STATUS | |
|---|---|
| SH | REV |
| 1 | — |
| 2 | — |

SEE SEPARATE PARTS LIST

NEXT SECT LTR: H

SEE PL

RIB INSTL — OUTBD CLOSURE

J 07878 X7224030

1/2

28 27 26

D

C

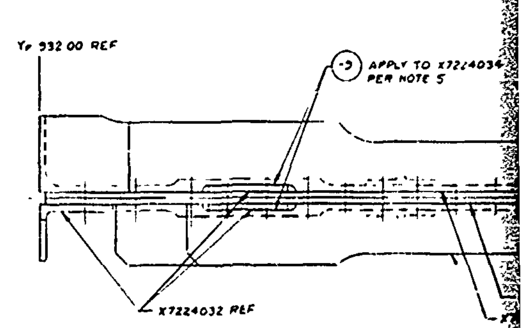


B

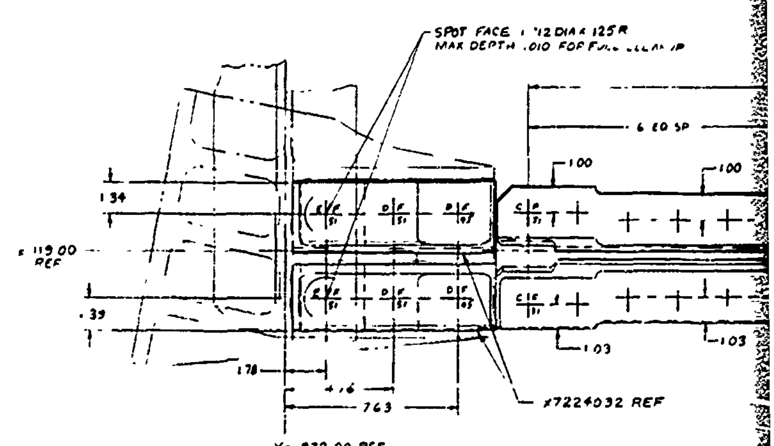


A

28 27 26

26 | 25 | 24 | 23

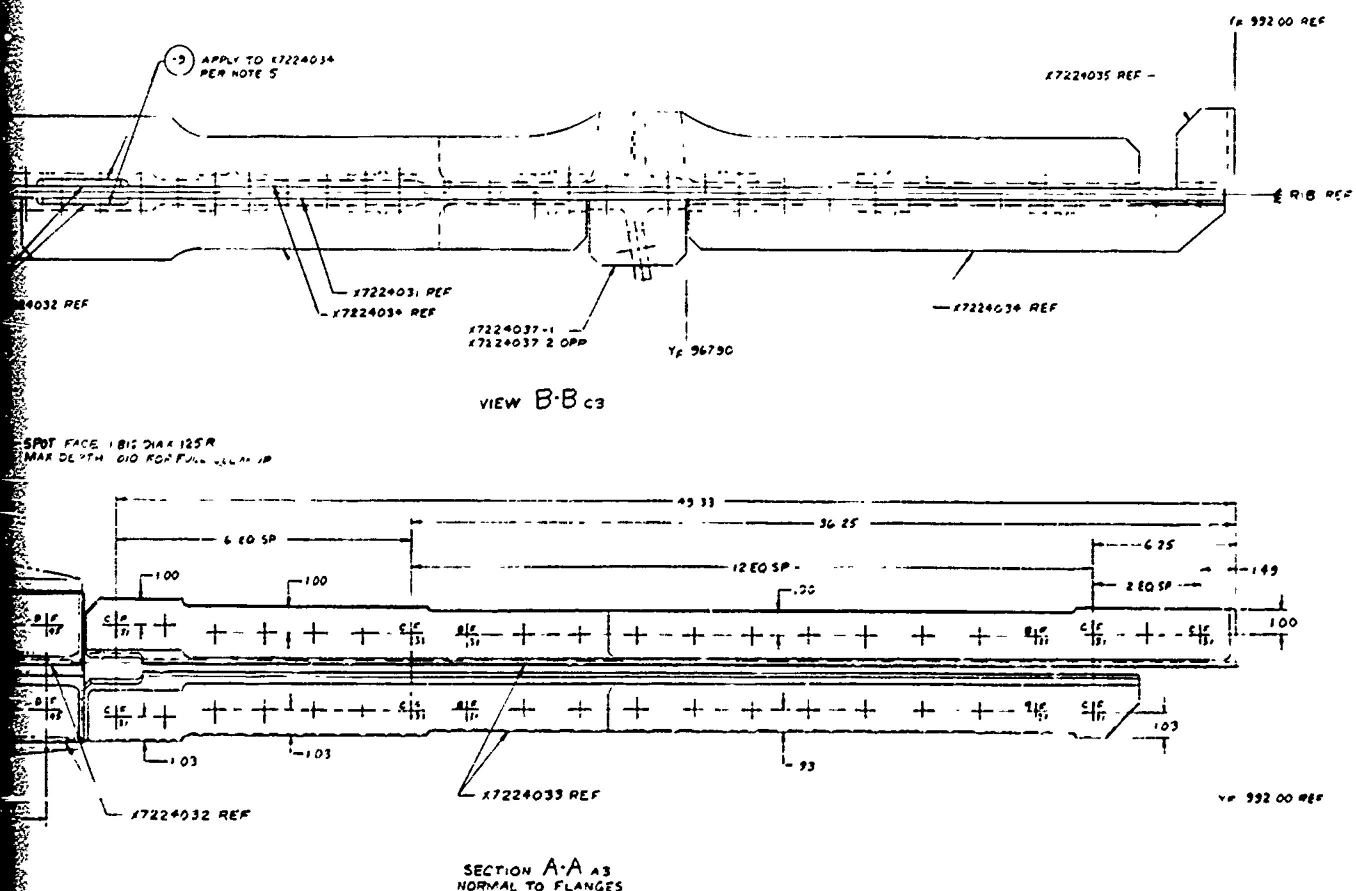


F33615-73-C-3001 | X7224030 | 2

25 | 24 | 23

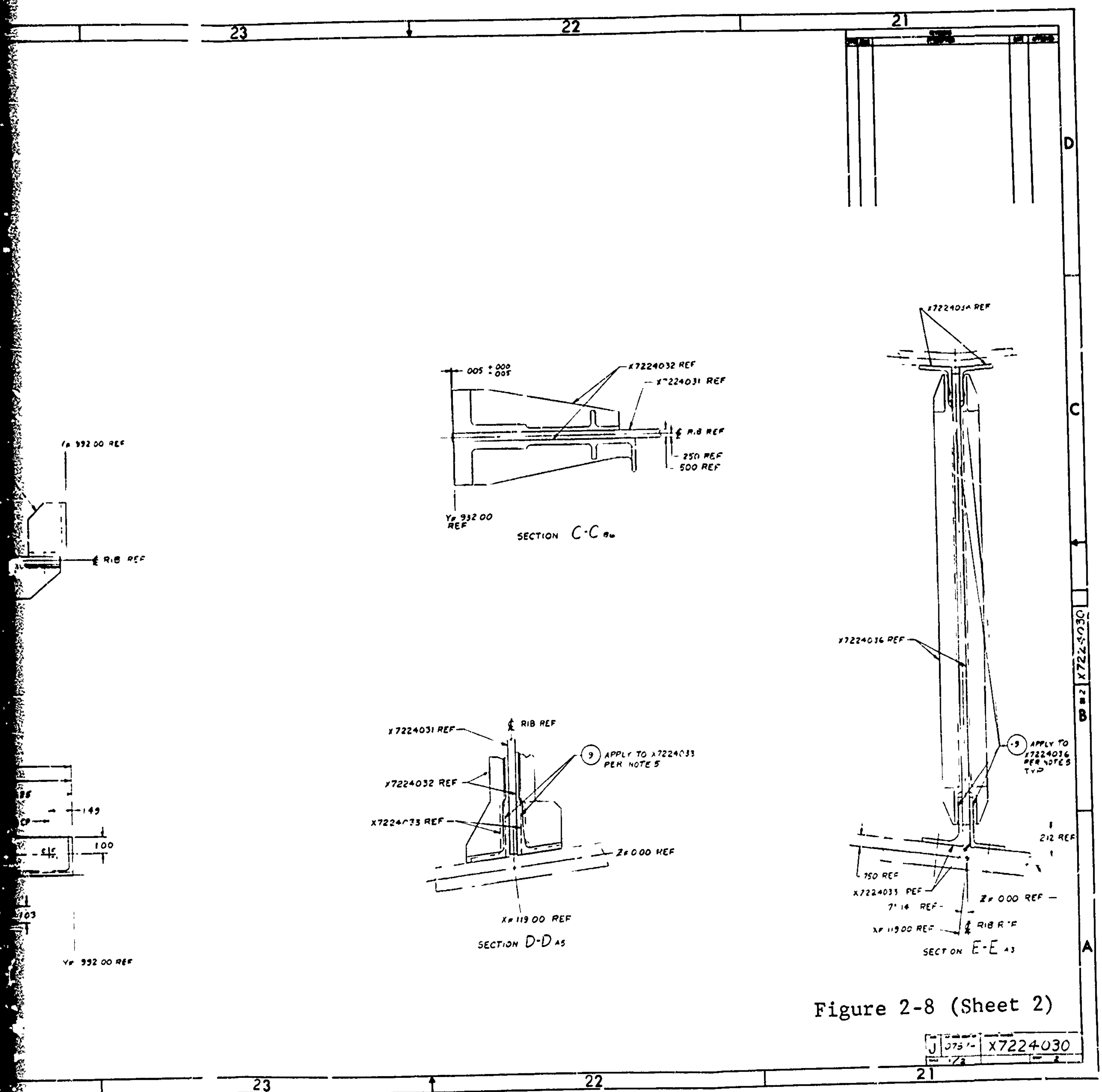


Figure 2-8 (Sheet 2)

- o symmetrically brazed three-element lower place
- o reconfigured internal bulkheads
- o material substitution and fabrication revision to the highly loaded shear webs.

These changes along with a complete description of each major component are discussed in the following paragraphs.

### 2.1.2.1 Lower Plate Assembly

The lower plate assembly (Figure 2-9, Drawing X7223730) consists of two symmetrically brazed Titanium sub-asssemblies with integral pivot lugs, lug reinforcing hubs, forward and aft bulkhead attach angles, outboard longeron splice fittings, stabilizing beam at $X_F$99, and centerline splice plates. These components are mechanically assembled using taper-lok fasteners for a minimal stress concentration intensity. The integral lug concept improves fabrication by eliminating the separate brazed assembly for the pivot lug and eliminates the critical fit between the lug and plate. The integral lug is also a more weight efficient configuration and improves structural reliability by deleting the dependence on mechanical fasteners for transferring the critical lug loads into the box structure. The symmetrically brazed concept permits the assembly to be used as either a left or right hand part, but requires separate bolt-on bulkhead attachment angles. Eccentric loading of the brazed joints is also minimized by the symmetrical design.

The brazed plate assembly shown in Figure 2-10 (Drawing X7223731) is constant thickness consisting of three lamina of beta-annealed 6AL-4V titanium which extend to include the pivot lug. The one-piece center lamina is a solid thin plate whereas the one-piece upper and lower elements are profiled into five crack stopper bars, inboard of the lug region. The plate assembly, as brazed, is symmetrical about its horizontal centerline. Local machining will be required after brazing to obtain identity as either a left or right hand part.

The aft longeron splice fitting consists of two elements of beta annealed 6A1-4V titanium, attached with fasteners to the brazed assembly. The upper element extends the full width of the plate and incorporates the vertical flange for attaching the closure rib. The lower element terminates after transferring the longeron load into the lower plate. This splice provides extra thickness to accommodate the baseline longeron interface

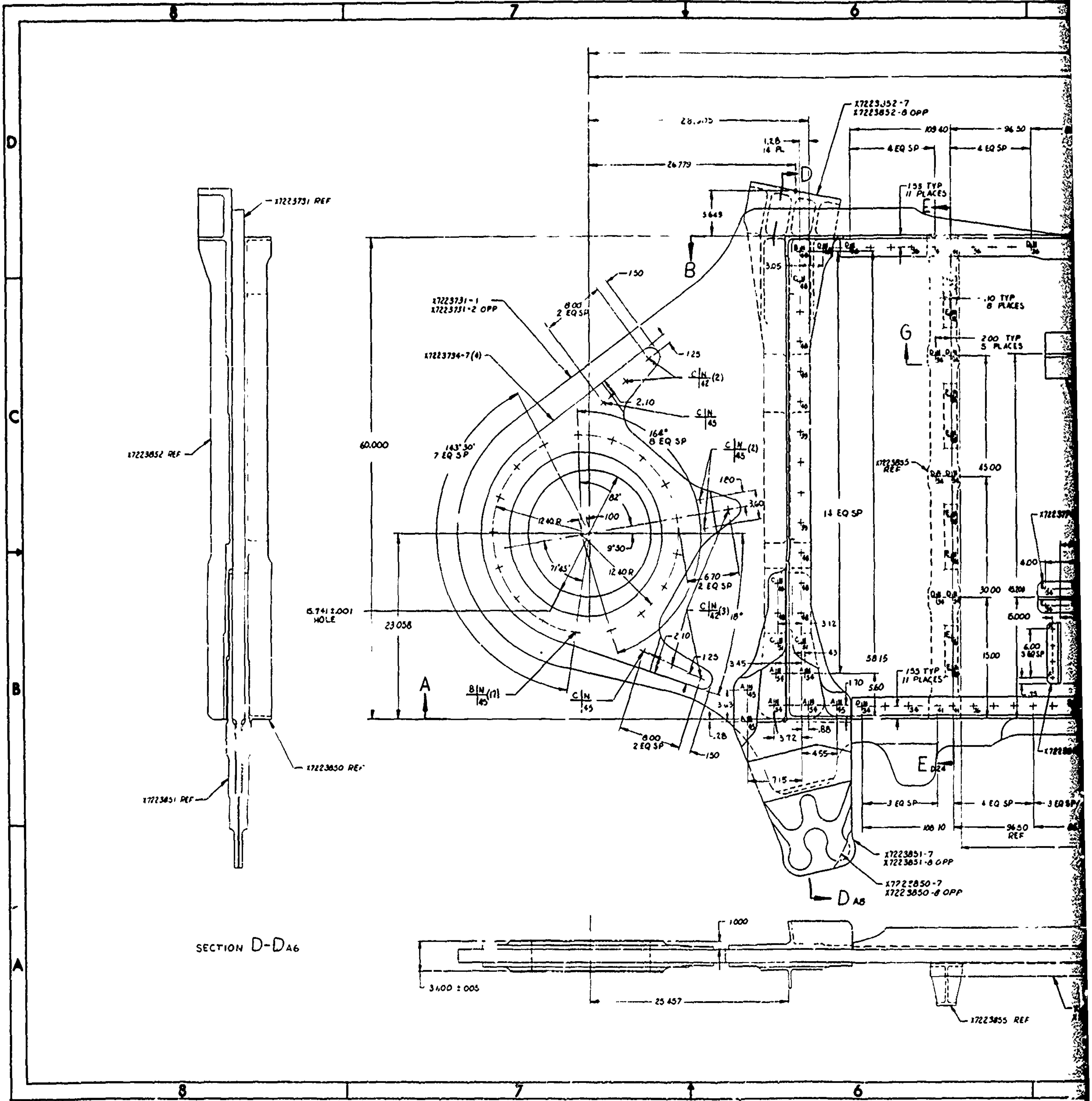
SECTION D-D A6
X7223731 REF
X7223852 REF
X7223850 REF
X7223851 REF
X7223852-7
X7223852-8 OPP
X7223731-1
X7223731-2 OPP
X7223734-7(4)
X7223855 REF
X7223851-7
X7223851-8 OPP
X7223850-7
X7223850-8 OPP
6.741 ± .001 HOLE
60.000
23.058
14 EQ SP
.155 TYP 11 PLACES
.10 TYP 8 PLACES
.200 TYP 5 PLACES
3.600 ± .005
25.457

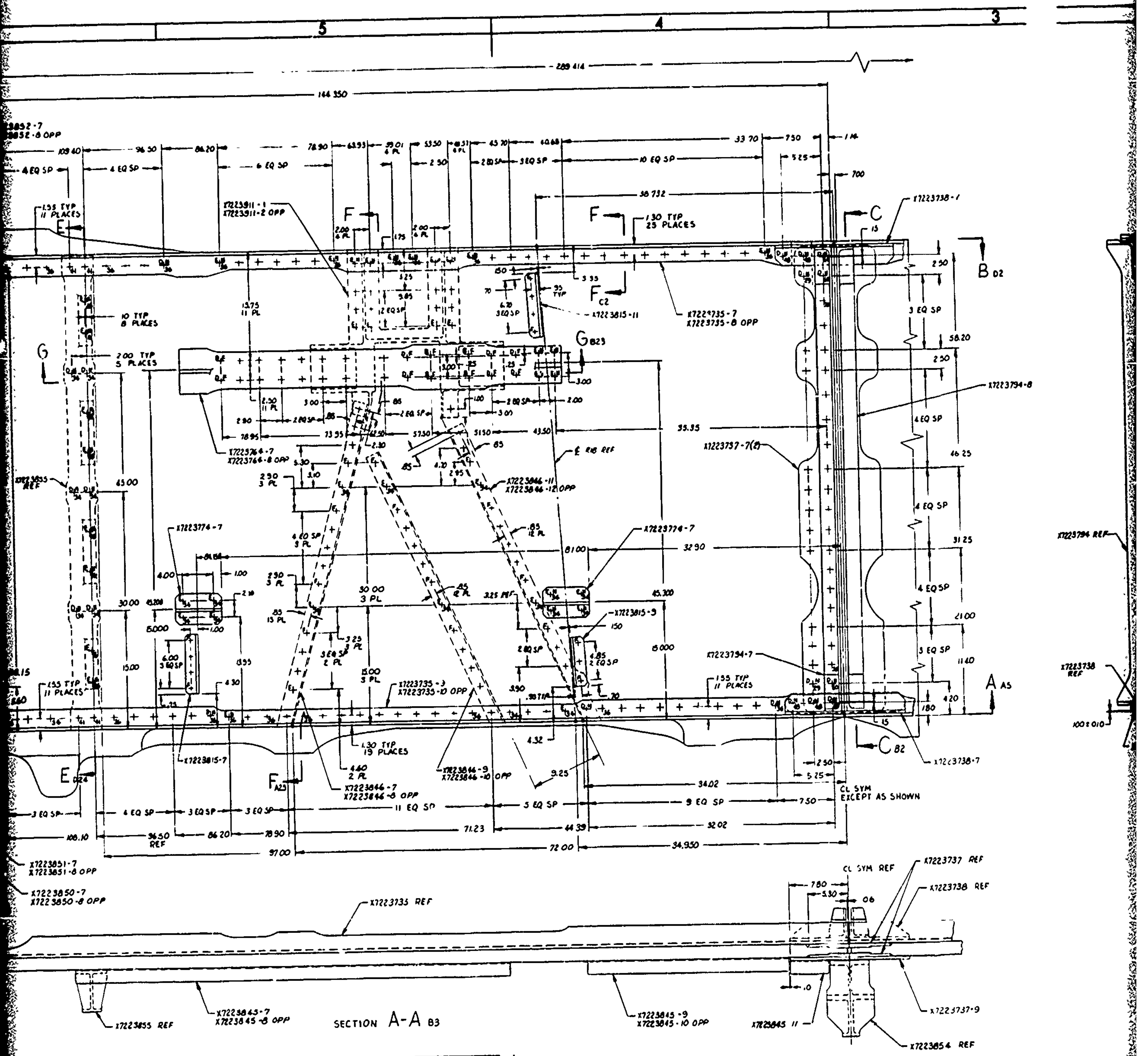


| | | | |
|---|---|---|---|
| F33615 73-C-3001 | | X7223730 | 1 |

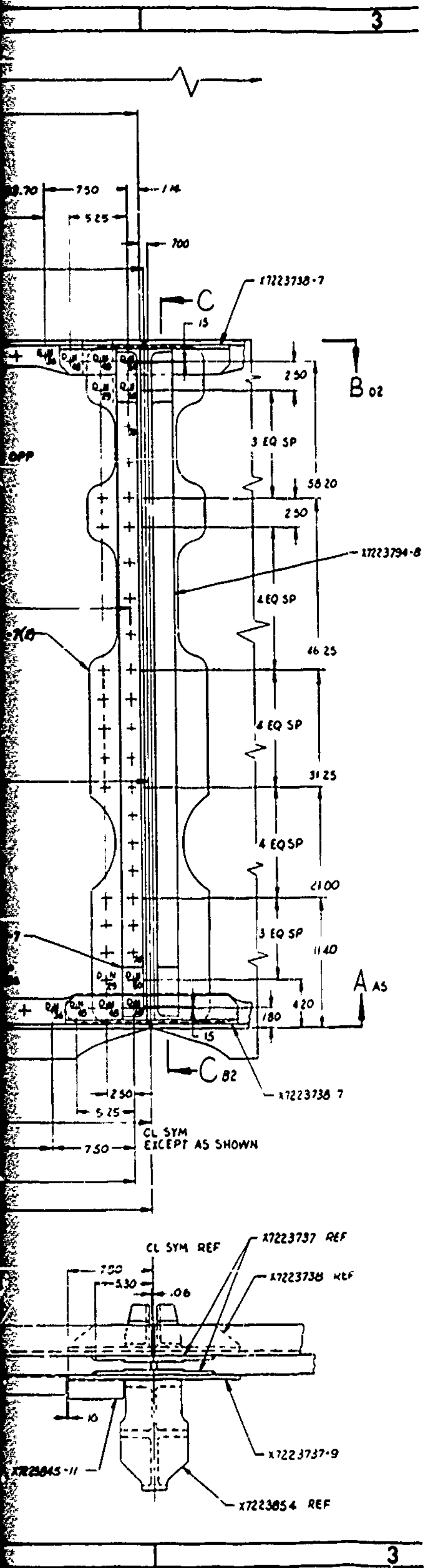


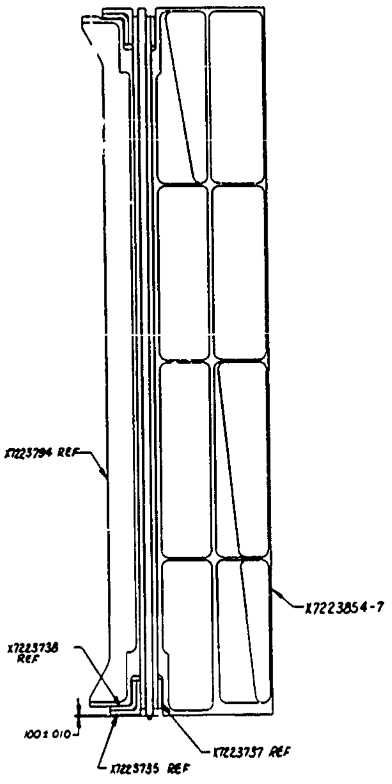


SECTION C-C B3

5. BOLT CODE:

BASIC CODE — HEAD LOCATION (N) NEAR SIDE (F) FAR SIDE — GRIP LENGTH DASH NO.

| BASIC CODE | NOM DIA | BOLT | NUT 61755/ | WASHER UNDER HD | WASHER UNDER NUT | BOLT INSTL SPEC |
|---|---|---|---|---|---|---|
| A | 1 | X7223999-16 | C389-16 | 61756/P511- | X7223986-16 | X7223993-16 |
| B | 7/8 | -14 | -14 | - | -14 | -14 |
| C | 3/4 | -12 | -12 | -24 | -12 | -12 |
| D | 5/8 | -10 | -10 | -22 | -10 | -10 |
| E | 1/2 | -8 | -8 | -16 | -8 | -8 |
| F | 3/8 | X7223999-6 | C389-6 | 61756/P5H-10 | X7223986-6 | X7223993-6 |
| | | | | | | |

4 -1 CONTAINS FRACTURE CRITICAL DETAILS. RETAIN ORIGINAL DETAIL MATERIAL TRACEABILITY NUMBERS IN ACCORDANCE WITH X7224199.
3. SEALING MATERIALS AND METHODS OF APPLICATION PER X7224196.
2. APPLY -7 GENERAL SEALANT TO ALL FAYING SURFACES.
1 DIMENSIONS AND TOLERANCES PER USASI Y14.5.

NOTES ~ EXCEPT AS SHOWN

Figure 2-9 (Sheet 1)

SEE SEPARATE PARTS LIST

GENERAL DYNAMICS CONVAIR AEROSPACE DIVISION FORT WORTH OPERATION FORT WORTH TEXAS

SEE PL

NONE

LOWER PLATE, WING CARRYTHROUGH ASSY OF

J 07878 X7223730

28 27 26

D

C

B

A

28 27 26

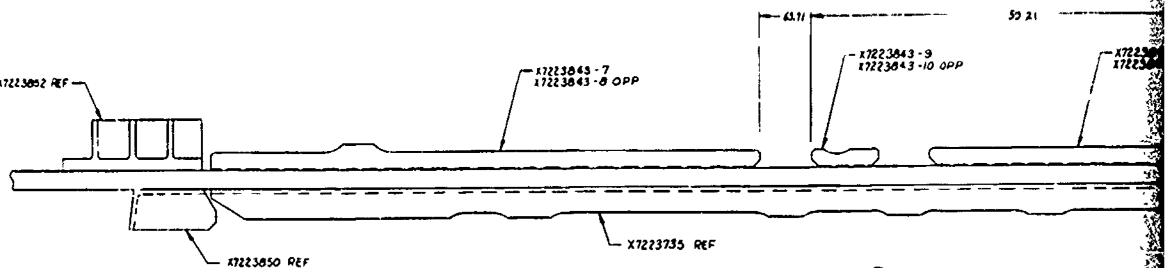


SECTION B-B

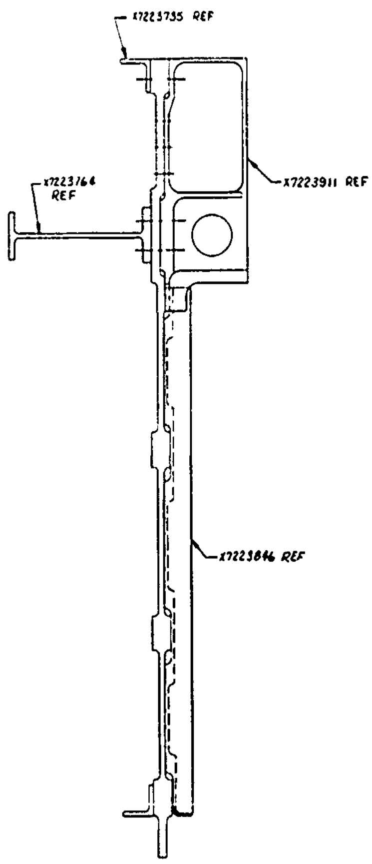


SECTION F-F B3

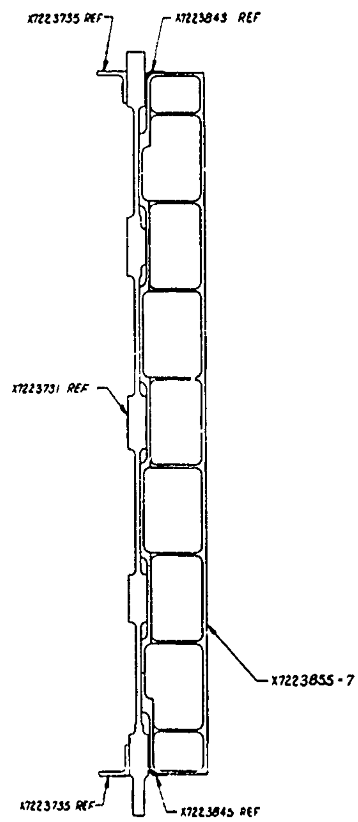


SECTION E-E B6

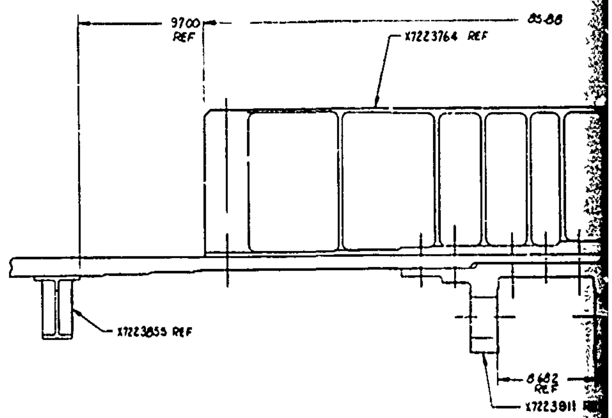


SECTION G-G

| CONTRACT NO. | REV | DWG NO | SH |
|---|---|---|---|
| F33615-73-C-3001 | | X7223730 | 2 |

25 24 23

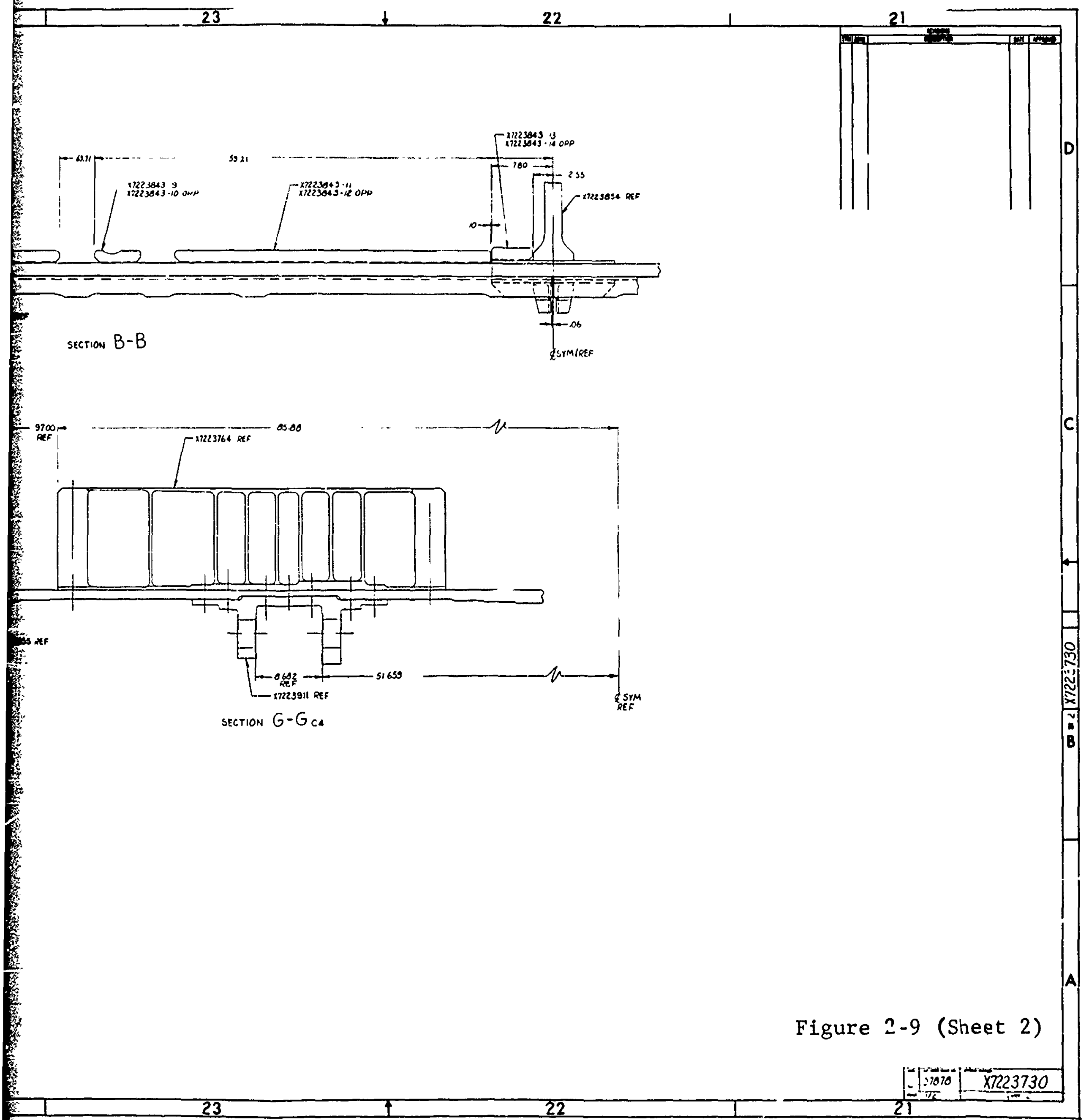


Figure 2-9 (Sheet 2)

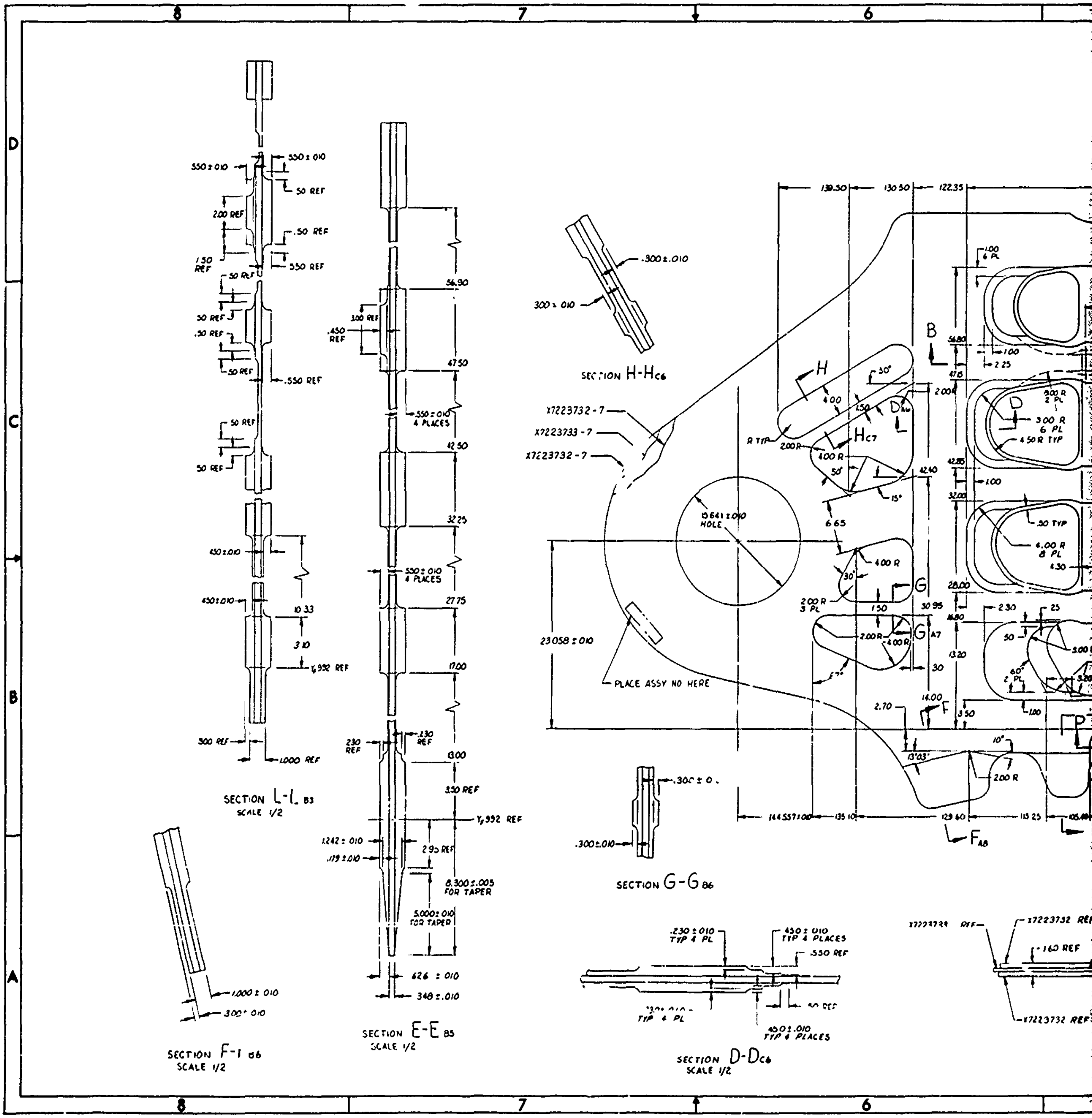
SECTION L-L B3
SCALE 1/2
SECTION E-E B5
SCALE 1/2
SECTION F-I B6
SCALE 1/2
SECTION H-H C6
SECTION G-G B6
SECTION D-D C6
SCALE 1/2
PLACE ASSY NO HERE
15.641±.010 HOLE
23.058±.010
X7223732-7
X7223733-7
X7223732-7

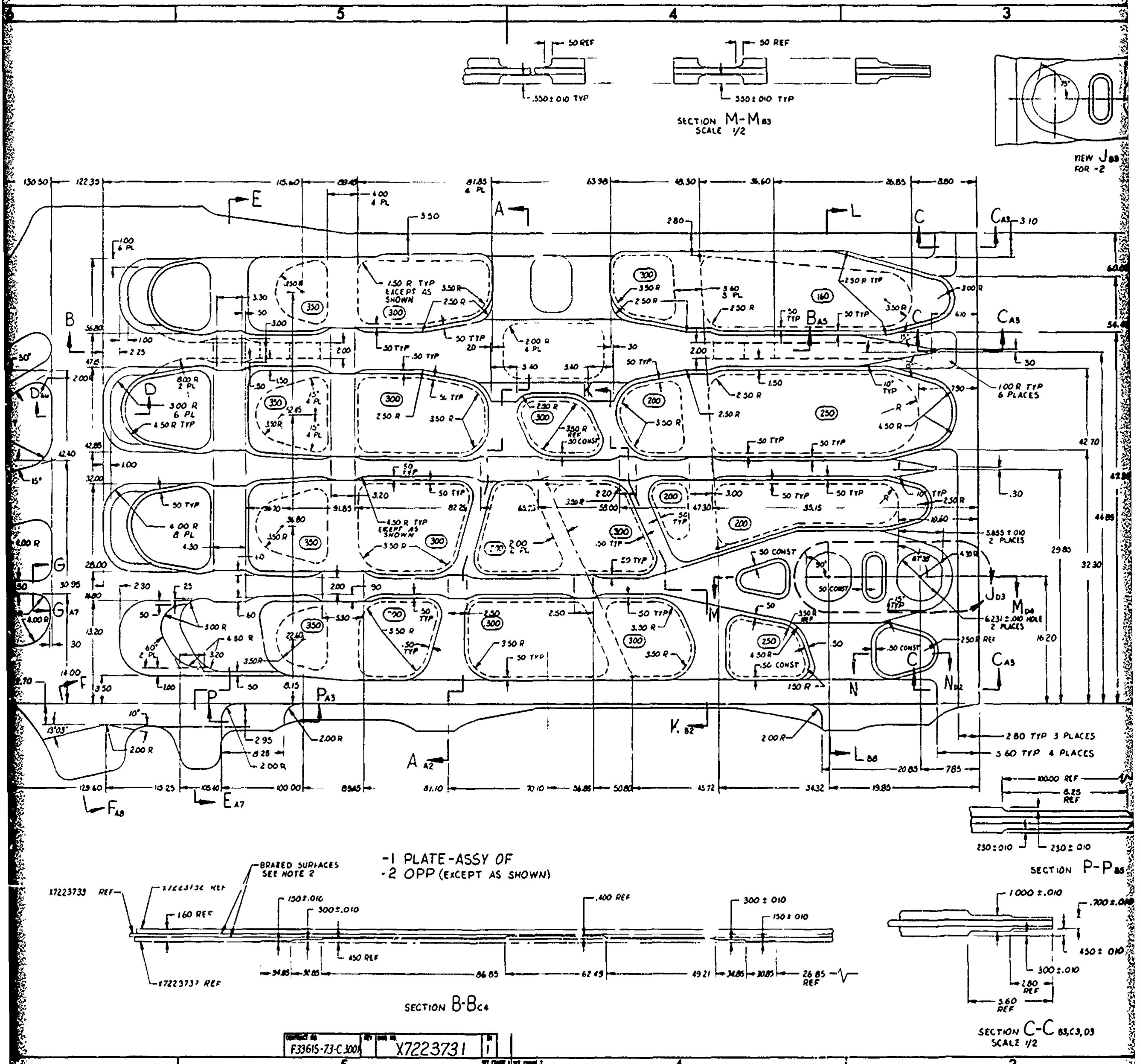
SECTION M-M B3
SCALE 1/2
VIEW J B3
FOR -2
-1 PLATE-ASSY OF
-2 OPP (EXCEPT AS SHOWN)
BRAZED SURFACES
SEE NOTE 2
SECTION B-B C4
SECTION P-P B5
SECTION C-C B3,C3,D3
SCALE 1/2
1.50 R TYP
EXCEPT AS
SHOWN
1.00 R TYP
6 PLACES
2.80 TYP 3 PLACES
5.60 TYP 4 PLACES
F33615-73-C-3001
X7223731
5
4
3

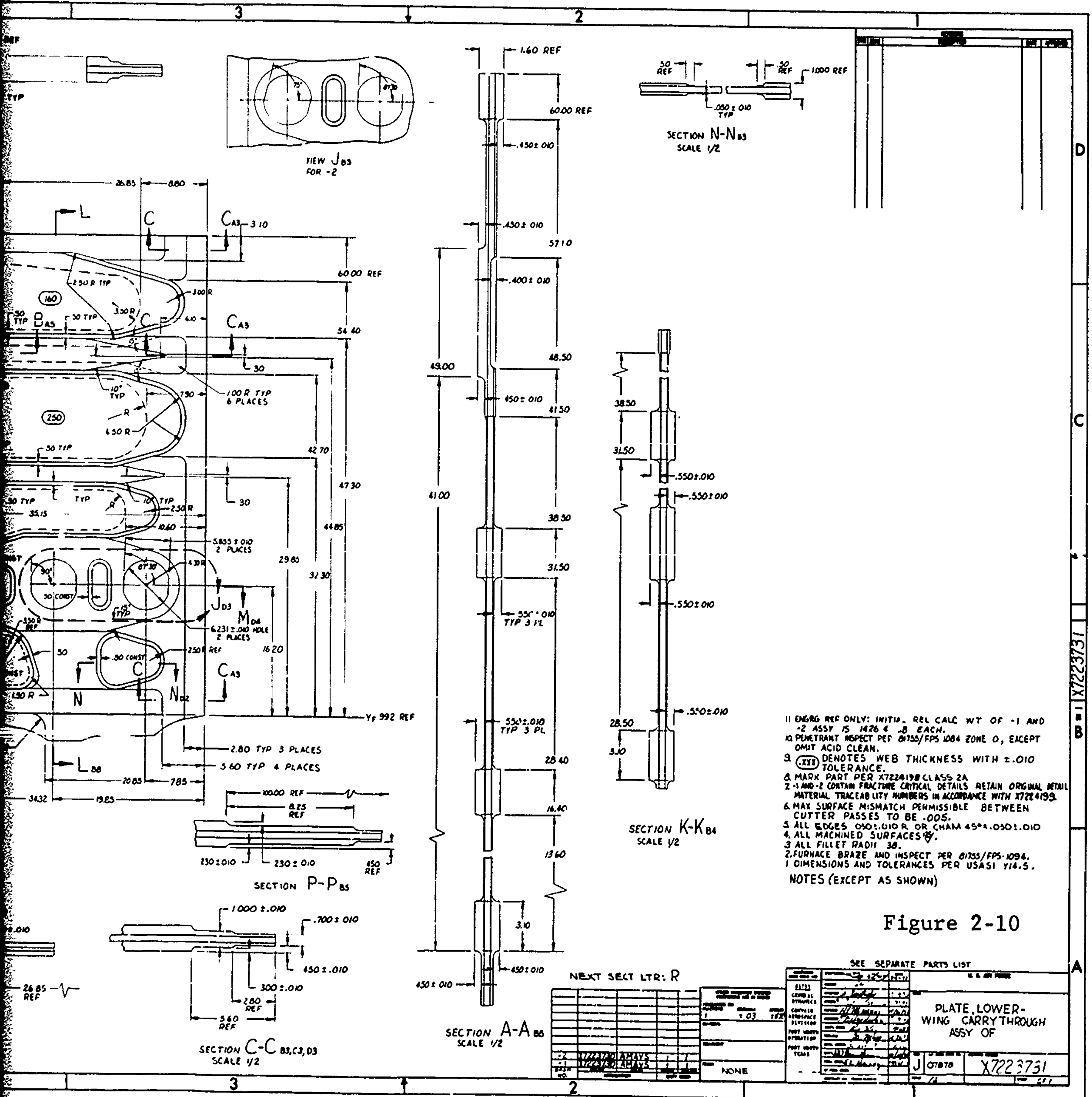

VIEW J B3
FOR -2
SECTION N-N B3
SCALE 1/2
SECTION K-K B4
SCALE 1/2
SECTION P-P B5
SECTION C-C B3,C3,D3
SCALE 1/2
SECTION A-A B6
SCALE 1/2
11 ENGRG REF ONLY: INITIAL REL CALC WT OF -1 AND -2 ASSY IS 1426 4 .8 EACH.
10 PENETRANT INSPECT PER 81755/FPS 1084 ZONE O, EXCEPT OMIT ACID CLEAN.
9 (.XXX) DENOTES WEB THICKNESS WITH ±.010 TOLERANCE.
8 MARK PART PER X7224198 CLASS 2A
7 -1 AND -2 CONTAIN FRACTURE CRITICAL DETAILS RETAIN ORIGINAL DETAIL MATERIAL TRACEABILITY NUMBERS IN ACCORDANCE WITH X7224199.
6 MAX SURFACE MISMATCH PERMISSIBLE BETWEEN CUTTER PASSES TO BE .005.
5 ALL EDGES .050±.010 R OR CHAM 45°×.050±.010
4 ALL MACHINED SURFACES
3 ALL FILLET RADII .38.
2 FURNACE BRAZE AND INSPECT PER 81755/FPS-1094.
1 DIMENSIONS AND TOLERANCES PER USASI Y14.5.
NOTES (EXCEPT AS SHOWN)
NEXT SECT LTR: R
SEE SEPARATE PARTS LIST
PLATE, LOWER-WING CARRYTHROUGH ASSY OF
NONE
X7223731


Figure 2-10

requirement, and it reduces the material width required in the lower plate from 84 inches to 73 inches.

The forward longeron splice fitting is integrally machined from 7050 aluminum plate and is mechanically fastened to the lower surface of the brazed lower plate. The fitting extends the full width of the lower plate and includes a vertical flange for attaching the support structure for the lower contoured fairing.

Separate bolt-on lug reinforcements are required to supplement the strength capability of the brazed assembly, and to maintain baseline bearing thickness at the pivot hole. The attaching taper-lok bolts are located in relatively low stressed areas and provide a positive control against element delaminations.

The reinforcement beams attached to the external surface of the lower plate at $X_F99$ are required for compression stability during negative loading conditions and extend to contour for support of the lower fairing. The beams have been redesigned from a built-up aluminum section to an integrally machined part of 7050 aluminum.

#### 2.1.2.2 Upper Plate Assembly

The upper plate assembly (Drawing X7223720, Figure 2-11) reacts the compression load introduced into the box structure by the pivot pins. Since the primary loading is compression, no fail-safe features are required. This structure is critical in compression stability.

The section outboard of $X_F84$ consists of integrally machined details electron-beam welded together and a bolt-on sandwich panel. The welded assembly includes the pivot lug, forward and aft partial width plate elements, and an outboard plate rail in the area of the closure rib. Beta annealed 6Al-4V titanium material was selected for the weld assembly to obtain its high fracture toughness because of the critical nature of the pivot lug and integral aft longeron tab. Although compression is the primary load, the pivot lug will experience some local tensile stresses, while the longeron tab is loaded primarily in tension. The sandwich panel is made of 6Al-4V-2Sn titanium for maximum strength and stiffness.

The intermediate section ($X_F39$ to $X_F84$) consists of integrally machined forward and aft partial width plates connected by a bolt-on sandwich panel. Aluminum was selected for both the plate

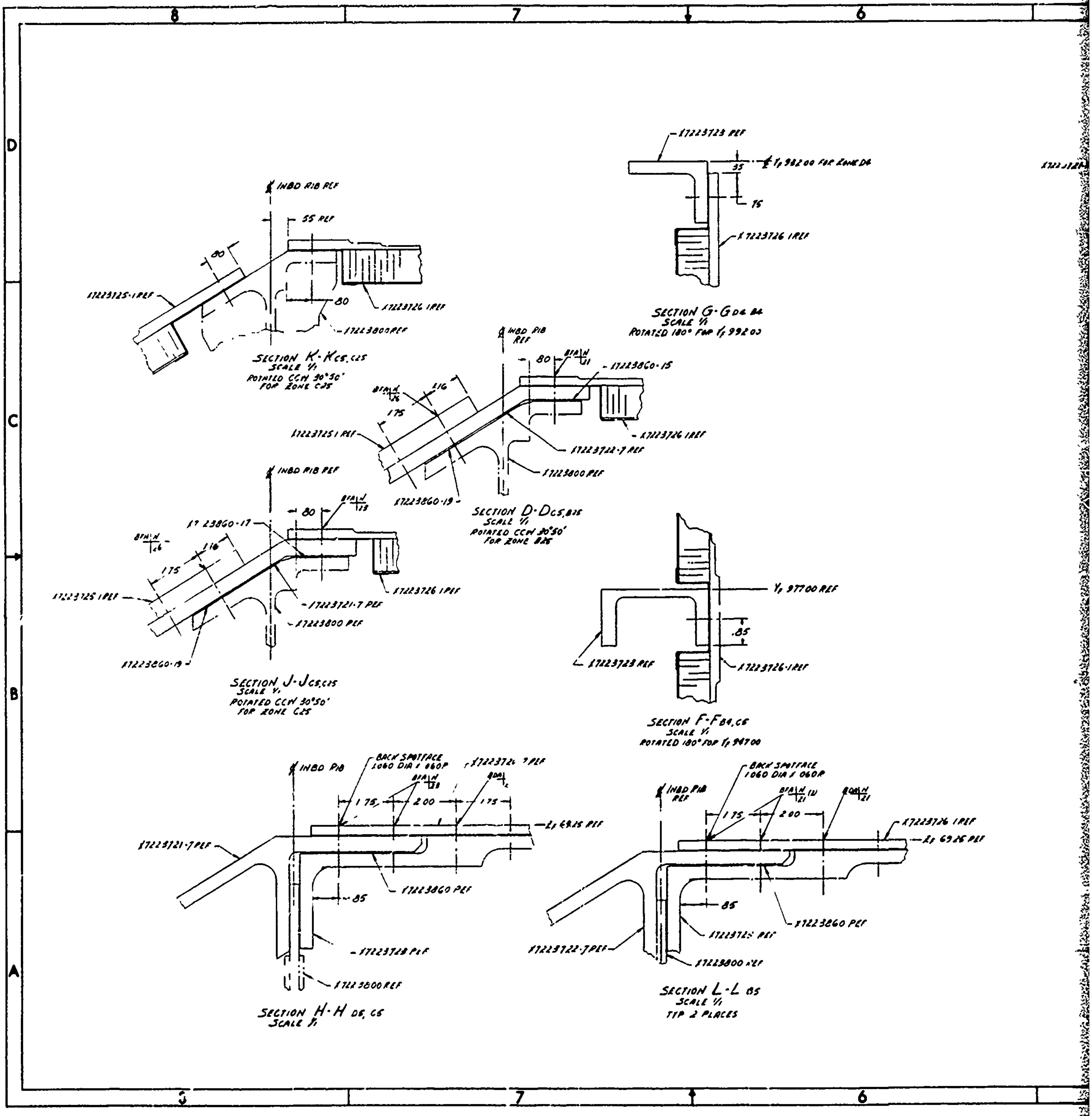

8
7
6
D
C
B
A
SECTION G-G D6, B6
SCALE 1/1
ROTATED 180° FOR Y, 992.00
SECTION K-K C5, C25
SCALE 1/1
ROTATED CCW 30°50' FOR ZONE C25
SECTION D-D C5, B25
SCALE 1/1
ROTATED CCW 30°50' FOR ZONE B25
SECTION J-J C5, C25
SCALE 1/1
ROTATED CCW 30°50' FOR ZONE C25
SECTION F-F B4, C6
SCALE 1/1
ROTATED 180° FOR Y, 977.00
SECTION H-H D6, C6
SCALE 1/1
SECTION L-L B5
SCALE 1/1
TYP 2 PLACES
INBD RIB REF
55 REF
X7223726 IREF
X7223800 REF
X7223726-1 REF
Y, 977.00 REF
BACK SPOTFACE 1.060 DIA X .060P
.85

| 5 | 4 | 3 |
|---|---|---|

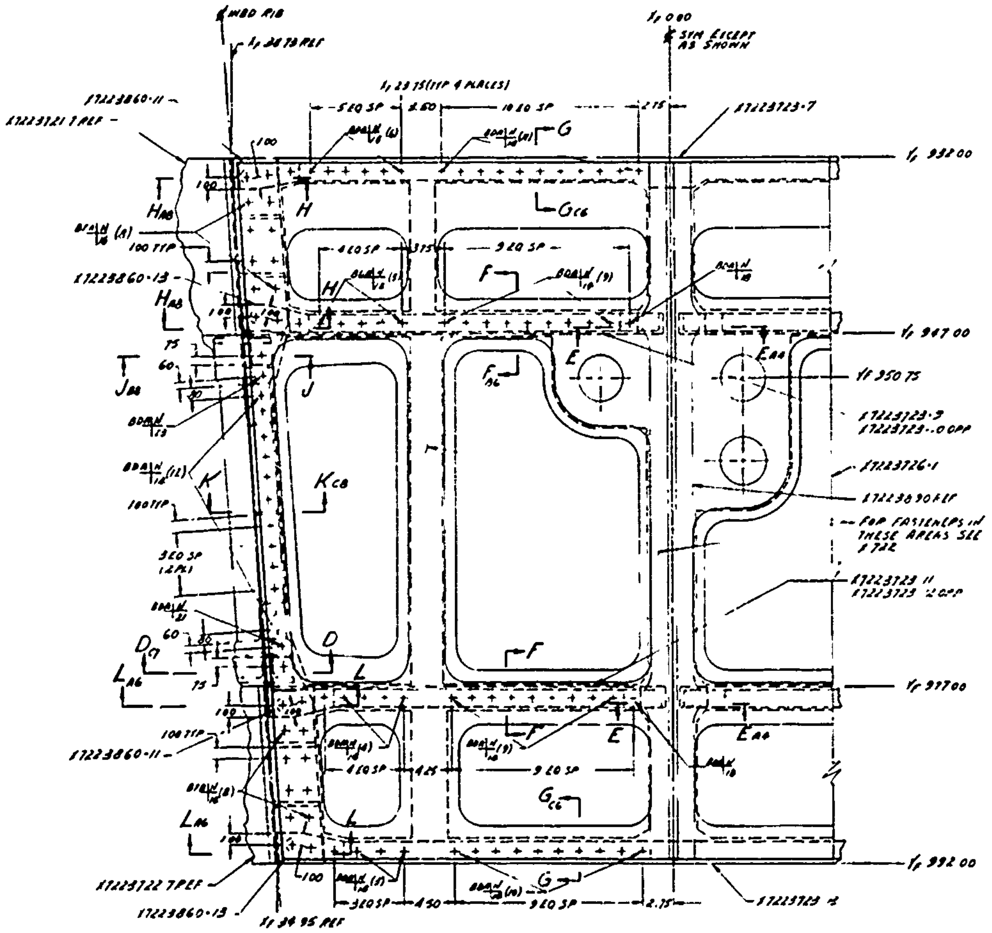

VIEW A-A D2

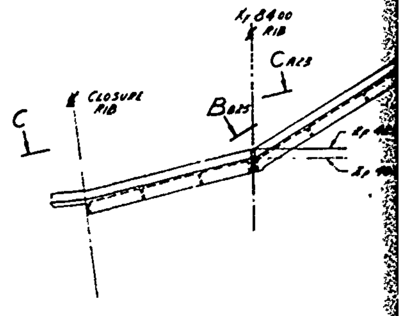

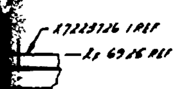

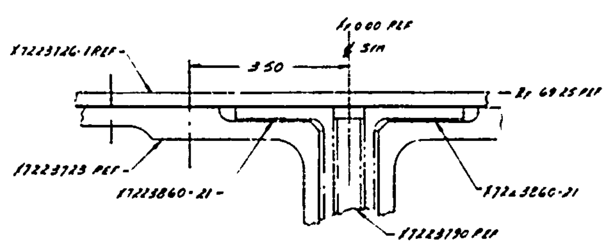

SECTION E-E B4, C4
SCALE 1/1

| | | |
|---|---|---|
| F33615-73C-3001 | X7223720 | 1 |

| 5 | 4 | 3 |
|---|---|---|

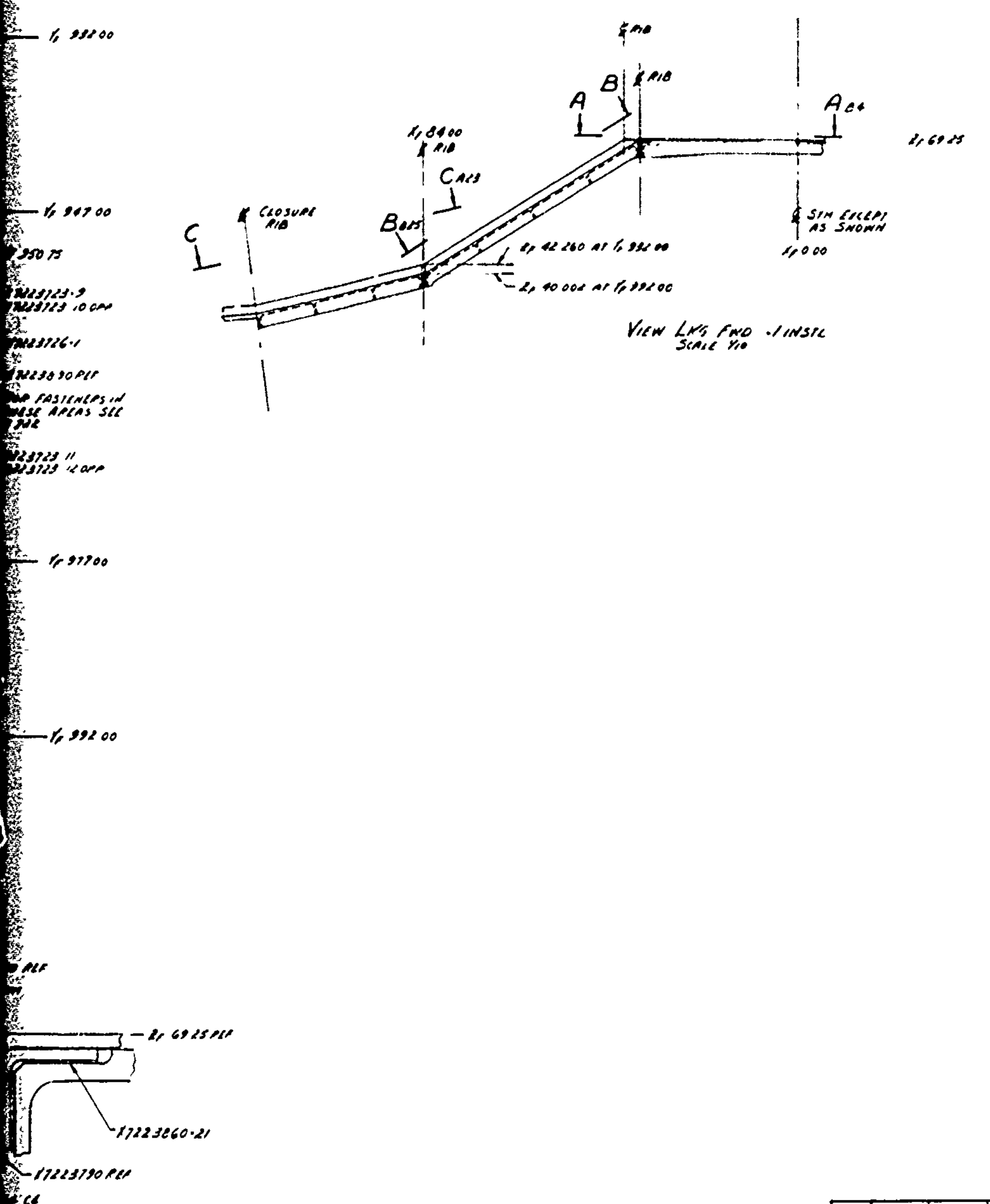


5 BOLT CODE:

BASIC CODE — HEAD LOCATION (N) NEAR SIDE (F) FAR SIDE — GRIP LENGTH DASH No

| BASIC CODE | HOLE DIA | BOLT | NUT A1755/ | WASHER UNDER HD | WASHER UNDER NUT | TORQUE PER A1755/MOD |
|---|---|---|---|---|---|---|
| BDA | .3770 .3796 | X7223996-6 | C077-6 | X7223992-6 | X7223994-6 | -6B |
| BFA | [illegible] | X7223996-8 | C077-8 | X7223992-8 | X7223994-8 | -8B |
| BHA | .6275 .6241 | X7223996-10 | C077-10 | X7223992-10 | X7223994-10 | -10B |
| BJA | .7526 .7491 | X7223996-12 | C077-12 | X7223992-12 | X7223994-12 | -12B |
| | | | | | | |
| | | | | | | |

4 SEALING MATERIALS AND METHODS OF APPLICATION PER X7224196

3 INSTALL ALL STRAIGHT SHANK FASTENERS WITH -7 GENERAL SEALANT

2 APPLY -7 GENERAL SEALANT TO ALL FAYING SURFACES

1 DIMENSIONS AND TOLERANCES PER USASI Y14.5

NOTES (EXCEPT AS SHOWN)

Figure 2-11 (Sheet 1)

SEE SEPARATE PARTS LIST

UPPER PLATE INSTL - $Y_f$ 932.00 TO $Y_f$ 992.00

X7223720

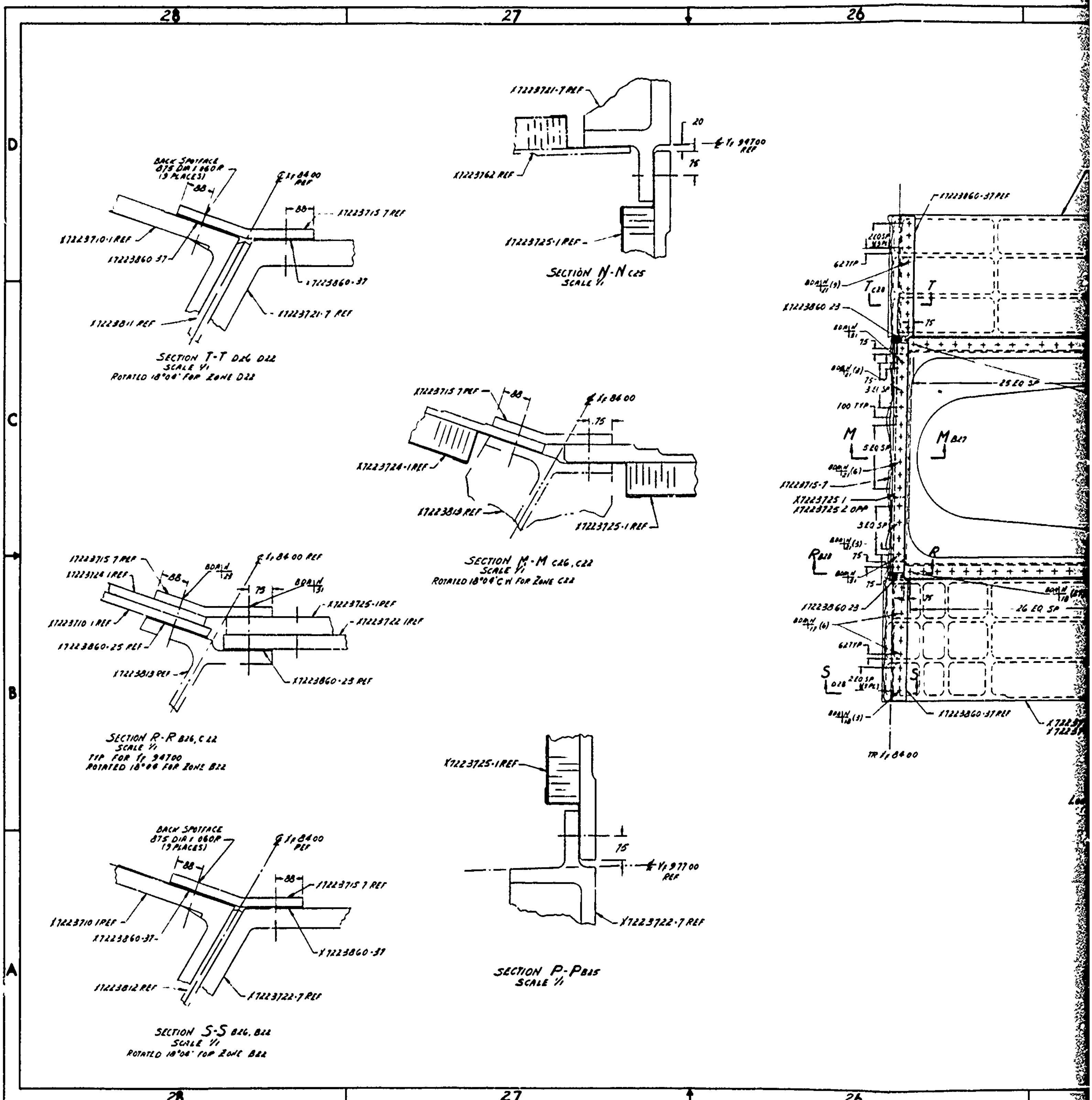
28
27
26
D
C
B
A
SECTION T-T D26 D22
SCALE 1/1
ROTATED 18°04' FOR ZONE D22
SECTION N-N C25
SCALE 1/1
SECTION M-M C26, C22
SCALE 1/1
ROTATED 18°04' C W FOR ZONE C22
SECTION R-R B26, C22
SCALE 1/1
TYP FOR Y1 94700
ROTATED 18°04' FOR ZONE B22
SECTION P-P B25
SCALE 1/1
SECTION S-S B26, B22
SCALE 1/1
ROTATED 18°04' FOR ZONE B22
BACK SPOTFACE
.875 DIA X .060R
(3 PLACES)
X7223725-1 REF
X7223722-7 REF

25 24 23

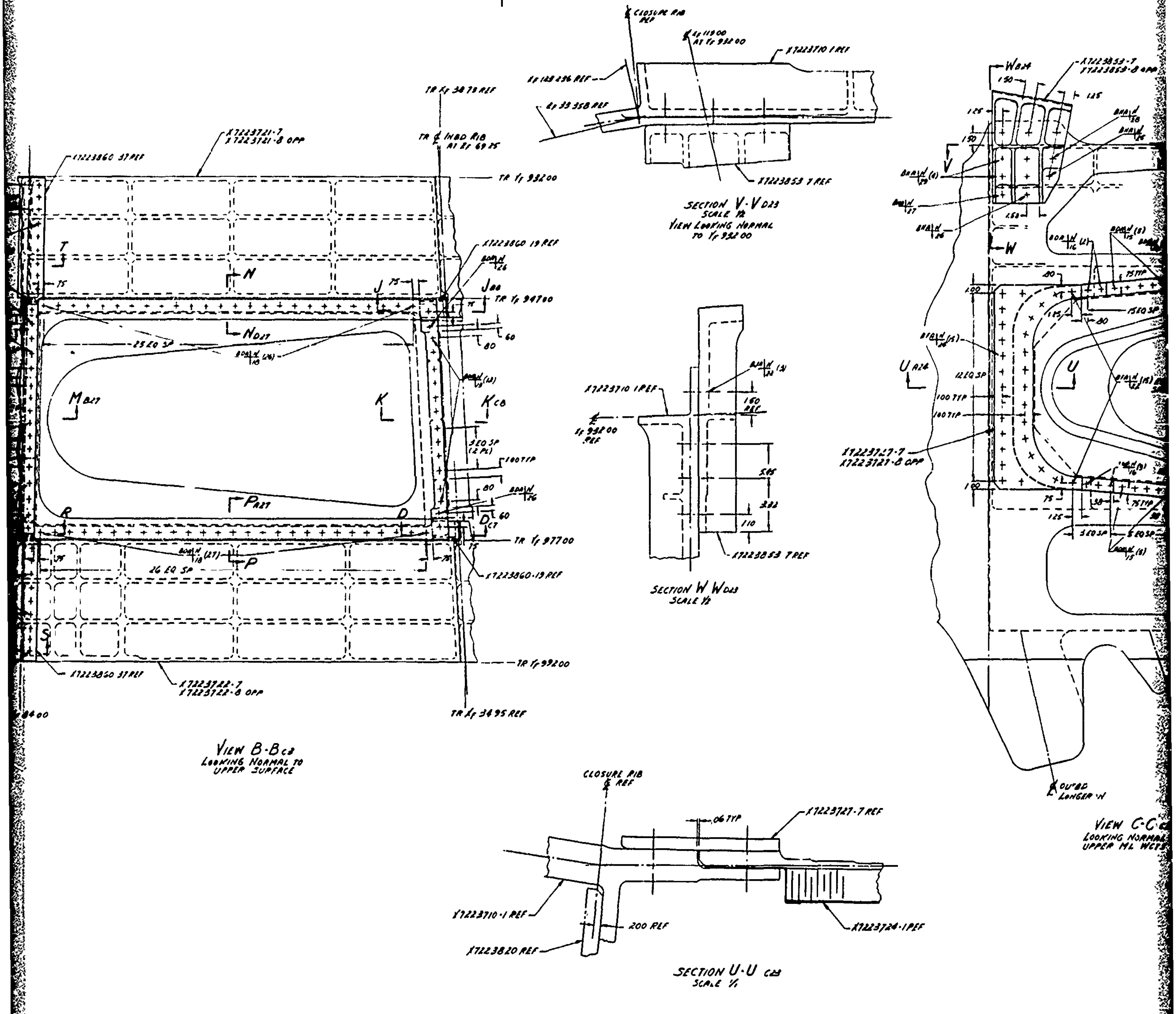


| CONTRACT NO. | REV | DWG NO. | SH |
|---|---|---|---|
| F33615 73 C-3001 | | X7223720 | 2 |

25 24 23

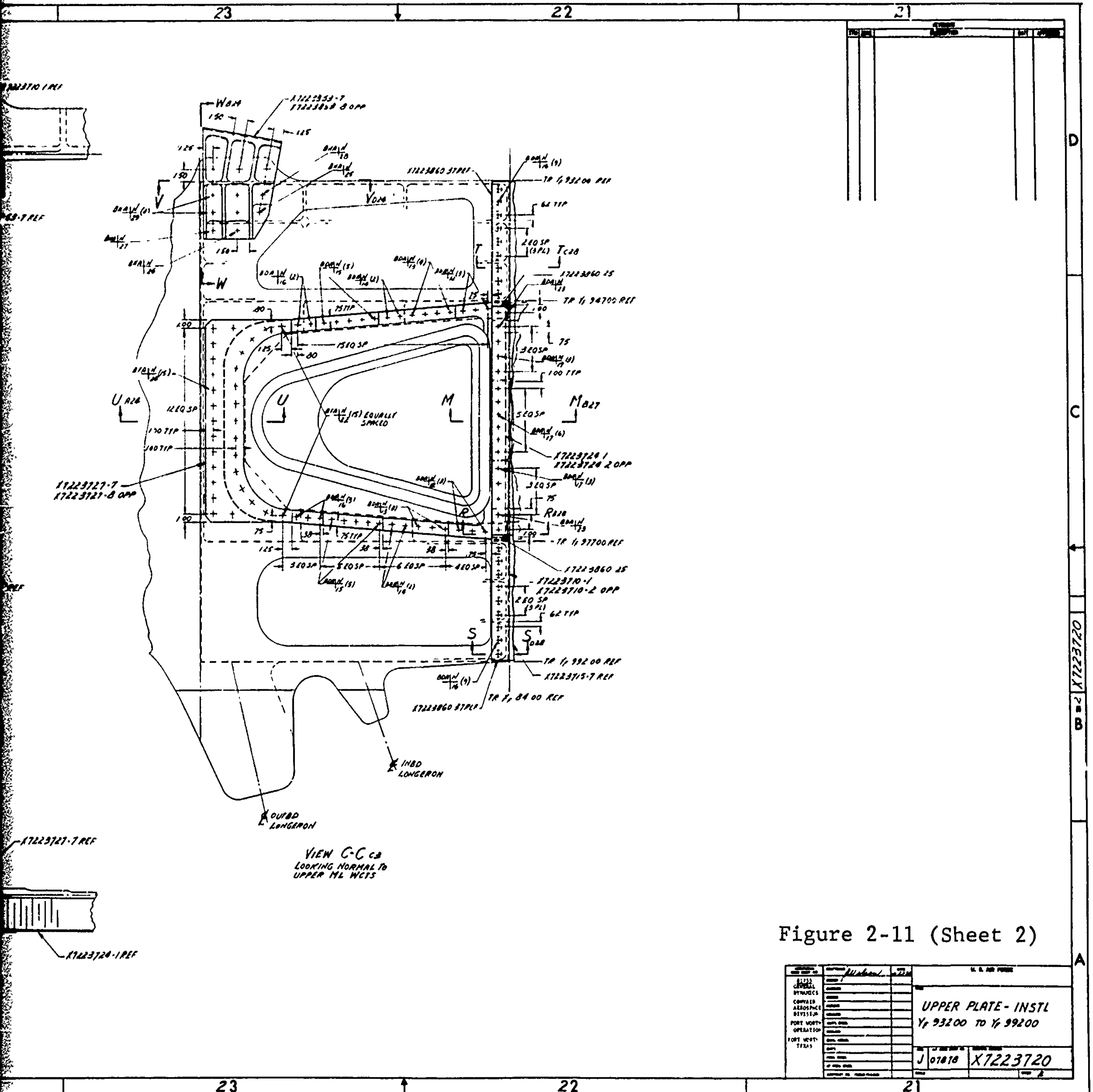


Figure 2-11 (Sheet 2)

elements and the sandwich panel to minimize cost. The heavier gages used for the aluminum structure also reduces the stiffening requirements to prevent buckling. 7050 aluminum with its superior strength and above average fracture toughness was used for the integrally machined plate elements. The sandwich panel is fabricated from 2024 aluminum sheet, reinforced with 5052 aluminum core.

The area inboard of $X_F$ 39 consists of a 2024 aluminum sandwich panel supported by 7050 aluminum rails at $Y_F$ 932, $Y_F$ 947, $Y_F$ 977, and $Y_F$ 992. Sandwich type construction is the most efficient structure in this region due to the low load density, the compression stability, and the fuel pressure requirements.

The intermediate section is mechanically attached to the outboard and inboard sections through tension splices which sandwich the ribs at $X_F$ 39 and $X_F$ 84. This type splice was employed to transfer the compressive loads through bearing, thus minimizing the fasteners requirement. Splices are required at these locations to accommodate the changes in direction of the upper surface. Integral flanges are provided for the attachment of the bulkheads and ribs. The upper plate has been configured to concentrate the axial load in the forward and aft plate elements to some extent. It is easier to stabilize this portion of the upper cover because of the bulkhead spacing.

The intermediate section deviates from the baseline structure in that it is located below contour. This was accomplished to eliminate costs associated with part fabrication to a contoured surface. A separate, non-structural fairing is required to achieve fuselage contour.

### 2.1.2.3 $Y_F$ 932 Bulkhead

The forward bulkhead at $Y_F$ 932 is shown in Figure 2-12 (Drawing X7223750). It reacts shear loads and fuel pressures, and distributes the inboard-outboard loads from the wing sweep actuator. The bulkhead also reacts the vertical kick loads from the MLG drag fitting. The two web elements outboard of $X_F$ 39 consist of beta annealed 6AL-4V titanium reinforced with 5052 aluminum core. The Phase Ib design utilized laminated sheets of Beta "A" titanium adhesively bonded together. Test results, however, indicated the crack growth characteristics of Beta "C" sheet were inadequate. Aluminum was considered for this portion of the bulkhead web. However, the lower portion of the webs receive high tensile stresses from the lower plate and the fatigue

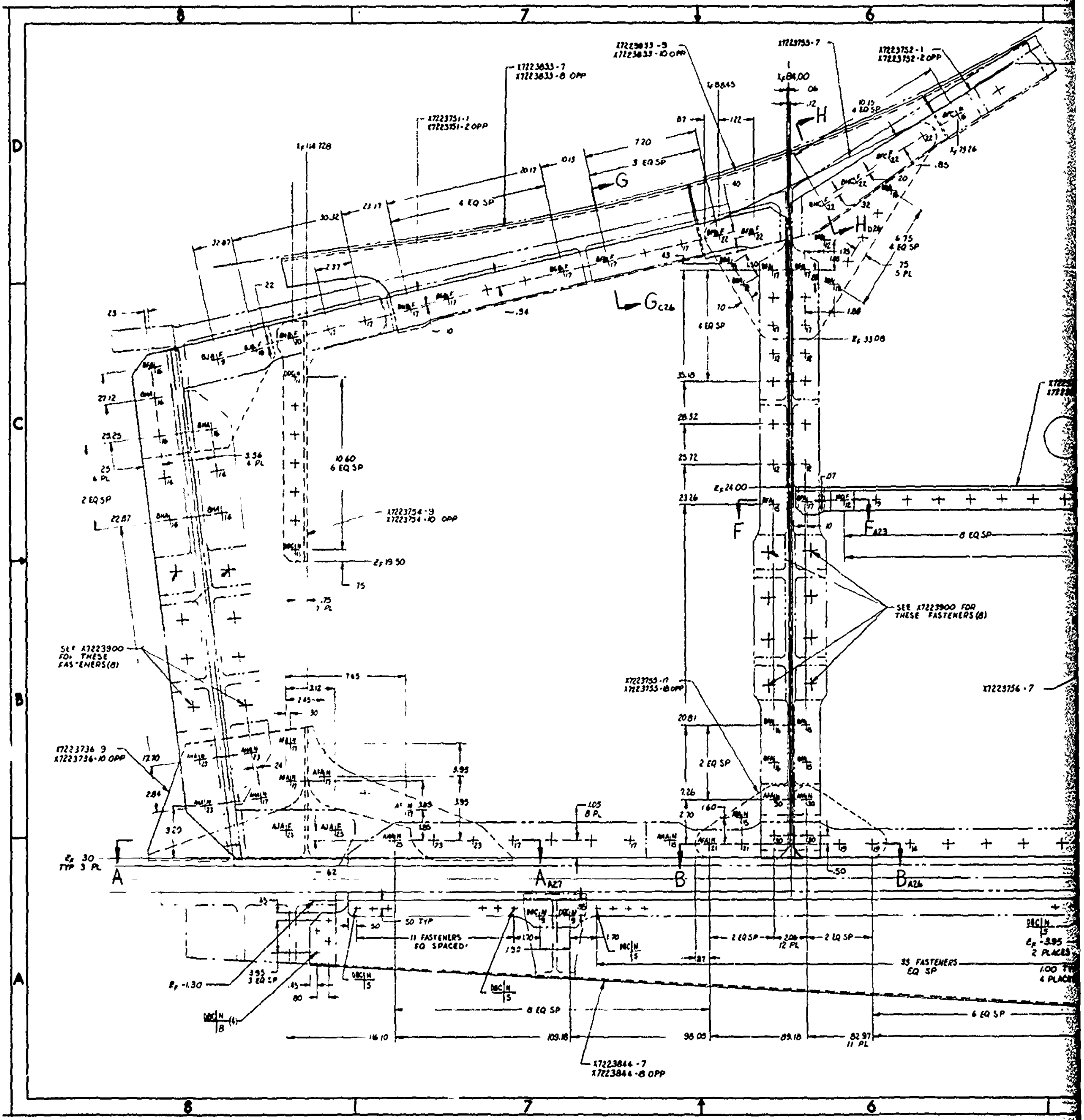

X7223833-9
X7223833-10 OPP
X7223755-7
X7223752-1
X7223752-2 OPP
X7223833-7
X7223833-8 OPP
X7223751-1
X7223751-2 OPP
X7223754-9
X7223754-10 OPP
SEE X7223900 FOR THESE FASTENERS (8)
X7223755-17
X7223755-18 OPP
X7223756-7
X7223736-9
X7223736-10 OPP
11 FASTENERS EQ SPACED
35 FASTENERS EQ SP
X7223844-7
X7223844-8 OPP

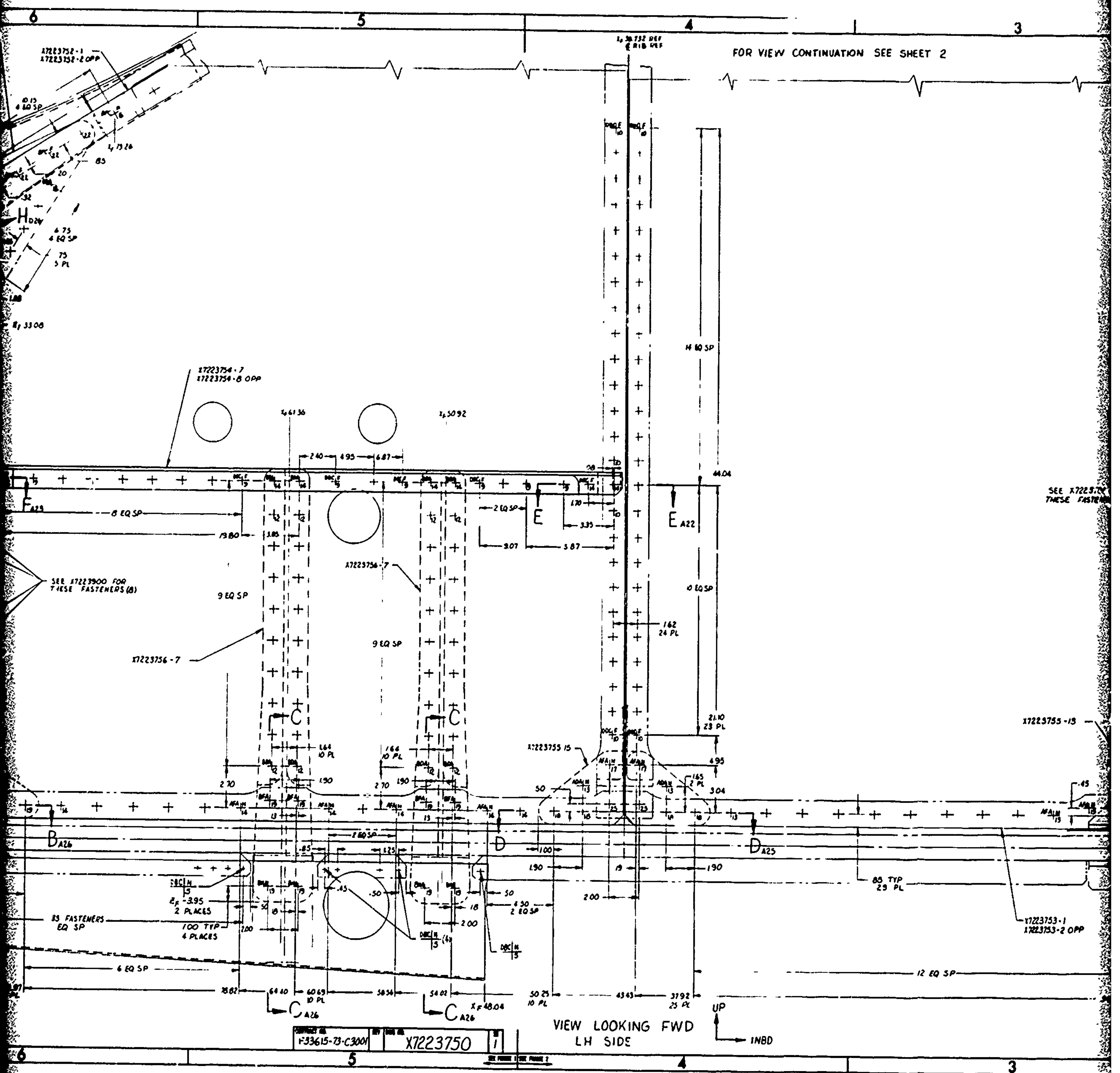
FOR VIEW CONTINUATION SEE SHEET 2
X7223752-1
X7223752-2 OPP
X7223754-7
X7223754-8 OPP
X7223756-7
X7223755-15
X7223755-13
X7223753-1
X7223753-2 OPP
SEE X7223900 FOR THESE FASTENERS (8)
8 EQ SP
9 EQ SP
14 EQ SP
10 EQ SP
12 EQ SP
6 EQ SP
2 EQ SP
162
24 PL
21.10
23 PL
85 TYP
25 PL
33 FASTENERS EQ SP
100 TYP
4 PLACES
2 PLACES
1.64
10 PL
44.04
4.95
3.04
19.80
3.07
3.87
3.35
2.70
1.90
2.00
50.25
10 PL
37.92
25 PL
60.69
10 PL
$X_F$ 48.04
E
$E_{A22}$
$F_{A23}$
$B_{A26}$
D
$D_{A25}$
C
$C_{A26}$
$H_{D24}$
UP
INBD
VIEW LOOKING FWD
LH SIDE
F33615-73-C3001
X7223750
1
6
5
4
3

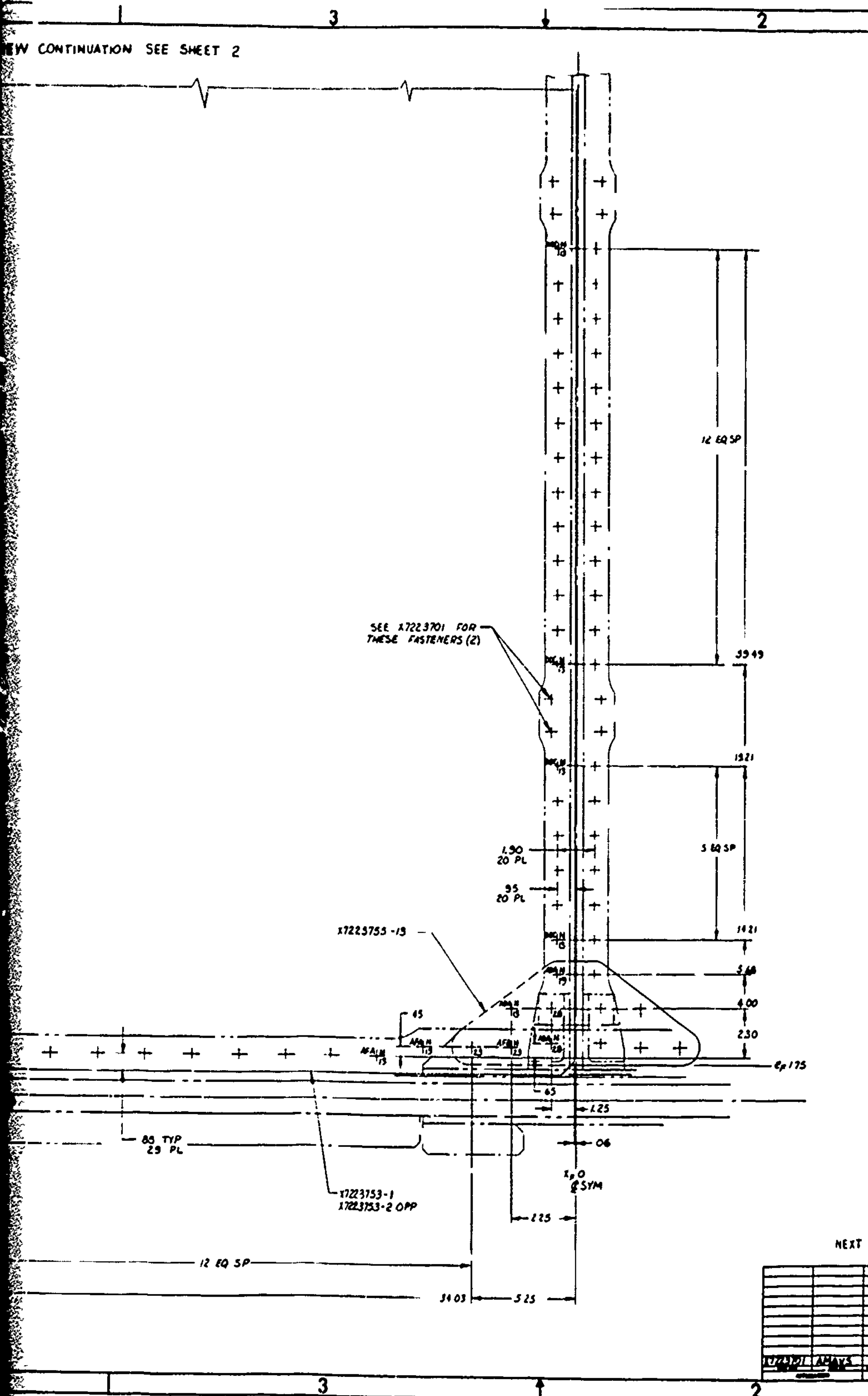


5. BOLT CODE.

BASIC CODE — HEAD LOCATION (N) NEAR SIDE (F) FAR SIDE — GRIP LENGTH DASH NO.

| BASIC CODE | HOLE DIA | BOLT | NUT 81755/ | WASHER UNDER HD | WASHER UNDER NUT | BOLT INSTL SPEC | TORQUE PER 81755/M016 |
|---|---|---|---|---|---|---|---|
| ADA | (1) | X7223999-6 | C389-6 | 81755/P511-10 | X7223986-6 | X7223993-6 | (2) |
| AFA | (1) | X7223999-8 | C389-8 | 81755/P511-16 | X7223986-8 | X7223993-8 | (2) |
| AHA | (1) | X7223999-10 | C389-10 | 81755/P511-22 | X7223986-10 | X7223993-10 | (2) |
| AJA | (1) | X7223999-12 | C389-12 | 81755/P511-24 | X7223986-12 | X7223993-12 | (2) |
| BDA | 3770 3746 | X7223996-6 | C077-6 | X7223992-6 | X7223994-6 | (2) | -6B |
| BFA | 5025 4996 | -8 | C077-8 | -8 | X7223994-8 | (2) | -8B |
| BFB | 5025 4996 | -8 | C356-8 C396-8B | -8 | X7223994-8 | (2) | -8B |
| BFC | 5025 4996 | -8 | C356-8 C396-8B | -8 | (2) | (2) | -8B |
| BGB | 5650 5617 | -9 | C356-9 C396-9B | -9 | X7223994-9 | (2) | -9B |
| BHA | 6275 6241 | -10 | C077-10 | -10 | X7223994-10 | (2) | -10B |
| BHB | 6275 6241 | -10 | C356-10 C396-10B | -10 | X7223994-10 | (2) | -10B |
| BHC | 6275 6241 | -10 | C356-10 C396-10B | -10 | (2) | (2) | -10B |
| BJB | 7525 7491 | X7223996-12 | C356-12 C396-12B | X7223992-12 | X7223994-12 | (2) | -12B |
| DBC | 2520 2496 | 81755/C020-8 | C2950-8 | X7223981-8 | (2) | (2) | -4A |
| DDC | 3770 3746 | 81755/C020-12 | C2950-12 | X7223981-12 | (2) | (2) | -6A |
| | | | | | | | |

(1) SEE BOLT INSTL SPEC
(2) NOT APPLICABLE

4. SEALING MATERIALS AND METHODS OF APPLICATION PER X7224196.
3. INSTALL ALL STRAIGHT SHANK FASTENERS WITH -7 GENERAL SEALANT.
2. APPLY -7 GENERAL SEALANT TO ALL FAYING SURFACES.
1. DIMENSIONS AND TOLERANCES PER USASI Y14.5.

NOTES (EXCEPT AS SHOWN)

Figure 2-12 (Sheet 1)

SEE SEPARATE PARTS LIST

NEXT SECTION LETTER: L

SEE PL

BULKHEAD INSTL-
WING CARRYTHROUGH,
$Y_F$ 932.00

07878 X7223750

X7223701

1 OF 2

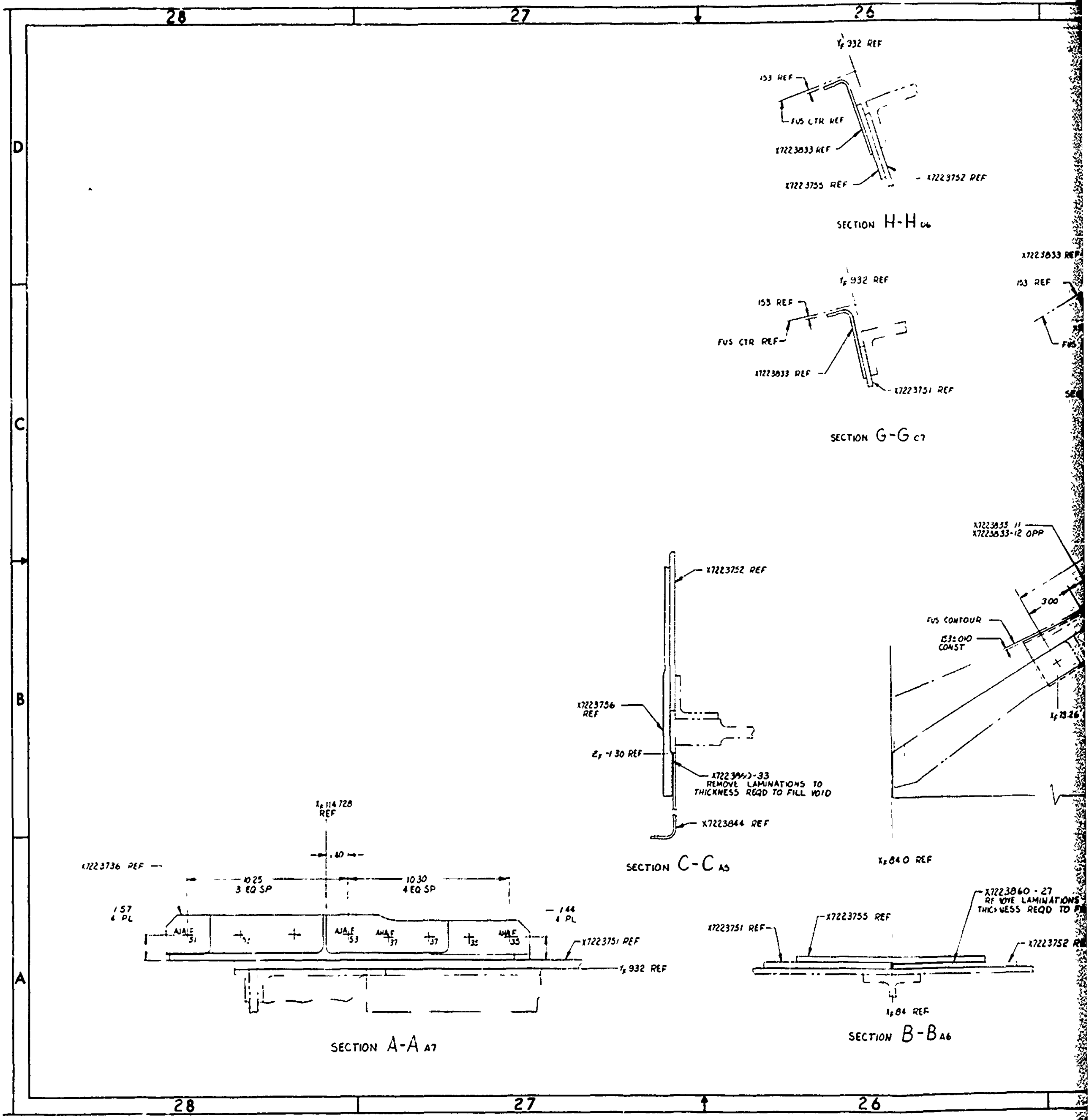

28
27
26
D
C
B
A
$Y_F$ 932 REF
153 REF
FUS CTR REF
X7223833 REF
X7223755 REF
X7223752 REF
SECTION H-H D6
$Y_F$ 932 REF
153 REF
FUS CTR REF
X7223833 REF
X7223751 REF
SECTION G-G C7
X7223833 REF
153 REF
X7223752 REF
X7223756 REF
$Z_F$ -1 30 REF
REMOVE LAMINATIONS TO THICKNESS REQD TO FILL VOID
X7223844 REF
SECTION C-C A5
X7223833-11
X7223833-12 OPP
300
FUS CONTOUR
153±.010 CONST
$X_F$ 84 0 REF
$X_F$ 114 728 REF
.40
X7223736 REF
10 25 3 EQ SP
10 30 4 EQ SP
1 57 4 PL
1 44 4 PL
X7223751 REF
$Y_F$ 932 REF
SECTION A-A A7
X7223860 - 27
X7223751 REF
X7223755 REF
X7223752 REF
$Y_F$ 84 REF
SECTION B-B A6

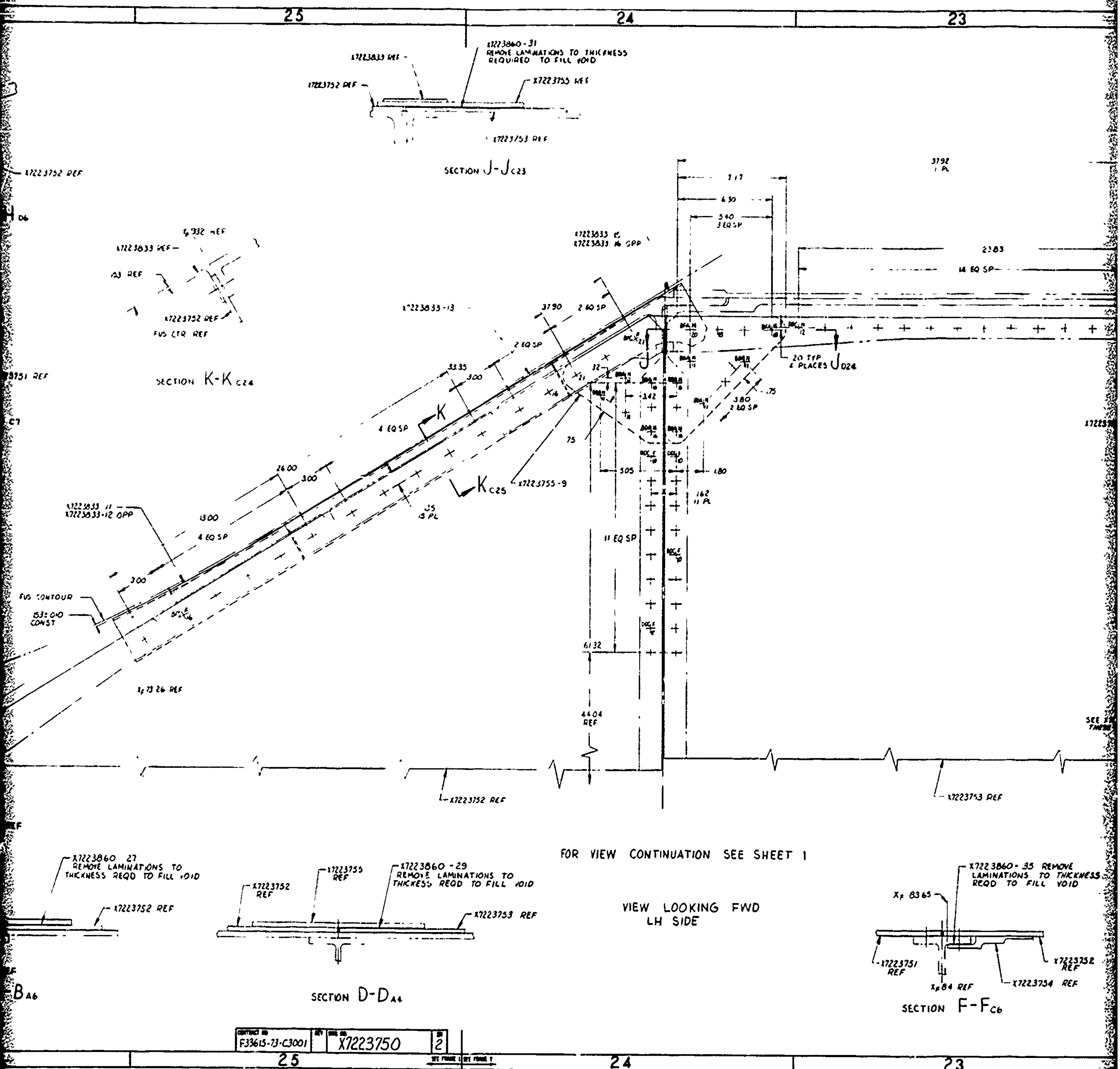

25
24
23
X7223860-31 REMOVE LAMINATIONS TO THICKNESS REQUIRED TO FILL VOID
X7223833 REF
X7223752 REF
X7223755 REF
X7223753 REF
SECTION J-J C23
X7223752 REF
X7223833 REF
SECTION K-K C24
X7223833-13
X7223755-9
X7223833-11
X7223833-12 OPP
FUS CONTOUR
4 EQ SP
2 EQ SP
3 EQ SP
14 EQ SP
11 EQ SP
20 TYP 4 PLACES
J D24
K C25
X7223752 REF
X7223753 REF
FOR VIEW CONTINUATION SEE SHEET 1
X7223860-27 REMOVE LAMINATIONS TO THICKNESS REQD TO FILL VOID
X7223752 REF
X7223755 REF
X7223860-29 REMOVE LAMINATIONS TO THICKESS REQD TO FILL VOID
X7223753 REF
SECTION D-D A4
VIEW LOOKING FWD LH SIDE
X7223860-35 REMOVE LAMINATIONS TO THICKNESS REQD TO FILL VOID
X7223751 REF
X7223752 REF
X7223754 REF
SECTION F-F C6
B A6
F33615-73-C3001
X7223750
2

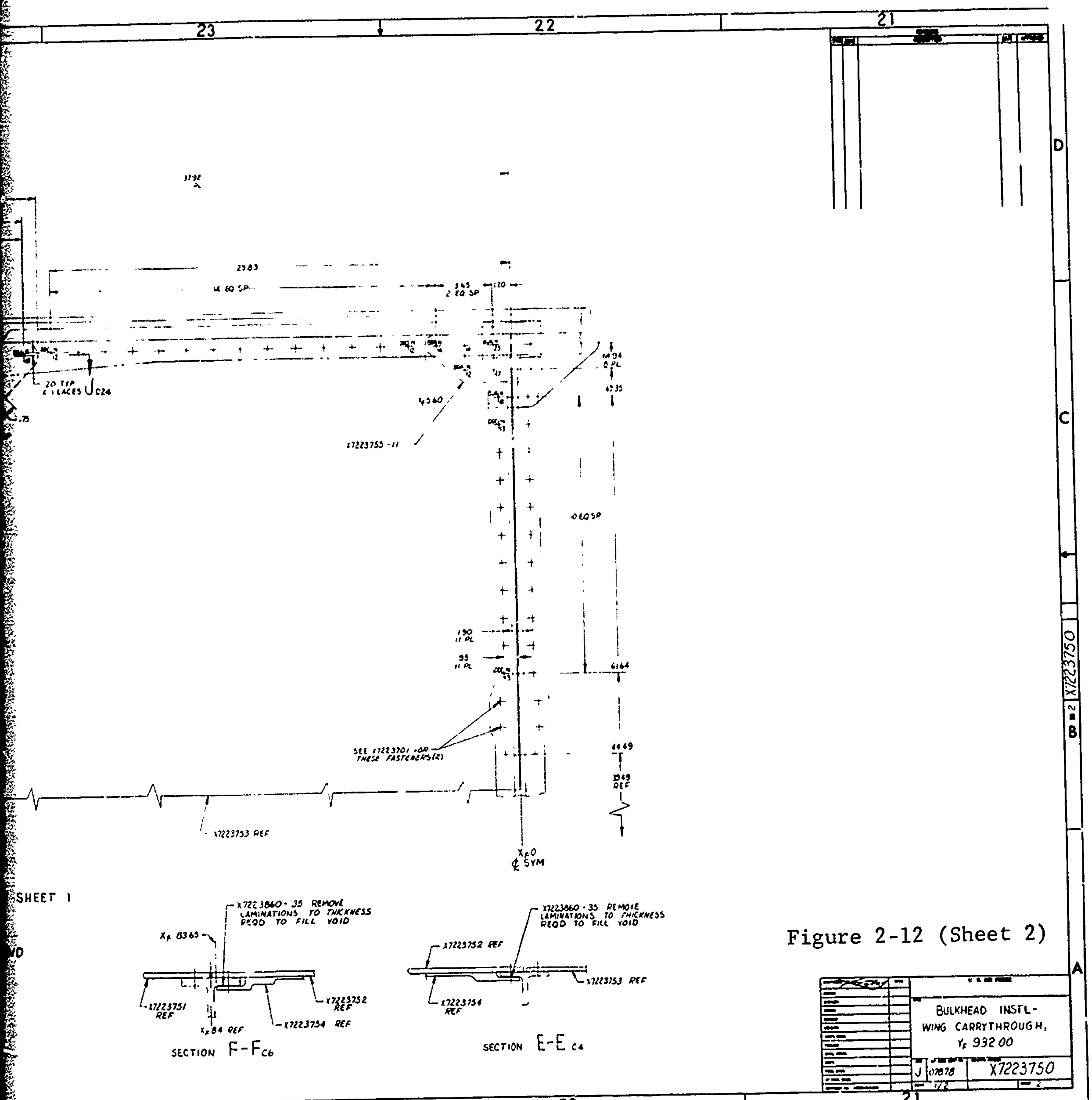


Figure 2-12 (Sheet 2)

allowables for aluminum would not permit its use in conjunction with the titanium lower plate.

The panel inboard of $Y_F$ 947 experiences relatively low load intensity, permitting the use of lower cost aluminum construction. 2024 aluminum sheet reinforced with 5052 core is used for this panel. This panel interfaces with the weapons bay wall and the rotary launcher fitting.

### 2.1.2.4 Internal Bulkheads

The internal bulkheads, located at $Y_F$ 947 and $Y_F$ 977, have been changed to "arched" configurations as shown in Figures 2-13 and 2-14 (drawing X7223760 and X7223770 respectively). The arched concept permits the use of lower cost aluminum construction by deleting the strain compatibility requirement with the titanium lower plate. Fastener reduction is also accomplished in the fatigue critical lower plate by eliminating the attachment of these bulkheads. The internal beam and its necessary attachments through the lower plate are still required, however, at $Y_F$ 947 to support the MLG drag brace fitting.

### 2.1.2.5 $Y_F$ 992 Bulkhead

The aft bulkhead is shown in Figure 2-15 (Drawing X7223780) and is similar to the $Y_F$ 932 bulkhead in type of material and fabrication. The only exception is the panel inboard of $X_F$39. Due to the higher axial stresses near the lower surface and the loads introduced by the MLG side load fitting, titanium was required for this panel. In addition to the MLG side load fitting, support is also provided to the MLG trunion fittings at $X_F$72 and $X_F$95.5. Access into the box structure is also provided in this bulkhead.

### 2.1.2.6 Outboard Closure Rib

The outboard closure rib (drawing X7223820, Figure 2-16) is a fracture critical part designed to safe life requirements. The rib reacts torsional shear loads introduced by the pivot lugs, distributes the kick load from the wing sweep actuator attach fitting and resists fuel pressure loads. Beta annealed 6AL-4V titanium is used for the web and bolt-on fittings which distribute the actuator kick loads into the web. The web is reinforced with several bolt-on 7050 aluminum stiffeners.

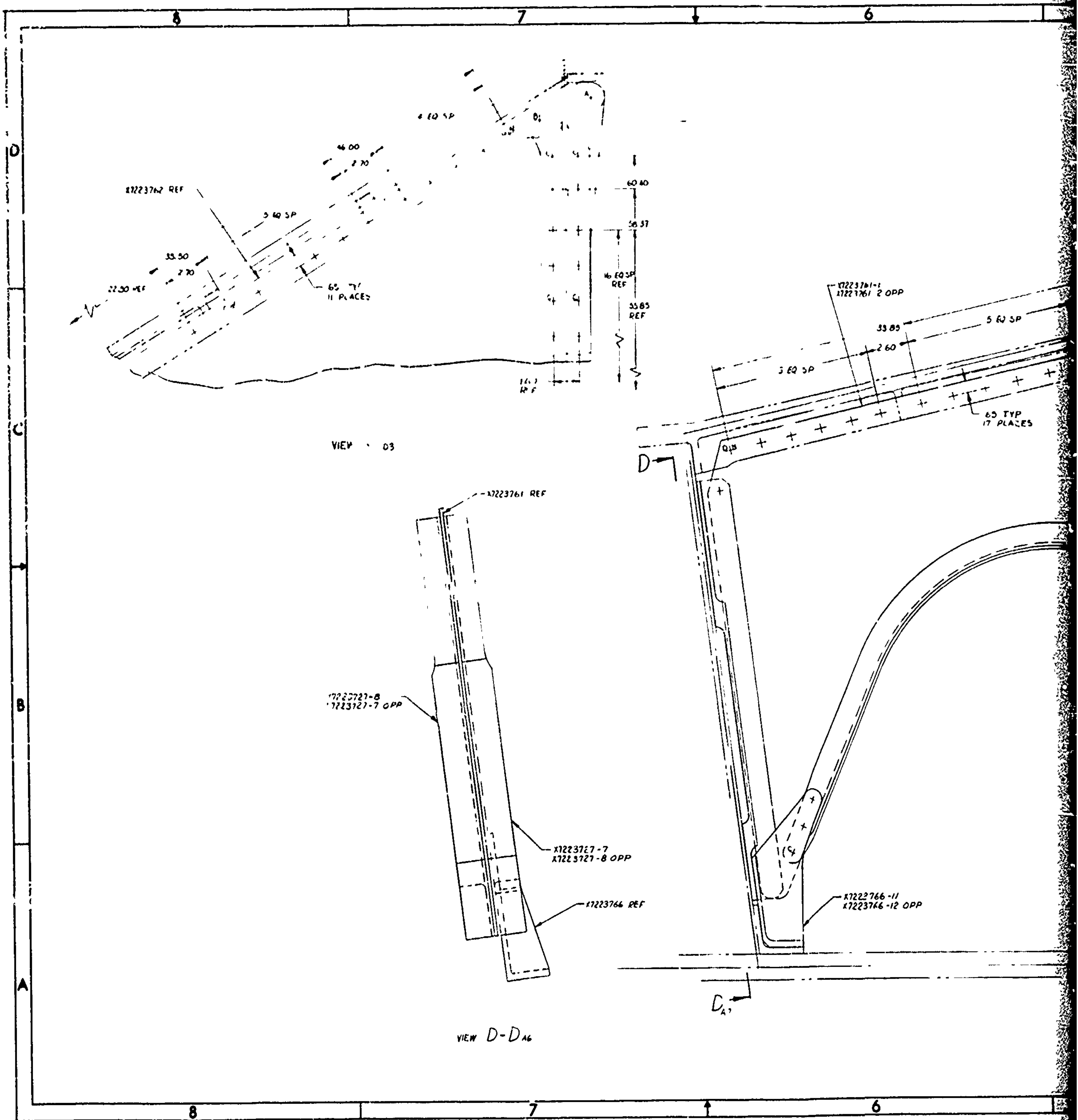
X7223762 REF
5 EQ SP
4 EQ SP
46.00
2.70
35.50
22.50 REF
.65 TYP
11 PLACES
60.60
56.37
16 EQ SP
REF
35.85
REF
VIEW
X7223761 REF
X7223727-8
X7223727-7 OPP
X7223727-7
X7223727-8 OPP
X7223766 REF
VIEW D-D A6
X7223761-1
X7223761-2 OPP
33.85
5 EQ SP
2.60
5 EQ SP
.65 TYP
17 PLACES
X7223766-11
X7223766-12 OPP

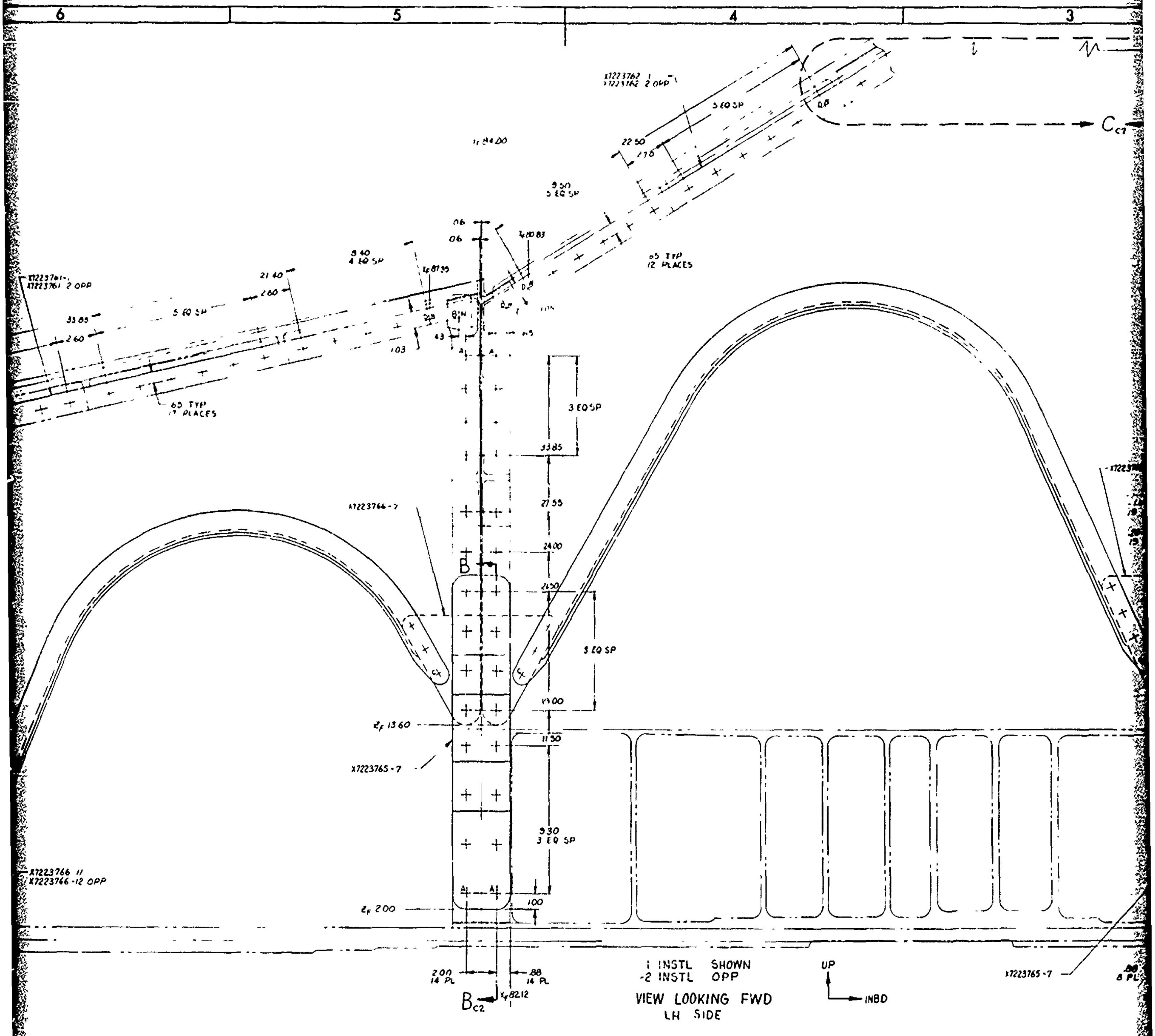


| CONTRACT NO. | REV | DWG NO | SH |
|---|---|---|---|
| F33615-73 C 3001 | | X7223760 | 1 |

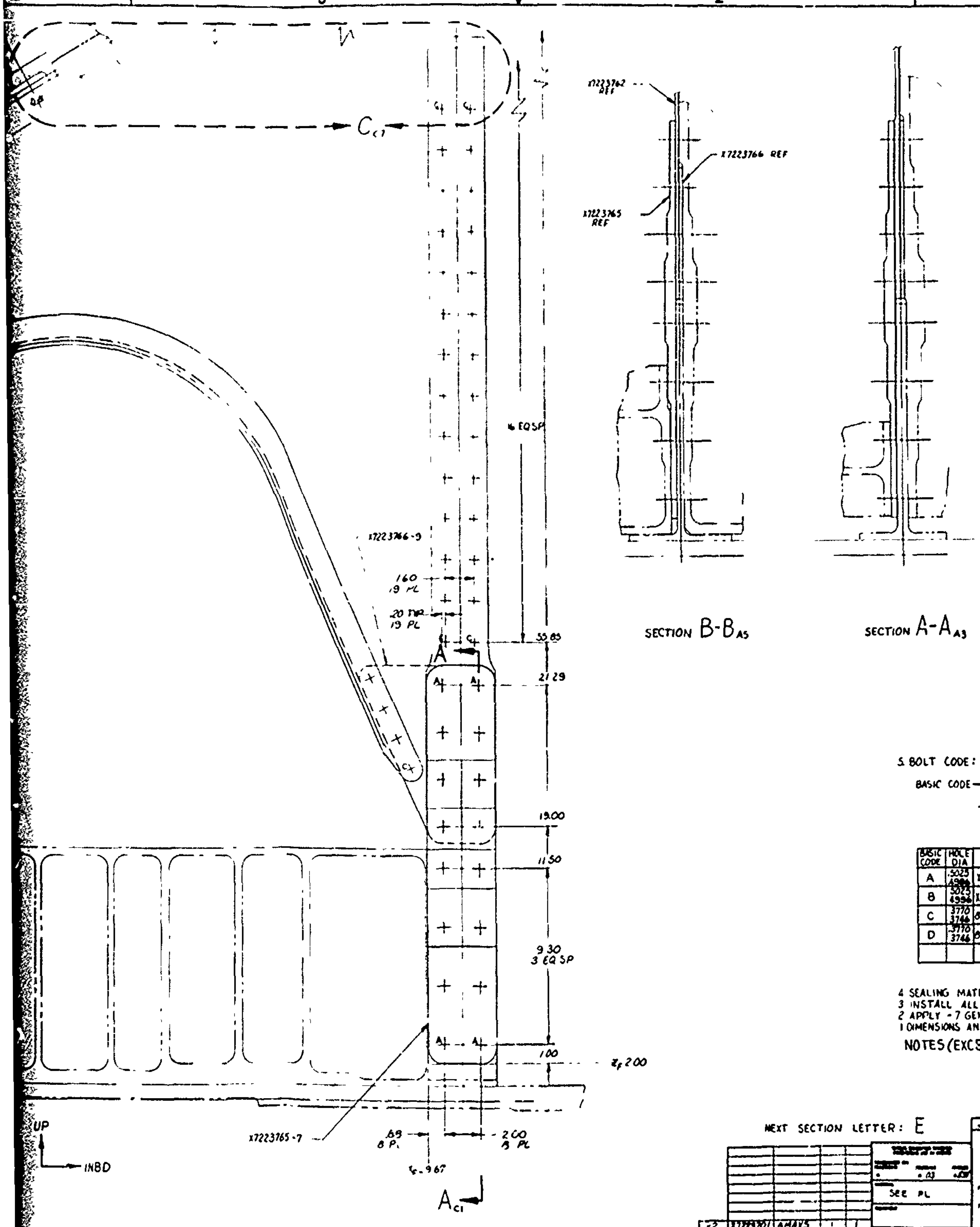


5 BOLT CODE:

BASIC CODE — HEAD LOCATION (N) NEAR SIDE (F) FAR SIDE — GRIP LENGTH DASH NO

| BASIC CODE | HOLE DIA | BOLT | NUT 81755/ | WASHER UNDER HD | WASHER UNDER NUT | TORQUE PER 81755/M016 |
|---|---|---|---|---|---|---|
| A | .5025 .4996 | X7223996-8 | C077-8 | X7223992-8 | X7223994-8 | -8B |
| B | .5025 .4996 | X7223996-8 | C396-8 C396-8B | X7223992-8 | | -8B |
| C | .3770 .3746 | 81755/C020-12 | C2950-12 | X7223991-12 | | -6A |
| D | .3770 .3746 | 81755/C020 12 | C396-6 C396-6B | X7223991-12 | | -6A |
| | | | | | | |

4 SEALING MATERIALS AND METHODS OF APPLICATION PER X7224196.
3 INSTALL ALL FASTENERS WITH -7 GENERAL SEALANT.
2 APPLY -7 GENERAL SEALANT TO ALL FAYING SURFACES.
1 DIMENSIONS AND TOLERANCES PER USASI Y14.5

NOTES (EXCEPT AS SHOWN)

Figure 2-13

SEE SEPARATE PARTS LIST

NEXT SECTION LETTER: E

SEE PL

BULKHEAD INSTL-
WING CARRYTHROUGH,
$Y_F$ 947.00

J 07878 X7223760

X7223760

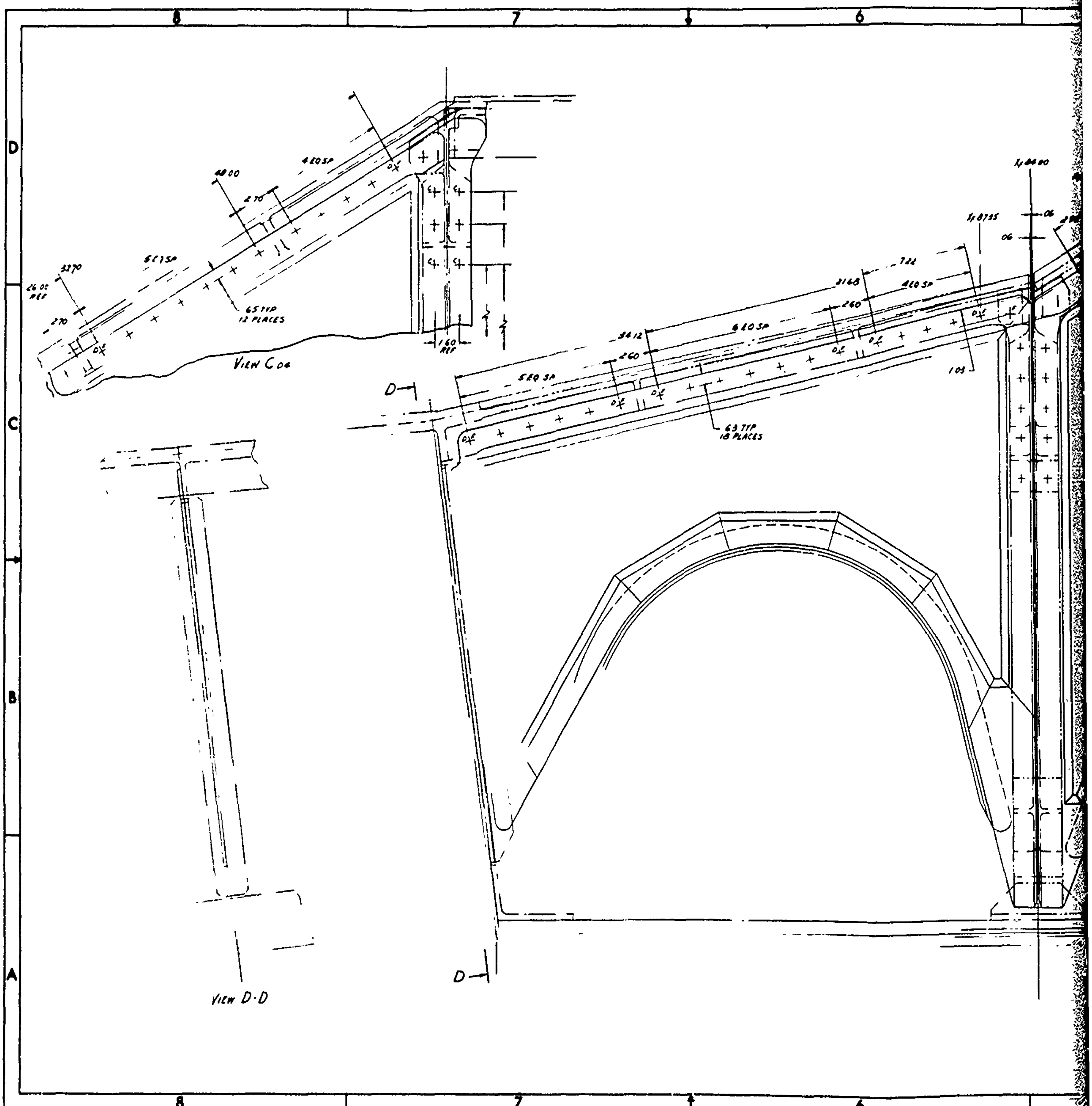
VIEW D-D
65 TYP
12 PLACES
63 TYP
18 PLACES
5 EQ SP
6 EQ SP
4 EQ SP
D
D

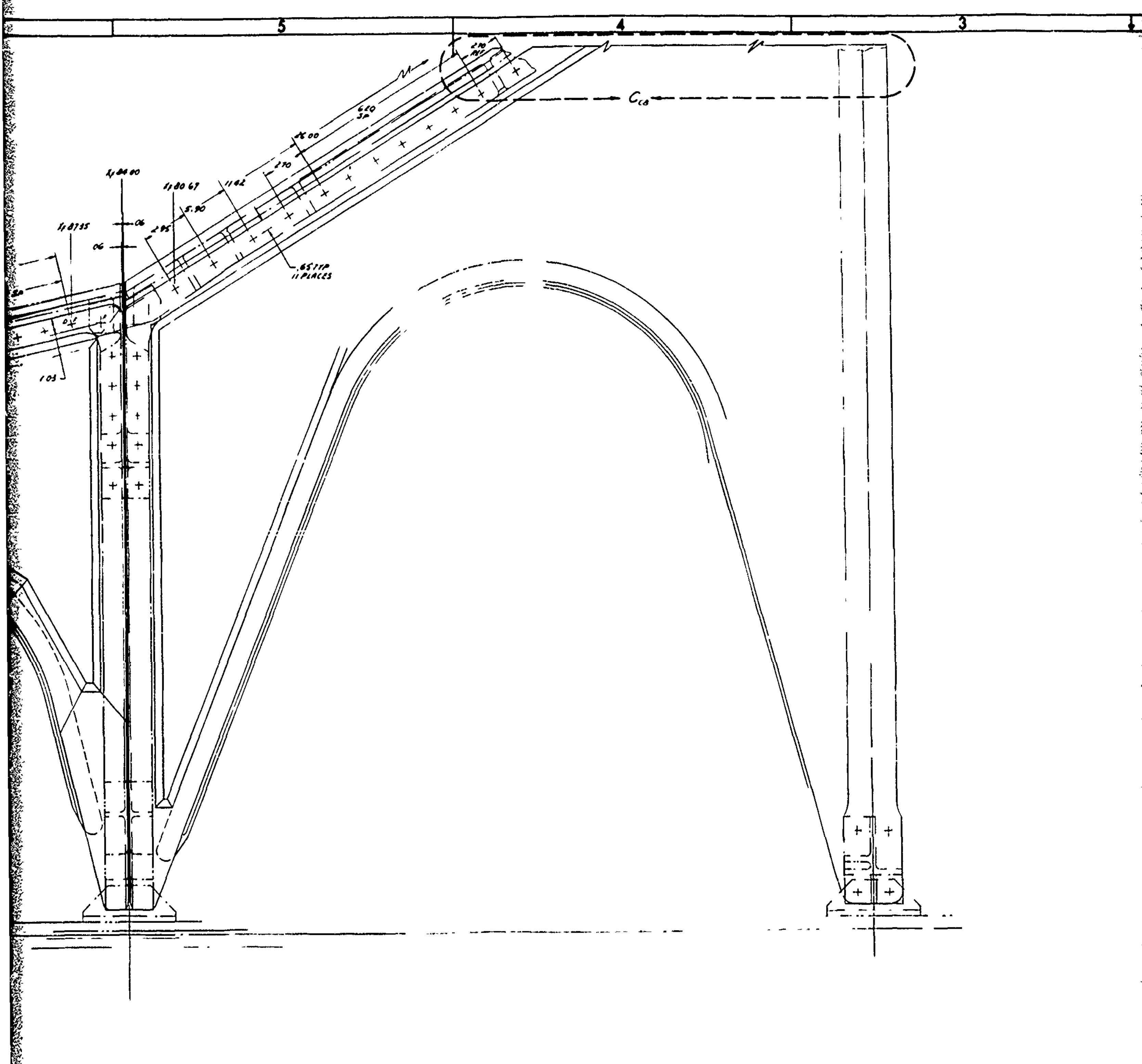

5
4
3
.65 TYP
11 PLACES
6 EQ SP

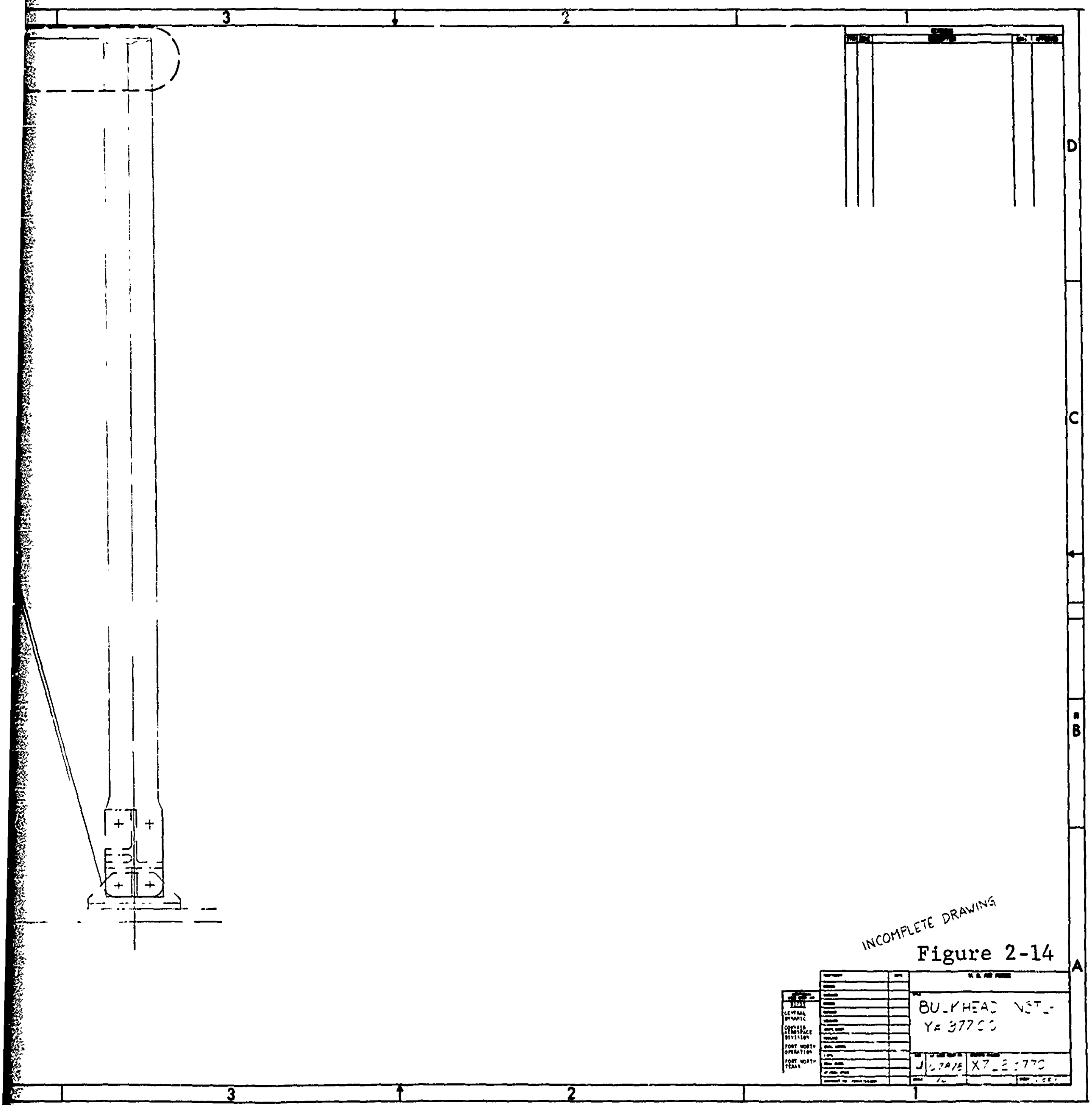

INCOMPLETE DRAWING
BULKHEAD
CONVAIR AEROSPACE DIVISION
FORT WORTH OPERATION
FORT WORTH TEXAS


Figure 2-14

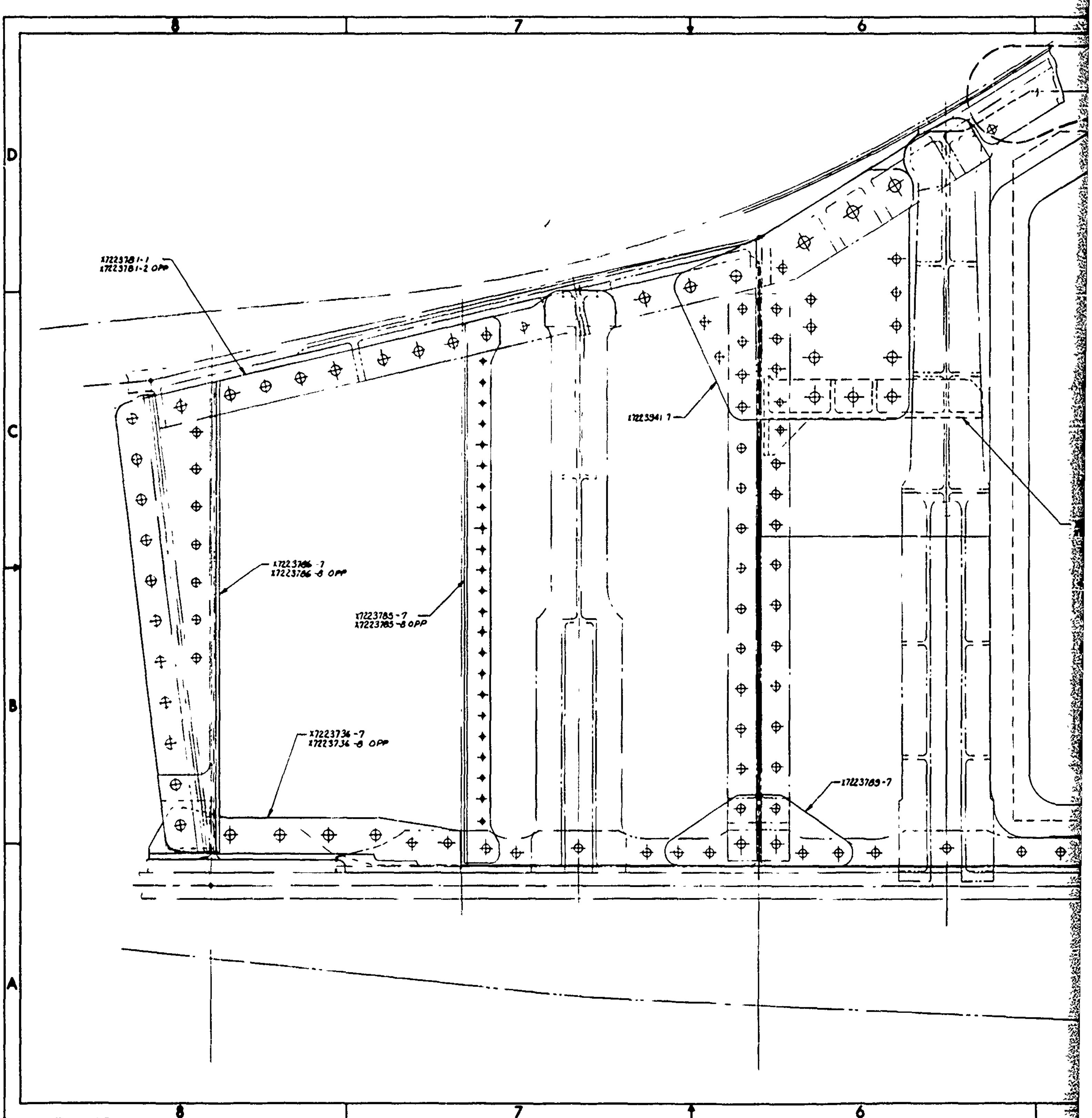

8
7
6
D
C
B
A
X7223781-1
X7223781-2 OPP
X7223786-7
X7223786-8 OPP
X7223785-7
X7223785-8 OPP
X7223734-7
X7223734-8 OPP
X7223941-7
X7223789-7

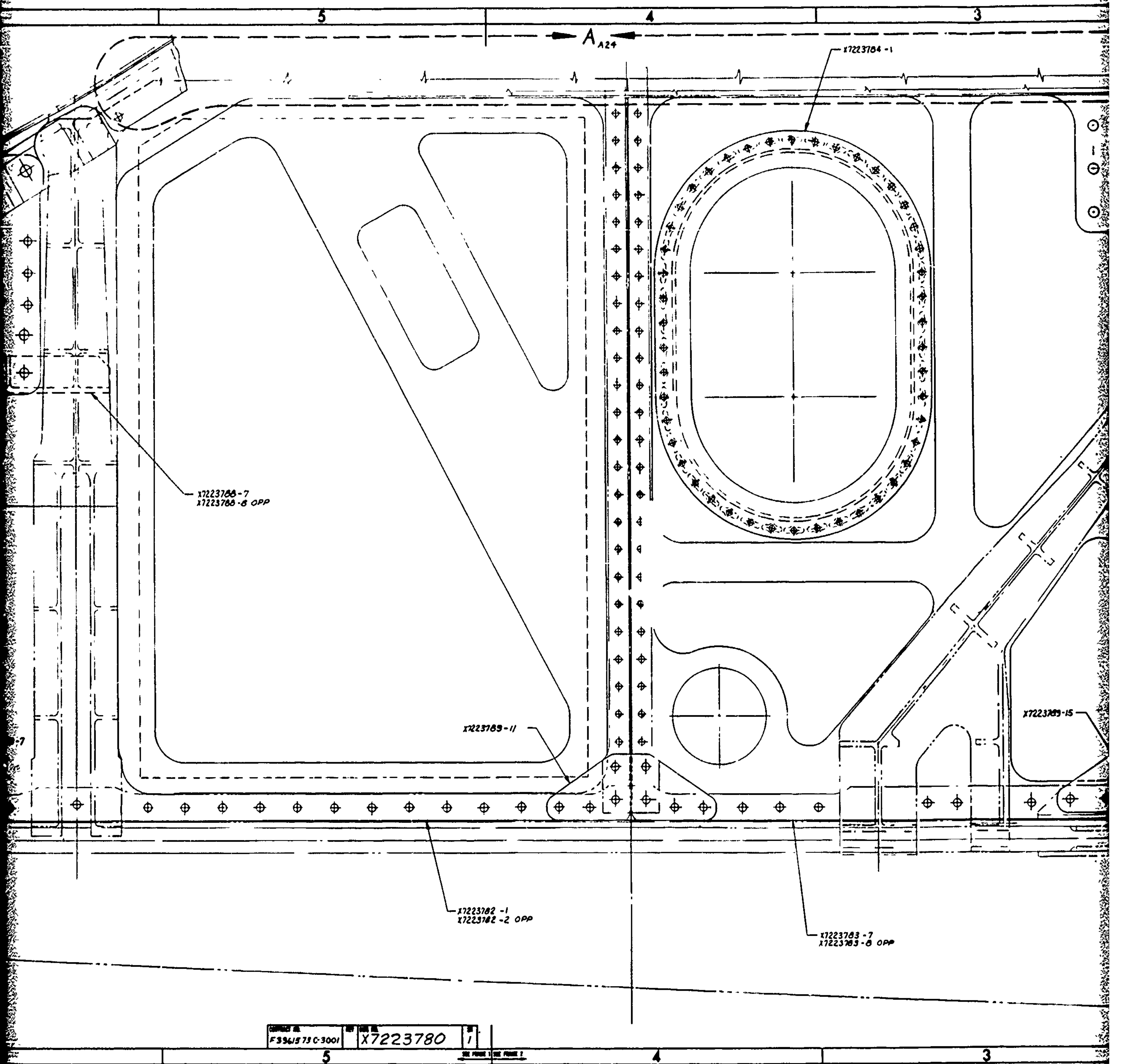
5
4
3
A A24
X7223784-1
X7223788-7
X7223788-8 OPP
X7223789-11
X7223789-15
X7223782-1
X7223782-2 OPP
X7223783-7
X7223783-8 OPP
F33615 73 C-3001
X7223780
1
5
4
3

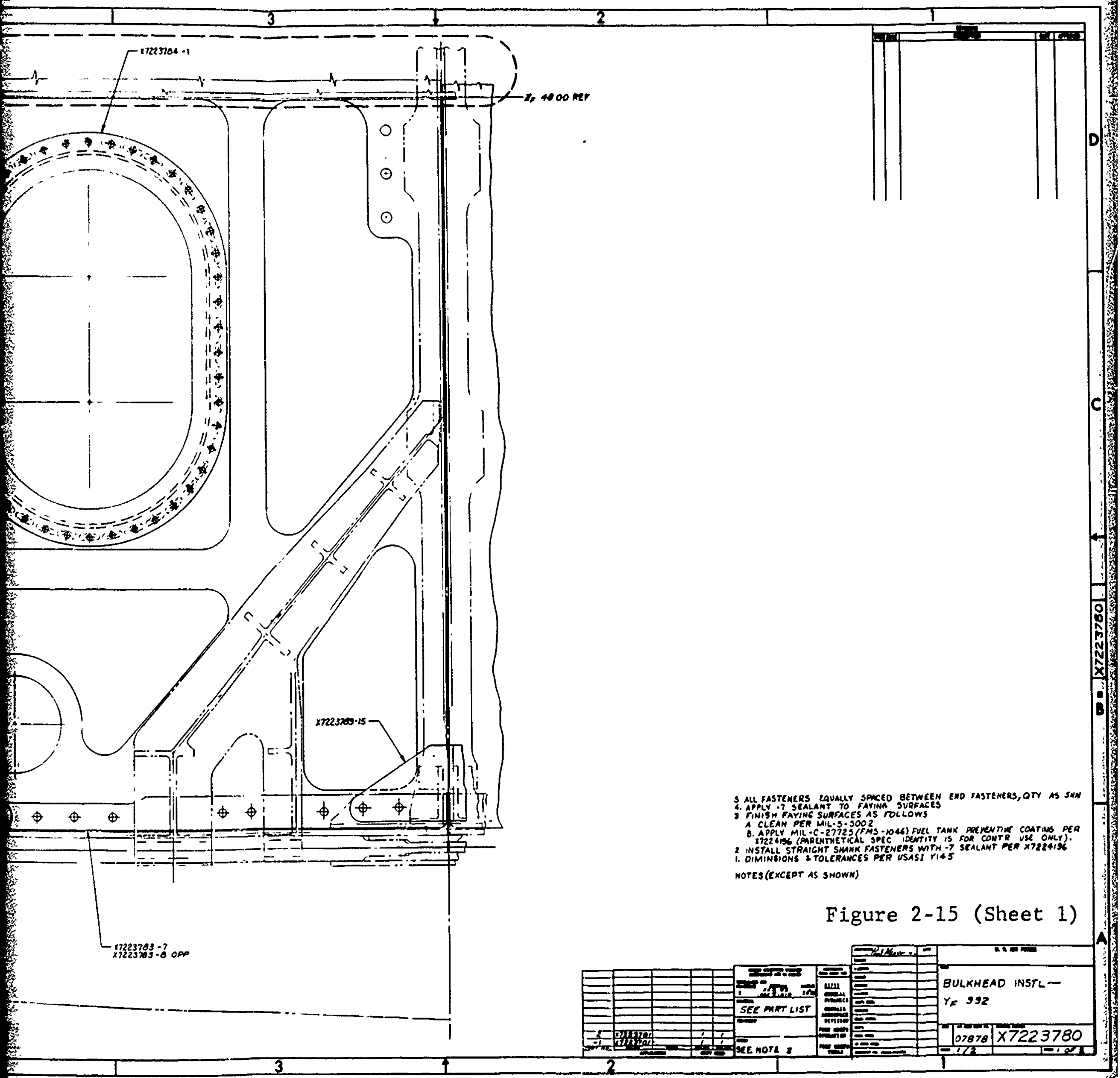


Figure 2-15 (Sheet 1)

28 27 26

D

C

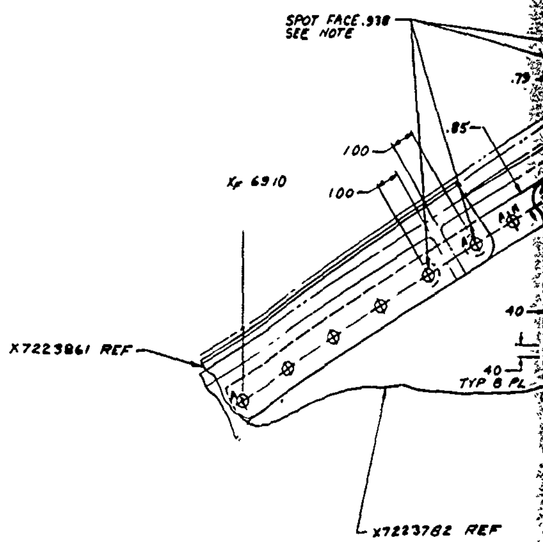


B

A

28 27 26

| 25 | 24 | 23 |
|---|---|---|

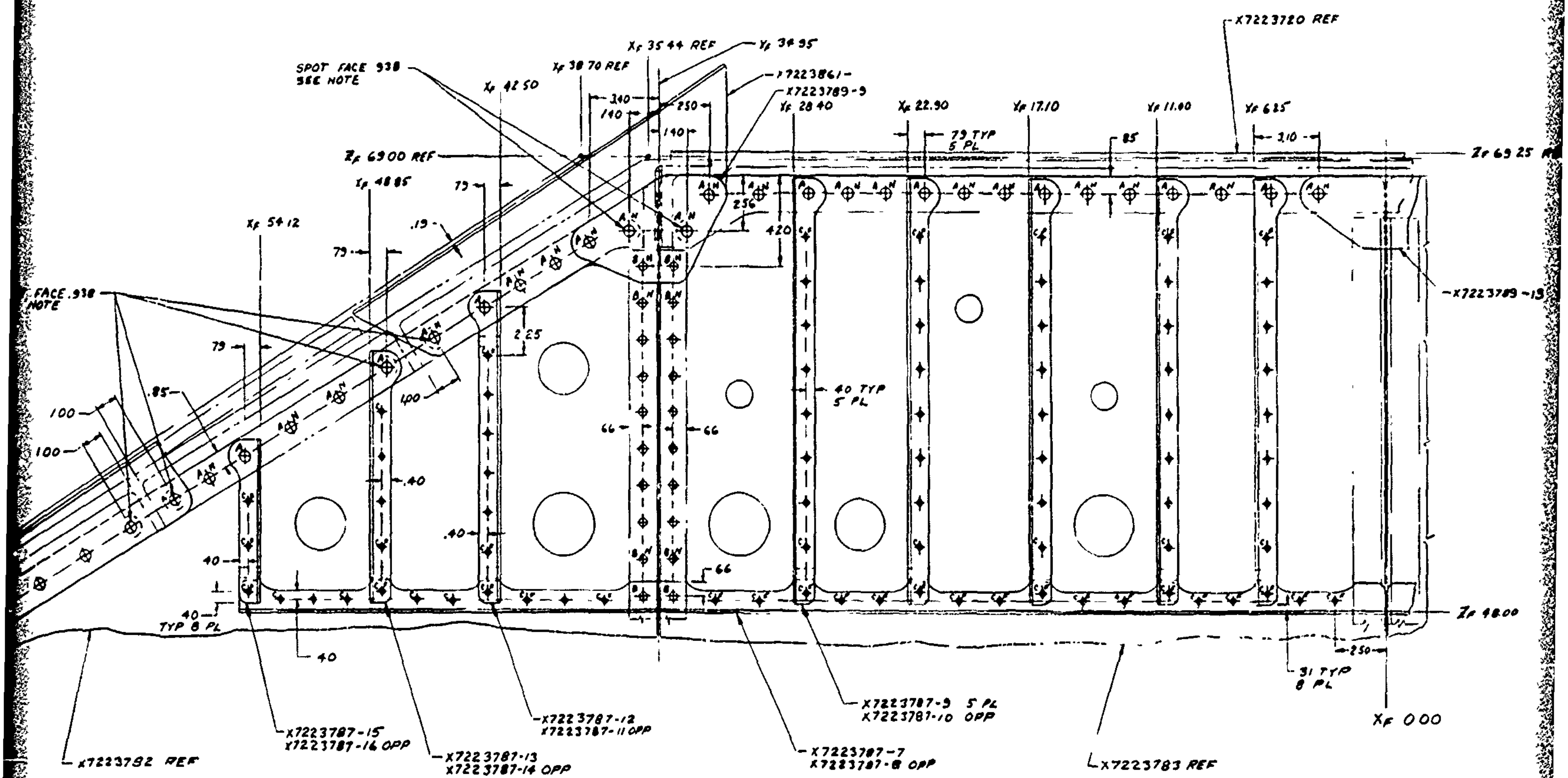


VIEW A

| CONTRACT NO. | DWG NO. | |
|---|---|---|
| F33615-73 C-3001 | X7223780 | E |

| 25 | 24 | 23 |
|---|---|---|

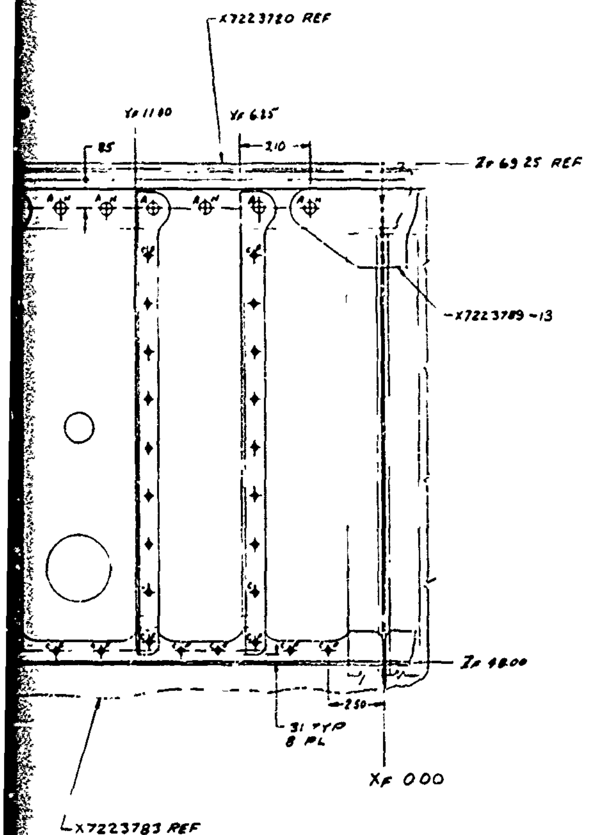


Figure 2-15 (Sheet 2)

C7878 X7223780

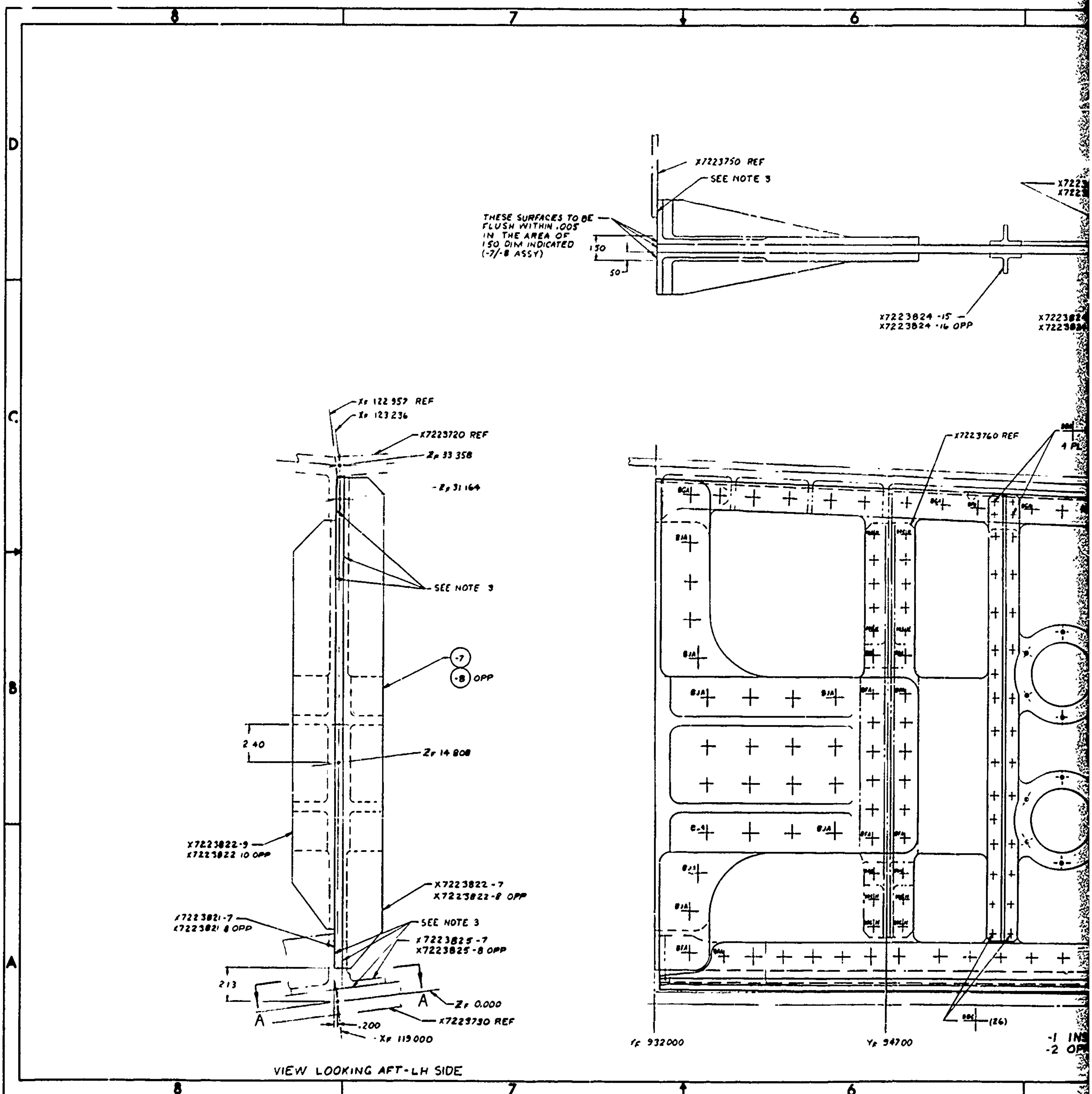
8
7
6
D
C
B
A
X7223750 REF
SEE NOTE 3
THESE SURFACES TO BE FLUSH WITHIN .005 IN THE AREA OF 150 DIM INDICATED (-7/-8 ASSY)
150
50
X7223824 -15
X7223824 -16 OPP
XF 122 957 REF
XF 123 236
X7223720 REF
ZF 33 358
ZF 31 164
SEE NOTE 3
-7
-8 OPP
2 40
ZF 14 808
X7223822-9
X7223822 10 OPP
X7223822 -7
X7223822 -8 OPP
X7223821-7
X7223821 8 OPP
SEE NOTE 3
X7223825 -7
X7223825 -8 OPP
213
A
A
ZF 0.000
X7223730 REF
.200
XF 119000
VIEW LOOKING AFT-LH SIDE
X7223760 REF
(26)
YF 932000
YF 94700
-1 INS
-2 OP

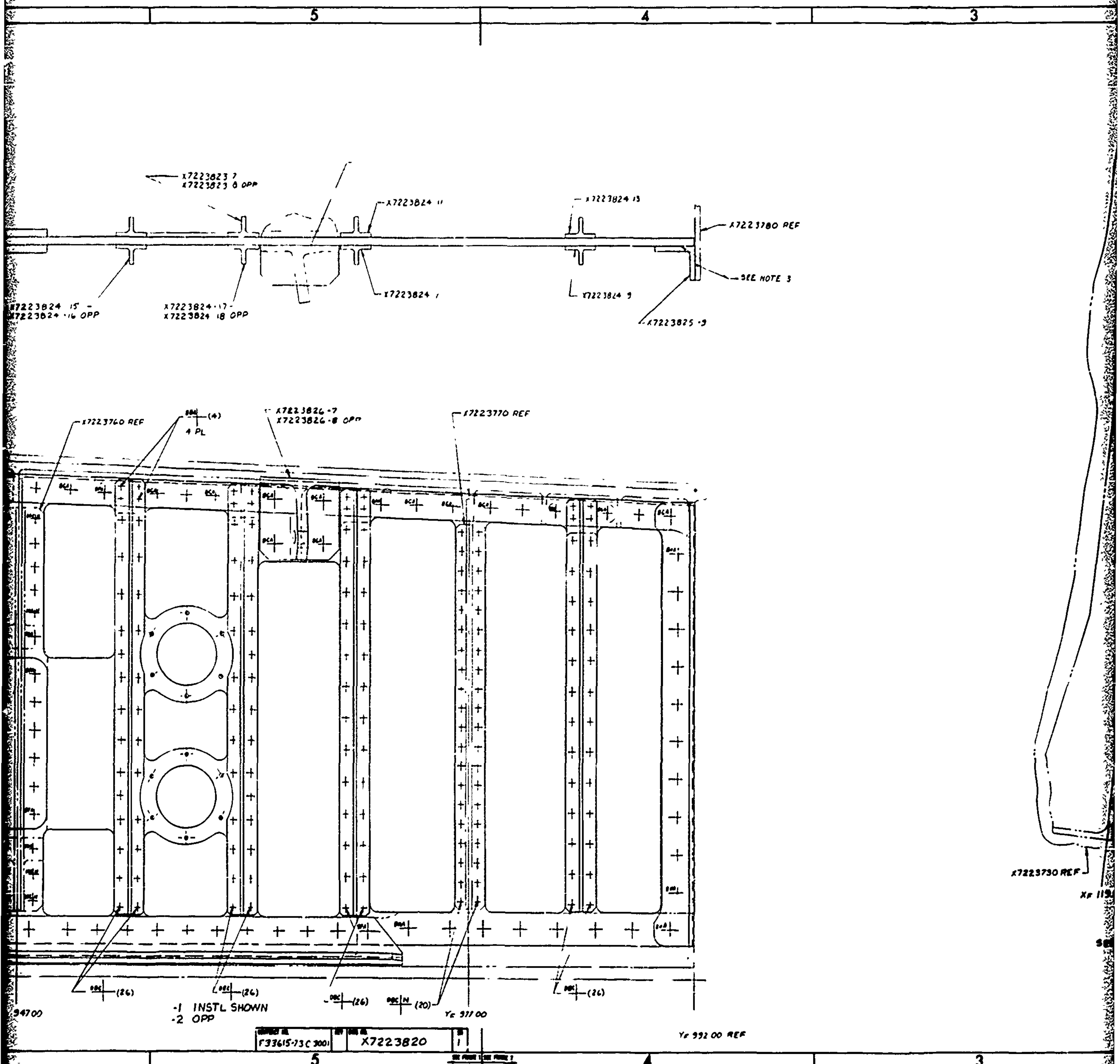
5
4
3
X7223823 7
X7223823 8 OPP
X7223824 11
X7223824 13
X7223780 REF
SEE NOTE 3
X7223824 15
X7223824 16 OPP
X7223824 17
X7223824 18 OPP
X7223824 1
X7223824 9
X7223825 5
X7223760 REF
4 PL
X7223826-7
X7223826-8 OPP
X7223770 REF
X7223730 REF
(26)
(20)
-1 INSTL SHOWN
-2 OPP
94700
Yr 971 00
Yr 992 00 REF
F33615-73C 3001
X7223820

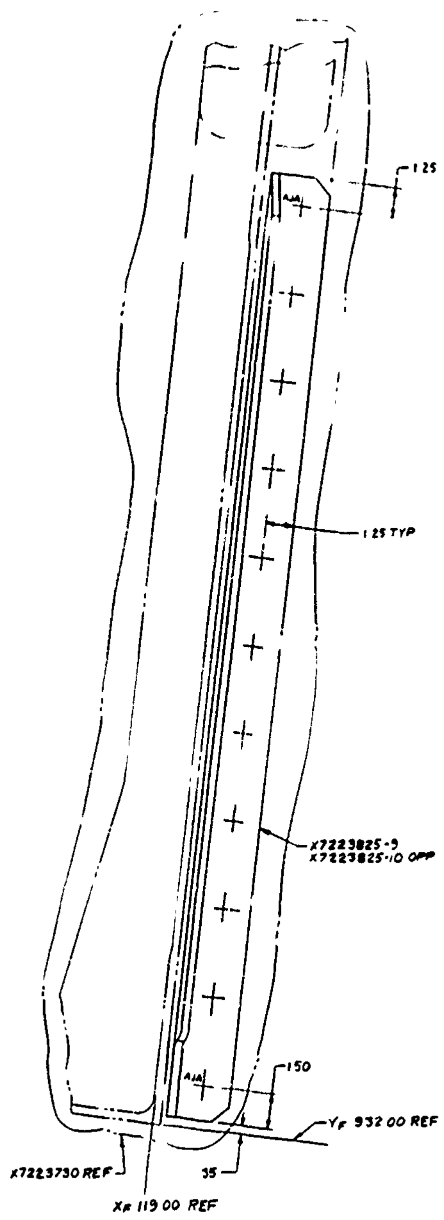


SECTION A-A

6 FASTENER CODE

BASIC CODE
HEAD LOCATION (N) NEAR (F) FAR
GRIP LENGTH DASH NO

| BASIC CODE | HOLE DIA | BOLT OR PIN | NUT | WASHER HEAD SIDE | WASHER NUT SIDE | TORQUE IN-LB | INSTL SPEC |
|---|---|---|---|---|---|---|---|
| AJA | △ | X7223999-12 ◇ | B1755/C389-12 | B1755/P611 24 | X7223986-12 | △ | X7223993 |
| BBA | .2520 .2496 | X7223996-4-◇ | B1755/C077-4 | X7223992-4 | X7223994-4 | 100 50 | NONE |
| BDA | .3770 .3746 | X7223996-6-◇ | B1755/C077 6 | X7223992-6 | X7223994-6 | 390 160 | NONE |
| BFA | .5025 .4996 | X7223996-8 ◇ | B1755/C077 8 | X7223992-8 | X7223994-8 | 1100 480 | NONE |
| BGA | .5650 .5617 | X7223996-9-◇ | B1755/C077-9 | X7223992-9 | X7223994-9 | 1600 800 | NONE |
| BHA | .6275 .6241 | X7223996-10-◇ | B1755/C077 10 | X7223992-10 | X7223994 10 | 2400 1100 | NONE |
| BJA | .7525 .7491 | X7223996-12-◇ | B1755/C077-12 | X7223992-12 | X7223994 12 | 5000 2300 | NONE |
| DBC | .2520 .2496 | B1755/C020-8-◇ | B1755/2950 8 | X7223991-8 | NONE | 60 30 | NONE |
| DDC | .3770 .3746 | B1755/C020-12-◇ | B1755/2950-12 | X7223991-12 | NONE | 240 [illegible] | NONE |
| | | | | | | | |
| | | | | | | | |

△ SEE INSTL SPEC
◇ DENOTES GRIP DASH NO

5 ALL FASTENERS EQUALLY SPACED BETWEEN END FASTENERS, QTY AS SHOWN
4 APPLY -9 SEALANT TO FAYING SURFACES
3 FINISH FAYING SURFACES AS FOLLOWS:
A CLEAN PER MIL-S-5002
B APPLY MIL-C-27725 (FMS 1046) FUEL TANK PREVENTIVE COATING PER X7224196 (PARENTHETICAL SPEC IDENTY IS FOR CONTR USE ONLY)
2 INSTALL STRAIGHT SHANK FASTENERS WITH -9 SEALANT PER X7224196
1 DIMENSIONS & TOLERANCES PER ASASI Y14.5

NOTES (EXCEPT AS SHOWN)

Figure 2-16

NEXT SECT LTR B

U.S. AIR FORCE

GENERAL DYNAMICS CONVAIR AEROSPACE DIVISION FORT WORTH TEXAS

RIB INSTL-CLOSURE, XF 119, CANTED

E 07878 X7223820

-2 X7223701 AMAV5
-1 X7223701 AMAV5

### 2 1.2.7 Outboard Intermediate Rib

The outboard intermediate rib at $X_F84$ is shown in the box assembly drawing, X7223701, Figure 2-17. It is designed to react a combination of torsional shear loads, fuel slosh loads, kick loads due to the directional change of the upper plate, and the wing sweep actuator fitting load. This rib is a four element component configured to provide adequate access into the outboard portion of the box and to allow adequate fuel flow.

Aluminum construction satisfies the structural requirements of the rib and provides the minimum fabrication and material cost. The upper and lower center beams and the forward panel are integrally machined from 7050 plate. The aft panel is a sandwich panel consisting of a one-piece 7050 aluminum frame, 2024 aluminum face sheets and 5052 aluminum core.

### 2.1.2.8 Inboard Intermediate Rib

The inboard intermediate rib is also shown on the assembly drawing X7223701, Figure 2-17. The rib is located on the break of the upper cover (approximately $X_F38$) to react the resulting kick loads. In addition, the ribs experiences fuel slosh loads and secondary shear loads. The internal bulkheads terminate here, their load being transferred into the rib for redistribution. The rib is a four element component configured to provide adequate access into the outer portion of the box structure and to allow fuel flow.

The forward and aft sections are sandwich panels with 7050 aluminum slug type edge members and 2024 aluminum face sheets. The vertical attaching flanges are integral with the slug edge members. The upper and lower beams are integrally machined from 7050 aluminum plate.

### 2.1.2.9 Centerline Rib

The centerline rib is also shown on the assembly drawing, X7223701, Figure 2-17. This rib divides the left and right hand fuel tanks and, in addition to this fuel pressure loading, reaction is provided for the weapons launcher loads and kick loads from the MLG side brace fitting. The rib consists of an aluminum sandwich panel with 7050 slug type edge members. The forward and aft edge members are integrally machined with the attach flanges at $Y_F932$ and $Y_F992$. The skins are 2024 aluminum.

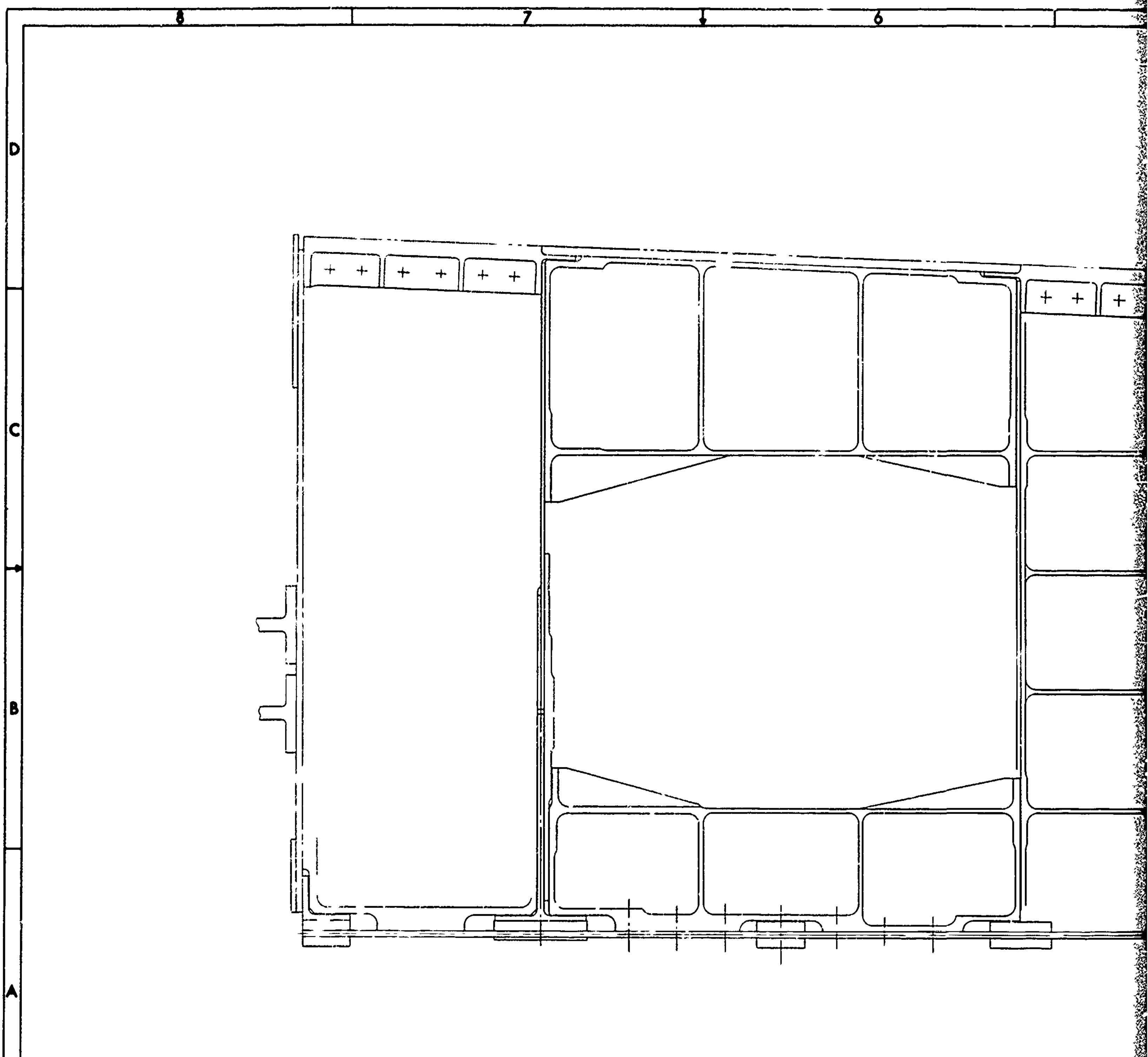

8
7
6
D
C
B
A

5 4 3

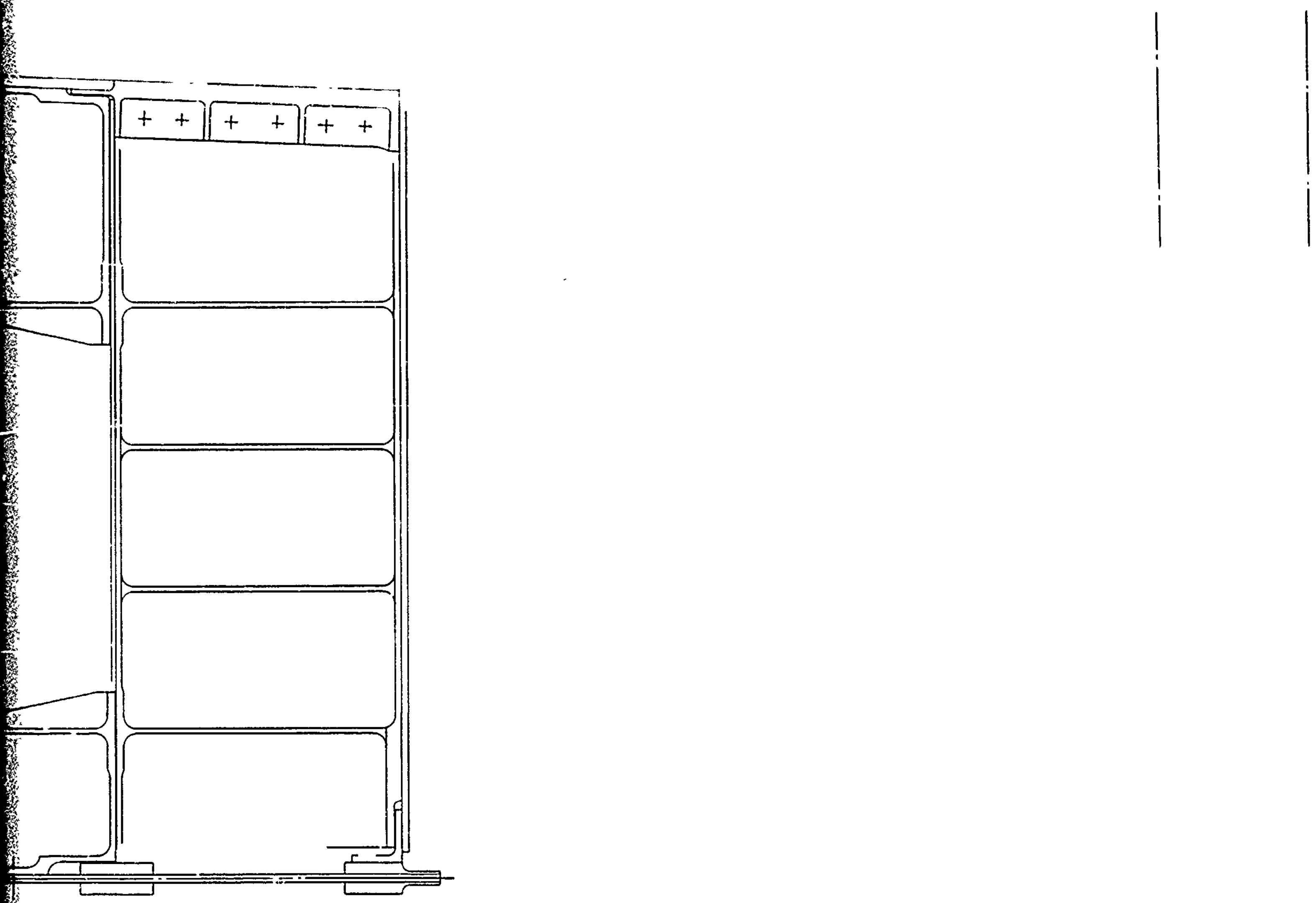

| CONTRACT NO. | REV | DWG NO. | SH |
| --- | --- | --- | --- |
| F33615-73-C-3001 | | X7223701 | 1 |

5 4 3

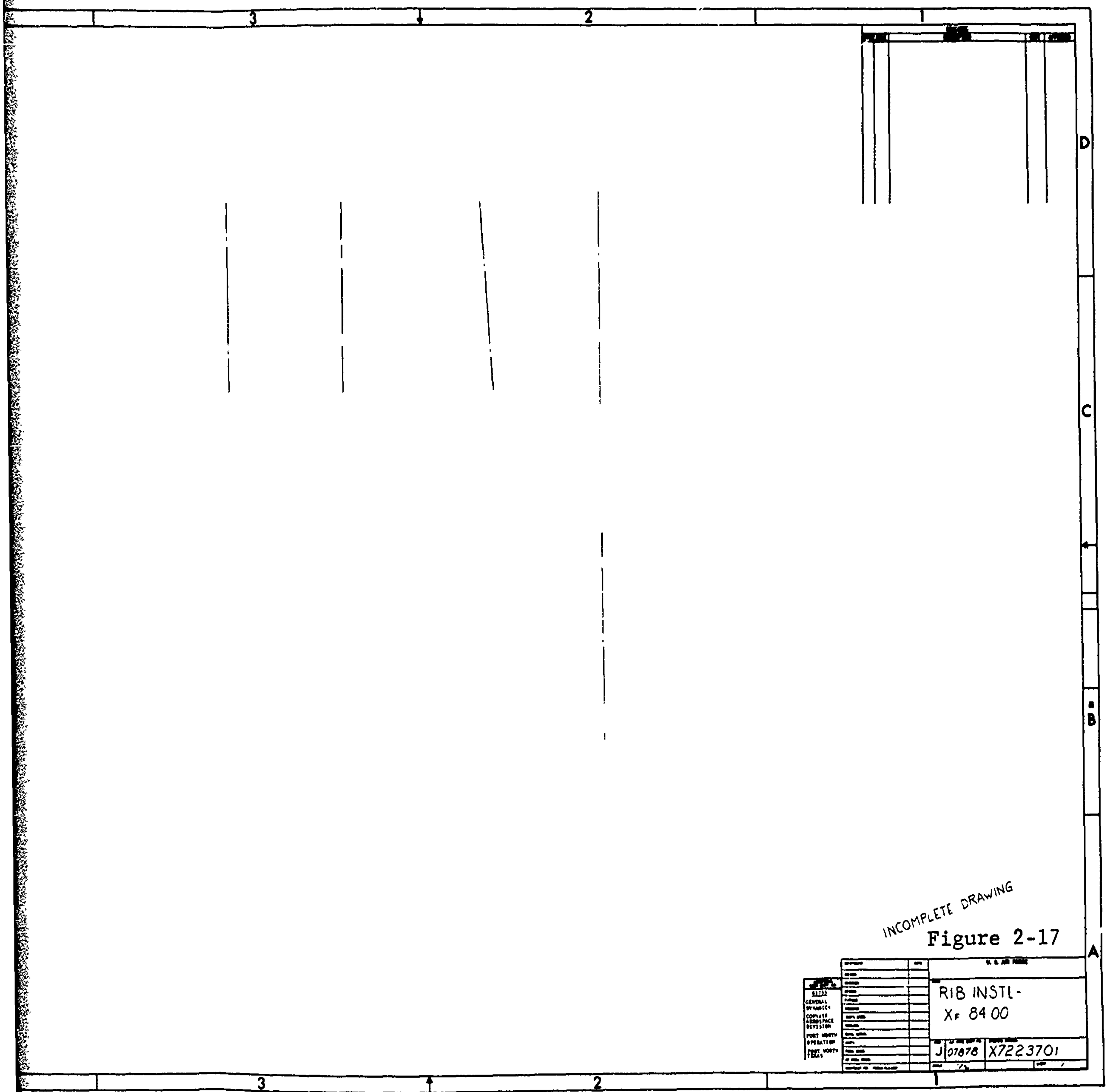


Figure 2-17

## 2.2 STRUCTURAL ANALYSIS

A variety of tasks were accomplished by stress analysis personnel during Phase II. The major accomplishments are summarized in the following list:

1. Converted updated design loads from the form furnished by Rockwell International to a form useable for Convair Aerospace finite element analysis, including determination of loads required for static balance.

2. Performed finite element analysis of the various FSIL and NBB configurations to determine internal loads and stresses for the complete carrythrough structure.

3. Performed additional fine grid finite element analysis for local areas to determine more detailed stress and load distributions and/or critical buckling loads.

4. Provided assistance to design personnel during final structural member sizing to assure adequate static and fatigue strength.

5. Provided stress data for fatigue and fracture analysis.

6. Continued stiffness studies.

7. Performed additional damage tolerance analyses for FSIL using finite element procedures.

8. Performed detailed stress analysis of parts shown on drawings being prepared for release for manufacture.

9. Participated in test planning, test part manufacture, testing, and interpretation of resulting data.

10. Performed finite element analysis of the simulated fuselage and fuselage test fixture to arrive at a configuration that would properly load the carrythrough structure during test.

11. Furnished internal loads from model of item 10. to test lab for design of upper test fixture structure.

12. Performed detailed stress analysis of simulated fuselage parts being released for manufacture.

13. Prepared inputs for necessary status and interim reports and the May and November, 1973 design reviews.

In many instances, the accomplishments represented a continuation of tasks begun in Phase Ib. Because of the large amount of computer data and manual stress analysis data generated, it is not feasible to include it in this report. The current data is retained on file by the contractor for review. In specific instances, in response to requests from AFFDL, data tapes were furnished to the interested parties through ADPO (Advanced Development Program Office). Where necessary for clarity of presentation, examples of data are included herein.

### 2.2.1 Design Loads

As noted in AFFDL-TR-73-40, Section 2.2.1, RI furnished loads data for 11 basic design conditions and two stiffness conditions. For the initial portion of the Phase II effort, the conditions described in Section 2.2.1 of AFFDL-TR-73-40 were used and,for brevity, they are not repeated here. For the latter portion of the design effort, updated technical data was provided which reflected deletion of the wing intrusion, increased pitching moments at the pivot and other load changes, and gross weight increase. For design purposes, the gross weight increase was covered through the stipulation by AFFDL that all flight loads be increased by 10% for analysis purposes. The 10% increase was considered where pertinent in the actual stress analysis, but it is not included in the loads actually used for finite element model input nor in loads summarized in this report.

The updated data was received in a period from approximately 8/23/73 to 10/15/73 and consisted of the following information:

1. Wing pivot loads shown in an excerpt from NARSAP 39 station Model data dated 4/23/73.

2. Interface loads contained in NA-73-510 NARSAP internal loads document.

3. Maximum gear actuator load obtained verbally - 250,000 lbs.

4. Main landing gear emergency hydraulic actuator loads in graphical form.

5. Wing sweep actuator vertical load and overwing fairing loads transmitted to Convair from ADPO.

6. Preliminary carrythrough box interface loads in the form of a Xerox copy produced from view graph presentation materials. Since these were only used for interim studies prior to receipt of NARSAP data, they are not reproduced in this report.

The final set of loads used for Phase II analysis was obtained from the following sources:

1. Shear flows - NARSAP values from NA 73-510 ratioed by
   $(|q_{ASKA}|/|q_{NARSAP}|)$ TFD-72-838

2. Longeron loads - Based on NARSAP values from NA 73-510.

3. Wing pivot loads - From NARSAP 39 station model data dated 4/23/73.

4. Wing sweep actuator loads - Loads from TFD-72-835 and TFD-72-838, App. A, ratioed by $\frac{M_Z \text{ NARSAP 39 Sta Data}}{M_{Z \text{PH. Ib}}}$, plus values from item 5. above.

5. Weapon launcher loads - Values from TFD-72-838 with Appendices A and B and TFD-72-835.

6. Landing gear loads - Values from TFD-72-838 with appendices for overall box analysis. These values were chosen rather than those presented in TFD-72-835 since the former were, presumably, those found by RI to be the most critical. The loads chosen apparently include no gear actuator loads. For local areas, values from TFD-72-835 were used.

7. Fuel pressures - Based on TFD-72-840 information.

8. Aerodynamic pressures - Values from TFD-72-835

9. Stiffness condition loads - Values from TFD-72-1176.

10. Overwing fairing loads - Values transmitted to Convair by ADPO.

11. Main landing gear emergency hydraulic actuator cylinder loads - Values from RI plots assumed to act separately for local design only.

12. Main landing gear actuator loads - Value noted previously taken as acting separately for local design only.

The data in TFD-72-835 (weapons launcher loads) and TFD-72-840 are not directly applicable to specific flight conditions because fuel and armament loadings for the design conditions were not made available.

A summary of load conditions used for overall box analysis is shown in Table II- 1. As noted, AS8C was used instead of AS8000 since insufficient data was available in NA-73-510 to allow breaking the latter down into symmetric and antisymmetric portions.

The revised baseline loads data is shown in Section 2.2.1.1. These loads do not include a 10% increase in gross weight. The internal loads represent the deletion of the wing intrusion and other changes.

2.2.1.1 Baseline Loads

1. Wing pivot loads from the NARSAP 39 station data are shown in Table II- 3.

2. Wing carrythrough structure - fuselage interface loads were supplied in the form of NARSAP math model internal loads data. The required interface loads were obtained or derived from this data. The interface loads are shown in Tables II- 4 through II- 7. The net NARSAP shears and moments are summarized for reference in Table II-8.

3. Wing sweep actuator loads derived from RI data are shown in Table II-9.

4. Landing gear loads are shown in Table II-10.

5. Weapons launcher loads are shown in Table II-11.

6. Main landing gear emergency hydraulic actuator cylinder loads are shown in Figure 2-22.

7. Wing sweep actuator vertical load and overwing fairing loads are shown in Table II-12.

8. The fuel pressures used in combination with the flight conditions are shown in Figure 2-23.

9. The upper cover aerodynamics pressures are as follows:

Table II-1 OVERALL LOAD CONDITION SUMMARY

| CONVAIR[1,2,3] COND. NO. | NARSAP COND. NO. | CONDITION DESCRIPTION | WING POSITION |
|---|---|---|---|
| AS1000<br>AS1000A | 660331<br>660332 | Abrupt Roll, 3G Limit | 67.5° |
| AS2000 | 110021 | Steady Pitch, 2G, Flaps Down | 15 |
| AS3000 | 161432 | Steady Pitch, 3G | 67.5 |
| AS4000 | 110301 | Steady Pitch, OG, Spoilers | 15 |
| AS5000 | 112120 | Steady Pitch, 2G, Slats | 15 |
| AS6000 | 810012 | 2 Pt. Braked Roll, 1G | 15 |
| AS7000 | 880025 | Taxi, 2G | 15 |
| AS8000[4]<br>AS8000A | 880012 | Ground Turning, 1G | 15 |
| AS9000[5] | 122222 | Steady Pitch, 2G | 25 |
| AS10000 | 160337 | Steady Pitch, 3G, Low Level | 67.5 |
| AS11000 | 160316 | Steady Pitch, 1G | 67.5 |

NOTES:
1. PIVOT LOADS TAKEN FROM NARSAP 39 STA. DATA DTD. 4/23/73
2. ARMAMENT AND LANDING GEAR LOADS ASSUMED TO REMAIN AS IN TFD-72-838 AND TFD-72-838 APP. A
3. SWEEP ACTUATOR LOADS OBTAINED BY $M_Z$ RATIO USING TFD-72-835 AND TFD-72-838 APP. A AND NARSAP 39 STA. DATA DTD. 4/23/73
4. ASKA 8C TO BE USED UNTIL ASKA DATA IS RECEIVED FOR AS8000
5. NARSAP 122222 USED BECAUSE PIVOT LOADS EXCEEDED 122221
6. SEE TABLE II-2 FOR NARSAP CONDITION NUMBER DESCRIPTION.

## TABLE II-2 - NARSAP CONDITION NUMBER DESCRIPTION

6 DIGIT NUMBER - A B C D E S

A. <u>TYPE CONDITION</u>

1. STEADY PITCH
2. PITCHING ACCELERATION
3. VERTICAL GUST
4. LATERAL GUST
5. YAW MANEUVER
6. ROLL MANEUVER
7. LANDING
8. TAXI
9. NUCLEAR BLAST

B. <u>WING POSITION - $\Lambda$</u>

0. EXTENDED OR UNDEFINED
1. $15^{o}$
2. $25^{o}$
3. $35^{o}$
4. $45^{o}$
5. $55^{o}$
6. $65 - 67.5^{o}$

C. <u>ALTITUDE</u>

0. SEA LEVEL TO 9999' OR UNDEFINED
1. 10000 - 19999'
2. 20000 - 29999'
3. 30000 - 39999'
4. 40000 - 49999'
5. 50000 - 59999'
6. 60000'+

D. <u>VELOCITY</u> - MACH NO.

0. ZERO OR UNDEFINED
1. 0.01 - 0.69
2. 0.70 - 0.84
3. 0.85 - 0.99
4. 1.00 - 1.49
5. 1.50 - 1.99
6. 2.00 - 2.19
7. 2.20+

E. <u>LOAD FACTOR</u> 'g'

0. ZERO OR UNDEFINED

1.—8. APPROXIMATE 'g' LEVEL

9. NEGATIVE 'g' LEVEL

S. <u>SEQUENCE NUMBER</u>

0. NORMAL

1.— 9. IF THERE ARE SIMILAR CONDITIONS

TABLE II-3 - ULTIMATE NARSAP 39 STA. WING PIVOT LOADS (4-23-73)

| CONDITION | ___ | $P_Z$ KIPS | $M_X$ IN. LB./$10^6$ | $M_Y$ IN. LB./$10^6$ | $M_Z$ IN. LB./$10^6$ |
|---|---|---|---|---|---|
| AS 1000<br>1000A | 67.5<br>67.5 | 264.28 | 44.07 | -74.16 | -12.68 |
| AS 2000 | 15 | 344.26 | 102.22 | -26.79 | -4.24 |
| AS 3000 | 67.5 | 233.50 | 39.70 | -70.57 | -5.06 |
| AS 4000 | 15 | -96.26 | -37.41 | 6.52 | 24.45 |
| AS 5000 | 15 | 294.86 | 93.35 | -12.83 | -22.20 |
| AS 6000 | 15 | -43.15 | -11.70 | 2.72 | -7.53 |
| AS 7000 | 15 | -74.34 | -19.49 | 4.42 | 0 |
| AS 8000<br>8000A | 15<br>15 | -37.17 | -9.75 | 2.21 | 0 |
| AS 9000 | 25 | 314.01 | 96.57 | -31.65 | -4.49 |
| AS 10000 | 67.5 | 298.15 | 51.37 | -88.33 | -12.55 |
| AS 11000 | 67.5 | 20.82 | 4.56 | -1.87 | 24.00 |

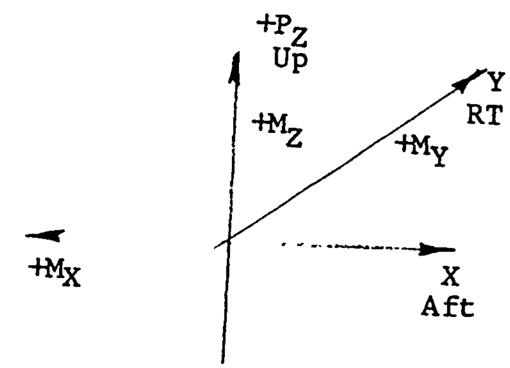

TABLE II-4

$Y_F$ 932 Bulkhead Longeron Load Summary

| Condition | | (1) | | | (2) | | | (3) | | | (6) | | | (7) | | | (9) | | |
|---|---|---|---|---|---|---|---|---|---|---|---|---|---|---|---|---|---|---|---|
| NARSAP | Convair | $F_x$ | $F_y$ | $F_z$ | $F_x$ | $F_y$ | $F_z$ | $F_x$ | $F_y$ | $F_z$ | $F_x$ | $F_y$ | $F_z$ | $F_x$ | $F_y$ | $F_z$ | $F_x$ | $F_y$ | $F_z$ |
| 660331,2 | 1000S | 0 | 68889 | 0 | 4513 | 23786 | 0 | 46720 | 246217 | -18516 | 1909 | -62168 | 1436 | 2035 | -158727 | 4233 | 0 | -117998 | 787 |
| 660331,2 | 1000A | 0 | 4269 | 0 | 2412 | 12712 | 0 | 2943 | 15512 | -1167 | 290 | -9443 | 218 | 62 | -4809 | 128 | 0 | 0 | 0 |
| 110021 | 2000 | 0 | 213869 | 0 | 45183 | 238121 | 0 | 19854 | 104630 | -7868 | 2836 | -92387 | 2134 | 3563 | -277963 | 7413 | 0 | -186286 | 1243 |
| 161432 | 3000 | 0 | 72294 | 0 | 3154 | 16621 | 0 | 49013 | 258302 | -19424 | 1881 | -61279 | 1416 | 2075 | -161870 | 4317 | 0 | -124067 | 828 |
| 110301 | 4000 | 0 | 4455 | 0 | -9313 | -49081 | 0 | -12372 | -65200 | 4903 | -853 | 27797 | -642 | -638 | 49776 | -1328 | 0 | 32254 | -215 |
| 112120 | 5000 | 0 | 162451 | 0 | 41608 | 219279 | 0 | 16227 | 85518 | -6431 | 2648 | -86264 | 1993 | 2968 | -231549 | 6175 | 0 | -149434 | 997 |
| 810012 | 6000 | 0 | -120889 | 0 | 16249 | 85632 | 0 | 8158 | 42994 | -3233 | 462 | -15052 | 348 | 507 | -39566 | 1055 | 0 | -40888 | 273 |
| 880025 | 7000 | 0 | 80647 | 0 | 23050 | 121477 | 0 | 4757 | 25071 | -1885 | 920 | -29952 | 692 | 1525 | -118993 | 3174 | 0 | -78250 | 522 |
| 880012S | 8S | 0 | 37937 | 0 | 14378 | 75773 | 0 | -1953 | -10291 | 774 | 422 | -13756 | 318 | 549 | -42821 | 1142 | 0 | -46842 | 312 |
| 980012A | 8A | 0 | 22487 | 0 | 17585 | 92676 | 0 | 10423 | 54931 | -4131 | -815 | 26535 | -613 | -333 | 26006 | -694 | 0 | 0 | 0 |
| 122222 | 9000 | 0 | 176364 | 0 | 36091 | 190205 | 0 | 22287 | 117453 | -8832 | 2464 | -80258 | 1854 | 3089 | -240967 | 6427 | 0 | -162797 | 1086 |
| 160337 | 10000 | 0 | 90576 | 0 | 5426 | 28593 | 0 | 62857 | 331261 | -24911 | 2525 | -82251 | 1900 | 2698 | -210428 | 5612 | 0 | -157752 | 1052 |
| 160316 | 11000 | 0 | 56451 | 0 | 990 | 5217 | 0 | -8951 | -47172 | 3547 | -250 | 8346 | -193 | 181 | -14138 | 377 | 0 | -8704 | 58 |

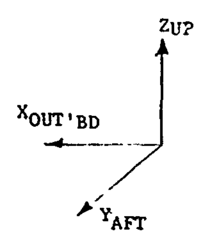


NOTES:
1) $F_y$ values obtained from NARSAP data (NA-73-510 & TFD-72-838); $F_x$ and $F_z$ values derived from longeron geometry.
2) All loads are lbs. ult.
3) Longeron (9) on ℄ listed as 1/2 of total load.
4) Positive sign convention per sketch.
5) See Fig. 2-18 for longeron locations.

NOTES:
1. LONGERON
2. DUMMY LONGERON
3. SHEAR PATH NODE
4. NUMBERS IN PARENTHESIS ARE NARSAP LONGERON AND SHEAR FLOW DESIGNATIONS; ALL OTHERS ARE ASKA DESIGNATIONS.
5. SHEAR FLOW DIRECTION COINCIDES WITH NARSAP CONVENTION.

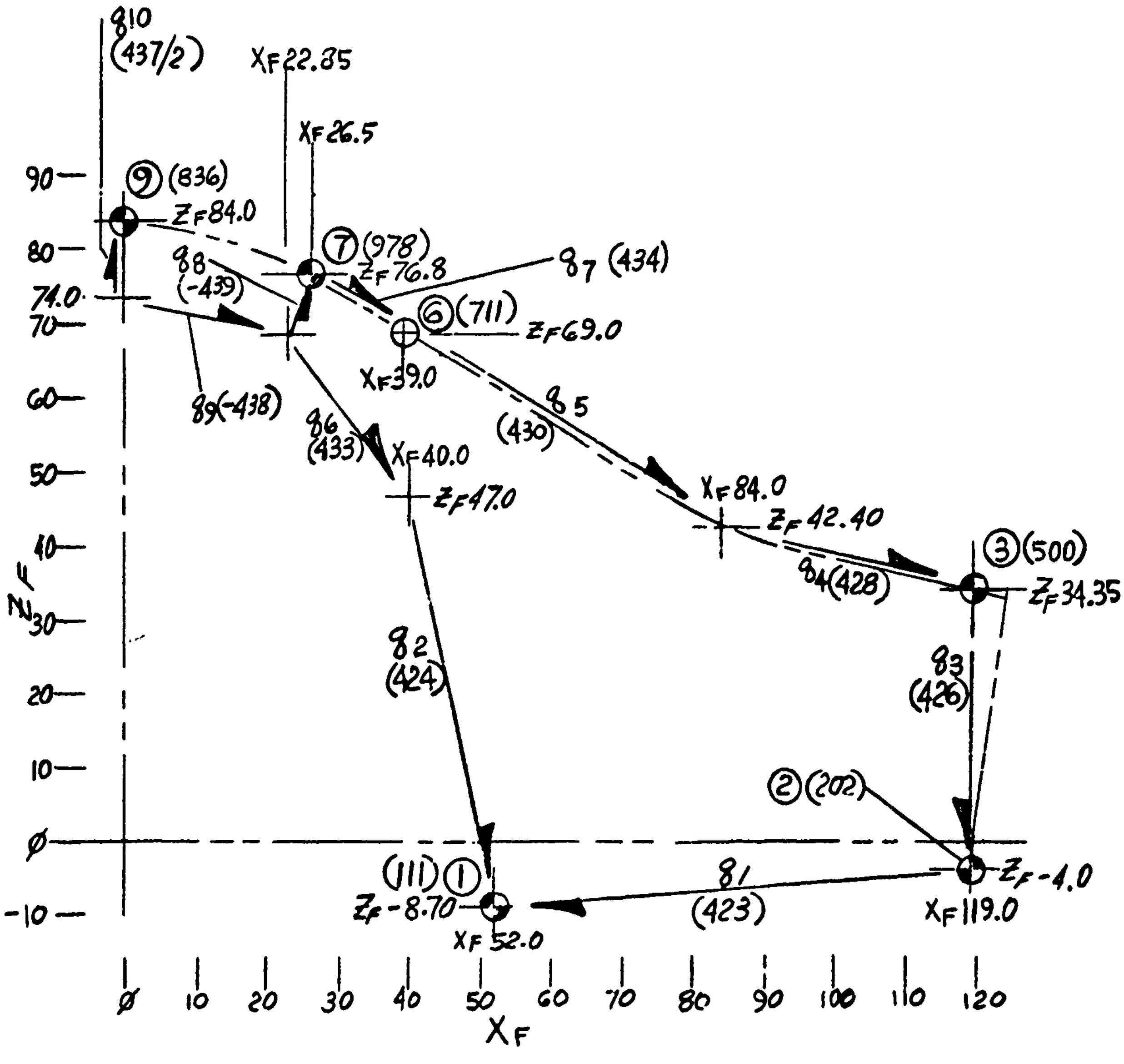


Figure 2-18 NARSAP-ASKA MATH MODEL INTERFACE LOAD GEOMETRY $Y_F$ 932 BULKHEAD

TABLE II-5

$Y_F$ 932 NARSAP Shear Flow Summary

| Condition NARSAP | Condition Convair | $q_1$ | $q_2$ | $q_3$ | $q_4$ | $q_5$ | $q_6$ | $q_7$ | $q_8$ | $q_9$ | $q_{10}$ |
|---|---|---|---|---|---|---|---|---|---|---|---|
| 660331,2 | 1000S | 140.7 | -201.52 | -1166.49 | 1774.25 | 1774.25 | -277.26 | 1097.77 | -76.26 | -103.69 | -17.10 |
| 660331,2 | 1000A | -8.81 | 37.81 | -157.82 | 25.02 | 25.02 | 38.62 | -216.76 | -152.62 | -72.58 | 0 |
| 110021 | 2000 | 466.9 | 102.9 | 917.5 | 2162.8 | 2162.8 | 30.9 | 1459.7 | -633.9 | -160.2 | -30.6 |
| 161432 | 3000 | 151.25 | -239.84 | -1315.98 | 1745.95 | 1745.95 | -320.28 | 1108.95 | -51.84 | -107.46 | -18.2 |
| 110301 | 4000 | -139.76 | 168.98 | -306.33 | -936.23 | -936.23 | 206.21 | -530.86 | -124.76 | 32.9 | 1.38 |
| 112120 | 5000 | 278.94 | 5.94 | 689.78 | 1817.20 | 1817.20 | -66.26 | 1075.4. | -461.43 | -147.26 | -20.05 |
| 810012 | 6000 | -306.51 | -391.41 | 714.03 | 826.48 | 826.48 | -223.34 | 761.68 | 58.03 | -18.46 | -13.685 |
| 880025 | 7000 | 179.5 | 700.7 | 997.2 | 875.6 | 875.6 | 754.9 | 651.7 | -967.5 | -25.0 | -29.2 |
| 880012S | 8 S | 57.50 | 211.74 | 637.85 | 299.65 | 299.65 | 331.59 | 260.74 | -273.71 | 267.60 | -436.98 |
| 880012A | 8 A | 66.16 | -100.04 | 151.16 | 338.61 | 338.61 | -143.41 | 543.94 | 382.29 | 96.66 | 0 |
| 122222 | 9000 | 363.9 | 9.6 | 517.5 | 1968.7 | 1968.7 | -72.2 | 1357.9 | -444.9 | -142.0 | 25.1 |
| 160337 | 10000 | 186.9 | -231.4 | -1596.0 | 2318.0 | 2318.0 | -330.1 | 1426.7 | -150.9 | -136.7 | -24.0 |
| 160316 | 11000 | -26.28 | 99.63 | -49.40 | -373.47 | -373.47 | 105.13 | -90.17 | -142.61 | -6.62 | -2.70 |

Notes:
1) All loads are lbs/in Ult.
2) $q_{10}$ on ℄ listed as 1/2 of total shear flow
3) Positive sign convention and location for shear flow depicted on Figure 2-18
4) Values from NA-73-510 & TFD-72-838

TABLE II-6 $Y_F$ 992 LONGERON LOADS SUMMARY Sheet 1

| Condition | | (11) | | | (12) | | | (15) | | | (16) | | | (17) | | |
|---|---|---|---|---|---|---|---|---|---|---|---|---|---|---|---|---|
| NARSAP | Convair | $F_x$ | $F_y$ | $F_z$ | $F_x$ | $F_y$ | $F_z$ | $F_x$ | $F_y$ | $F_z$ | $F_x$ | $F_y$ | $F_z$ | $F_x$ | $F_y$ | $F_z$ |
| 660331,2 | 1000 S | 0 | -64347 | 0 | 0 | 994 | 0 | 303883 | -1310464 | -21990 | 72622 | -188815 | -3168 | -215113 | 927649 | -1633 |
| 660331,2 | 1000 A | 0 | 0 | 0 | 0 | 0 | 0 | 53409 | -230322 | -3865 | 38886 | -101102 | -1696 | -63493 | 273805 | -482 |
| 110021 | 2000 | 0 | -76268 | 0 | 0 | 2285 | 0 | 201789 | -870194 | -14602 | 70038 | -182097 | -3056 | -83197 | 358778 | -631 |
| 161432 | 3000 | 0 | -66700 | 0 | 0 | 1457 | 0 | 329740 | -1421968 | -23861 | 75983 | -197553 | -3315 | -230441 | 993752 | -1749 |
| 110301 | 4000 | 0 | 27187 | 0 | 0 | 2188 | 0 | -38457 | 165842 | 2783 | -25019 | 65048 | 1092 | 31575 | -136163 | 240 |
| 112120 | 5000 | 0 | -75030 | 0 | 0 | -201 | 0 | 118325 | -510263 | -8562 | 55635 | -144650 | -2427 | -49564 | 213741 | -376 |
| 810012 | 6000 | 0 | -130164 | 0 | 0 | -8986 | 0 | 129697 | -559306 | -9385 | 56116 | -145899 | -2448 | -71389 | 307856 | -542 |
| 880025 | 7000 | 0 | -100476 | 0 | 0 | -5242 | 0 | 130657 | -563445 | -9455 | 58679 | -152564 | -2560 | -73703 | 317834 | -55[illegible] |
| 880012 S | 8 S | 0 | -71,850 | 0 | 0 | 417 | 0 | 46,452 | -200,319 | -3361 | 28,148 | -73,184 | -1228 | -16,440 | 70,897 | -125 |
| 880012 A | 8 A | 0 | 0 | 0 | 0 | 0 | 0 | 35,766 | -154,238 | -2588 | 16,919 | -43,989 | -738 | -1386 | 5977 | -11 |
| 122222 | 9000 | 0 | -71112 | 0 | 0 | 2096 | 0 | 204359 | -881274 | -14788 | 65468 | -170215 | -2856 | -98092 | 423012 | -745 |
| 160337 | 10000 | 0 | -78379 | 0 | 0 | 2025 | 0 | 406900 | -1754710 | -29444 | 94972 | -246925 | -4143 | -286869 | 1237092 | -2177 |
| 160316 | 11000 | 0 | 5468 | 0 | 0 | 3212 | 0 | 10608 | -45745 | -768 | -8924 | 23202 | 389 | 7418 | -31988 | 56 |

NOTES: (1) $F_y$ values obtained from NARSAP data (NA 73-510 and TF072-838); $F_x$ and $F_z$ values derived from longeron geometry.

(2) $F_y$ values do <u>not</u> include balance load contribution.

(3) All values are lbs ult.

(4) Values for longerons on ℄ are listed as 1/2 of total.

(5) Positive sign convention per sketch.

(6) See Fig. 2-19 for longeron locations.

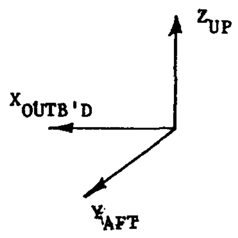

TABLE II-6 $Y_F$ 992 LONGERON LOADS SUMMARY Sheet 2

| Convair | 18 | | | 21 | | | 22 | | | 23 | | | 24 | | | 25 | | |
|---|---|---|---|---|---|---|---|---|---|---|---|---|---|---|---|---|---|---|
| | $F_x$ | $F_y$ | $F_z$ | $F_x$ | $F_y$ | $F_z$ | $F_x$ | $F_y$ | $F_z$ | $F_x$ | $F_y$ | $F_z$ | $F_x$ | $F_y$ | $F_z$ | $F_x$ | $F_y$ | $F_z$ |
| 1000 S | -22487 | 53468 | 6151 | 0 | 52008 | -1035 | 0 | 178964 | 0 | 0 | 66539 | 0 | 0 | 250326 | 2013 | 0 | 28681 | 0 |
| 1000 A | -1350 | 3511 | 369 | 0 | 7004 | -139 | 0 | 12137 | 0 | 0 | -3292 | 0 | 0 | 0 | 0 | 0 | 0 | 0 |
| 2000 | -8231 | 21402 | 2252 | 0 | 86457 | -1720 | 0 | 227698 | 0 | 0 | 85908 | 0 | 0 | 304258 | 2446 | 0 | 41772 | 0 |
| 3000 | -24056 | 62546 | 6580 | 0 | 57740 | -1149 | 0 | 195952 | 0 | 0 | 71478 | 0 | 0 | 272513 | 2191 | 0 | 30791 | 0 |
| 4000 | 1055 | -2742 | -288 | 0 | -6848 | 136 | 0 | -38052 | 0 | 0 | -14034 | 0 | 0 | -56938 | -458 | 0 | -5489 | 0 |
| 5000 | -2667 | 6934 | 730 | 0 | 56475 | -1124 | 0 | 161427 | 0 | 0 | 55443 | 0 | 0 | 208561 | 1677 | 0 | 27563 | 0 |
| 6000 | -8733 | 22706 | 2389 | 0 | 49159 | -978 | 0 | 171591 | 0 | 0 | 18752 | 0 | 0 | 192362 | 1547 | 0 | 1702 | 0 |
| 7000 | -15050 | 39131 | 4117 | 0 | 54794 | -1090 | 0 | 173730 | 0 | 0 | 31393 | 0 | 0 | 190802 | 1534 | 0 | 14043 | 0 |
| 8 S | -5004 | 13,011 | 1369 | 0 | 22,148 | -441 | 0 | 112,143 | 0 | 0 | 1374 | 0 | 0 | 129,575 | 1042 | 0 | -4212 | 0 |
| 8 A | 1596 | -4151 | -437 | 0 | -1236 | 25 | 0 | 16,755 | 0 | 0 | -3907 | 0 | 0 | 0 | 0 | 0 | 0 | 0 |
| 9000 | -9589 | 24933 | 2623 | 0 | 78945 | -1571 | 0 | 207176 | 0 | 0 | 77180 | 0 | 0 | 272412 | 2190 | 0 | 36845 | 0 |
| 10000 | -28803 | 74888 | 7879 | 0 | 64939 | -1292 | 0 | 235334 | 0 | 0 | 89208 | 0 | 0 | 337269 | 2712 | 0 | 39261 | 0 |
| 11000 | 181 | -470 | -49 | 0 | 19010 | -378 | 0 | 15446 | 0 | 0 | 596[illegible] | 0 | 0 | 2058 | 17 | 0 | 3846 | 0 |

NOTES: 1. ⊕ LONGERON
2. ┼ SHEAR PATH NODE
3. NUMBERS IN PARENTHESIS ARE NARSAP LONGERON AND SHEAR FLOW DESIGNATIONS; ALL OTHERS ARE ASKA DESIGNATIONS.
4. SHEAR FLOW DIRECTION COINCIDES WITH NARSAP CONVENTION.

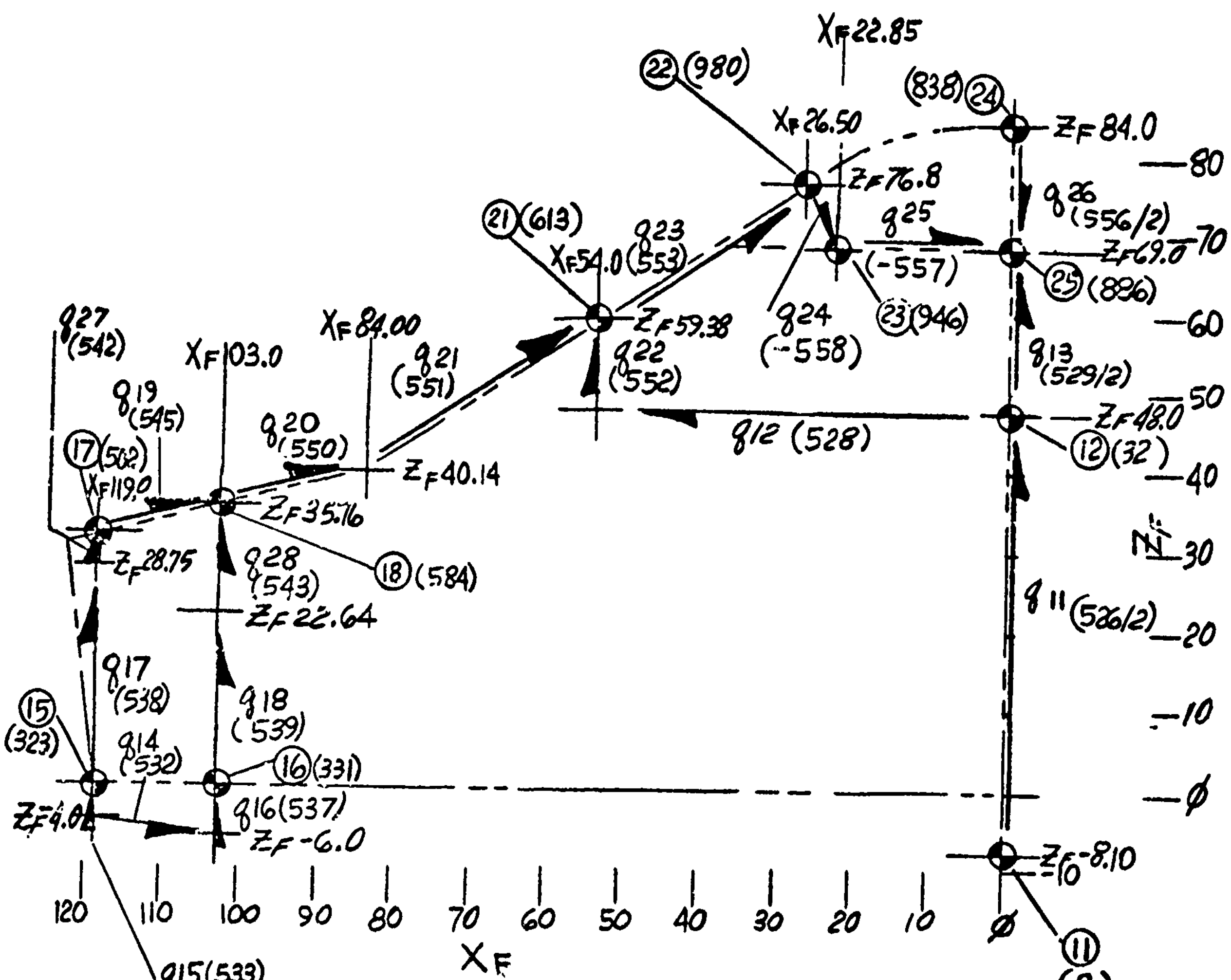


Figure 2-19 NARSAP-ASKA MATH MODEL INTERFACE LOAD GEOMETRY $Y_F$ 992 BULKHEAD

TABLE II-7 SHEET 1

$Y_F$ 992 NARSAP SHEAR FLOW SUMMARY

| Condition | | $q_{11}$ | $q_{12}$ | $q_{13}$ | $q_{14}$ | $q_{15}$ | $q_{16}$ | $q_{17}$ | $q_{18}$ |
|---|---|---|---|---|---|---|---|---|---|
| NARSAP | Convair | | | | | | | | |
| 660331,2 | 1000 S | -249.97 | -27.37 | -115.85 | -825.58 | 9729.17 | 2480.21 | -8439.48 | -174.40 |
| 660331,2 | 1000 A | 0 | -503.18 | 0 | 682.18 | 685.45 | 1570.13 | -2958.79 | 60.73 |
| 110021 | 2000 | -303.2 | -134.9 | -174.5 | 904.4 | 5757.6 | 3073.6 | -5196.5 | 482.6 |
| 161432 | 3000 | -490.31 | 2.97 | -125.70 | -443.53 | 10550.38 | 2608.74 | -9074.97 | -175.04 |
| 110301 | 4000 | 317.86 | 131.45 | 17.82 | -328.92 | -635.63 | -1203.01 | 1446.47 | -231.18 |
| 112120 | 5000 | -762.54 | -168.25 | -222.33 | 559.11 | 2833.12 | 2498.9 | -3621.6 | 394.45 |
| 810012 | 6000 | -1886.29 | -475.03 | -477.25 | 208.38 | 4246.14 | 1577.33 | -2443.24 | -719.62 |
| 880025 | 7000 | -685.75 | -274.2 | -442.0 | 304.6 | 4089.2 | 1550.3 | -2941.5 | -941.2 |
| 880012 S | 8 S | -561.40 | -271.82 | -343.13 | 41.57 | 1828.64 | 680.09 | -668.10 | -489.52 |
| 880012 A | 8 A | 0 | 63.54 | 0 | -65.41 | 1399.46 | 346.35 | -418.15 | -306.99 |
| 122222 | 9000 | -289.7 | -97.5 | -180.2 | 661.6 | 5763.5 | 2785.3 | -5731.4 | 365.7 |
| 160337 | 10000 | -285.3 | -5.0 | -113.2 | -796.1 | 12621.4 | 3401.1 | -11470.6 | -114.6 |
| 160316 | 11000 | 145.2 | 143.48 | -71.38 | -217.74 | 518.87 | -499.18 | -453.04 | -115.34 |

NOTES: (1) All loads are lbs/in ult.

(2) Values for shear flows on ℄ are listed as 1/2 of total.

(3) Positive sign convention and locations for shear flows depicted on Fig. II-19

(4) Values from NA-73-510 and TFD-72-838.

TABLE II-7 SHEET 2

$Y_F$ 922 NARSAP SHEAR FLOW SUMMARY

| Condition | | $q_{19}$ | $q_{20}$ | $q_{21}$ | $q_{22}$ | $q_{23}$ |
|---|---|---|---|---|---|---|
| NARSAP | Convair | | | | | |
| 660331,2 | 1000 S | 1388.48 | 962.44 | 962.44 | -185.65 | -562.09 |
| 660331,2 | 1000 A | -56.97 | -35.22 | -35.22 | -416.03 | 471.05 |
| 110021 | 2000 | -1567.7 | -584.8 | -584.8 | -216.4 | -399.8 |
| 161432 | 3000 | 1527.57 | 1031.54 | 1031.54 | -179.54 | 641.63 |
| 110301 | 4000 | 62.98 | -150.82 | -150.82 | 84.74 | -42.48 |
| 112120 | 5000 | -1620.23 | -754.89 | -754.89 | -161.98 | -666.47 |
| 810012 | 6000 | 1225.40 | 344.86 | 344.86 | -650.60 | 67.63 |
| 880025 | 7000 | 837.6 | 33.4 | 33.4 | -565.8 | -188.4 |
| 880012 S | 8 S | 627.28 | -2.45 | -2.45 | -408.93 | -209.04 |
| 880012 A | 8 A | 137.94 | -67.20 | -67.20 | 19.38 | -72.05 |
| 122222 | 9000 | -1351.3 | -529.8 | -529.8 | -183.9 | -383.4 |
| 160337 | 10000 | 2032.9 | 1417.1 | 1417.1 | -216.9 | 920.4 |
| 160316 | 11000 | -878.37 | -709.99 | -709.99 | 100.36 | -454.15 |

TABLE II-7 SHEET 3

$Y_F$ 992 NARSAP SHEAR FLOW SUMMARY

| Condition | | $q_{24}$ | $q_{25}$ | $q_{26}$ | $q_{27}$ | $q_{28}$ |
|---|---|---|---|---|---|---|
| NARSAP | Convair | | | | | |
| 660331,2 | 1000 S | -92.36 | -788.46 | -667.16 | -8439.48 | -174.40 |
| 660331,2 | 1000 A | -174.80 | 209.44 | 0 | -2958.79 | 60.73 |
| 110021 | 2000 | -586.1 | 694.4 | -607.85 | -5196.8 | 482.6 |
| 161432 | 3000 | -67.89 | 861.13 | -720.99 | -9074.97 | -175.04 |
| 110301 | 4000 | 21.34 | -183.53 | 174.64 | 1446.47 | -231.18 |
| 112120 | 5000 | -482.07 | 380.79 | -225.56 | -3621.6 | 394.45 |
| 810012 | 6000 | 788.5 | 761.89 | -31.69 | -2443.24 | -719.62 |
| 880025 | 7000 | 433.5 | 645.3 | -89.3 | -2941.5 | -941.2 |
| 880012 S | 8 S | 690.37 | 437.05 | 199.73 | -562.31 | -544.45 |
| 880012 A | 8 A | 185.47 | 98.97 | 0 | -325.07 | -309.05 |
| 122222 | 9000 | -530.9 | 626.0 | -512.7 | -5731.4 | 365.7 |
| 160337 | 10000 | -58. | 1088.9 | -985.0 | 11470.6 | -114.6 |
| 160316 | 11000 | -286.47 | -126.03 | 176.47 | -453.04 | -115.34 |

TABLE II - 8 NARSAP ULT. A/P LOADS APPLIED TO BOX

| CONVAIR NO. | NARSAP NO. | STA 932 FWD LB | STA 932 SHEAR SIDE LB | STA 932 VERTICAL LB | STA 932 PITCHING MOMENT | STA 932 YAWING MOMENT | STA 932 ROLLING MOMENT | STA 992 FWD LB | STA 992 SHEAR SIDE LB | STA 992 VERTICAL LB | STA 992 PITCHING MOMENT IN LB | STA 992 YAWING MOMENT IN LB | STA 992 ROLLING MOMENT IN LB |
|---|---|---|---|---|---|---|---|---|---|---|---|---|---|
| 1000 | 660331 | 0 | -7950 | -28,238 | -37,264,378 | -6,169,861 | -1,247,127 | 0 | 9,530 | 384,171 | -153,691,102 | -8,505,683 | -17,545,966 |
| 2000 | 110021 | | | -261,654 | -85,179,070 | | | | | 302,532 | -139,980,022 | | |
| 3000 | 161432 | | | -9,320 | -37,816,322 | | | | | 408,054 | -166,296,840 | | |
| 4000 | 110301 | | | -71,136 | 12,737,960 | | | | | -67,108 | 28,079,361 | | |
| 5000 | 112120 | | | -194,536 | -71,283,787 | | | | | 277,323 | -93,399,775 | | |
| 6000 | 810012 | 175,539 | 0 | -70,855 | -10,653,008 | | | | | 283,189 | -89,953,927 | | |
| 7000 | 880025 | | | -275,259 | -36,210,178 | | | -160,455 | 0 | 317,878 | -95,830,749 | | |
| 8000 | 880012 | 0 | -68,739 | -119,591 | -13,439,030 | | | | | 158,939 | -47,915,364 | | |
| 9000 | 122222 | | | -199,698 | -71,962,921 | -24,040,657 | 7,019,259 | 0 | 79,245 | 343,513 | -132,972,792 | -31,802,619 | -3,416,067 |
| 10000 | 160337 | | | -37,928 | -49,231,786 | | | | | 496,506 | -204,432,574 | | |
| 11000 | 160316 | | | 19,455 | -6,745,465 | | | | | 90,478 | -4,463,323 | | |

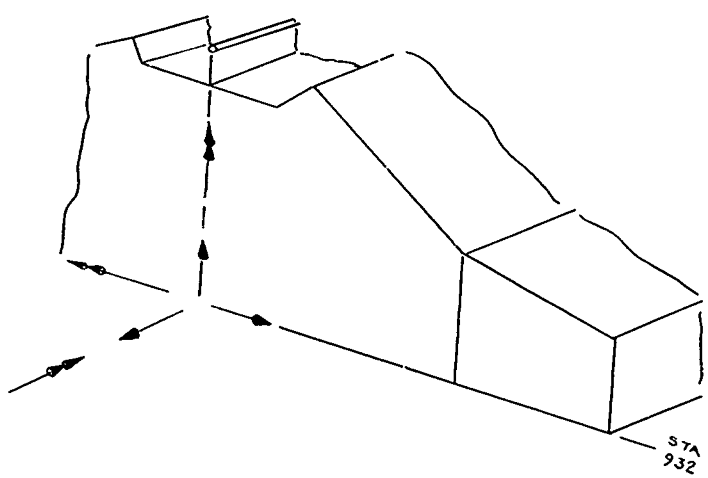


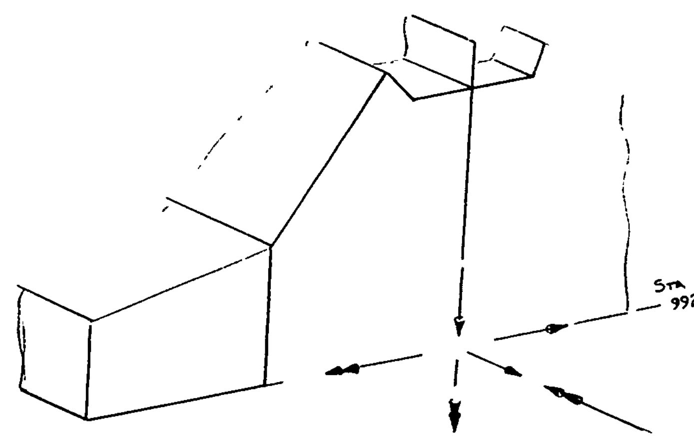

TABLE II-9

ULTIMATE LOADS APPLIED TO WING `WEEP ACTUATOR FITTING

| CONVAIR COND. | NAR COND. | $\Lambda$ DEG. | $F_X$ LBS ULT | $F_Y$ LBS ULT | $F_Z$ LBS ULT | RESULTANT LBS ULT |
|---|---|---|---|---|---|---|
| AS 1000S | 660331 | 67.5 | -215,895 | -156,390 | 7950 | -266,705 |
| AS 1000A | 660332 | | -78,840 | - 57,840 | 2895 | -97,392 |
| AS 2000 | 110021 | 15 | -80,685 | - 7770 | 2655 | -81,102 |
| AS 3000 | 161432 | 67.5 | -84,615 | - 61,290 | 3120 | -104,527 |
| AS 4000 | 110301 | 15 | 491,970 | 47,250 | -16,095 | 494,496 |
| AS 5000 | 112120 | 15 | -448,380 | -43,200 | 14,715 | -450,697 |
| AS 6000 | 810012 | 15 | -151,200 | -14,565 | 4965 | -151,981 |
| AS 7000 | 880025 | 15 | -390 | -45 | 0 | -392 |
| AS S | 880012 | 15 | -195 | -15 | 0 | -196 |
| AS A | | | 0 | 0 | 0 | 0 |
| AS 9000 | 122222 | 25 | -78,615 | -16,151 | 2621 | -80,300 REF.NOTE 1 |
| AS 10000 | 160337 | 67.5 | -285,887 | -207,074 | 10,524 | -353,160 REF. NOTE 1 |
| AS 11000 | 160316 | 67.5 | 669,585 | 485,010 | -24,630 | 827,155 |

NOTES:
(1) LOADS REVISED PER NAR LOADS PACKAGE RECEIVED 4 SEPT. 1973
(2) POSITIVE RESULTANT LOAD INDICATES ACTUATOR IS IN TENSION
(3) LOADS APPLIED AT $X_F$ 122.75, $Y_F$ 917.0, $Z_F$ 14.748 -- Ref. Fig. 2-45
(4) EFFECT OF PIVOT FRICTION NOT INCLUDED.

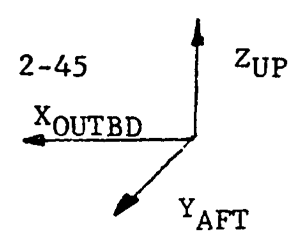

TABLE II-10

**MAIN LANDING GEAR FITTING ULTIMATE LOADS**

| CONDITION | OUTB'D TRUNNION LBS X $10^3$ | | | INB'D TRUNNION LBS X $10^3$ | | | SIDE BRACE LBS X $10^3$ | | | DRAG BRACE LBS X $10^3$ | | |
|---|---|---|---|---|---|---|---|---|---|---|---|---|
| | $F_X$ | $F_Y$ | $F_Z$ | $F_X$ | $F_Y$ | $F_Z$ | $F_X$ | $F_Y$ | $F_Z$ | $F_X$ | $F_Y$ | $F_Z$ |
| ASKA 6 | 0 | -153.369 | 312.524 | 0 | -114.233 | 312.568 | -236.130 | -81.558 | 272.869 | 236.130 | 558.178 | -622.562 |
| 7 | 0 | -162.31 | 432.549 | 0 | -77.855 | 222.874 | -119.164 | -41.286 | 137.7 | 119.164 | 281.669 | -314.166 |
| 8 | 0 | 31.99 | -150.708 | 0 | -117.436 | 346.692 | -177.288 | -56.933 | 204.865 | 60.226 | 142.357 | -158.782 |
| 8A | 0 | 41.356 | -177.538 | 0 | -118.069 | 349.06 | -180.446 | -58.277 | 208.514 | 57.099 | 134.966 | -150.538 |
| POINT OF LOAD APPLICATION | $X_F$95.5 | $Y_F$1000 | $Z_F$1.0 | $X_F$72 | $Y_F$1000 | $Z_F$1.0 | $X_F$23 | $Y_F$1000 | $Z_F$1.0 | $X_F$56.0 | $Y_F$947.0 | $Z_F$-4.5 |

NOTES:

(1) Loads Listed as Applied to CTB Fittings --- One Side --- Per TFD-72-838

(2) Loads Are in "ASKA" Model Reference System (Ref. Sketch)

(3) "A" Designates Anti-symmetric Portion of Unsymmetrical Load Condition

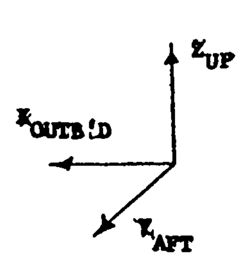

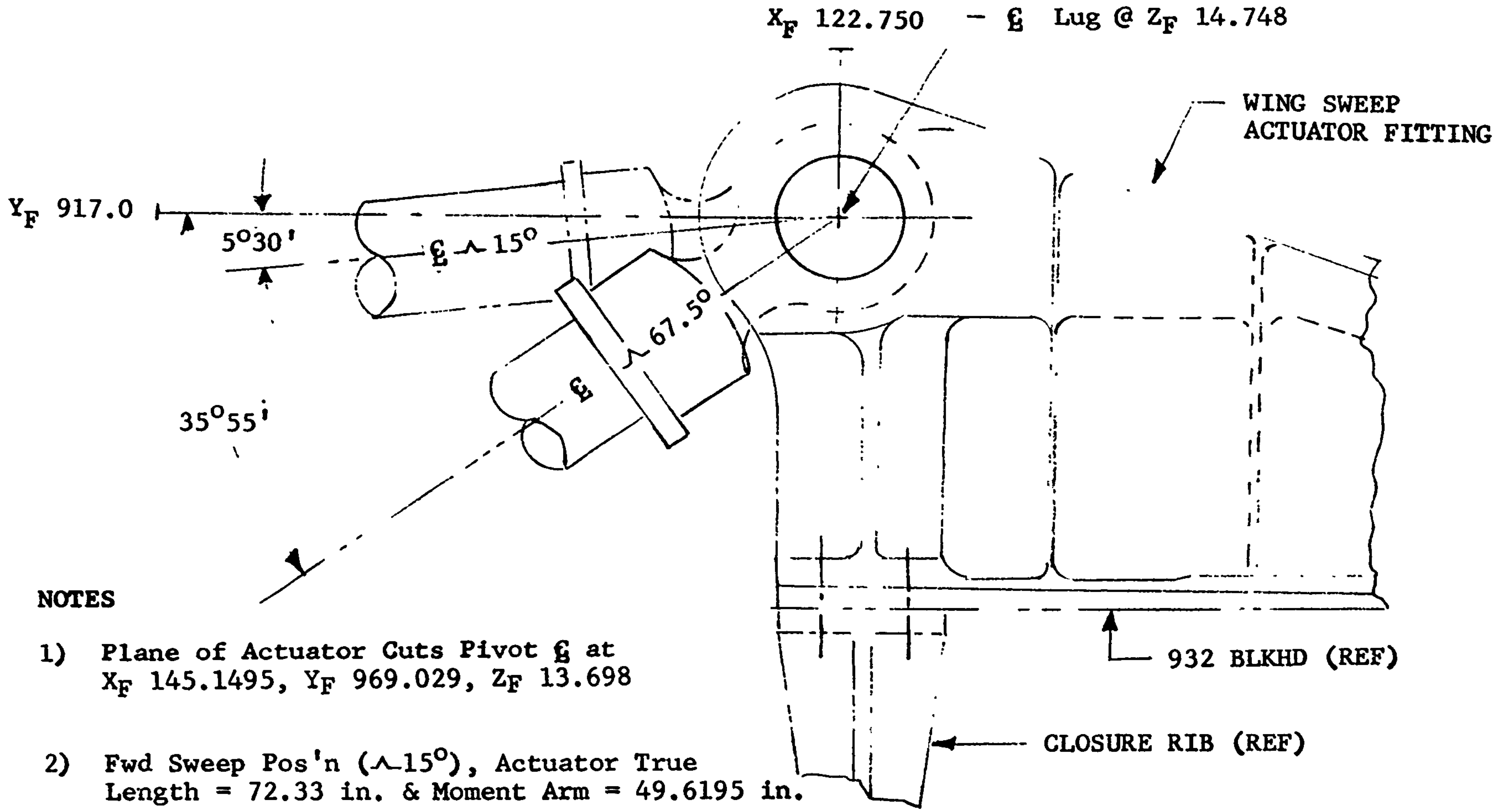


NOTES

1) Plane of Actuator Cuts Pivot ℄ at $X_F$ 145.1495, $Y_F$ 969.029, $Z_F$ 13.698

2) Fwd Sweep Pos'n ($\Lambda$ 15°), Actuator True Length = 72.33 in. & Moment Arm = 49.6195 in.

3) Aft Sweep Pos'n ($\Lambda$ 67.5°), Actuator True Length = 109.0426 in. & Moment Arm = 29.0 in.

FIGURE 2-20

WING SWEEP ACTUATOR GEOMETRY

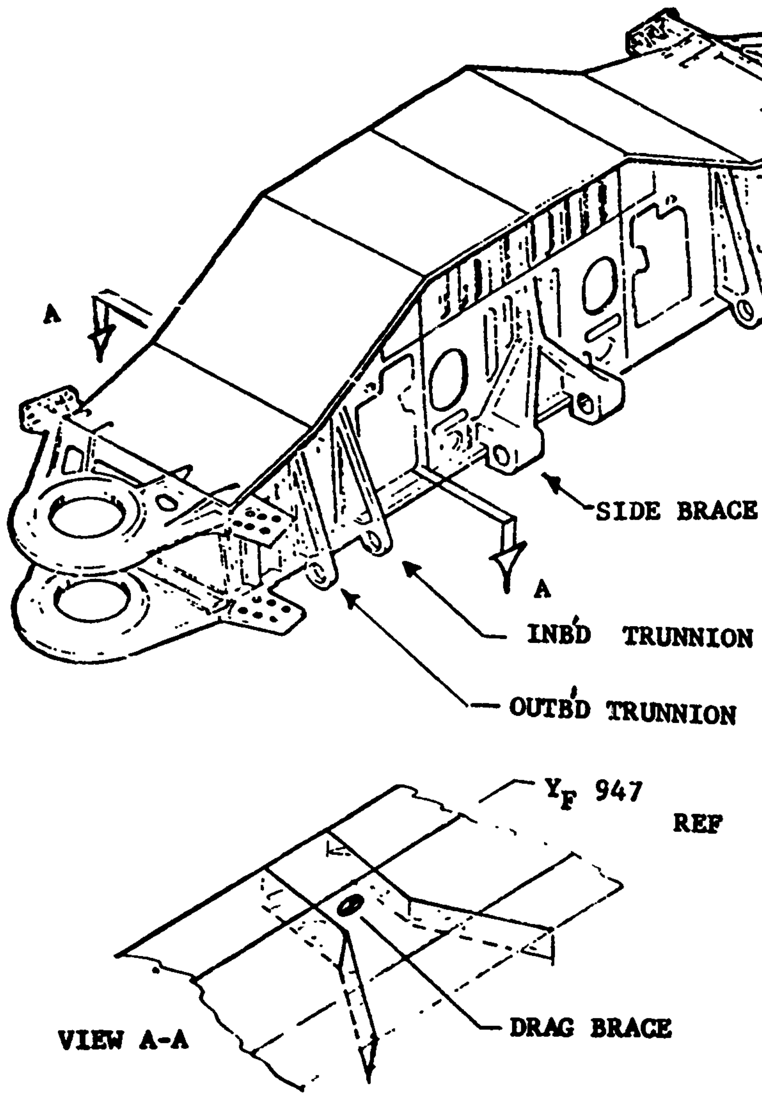


| ITEM | $X_F$ | $Y_F$ | $Z_F$ |
|---|---|---|---|
| OUTBD TRUNNION | 95.5 | 1000 | 1.0 |
| INBD TRUNNION | 72.0 | 1000 | 1.0 |
| SIDE BRACE | 23.0 | 1000 | 1.0 |
| DRAG BRACE | 56.0 | 947.0 | -4.5 |

FIGURE 2-21 MAIN LANDING GEAR FITTING GEOMETRY

TABLE II-11

ULTIMATE WEAPONS LAUNCHER LOADS
(HALF BOX)

| CONDITION | $F_X$ LBS | $F_Y$ LBS | $F_Z$ LBS |
|---|---|---|---|
| ASKA 1000S | 0 | 0 | 0 |
| 1000A | 0 | 0 | 0 |
| 2000 | 0 | 0 | -13,462 |
| 3000 | 0 | 0 | -20,193 |
| 4000 | 0 | 0 | 0 |
| 5000 | 0 | 0 | -13,462 |
| 6000 | 0 | 0 | -5,040 |
| 7000 | 0 | 0 | -13,427 |
| 8S | 0 | 0 | -6,731 |
| 8A | 0 | 0 | 0 |
| 9000 | 0 | 0 | -13,462 |
| 10000 | 0 | 0 | -20,193 |
| 11000 | 0 | 0 | -6,731 |

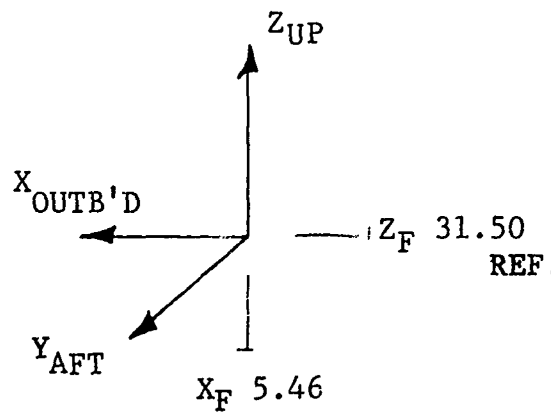


NOTES: 1) Loads listed as applied to CTB --- One Side --- Per TFD-72-838

2) Loads are in "ASKA" Reference System (Ref Sketch)

3) "A" Designates anti-symmetric portion of unsymmetrical load condition.

Table II-12

OVERWING FAIRING AND SUPPLEMENTARY WING SWEEP ACTUATOR LOADS FROM AFFDL 10/12/73

| ITEM | LOCATION | | | VALUE | |
|---|---|---|---|---|---|
| OVERWING FAIRING LOADS | $X_F$ | $Y_F$ | $Z_F$ | $F_Z$ | $M_Y$ |
| FORWARD UPPER | 138.9 | 944.1 | 23.75 | 21,500 lbs | 491,000 in. lbs |
| AFT UPPER | 149.6 | 988.01 (1) | 30.00 | 15,195 | — |
| LOWER | 138.9 | 944.1 | -6.5 | 10,700 | 289,000 |
| SWEEP ACTUATOR DESIGN LOAD | SEE TABLE II-9 | | | 30,000 | 0 |

NOTES: (1) Given as 998.026 in original data.
(2) All loads ultimate

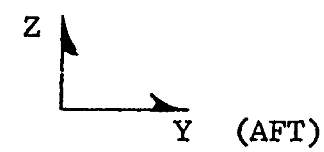

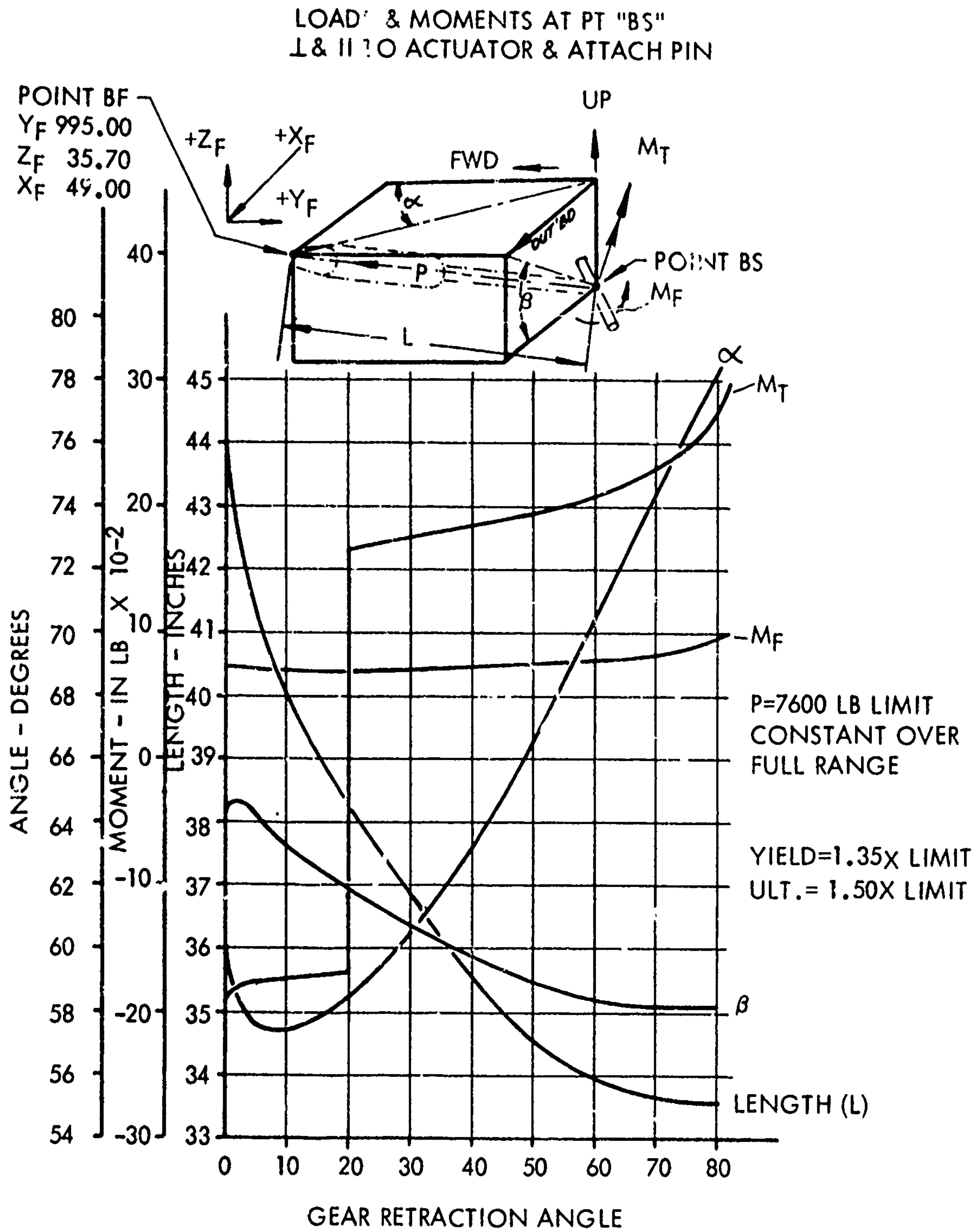


Figure 2-22 MAIN LANDING GEAR EMERGENCY HYD. ACTUATOR CYL. LOADS & GEOMETRY VS. GEAR ROTATION

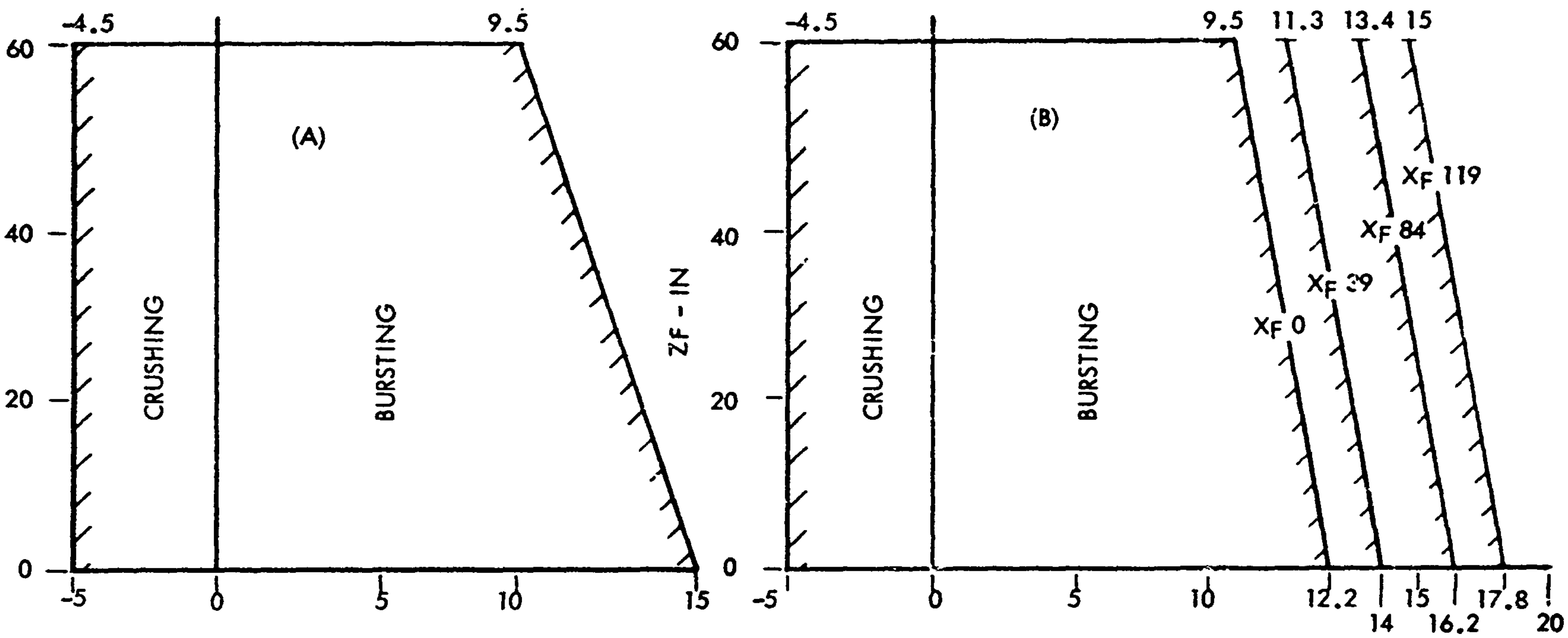


NOTES:

1. USE (A) FOR COMBINATION WITH FLT. CONDS. ON TANK BOUNDARIES. ALL $X_F$ & $Y_F$ EXCEPT FOR Og WHERE MAX. BURSTING PRESSURE IS TO BE 8.25 PSIG. (REFUELING)
2. USE (B) VALUES ACTING SEPARATELY FOR LOCAL DESIGN OF TANK BOUNDARIES. ALL $Y_F$.
3. FOR SLOSH PRESSURE USE 2.25 (F-111 DATA)
4. ALL PRESSURES ULTIMATE

Figure 2-23 FUEL TANK PRESSURES - AMAVS

| | ℄ | $Y_F$ 115 |
|---|---|---|
| ASKA 2 | .75 PSI | 1.80 PSI |
| ASKA 3 | 2.55 | 2.55 |
| ASKA 10 | 3.0 | 4.5 |

As specified in TFD-72-835, room temperature was used for all design conditions.

### 2.2.1.2 Static Balance

The application to the carrythrough box of all of the design loads supplied by RI does not result in a statically balanced structure. This fact was recognized by RI as has been previously discussed on page 2-179 of AFFDL-TR-73-40.

Small additional unbalances are present in the Convair model because of geometric differences such as longeron load application points at estimated longeron centroids instead of at the NARSAP longeron load locations. The balancing procedure used by Convair was as follows:

1. Symmetrical conditions or symmetrical portions of unsymmetrical conditions - The vertical force and pitching moment unbalance at $Y_F$ 992. resulting from applying the design loads, was determined utilizing the HP9820 calculator. A force equal and opposite to one-half of the vertical unbalance was applied at the launcher fitting on $Y_F$ 932 and to the inboard trunnion location ($X_F$ 72, $Y_F$ 992). The net remaining pitching unbalance was nullified by altering the fore and aft components of the $Y_F$ 992 longeron loads in a manner similar to that used by RI. Since the fore and aft adjustment loads are small compared to the fore and aft ($F_Y$) longeron loads, no attempt was made to adjust the vertical and horizontal components of the longeron load ($F_x$, $F_z$).

   Condition AS6000 produces a fore and aft load unbalance as well as a pitching unbalance. Equilibrium was achieved by adjusting the longeron loads at 992 for both pitching moment and longitudinal force balance. The balance loads were determined as follows:

   (a) The incremental longeron loads produced by $Y_F$ 992 AS6000 moment were obtained by multiplying the longeron loads for a pure moment conditions AS10000 by the moment ratio, $M_{AS6000}/M_{AS10000}$.

(b) The incremental longeron loads produced by axial load were obtained by subtracting the incremental load due to moment obtained in (a) from the total AS6000 longeron load.

(c) Adjusted moment longeron loads were obtained by multiplying the values of (a) by $M_{REQ'D\ AS6000}/P_{AS6000}$.

(d) The incremental longeron loads required for fore and aft force balance were obtained by multiplying the values of (b) by REQ'D $P_{AS6000}/P_{AS6000}$.

(e) The results of (b), (c), and (d) were added together to obtain the final longeron loads at 992 for overall balance.

A final overall force and moment summation including adjusted loads was made with the HP9820 to assure that equilibrium existed.

2. Antisymmetric conditions - Conditions AS1000A and AS8A are the antisymmetric portions which combine with AS1000S and AS8S to form the two asymmetrical design load conditions. For the antisymmetrical cases, static balance must be achieved in the yaw ($M_z$), roll ($M_y$) and lateral ($F_x$) directions. A simplified balancing procedure was developed which forced equilibrium by altering the lug loads. This alteration was deemed acceptable because the incremental lug loads resulting from balancing AS1000A and AS8A are insignificant compared to the critical lug design conditions. Yaw ($M_z$) balance was achieved by adding couple loads at the lugs and the centerline longerons. The yaw couple was created in the $Z_F$ 15.0605 plane and the couple forces were then beamed out to the lugs and longerons. The lateral load unbalance was reacted with an equal and opposite load on the lugs. This load was divided equally between the upper and lower lugs. Finally, roll unbalance (including the effects of the lateral balance load) was nullified with a lateral couple load on the lugs.

A summary of the final fuselage shears and moments and the required vertical balance load for each condition is given in Table II-13. It should be noted that these values are for a total WCTS and combine the symmetric and antisymmetric portion of AS1000 and AS8 to yield total load conditions.

TABLE II-13

SUMMARY OF BULKHEAD SHEARS, MOMENTS, AND VERTICAL BALANCE LOAD FOR DESIGN CONDITIONS

| CONDITION | DESCRIPTION | $\Lambda$ | $V_Z$ 932 | $M_X 932 \times 10^{-6}$ | $V_Z 992$ | $M_X 992 \times 10^{-6}$ | $F_Z$ 962 (BAL) |
|---|---|---|---|---|---|---|---|
| AS 1000 | ABRUPT ROLL | 67.5° | - 25,012 | -35.721 | -429,888 | 158.056 | - 20,954 |
| AS 2000 | 2G FLAPS DOWN | 15° | -261,394 | -83.138 | -307,544 | 140.849 | - 92,980 |
| AS 3000 | 3G , 11,000 FT. | 67.5° | - 5,878 | -36.217 | -443,640 | 168.601 | 22,802 |
| AS 4000 | 0G, SPOILERS OPEN 70° | 15° | 70,880 | 12.300 | 83,056 | - 24.793 | 38,692 |
| AS 5000 | 2G, SLATS OPEN 20° | 15° | -194,288 | -69.601 | -318,666 | 95.155 | - 50,308 |
| AS 6000 | 2 PT. BRAKED ROLL | 15° | - 71,314 | -10.532 | -389,894 | 88.227 | 6,812 |
| AS 7000 | 2G TAXI | 15° | -276,172 | -35.405 | -321,246 | 97.754 | -184,848 |
| AS 8 | GROUND TURNING | 15° | -138,402 | -17.986 | -161,176 | 49.261 | - 63,300 |
| AS 9000 | 2G , 20,000 FT. | 25° | -198,970 | -70.142 | -348,038 | 134.082 | - 55,094 |
| AS 10000 | 3G , S.L. | 67.5° | - 33,604 | -47.173 | -502,292 | 214.630 | - 20,200 |
| AS 11000 | 1G , S.L. | 67.5° | 19,238 | - 6.729 | - 84,208 | 9.615 | 36,894 |

NOTES: (1) SHEARS ARE POUNDS ULT. AND MOMENTS ARE IN.- POUNDS ULT. FOR TOTAL CTB

(2) LISTED SHEARS AT $Y_F$932 and $Y_F$992 ARE INTERFACE SHEARS AND DO NOT INCLUDE ARMAMENT OR LANDING GEAR LOADS.

(3) LISTED MOMENTS AT $Y_F$992 INCLUDES BALANCE CONTRIBUTION.

(4) REFERENCE SKETCH FOR POSITION SIGN CONVENTION.

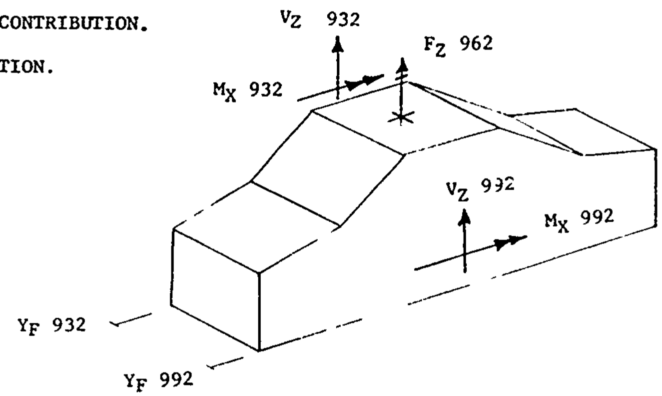

### 2.2.2 Node Point Loads for Math Models

In order to apply the design loads to the carrythrough structure math model, it was necessary to convert the basic RI loads data of paragraph 2.2.1 to panel point loads. The panel point loads were developed initially for the FSIL model. For use on the NBB model they were modified as necessary to match the loading points where commonality did not exist.

The first step consisted of geometry definition. The following assumptions were made in the geometry selection:

1. Longeron loads act at the estimated centroid of the RI longeron material based on RI drawings.

2. Shear flows act at the intersection of the actual fuselage webs and skins with the carrythrough structure as shown on RI drawings.

Figures 2- 24 and 2- 25 show the basic Convair Aerospace geometry used at $Y_F$ 932 and $Y_F$ 992 for panel point load computation.

The geometry shown in Figures 2-25 and 2-25 gives shear path lengths and directions that are somewhat different from the NARSAP model. For this reason and because the updated shear flow data was furnished in NARSAP rather than ASKA form, the following shear flow adjustments were made:

1. NARSAP shear flows shown in Tables II- 5 and II- 7 which are average panel values, were corrected to ASKA values using the ratios between NARSAP and ASKA values found in TFD-72-838 (Section 2.2.1).

2. The shear flows of item 1. were further adjusted to yield vertical force sums at $Y_F$ 932 and $Y_F$ 992 that were equal to the corresponding RI sums (prior to static balance corrections discussed in 2.2.1.2).

These adjustments were accomplished using HP9820 procedures. The results are summarized in Tables II-14 and II-15. The horizontal force sums at $Y_F$ 932 and $Y_F$ 992 were approximately the same as the corresponding RI sums.

The NMAVS shear flows along with the NARSAP longeron loads from Tables II-4 and II-6 were then entered into another HP 9820 program which computes the forces due to shear flows, distributes

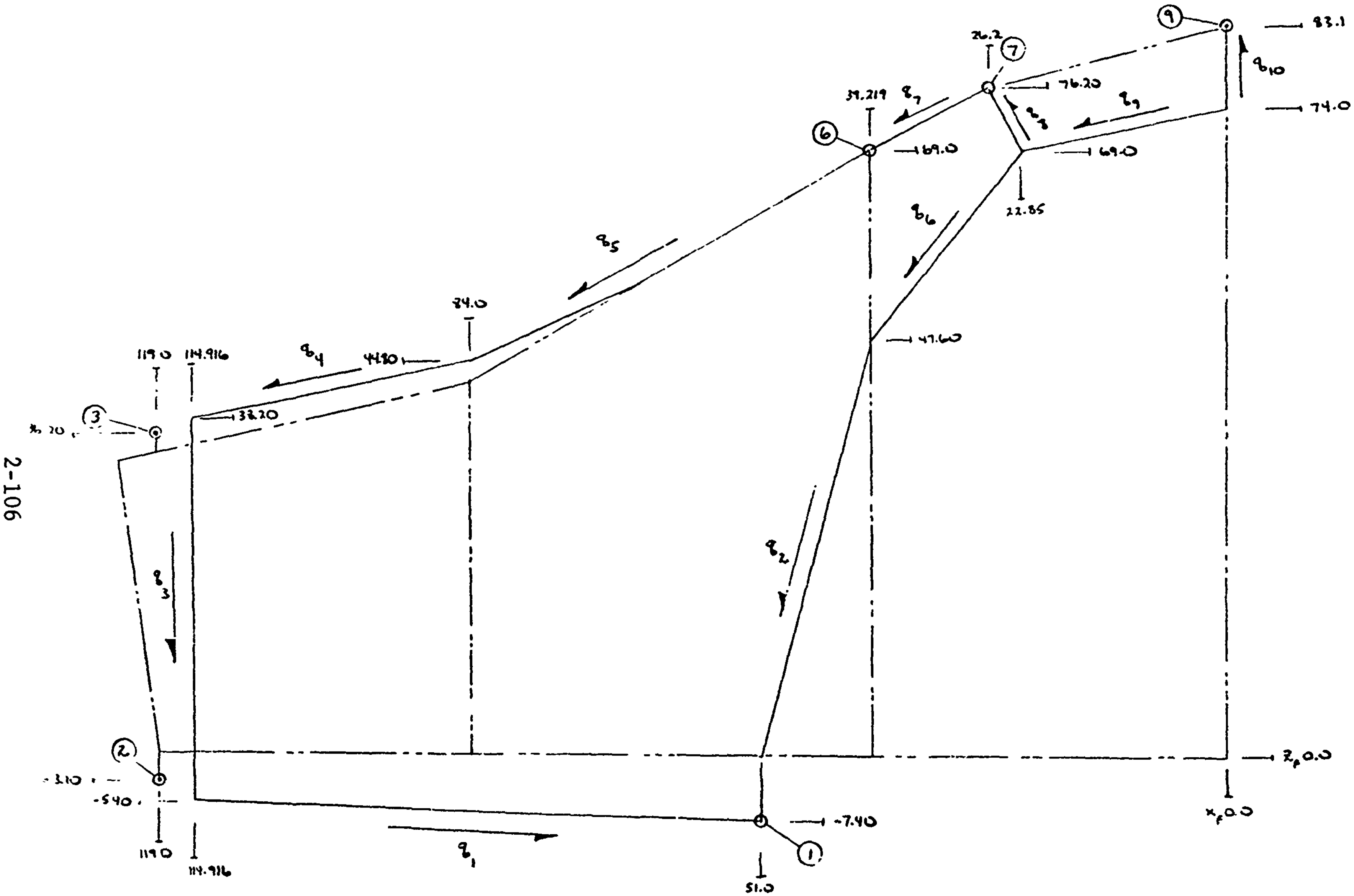


FIGURE 2-24

$Y_F$ 932 GEOMETRY FOR CAD PANEL POINT LOADS RESOLUTION

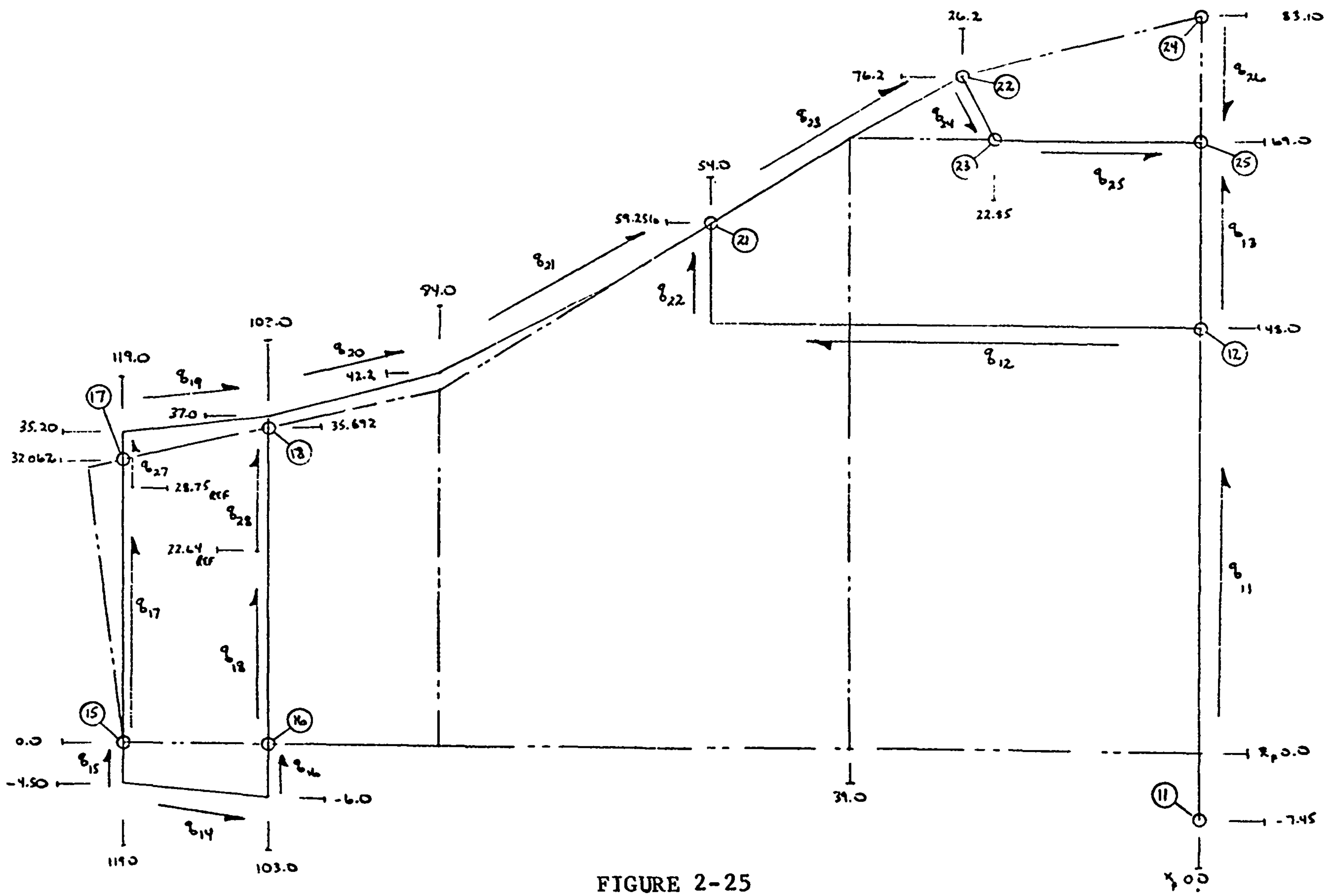


FIGURE 2-25

$Y_F$ 992 GEOMETRY FOR CAD PANEL POINT LOADS RESOLUTION

TABLE II-14

AMAVS $Y_F$932 Bulkhead Shear Flow Summary

Input for Node Point Distribution

| Convair Condition | $q_1$ | $q_2$ | $q_3$ | $q_4$ | $q_5$ | $q_6$ | $q_7$ | $q_8$ | $q_9$ | $q_{10}$ |
|---|---|---|---|---|---|---|---|---|---|---|
| 1000 S | 330.64 | -204.15 | -1104.81 | 2363.35 | 1745.72 | -285.06 | 1210.48 | - 93.74 | -103.69 | -19.29 |
| 1000 A | -20.70 | 33.30 | -149.47 | 33.33 | 24.62 | 39.71 | -239.01 | -187.61 | -72.58 | 0 |
| 2000 | 1097.21 | 104.24 | 868.98 | 2880.91 | 2128.02 | 31.77 | 1609.57 | -779.22 | -160.20 | -34.51 |
| 3000 | 355.44 | -242.97 | -1246.39 | 2325.66 | 1717.88 | -329.29 | 1222.81 | -63.72 | -107.46 | -20.53 |
| 4000 | -328.43 | 171.19 | -290.13 | -1247.09 | -921.18 | 212.01 | -585.36 | -153.36 | 32.90 | 1.56 |
| 5000 | 655.51 | 5.56 | 653.30 | 2420.56 | 1787.98 | -68.12 | 1185.83 | -567.21 | -147.26 | -22.62 |
| 6000 | -720.30 | -396.52 | 676.27 | 1100.90 | 813.19 | -229.62 | 839.88 | 71.33 | -18.46 | -15.44 |
| 7000 | 421.82 | 709.84 | 944.47 | 1166.33 | 861.52 | 776.13 | 718.61 | -1189.30 | -25.00 | -32.94 |
| 8 S | 135.13 | 315.80 | 604.12 | 399.14 | 294.83 | 340.88 | 286.97 | -336.46 | 267.61 | -492.89 |
| 8 A | 155.48 | -101.35 | 143.17 | 451.04 | 333.17 | -147.43 | 599.80 | 469.93 | 96.67 | 0 |
| 9000 | 854.46 | 7.7 | 490.13 | 2622.37 | 1937.04 | -74.23 | 1497.32 | -546.89 | -142.00 | -28.31 |
| 10000 | 439.21 | -234.42 | -1511.60 | 3087.65 | 2280.73 | -339.38 | 1573.18 | -185.49 | -136.70 | -27.07 |
| 11000 | -61.76 | 100.93 | -46.79 | -497.47 | -367.46 | 108.09 | -99.43 | -175.30 | -6.52 | -3.05 |

NOTES: (1) All values are lbs/in ult.

(2) Values for shear flow on ℄ are listed as 1/2 of total.

(3) Positive sign convention and location for shear flows depicted on Fig. 2-24.

TABLE II - 15

AMAVS $Y_F$992 BULKHEAD SHEAR FLOW SUMMARY Sheet 1

| Convair Condition | $q_{11}$ | $q_{12}$ | $q_{13}$ | $q_{14}$ | $q_{15}$ | $q_{16}$ | $q_{17}$ | $q_{18}$ | $q_{19}$ |
|---|---|---|---|---|---|---|---|---|---|
| 1000 S | -251.18 | -27.37 | -118.10 | -2225.00 | 8727.07 | 3343.65 | -6785.93 | -144.05 | 7096.83 |
| 1000 A | 0 | -503.18 | 0 | 1838.53 | 614.85 | 2116.74 | -2379.07 | 50.16 | -291.19 |
| 2000 | -304.66 | -134.90 | -177.89 | 2437.43 | 5164.57 | 4143.61 | -4178.35 | 398.60 | -8012.86 |
| 3000 | -492.68 | 2.97 | -128.14 | -1195.35 | 9463.69 | 3516.92 | -7296.91 | -144.57 | 7807.75 |
| 4000 | 319.39 | 131.45 | 18.17 | -886.47 | -570.16 | -1621.81 | 1163.06 | -190.94 | 321.90 |
| 5000 | -766.22 | -168.25 | -226 65 | 1506.85 | 2541.31 | 3368.84 | -2912.02 | 325.80 | -8281.35 |
| 6000 | -1895.39 | -475.03 | -486.53 | 561.60 | 3808.79 | 2126.45 | -1964.54 | -594.37 | 6263.29 |
| 7000 | -689.06 | -274.20 | -450.60 | 820.92 | 3668.01 | 2090.01 | -2365.17 | -777.38 | 4281.16 |
| 8 S | -564 12 | -271.82 | -349.79 | 112.03 | 1640.29 | 916.85 | -537.20 | -404.33 | 3206.16 |
| 8 A | 0 | 63.53 | 0 | -176.31 | 1255.32 | 466.92 | -336.22 | -253.56 | 705.04 |
| 9000 | -291.10 | -97.50 | -183.70 | 1783.06 | 5169.86 | 3754.95 | -4608.45 | 302.05 | -6906.79 |
| 10000 | -286.68 | -5.00 | -115.40 | -2145.55 | 11321.40 | 4585.12 | -9223.17 | -94.65 | 10390.60 |
| 11000 | 145.90 | 143.48 | -72.7 | -586.83 | 465.43 | -672.96 | -364.28 | -95.27 | -4489.54 |

NOTES: (1) All loads are lbs/in ult.

(2) Values for shear flow on ℄ are listed as 1/2 of total.

(3) Positive sign convention and location for shear flows depicted on Figure 2-25

TABLE II - 15
AMAVS $Y_F$992 BULKHEAD SHEAR FLOW SUMMARY Sheet 2

| Convair Condition | $q_{20}$ | $q_{21}$ | $q_{22}$ | $q_{23}$ | $q_{24}$ | $q_{25}$ | $q_{26}$ | $q_{27}$ | $q_{28}$ |
|---|---|---|---|---|---|---|---|---|---|
| 1000 S | 345.14 | 864.04 | -177.01 | -611.24 | -100.02 | -788.46 | -749.07 | -10471.37 | -262.56 |
| 1000 A | -12.63 | -31.62 | -396.68 | 512.24 | -189.31 | 209.44 | 0 | -3671.15 | 91.43 |
| 2000 | -209.72 | -525.01 | -206.33 | -434.76 | -634.74 | 694.40 | -682.48 | -6447.98 | 726.57 |
| 3000 | 369.92 | 926.08 | -171.19 | 697.73 | -73.52 | 861.13 | -809.51 | -11259.86 | -263.53 |
| 4000 | -54.09 | -135.40 | 80.80 | -46.19 | 23.11 | -183.53 | 196.08 | 1794.72 | -348.05 |
| 5000 | -270.71 | -677.71 | -154.44 | -724.75 | -522.08 | 380.79 | -253.25 | -4493.54 | 593.86 |
| 6000 | 123.67 | 309.60 | -620.33 | 73.54 | 853.94 | 761.89 | -35.58 | -3031.47 | -1083.41 |
| 7000 | 11.98 | 29.99 | -539.48 | -204.87 | 469.48 | 645.30 | -100.26 | -3649.70 | -1417.00 |
| 8 S | -.88 | -2.20 | -389.90 | -227.33 | 747.67 | 437.05 | 224.25 | -697.69 | -819.68 |
| 8 A | -24.10 | -60.34 | 18.47 | -78.36 | 200.86 | 98.97 | 0 | -403.34 | -465.28 |
| 9000 | -189.99 | -475.63 | -175.34 | -416.92 | -574.96 | 626.00 | -575.64 | -7111.29 | 550.57 |
| 10000 | 508.19 | 1272.22 | -206.81 | 1000.88 | -62.81 | 1088.90 | -1105.93 | -14233.26 | -172.53 |
| 11000 | -254.61 | -637.40 | 95.69 | -493.86 | -310.24 | -126.03 | 198.14 | -562.11 | -173.65 |

these to the node points, and adds the X and Z components of the longeron loads to the shear flows where applicable.

Using the pivot loads from Table II-3 and sweep actuator loads from Table II-9 simultaneous equations were written and solved to obtain lug loads in the place of the lugs and shear link load. The problem is statically determinate from the six force and moment equations available, but the number of equations was reduced to five by utilizing the sweep actuator loads from Table II-9 as known values rather than utilizing $M_z$ from Table II-3 and formulating the problem with the sweep actuator load as an unknown. A sketch of the geometry used is shown in Figure 2-26. The results are summarized in Table II-16. The inplane values were then resolved in the math model global coordinate system. A summary of the resolved loads is shown in Table II-17. These loads were then distributed over the lug panel points. Only the X and Y components of the upper lug loads were applied to the math model because the required Z boundary restraints of TN1 produced Z components. (See AFFDL-TR-73-40.) Sweep actuator loads applied to the actuator pivot point were beamed in a rational manner to panel points on the closure rib and on the $X_F$ 84 rib.

Link loads were applied at a panel point coincident to the closure rib and the upper cover at $X_F$ 123.06, $Y_F$ 969.5, $Z_F$ 31.985.

Landing gear loads were beamed in a rational manner to appropriate panel points.

All of the panel point loads for a given condition were then applied to a freebody of the wing carrythrough structure and forces and moments were summed, with the moment center being $Y_F$ 992, $Z_F$ 0. Utilizing the results of this operation (i.e., net WCTS unbalance), balance loads were calculated and applied as discussed in Section 2.2.1.2. After integrating the balance loads into the panel point loads, the balance was rechecked. A set of panel point loads for a typical condition (AS2000) are shown in Table II-18.

In using procedure TN1, forces cannot be applied to nodes which have been put in boundary. Consequently, force components in the direction of boundary restraints at boundary nodes were not entered as applied loads in the TN1 input. The omitted values are circled on the AS2000 data sheets presented.

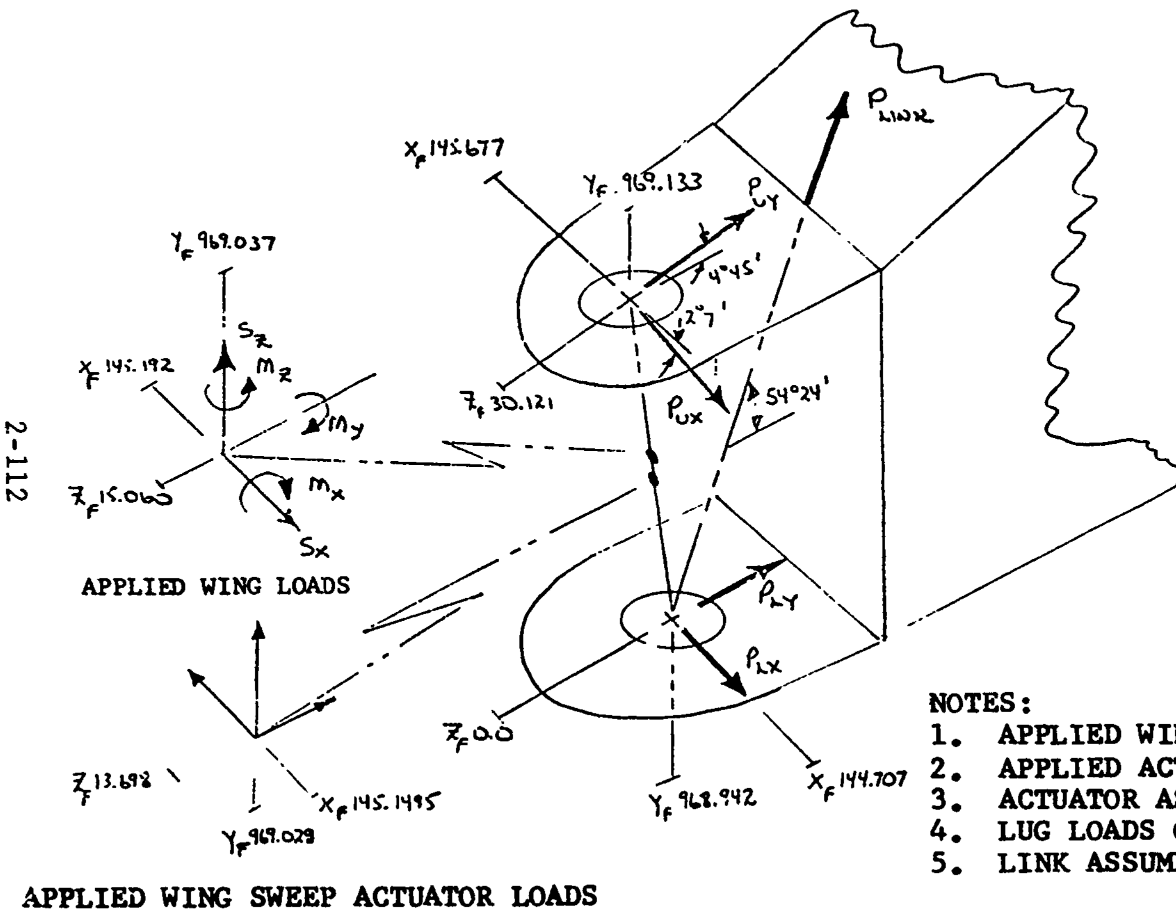


NOTES:
1. APPLIED WING LOADS, REFERENCE TABLE II-5
2. APPLIED ACTUATOR LOADS, REFERENCE TABLE II-5
3. ACTUATOR ASSUMED IN TENSION
4. LUG LOADS ORIENTED AS SHOWN IN PLANE OF LUGS
5. LINK ASSUMED IN COMPRESSION

Figure 2-26 GEOMETRY FOR DETERMINATION OF WCTS LUG LOADS

TABLE II-16

SUMMARY OF APPLIED IN-PLANE LUG LOADS AND SHEAR LINK LOADS

| CONVAIR COND. | $\Lambda$ | $P_{UX}$ LBS.ULT. | $P_{UY}$ LBS.ULT. | $P_{LX}$ LBS.ULT. | $P_{LY}$ LBS.ULT | $P_{LINK}$ LBS.ULT. |
|---|---|---|---|---|---|---|
| AS 1000 | 67.5° | -2,114,632 | 1,263,002 | 2,269,787 | -1,508,652 | 58,129 |
| 1000A | 67.5° | -252,646 | 74,596 | 309,616 | -158,950 | 9883 |
| AS 2000 | 15° | -887,383 | 3,373,592 | 894,619 | -3,464,658 | 36,416 |
| AS 3000 | 67.5° | -2,317,083 | 1,287,388 | 2,376,995 | -1,395,188 | 47,017 |
| AS 4000 | 15° | 195,488 | -1,022,949 | -242,745 | 1,503,300 | 14,394 |
| AS 5000 | 15° | -407,444 | 2,909,325 | 450,378 | -3,365,895 | 30,002 |
| AS 6000 | 15° | 82,890 | -459,645 | -97,002 | 311,963 | -8606 |
| AS 7000 | 15° | 146,922 | -650,758 | -146,796 | 659,071 | -18,538 |
| AS 8000 | 15° | 73,476 | -325,376 | -73,413 | 329,532 | -9269 |
| 8000A | 15° | 0 | 0 | 0 | 0 | 0 |
| AS 9000 | 25° | -1,045,068 | 3,185,941 | 1,060,580 | -3,260,942 | 11,640 |
| AS 10000 | 67.5° | -2,841,164 | 1,585,370 | 3,046,589 | -1,902,974 | 63,309 |
| AS 11000 | 67.5° | -282,831 | 458,220 | -202,482 | 215,047 | -3675 |

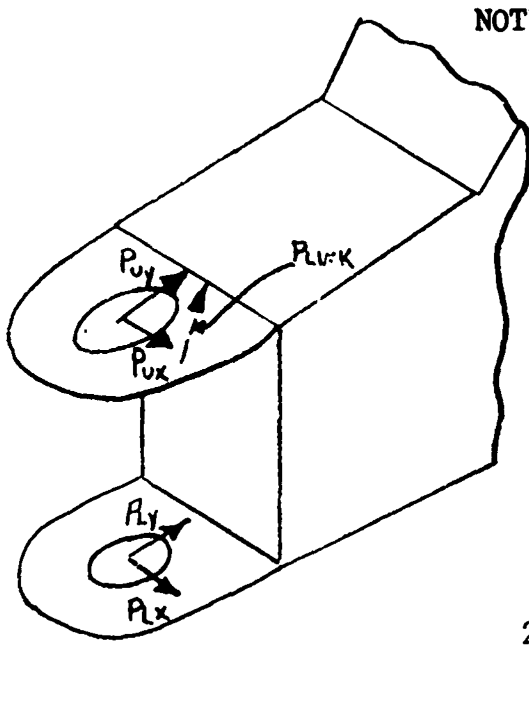

NOTES: (1) POSITIVE CONVENTION SHOWN

(2) LUG LOADS ARE IN PLANE OF LUG

(3) LOADS INCLUDE EFFECT OF WING SWEEP ACTUATOR

(4) SHEAR LINK LOADS SHOWN ARE AS APPLIED TO WCTS; SKETCH INDICATES COMPRESSIVE LINK LOAD

TABLE II-17

Summary of Applied Pivot Loads in Global Coordinate System

| Convair Condition | $\Lambda$ | UPPER LUG | | | LOWER LUG | | | SHEAR LINK | | |
|---|---|---|---|---|---|---|---|---|---|---|
| | | $F_x$ | $F_y$ | $F_z$ | $F_x$ | $F_y$ | $F_z$ | $F_x$ | $F_y$ | $F_z$ |
| 1000 S | 67.5° | -1,258,670 | -2,113,194 | 182,683 | 1,508,652 | 2,269,787 | 0 | -33,797 | 0 | 47,294 |
| 1000 A ▷ | 67.5° | -7,576 | -241,876 | 9,568 | 132,162 | 320,214 | 0 | -5,746 | 0 | 13,981 |
| 2000 | 15° | -3,362,021 | -886,780 | 312,138 | 3,464,658 | 894,619 | 0 | -21,173 | 0 | 29,628 |
| 3000 | 67.5° | -1,282,972 | -2,315,507 | 192,178 | 1,395,188 | 2,376,995 | 0 | -27,336 | 0 | 38,254 |
| 4000 | 15° | 1,019,440 | 195,355 | -91,930 | -1,503,300 | -242,745 | 0 | -8,369 | 0 | 11,711 |
| 5000 | 15° | -2,899,346 | -407,167 | 255,968 | 3,365,895 | 450,378 | 0 | -17,443 | 0 | 24,410 |
| 6000 | 15° | 458,068 | 82,834 | -41,124 | -311,963 | -97,002 | 0 | 5,004 | 0 | -7,002 |
| 7000 | 15° | 648,526 | 146,822 | -59,315 | -659,071 | -146,796 | 0 | 10,778 | 0 | -15,083 |
| 8 S | 15° | 324,260 | 73,426 | -29,658 | -329,532 | -73,413 | 0 | 5,389 | 0 | -7,541 |
| 8 A ▷ | 15° | -42,770 | -26,027 | 4,516 | 51,636 | -26,027 | 0 | 0 | 0 | -4,516 |
| 9000 | 25° | -3,175,013 | -1,044,357 | 302,422 | 3,260,94[illegible] | 1,060,580 | 0 | -6,768 | 0 | 9,470 |
| 10000 | 67.5° | -1,579,932 | -2,839,232 | 236,209 | 1,902,974 | 3,046,589 | 0 | -36,808 | 0 | 51,509 |
| 11000 | 67.5° | -456,648 | -282,639 | 48,390 | -215,047 | -202,482 | 0 | 2,137 | 0 | -2,990 |

NOTES:
(1) All loads are lbs ult.
(2) Loads include effect of wing sweep actuator.
(3) Loads are listed as applied to WCTS.
(4) Reference sketch for positive sign convention.
(5) ▷ Assymmetric conditions include balance loads applied to lugs.

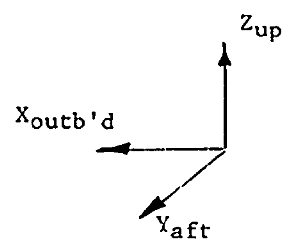

Table II-18 PANEL POINT LOADS, CONDITION AS 2000

## I LUG LOADS

### UPPER LUG LOADS

NBB MODEL
COND AS
2000
DATE
90573

TOTAL LUG FX=
-3362021
TOTAL LUG FY=
-886780

| | NODE | +FX ACTS OUTBD<br>+FY ACTS AFT | |
|---|---|---|---|
| $F_x$ | 882 | FX4= | -531199.318 |
| | 883 | FX5= | -726196.536 |
| | 885 | FX6= | -847229.292 |
| | 886 | FX7= | -726196.536 |
| | 887 | FX8= | -531199.318 |
| $F_y$ | 901 | FY1= | -140111.240 |
| | 880 | FY2= | -191544.480 |
| | 881 | FY3= | -223468 |
| | 882 | FY4= | -191544.480 |
| | 883 | FY5= | -140111.240 |

### LOWER LUG LOADS

NBB MODEL
COND AS
2000
DATE
90573

TOTAL LUG FX=
3464658
TOTAL LUG FY=
894619

| | NODE | +FX ACTS OUTBD<br>+FY ACTS AFT | |
|---|---|---|---|
| $F_x$ | 896 | FX10= | 547415.964 |
| | 908 | FX11= | 748366.128 |
| | 916 | FX12= | 873093.816 |
| | 884 | FX1= | 748366.128 |
| | 907 | FX2= | 547415.964 |
| $F_y$ | 874 | FY7= | 141349.802 |
| | 875 | FY8= | 193237.704 |
| | 876 | FY9= | 225443.988 |
| | 896 | FY10= | 193237.704 |
| | 903 | FY11= | 141349.802 |

END COND AS

## II SHEAR LINK

| NODE | $F_x$ | $F_y$ | $F_z$ |
|---|---|---|---|
| 751 | -10587 | 0 | 14814 |
| 753 | -10587 | 0 | 14814 |

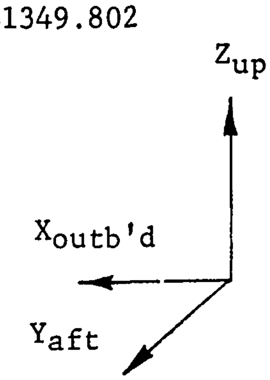

TABLE II - 18 Cont'd.

NODE POINT LOADS

COND 2000
MODEL N.B.B.

## III WING SWEEP ACTUATOR FITTING LOADS

| NODE | $F_X$ | $F_Y$ | $F_Z$ |
|---|---|---|---|
| 737 | -39439 | -20338 | 1382 |
| 739 | -41246 | -20690 | 1382 |
| 510 | 0 | 16604 | -54 |
| 513 | 0 | 16604 | -54 |

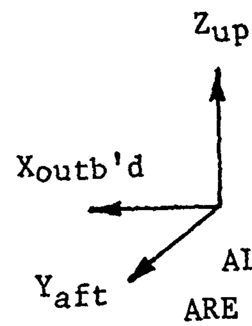


ALL LOADS ARE LBS ULT.

NOTES:
1. These values for use with TN1 program.
2. Values shown are loads fitting applies to CTB.
3. Revised 17 May 73 for latest geometry.

## IV LANDING GEAR FITTINGS

| TRUNNIONS | NODE | $F_X$ | $F_Y$ | $F_Z$ |
|---|---|---|---|---|
| | 606 | 0 | 0 | 0 |
| OUTBOARD | 627 | 0 | 0 | 0 |
| INBOARD | L.G. | 0 | 0 | 0 |
| | BAL. | 0 | 0 | -23245 |
| | 467 | 0 | 0 | -23245 |
| | 420 | 0 | 0 | 0 |

TABLE II - 18 Cont'd.

MODE POINT LOADS

COND. 2000
MODEL N.B.B.

IV CONT.

| SIDE BRACE FITTING | NODE | $F_X$ | $F_Y$ | $F_Z$ |
|---|---|---|---|---|
| Lo L/H | 296 | 0 | 0 | 0 |
| Lo R/H | 291 | 0 | 0 | 0 |
| Up $\mathbb{C}_L$ :LD GR | X | 0 | 0 | 0 |
| SHEAR | X | 0 | 0 | -3549 |
| TOTAL | 116 | 0 | 0 | -3549 |

DRAG BRACE:

| NODE | $F_X$ | $F_Y$ | $F_Z$ |
|---|---|---|---|
| 476 | 0 | 0 | 0 |
| 257 | 0 | 0 | 0 |
| 277 | 0 | 0 | 0 |
| 317 | 0 | 0 | 0 |
| 279 | 0 | 0 | 0 |
| 347 | 0 | 0 | 0 |
| 390 | 0 | 0 | 0 |
| 397 | 0 | 0 | 0 |
| 398 | 0 | 0 | 0 |

TABLE II - 18 Cont'd

NODE POINT LOADS

COND. 2000
MODEL N.B.B.

V ARMAMENT LOADS.

| NODE | LOAD SOURCE | $F_X$ | $F_Y$ | $F_Z$ |
|---|---|---|---|---|
| | ARM | 0 | 0 | -6731 |
| | BAL. | 0 | 0 | -11623 |
| 14 | | 0 | 0 | -18354 |
| | ARM | 0 | 0 | -6731 |
| | BAL. | 0 | 0 | -11623 |
| 17 | | 0 | 0 | -18354 |

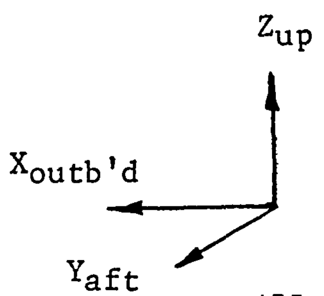


ALL LOADS LBS ULT.

TABLE II - 18 Cont'd.

$Y_F$ 932 FW BLKHD NODE POINT LOADS

COND. 2000 NBB (ALL LDS ULT)

| 9820 NODE NO. | NODE NO. | $F_X$ | $F_Y$ | $F_Z$ |
|---|---|---|---|---|
| 1 | 3 | 0 | -186286 | 1086 |
| 2 | 9 | -921 | 0 | 42 |
| 3 | 35 | -1687 | 0 | +313 |
| 4 | 92 | -1955 | 0 | -2943 |
| 5 | 95 | 12925 | -277963 | -1187 |
| 6 | 162 | 26361 | -92387 | -8630 |
| 7 | 231 | 27154 | 0 | -16237 |
| 8 | 359 | 24132 | 0 | -12321 |
| 9 | 461 | 20216 | 0 | -9534 |
| 10 | 499 | 20814 | 0 | -7142 |
| 11 | 545 | 18351 | 0 | -3918 |
| 12 | 601 | 16940 | 0 | -3601 |
| 13 | 626 | 20512 | 0 | -4379 |
| 14 | 646 | 17170 | 0 | -3659 |
| 15 | 685 | 5647 | 0 | -2844 |
| 16 | 714 | 0 | 104630 | -7868 |
| 16 1/2 | 716 | 19854 | 0 | 0 |
| 17 | 678 | 0 | 0 | -4166 |
| 17 1/2 | 761 | 0 | 0 | -4489 |
| 18 | 687 | 0 | 0 | -10793 |

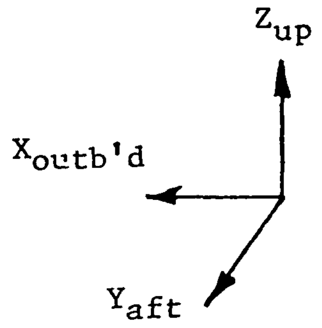


$\Sigma F_x = 240,690$

$\Sigma F_y = -13$

$\Sigma F_z = -130,697$

ALL LDS LB ULT.

XX IN BOUNDARY

TABLE II - 18 Cont'd

$Y_F$ 932 FWD BLKHD NODE POINT LOADS Cont'd

COND. 2000 NBB (ALL LDS ULT)

| 9820 NODE NO. | NODE NO. | $F_X$ | $F_Y$ | $F_Z$ |
|---|---|---|---|---|
| 19 | 688 | 0 | 0 | -8307 |
| 20 | 719 | 0 | 0 | -41128 |
| | 743 | 45183 | 0 | 0 |
| 21 | 733 | 0 | 238121 | 34246 |
| 22 | 710 | -955 | 0 | -2412 |
| 23 | 690 | -2919 | 0 | -203 |
| 24 | 663 | -3489 | 0 | -247 |
| 25 | 602 | -2875 | 0 | -203 |
| 26 | 586 | -3116 | 0 | -219 |
| 27 | 516 | -4169 | 0 | -291 |
| 28 | 448 | -5486 | 0 | -384 |
| 29 | 382 | -5684 | 0 | -400 |
| 30 | 315 | -2662 | 187737 | -567 |
| 31 | 266 | 288 | 26135 | -1637 |
| 32 | 251 | 630 | 0 | -2481 |
| 33 | 237 | 432 | 0 | -1482 |

TABLE II - 18 Cont'd

$Y_F$ 992 AFT BLKHD NODE POINT LOADS

COND. 2000 NBB (ALL LDS ULT)

| 9820 NODE NO. | NODE NO. | $F_X$ | $F_Y$ 1 | $F_Z$ |
|---|---|---|---|---|
| 1 | 207 | 0 | -77257 | -1135 |
| 2 | 220 | 0 | 0 | -2963 |
| 3 | 181 | 0 | 0 | -5286 |
| 4 | | | | |
| 5 | | | | |
| 6 | 55 | 0 | 0 | -3123 |
| 7 | 26 | -287 | 2315 | -1839 |
| 8 | 30 | 0 | 0 | -1868 |
| 9 | 36 | -1476 | 42314 | 3945 |
| 10 | 21 | 0 | 308205 | 7257 |
| 11 | 48 | -3472 | 0 | 0 |
| 12 | 70 | -4253 | 0 | 0 |
| 13 | 88 | -4462 | 0 | 0 |
| 14 | 85 | -1142 | 87022 | 2285 |
| 15 | | | | |
| 16 | 33 | -1500 | 0 | 0 |
| 17 | 66 | -1710 | 0 | 0 |
| 18 | | | | |

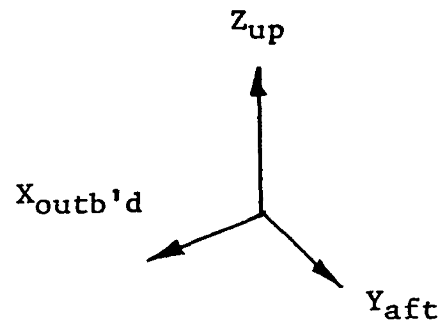


$F_x$ = 214,700

$F_y$ = 0.0

$F_z$ = 153,772

All loads are lbs. ult.

xx — In Boundary

1 $F_y$ modified to to force balance

TABLE II - 18 Cont'd.

$Y_F$ 992 AFT BLKHD NODE POINT LOADS Cont'd

COND. 2000 NBB (ALL LDS ULT.)

| 9820 NODE NO. | NODE NO. | FX | FY 1 | FZ |
|---|---|---|---|---|
| 19 | 123 | -1069 | 0 | 0 |
| 20 | 174 | -1248 | 0 | 0 |
| 21 | 235 | -1032 | 0 | 0 |
| 22 | 267 | -438 | 0 | -1161 |
| 23 | 94 | 3784 | 230651 | 720 |
| 24 | 164 | 4630 | 0 | -5495 |
| 25 | 201 | 3326 | 0 | -2117 |
| 26 | 258 | 4301 | 87578 | -5619 |
| 27 | 371 | 4725 | 0 | -2809 |
| 28 | 418 | 4988 | 0 | -2636 |
| 29 | 542 | 4356 | 0 | -1996 |
| 30 | 594 | 1992 | 0 | -545 |
| 31 | 642 | 16813 | 0 | -3464 |
| 32 | 686 | 31250 | 0 | -7212 |
| 33 | 715 | 15224 | 0 | -13585 |
| 34 | 724 | -83197 | 363432 | -24069 |
| 35 | 736 | 0 | 0 | -30720 |
| 36 | 725 | 0 | 0 | -32382 |

TABLE II - 18 Cont'd

$Y_F$ 992 AFT BLKHD NODE POINT LOADS Cont'd.

COND. 2000 NBB (ALL LDS ULT.)

| 9820 NODE NO. | NODE NO. | $F_X$ | $F_Y$ 1 | $F_Z$ |
|---|---|---|---|---|
| 37 | 732 | 0 | 0 | -40112 |
| 38 | 763 | 199991 | -881481 | -28052 |
| 39 | 731 | -7008 | 0 | 10731 |
| 40 | 712 | -16063 | 0 | -1828 |
| | 708 | -3436 | 0 | 0 |
| 41 | 668 | -9078 | 0 | 11492 |
| 42 | 660 | 69122 | -184459 | 11766 |
| 43 | 658 | 0 | 0 | 3827 |
| 44 | 657 | 0 | 0 | 3886 |
| 45 | 638 | 0 | 0 | 5466 |
| 46 | 641 | -8231 | 21680 | 5703 |

### 2.2.3 NBB Stress Analysis

The stress analysis of the "No-Box Box" configuration during Phase II consisted of three primary areas of effort:

1. Finite element modeling of the complete carrythrough box.

2. Finite element and other computer based analysis for local areas.

3. Manual stress analysis conducted as a continuing part of the support of on-board design and production drawing analysis.

Where buckling or static strength considerations governed fastener or member sizes, a 10% positive margin of safety was maintained to allow for the gross weight increase (Section 2.2.1). In areas where fatigue was critical, reduced allowable ultimate stresses were used (Section 2.3 ). Material properties were taken from standard sources such as MIL-HDBK5 and from data generated specifically for the less common materials used for AMAVS design (Section 2.4 ).

#### 2.2.3.1 <u>Overall Box Analysis</u>

To obtain a consistent set of internal loads and stresses for the overall carrythrough box, finite element models were constructed for use with Convair Computer Procedure TN1 (Ref. AFFDL-TR-73-40, Par. 2.2.2.1). Membrane and bar elements were used. The models had approximately 868 nodes and 1942 elements. Because of relatively major changes in the configuration and load updating, several model iterations were made. The current conditions run with the model available during drawing sign out are summarized in Table II-19. An updated model will be developed when production drawings are substantially completed in order to verify or revise the final design prior to fabrication.

#### 2.2.3.2 <u>Local Areas - Computer Analysis</u>

Local area analyses using finite element procedures included the following:

1. Upper lug stability checks - NASTRAN procedure. Includes upper lug and upper plate inboard to $X_F$ 84.

2. Closure rib stability checks - NASTRAN procedure.

TABLE II-19

NBB TN1 LOG
CURRENT DESIGN LOAD CONDITIONS

| RUN DESIGNATION | JOB NO. | DATE | CHARGE TIME | CONDITIONS |
|---|---|---|---|---|
| NBB 4-1 | 18495 | 9/14/73 | 48.22 MIN | AS 2000, 7000, 9000, 10000 |
| NBB 4-2 | 185362 | 9/21/73 | 48.58 MIN | AS 4000, 5000, 6000, 11000 |
| NBB 4-3 | 185363 | 9/21/73 | 71.13 MIN | AS 1000 L/H, 1000 R/H, 3000 |

3. Lower lug stress distribution - TLO linear strain procedure. (See AFFDL-TR-73-40 Par. 2.2.2.2 for TLO description.)

4. Lower aft outboard longeron tab stress distribution - TLO procedure.

5. Lower plate material distribution studies - TR4 procedure (essentially same as TN1).

6. $Y_F$ 992 bulkhead transition radius stress distribution - TLO procedure.

7. Sandwich panel load introduction studies - TN1.

### 2.2.3.3 Detailed Manual Stress Analysis

The computer analyses discussed in Sections 2.2.4.1 and 2.2.4.2 were supplemented by conventional manual stress analyses in the following general areas. Where feasible, the HP 9820 capability was used to make various standard solutions. Internal loads were derived from the finite element models in most cases.

1. Determination of net section stresses.

2. Fastener pattern checks.

3. Computation of margins of safety.

4. Stability analyses for plates, sandwich panels, and stiffeners.

5. Splice analyses.

6. Fitting analyses.

## 2.2.4 Fail Safe Integral Lug

As in the case of the NBB configuration, the stress analysis of the FSIL configuration consisted of three primary areas of effort (See 2.2.3). Although the NBB configuration was chosen for production, the FSIL was also analyzed during Phase II since both configurations were carried well into the final design stage before configuration selection.

2.2.4.1 Overall Box Analysis

Convair procedure TN1 was used with finite element models of the overall box. Membrane and bar elements were used. The models had approximately 801 nodes and 1790 elements. Several model iterations were made. A summary of the last set of conditions run prior to configuration selection is shown in Table II-20.

2.2.4.2 Local Areas - Computer Analysis

Local area analyses using finite element procedures included the following:

1. Lower lug stress distributions - TLO linear strain procedure.

2. Upper lug stability checks - A3S procedure (Ref. Par. 2.2.2.5, AFFDL-TR-73-40).

3. Upper forward outboard plate stability check - NASTRAN and A3S procedures.

4. Lower plate damage tolerance studies - overall TN1 model with elements cut to simulate crack.

5. Braze shear and peel stress studies - TLO linear strain procedure.

2.2.4.3 Detailed Manual Stress Analysis

The discussion for NBB para. 2.2.4.3, is generally applicable to FSIL also.

## 2.2.5 Common and Miscellaneous

2.2.5.1 Common Items

Stress analyses using conventional methods were performed for the sweep actuator fitting, the MLG drag brace fitting, the MLG side brace fitting and the MLG inboard and outboard trunnion fittings. These items were substantially common to both configurations. Additional analyses were performed to assure that changes made to tailor the parts for NBB were structurally adequate.

TABLE II-20

FSIL TN1 LOG
CURRENT DESIGN LOAD CONDITIONS

| RUN DESIGNATION | JOB NO. | DATE | CHARGE TIME | CONDITIONS | REMARKS |
|---|---|---|---|---|---|
| FSIL-6-1 | 184936 | 9/14/73 | 31.90 MIN. | AS 2000, 7000, 9000, 10000 | QUAD ELEMENTS SIMULATED WITH RECTANGULAR ELEMENTS (SEE BELOW) |
| FSIL-6-2 | 184944 | 9/14/73 | 32.50 MIN. | AS 4000, 5000, 6000, 11000 | SAME AS 6-1 |
| FSIL-6-3 | 184948 | 9/24/73 | 45.43 MIN | AS 1000 L/H, 1000 R/H,3000 | SAME AS 6-1 |
| FSIL-6-1 | 184936 | 9/26/73 | 34.06 MIN | AS 2000, 7000, 9000, 10000 | RERUN TO CORRECT ELEMENT SIMULATION (SEE NOTES) |

NOTES: QUAD ELEMENTS ON OUBD END OF [illegible] 932 BULKHEAD INCORRECTLY IDENTIFIED IN TNI PROGRAM AS RECTANGULAR ELEMENTS. FSIL-6-1 CONTAINS CRITICAL LOAD CONDITIONS FOR THIS STRUCTURE AND WAS RERUN TO OBTAIN CORRECT INTERNAL LOADS. OTHER CONDITIONS NOT CRITICALLY AFFECTED BY THIS SITUATION.

2.2.5.2 Miscellaneous

The following items were included in miscellaneous analyses:

1. 603FTB052 test specimen (Manual).

2. 603FTB053 test specimen (Manual).

3. 603FTB035 test specimen (TNI)

4. Studies of grid size effects (NASTRAN).

5. 603FTB004 test specimen (TLO).

## 2.2.6 Stiffness Analysis

As discussed in Para. 2.2.7 of AFFDL-TR-73-40, a stiffness requirement was furnished in the form of allowable stored elastic energy (.0739 x $10^8$ in.lbs.). The value found for the FSIL 5-3 model was .0848 x $10^8$ in.lbs. and for the NBB3-3 model it was .0661 x $10^8$ in.lbs. New runs were not made for the wing intrusion deletion configuration because ASKA stiffness conditions were not furnished to Convair. A review of box torsional deflections as reflected in relative Y deflections for the upper and lower lugs was made for AS10000 and AS10. The deflections were found to be larger for AS10000, but when the deflections were normalized on pitching moment, it was found that the NBB4 and FSIL 6 series models deflected less per inch-pound than the earlier models, i.e. they were stiffer. It was concluded, therefore, that with the deletion of the wing intrusion less virtual energy storage would occur than before so that FSIL would approach the requirement more closely while NBB would have an even greater stiffness margin.

## 2.2.7 Effect of Updated Loads on Weight

TNI models were run and the first cycle resized weights were obtained in order to gain some insight into the effect of the deletion of the wing intrusion and the load updating. The results obtained are shown in Table II-21. It may be seen that for the 67.5° condition, the weight increase on the FSIL is 284 lbs./AP and 336 lbs./AP for the NBB. It should be noted that the model box input weights are to be considered in a relative manner only. The effects of the 10% gross weight increase are not included in these values.

Table II-21 EFFECTS OF UPDATED LOADS

| MODEL RUN | CONDITION | INPUT WEIGHT | RESIZED WEIGHT | WEIGHT CHANGE 1/2 BOX | WT.CHG. AP |
|---|---|---|---|---|---|
| FSIL-5-1 No. 2 | ASKA 2 | 3853 lbs./1/2 box | 2111 lbs./1/2 box | -4 lbs. | Neg. |
| FSIL-6-1 | AS2000 | 3853 | 2107 | | |
| FSIL-5-1 No. 2 | ASKA 10 | 3853 | 1784 | +142 | +284 lbs |
| FSIL-6-1 | AS10000 | 3853 | 1926 | | |
| NBB-3-1 No. 2 | ASKA 2 | 4424 | 2438 | -3 | Neg. |
| NBB-4-1 | AS2000 | 4424 | 2435 | | |
| NBB-3-1 No. 2 | AS10 | 4424 | 2039 | +168 | +336 |
| NBB-4-1 | AS10000 | 4424 | 2207 | | |

Notes: 10% Gross Wt. Change Not Included

### 2.2.8 Simulated Fuselage

The structure referred to as the simulated fuselage consists of the two components of the test fixture which are adjacent to the WCTS. These components extend forward to $Y_F$ 850 and aft to $Y_F$ 1050. The simulated fuselage is designed such that loads applied to the WCTS are similar to the RI NARSAP math model results. In addition to required stiffness, sufficient strength is provided for static and fatigue loadings.

Several TNI math models of the upper test fixture - simulated fuselage - carrythrough structure combinations were set up and iterated to obtain longeron loads and shear flows to compare with the NARSAP results. These models are similar to the Phase Ib models (See AFFDL TR-73-40) except for the following differences:

1. Models with both FSIL and NBB boxes were run.

2. The simulated fuselage plate elements were changed to "shear only plate" which is the same type of element used in the NARSAP model.

3. The bulkhead at Sta. 1050 was changed from a full fuselage cross section planform to a configuration that reflects the cut out for the landing gear

4. Longeron and web materials, areas, and thicknesses were adjusted on an iterative basis to obtain NARSAP load distributions.

5. Wing intrusion provisions were removed.

A computer drawing of a typical model is shown in Figure 2-27. The comparison of the two Convair models and the NARSAP model are shown in Table II-22 and Table 2-23. Figures 2-28 and 2-29 give the location of the math model load points referred to in the tables. For an overall review of the test set up see Section III.

The load comparisons indicate relatively good agreement for longeron loads and shear flows in the high load carrying regions.

Where appropriate, reduced ultimate material allowables were used to assure adequate fatigue life. Where required, allowance was also made for the required 10% gross weight increase effect.

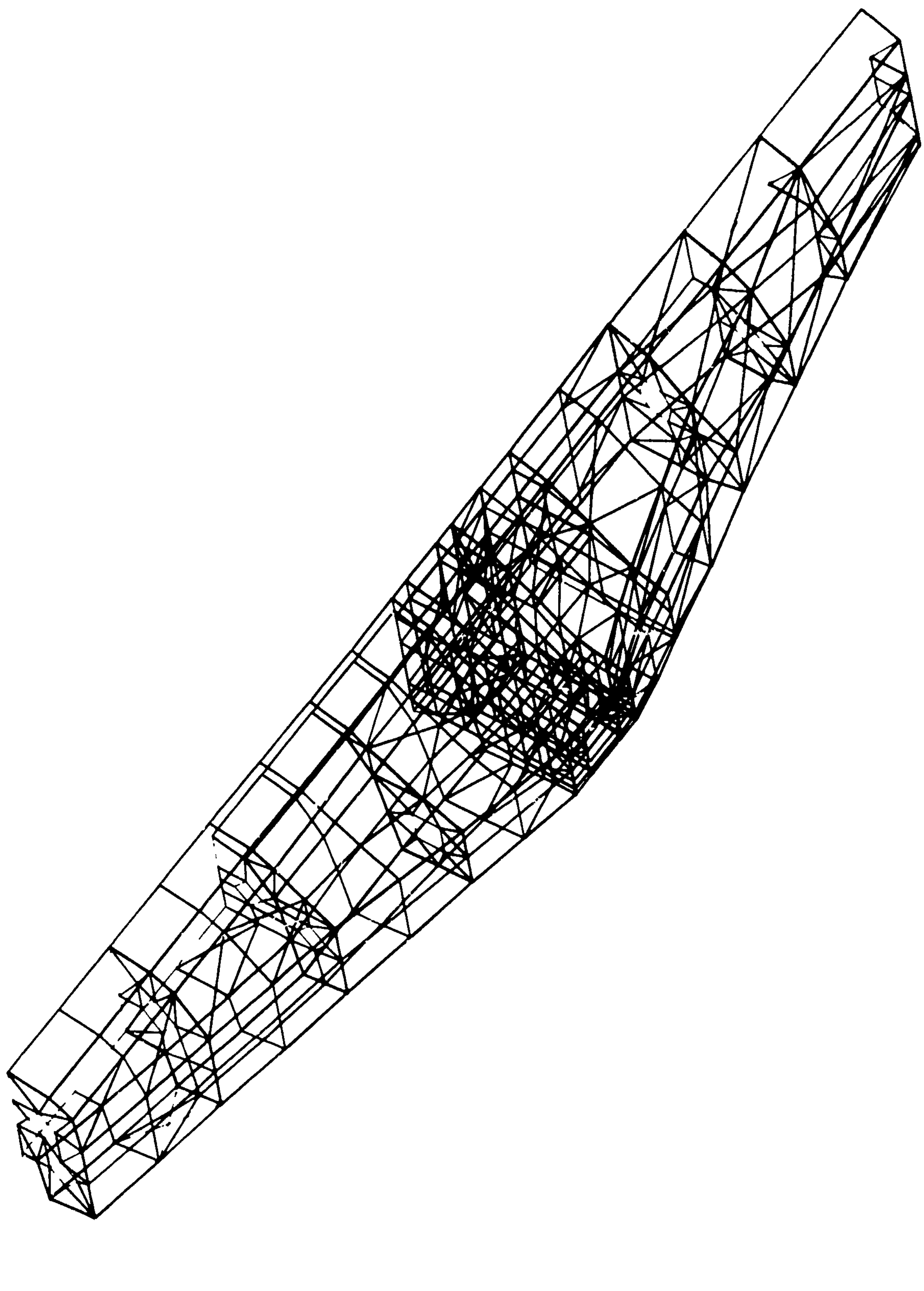

Figure 2-27 SIMULATED FUSELAGE MATH MODEL

Table II-22 CONVAIR AND NARSAP SHEAR FLOW - LBS./IN.

| | AS 2000 | | | AS 7000 | | | AS 9000 | | | AS 10000 | | |
|---|---|---|---|---|---|---|---|---|---|---|---|---|
| | FSIL | NBB | NARSAP | FSIL | NBB | NARSAP | FSIL | NBB | NARSAP | FSIL | NBB | NARSAP |
| 1 | 455 | 409 | 467 | -180 | -115 | 179 | 475 | 410 | 364 | 714 | 545 | 187 |
| 2 | -108 | -54 | 103 | 807 | 844 | 701 | -170 | -132 | 8 | -341 | -348 | -231 |
| 3 | 709 | 912 | 917 | 1097 | 905 | 997 | 255 | 503 | 517 | -1837 | -1379 | -1596 |
| 4 | 2136 | 1852 | 2163 | 515 | 582 | 876 | 1949 | 1670 | 1969 | 2075 | 1754 | 2318 |
| 5 | 2386 | 2058 | 2163 | 553 | 628 | 876 | 2193 | 1869 | 1969 | 2437 | 2038 | 2318 |
| 6 | -61 | 14 | 31 | 949 | 989 | 755 | -139 | -83 | -72 | -333 | -324 | -330 |
| 7 | 941 | 1115 | 1460 | 455 | 502 | 652 | 857 | 999 | 1358 | 914 | 1020 | 1427 |
| 8 | 670 | 505 | 634 | 375 | 407 | 967 | 574 | 411 | 445 | 462 | 250 | 151 |
| 9 | 650 | 565 | 160 | 82 | 84 | 25 | 592 | 515 | 142 | 632 | 561 | 137 |
| 10 | 100 | -100 | -61 | -604 | -316 | -58 | 146 | -32 | -50 | 288 | 120 | -48 |
| 11 | 2267 | 2422 | -606 | -1910 | -2040 | -1371 | 1878 | 2020 | -579 | 1576 | 1625 | -571 |
| 12 | 370 | 533 | -135 | -650 | -803 | -274 | 294 | 418 | -97 | -396 | -337 | -5 |
| 13 | 1758 | 1630 | -349 | -994 | -710 | -884 | 1440 | 1364 | -360 | 1572 | 1816 | -226 |
| 14 | 2415 | 440 | 904 | -647 | -685 | 305 | 1790 | 189 | 662 | -1517 | -1617 | -796 |
| 15 | -1611 | 445 | 5757 | 1185 | 1272 | 4089 | -951 | 721 | 5764 | 3639 | 3762 | 12621 |
| 16 | 3578 | -161 | 3074 | 437 | 307 | 1550 | 2963 | -57 | 2785 | 929 | 710 | 3401 |
| 17 | -6909 | -7228 | -5197 | -1517 | -1827 | -2941 | -6942 | -7205 | -5731 | -10570 | -10583 | -11470 |
| 18 | 469 | 495 | 483 | -1571 | -1430 | -941 | 193 | 183 | 366 | -1132 | -1314 | -114 |
| 19 | -4492 | -3926 | -1568 | 1209 | 1111 | 838 | -3807 | -3368 | 1351 | 748 | 385 | 2032 |
| 20 | -2024 | -1385 | -585 | 472 | 426 | 33 | -1615 | -1064 | -530 | 1554 | 1650 | 1417 |
| 21 | -2049 | 1614 | -585 | -103 | -106 | 33 | -1734 | -1366 | -530 | 687 | 742 | 1417 |
| 22 | 225 | 367 | -216 | -602 | -741 | -566 | 170 | 277 | -184 | -173 | -299 | -217 |
| 23 | -536 | -612 | -400 | -57 | -191 | -188 | -452 | -532 | -383 | 596 | 460 | 920 |
| 24 | 476 | 350 | 694 | -706 | -730 | 645 | 349 | 233 | 626 | -295 | -460 | 1089 |
| 25 | -212 | -389 | -694 | -917 | -949 | -645 | -252 | -404 | -626 | -970 | -1106 | -1089 |
| 26 | -2346 | -2078 | -1216 | 632 | 494 | -179 | -1966 | -1728 | -1025 | -2002 | -1846 | -1970 |

Table II-23 CONVAIR AND NARSAP LONGERON LOADS - KIPS

| | AS 2000 | | | AS 7000 | | | AS 9000 | | | AS 10000 | | |
|---|---|---|---|---|---|---|---|---|---|---|---|---|
| | FSIL | NBB | NARSAP | FSIL | NBB | NARSAP | FSIL | NBB | NARSAP | FSIL | NBB | NARSAP |
| 141 | -123 | -140 | -214 | - 47 | - 56 | - 81 | -105 | -117 | -176 | - 78 | - 71 | - 94 |
| 146 | 199 | 202 | 186 | 82 | 86 | 78 | 174 | 176 | 163 | 159 | 159 | 158 |
| 148 | 302 | 293 | 278 | 114 | 119 | 119 | 264 | 255 | 241 | 237 | 223 | 210 |
| 150 | 102 | 77 | 92 | 24 | 25 | 30 | 91 | 67 | 80 | 90 | 64 | 82 |
| 157 | -227 | -173 | -105 | 3 | -20 | -25 | -239 | -182 | -117 | -433 | -356 | -331 |
| 162 | -253 | -259 | -238 | -177 | -154 | -121 | -185 | -198 | -190 | 25 | -19 | -29 |
| | | | | | | | | | | | | |
| 256 | 291 | 280 | 304 | 206 | 199 | 191 | 263 | 253 | 272 | 319 | 315 | 337 |
| 257 | 40 | 26 | 42 | -4 | -9 | 14 | 34 | 20 | 37 | 12 | -4 | 39 |
| 258 | 1 | -6 | 2 | -10 | -14 | -5 | 0 | -7 | 2 | -7 | -18 | 2 |
| 259 | 274 | 282 | 228 | 190 | 197 | 174 | 249 | 256 | 207 | 289 | 303 | 235 |
| 260 | 76 | 77 | 86 | 31 | 32 | 31 | 68 | 68 | 77 | 72 | 70 | 89 |
| 262 | 97 | 79 | 86 | 69 | 66 | 55 | 89 | 73 | 79 | 85 | 85 | 65 |
| 266 | 51 | 75 | 21 | 57 | 56 | 39 | 60 | 83 | 25 | 139 | 167 | 75 |
| 267 | 274 | 334 | 359 | 254 | 279 | 318 | 345 | 399 | 423 | 1296 | 1300 | 1237 |
| 275 | -812 | -934 | -870 | -543 | -577 | -563 | -832 | -935 | -881 | -1822 | -1842 | -1755 |
| 282 | -174 | -110 | -182 | -122 | -120 | -153 | -164 | -114 | -170 | -236 | -242 | -247 |
| 286 | -120 | -103 | -77 | -127 | -109 | -100 | -111 | -96 | -71 | -148 | -133 | -78 |

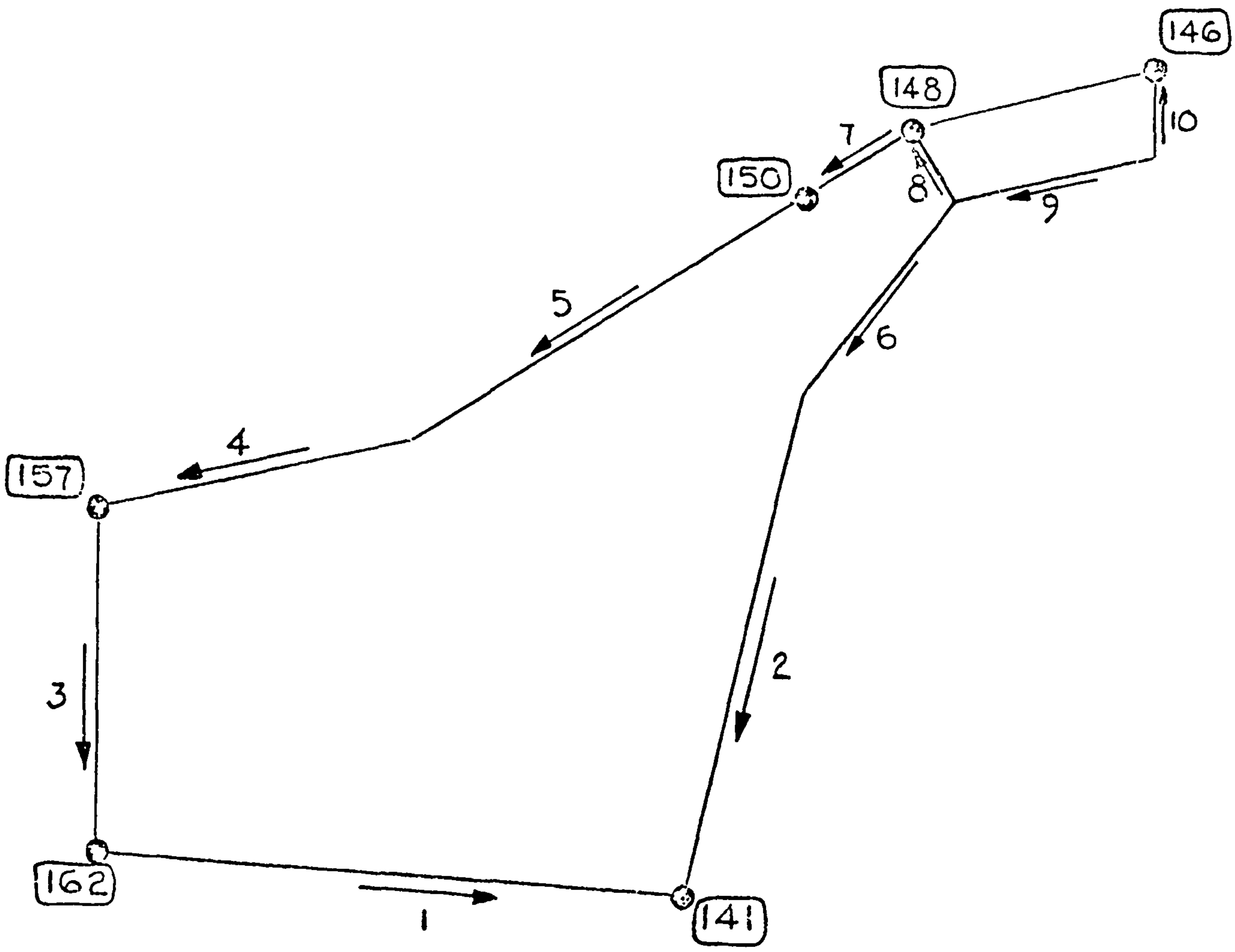


Figure 2-28 FORWARD SIMULATED FUSELAGE SHEAR FLOW AND LONGERON LOCATION DIAGRAM - $Y_F$891-932

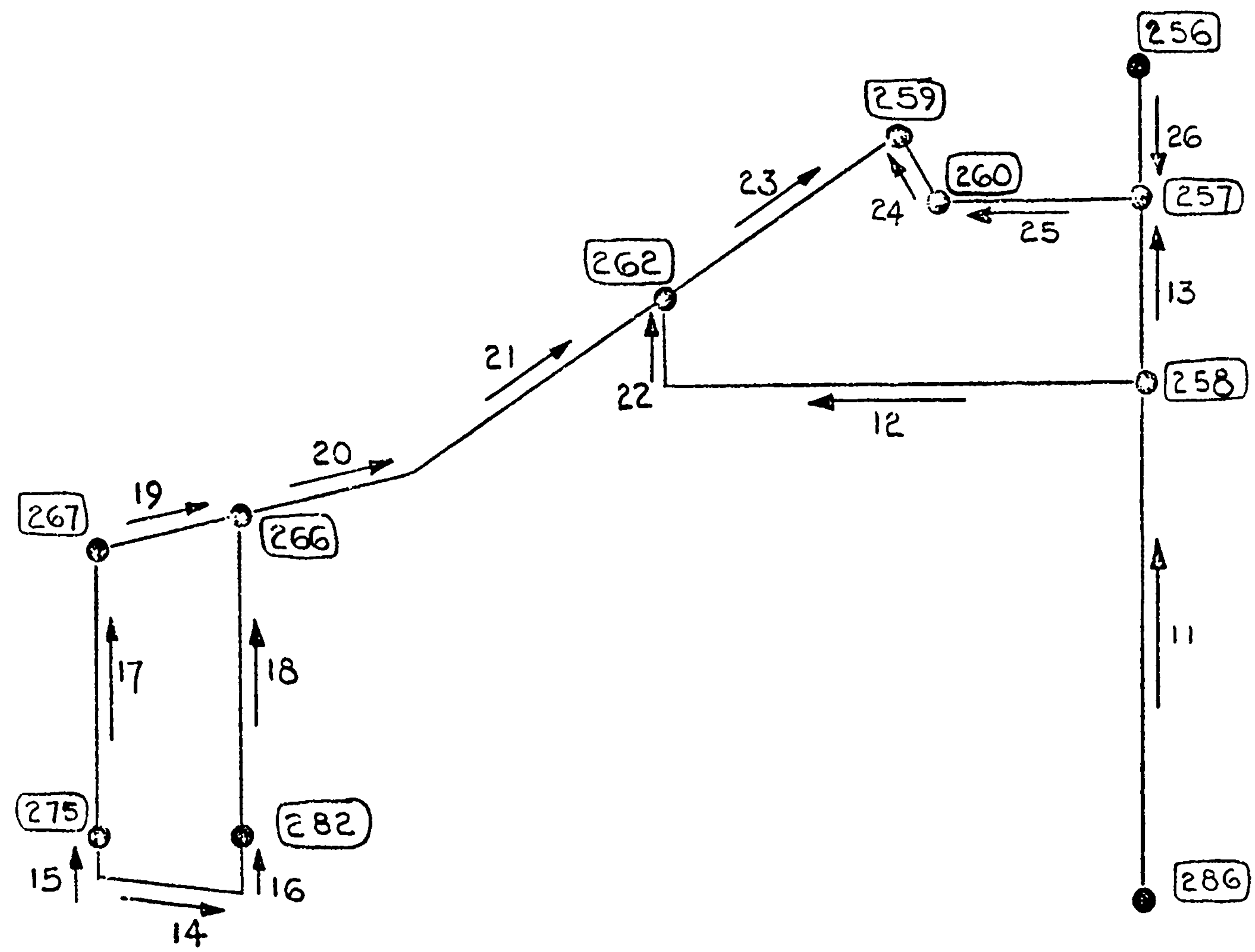


Figure 2-29 AFT SIMULATED FUSELAGE SHEAR FLOW AND LONGERON LOCATION DIAGRAM $Y_F$992-1021

## 2.3 FATIGUE AND FRACTURE ANALYSIS

Fatigue and fracture analyses were conducted to substantiate the ability of the FSIL and the NBB designs to meet the fatigue and fracture requirements specified for the baseline aircraft. The fatigue loads spectrum, the fatigue requirements, and the fracture mechanics design requirements are summarized in report AFFDL-TR-73-1.

### 2.3.1 Fatigue Analysis

Fatigue allowables were determined for both WCTS designs using the results of the stress analysis, the fatigue loads spectrum, and fatigue S/N test data. The fatigue analysis method is based on Miner's theory of cumulative damage. Fatigue allowables are based on net section effective (Von Mises yield criterion) stresses.

#### 2.3.1.1 Fatigue Test Data - Basic Materials

Conventional S/N fatigue tests were conducted on beta annealed 6Al-4V titanium plate, 10 Nickel steel plate, and Beta C titanium sheet. Flat specimens of three configurations were used: smooth ($K_T = 1$), center hole ($K_T = 2.4$), and edge notched ($K_T = 5.0$). Tests were conducted at three R ratios: R = 0.1, 0.5, and -0.5. Twenty specimen S/N curves were developed for $K_T$ of 2.4 and 5.0 at each R ratio and for $K_T = 1$ at R = 0.1. Material was oriented in the longitudinal grain direction. Fatigue properties in the longtransverse direction were spot checked by testing 5 LT specimens at each of two stress levels for $K_T = 2.4$, R = 0.1, and $K_T = 5.0$, R = 0.1.

The fatigue test data were reduced to a form suitable for computer input by constructing constant life fatigue diagrams for $K_T = 2.4$ and 5.0. Subsequently, these diagrams were used to construct a family of fatigue curves: alternating stress, $S_A$, vs cycles to failure, N, for a series of mean stress levels, $S_M$. The results are summarized in Figures 2-30 thru 2-49 as follows:

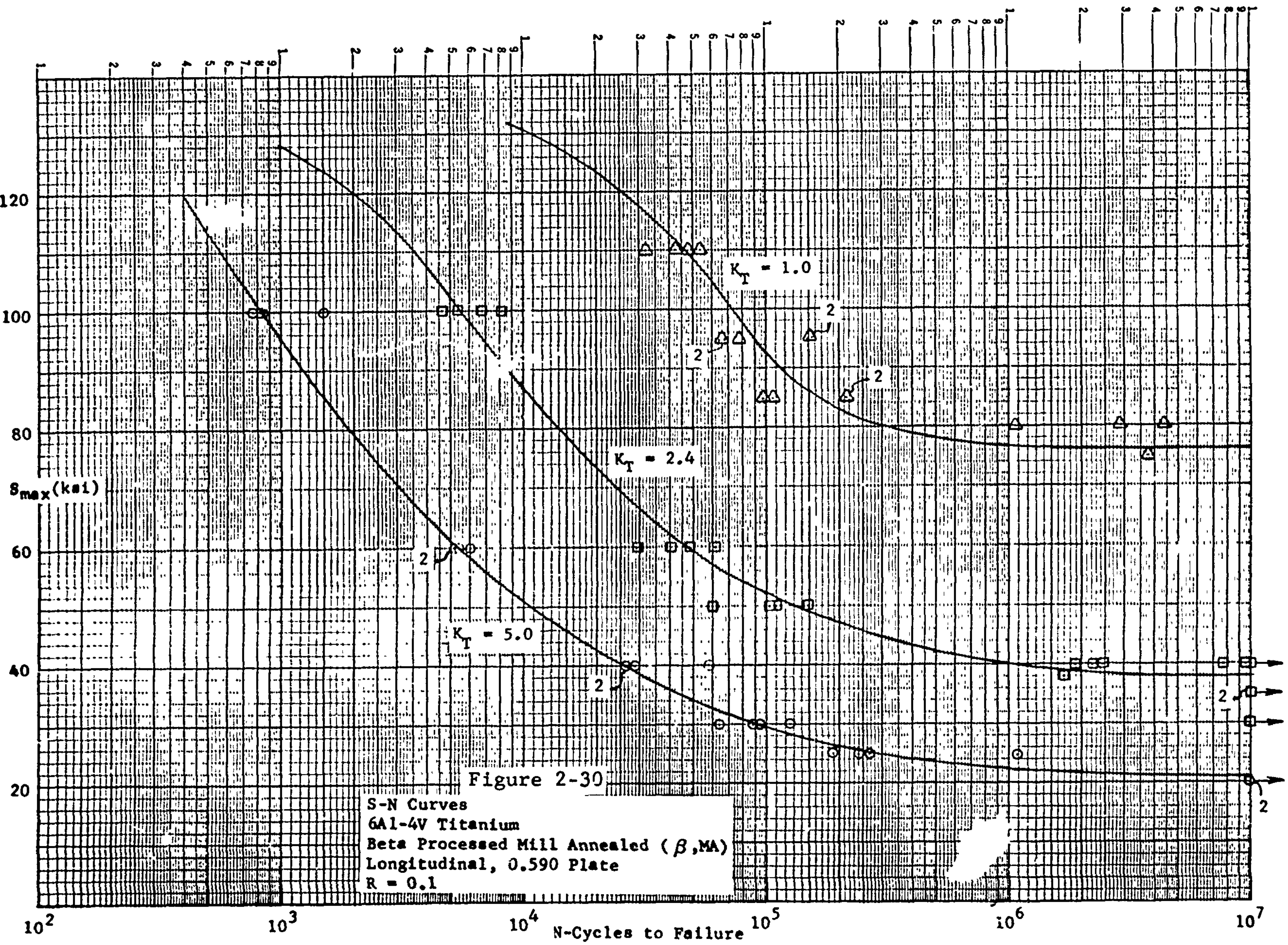


Figure 2-30

S-N Curves
6Al-4V Titanium
Beta Processed Mill Annealed ($\beta$,MA)
Longitudinal, 0.590 Plate
R = 0.1

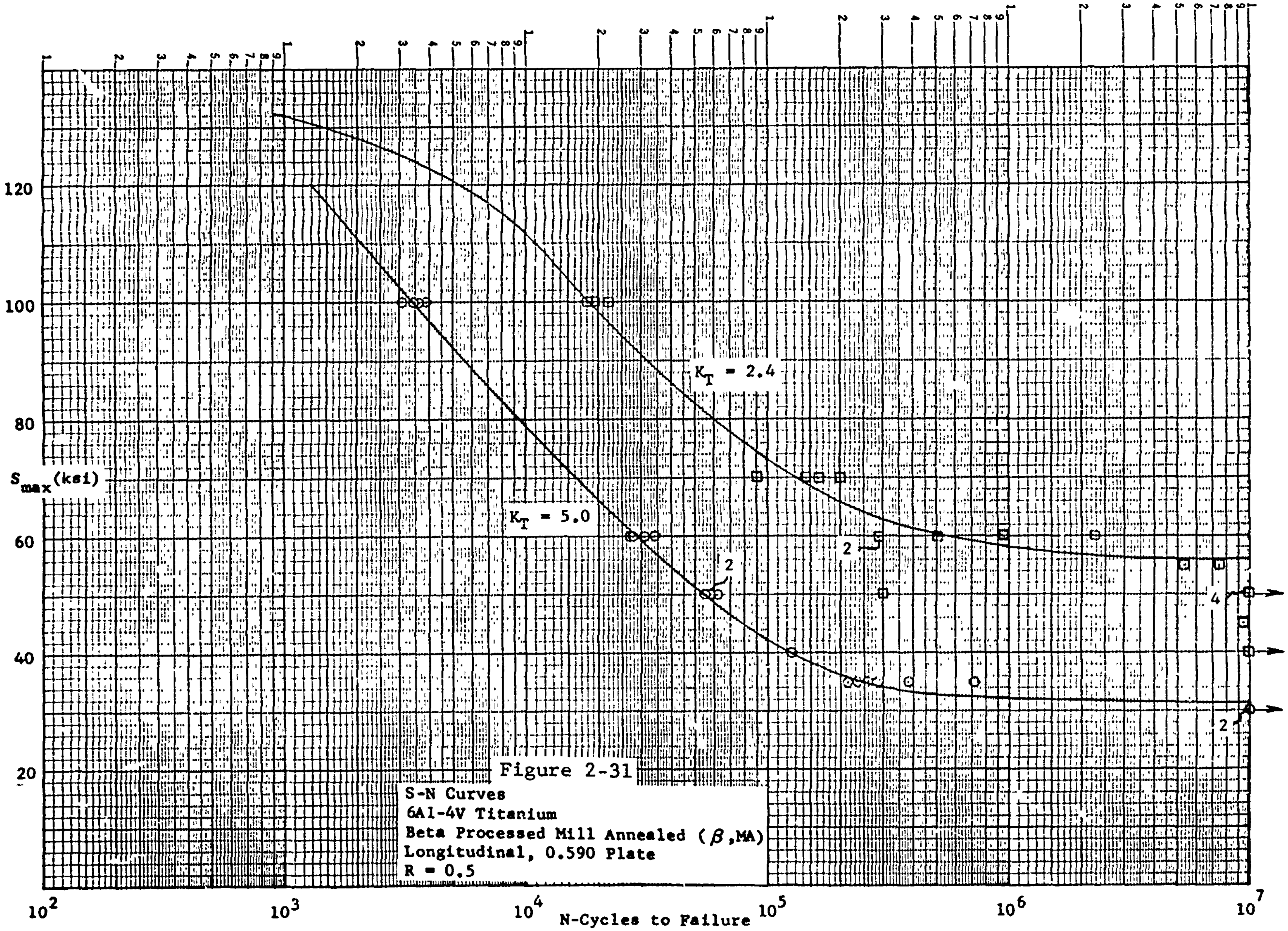


Figure 2-31
S-N Curves
6Al-4V Titanium
Beta Processed Mill Annealed ($\beta$,MA)
Longitudinal, 0.590 Plate
R = 0.5

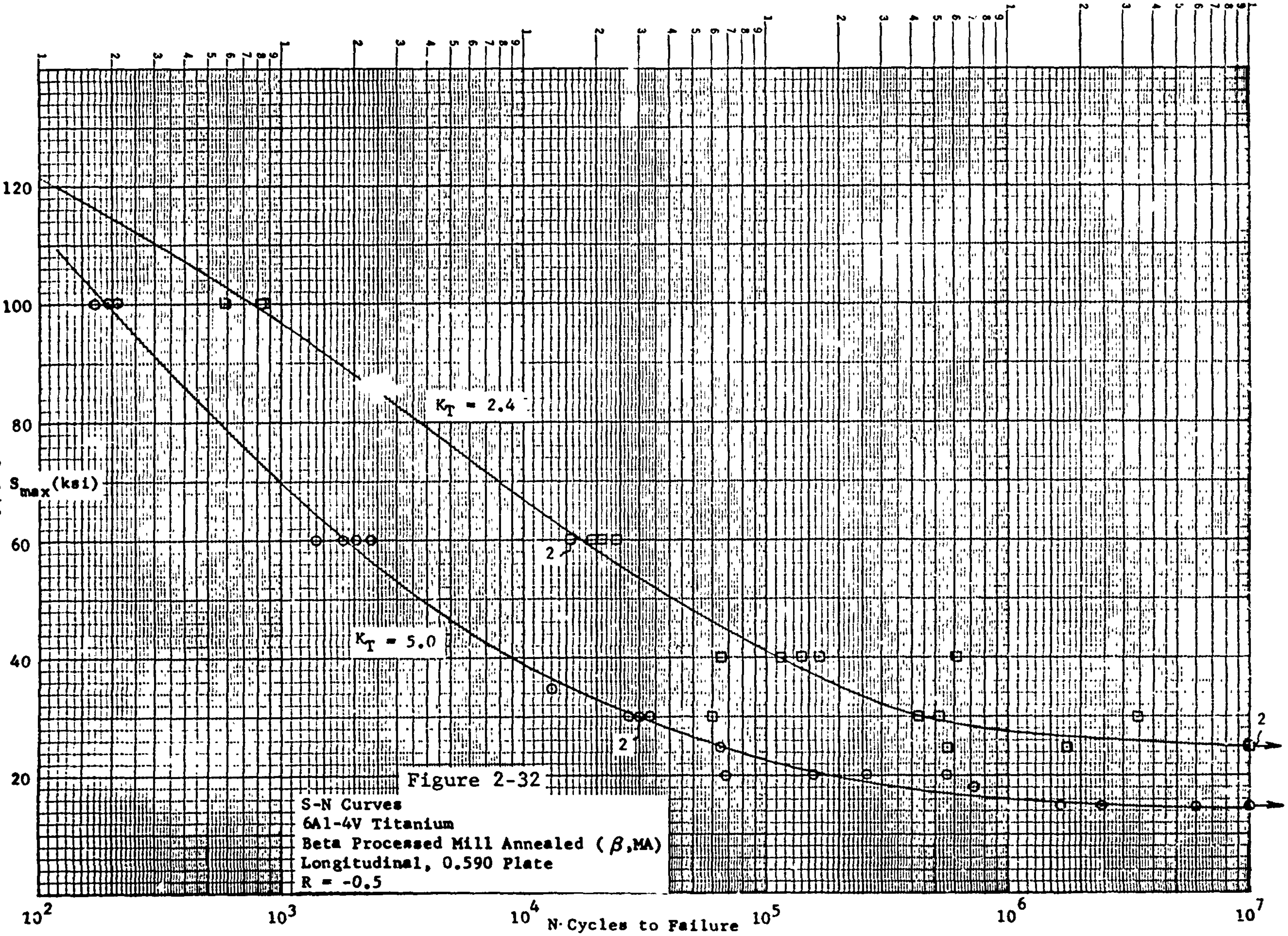


Figure 2-32

S-N Curves
6Al-4V Titanium
Beta Processed Mill Annealed ($\beta$,MA)
Longitudinal, 0.590 Plate
R = -0.5

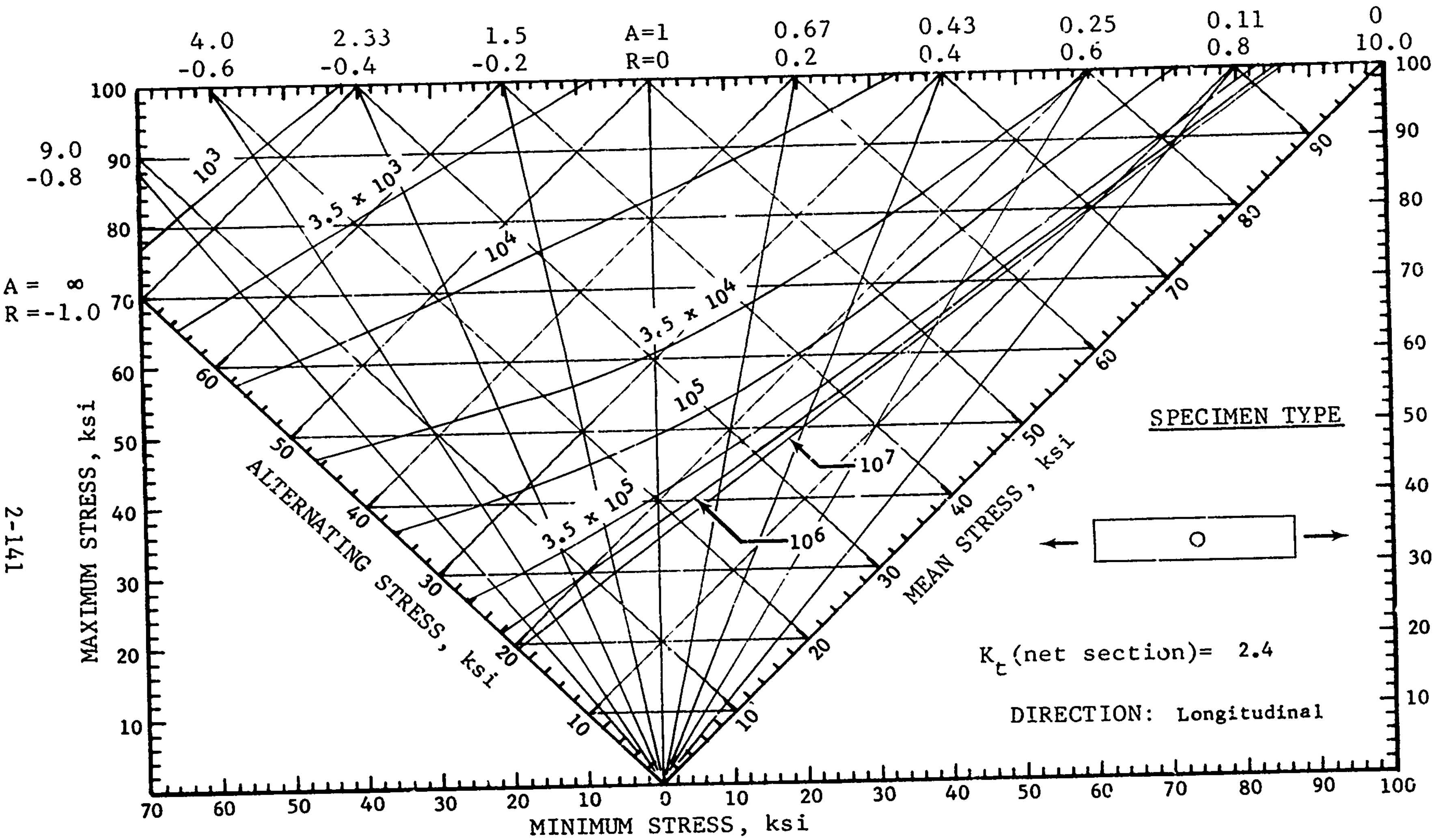


MATERIAL: 6Al-4V Ti
Beta Prcsd Mill Anld ($\beta$,MA)
FORM: 0.590 Plate

$F_{tu}$ = 130  $F_{ty}$ = 116
$F_{ntu}$ = 133  % El.= 9

TEST CONDITIONS

CYCLIC RATE: 1800 cpm
TEMPERATURE: Room

Date: October 1973

DATA SOURCE: AMAVS

Figure 2-33 CONSTANT LIFE FATIGUE DIAGRAM FOR BETA ANNEALED 6AL-4V TITANIUM $K_T$ = 2.4

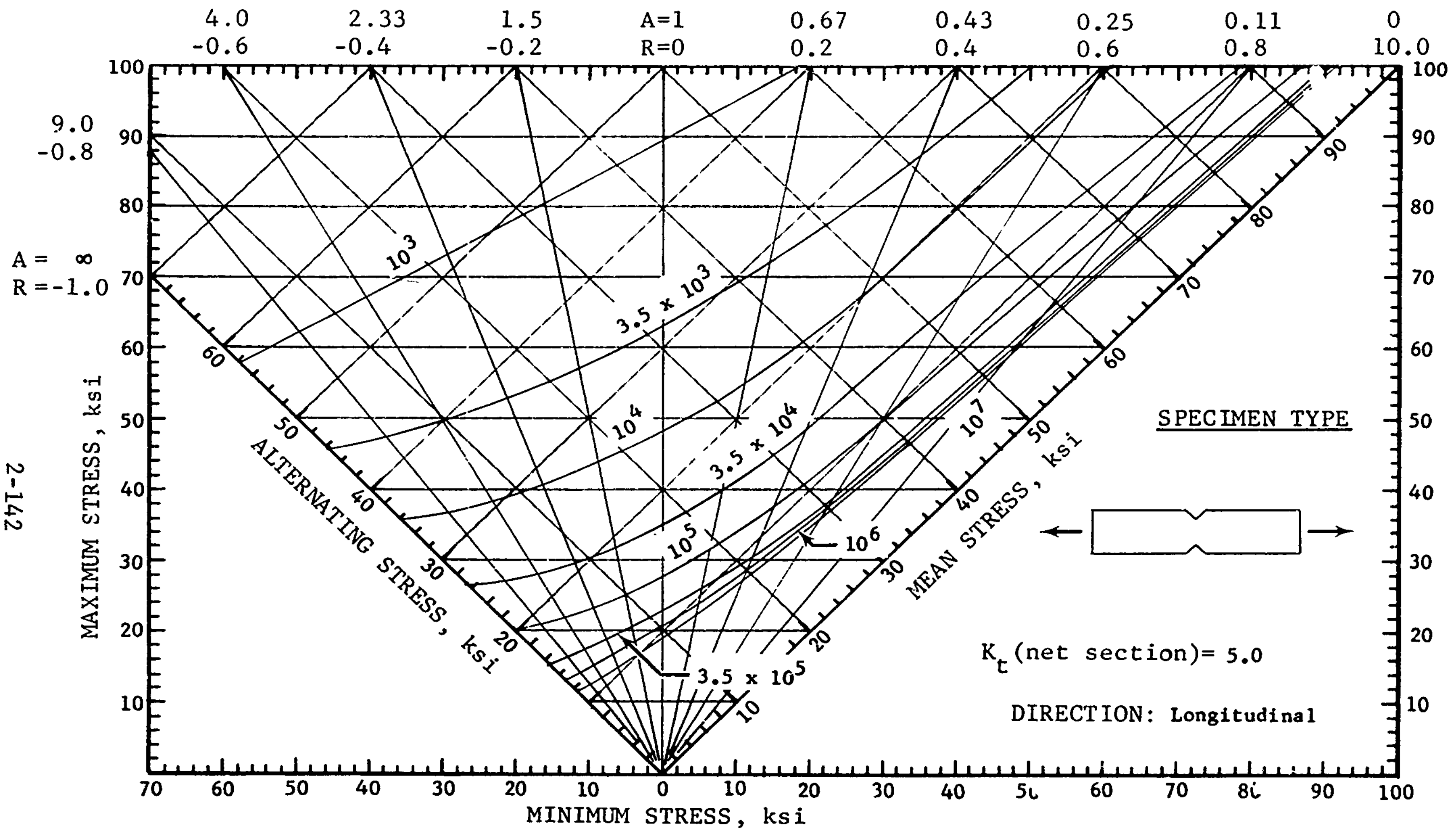


MATERIAL: 6Al-4V Ti
Beta Prcsd Mill Anld ($\beta$,MA)
FORM: 0.590 Plate

$F_{tu} = 130$ $F_{ty} = 116$
$F_{ntu} = 147$ % El. = 9

TEST CONDITIONS

CYCLIC RATE: 1800 cpm
TEMPERATURE: Room

DATA SOURCE: AMAVS

Date: October 1973

Figure 2-34 CONSTANT LIFE FATIGUE DIAGRAM FOR BETA ANNEALED 6AL-4V TITANIUM, $K_T = 5$

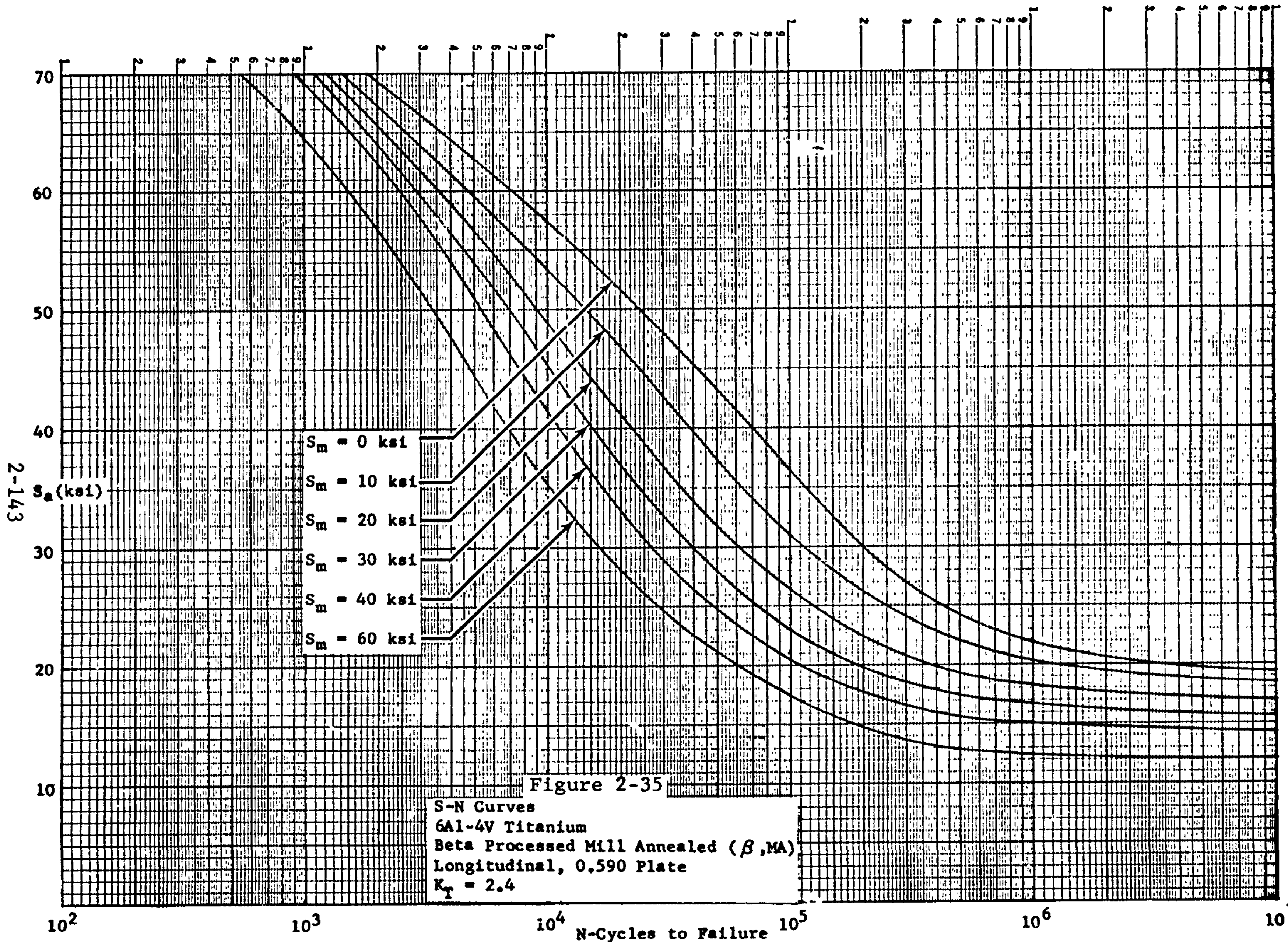


Figure 2-35

S-N Curves
6Al-4V Titanium
Beta Processed Mill Annealed ($\beta$, MA)
Longitudinal, 0.590 Plate
$K_T$ = 2.4

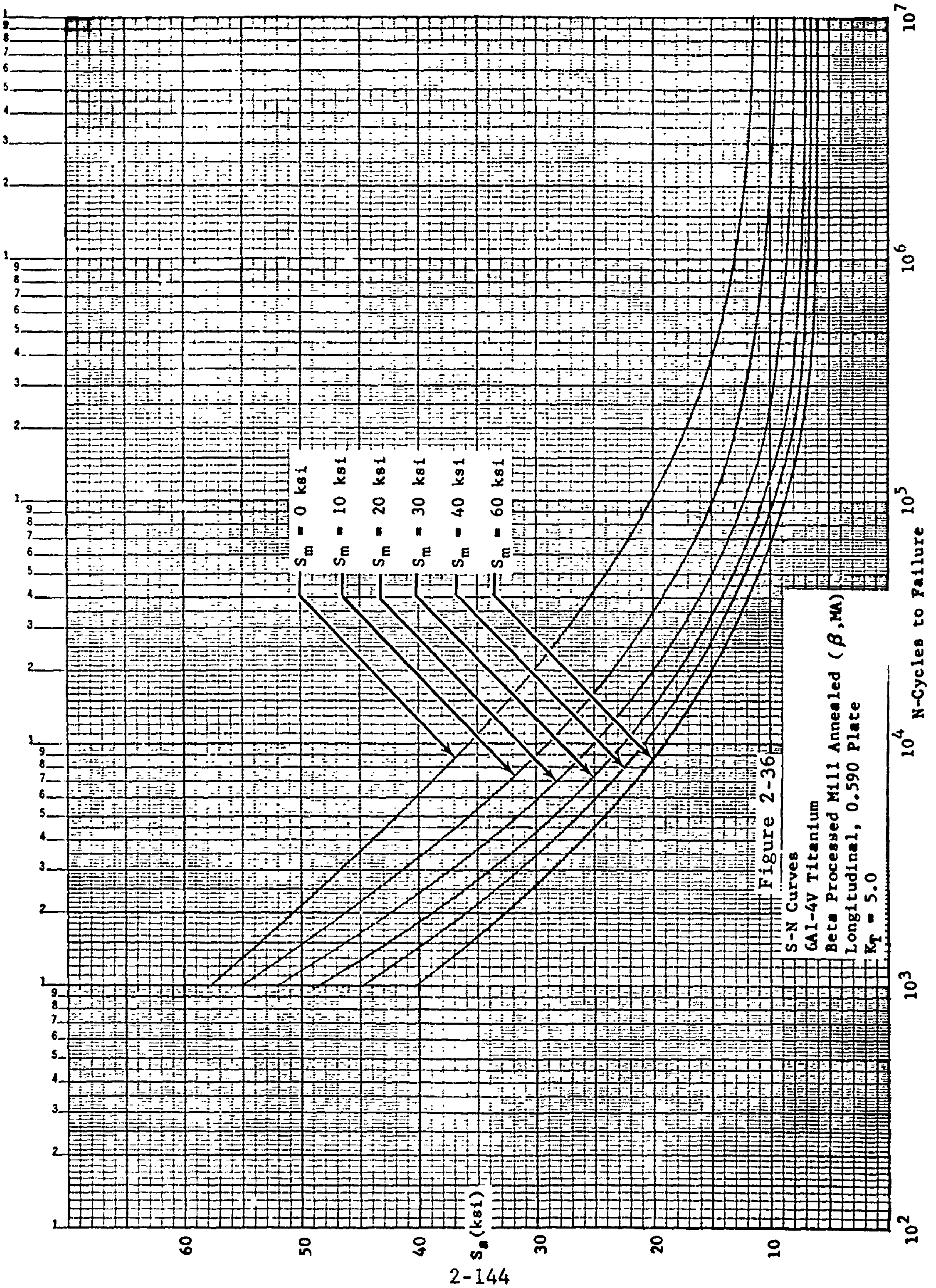


Figure 2-36

S-N Curves
6Al-4V Titanium
Beta Processed Mill Annealed ($\beta$,MA)
Longitudinal, 0.590 Plate
$K_T$ = 5.0

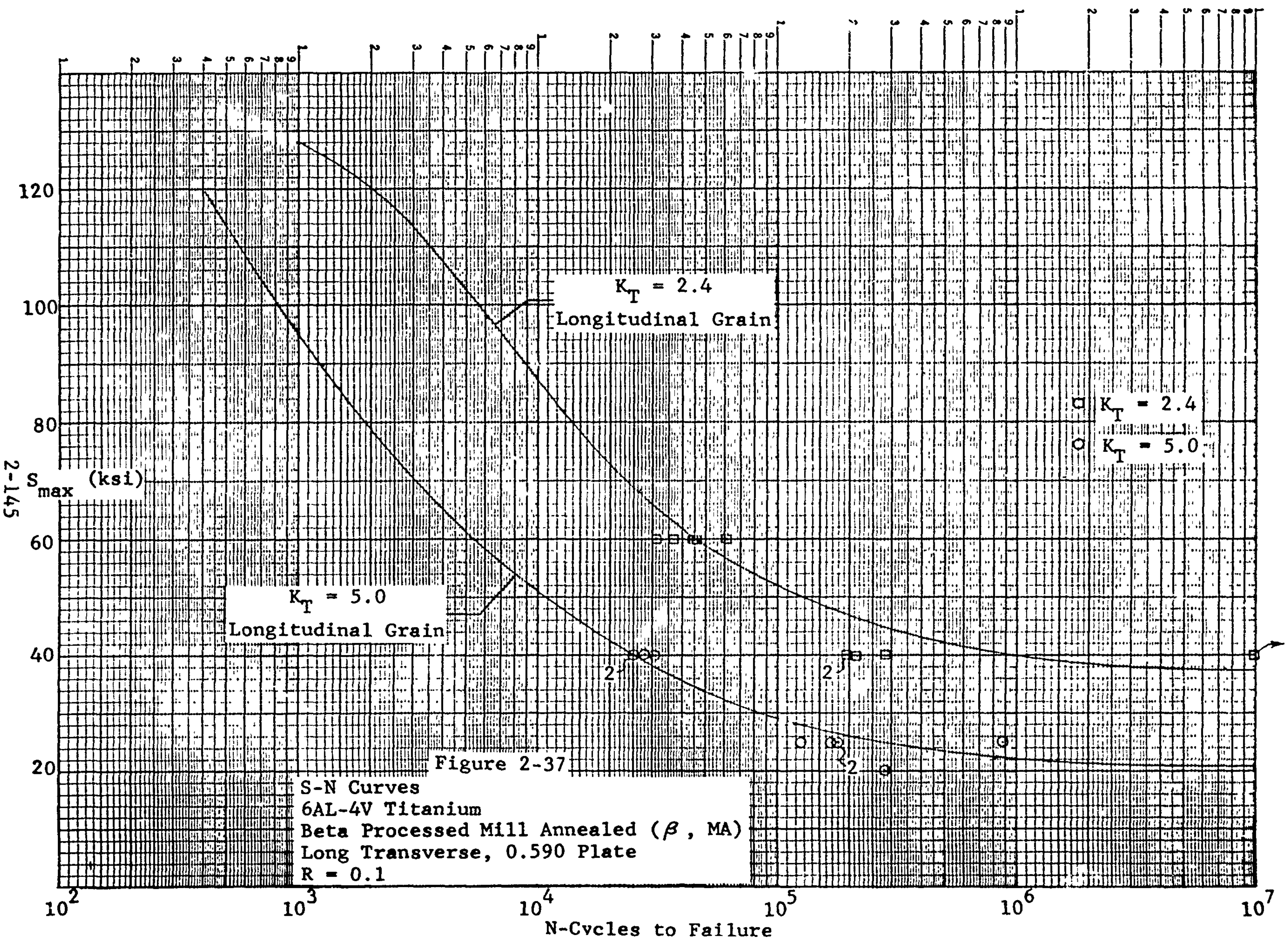


Figure 2-37
S-N Curves
6AL-4V Titanium
Beta Processed Mill Annealed ($\beta$, MA)
Long Transverse, 0.590 Plate
R = 0.1

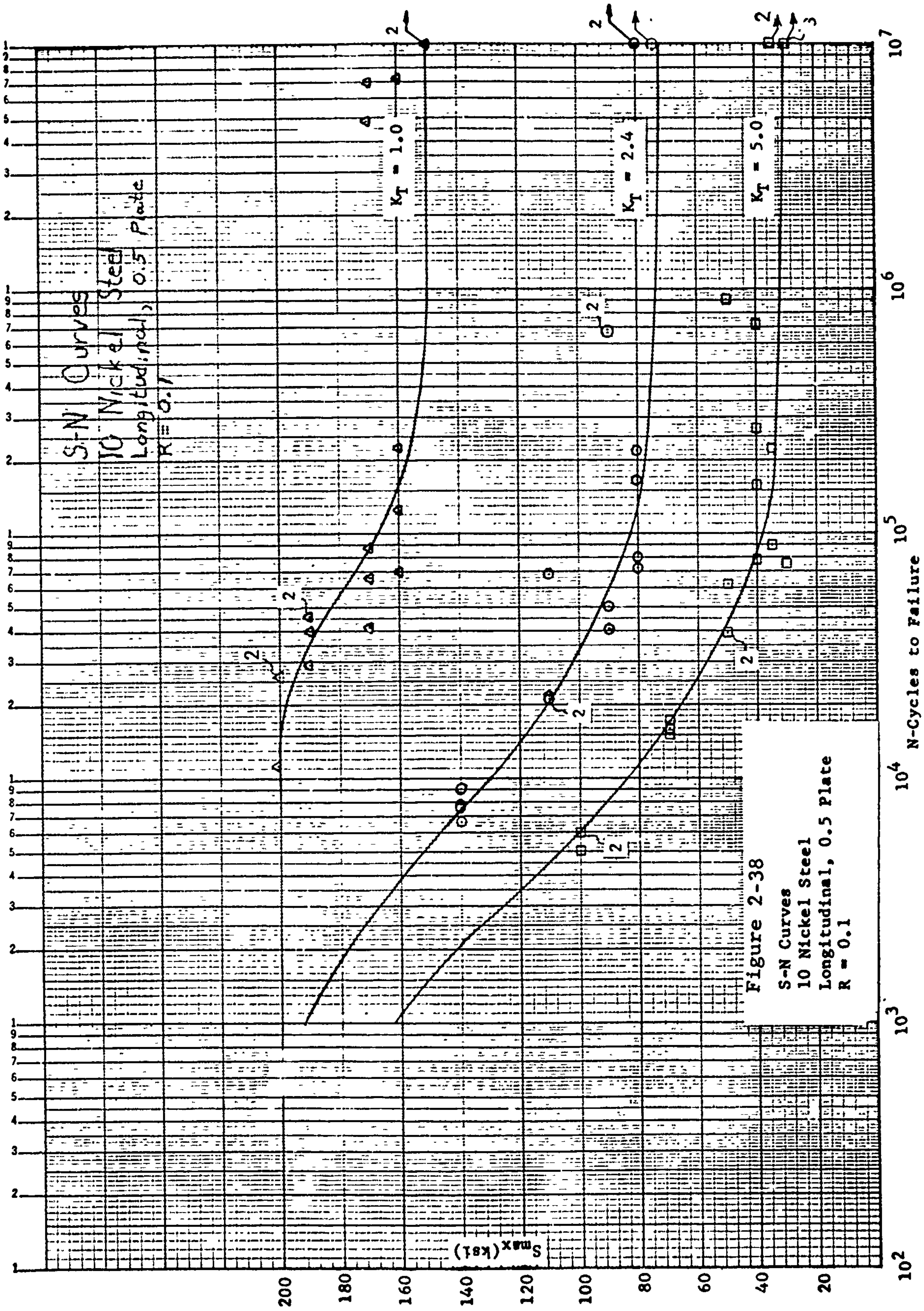


Figure 2-38
S-N Curves
10 Nickel Steel
Longitudinal, 0.5 Plate
R = 0.1

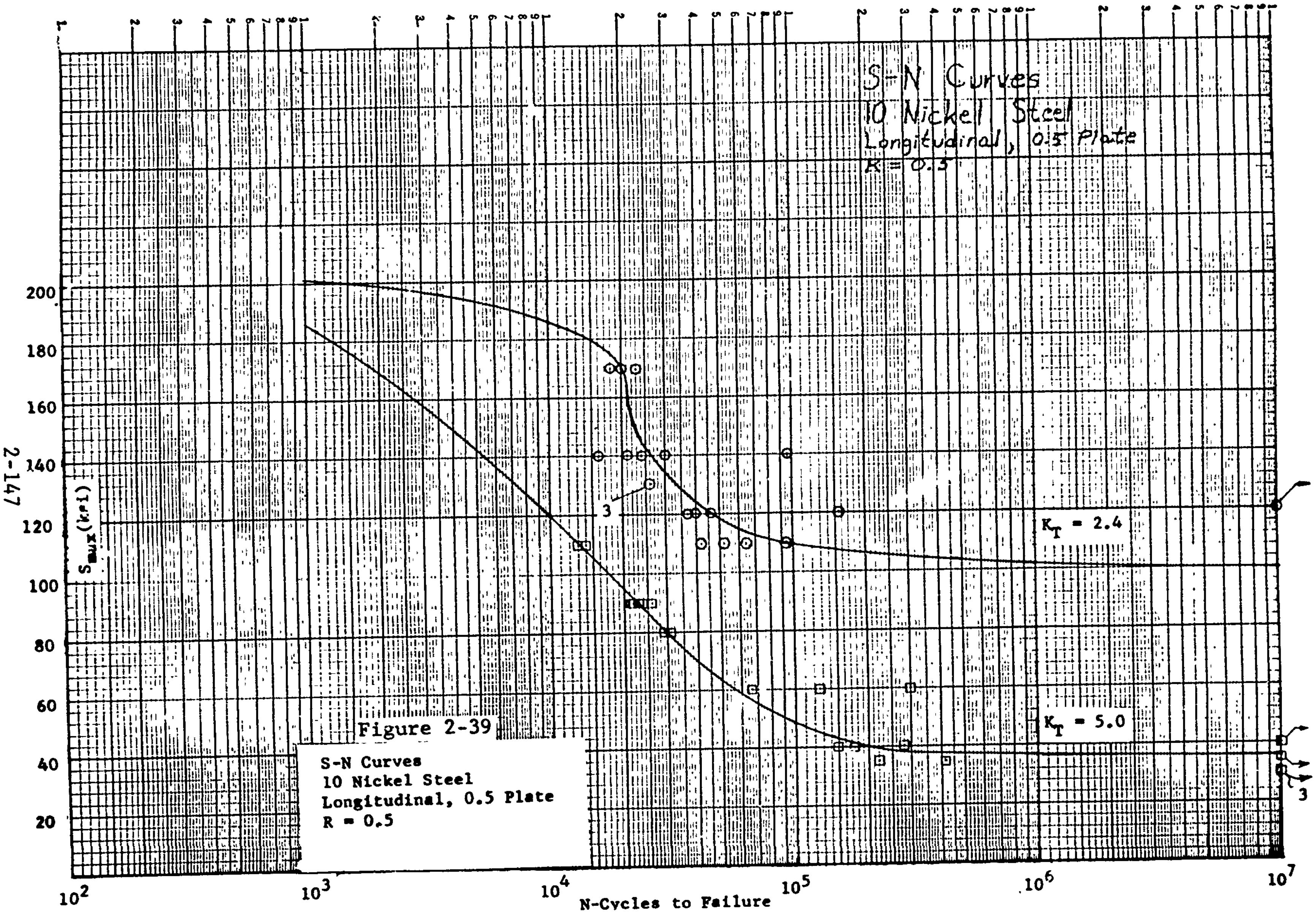


Figure 2-39

S-N Curves
10 Nickel Steel
Longitudinal, 0.5 Plate
R = 0.5

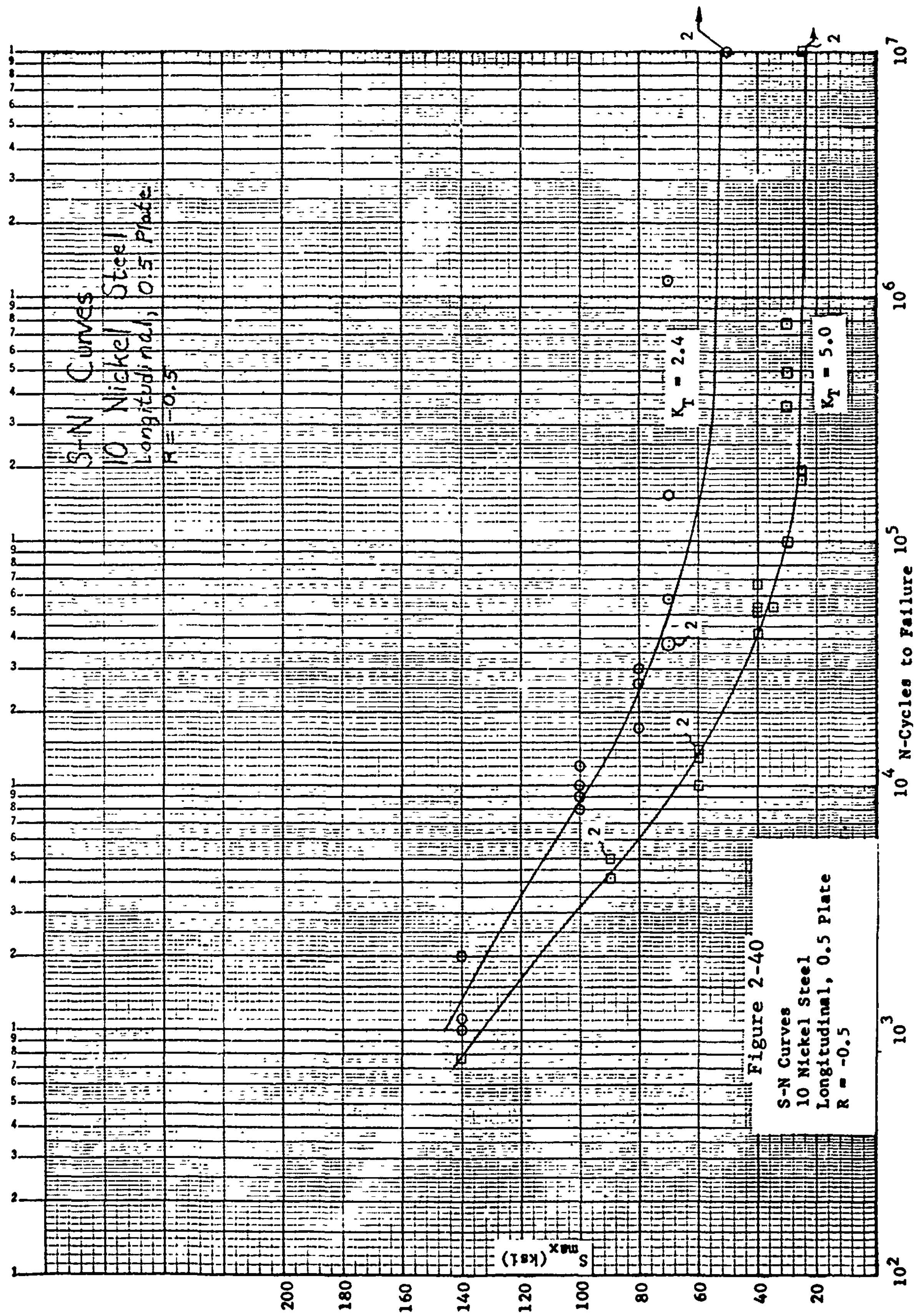


Figure 2-40
S-N Curves
10 Nickel Steel
Longitudinal, 0.5 Plate
R = -0.5

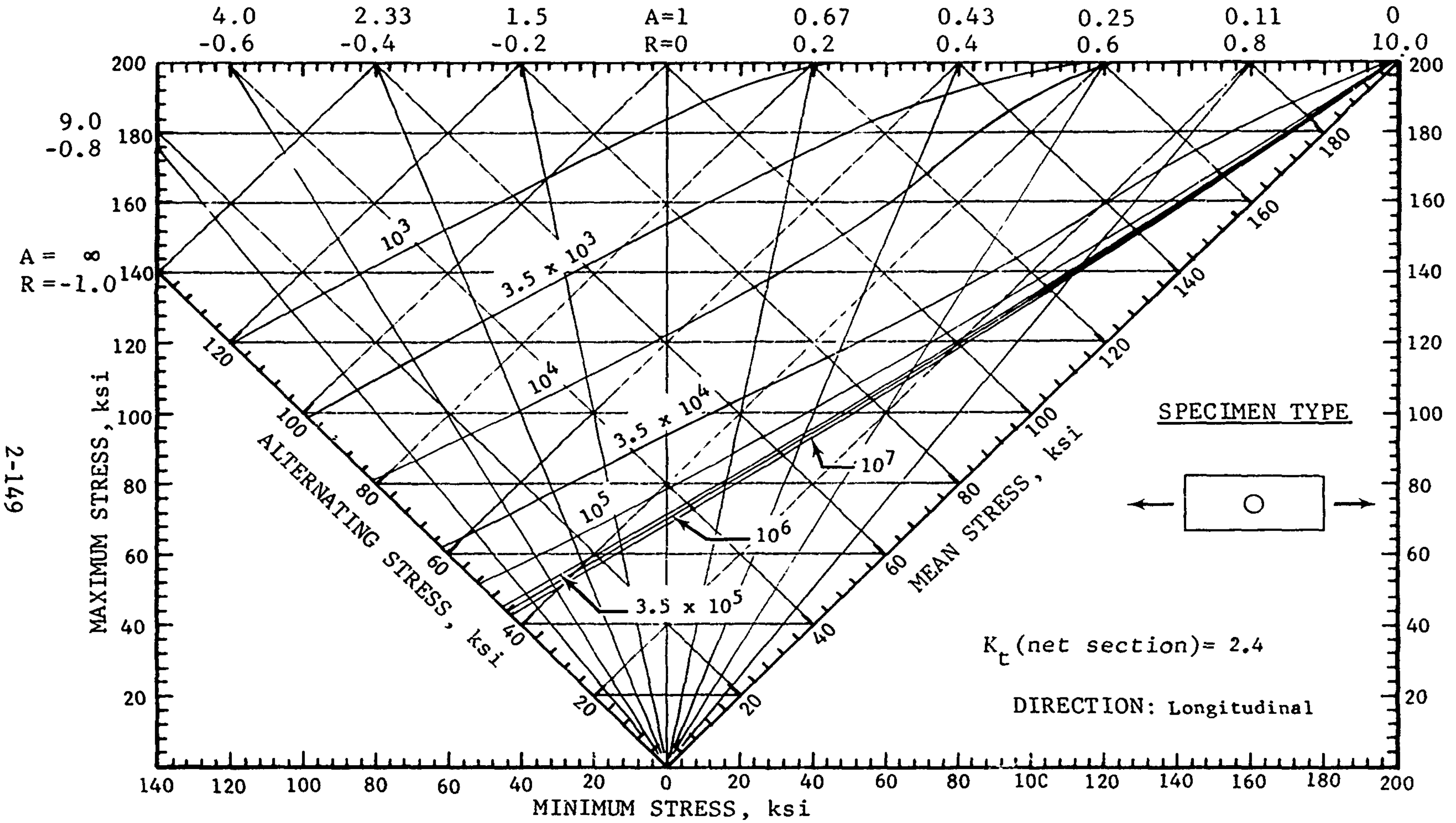


MATERIAL: 10 Ni Steel    $F_{tu} = 197$    $F_{ty} = 183$

FORM: 0.5 Plate    $F_{ntu} = 202$    % El. = 16

TEST CONDITIONS

CYCLIC RATE: 1800 cpm

TEMPERATURE: Room

DATA SOURCE: AMAVS    Date: October 1973

Figure 2-41 CONSTANT LIFE FATIGUE DIAGRAM FOR 10 NI STEEL, $K_T = 2.4$

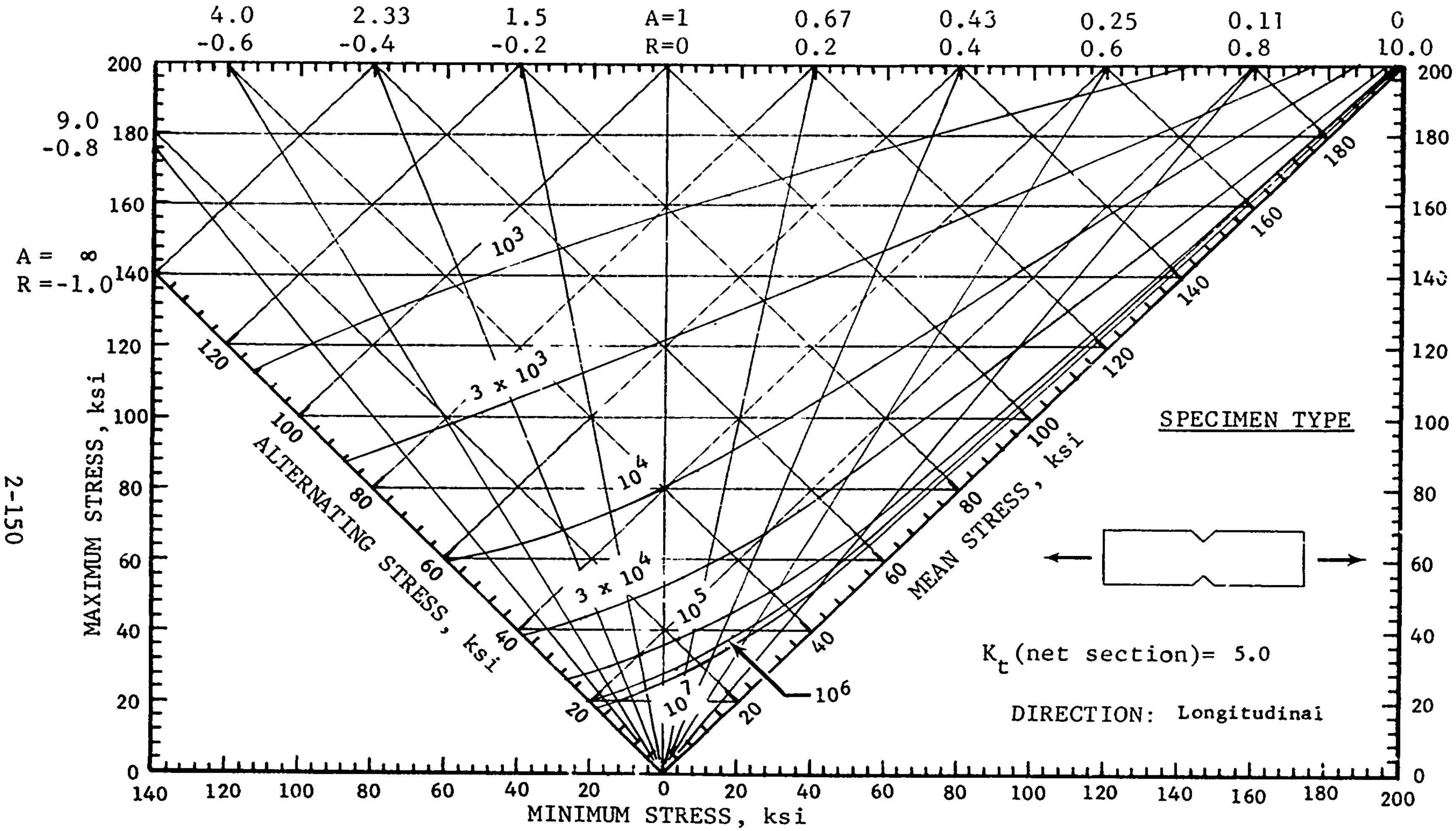


MATERIAL: 10 Ni Steel $F_{tu}$ = 197 $F_{ty}$ = 183

FORM: 0.5 Plate $F_{ntu}$ = 220 % El. = 16

TEST CONDITIONS

CYCLIC RATE: 1800 cpm

TEMPERATURE: Room

DATA SOURCE: AMAVS

Date: October 1973

Figure 2-42 CONSTANT LIFE FATIGUE DIAGRAM FOR 10 NI STEEL, $K_T$ = 5

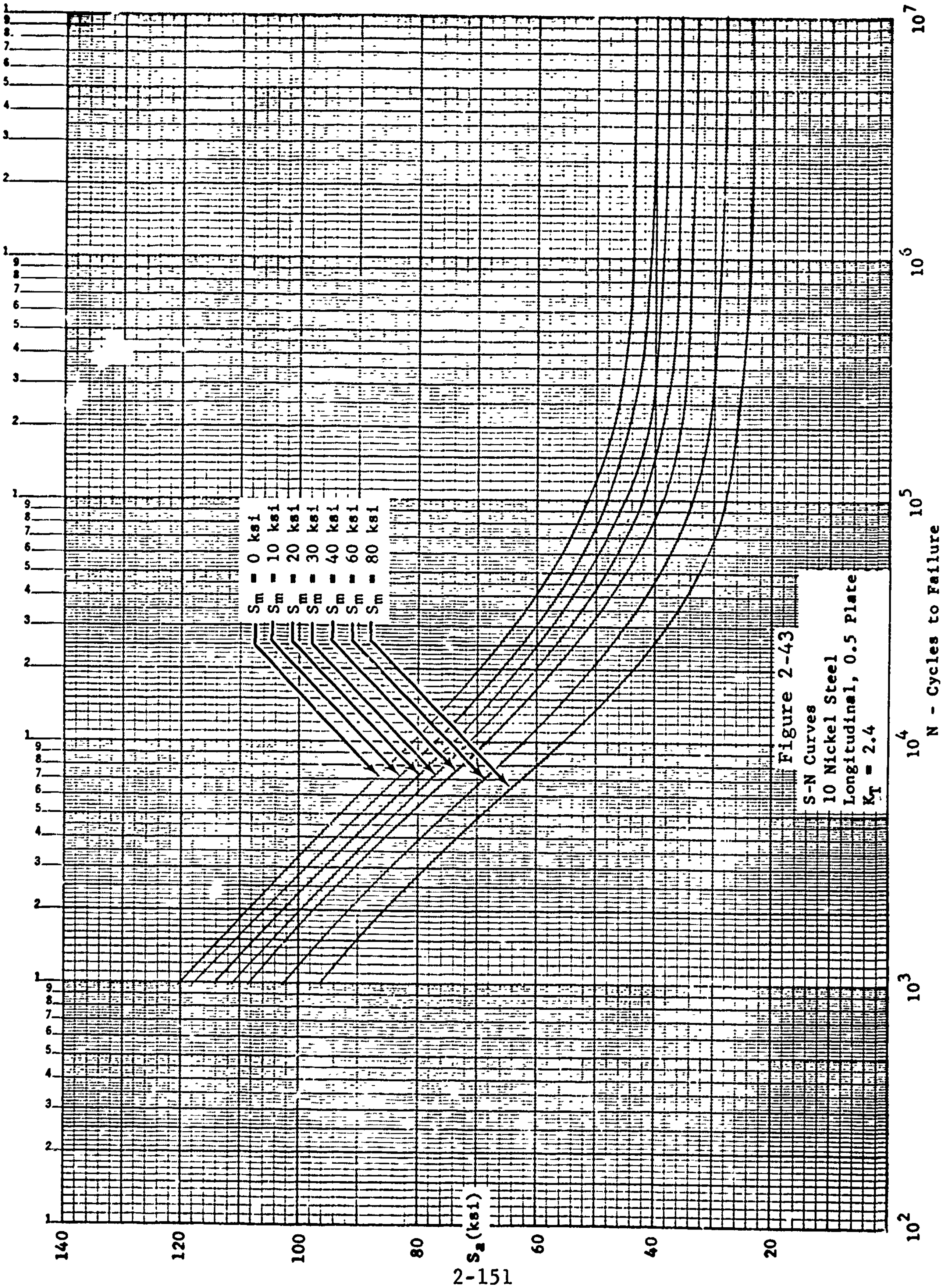


Figure 2-43
S-N Curves
10 Nickel Steel
Longitudinal, 0.5 Plate
$K_T$ = 2.4

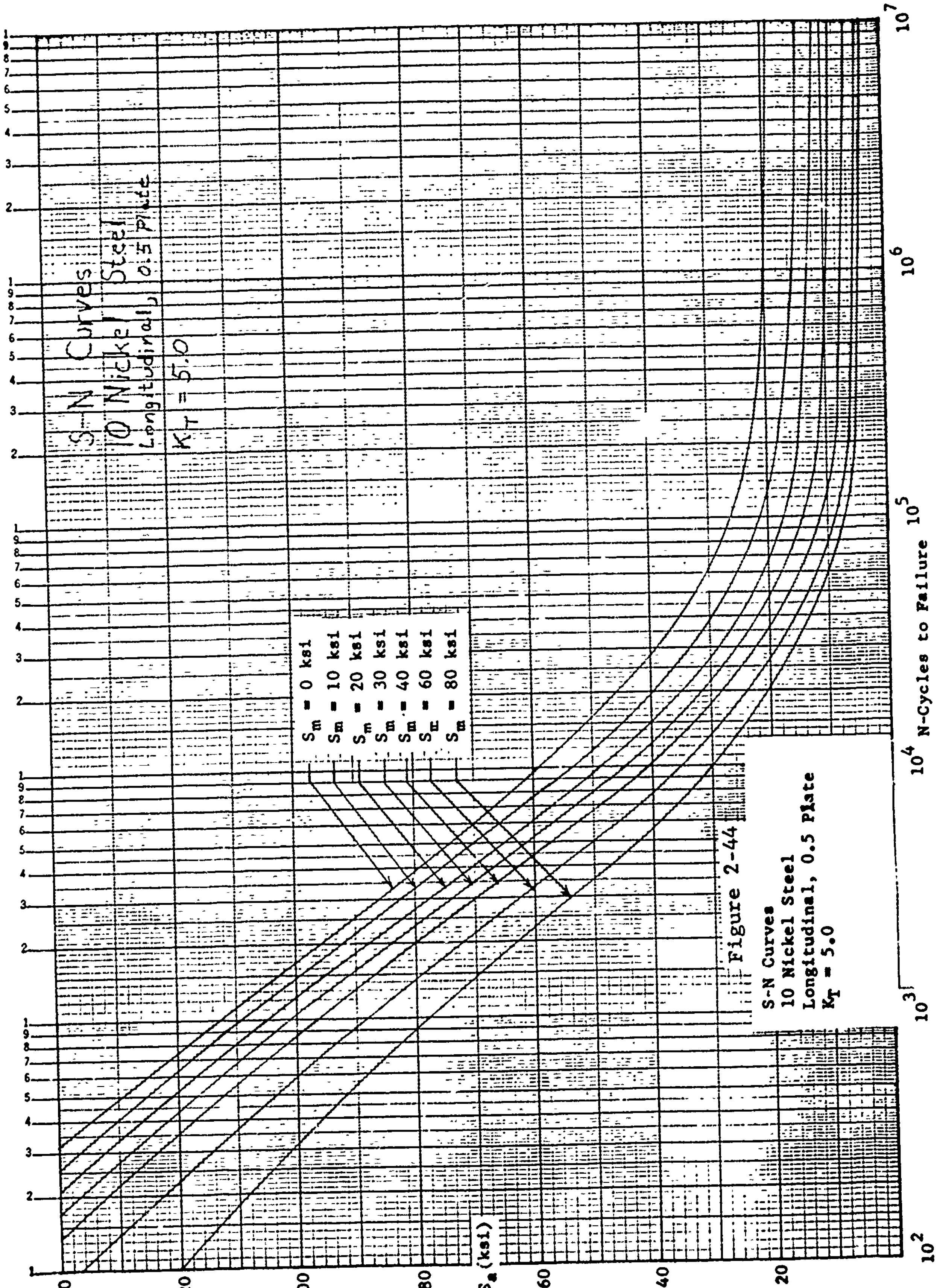


Figure 2-44
S-N Curves
10 Nickel Steel
Longitudinal, 0.5 Plate
$K_T = 5.0$

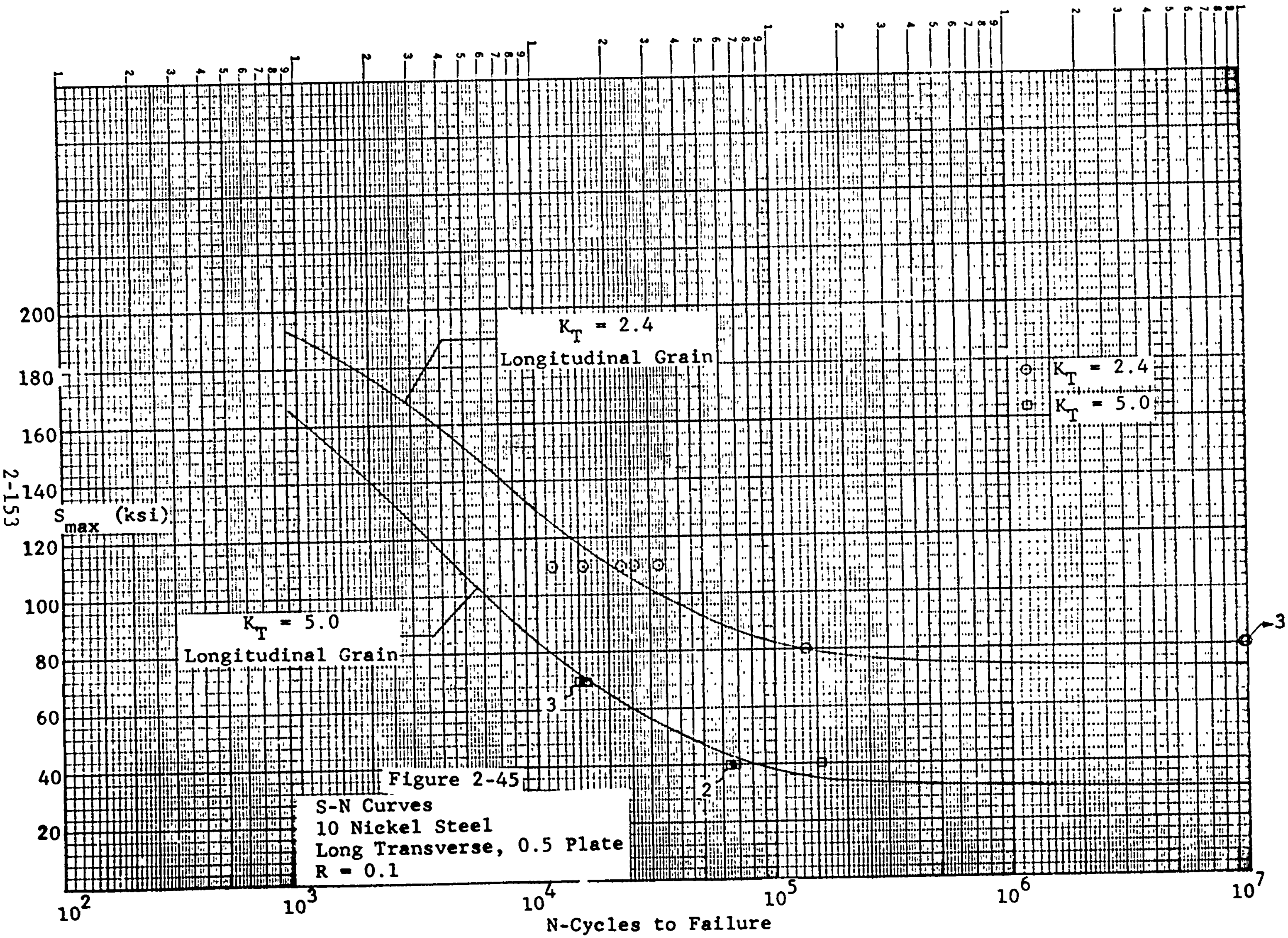


Figure 2-45
S-N Curves
10 Nickel Steel
Long Transverse, 0.5 Plate
R = 0.1

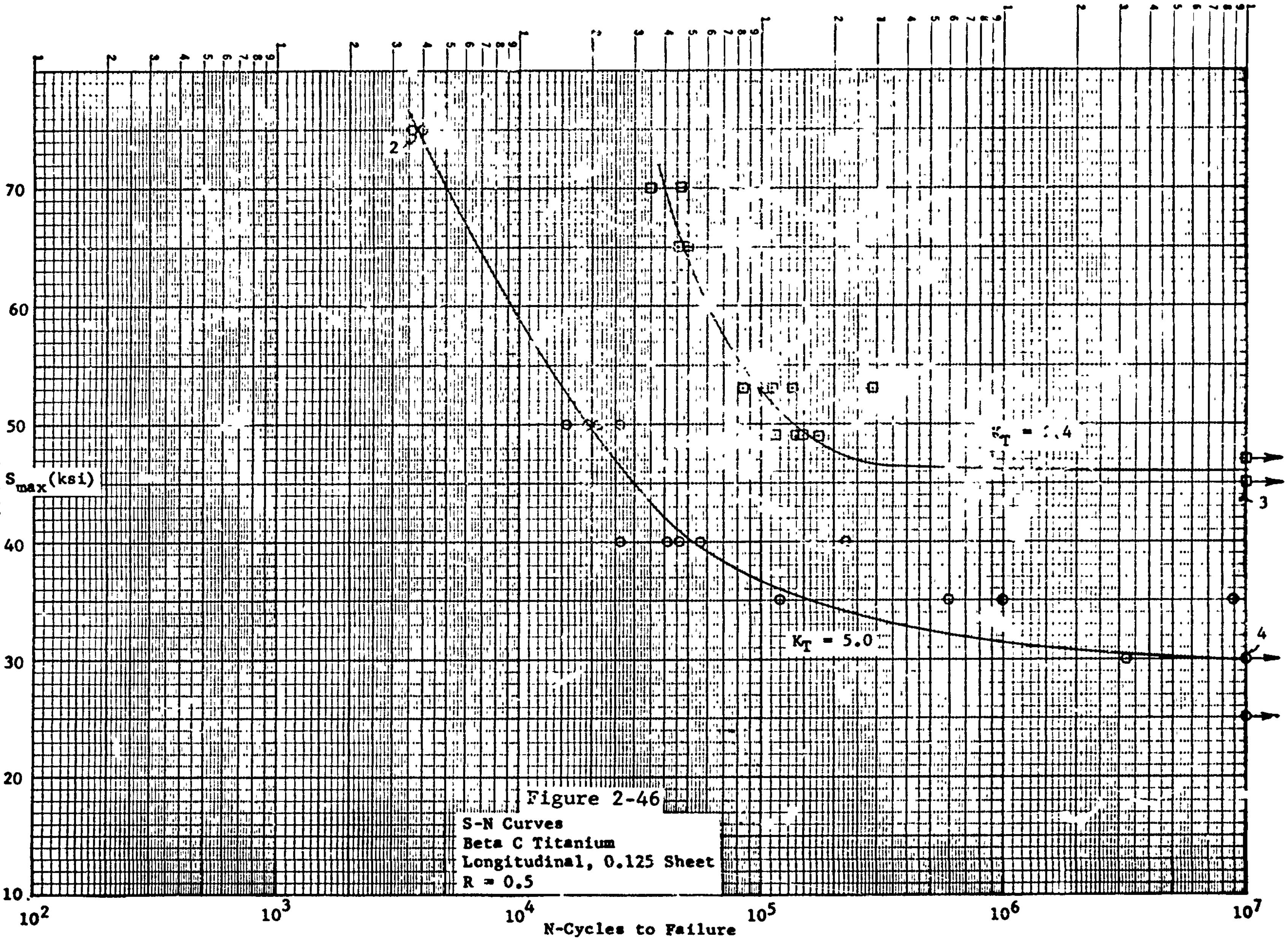


Figure 2-46
S-N Curves
Beta C Titanium
Longitudinal, 0.125 Sheet
R = 0.5

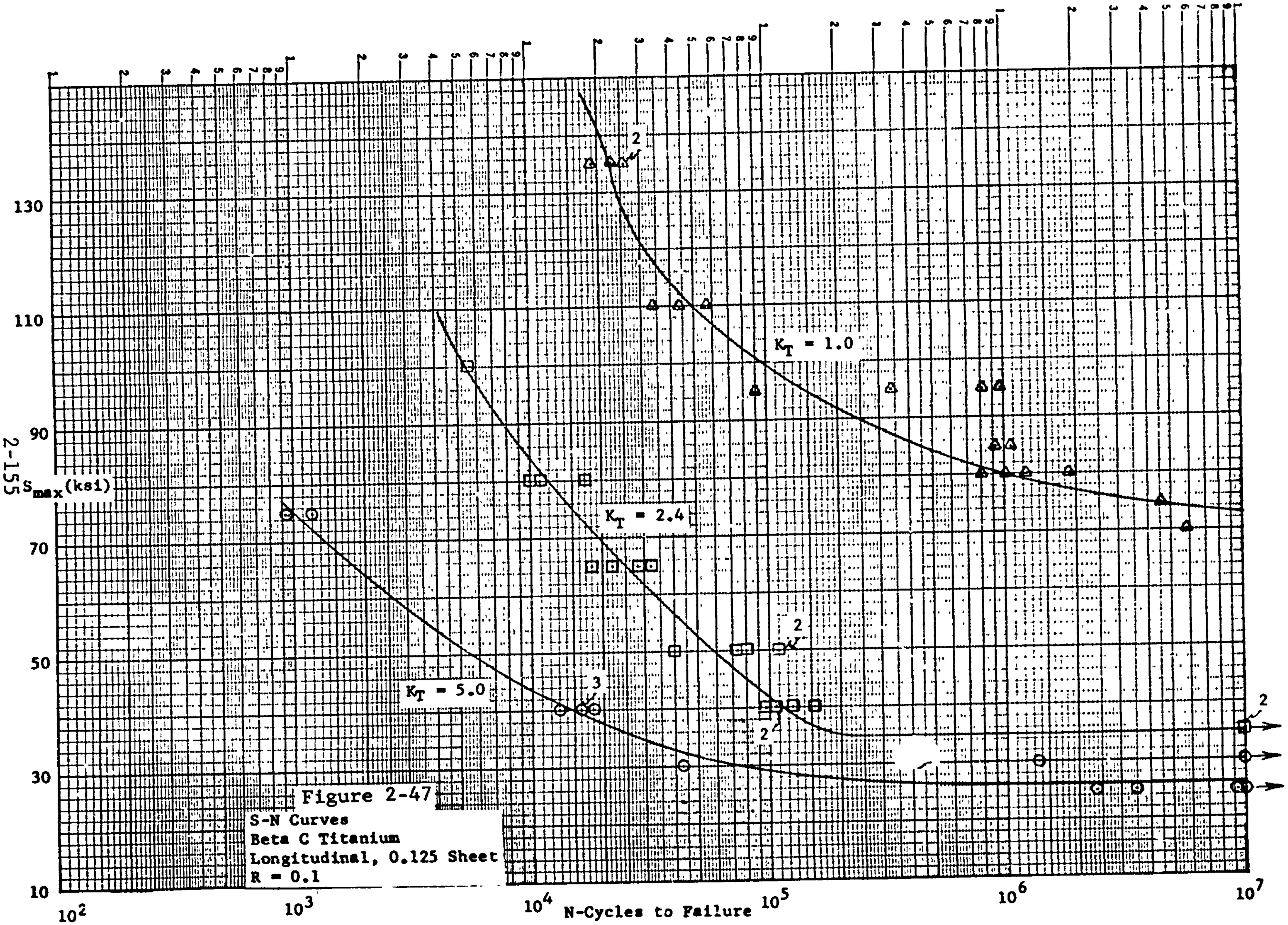


Figure 2-47
S-N Curves
Beta C Titanium
Longitudinal, 0.125 Sheet
R = 0.1

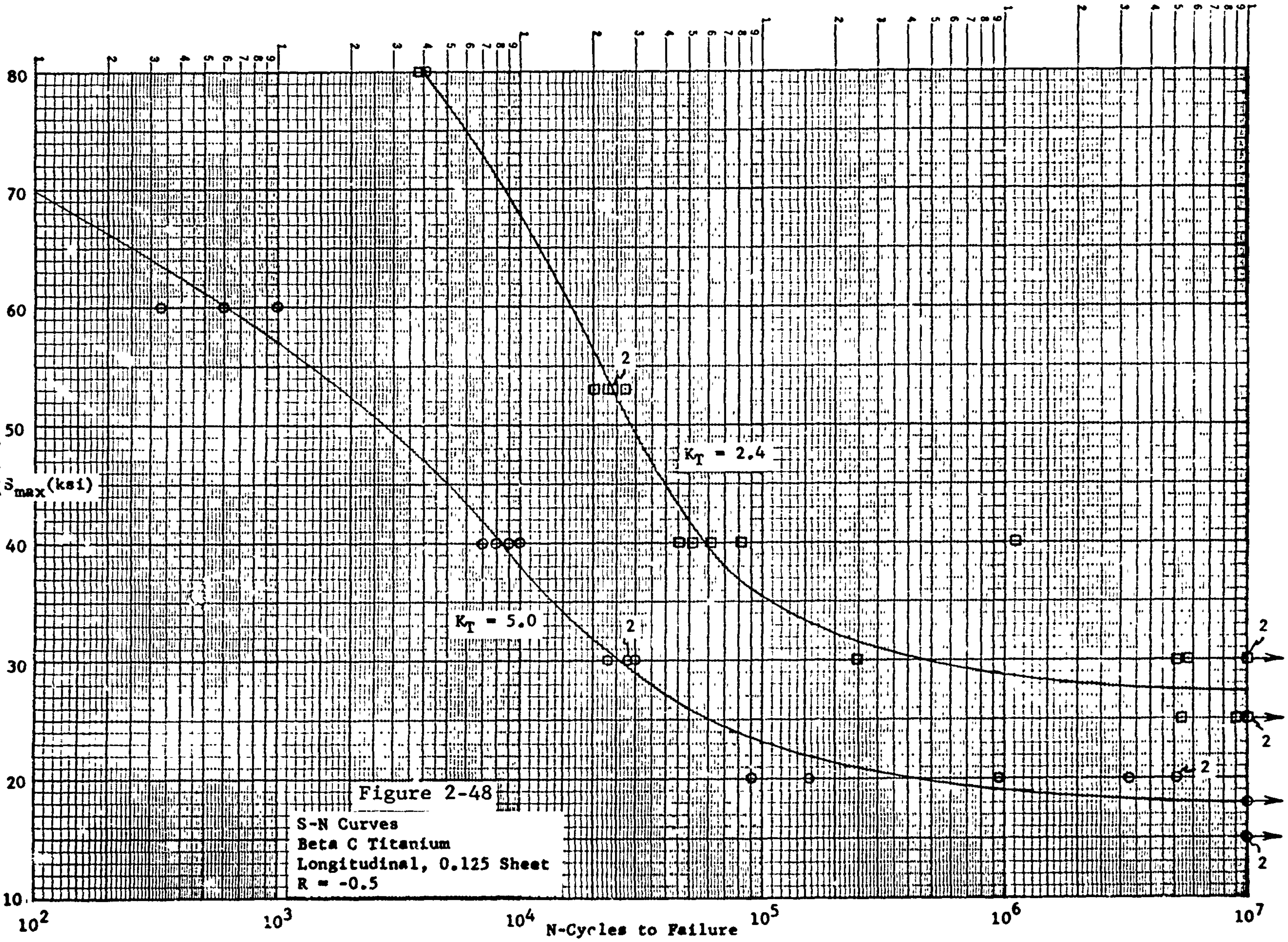


Figure 2-48

S-N Curves
Beta C Titanium
Longitudinal, 0.125 Sheet
R = -0.5

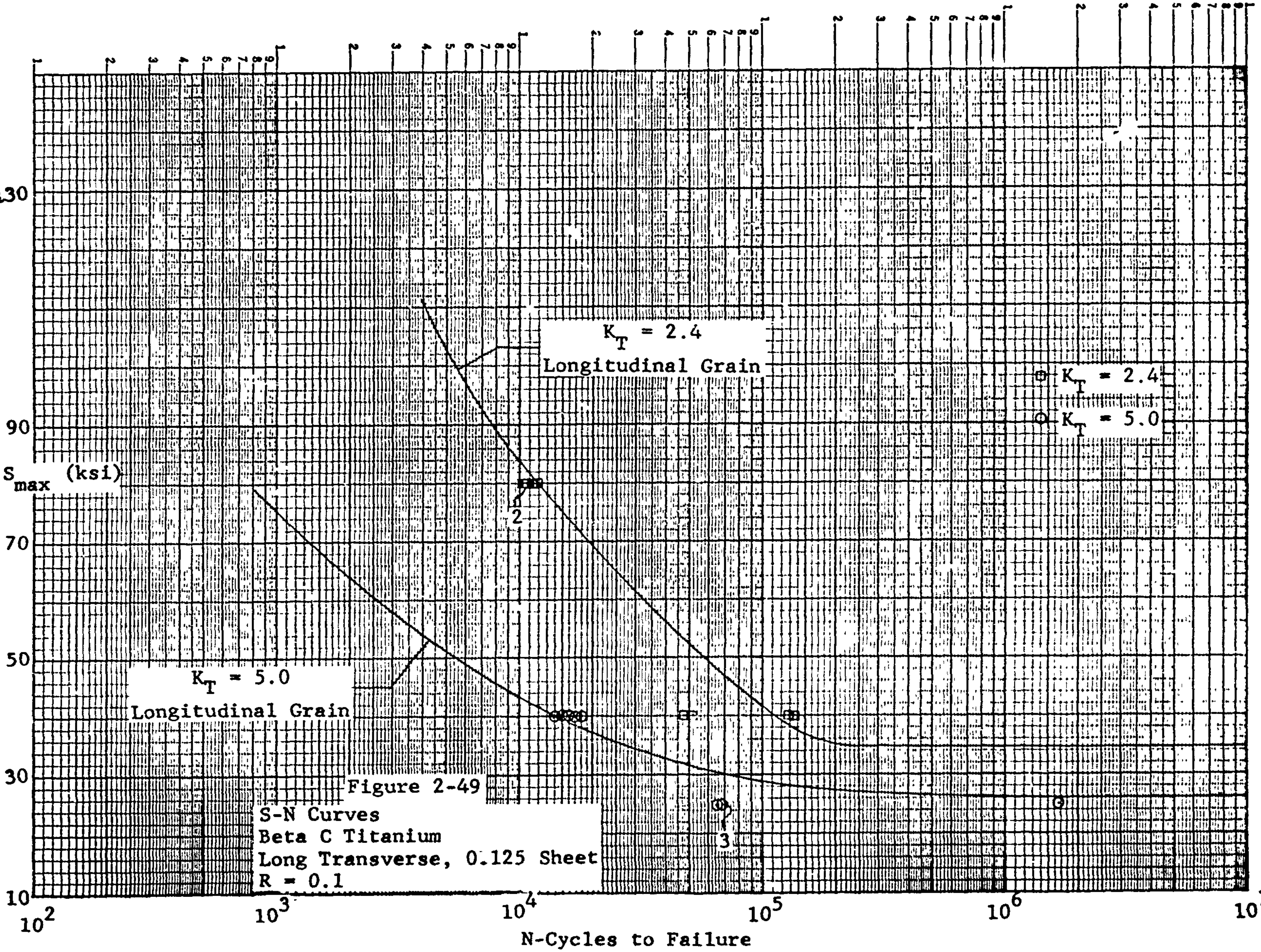


Figure 2-49
S-N Curves
Beta C Titanium
Long Transverse, 0.125 Sheet
R = 0.1

| Material | Type | Figures |
|---|---|---|
| Ti 6Al-4V ($\beta$,MA) | S/N Data | 2-30, 2-31, 2-32 |
| " | Constant Life Diagrams | 2-33, 2-34 |
| " | $S_A$ vs N Curves | 2-35, 2-36 |
| " | Long Transverse Data | 2-37 |
| 10 Ni Steel | S/N Data | 2-38, 2-39, 2-40 |
| " | Constant Life Diagrams | 2-41, 2-42 |
| " | $S_A$ vs N Curves | 2-43, 2-44 |
| " | Long Transverse Data | 2-45 |
| Beta C | S/N Data | 2-46, 2-47, 2-48 |
| " | Long Transverse Data | 2-49 |

The 10 Ni steel fatigue data at $K_T$ = 5.0 were significantly lower than expected. Tests on round notched specimens with $K_T$ = 5 were conducted to determine if the edge notched specimens were more severe at a given $K_T$ level than the round notch specimens commonly used. As shown in Figures 2-50,51, and 52, the test data from round and flat specimens are essentially the same at R = -0.5 and R = 0.1; however, at R = 0.5 the endurance limit of the round specimens is 55 KSI vs 35 KSI for the flat specimens.

### 2.3.1.2 Fatigue Test Data - Weldments

Fatigue tests were conducted on EB welds in beta annealed 6Al-4V titanium (1/2, 1 and 2 in. thick) and GTA welds in 10 Nickel steel plate (.625 in. thick). Flat specimens with $K_T$ = 1 were tested at R = 0.1 and R = 0.5 (10 Ni only). The weld line was located normal to the applied load in the center of the test section.

The fatigue test data were compared with data obtained for the base metal. Comparison plots are shown in Figure 2-53 for EB welded titanium and in Figure 2-54 for GTA welded steel. Notice that in both cases welding does impair the $K_T$ = 1 fatigue resistance, but the welded specimens have better fatigue lives than the open hole specimens.

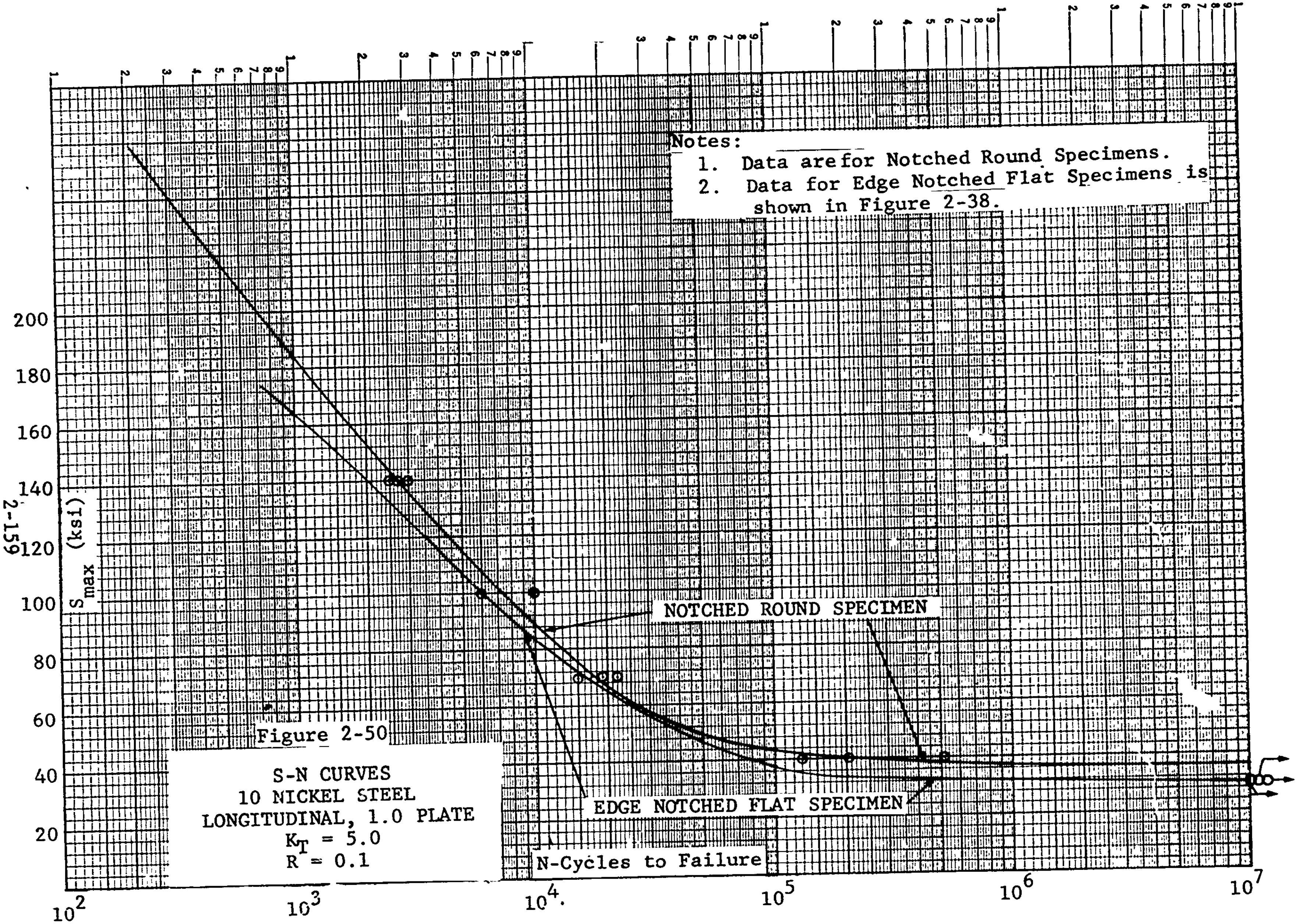


Figure 2-50

S-N CURVES
10 NICKEL STEEL
LONGITUDINAL, 1.0 PLATE
$K_T = 5.0$
$R = 0.1$

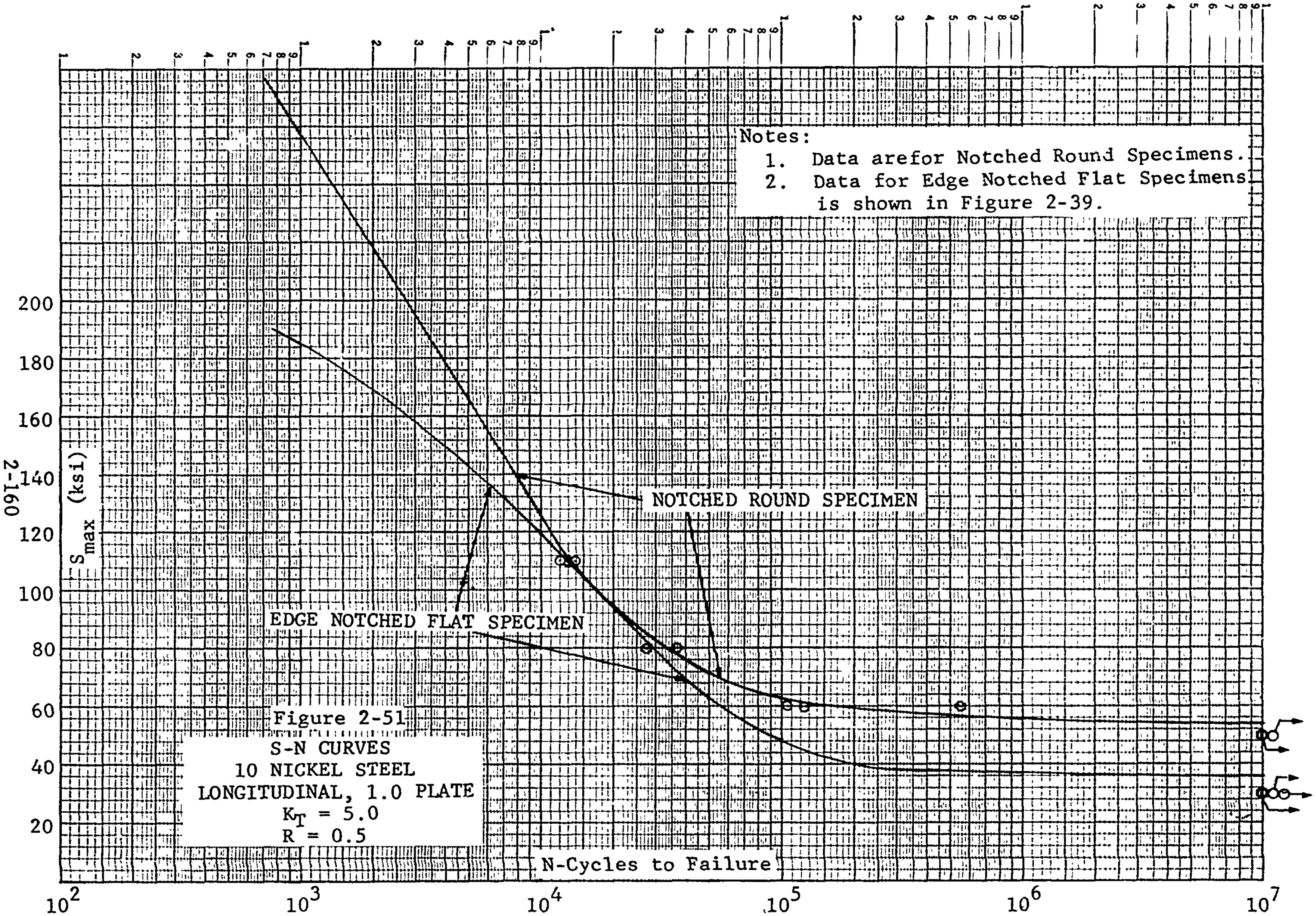


Figure 2-51
S-N CURVES
10 NICKEL STEEL
LONGITUDINAL, 1.0 PLATE
$K_T = 5.0$
$R = 0.5$

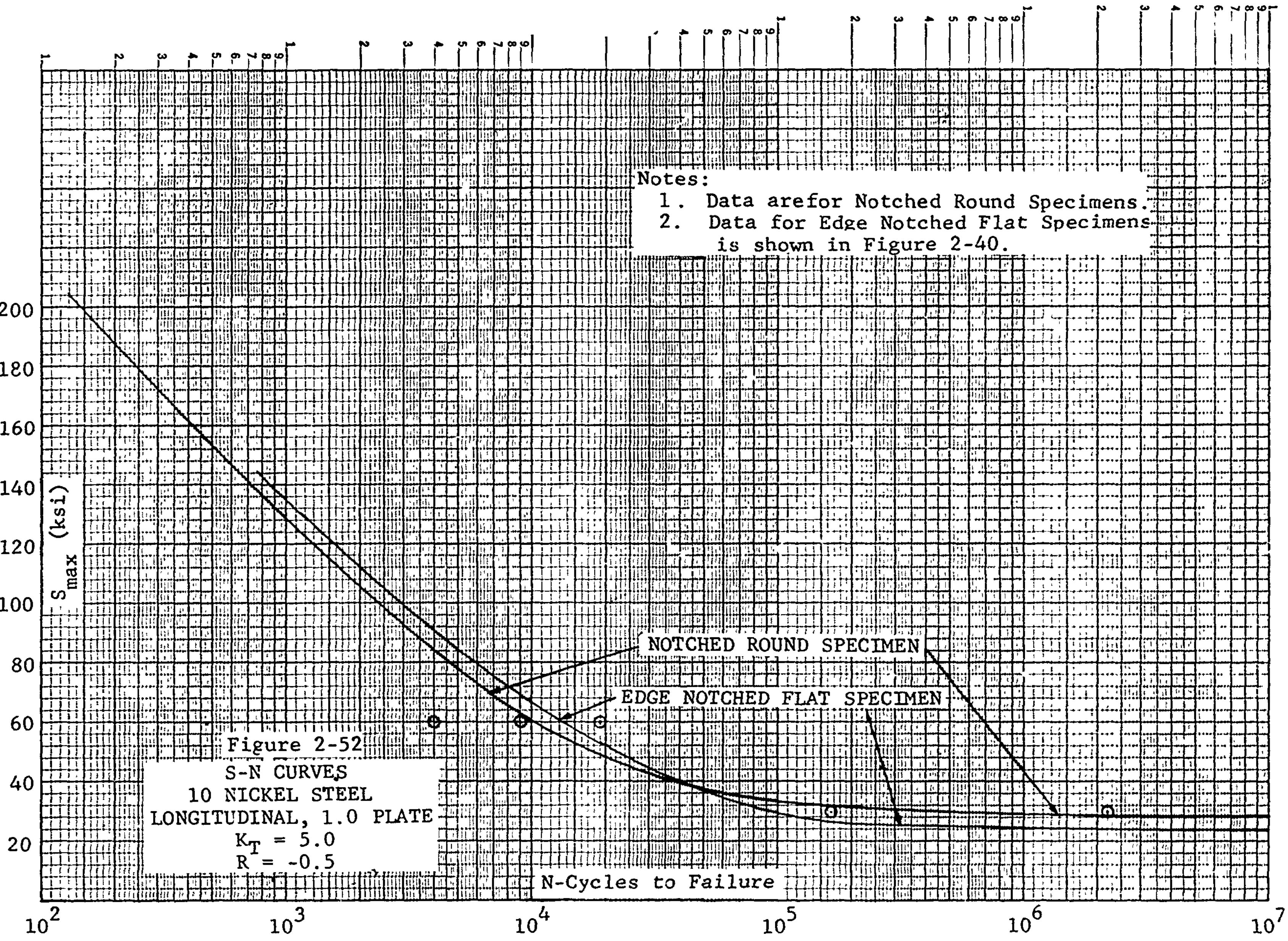


Figure 2-52
S-N CURVES
10 NICKEL STEEL
LONGITUDINAL, 1.0 PLATE
$K_T = 5.0$
$R = -0.5$

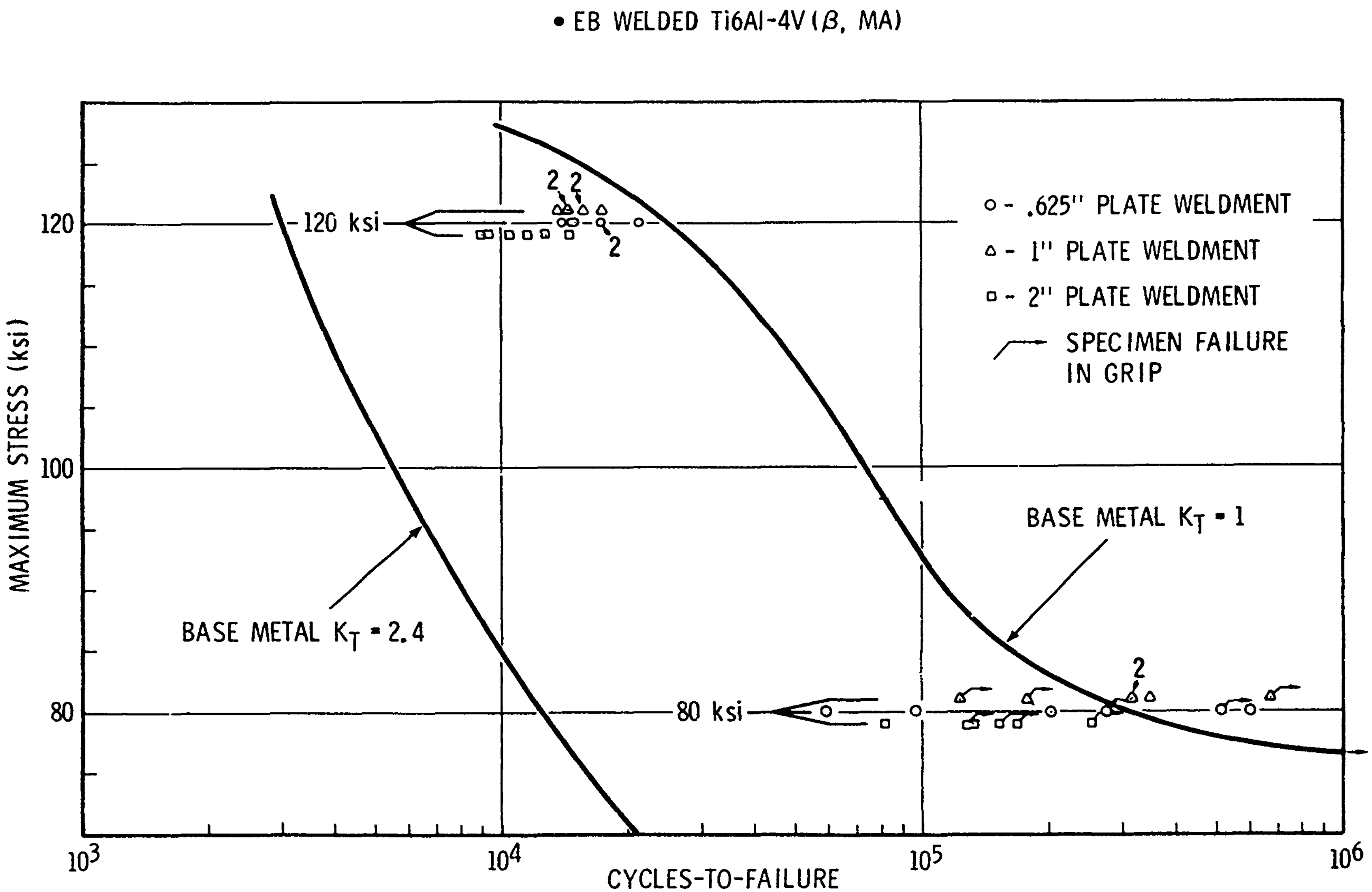


Figure 2-53 FATIGUE DATA SUMMARY

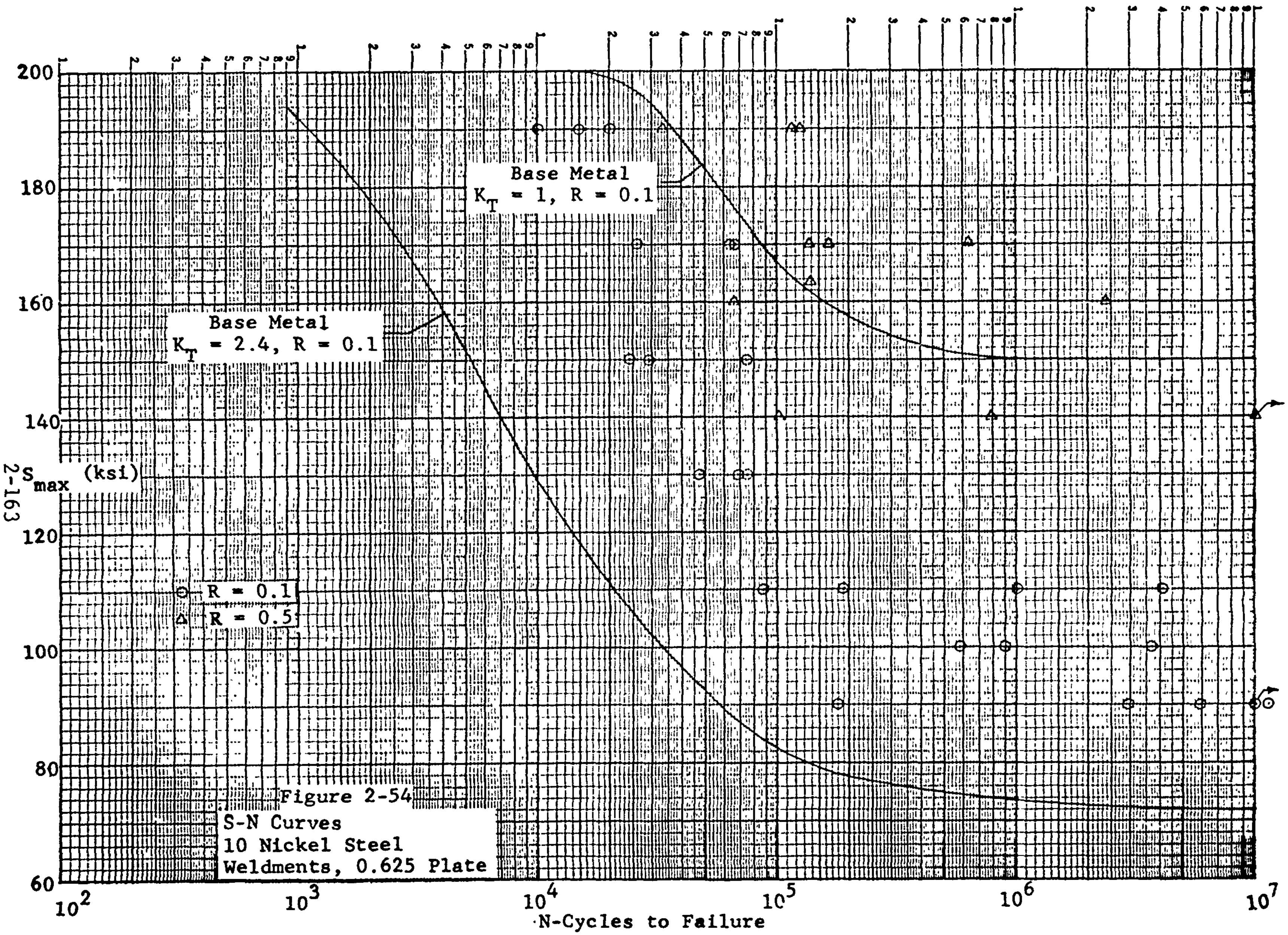

Figure 2-54
S-N Curves
10 Nickel Steel
Weldments, 0.625 Plate

### 2.3.1.3 Fatigue Allowables

Fatigue allowables were determined for beta annealed 6Al-4V titanium and 10 Ni steel subjected to seven representative stress spectra. The spectra represent parts of the WCTS which are critical in forward sweep (spectra 1, 3 and 6), $25^{\circ}$ sweep (spectrum 2), aft sweep (spectra 5 and 7), and ground (spectrum 4) conditions. The results for $K_T = 2.4$ and 5.0 are summarized in Table II-24. Notice that at $K_T = 2.4$ both materials can be worked to their static strength. Based on the $K_T = 2.4$ results, the fatigue allowable for these materials at all locations where $K_T \leq 2$ were set equal to the static strength of the material. The fatigue allowables at $K_T = 5$ ranged from 55 to 70% of $F_{tu}$ for both materials. The $K_T = 5$ allowables were used for lugs, splices, and open holes. Whenever the stresses exceeded the $K_T = 5$ allowable, Taper-lok fasteners were required. Allowables for structural areas where holes with Taper-lok fasteners are the principal stress concentration points were intermediate between the $K_T = 2.4$ and $K_T = 5$ values: 100 KSI for beta annealed 6Al-4V titanium and 150 KSI for 10 Nickel steel. Aluminum allowables were established using the preliminary design allowables methodology discussed in AFFDL-TR-73-40 for the specific alloys of interest, 2024-T851 and 7050-T7351.

Fatigue allowables for the lugs were based on sizing procedures successfully applied during the F-111 program. The net section stress is determined using the maximum applied load and the minimum cross-sectional area. The maximum allowable net section stress was determined from fatigue analysis using $K_T = 5$ S/N data and a lug stress spectrum. The lug stress spectrum was developed assuming that the minimum lug cross-section receives the highest stress in each of the flight configurations, i.e., at different wing sweeps the critical location remains the same. It was further assumed that the limit stresses for each flight condition in the fatigue spectrum (ASKA 2, 10, 5, 9) were equal and the minimum applied stress was equal to zero. Using these procedures, the lug stress allowables were 77 KSI for FSIL and 131 KSI for the NBB.

Fatigue allowables for welded joints were based on the design requirement that all welds be located remote from stress concentrations. A factor of .85 on $F_{tu}$ was used for the weld joint allowable. This is considered conservative because all weld fatigue test data were superior to the open-hole data. Fatigue analysis based on open-hole ($K_T = 2.4$) data indicates that both materials can be worked to 100% $F_{tu}$.

Fatigue allowables used in final design are summarized in Table II-25 (FSIL) and Table II-26 (NBB).

Table II-24 FATIGUE ALLOWABLES FOR SEVEN SPECTRA REPRESENTATIVE OF FSIL AND NBB LOWER COVERS

| SPECTRUM NO. | RELATIVE STRESS ASKA* 10 | ASKA 2&5 | ASKA 9 | ASKA 7 | TI6AL-4V($\beta$,MA) $K_T$=2.4 KSI | $K_T$=5 KSI | 10 NI STEEL $K_T$=2.4 KSI | $K_T$=5 KSI |
|---|---|---|---|---|---|---|---|---|
| 1 | .45 | 1.0 | .73 | 0 | 130 | 81 | 190 | 115 |
| 2 | .58 | .88 | 1.0 | -.34 | ↑ | 82 | ↑ | 110 |
| 3 | .76 | 1.0 | .84 | -.20 | | 84 | | 123 |
| 4 | .68 | 1.0 | .83 | -.56 | | 75 | | 113 |
| 5 | 1.0 | .78 | .81 | -.06 | | 87 | | 120 |
| 6 | .81 | 1.0 | .90 | -.13 | ↓ | 81 | ↓ | 112 |
| 7 | 1.0 | .86 | .66 | -.14 | 130 | 85 | 190 | 112 |

Table II-25 FATIGUE ALLOWABLES FOR FAIL SAFE INTEGRAL LUG CONFIGURATION

| Material | Part | Allowable |
|---|---|---|
| Ti 6Al-4V ($\beta$,MA) | Lower Lug | 77 KSI (Net Section Stress) |
| ↓ | Centerline Splice | 80 KSI |
| | All Welds | 106 KSI |
| | Other Tension Members ($K_T \geq 2$) | 100 KSI |
| | Upper Out'bd Longeron Splice | 90 KSI |
| | Other Structure | Static Design |
| 7050 | All Tension Member ($K_T > 2$) | 45 KSI |
| 2024 | Other Parts | Static Design |

Table II-26 FATIGUE ALLOWABLES FOR THE NO-BOX CONFIGURATION

| Material | Part | Allowable |
| --- | --- | --- |
| 10 Ni Steel | Lower Lug | 131 KSI (Net Section Stress) |
| | All Welds | 166 KSI |
| | Upper Out'bd Longeron Splice | 130 KSI |
| | Other tension members $K_T > 2$ | 150 |
| | Other structure | Static Design |
| 7050, 2024 | All tension members $K_T > 2$ | 45 KSI |
| | Other Parts | Static design |
| Ti 6Al-4V ($\beta$,MA) | Splices @ $X_F 39$, $Z_F 0$ | 87 KSI |
| | Splices @ $X_F$ 84, $Z_F 0$ | 77 KSI |
| | Other Tension Members ($K_T > 2$) | 100 KSI |
| | Other Structure | Static Design |

### 2.3.2 Fatigue Crack Growth Test Data

The crack growth analysis is based on data for the two materials of principal interest: beta annealed 6Al-4V titanium and 10 Ni steel. Constant amplitude tests were conducted in dry air at 360 cpm and in sump tank water at 6 and 60 cpm. Spectrum tests were conducted using tensile panels with either surface flaws in open structure or quarter circle cracks extending from one edge of a hole. Specimens were tested using four distinct spectra representing two control points and two truncation levels.

#### 2.3.2.1 Constant Amplitude Tests

Constant amplitude fatigue crack growth tests were conducted on beta annealed 6Al-4V titanium plate, 10 Nickel steel plate, and Beta C titanium sheet. The test data for beta annealed 6Al-4V titanium plate were presented in AFFDL-TR-73-77. For 10 Ni steel, 10 of 13 crack growth curves were presented in the same report. The other three tests are shown along with the curves of the equations used in the crack growth analysis in Figure 2-55. Notice that the analysis lines are conservative interpretations of the test data, particularly at growth rates below 2 x $10^{-6}$ inch per cycle where the cracks grow slower in sump tank water than in dry air. The test data for Beta C titanium are presented in Figures 2-56, 57, and 58; a single Forman equation fits all of the test data for both dry air and sump tank water:

$$\frac{da}{dN} = \frac{2.3 \times 10^{-7} \Delta K^{2.63}}{(1-R)\ 70- \Delta K}$$

#### 2.3.2.2 Spectrum Load Tests

The results of the spectrum environmental test program are summarized in Table II-27. Crack growth analyses based on the Wheeler model were conducted to develop an analytical correlation for each set of test data. Available data and preliminary analytical correlations were presented in AFFDL-TR-73-77. The analytical correlations for beta annealed 6Al-4V titanium were modified in accordance with the procedures outlined in Section 2.3.3; the test data and correlations are presented in Figures 2-59 - 2-65. The analytical correlations for 10 Ni Steel have remained unchanged; the test data obtained since the Second Interim Report are shown in Figures 2-66, 2-67 and 2-68.

Table II-27 SPECTRUM-ENVIRONMENTAL CRACK GROWTH TESTS

| MATERIAL | ENVIRONMENT | SPECTRUM | SPECIMEN | RESULTS m = |
|---|---|---|---|---|
| Ti6Al-4V(β,MA) | DRY AIR | 1 | SF | 1.8 |
| | DRY AIR | 2 | SF | 1.6 |
| | DRY AIR | 1 | CH | 1.4 |
| | DRY AIR | 2 | CH | 0.7 |
| | SUMP TANK WATER | 1 | SF | 1.9 |
| | | 1* | SF | 1.7 |
| | | 2* | SF | 1.8 |
| 10 Ni Steel | DRY AIR | 1 | SF | 0.8 |
| | DRY AIR | 2 | SF | 0.8 |
| | DRY AIR | 1 | CH | 0.9 |
| | DRY AIR | 2 | CH | 0.9 |
| | DRY AIR | 1* | SF | 0.5 |
| | DRY AIR | 2* | SF | 0.6 |
| | SUMP TANK WATER | 1 | SF | 1.0 |
| | | 1* | SF | 0.8 |
| | | 2* | SF | 1.2 |

• SURFACE FLAW SPECIMEN (SF)

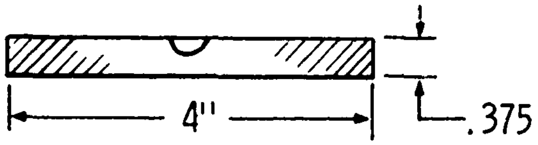


• CRACKED HOLE SPECIMEN (CH)

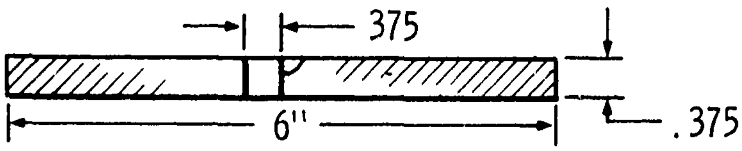


Note: Spectra 1* and 2* are untruncated versions of Spectra 1 and 2, respectively

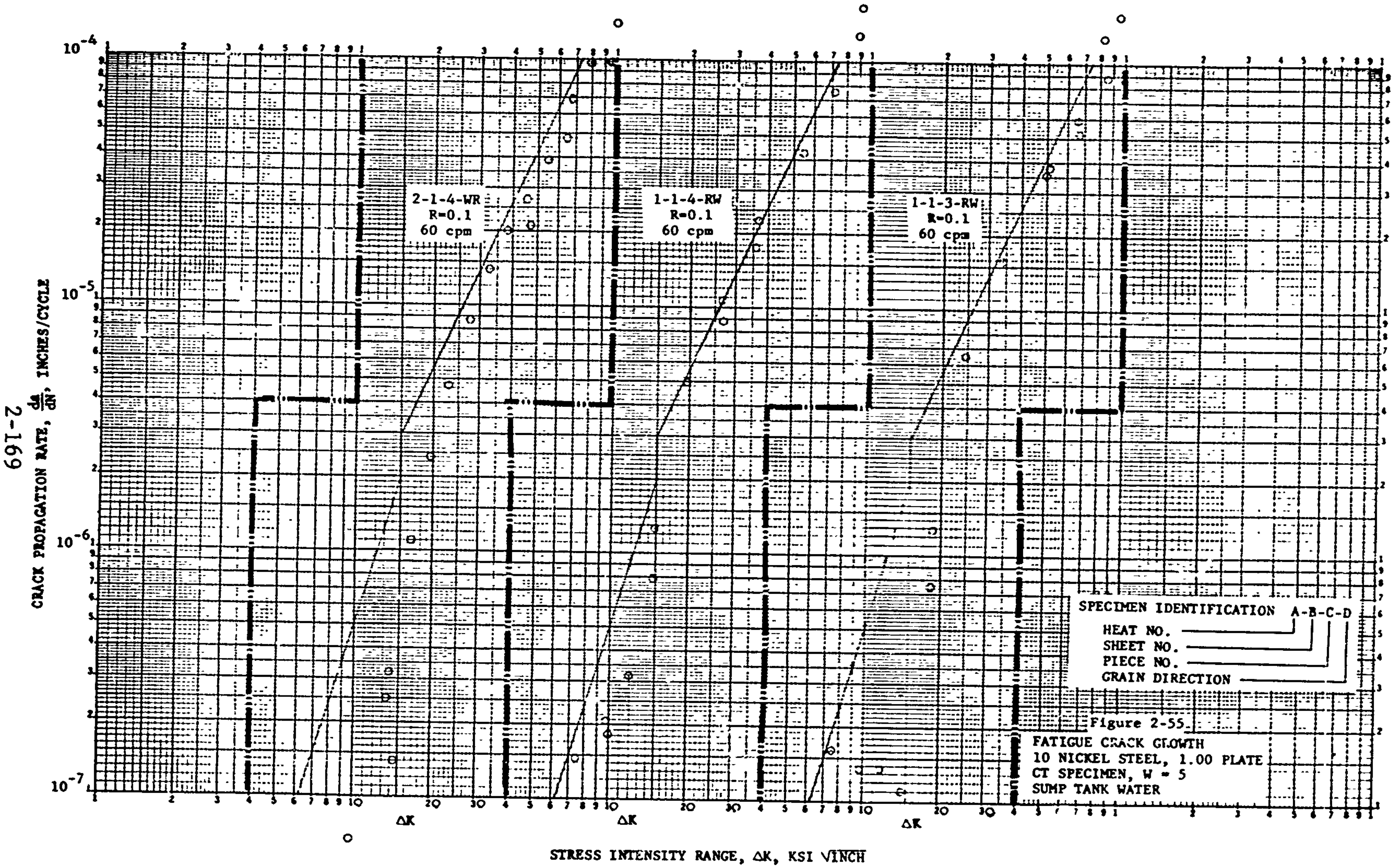


Figure 2-55.
FATIGUE CRACK GROWTH
10 NICKEL STEEL, 1.00 PLATE
CT SPECIMEN, W = 5
SUMP TANK WATER

Note: Lines represent Forman equations used in the crack growth analysis.

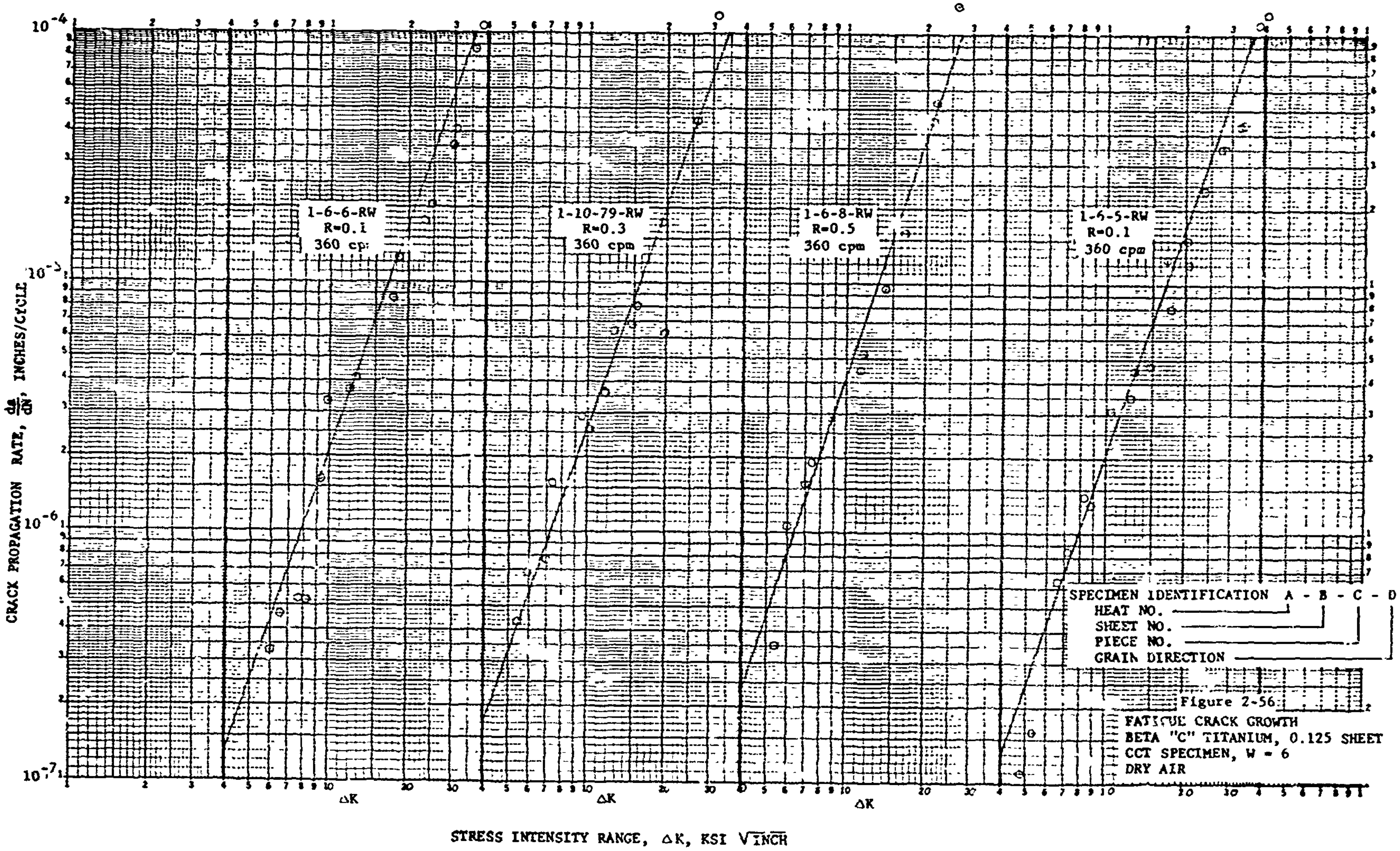

Figure 2-56
FATIGUE CRACK GROWTH
BETA "C" TITANIUM, 0.125 SHEET
CCT SPECIMEN, W = 6
DRY AIR

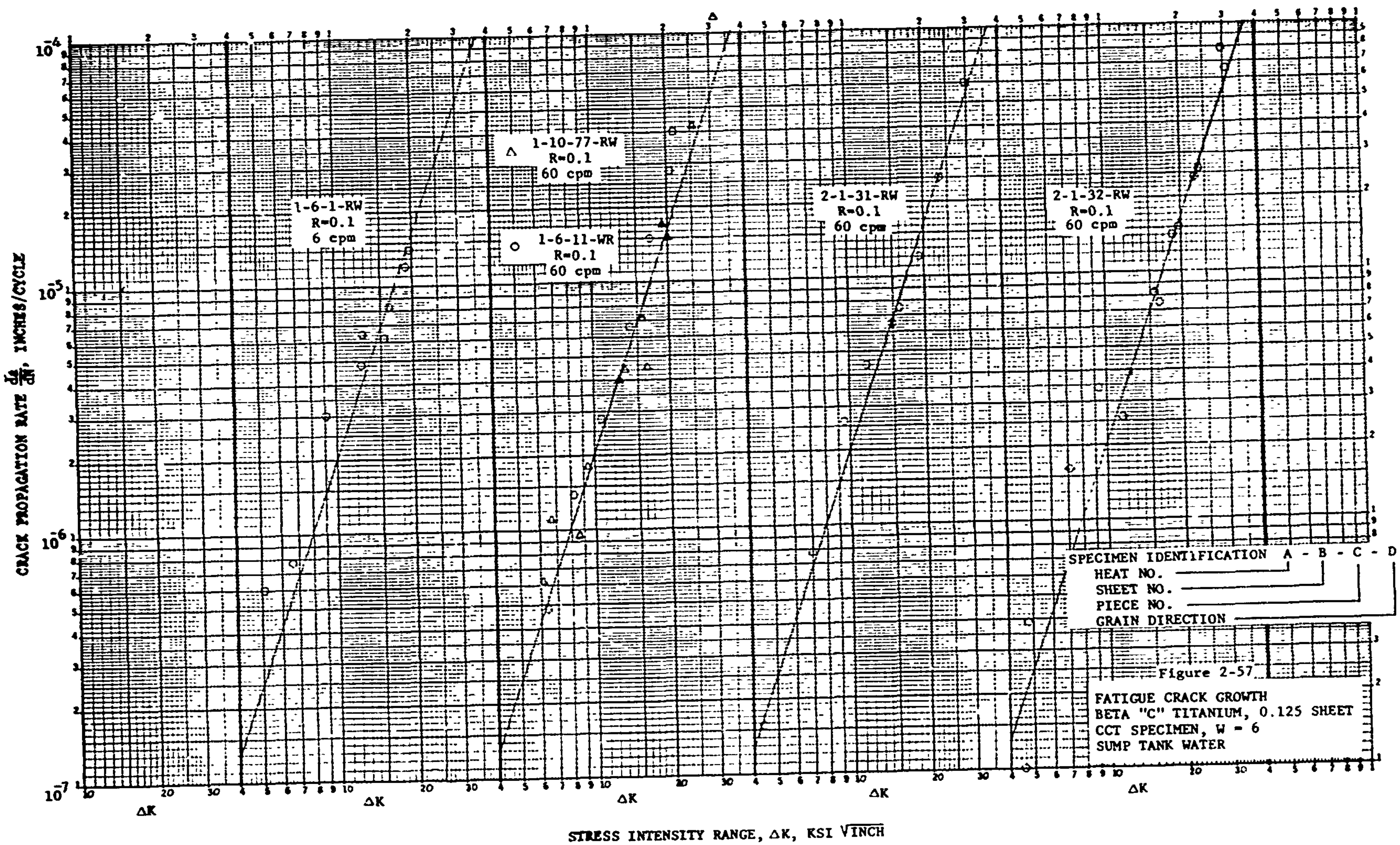


Figure 2-57

FATIGUE CRACK GROWTH
BETA "C" TITANIUM, 0.125 SHEET
CCT SPECIMEN, W = 6
SUMP TANK WATER

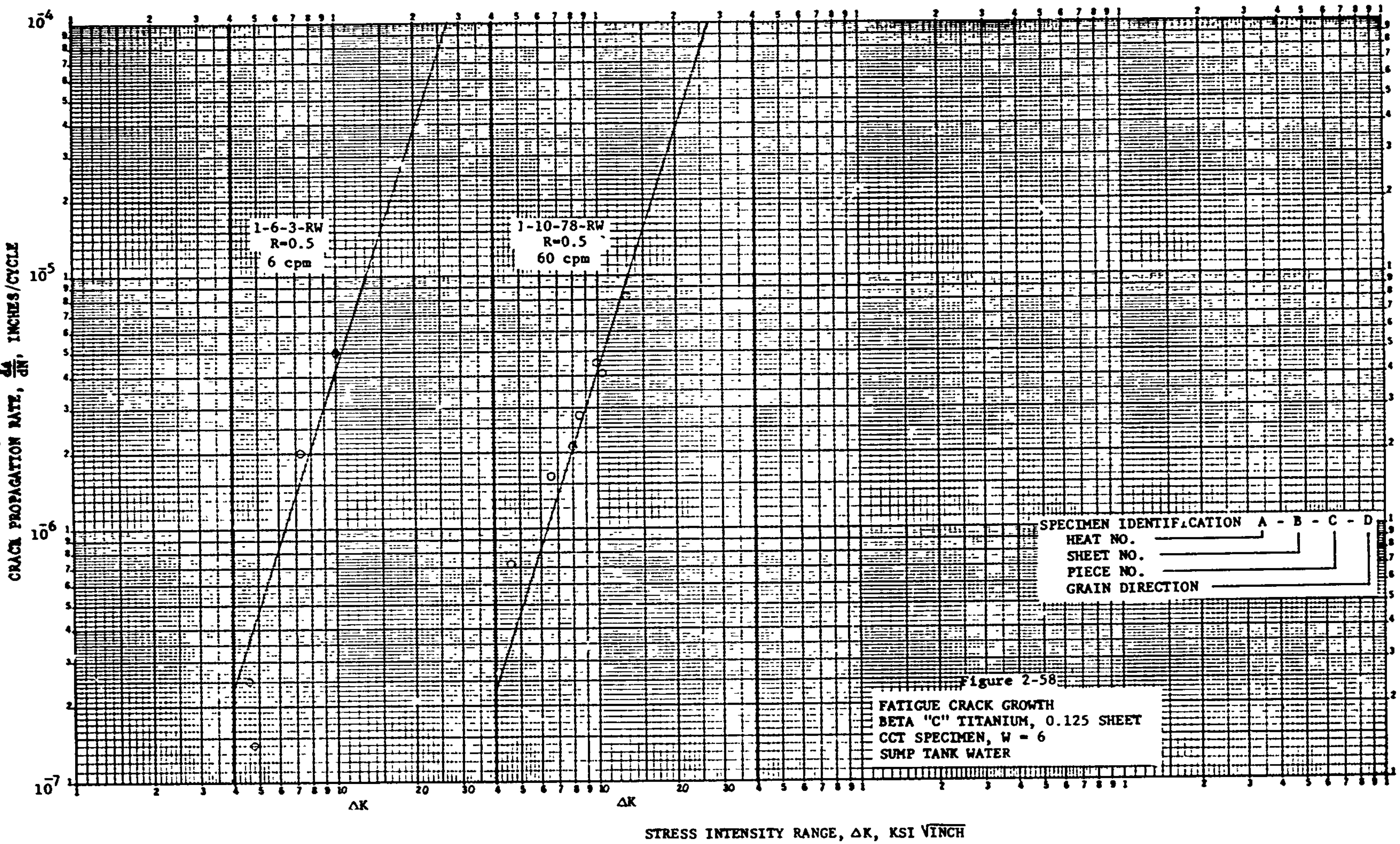


Figure 2-58

FATIGUE CRACK GROWTH
BETA "C" TITANIUM, 0.125 SHEET
CCT SPECIMEN, W = 6
SUMP TANK WATER

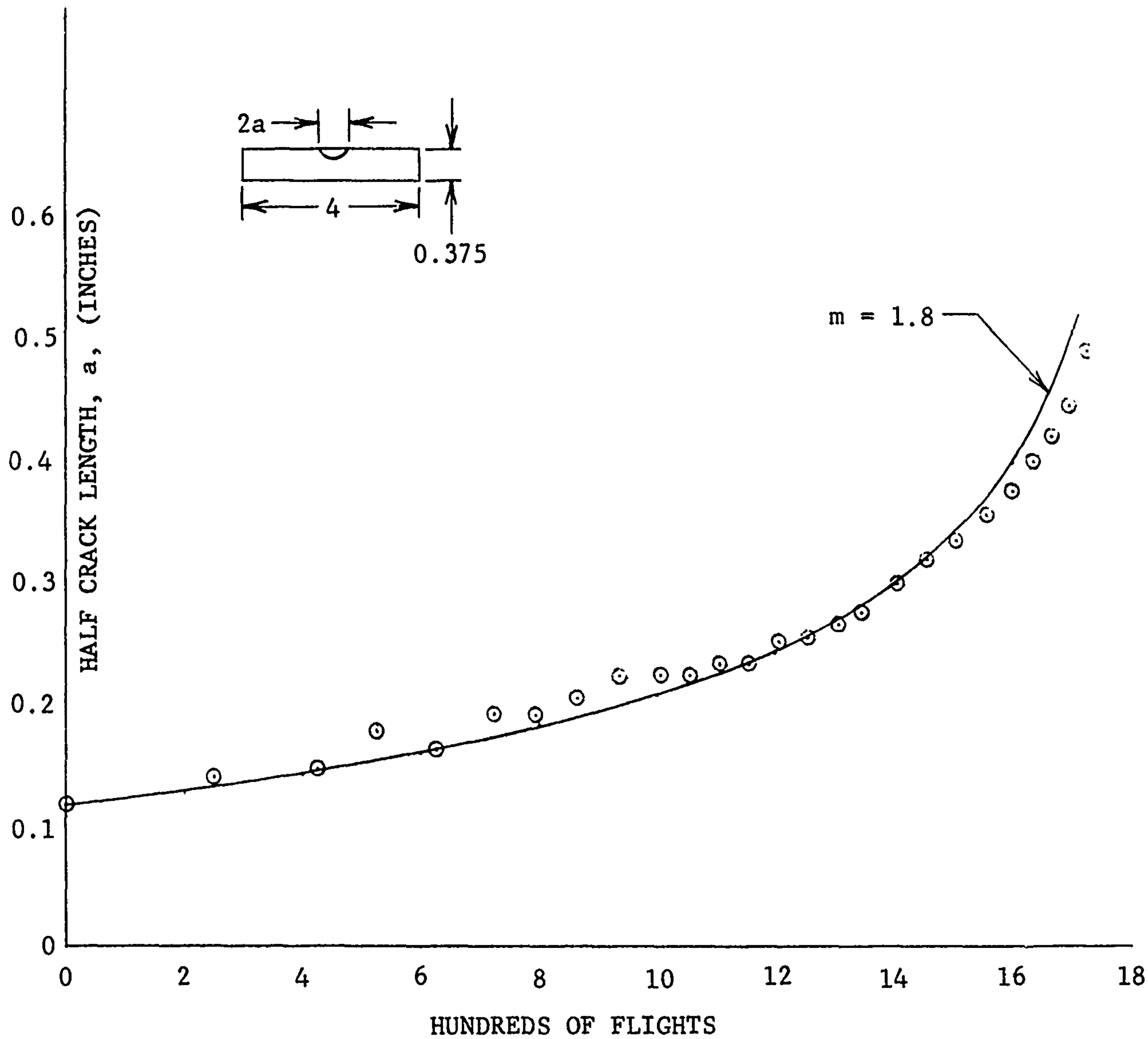


Figure 2-59

CRACK GROWTH TEST
BETA ANNEALED 6AL-4V TITANIUM
FTJ10940-153
SPECTRUM NO. 1 ( $\sigma_{max}$ = 79.82 KSI)
DRY AIR
SEMICIRCULAR SURFACE FLAW

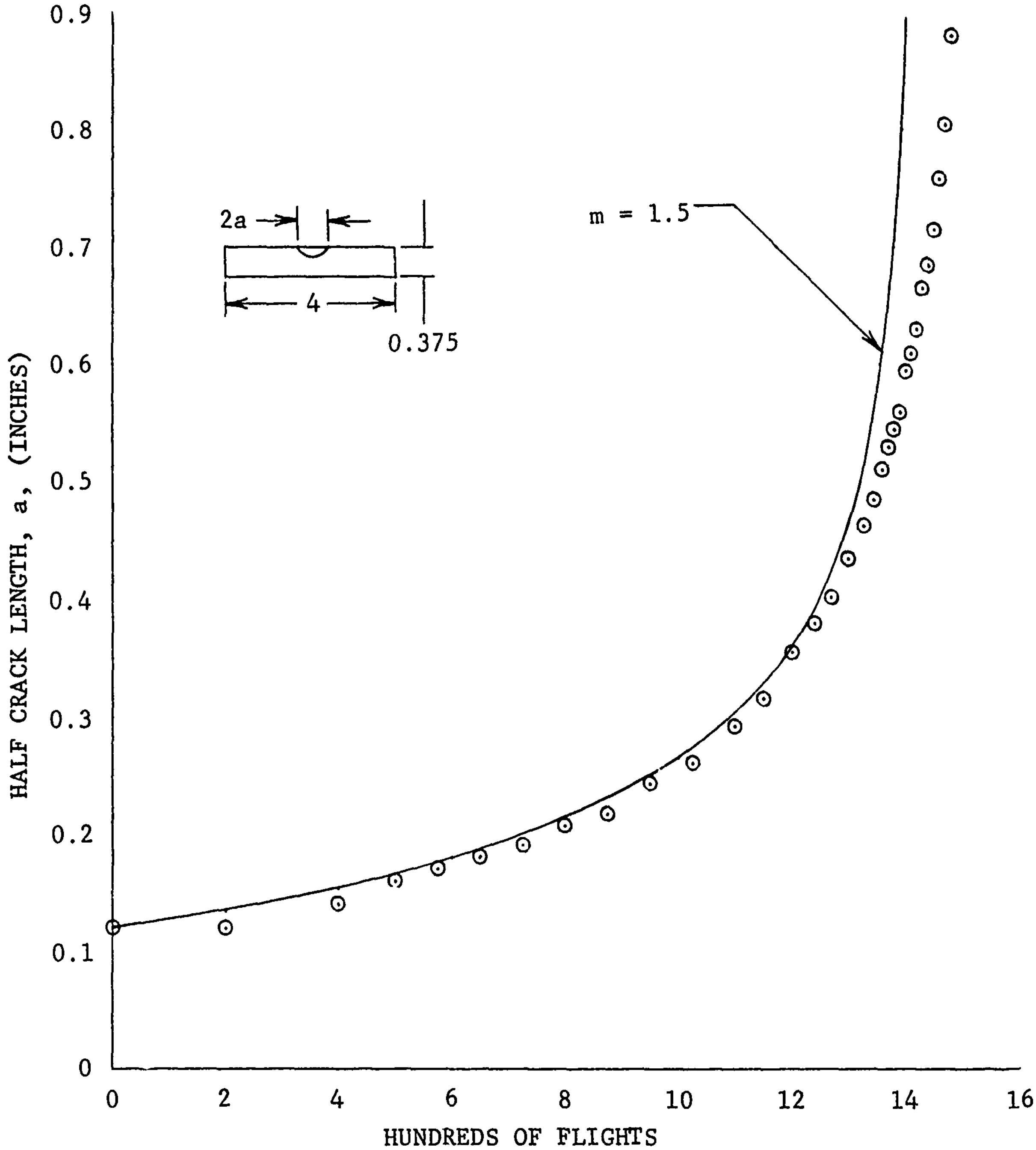


Figure 2-60

CRACK GROWTH TEST
BETA ANNEALED 6AL-4V TITANIUM
FTJ10940-153
SPECTRUM NO. 2 ($\sigma_{max}$ = 68.89 KSI)
DRY AIR
SEMICIRCULAR SURFACE FLAW

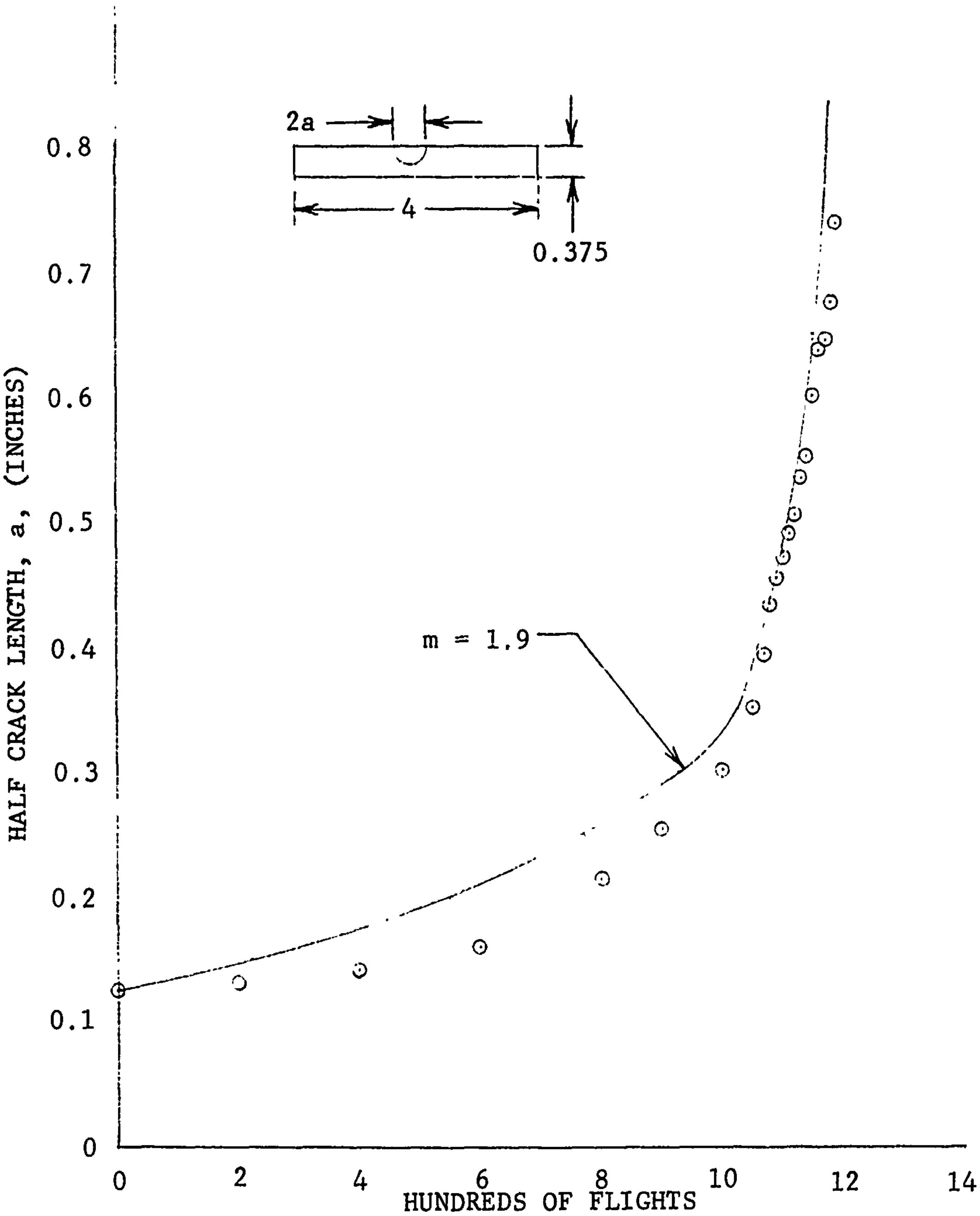


Figure 2-61

CRACK GROWTH TEST
BETA ANNEALED 6AL-4V TITANIUM
FTJ10940-153
SPECTRUM NO. 1 ($\sigma_{max}$ = 79.82 KSI)
SUMP TANK WATER
SEMICIRCULAR SURFACE FLAW

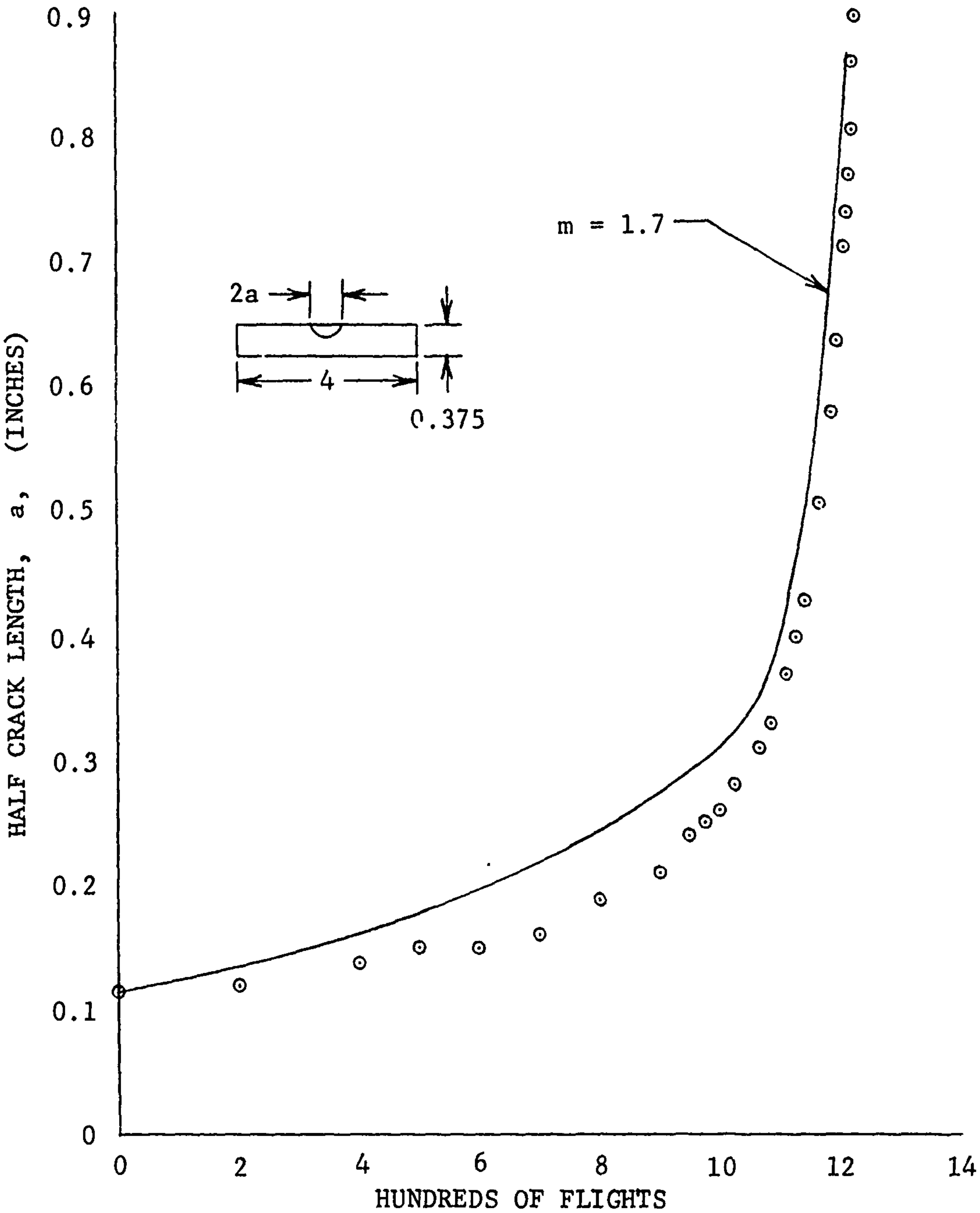


Figure 2-62

CRACK GROWTH TEST
BETA ANNEALED 6AL-4V TITANIUM
FTJ10940-153
SPECTRUM NO. 1 * ($\sigma_{max}$ = 79.82 KSI)
SUMP TANK WATER
SEMICIRCULAR SURFACE FLAW

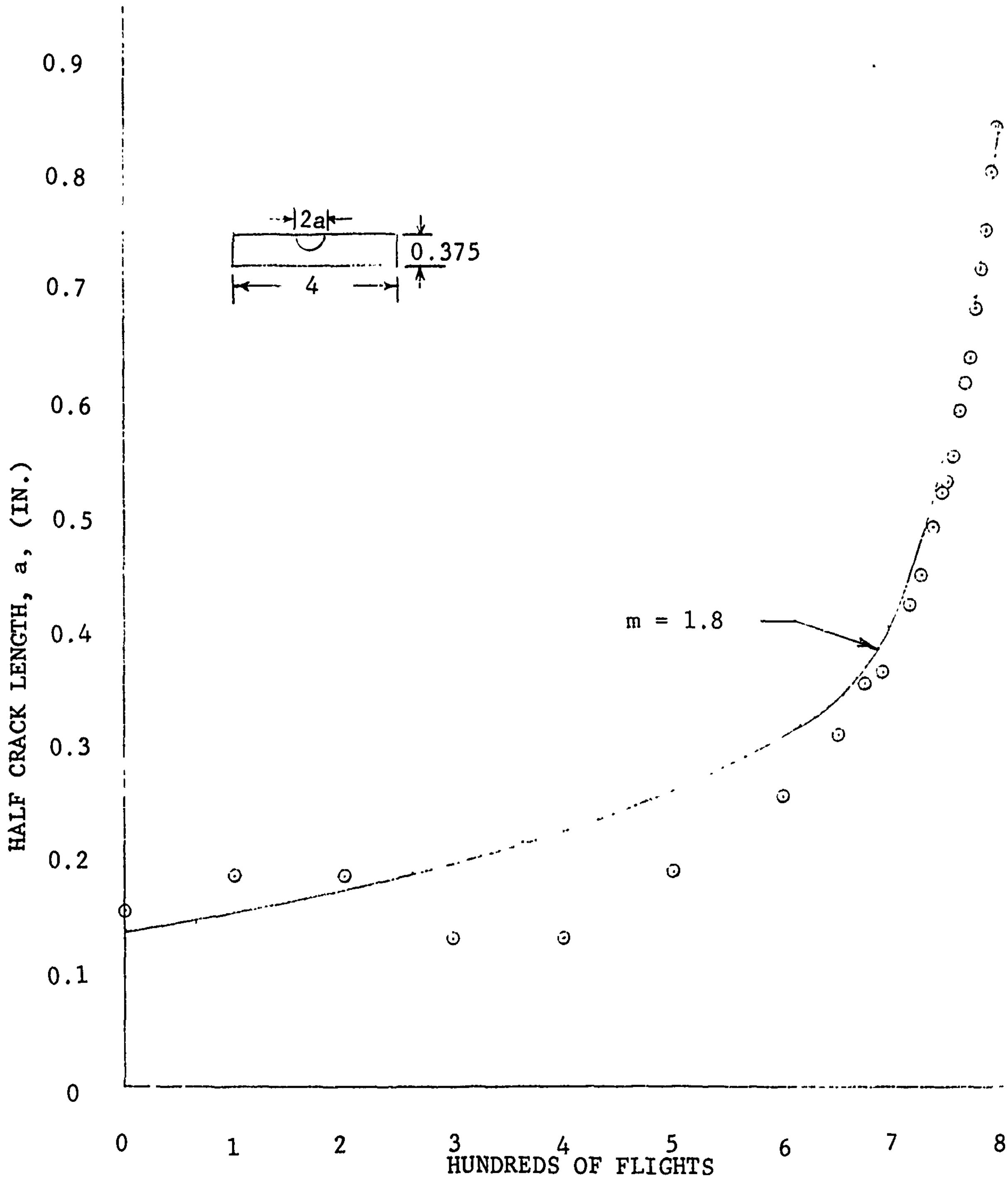


Figure 2-63

CRACK GROWTH TEST
BETA ANNEALED 6AL-4V TITANIUM
FTJ10940-153
SPECTRUM NO. 2 * ($\sigma_{max}$ = 68.89 KSI)
SUMP TANK WATER
SEMICIRCUIAR SURFACE FLAW

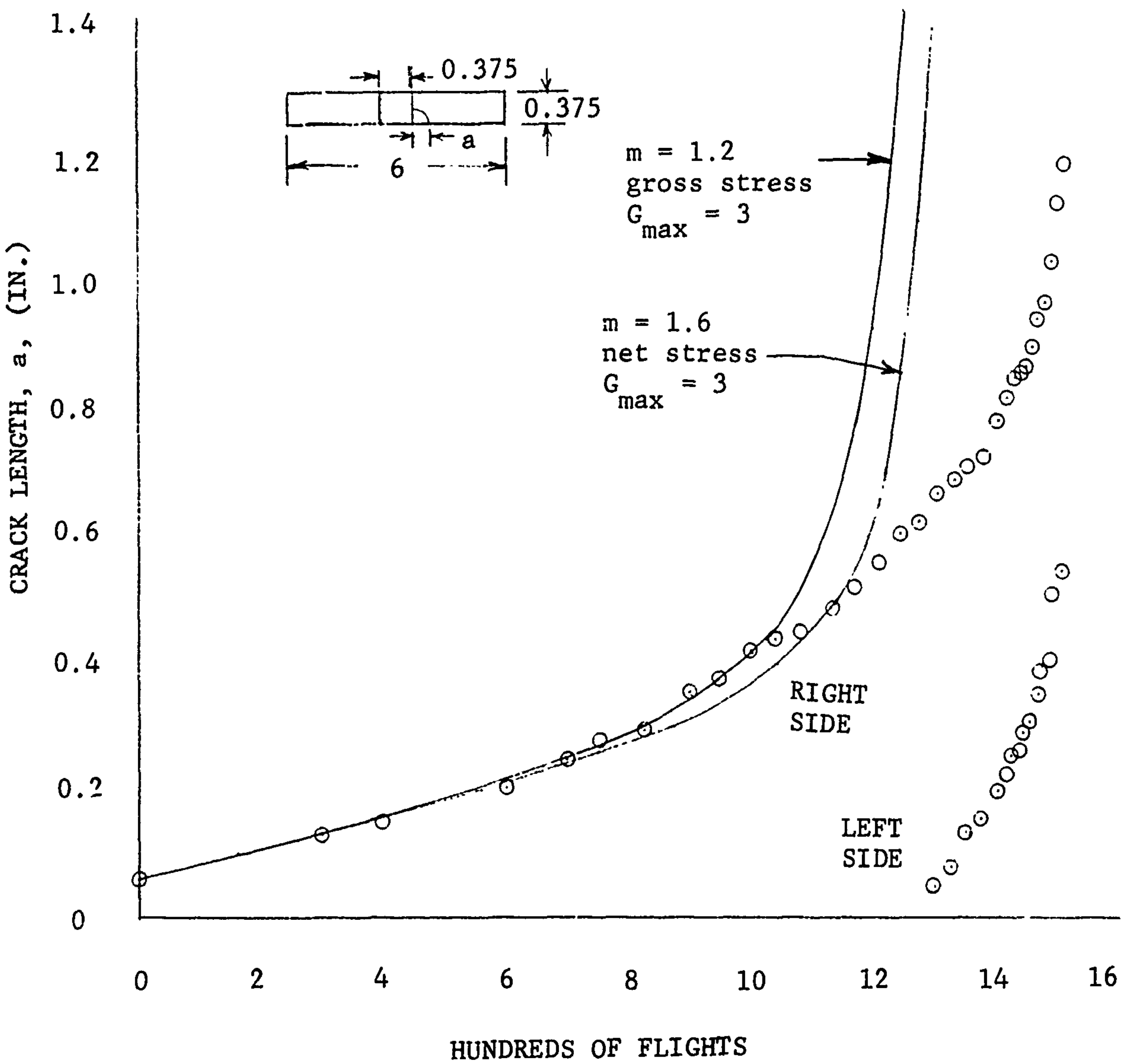


Figure 2-64

CRACK GROWTH TEST
BETA ANNEALED 6AL-4V TITANIUM
FTJ10940-152
SPECTRUM NO. 1 ($\sigma_{max}$ = 79.82 KSI)
DRY AIR
QUARTER CIRCULAR CORNER CRACK

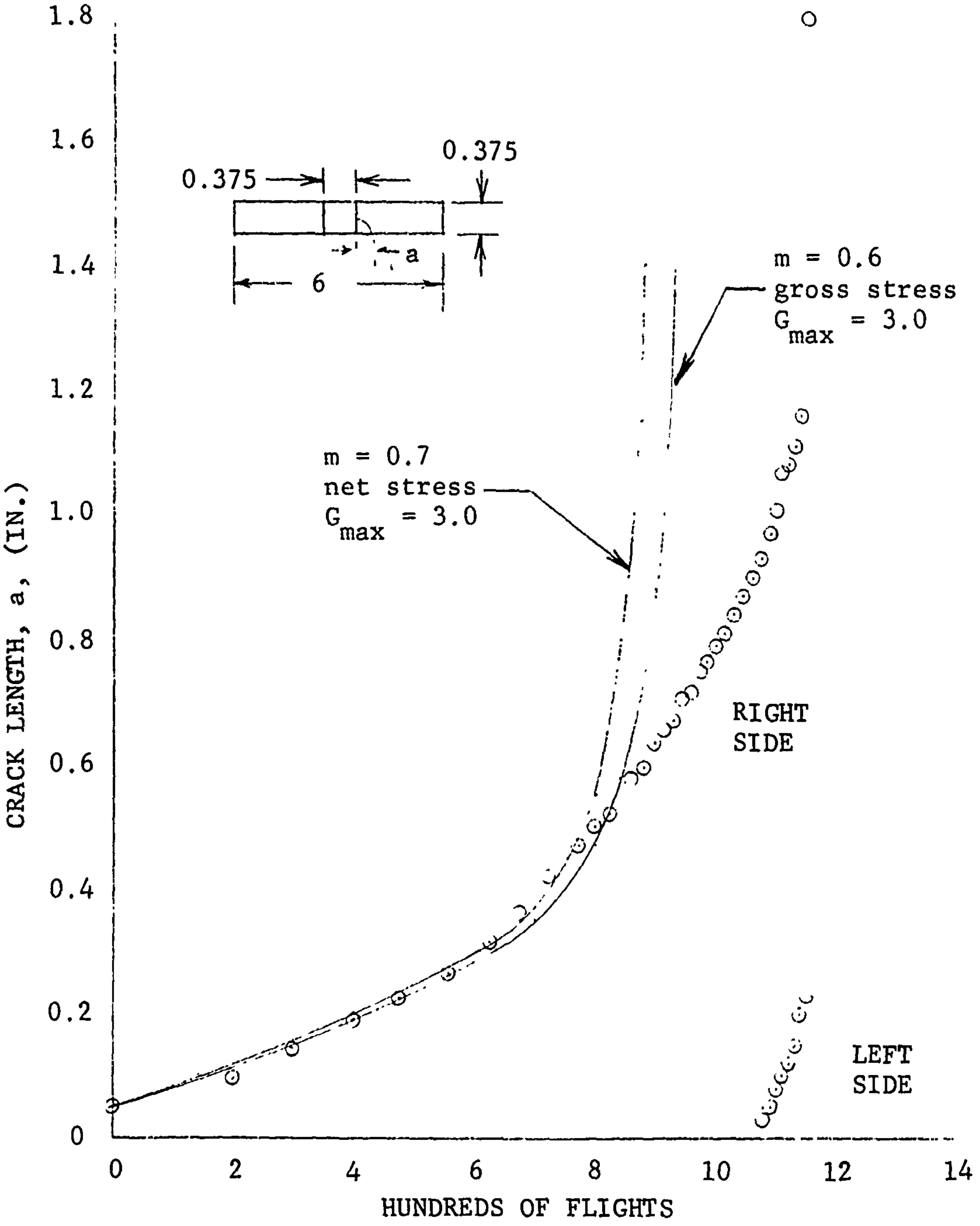


Figure 2-65

CRACK GROWTH TEST
BETA ANNEALED 6AL-4V TITANIUM
FTJ10940-152
SPECTRUM NO. 2 ($\sigma_{max}$ = 68.89 KSI)
DRY AIR
QUARTER CIRCULAR CORNER CRACK

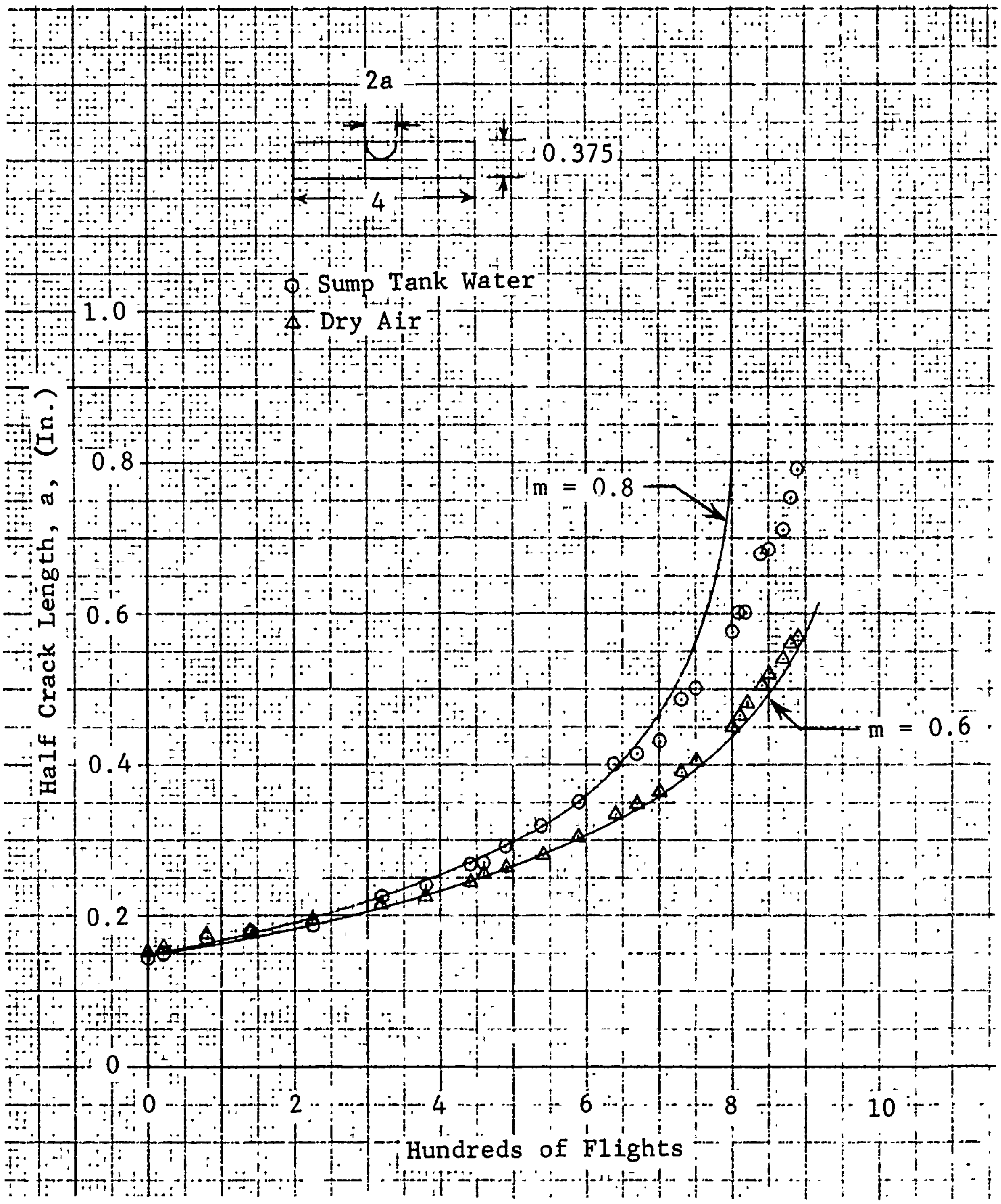


Figure 2-66

CRACK GROWTH TEST
10 NICKEL STEEL
FTJ10940-185
SPECTRUM NO. 1 * ($\sigma_{max}$ = 120 KSI)
SEMICIRCULAR SURFACE FLAW

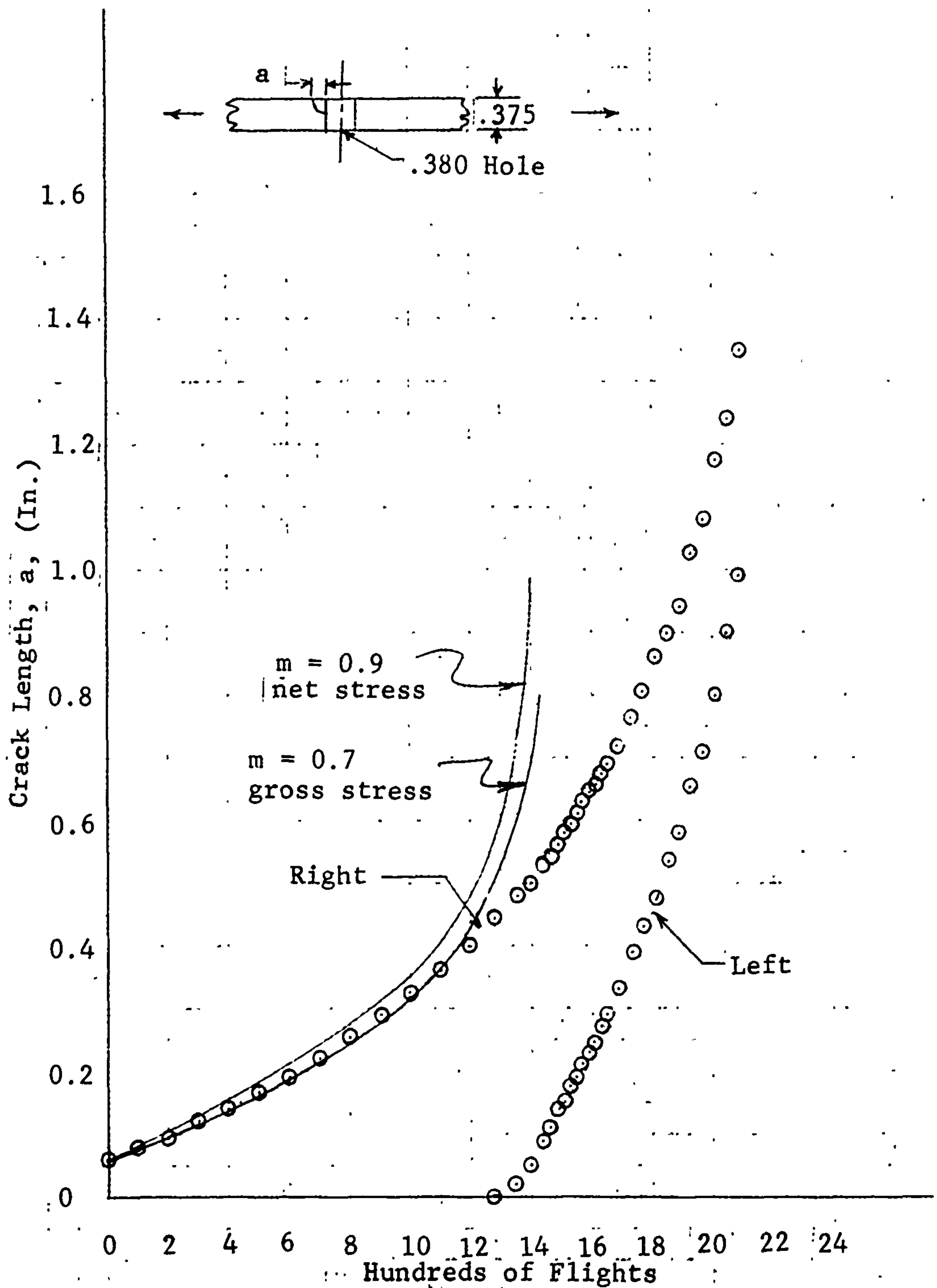


Figure 2-67

CRACK GROWTH TEST
10 NICKEL STEEL
FTJ10940-186
SPECTRUM NO. 1 ($\sigma_{max}$ = 120 KSI)
DRY AIR
QUARTER CIRCULAR CORNER CRACK

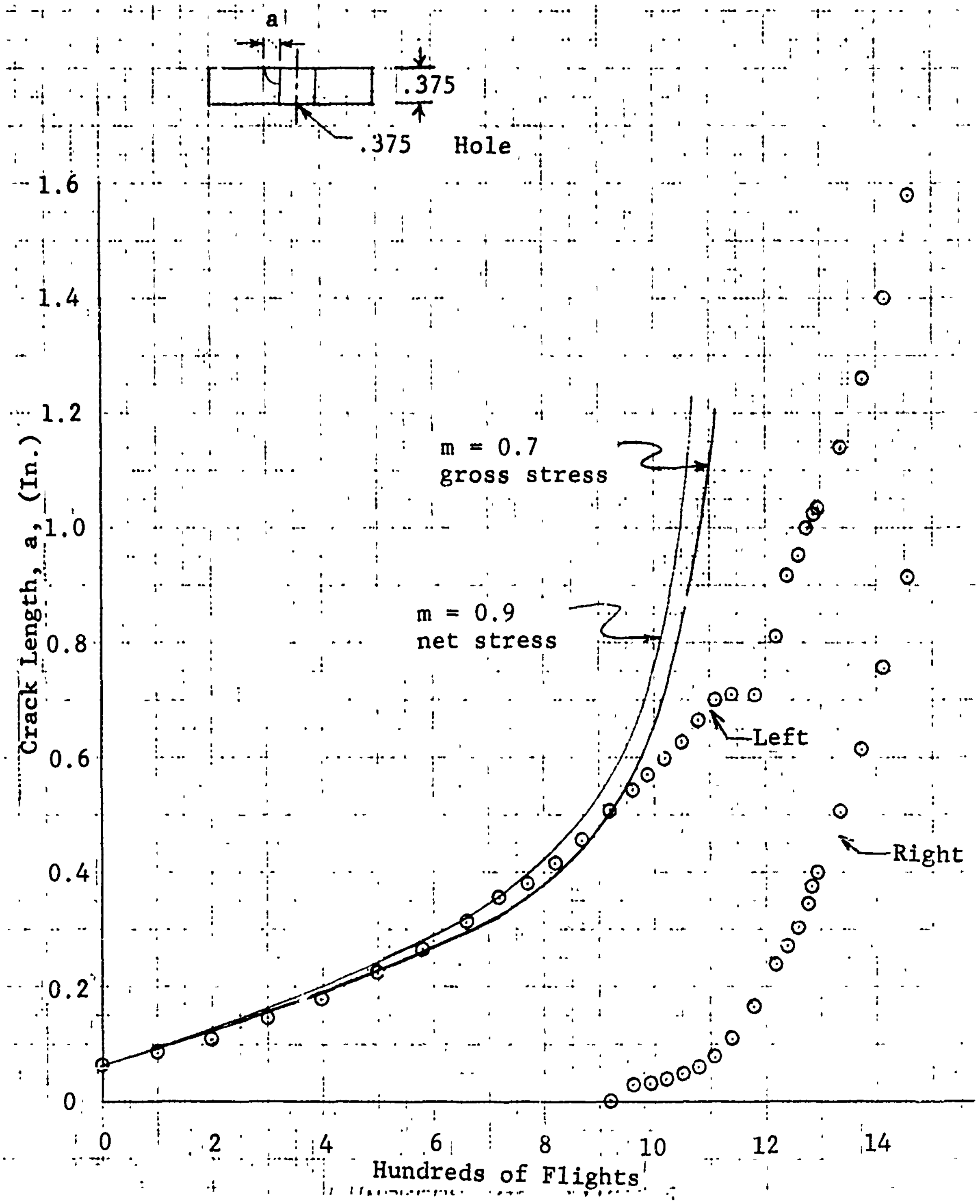


Figure 2-68

CRACK GROWTH TEST
10 NICKEL STEEL
FTJ10940-186
SPECTRUM NO. 2 ($\sigma_{max}$ = 103.6 KSI)
DRY AIR
QUARTER CIRCULAR CORNER CRACK

### 2.3.3 Crack Growth Analysis

Crack growth analyses were conducted on both WCTS designs using the results of the stress analysis, the fatigue loads spectrum and fracture mechanics test data. The Wheeler retardation model was used to account for spectrum retardation and environmental effects to the extent observed in the spectrum-environmental test program.

A modified version of the Air Force computer program CRACKS was used for the crack growth analyses. The modifications are discussed in report AFFDL-TR-73-1. The CRACKS program is based on a linear accumulation of incremental crack growth, i.e.

$$\frac{da}{dN} = f(\Delta K) \tag{1}$$

$$a_n = a_o + \sum_{i=1}^{n} \left(\frac{da}{dN}\right)_i \tag{2}$$

where $a_o$ = initial crack length

$a_n$ = crack length after n cycles

The functional relationship between crack growth rate da/dN, and the stress intensity range, $\Delta K$, is established empirically from the constant amplitude crack growth test data. As presented in Section 2.3.2.1, this relationship is expressed in terms of one or more equations of either the Paris or the Forman type. Environmental enhanced crack growth is accounted for by use of the appropriate da/dN data.

The Wheeler model was used to account for spectrum retardation effects, i.e., the growth rate reduction following a peak overload. The Wheeler model was incorporated into the CRACKS program by modifying Equation 2 as follows:

$$a_n = a_o + \sum_{i=1}^{n} C_{Pi} \left(\frac{da}{dN}\right)_i \tag{3}$$

Where $C_{Pi}$ is the spectrum retardation factor

$$C_{Pi} = \left[\frac{R_Y}{a_p - a}\right]^m \qquad \text{for } a + R_Y < a_p$$

$$C_{Pi} = 1 \qquad \text{for } a + R_Y \geq a_p \tag{4}$$

where a, $a_p$ and $R_Y$ are defined in the sketch

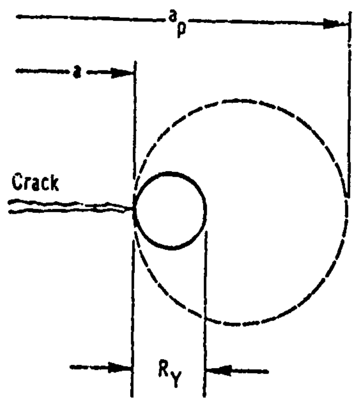


$$R_Y = \frac{1}{6\pi} \left(\frac{K}{\sigma_{ys}}\right)^2$$

The retardation exponent, m, is an empirical constant determined on the basis of the spectrum environmental crack growth tests discussed in Section 2.3.2.2. The best-fit m value is obtained by generating a family of crack growth curves using the test spectrum, the appropriate da/dN data and a series of m values. The analysis curve that most closely approximates the experimental data sets the m value. The analysis curves shown in Figures 2-59 through 2-68 represent the best-fit m values for beta annealed 6Al-4V titanium and 10 Ni steel.

Equation (3) implies cycle-by-cycle summation of the incremental crack growth. To improve efficiency, the CRACKS program uses a Runge Kutta integration of the da/dN curves over an interval of fatigue cycles at a constant load level within the fatigue spectrum. This procedure is extremely accurate but requires several computational steps. Further efficiency improvements were achieved for the AMAVS program by using a single-step integration procedure, i.e.

$$a_n = a_o + \sum_{i=1}^{EN} C_{Pi} \left(\frac{da}{dN}\right)_i \Delta N_i \tag{5}$$

where $\Delta Ni$ is the number of cycles in the $i^{th}$ spectrum load level and the incremental crack growth within each load level is summed over the range of load levels applied (i = 1 to EN).

Use of Equation 5 resulted in a four-fold savings in computer run time, however, computer run times were still too long. Satisfactory length computer runs (approx. 1 minute per 1280 flights) were achieved by converting the flight-by-flight spectrum to a 10 flight block spectrum. Comparative runs indicated that crack growth rates were essentially the same for both spectra. The block spectrum was slightly conservative because more retardation occurred in the flight-by-flight spectrum.

### 2.3.4 Fracture Analysis of Selected Control Points

Fracture analyses were conducted on 10 control points in the FSIL WCTS and 9 in the NBB configuration. Primary tensile-loaded elements of the WCTS were identified as control points based on the evaluation of finite element math model stresses, stress analysis results and design details. Surveys of the stress distributions for the five fatigue spectrum conditions (ASKA Conditions 2, 10, 5, 9 and 7, representing post-takeoff, TFR, prelanding, climb/cruise, and ground/taxi, respectively) were considered in the selection of control points.

A worksheet was prepared for each control point showing a sketch of the location and dimensions of the control point, part identification, material, damage tolerance category, and inspectability category. These control point data are supplemented with tabulated information which includes the stresses (maximum principal and effective) for each condition in the fatigue loads spectrum; maximum spectrum, limit, net ultimate, and allowable stress levels; initial and critical crack sizes; and type of crack (cracked hole, surface crack, etc.) considered at each control point.

Areas of the WCTS approaching and/or exceeding the following established gross section limit stress levels were selected as primary fracture control points.

| | |
|---|---|
| o Ti 6Al-4V ($\beta$,MA) | 67 ksi - maximum<br>53 ksi - typically |
| o 10 Ni Steel | 100 ksi - maximum<br>80 ksi - typically |
| o 7075 Al<br>2024 Al | 30 ksi - maximum |

Using the gross section limit stress levels noted above, critical crack sizes, $a_c$ were calculated using the following crack models.

o For part thru cracks adjacent to holes:

$$K_{IC} = \sigma \sqrt{\frac{\pi a_c}{Q}} \; M_K \; G_{KT}$$

$$a_c = \frac{Q}{\pi} \left[\frac{K_{IC}}{M_K \sigma G_{KT}}\right]^2$$

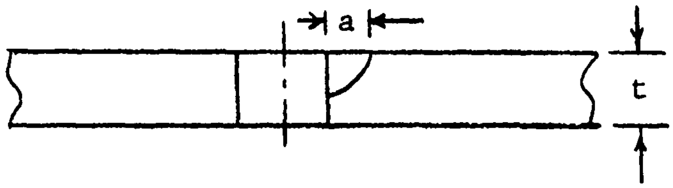


where Q = Flaw Shape Factor = $2.46 - .212\ (\sigma/\sigma_{ys})^2$
$M_K$ = Back Face Correction Factor
$G_{KT}$ = Stress Gradient Factor

o For thru-the-thickness cracks adjacent to holes:

$$K_{IC} = \sigma \sqrt{\frac{(a_c + d)}{2}} \; G_{KT}$$

$$a_c = \frac{2}{\pi} \left[\frac{K_{IC}}{G_{KT}\sigma}\right]^2 - d$$

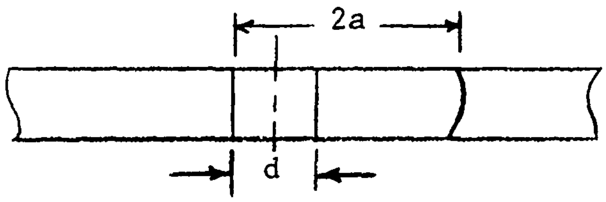


o For thru-the-thickness cracks with a finite width correction.

$$K_{IC} = \sigma\sqrt{\pi a}\,\sqrt{\operatorname{Sec}\frac{\pi a}{W}}$$

$$a_c = \frac{1}{\pi}\left(\frac{K_{IC}}{\sigma}\right)^2 \frac{1}{\operatorname{Sec}\frac{\pi a}{W}}$$

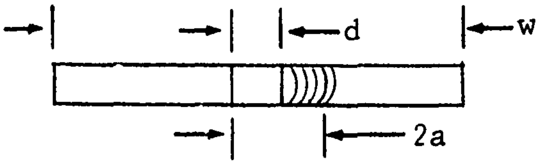


The following material properties were used in developing critical crack sizes:

<u>10 Ni Steel</u>

$K_{IC}$ = 200 ksi$\sqrt{in}$

$\sigma_{ys}$ = 175 ksi

E = 28.0 x $10^6$ psi

<u>Ti 6AL-4V ( $\beta$,MA)</u>

$K_{IC}$ = 80 ksi $\sqrt{in}$

$\sigma_{ys}$ = 115 ksi

E = 16.3 x $10^6$ psi

Critical crack sizes were calculated using stress levels corresponding to the maximum service spectrum stress or the limit load stress whichever was the greatest. For the control points considered herein, the highest stress was consistently the limit load stress; i.e., 2/3 ultimate gross section stress. Figure 2-69 shows a typical critical crack length, in this case a thru-the-thickness crack, for gross section limit stresses of 60 ksi to 130 ksi. For control points in the WCTS, $a_c$ typically was less than 4.0 inches. For cases where $a_c$ >4 inches, it was assumed that other factors such as structural geometry, loads redistribution, etc., would dominate.

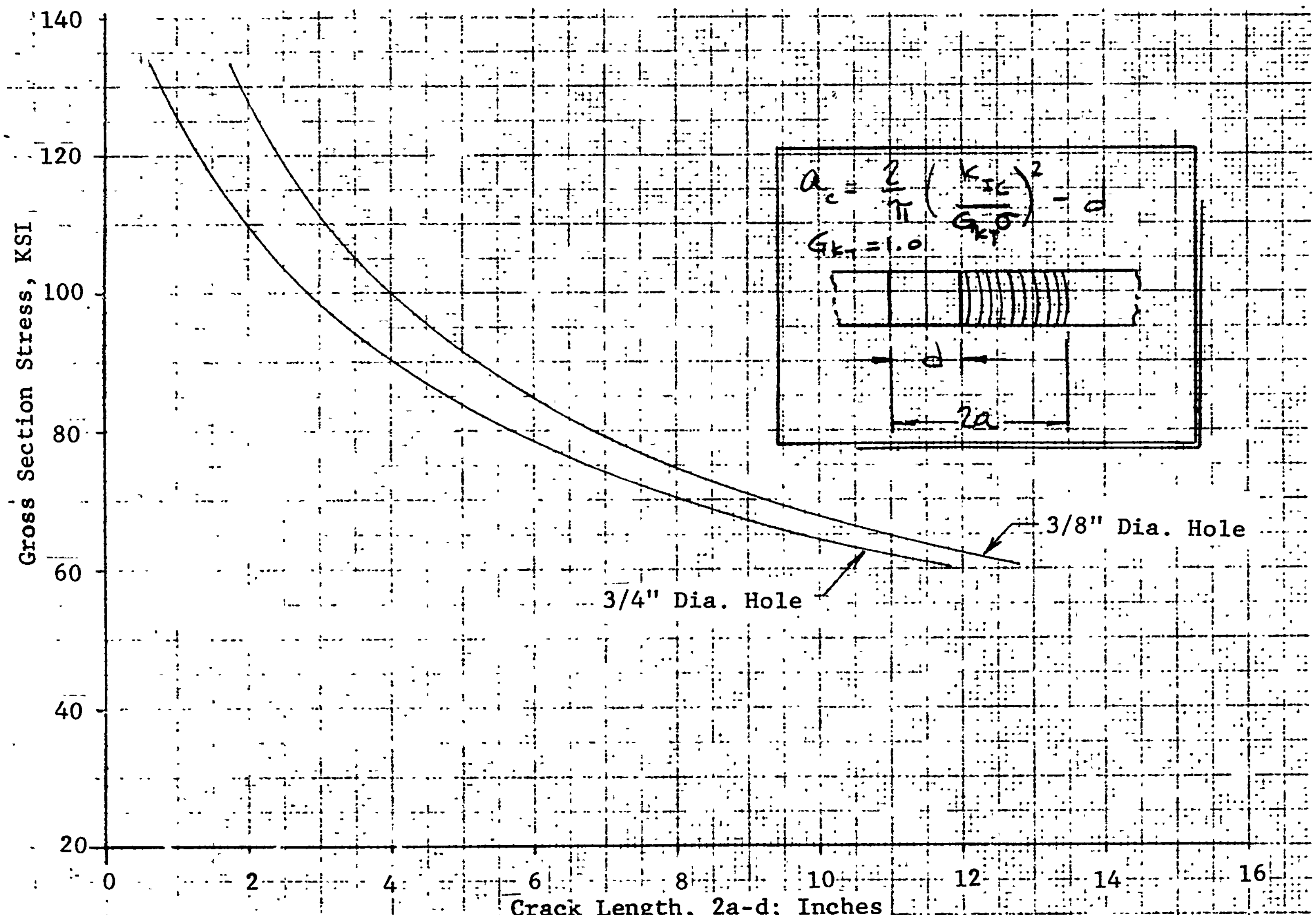


Figure 2-69 CRITICAL CRACK LENGTH VS. GROSS SECTION STRESS THRU THE THICKNESS CRACK IN 10 NI STEEL; $K_{IC}$ = 200 KSI IN.

### 2.3.4.1 FSIL Fracture Analysis

Fracture analyses were conducted on the following 10 FSIL configuration control points.

1. Control Point 1, Figure 2-70, Aft Outboard Corner, Upper Plate at Weld Line.

   Crack growth analyses were conducted at the $X_F$ 124.75 weld line using EB da/dN data. A 0.15-inch initial crack length, a crack retardation exponent, m = o, and a sump tank water environment were used for these analyses. Results indicated that the initial crack length was less than 0.15-inches for 100% and 90% stress levels of the five fatigue spectrum conditions. An initial crack length greater than 0.15-inches with a critical length of 1.00-inches was calculated for an 80% stress level. Further work is needed to qualify this location.

2. Control Point 2, Figure 2-71, $Y_F$ 992 Bhd, Outboard, Lower Attach Angle.

   A crack growth analysis was conducted for a cracked hole at $X_F$54 using an 0.15-inch initial crack length, a crack retardation exponent m = 0.7, and a sump tank water environment. A critical crack length of 0.87 inches was calculated.

3. Control Point 3, Figure 2-72, Lower Plate, Aft Longeron, Outboard Lower

4. Control Point 4, Figure 2-73, Lower Plate, Lug

5. Control Point 5, Figure 2-74, Lower Plate, Centerline Splice

6. Control Point 6, Figure 2-75, $Y_F$992 Bhd, Inboard, Fuel Transfer Hole, $X_F$39

7. Control Point 7, Figure 2-76, $Y_F$932 Bhd, Forward Outboard, Lower Attach Angle

8. Control Point 8,
   - o Rib ($X_F$ 119)
   - o Sweep Actuator Fitting
   - o Sweep Actuator Fitting Support

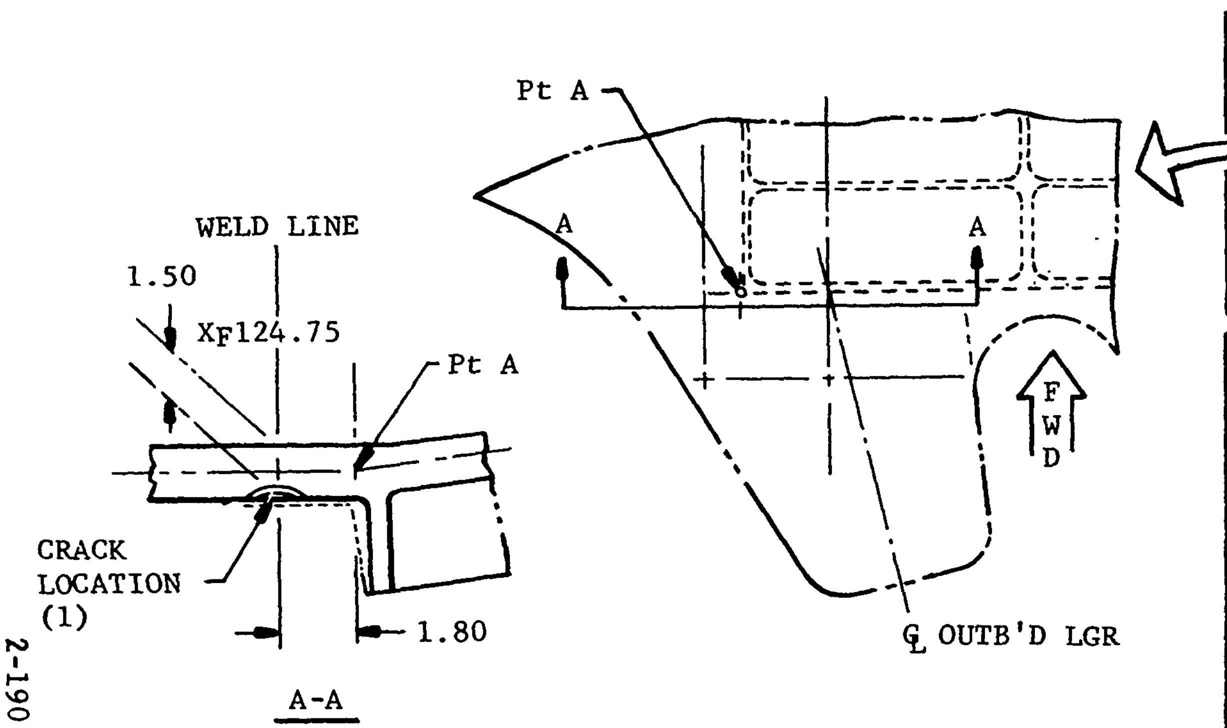


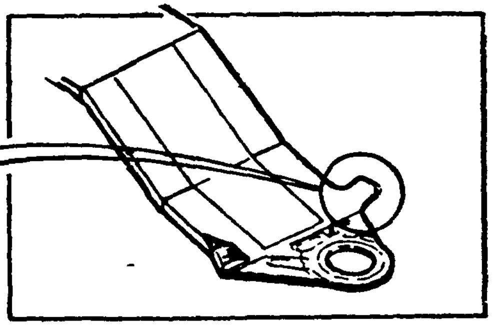

**PART IDENTIFICATION**
X7223710 UPPER LUG/PLATE WELD ASSY

**LOCATION**
$X_F$124.75; $Y_F$992; $Z_F$ 32

**MATERIAL**
Ti 6AL-4V (β, MA)

**DAMAGE TOLERANCE CATEGORY**
SAFE CRACK GROWTH

**INSPECTABILITY**
DEPOT LEVEL

| CRACK LOCATION | ANALYSIS * | GROSS SECTION ULTIMATE DESIGN STRESSES FOR ASKA CONDITIONS IN FATIGUE SPECTRUM, KSI | | | | | | STRESS, KSI | | | | CRACK SIZE, INCHES | | CRACK TYPE |
|---|---|---|---|---|---|---|---|---|---|---|---|---|---|---|
| | | ** | 2 | 10 | 5 | 9 | 7 | MAXIMUM SPECTRUM* | GROSS SEC LIMIT* | NET SECT. ULTIMATE* | ALLOWABLE | INITIAL | CRITICAL | |
| (1) | FRAC-TURE | M | -25 | 106 | -44 | -17 | 28 | 46.7 | 70.7 | N.A. | >80 | <.15 | 0.72 | SC |

* Gross section principal stresses used for fracture analysis.
Net section effective stresses used for fatigue analysis.
** Type stress--M: Maximum Principal Stress
E: Effective Stress

Figure 2-70 FSIL CONTROL POINT 1; UPPER PLATE, AFT OUTBOARD WELD LINE

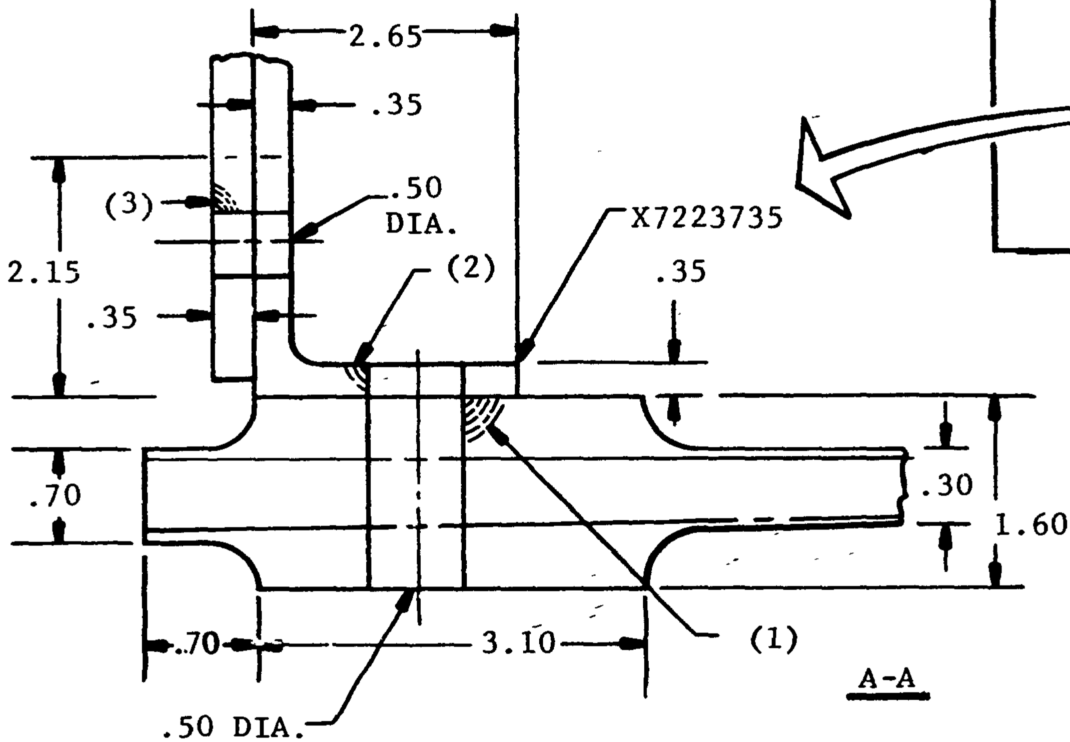


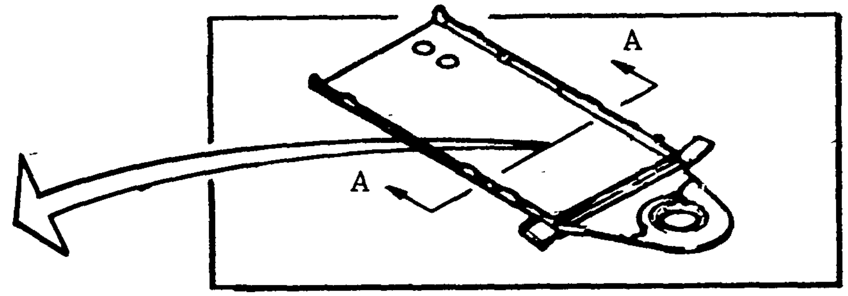


**PART IDENTIFICATION**
X7223735 ATTACH ANGLE

**LOCATION**
$X_F$54-72; $Y_F$992; $Z_F$ 0

**MATERIAL**
6AL-4V Ti (β, MA)

**DAMAGE TOLERANCE CATEGORY**
(1), (2) FAIL SAFE
(3) SAFE CRACK GROWTH

**INSPECTABILITY**
DEPOT LEVEL

| CRACK LOCATION | ANALYSIS * | GROSS SECTION ULTIMATE DESIGN STRESSES FOR ASKA CONDITIONS IN FATIGUE SPECTRUM, KSI | | | | | | STRESS, KSI | | | | CRACK SIZE, INCHES | | CRACK TYPE |
|---|---|---|---|---|---|---|---|---|---|---|---|---|---|---|
| | | ** | 2 | 10 | 5 | 9 | 7 | MAXIMUM SPECTRUM* | GROSS SEC LIMIT* | NET SECT. ULTIMATE* | ALLOWABLE | INITIAL | CRITICAL | |
| (1) | FRACTURE | M | 81.07 | 34.75 | 81.07 | 73.02 | 2.35 | 49.80 | 54.07 | N.A. | >100 | - | - | CH |
| (2) | | | | | | | | | | | | - | - | CH |
| 3 | FATIGUE | E | 81.07 | 34.75 | 81.07 | 73.02 | 2.35 | 60.26 | N.A. | 98.09 | 100 | >0.15 | 0.870 | CH |

* Gross section principal stresses used for fracture analysis.
Net section effective stresses used for fatigue analysis.
** Type stress--M: Maximum Principal Stress
E: Effective Stress

Figure 2-71 FSIL CONTROL POINT 2; FSIL $Y_F$ 992 BULKHEAD ATTACH ANGLE

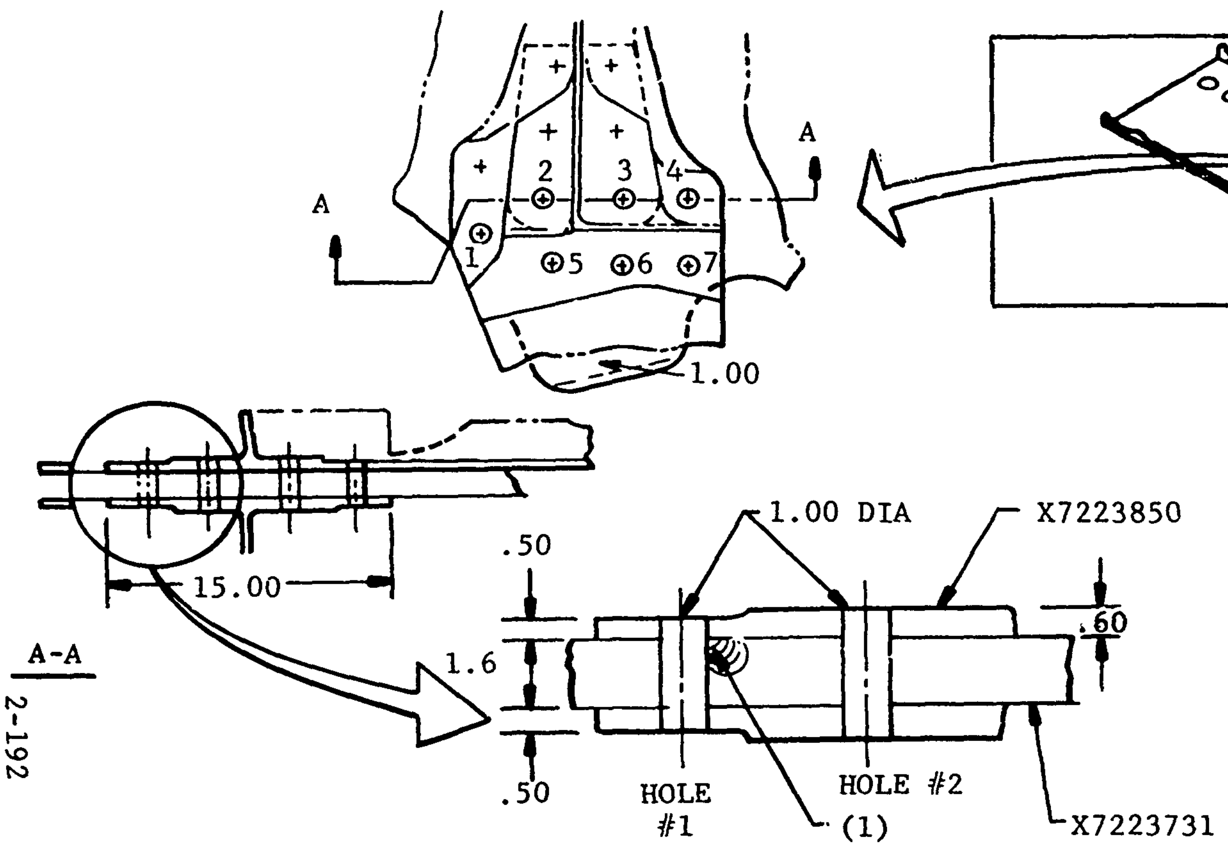


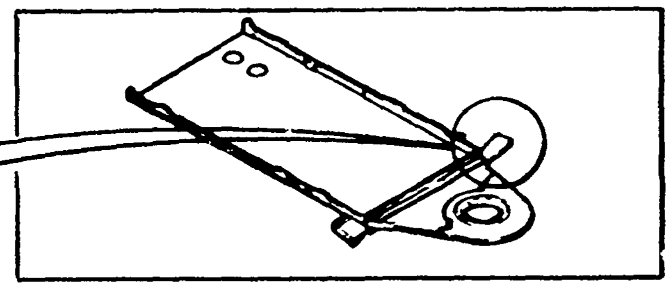

**PART IDENTIFICATION**
X7223850 LGR/X7223730 LWR PLATE ASSY

**LOCATION**
$X_F119$; $Y_F992$; $Z_F0$

**MATERIAL**
6AL-4V Ti (β,MA)

**DAMAGE TOLERANCE CATEGORY**
FAIL SAFE

**INSPECTABILITY**
DEPOT LEVEL

| CRACK LOCATION | ANALYSIS * | GROSS SECTION ULTIMATE DESIGN STRESSES FOR ASKA CONDITIONS IN FATIGUE SPECTRUM, KSI | | | | | | STRESS, KSI | | | | CRACK SIZE, INCHES | | CRACK TYPE |
|---|---|---|---|---|---|---|---|---|---|---|---|---|---|---|
| | | ** | 2 | 10 | 5 | 9 | 7 | MAXIMUM SPECTRUM* | GROSS SEC LIMIT* | NET SECT. ULTIMATE* | ALLOWABLE | INITIAL | CRITICAL | |
| (1) | FRACTURE | M | 43 | -109 | 43 | 34 | -24 | 26.41 | 28.68 | N.A. | >100 | >0.15 | >4.8 | CH |
| | FATIGUE | E | 55 | 105 | 55 | 47 | 22 | 48.07 | N.A. | 52.20 | 100 | | | |

* Gross section principal stresses used for fracture analysis.
Net section effective stresses used for fatigue analysis.
** Type stress--M: Maximum Principal Stress
E: Effective Stress

Figure 2-72 FSIL CONTROL POINT 3; $Y_F$ 992 BULKHEAD, AFT LOWER, OUTBOARD

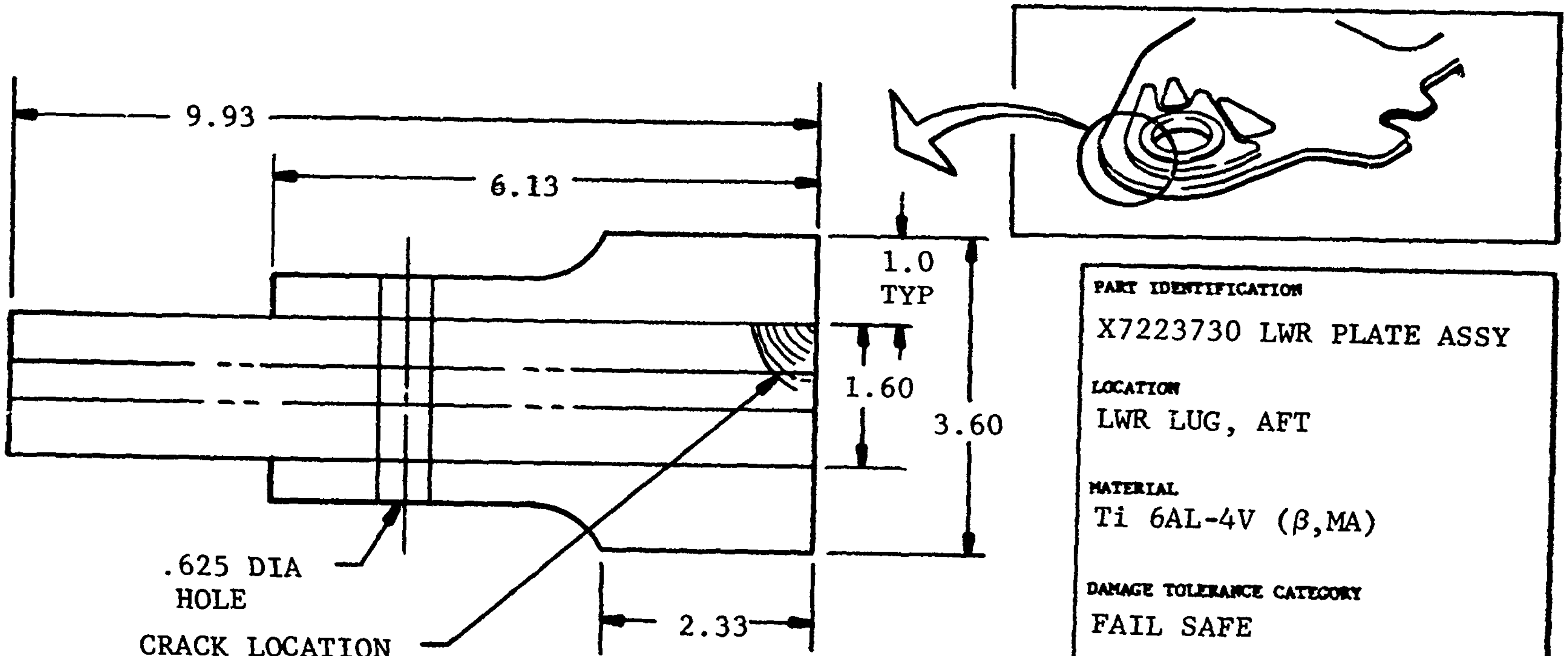


PART IDENTIFICATION
X7223730 LWR PLATE ASSY

LOCATION
LWR LUG, AFT

MATERIAL
Ti 6AL-4V (β,MA)

DAMAGE TOLERANCE CATEGORY
FAIL SAFE

INSPECTABILITY
DEPOT LEVEL

| CRACK LOCATION | ANALYSIS * | GROSS SECTION ULTIMATE DESIGN STRESSES FOR ASKA CONDITIONS IN FATIGUE SPECTRUM, KSI | | | | | | STRESS, KSI | | | | CRACK SIZE, INCHES | | CRACK TYPE |
|---|---|---|---|---|---|---|---|---|---|---|---|---|---|---|
| | | ** | 2 | 10 | 5 | 9 | 7 | MAXIMUM SPECTRUM* | GROSS SEC LIMIT* | NET SECT. ULTIMATE* | ALLOWABLE | INITIAL | CRITICAL | |
| (1) | FRACTURE | m | 105 | 70 | 101 | 100 | -4 | 62 | 70 | N.A. | >78 | >.15 | - | EC |
| | FATIGUE | e | 60 | 66 | 54 | 58 | -5 | 66 | N.A. | 71 | 78 | | | |

* Local gross section principal stresses used for fracture analysis.
Average net section effective stresses used for fatigue analysis.

** Type Stress . . . m: local max principal stress
e: average net section effective stress

Figure 2-73 FSIL CONTROL POINT 4; LOWER LUG

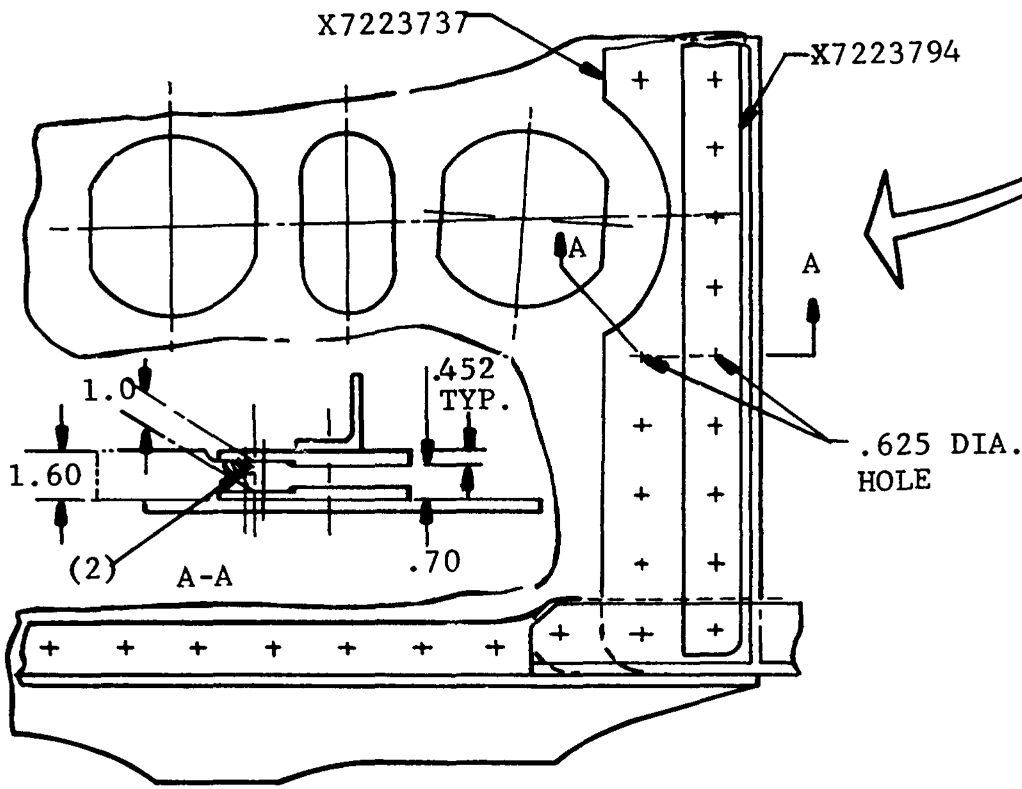


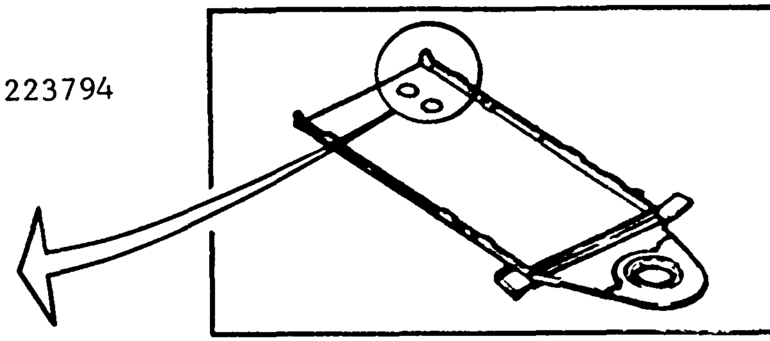

PART IDENTIFICATION
X7223730 LWR PLATE ASSY

LOCATION
$X_F0$; $Y_F980$; $Z_F0$

MATERIAL
Ti 6AL-4V ($\beta$,MA)

DAMAGE TOLERANCE CATEGORY
FAIL SAFE

INSPECTABILITY
DEPOT LEVEL

| CRACK LOCATION | ANALYSIS * | GROSS SECTION ULTIMATE DESIGN STRESSES FOR ASKA CONDITIONS IN FATIGUE SPECTRUM, KSI | | | | | | STRESS, KSI | | | | CRACK SIZE, INCHES | | CRACK TYPE |
|---|---|---|---|---|---|---|---|---|---|---|---|---|---|---|
| | | ** | 2 | 10 | 5 | 9 | 7 | MAXIMUM SPECTRUM* | GROSS SEC LIMIT* | NET SECT. ULTIMATE* | ALLOWABLE | INITIAL | CRITICAL | |
| (1) | FRACTURE | M | 54.88 | 33.78 | 51.50 | 48.27 | 2.36 | 31.64 | 36.60 | N.A. | >80 | - | - | CH |
| | | | | | | | | | | | | >0.15 | >4.0 | CH |
| | FATIGUE | E | 54.88 | 33.78 | 51.50 | 48.27 | 2.36 | 40.18 | N.A. | 60.70 | 80 | - | - | CH |

* Gross section principal stresses used for fracture analysis.
Net section effective stresses used for fatigue analysis.
** Type stress--M: Maximum Principal Stress
E: Effective Stress

Figure 2-74 FSIL CONTROL POINT 5; LOWER PLATE AND SPLICE

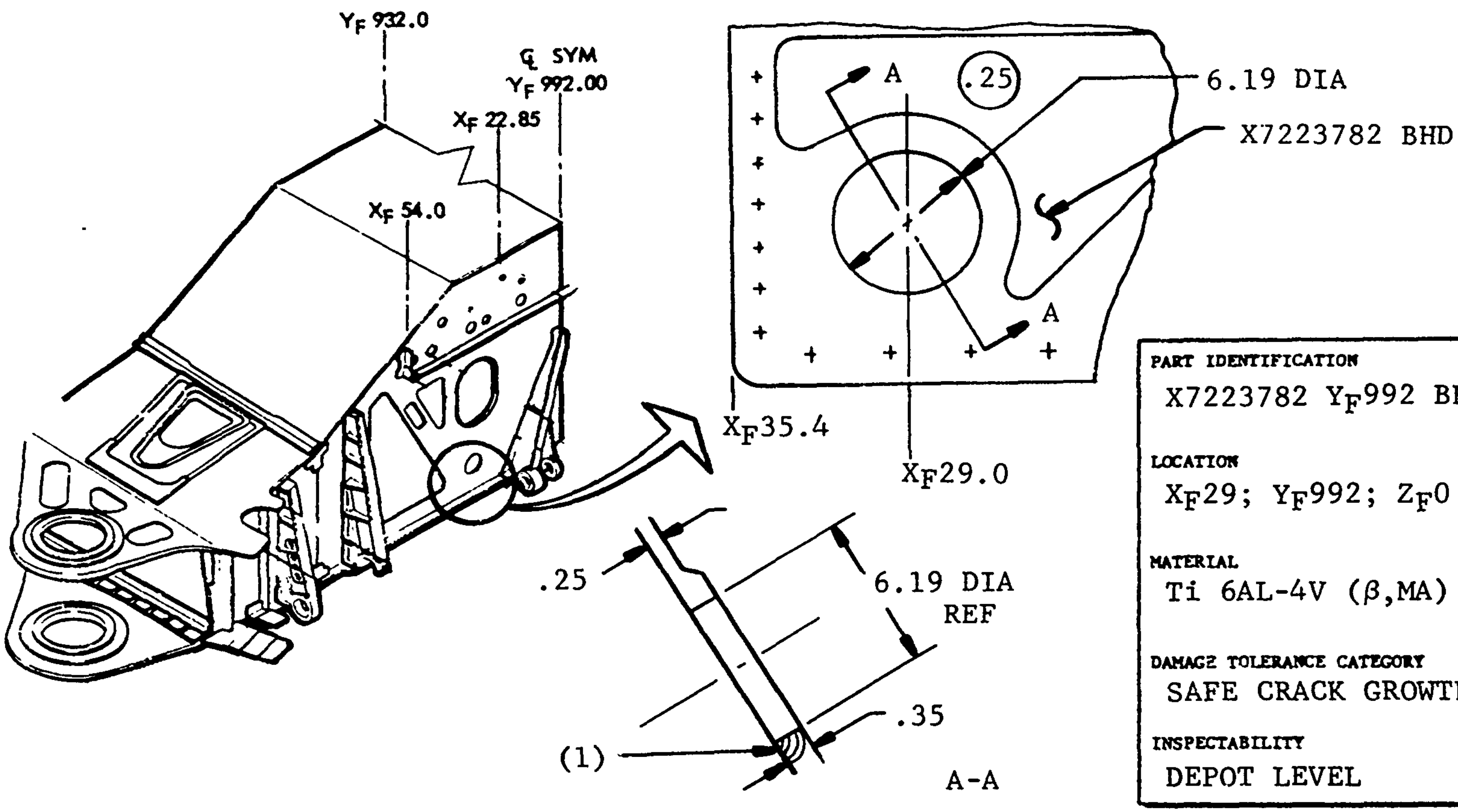


**PART IDENTIFICATION**
X7223782 $Y_F$992 BHD

**LOCATION**
$X_F$29; $Y_F$992; $Z_F$0

**MATERIAL**
Ti 6AL-4V (β,MA)

**DAMAGE TOLERANCE CATEGORY**
SAFE CRACK GROWTH

**INSPECTABILITY**
DEPOT LEVEL

| CRACK LOCATION | ANALYSIS * | GROSS SECTION ULTIMATE DESIGN STRESSES FOR ASKA CONDITIONS IN FATIGUE SPECTRUM, KSI | | | | | | STRESS, KSI | | | | CRACK SIZE, INCHES | | CRACK TYPE |
|---|---|---|---|---|---|---|---|---|---|---|---|---|---|---|
| | | ** | 2 | 10 | 5 | 9 | 7 | MAXIMUM SPECTRUM* | GROSS SEC LIMIT* | NET SECT. ULTIMATE* | ALLOWABLE | INITIAL | CRITICAL | |
| (1) | FRACTURE | M | 72 | 44 | 65 | 65 | 10 | 40.87 | 48.02 | N.A. | >80 | >0.15 | 0.63 | EC |
| | FATIGUE | E | 72 | 44 | 65 | 65 | 10 | 48.23 | N.A. | 56.67 | 80 | | | |

* Gross section principal stresses used for fracture analysis.
Net section effective stresses used for fatigue analysis.
** Type stress--M: Maximum Principal Stress
E: Effective Stress

Figure 2-75 FSIL CONTROL POINT 6; $Y_F$ 992 BULKHEAD, INBOARD

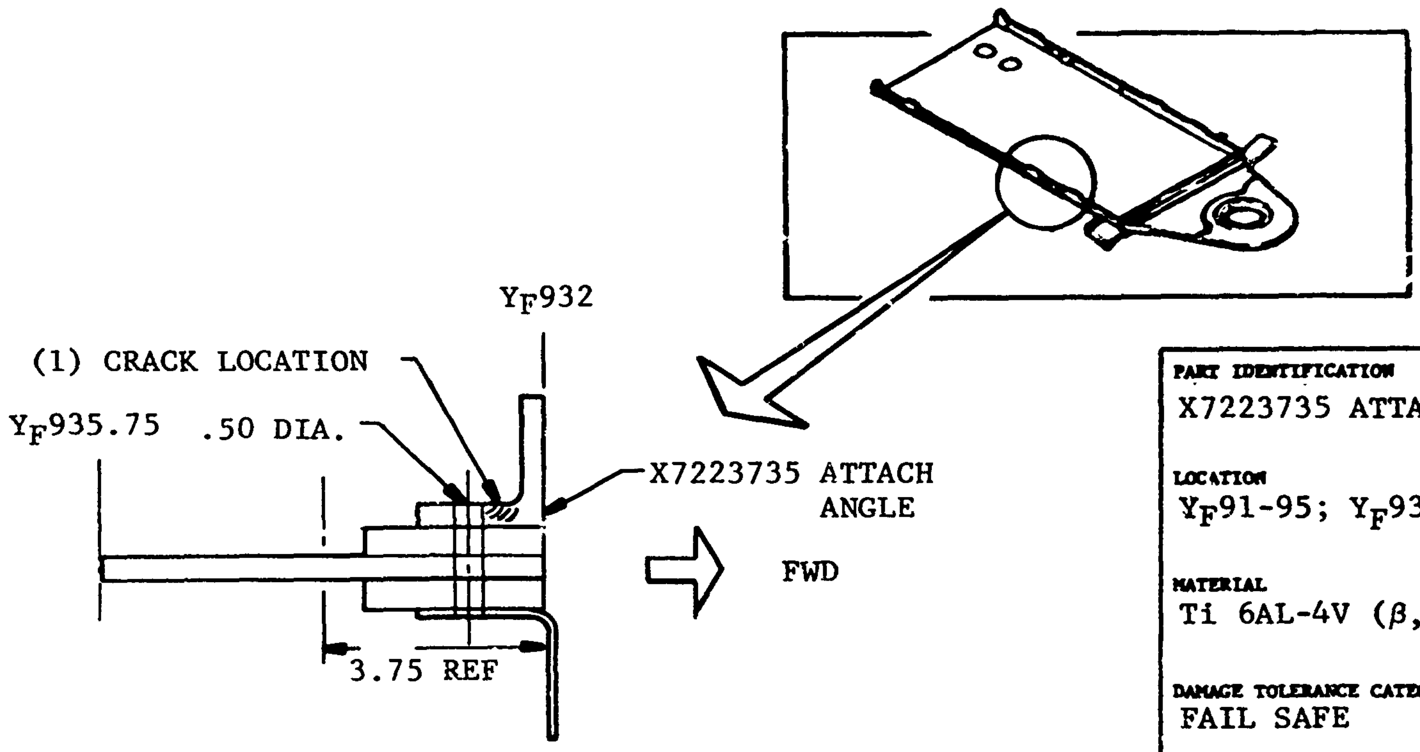


**PART IDENTIFICATION**
X7223735 ATTACH ANGLE

**LOCATION**
$Y_F91$-95; $Y_F932$; $Z_F0$

**MATERIAL**
Ti 6AL-4V ($\beta$,MA)

**DAMAGE TOLERANCE CATEGORY**
FAIL SAFE

**INSPECTABILITY**
DEPOT LEVEL

| CRACK LOCATION | ANALYSIS * | GROSS SECTION ULTIMATE DESIGN STRESSES FOR ASKA CONDITIONS IN FATIGUE SPECTRUM, KSI | | | | | | STRESS, KSI | | | | CRACK SIZE, INCHES | | CRACK TYPE |
|---|---|---|---|---|---|---|---|---|---|---|---|---|---|---|
| | | ** | 2 | 10 | 5 | 9 | 7 | MAXIMUM SPECTRUM* | GROSS SEC LIMIT* | NET SECT. ULTIMATE* | ALLOWABLE | INITIAL | CRITICAL | |
| (1) | FRACTURE | M | 51 | 58 | 38 | 49 | -9 | 28.95 | 38.69 | N.A. | >80 | >0.15 | 0.94 | CH |
| | FATIGUE | E | 70 | 79 | 52 | 67 | -13 | 39.71 | N.A. | 79.46 | 80 | | | |

* Gross section principal stresses used for fracture analysis.
Net section effective stresses used for fatigue analysis.
** Type stress--M: Maximum Principal Stress
E: Effective Stress

Figure 2-76 FSIL CONTROL POINT 7; $Y_F$ 932 BULKHEAD, LOWER OUTBOARD ATTACH ANGLE

- X7223821 - Web-Closure Rib, Outboard.
  Based on gross section limit stresses below 60 ksi at localized areas; the closure rib was considered not to be fracture critical.

- X7223822 Actuator Support Fitting
  Low stress levels in the support fitting did not deem critical crack length calculations of this part.

- X7223901 Sweep Actuator Fitting
  Based on gross section limit stresses below 60 ksi, the actuator fitting was not considered critical.

9. Control Point 9, MLG Trunnion, Fittings

   A survey of MLG trunnion fitting stresses indicated that these fittings are not fracture critical.

10. Control Point 10, Lower Plate, Fwd. Longeron, Outboard Lower

    This control point is similar to Control Point 3. Based on lower stresses (approximately 56%) in comparison to control point 3, this area was not considered critical.

2.3.4.2 NBB Fracture Analysis

Fracture analyses were conducted on nine NBB configuration control points. A listing of these points follows.

1. Control Point 1, Figure 2-77, $Y_F$ 992 Bhd. Inboard, Fuel Transfer Hole, $X_F$ 29.

2. Control Point 2, Figure 2-78, Lower Plate, Lug - Wing Pivot Bore

3. Control Point 3, Figure 2-79, Lower Plate, Fwd Inboard, Bolt Hole

4. Control Point 4, Figure 2-80, Lower Plate Assembly; Aft. Outboard Cutout, $X_F$ 68-72; $Y_F$ 992, $Z_F$ 0

5. Control Point 5, Figure 2-81, $Y_F$ 932 Bhd, Lower Attach Angle, $X_F$ 65, $X_F$ 72; $Z_F$ 0

6. Control Point 6, Figure 2-82, Upper Lug Installation, Aft Corner, $X_F$ 119

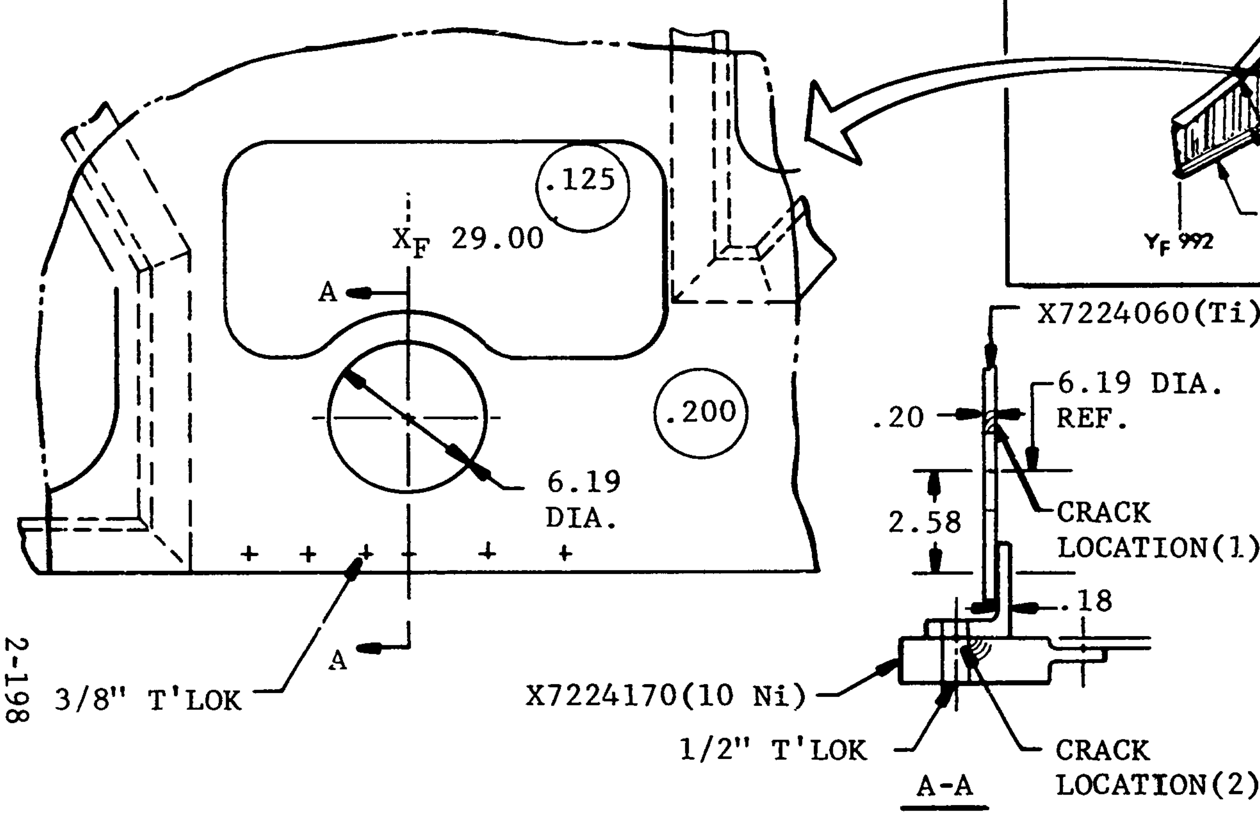


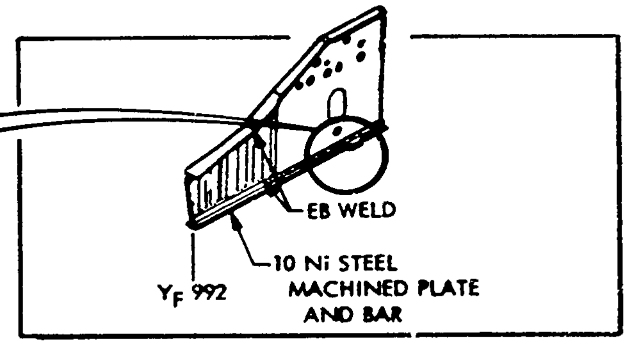


**PART IDENTIFICATION**
X7224060, $Y_F$992 BHD, WEB
X7224170, LWR PLATE ASSY

**LOCATION**
$X_F$29, $Y_F$992, $Z_F$0

**MATERIAL**
(1) Ti 6AL-4V ($\beta$,MA)
(2) 10 Ni STEEL

**DAMAGE TOLERANCE CATEGORY**
SAFE CRACK GROWTH

**INSPECTABILITY**
VISUAL; DEPOT LEVEL

| CRACK LOCATION | ANALYSIS * | GROSS SECTION ULTIMATE DESIGN STRESSES FOR ASKA CONDITIONS IN FATIGUE SPECTRUM, KSI | | | | | | STRESS, KSI | | | | CRACK SIZE, INCHES | | CRACK TYPE |
|---|---|---|---|---|---|---|---|---|---|---|---|---|---|---|
| | | ** | 2 | 10 | 5 | 9 | 7 | MAXIMUM SPECTRUM* | GROSS SEC LIMIT* | NET SECT. ULTIMATE* | ALLOWABLE | INITIAL | CRITICAL | |
| (1) | FRACTURE | M | 41.9 | 26.9 | 39.9 | 36.6 | 8.0 | 24.55 | 27.92 | N.A. | > 80 | >0.15 | 0.71 | EC |
| | FATIGUE | E | 41.9 | 26.9 | 39.9 | 36.6 | 8.0 | 46.62 | N.A. | 69.86 | 80 | | | |
| (2) | FRACTURE | M | 71.9 | 46.2 | 68.6 | 62.9 | 13.8 | 42.18 | 47.96 | N.A. | >150 | >.015 | 2.89 | CH |
| | FATIGUE | E | 71.9 | 46.2 | 68.6 | 62.9 | 13.8 | 80.09 | N.A. | 120 | 150 | | | |

* Gross section principal stresses used for fracture analysis.
Net section effective stresses used for fatigue analysis.
** Type stress--M: Maximum Principal Stress
E: Effective Stress

Figure 2-77 NBB CONTROL POINT 1; $Y_F$ 992 BULKHEAD, LOWER PLATE

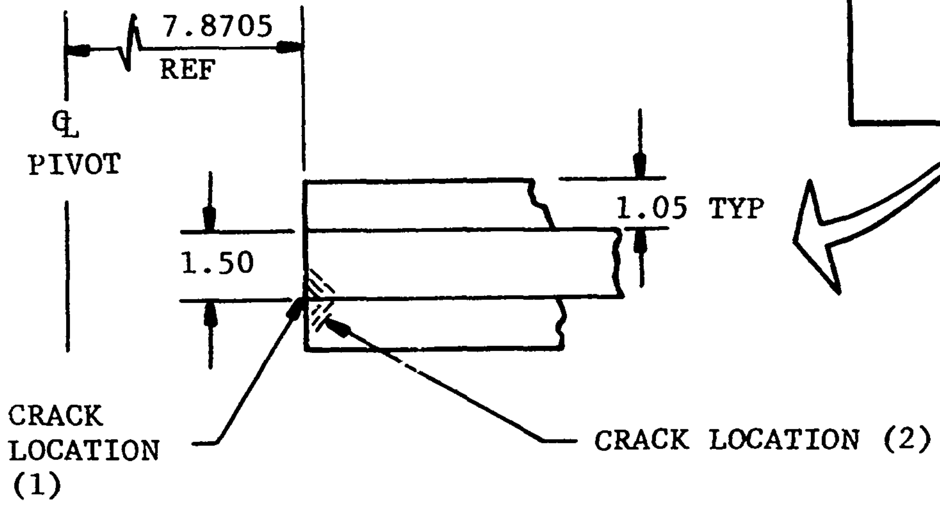


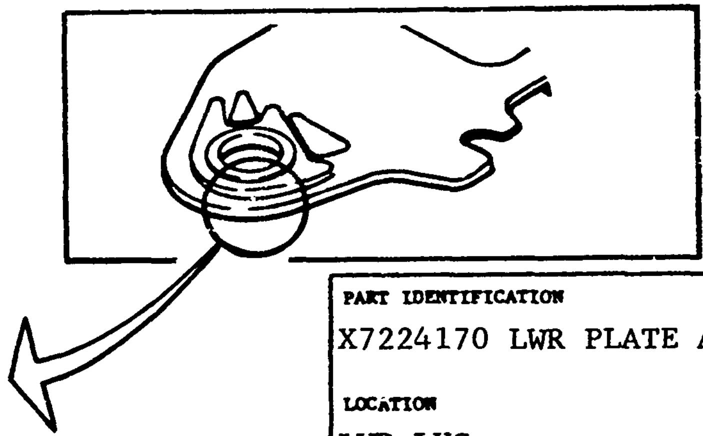

**PART IDENTIFICATION**
X7224170 LWR PLATE ASSY

**LOCATION**
LWR LUG

**MATERIAL**
10 Ni STEEL

**DAMAGE TOLERANCE CATEGORY**
SAFE CRACK GROWTH

**INSPECTABILITY**
DEPOT LEVEL

| CRACK LOCATION | ANALYSIS * | GROSS SECTION ULTIMATE DESIGN STRESSES FOR ASKA CONDITIONS IN FATIGUE SPECTRUM, KSI | | | | | | STRESS, KSI | | | | CRACK SIZE, INCHES | | CRACK TYPE |
|---|---|---|---|---|---|---|---|---|---|---|---|---|---|---|
| | | ** | 2 | 10 | 5 | 9 | 7 | MAXIMUM SPECTRUM* | GROSS SEC LIMIT* | NET SECT. ULTIMATE* | ALLOWABLE | INITIAL | CRITICAL | |
| (1) | FRACTURE | m | 137 | 35 | 140 | 118 | 4 | 86 | 93 | N.A. | - | # | # | EC |
| (2) | FATIGUE | e | 110 | 47 | 109 | 97 | -6 | 67 | N.A. | 110 | 131 | - | - | - |

* Local gross section principal stresses used for fracture analysis.
Average net section effective stresses used for fatigue analysis.

** Type Stress . . . m: local max principal stress
e: average net section effective stress

# Fine grid analysis not complete.

Figure 2-78 NBB CONTROL POINT 2; LOWER LUG, AFT

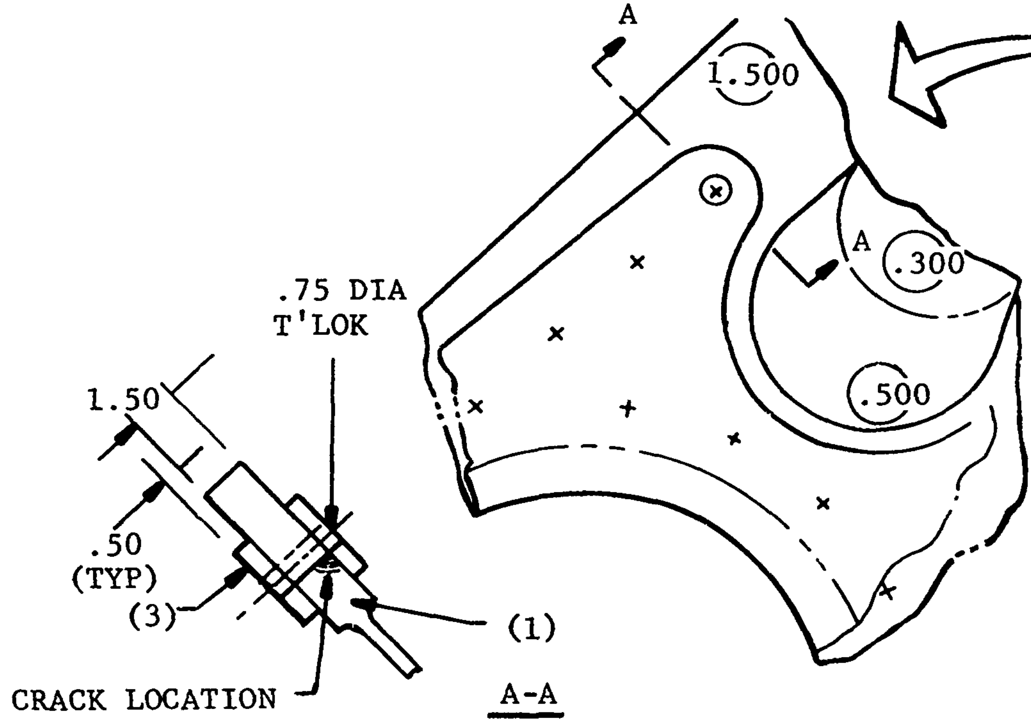


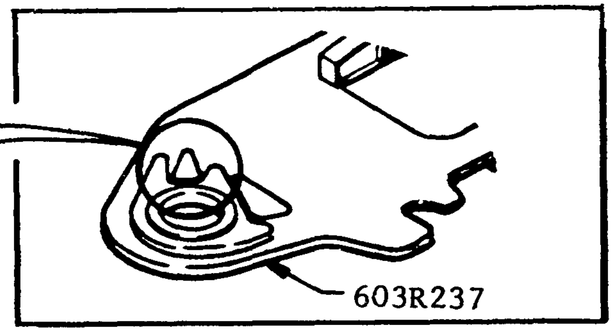


**PART IDENTIFICATION**
X7224170

**LOCATION**
$X_F$141.18; $Y_F$951.48:$Z_F$0

**MATERIAL**
10 Ni STEEL

**DAMAGE TOLERANCE CATEGORY**
SAFE CRACK GROWTH

**INSPECTABILITY**
VISUAL & DEPOT LEVEL

| CRACK LOCATION | ANALYSIS * | GROSS SECTION ULTIMATE DESIGN STRESSES FOR ASKA CONDITIONS IN FATIGUE SPECTRUM, KSI | | | | | | STRESS, KSI | | | | CRACK SIZE, INCHES | | CRACK TYPE |
|---|---|---|---|---|---|---|---|---|---|---|---|---|---|---|
| | | ** | 2 | 10 | 5 | 9 | 7 | MAXIMUM SPECTRUM* | GROSS SEC LIMIT* | NET SECT. ULTIMATE* | ALLOWABLE | INITIAL | CRITICAL | |
| (1) | FRACTURE | M | 114 | 121 | 100 | 106 | -16 | 64.71 | 80.71 | N.A. | >150 | >.15 | >4.0 | CH |
| | FATIGUE | E | 113 | 121 | 99 | 105 | 16 | 77.65 | N.A. | 145.2 | 150 | | | |

* Gross section principal stresses used for fracture analysis.
Net section effective stresses used for fatigue analysis.
** Type stress--M: Maximum Principal Stress
E: Effective Stress

Figure 2-79 NBB CONTROL POINT 3; LOWER PLATE, LUG

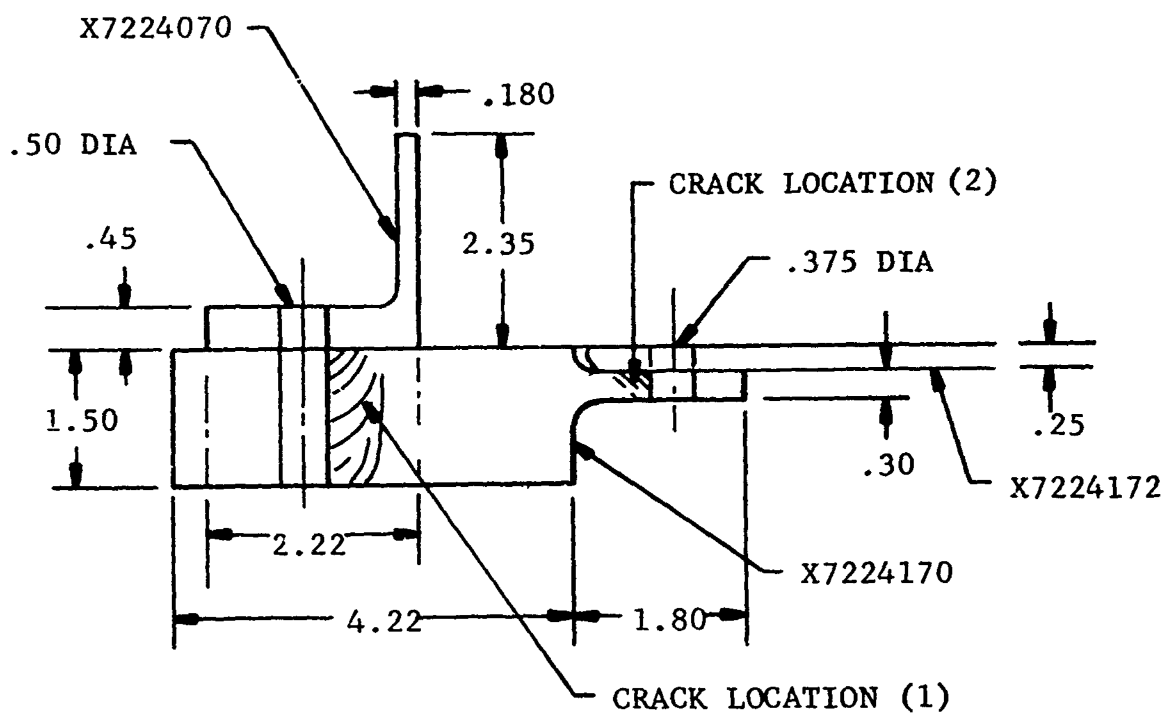


**PART IDENTIFICATION**
X7224170 LWR PLATE ASSY
X7224172 LWR PLATE, WEB

**LOCATION**
$X_F 68$; $Y_F 992$; $Z_F 0$

**MATERIAL**
10 Ni STEEL

**DAMAGE TOLERANCE CATEGORY**
SAFE CRACK GROWTH

**INSPECTABILITY**
DEPOT LEVEL

| CRACK LOCATION | ANALYSIS * | GROSS SECTION ULTIMATE DESIGN STRESSES FOR ASKA CONDITIONS IN FATIGUE SPECTRUM, KSI | | | | | | STRESS, KSI | | | | CRACK SIZE, INCHES | | CRACK TYPE |
|---|---|---|---|---|---|---|---|---|---|---|---|---|---|---|
| | | ** | 2 | 10 | 5 | 9 | 7 | MAXIMUM SPECTRUM* | GROSS SEC LIMIT* | NET SECT. ULTIMATE* | ALLOWABLE | INITIAL | CRITICAL | |
| (1) | FRACTURE | M | 127.1 | 60.5 | 122.7 | 110.5 | -14.9 | 75.37 | 84.78 | N.A. | >150 | >.15 | >1.82 | CH |
| (2) | FATIGUE | E | 125.4 | 59.6 | 121.0 | 108.7 | 20.2 | 88.94 | N.A. | 150 | 150 | >.15 | 0.92 | SC |

* Gross section principal stresses used for fracture analysis.
Net section effective stresses used for fatigue analysis.
** Type stress--M: Maximum Principal Stress
E: Effective Stress

Figure 2-80 NBB CONTROL POINT 4; LOWER PLATE, AFT OUTBOARD CUTOUT

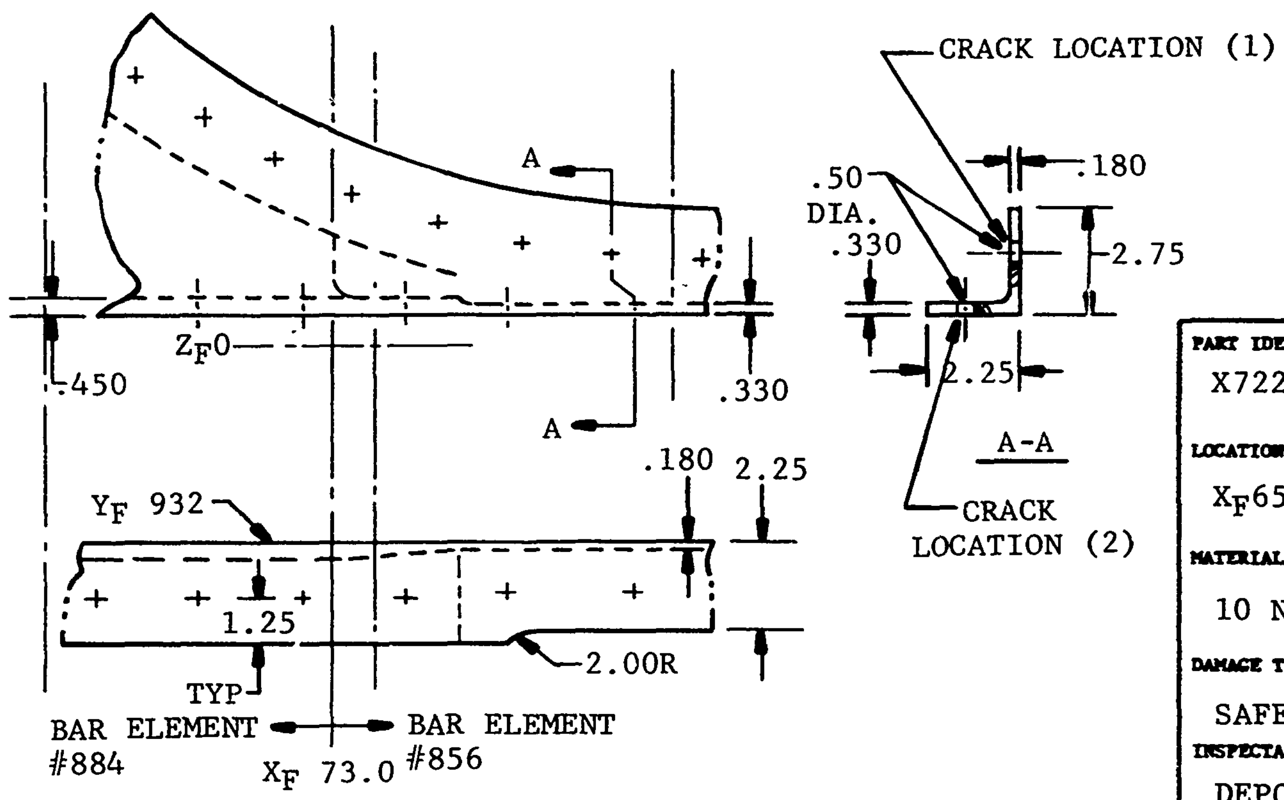


| PART IDENTIFICATION |
|---|
| X7224090 BHD. |
| LOCATION |
| $X_F65$-$X_F72$; $Y_F932$; $Z_F1$ |
| MATERIAL |
| 10 Ni STEEL |
| DAMAGE TOLERANCE CATEGORY |
| SAFE CRACK GROWTH |
| INSPECTABILITY |
| DEPOT LEVEL |

| CRACK LOCATION | ANALYSIS * | GROSS SECTION ULTIMATE DESIGN STRESSES FOR ASKA CONDITIONS IN FATIGUE SPECTRUM, KSI | | | | | | STRESS, KSI | | | | CRACK SIZE, INCHES | | CRACK TYPE |
|---|---|---|---|---|---|---|---|---|---|---|---|---|---|---|
| | | ** | 2 | 10 | 5 | 9 | 7 | MAXIMUM SPECTRUM* | GROSS SEC LIMIT* | NET SECT. ULTIMATE* | ALLOWABLE | INITIAL | CRITICAL | |
| (1) | FRACTURE | M | 93 | 69 | 70 | 87 | -22 | 52.79 | 62.03 | N.A. | >150 | >.15 | 1.66 | CH |
| (2) | FATIGUE | E | 93 | 69 | 70 | 87 | -22 | 67.36 | N.A. | 118.67 | 150 | >.15 | 1.34 | CH |

* Gross section principal stresses used for fracture analysis.
Net section effective stresses used for fatigue analysis.
** Type stress--M: Maximum Principal Stress
E: Effective Stress

Figure 2-81 NBB CONTROL POINT 5; $Y_F$ 932 BULKHEAD LOWER FLANGE

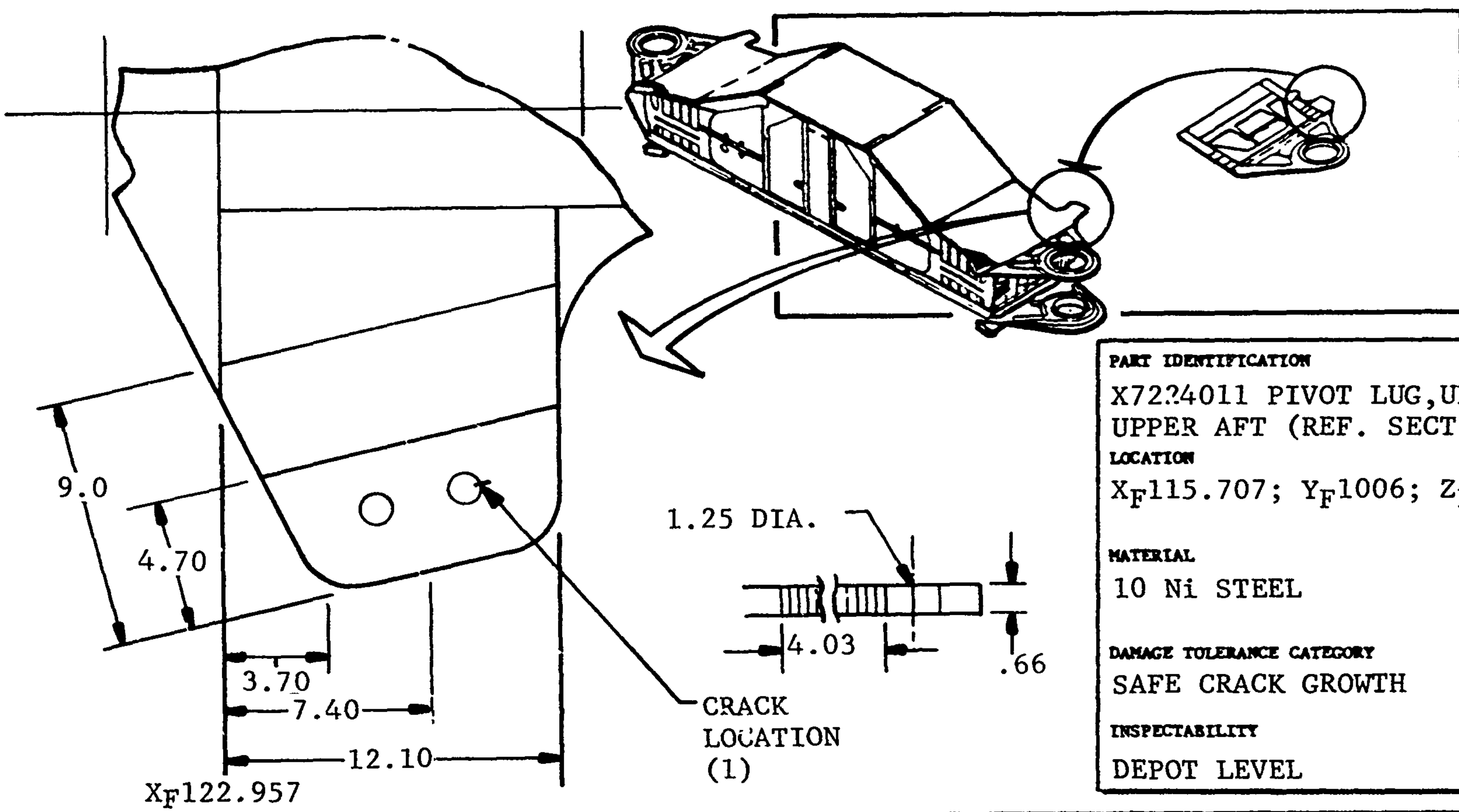


**PART IDENTIFICATION**
X72?4011 PIVOT LUG, UPPER UPPER AFT (REF. SECT. B-B)

**LOCATION**
$X_F$115.707; $Y_F$1006; $Z_F$

**MATERIAL**
10 Ni STEEL

**DAMAGE TOLERANCE CATEGORY**
SAFE CRACK GROWTH

**INSPECTABILITY**
DEPOT LEVEL

| CRACK LOCATION | * ANALYSIS | GROSS SECTION ULTIMATE DESIGN STRESSES FOR ASKA CONDITIONS IN FATIGUE SPECTRUM, KSI | | | | | | STRESS, KSI | | | | CRACK SIZE, INCHES | | CRACK TYPE |
|---|---|---|---|---|---|---|---|---|---|---|---|---|---|---|
| | | ** | 2 | 10 | 5 | 9 | 7 | MAXIMUM SPECTRUM* | GROSS SEC LIMIT* | NET SECT. ULTIMATE* | ALLOWABLE | INITIAL | CRITICAL | |
| (1) | FRACTURE | M | -84.8 | 84.8 | -85.7 | -44.4 | 31.3 | 37.0 | 56.6 | N.A. | > 150 | > .15 | > 4.0 | CH |
| | FATIGUE | E | 107.4 | 86.0 | 103.0 | 91.4 | 29.8 | 49.8 | N.A. | 114 | 150 | | | |

* Gross section principal stresses used for fracture analysis.
Net section effective stresses used for fatigue analysis.
** Type stress--M: Maximum Principal Stress
E: Effective Stress

Figure 2-82 NBB CONTROL POINT 6; NBB UPPER AFT, OUTBOARD

7. Control Point 7, X7224130 $X_F$ 84 Rib Assembly

A survey of maximum gross section stresses indicated very low stress distributions in the $X_F$ 84 rib. The maximum limit stress was 25 ksi. The rib assembly was not considered fracture critical.

8. Control Point 8, X7224030 $X_F$ 119 Closure Rib Assembly

A survey of stress levels in the closure rib indicated low stress distributions. The areas considered for this analysis are loaded by the sweep actuator fitting support attachment bolts and are therefore primarily loaded in shear. The maximum gross limit stress in the closure rib is 66 KSI.

9. Control Point 9, X7224170 Lower Plate, Forward Outboard Cutout; $X_F$ 68-72; $Y_F$ 940

This area is similar to control point 4. Since stress levels were lower than at $Y_F$ 992 (control point 4) this area was not considered a primary control point.

### 2.3.5 Fracture Control Plan

The fracture control plan was prepared and published (FZM-6068, 1 Feb. 1973) during Phase Ib. A brief overview of the plan was presented in the AMAVS Phase Ib Technical Report. During Phase II, steps were taken to implement the Fracture Control Plan prior to start of production. The Fracture Critical Parts List, Figure 2-83, was updated and the detailed Traceability requirements, Figure 2-84, were defined.

### 2.3.6 Finite Element Fracture Analysis

#### 2.3.6.1 <u>The Assumed Stress Hybrid-Model Finite Element Method</u>

The computer procedure (Convair code name UD1) based on the assumed stress hybrid-model finite element method for fracture mechanics analysis has been completely programmed and checked out. Improvements have also been made in efficiency, versatility, and applicability of the computer procedure during the Phase II reporting period of the AMAVS Program. The computer procedure calculates the crack tip stress intensity factors, then the nodal displacements, and finally the element stresses. For the assumed stress hybrid-model elements, element stresses at four corners are

FSIL Configuration

| | |
|---|---|
| X7223730-1 | Lower Plate Assembly |
| 31-1/2 | " " Brazed Assembly |
| 32-7 | " " Doubler |
| 33-7 | " " Web |
| 34-7 | " Lug Doubler |
| 35-7/-8,-9/-10 | $Y_F$ 932 & $Y_F$ 992 BHD Attach Angles |
| 36-7/-8,-9/-10 | $Y_F$ 932 & $Y_F$ 992 Gussets |
| 37-7 | Lower Plate ℄ Splice |
| X7223850-7/-8 | Closure Rib Attach Angle |
| 51-7/-8 | O.B. Aft Longeron Adapter |
| 52-7/-8 | Fwd Lower O.B. Longeron Fitting |
| X7223751-7/-8 | $Y_F$ 932 BHD Web, O.B. |
| X7223752-7/-8 | $Y_F$ 932 BHD Web, $X_F$ 39-84 |
| X7223765-7/-8 | $Y_F$ 947 BHD Lower Beam |
| X7223781-7/-8 | $Y_F$ 992 BHD Web O.B. |
| 82-7/-8 | $Y_F$ 992 BHD Web $X_F$ 35-84 |
| 83-7/-8 | $Y_F$ 992 BHD Web I.B. |
| X7223710-1/-2 | Upper Lug/Plate Weld Assembly |
| 11-7/-8 | Upper Lug |
| 12-7/-8 | Upper Plate - O.B. Fwd |
| 13-7/-8 | Upper Plate - O.B. Aft |
| 14-7/-8 | Upper Plate - O.B. Ctr |
| X7223853-7/-8 | Fwd Upper O.B. Longeron Fitting |
| X7223821-7/-8 | Web - Closure Rib |
| 22-7/-8,-9/-10 | Support - Actuator, Closure Rib |

No-Box Box Configuration

| | |
|---|---|
| X7224011-7/-8 | Pivot Lug - Upper |
| 60-1/-2 | $Y_F$ 992 Bhd Assembly |
| 61-7/-8 | $Y_F$ 992 Bhd-Inboard Web |
| 70-7/-8 | $Y_F$ 992 Bhd-Outboard Segment (Machined) |
| 71-1/-2 | $Y_F$ 992 Bhd-Outboard Segment (Welded) |
| 73-7/-8 | $Y_F$ 992 Bhd-Outboard Lower Cap |
| 75-7/-8 | $Y_F$ 992 Bhd-Outboard Web |
| 77-7 | $Y_F$ 992 Bhd-Inboard Lower Cap |
| 65-7/-8 | $Y_F$ 992 Bhd-Lower Cap Splice |
| X7224080-1/-2 | $Y_F$ 932 Bhd Assembly |
| 90-7/-8 | $Y_F$ 932 Bhd - Outboard Segment (Machined) |
| 91-1/-2 | " " " " " (Welded) |
| 93-7/-8 | " " " " Lower Cap |
| 95-7/-8 | " " " " Web |
| 97-7 | " " " - Inboard Lower Cap |
| 85-7/-8 | " " " - Outboard Gusset |
| 87-7/-8 | " " " - Lower Cap Splice |

Figure 2-83 FRACTURE CRITICAL PARTS LIST

No-Box Box Configuration (Continued)

| | |
|---|---|
| X7224155-7/-8 | Longeron Fitting - Upper Forward |
| X7224170-1/-2 | Lower Plate Assembly |
| 72-7/-8 | " " Panel $X_F$ 39-84 |
| 73-7/-8 | " " " $X_F$ 39R-39L |
| 75-7/-8 | Pivot Lug Lower |
| 76-7/-8 | " " " - Reinforcement |
| 77-7 | Lower Plate Splice - $Y_F$ 992 |
| 78-7 | Lower Plate Splice - $Y_F$ 932 |
| X7224180-7/-8 | Beam, MLG Drag Brace $Y_F$ 947 |
| X7224141-7/-8 | Closure Rib (Machined) |
| 43-7/-8,-9/-11 | Closure Rib (Details) |
| 44-7/-8 | Support - Actuator, Closure Rib Inbd. |
| 47-7/-8 | " " " " Outbd. |

Fittings

| | |
|---|---|
| X7223900-1/-2 | Wing Sweep Actuator Support Assy. |
| 01-7/-8 | " " " " " |
| 11-1/-2 | MLG Drag Strut Support Assy |
| 12-7/-8 | " " " " Inbd. Lug |
| 13-7/-8 | " " " Outbd. Lug |
| 14-7/-8 | " " " Extensions |
| 15-7/-8 | " " " Splice |
| X7223920-1/-2 | " " " Side Brace Support Assy. |
| 21-7/-8 | " " " " " Outbd Lug |
| 22-7/-8,-9/-10 | " " " " " Web |
| 23-7/-8 | " " " " " Beam |
| X7223930-7/-8 | " " " Trunnion $X_F$ 72 |
| 32-7/-8 | " " " Cap $X_F$ 72 |
| 31-7/-8 | " " " Trunnion $X_F$ 95.5 |

Figure 2-83 FRACTURE CRITICAL PARTS LIST (Continued)

| APPLICATION | | REVISIONS | | | |
|---|---|---|---|---|---|
| NEXT ASSY | USED ON | LTR | DESCRIPTION | DATE | APPROVED |

This drawing establishes the traceability requirements for Advanced Metallic Air Vehicle Structure parts when specifically called for on the Engineering Drawing.

1. Raw Material Information

Material for parts that require traceability will be purchased to specifications that define all traceability infomation which must be supplied by the producer.

2. Material Storage

Materials procured specifically for the AMAVS program requiring material traceability will be stored separately from materials procured for other programs.

3. Material Allocation Plan (MAP)

A material allocation plan (MAP) will be prepared by AMAVS Engineering for each sheet, plate or bar of incoming material requiring material traceability.

4. Material Serial Numbers

The MAP will assign each piece of incoming material a serial number coded as follows:

X X X
- X — Material Code
- X — Heat Number Code
- X — Sheet, Plate or Bar Number

| REV | - | - | | |
|---|---|---|---|---|
| SH | 1 | 2 | | |

REVISION STATUS OF SHEETS

| | | |
|---|---|---|
| UNLESS OTHERWISE SPECIFIED DIMENSIONS ARE IN INCHES TOLERANCES ON FRACTIONS ± DECIMALS .XX± .XXX± ANGLES ± | DRAFTSMAN E. Stern — DATE 7-10-73 | U.S. AIR FORCE |
| | CHECKER D. Bostick — 8-10-73 | |
| | ENGINEER N. H. Henry — 8/1/73 | TITLE Figure 2-84 Material Traceability Requirements for the AMAVS Program |
| MATERIAL | A F PROJ ENGR | |
| | CONTRACT NO F33615-73-C-3001 | |
| | AF DESIGN ACTIVITY AUTHENTICATION | SIZE A — AFCODE IDENT NO. 07878 — DRAWING NO. X7224199 |
| | E. K. [illegible] 9/-/73 | SCALE — SHEET 1 of 2 |

| REVISIONS | | | |
|---|---|---|---|
| SYM | DESCRIPTION | DATE | APPROVED |

4. (Cont)
The serial number shall be marked on incoming material prior to being placed in storage. The marking procedure will be specified on the MAP.

4.1 Material Codes:

A - Beta Annealed 6Al-4V titanium
B - 2024 or 2124 aluminum alloys
C - 10 Nickel Steel
D - Beta C titanium
E - 7050 aluminum

4.2 Heat Number Code

For each material, successive heats will be coded consecutively starting with the number one (1). Quality Assurance will maintain a record that correlates heat number and code number. The vendor and the full heat number will be recorded on the MAP.

4.3 Sheet, Plate or Bar Number

For each heat of material, each sheet, plate and/or bar will be consecutively numbered starting with the number one (1).

5. Part Traceability Number

Part traceability number is the piece serial number defined in step 4 along with the item number to identify the specific part, i.e.:

$$\underbrace{X - X - X}_{\text{Piece S/N}} \quad \underbrace{- X}_{\text{Item Number}}$$

This traceability number must be marked on the part during layout for the first cut operation and prior to material release.

6. Material Release

Production planning for traceable parts will specifically refer to the part traceability number as designated by the MAP. Material release for production of traceable parts will be by part traceability number.

7. Maintenance of Part Traceability Number

The part traceability number must be maintained on the part through all stages of manufacture and assembly. Loss of this identification at any stage of manufacture is cause for rejection of the part.

8. Traceability Records

For each traceable part, complete data documenting the heat number, material certification, production planning, inspection records, processing data sheets, discrepancy reports, etc., will be recorded, collected and maintained by Quality Assurance. These records will provide complete traceability from raw material through the completed assembly.

Figure 2-84 Sheet 2

| CODE IDENT NO. | SIZE | |
|---|---|---|
| 07878 | A | Material Traceability Requirements for the AMAVS Program |
| SCALE | | SHEET 2 of 2 |

calculated and printed. Triangular elements and general quadrilateral elements are based on conventional displacement assumptions and only the average stresses within the elements are calculated and printed. The computer procedure UD1 was reprogrammed to improve the overall efficiency in the following areas: (1) the maximum number of nodes in a structural simulation was increased from 250 to 350, (2) the maximum node separation was increased from 28 to 35, and (3) the solution algorithm of the program was improved.

2.3.6.2 Design Analysis by Computer Procedure UD1

In addition to a number of fracture analysis problems which have been reported in the First and Second Interim Reports of the AMAVS Program (AFFDL-TR-73-1 and AFFDL-TR-73-77), the following problems have been solved during Phase II, Final Design.

(1) A four-bay brazed lower plate with a center crack under uniform tension was analyzed. The stiffened panel shown in Figure 2-85 has a center crack in the web material with the center stiffener still remains intact. Figure 2-85 also shows the variation of crack tip stress intensity, $K_I$, versus half crack length, a. The center stiffener is assumed to be completely delaminated from the web material in the analysis.

(2) A fracture analysis was conducted on the brazed lower plate specimen, Drawing 603FTB035 "D". The test specimen is composed of a 0.5 inch web and two 0.6 inch stiffener panels brazed to the web plate. External loads of P = 2000 kips are applied to the structure along a line which is $4^o$ off the centerline of the structure as shown in Figures 2-86 and 2-87.

The finite element simulation is composed of hybrid-model finite elements, triangular elements and general quadrilateral elements. A typical finite element simulation of the test specimen is shown in Figure 2-88. Note that a crude simulation was used for the test fixtures. $K_I$ and $K_{II}$ were calculated at both crack tips and stresses were calculated throughout the entire panel. The following fracture analyses were made:

(1) A thru-crack embedded in the second bay of the lower panel specimen was analyzed. Figure 2-86 shows the structural arrangement as well as results from UD1 analyses with a = 2 inch, 4 inch, 5 inch and 6 inch. Both $K_I$ and $K_{II}$ vs. a were plotted in Figure 2-86. Note that the values plotted are for the crack tip on the right-hand side which are slightly greater than $K_I$

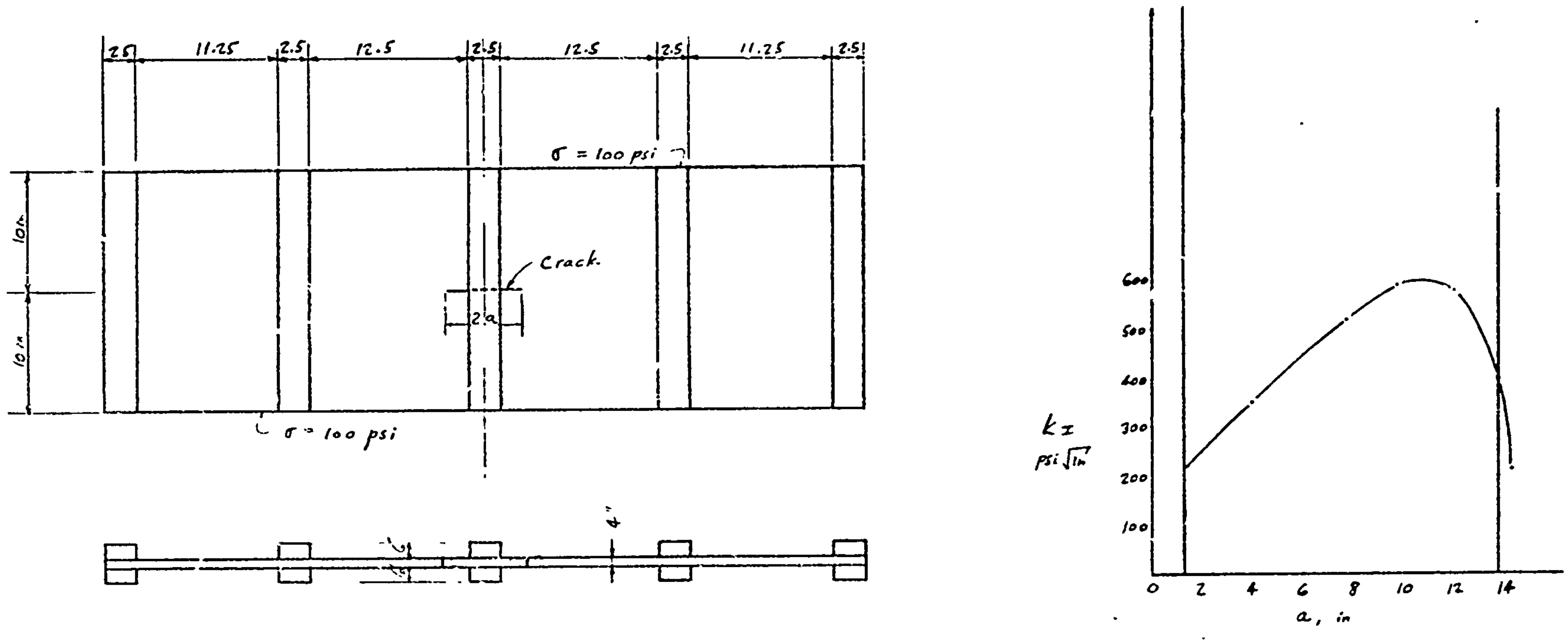


Figure 2-85 A FOUR BAY BRAZED PNL WITH A CENTER CRACK UNDER UNIFORM TENSION

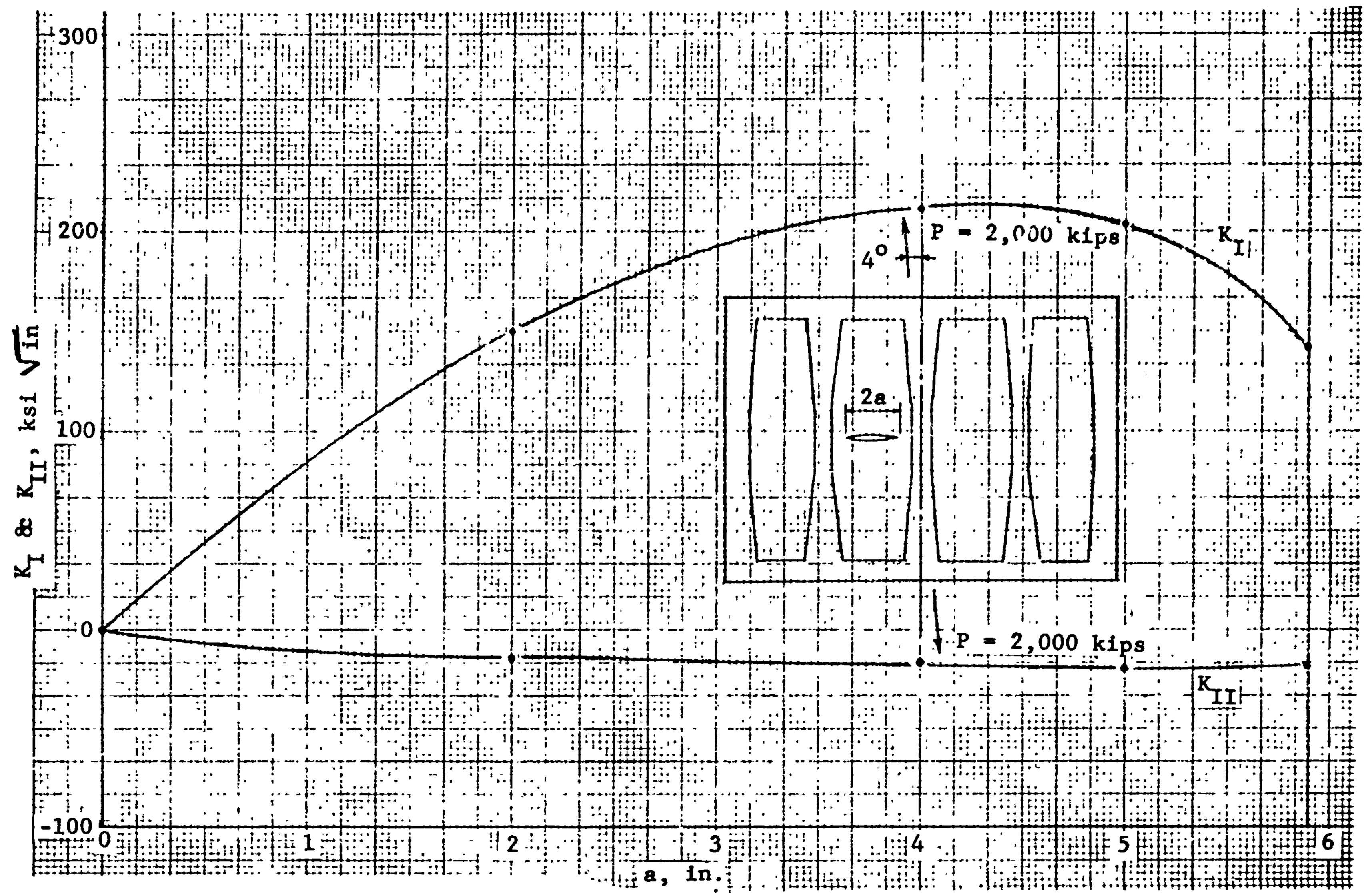


**Figure 2-86** $K_I$ and $K_{II}$ vs. a of an Eccentrically Cracked Lower Panel Specimen

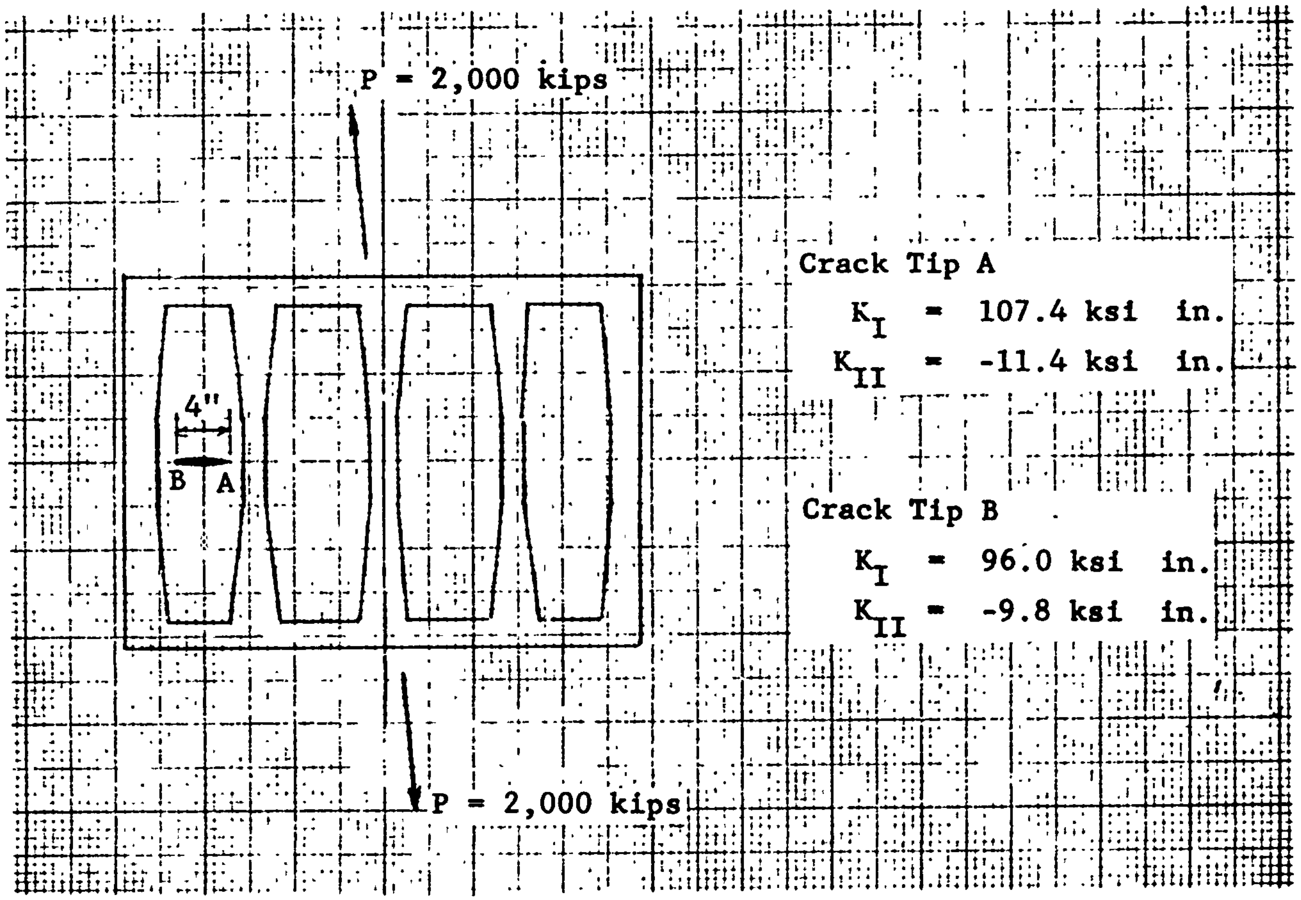


Figure 2-87 A Thru Crack Embeded in the First Bay of the Lower Panel Specimen

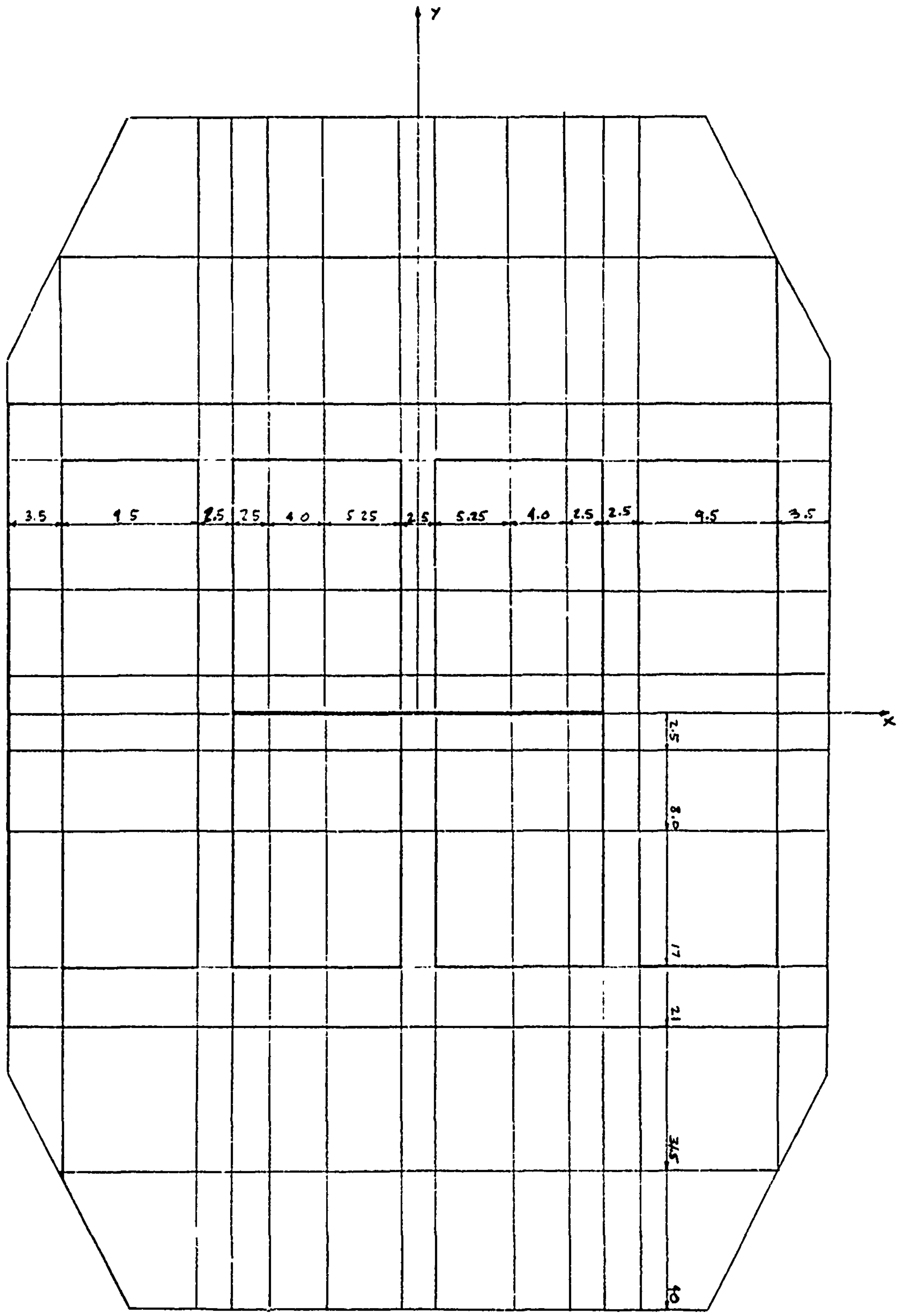


Figure 2-88 A TYPICAL FINITE ELEMENT SIMULATION OF THE BRAZED LOWER PLATE SPECIMEN

and $K_{II}$ of the crack tip on the left-hand side due to the eccentricity of the crack.

(2) A thru crack embedded in the first bay was analyzed. Only one problem was solved for a 4 inch crack. The results are shown in Figure 2-87.

(3) A center thru-crack embedded in the lower panel test specimen was analyzed. The structural arrangement and the results of $K_I$ and $K_{II}$ vs. a computed by UD1 are shown in Figure 2-89.

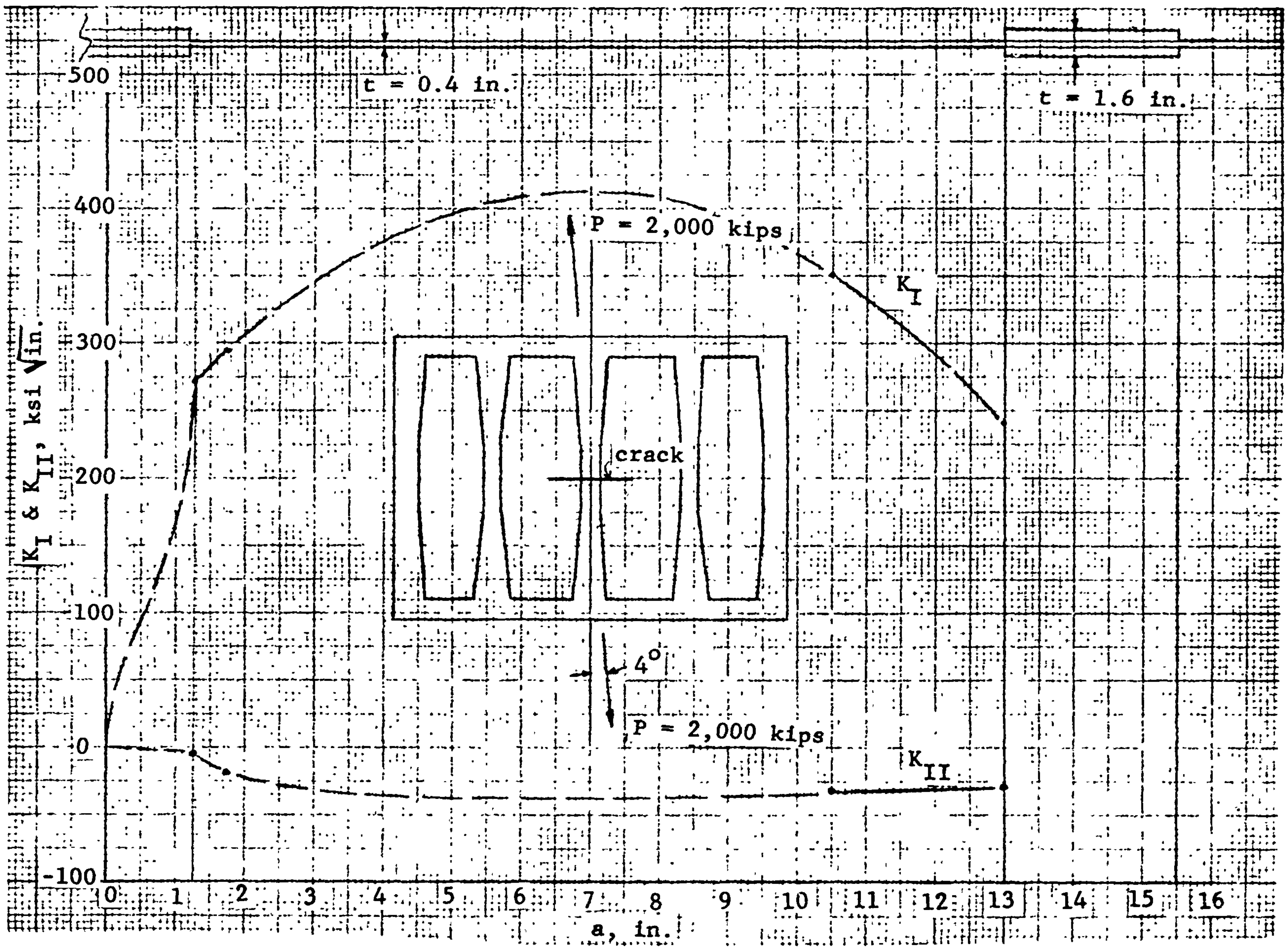


Figure 2-89 $K_I$ and $K_{II}$ vs. a of A Center Cracked Lower Panel Specimen

### 2.3.7 Fatigue Life Variability

The fatigue life variability of the following materials was evaluated:

10 Ni Steel Plate
Beta Annealed 6Al-4V Titanium Plate
Beta C Sheet
Silver-Brazed Beta Annealed 6Al-4V Titanium

For each material, a series of 20 specimens was flight-by-flight fatigue tested to establish the fatigue life distribution. The resulting test data (Figures 2-90 thru 2-93) were analyzed using maximum likelihood estimates (MLE) methods to determine the Weibull parameters. The shape parameter, $\alpha$, is a measure of the degree of variability and the characteristic life, $\beta$, is the number of flights for a 63.2% failure rate as defined by the untruncated Weibull distribution function:

$$F(t) = 1 - \exp\left[-(t/\beta)^{\alpha}\right]$$

where t = the fatigue life in cycles

F(t) = the fatigue life distribution

The test results indicate that Beta Annealed 6Al-4V Titanium and 10 Ni Steel have virtually identical characteristic fatigue lives when fatigue cycled to the same percentage of $F_{tu}$, 6126 and 6060 flights, respectively. However, the fatigue scatter was greater for 10 Ni Steel ($\alpha = 2.05$) than for the 6-4 Titanium ($\alpha = 3.06$). The characteristic fatigue life of Beta C, 2601 flights, was significantly lower than that of Ti 6Al-4V ($\beta$, MA) using the same stress spectrum, despite the greater strength of the Beta C ($F_{tu}$ = 185 KSI for Beta C vs 125 KSI for 6-4 Titanium). However, there was less scatter in the fatigue data for Beta C ($\alpha = 5.86$) than for 10 Ni Steel or Ti 6Al-4V ($\beta$, MA).

For silver alloy brazed pairs of Ti 6Al-4V ($\beta$,MA), the fatigue life variability ($\alpha = 7.96$), and the characteristic life ($\beta = 4563$ flights) were significantly lower than observed in single ply specimens. This was attributed to first-of-two type failures of parallel elements which tend to reduce scatter and decrease life. The decreased fatigue life was predicted to be 4803 flights for random pairs taken from the 20 single-ply specimens. Thus, most of the decrease in fatigue life can be attributed to a first-of-two failure mode as opposed to a degradation in fatigue strength due to brazing.

The fatigue life variability data were used to conduct a cursory evaluation of the two WCTS designs using the Whittaker reliability analysis model presented in AFML-TR-69-65. For the NBB, a location with a computed fatigue damage ($\sum n/N$) of .061, the reliability in a four-service life test program is .60. If there were four such points in the WCTS (i.e. with computed damage $\geq .061$) the computed reliability would be .36. For a fleet of 200 aircraft, the time to first failure would be 91 flights with a 50% probability. These predictions are considered unsatisfactory and are attributed to extrapolation of the Weibull plot to failure values not observed in the test program.

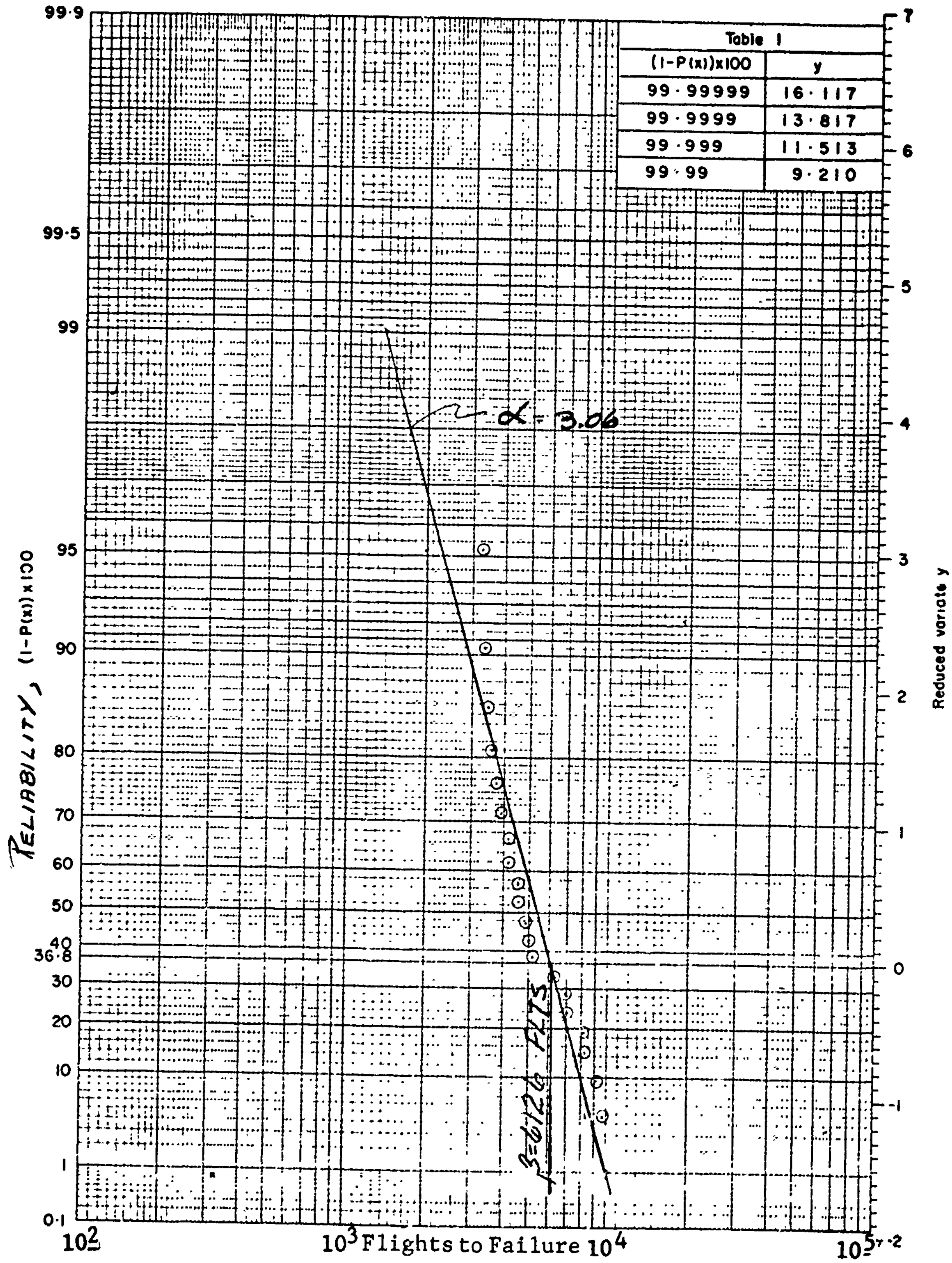


Figure 2-90 WEIBULL PLOT OF BETA ANNEALED 6AL-4V TITANIUM RELIABILITY TEST DATA

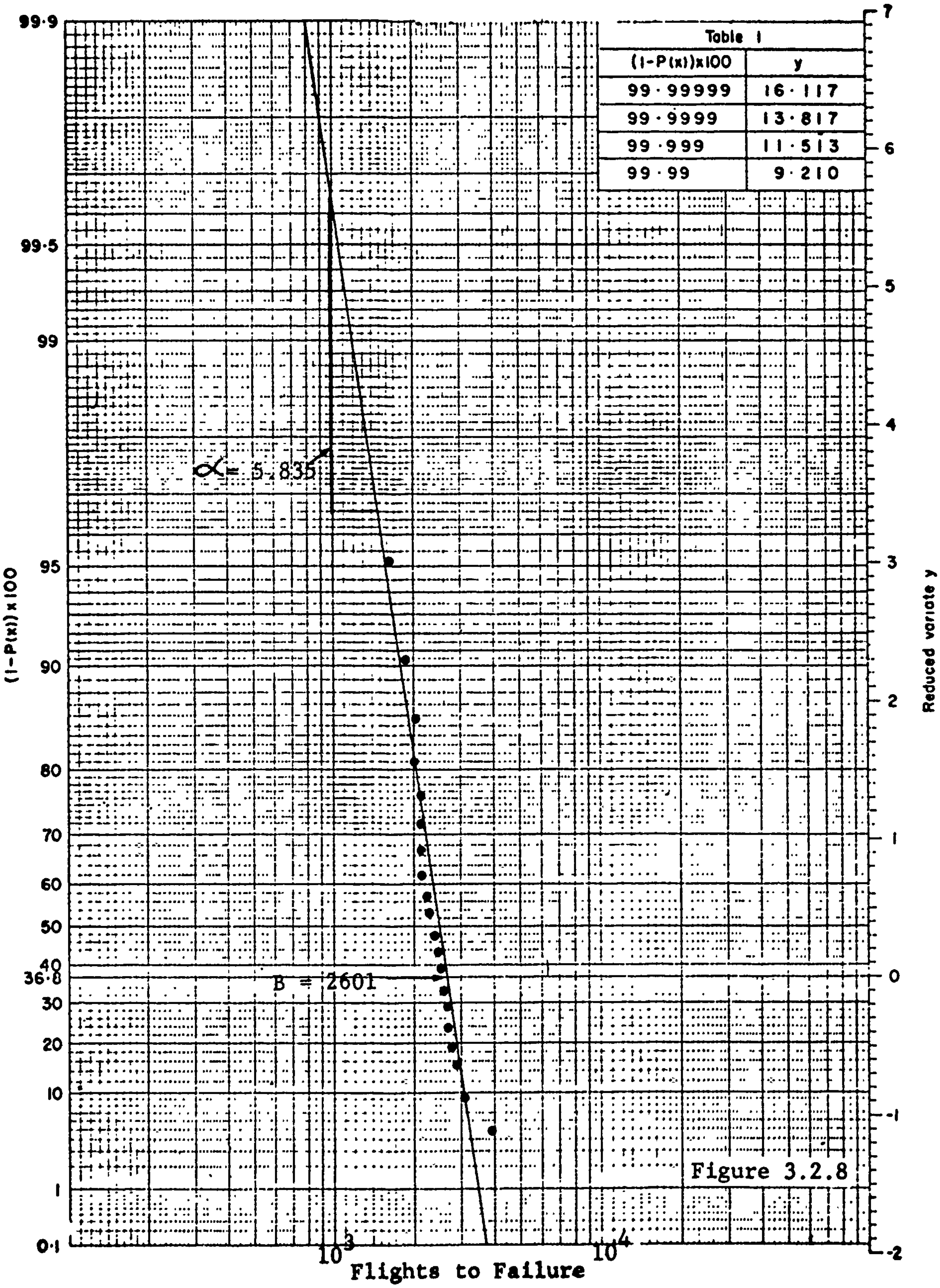


Figure 2-91 WEIBULL PLOT OF BETA C RELIABILITY TEST DATA

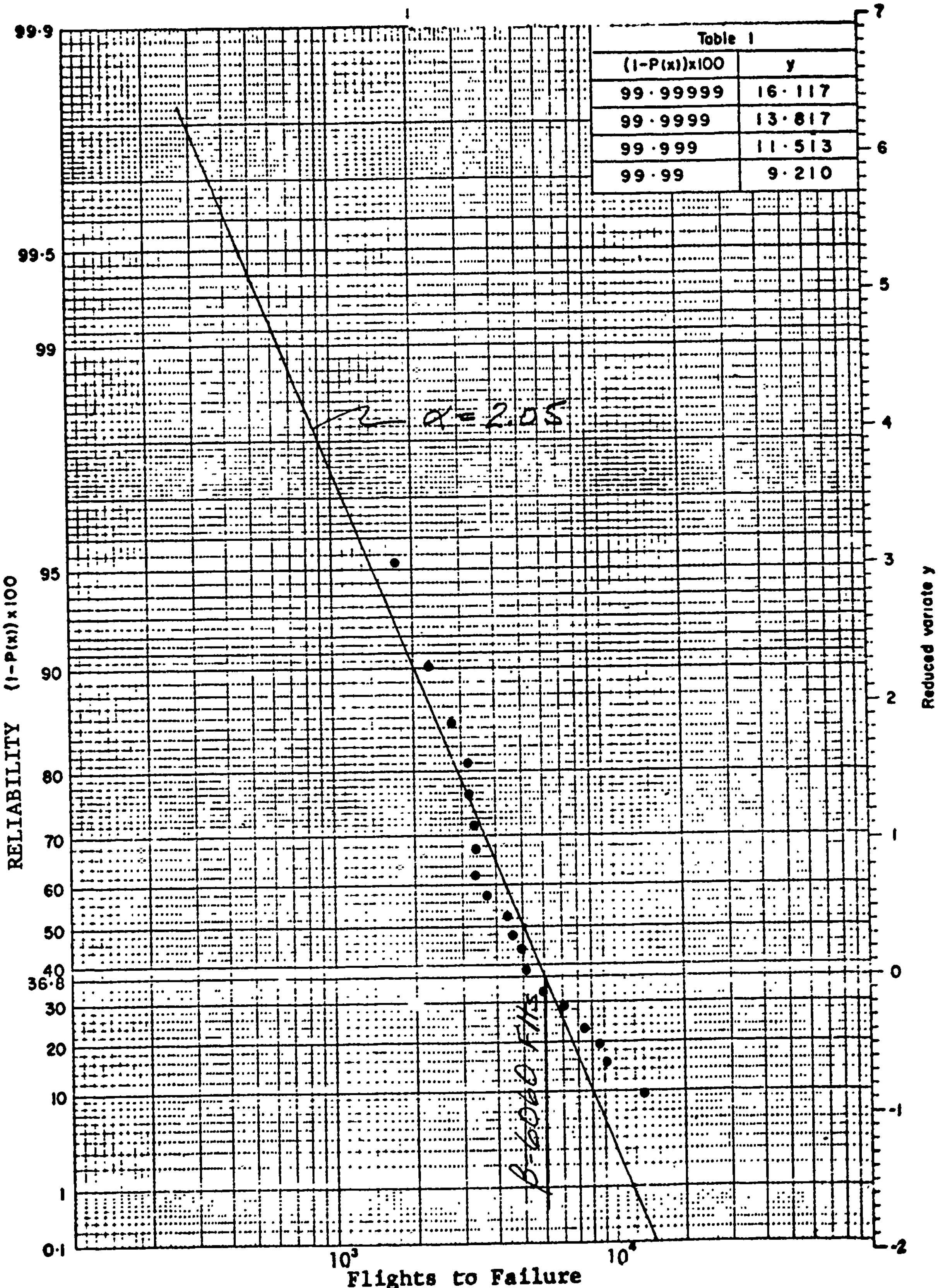


Figure 2-92 WEIBULL PLOT OF 10 NICKEL STEEL RELIABILITY TESTS

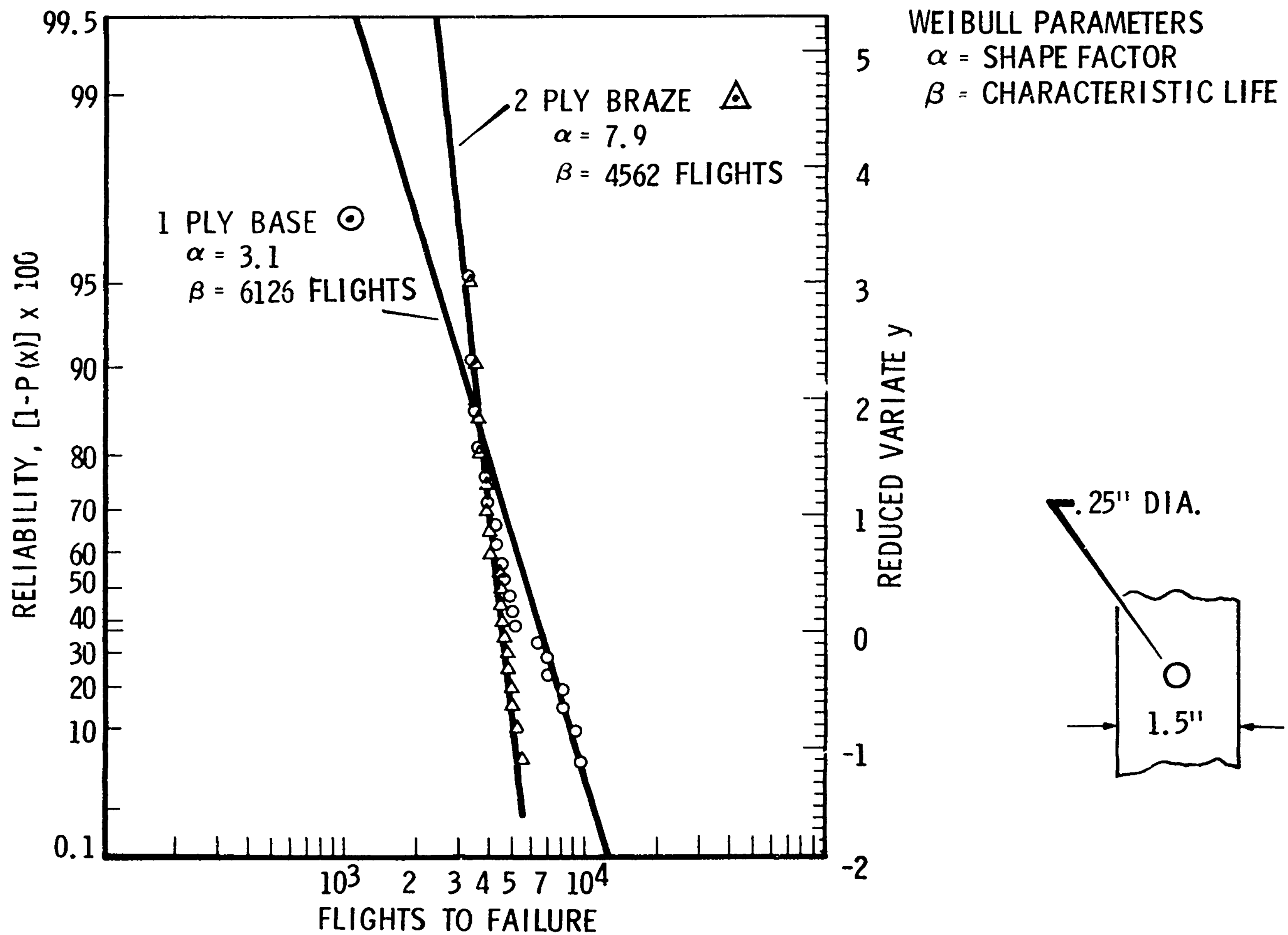


Figure 2-93 WEIBULL PLOT OF BETA ANNEALED 6AL-4V TITANIUM, SINGLE PLY AND 2 PLY BRAZE, RELIABILITY TEST DATA

## 2.4 MATERIALS ENGINEERING

### 2.4.1 Material Selection

The primary materials selected for use in the "No-Box" Box design are beta annealed 6Al-4V titanium, 10 Nickel steel and 7050 aluminum plate. Final design allowables based on test data, specification requirements, and vendor guarantees are shown in Tables II-28, II-29 and II-30, respectively.

### 2.4.2 Material Procurement

Beta Annealed 6Al-4V Titanium - Orders for all materials required for the FSIL design were placed during July and August and are scheduled for delivery during the last of December and the first half of January. Partial shipments have been received. Two vendors are participating in supplying this material, Reactive Metals Incorporated and Titanium Metals Corporation of America. The material on order for the FSIL configuration is more than adequate to support the "No-Box" Box design.

10 Nickel Steel - Orders for the material required to support the "No-Box" Box design were placed in September and first deliveries are scheduled to be received in January with completion in March. United States Steel Corporation is presently the only source for this material, with U. S. Steel doing the rolling and forging of the material and Latrobe Steel Company double vacuum melting (VIM plus VAR) of the ingot.

7050 Aluminum - Orders for the material required to support either configuration were placed in September, with delivery promised in early January. This material is a product of ALCOA and is being used in all applications requiring a starting thickness of 1.5 inches or greater.

Other Materials - Orders for long lead time items, such as 2024 aluminum, are being placed on an expedited basis. All orders for the 2024 aluminum required were placed during September and October and the majority of the requirements are being filled from warehouse stock. Orders for aluminum honeycomb core, adhesives, and other miscellaneous materials are in the process of being prepared.

Table II-28

**DESIGN ALLOWABLES**
**For Ti 6Al-4V**
**Beta Annealed Condition**
**(Ref. FMS-1109A)**

| FORM | PLATE | | | | |
|---|---|---|---|---|---|
| THICKNESS (Inches) | .188 - .500 | .501 - 1.000 | 1.001 - 2.000 | 2.001 - 2.500 | 2.501 - 4.000 |
| PROPERTY: | | | | | |
| $F_{tu}$(KSI) | 130 | 127 | 125 | 122 | 120 |
| $F_{ty}$(KSI) | 115 | 115 | 112 | 110 | 110 |
| $F_{cy}$(KSI) | 121 | 121 | 118 | 116 | 116 |
| $F_{su}$(KSI) | 87 | 85 | 83 | 81 | 80 |
| $F_{bru}$(KSI) | | | | | |
| e/D - 1.5 | 208 | 203 | 200 | 195 | 192 |
| e/D = 2.0 | 267 | 260 | 256 | 250 | 246 |
| $F_{bry}$(KSI) | | | | | |
| e/D = 1.5 | 140 | 140 | 136 | 134 | 134 |
| e/D = 2.0 | 170 | 170 | 166 | 163 | 163 |
| %Elong(L or LT) | 10 | 10 | 8 | 8 | 8 |
| E ($10^6$ psi) | | | 16.0 | | |
| $E_c$($10^6$ psi) | | | 16.4 | | |
| $K_{IC}$(KSI $\sqrt{inch}$) | | | 90(TYP) 80(MIN) | | |
| $K_{Iscc}$ (KSI $\sqrt{inch}$) typ | | | 60+ | | |
| $\rho$ (lbs/in$^3$) | | | .160 | | |

Table II-29

**DESIGN ALLOWABLES**

**For 10 Nickel Steel**

**(Ref. FMS-1111)**

| THICKNESS (Inches) | .375 - 2.00 | 2.01 - 4.00 | 4.01 - 8.00 |
|---|---|---|---|
| PROPERTY: | | | |
| $F_{tu}$ (KSI) | 190 | 190 | 190 |
| $F_{ty}$ (KSI) | 175 | 175 | 170 |
| $F_{cy}$ (KSI) | 184 | 184 | 179 |
| $F_{su}$ (KSI) | 121 | 121 | 121 |
| $F_{bru}$ (KSI) | | | |
| e/D = 1.5 | 274 | 274 | 274 |
| e/D = 2.0 | 368 | 368 | 368 |
| $F_{bry}$ (KSI) | | | |
| e/D = 1.5 | 245 | 245 | 240 |
| e/D = 2.0 | 291 | 291 | 282 |
| % Elong | 15 | 12 | 10 |
| Charpy V-Notch @ $0^{o}F$ (Ft.-Lbs.) | 60 | 50 | 40 |
| E ($10^6$ psi) | | 28.0 | |
| $E_C$ ($10^6$ psi) | | 28.0 | |
| $\rho$ (lbs/in$^3$) | | .284 | |
| $K_{IC}$ (KSI $\sqrt{\text{inch}}$) | | $>$ 180 | |
| $K_{Iscc}$ (KSI $\sqrt{\text{inch}}$) | | $>$150 | |

Table II-30
**DESIGN ALLOWABLES**
**7050 ALUMINUM ALLOY PLATE**

| TEMPER | | 7050-T7651 | 7050-T73651 | | | | |
|---|---|---|---|---|---|---|---|
| THICKNESS | | .250-1.00 | 1.01-2.00 | 2.01-3.00 | 3.01-4.00 | 4.01-5.00 | 5.01-6.00 |
| $F_{tu}$ (KSI) | L | 77 | 71 | 71 | 69 | 67 | 66 |
| | LT | 78 | 72 | 72 | 70 | 68 | 67 |
| | ST | | | 68 | 66 | 64 | 63 |
| $F_{ty}$ (KSI) | L | 69 | 63 | 63 | 60 | 58 | 56 |
| | LT | 67 | 63 | 63 | 60 | 58 | 56 |
| | ST | - | - | 59 | 56 | 54 | 53 |
| $F_{cy}$ (KSI) | L | 68 | 61 | 61 | 59 | 57 | 56 |
| | LT | 69 | 64 | 64 | 62 | 60 | 58 |
| | ST | - | - | 63 | 61 | 59 | 57 |
| $F_{su}$ (KSI) | | 44 | 41 | 42 | 42 | 41 | 41 |
| $F_{bru}$ (KSI) | e/D = 1.5 | 115 | 110 | 111 | 108 | 105 | 102 |
| | e/D = 2.0 | 150 | 144 | 142 | 137 | 133 | 129 |
| $F_{bry}$ (KSI) | e/D = 1.5 | 96 | 94 | 96 | 95 | 93 | 92 |
| | e/D = 2.0 | 112 | 109 | 112 | 109 | 106 | 105 |
| % Elong. | L | 7 | 9 | 9 | 9 | 9 | 8 |
| | LT | 7 | 6 | 6 | 6 | 5 | 5 |
| | ST | - | - | 2 | 2 | 2 | 2 |
| E ($10^6$ psi) | | | 10.3 | | | | |
| $E_C$ ($10^6$ psi) | | | 10.5 | | | | |
| $\rho$ (lbs/in$^3$) | | | .102 | | | | |
| $K_{IC}$ (KSI in.) (Typ) | | | 32 (L-T) 27 (T-L) 24 (S-L) | | | | |
| $K_{I_{scc}}$ (KSI in) | | | Resistant in T73651 temper 90-95% of $K_{IC}$ | | | | |

TENSILE DATA BASED ON ALCOA GREEN LETTER GL220(4-73)

### 2.4.3 Materials Testing

The status of the materials testing program is being reported in other sections of this report and is essentially complete. The data generated is being compiled in the Materials Property Data Report which is prepared and submitted incrementally at the end of each phase of the AMAVS program. The Phase Ib report (General Dynamics, Convair Aerospace Division Report FZM-6148) was submitted in April 1973 and the Phase II report is scheduled for submittal in January 1974. The design allowables noted in paragraph 2.4.1 and 2.4.5 and in subsection 2.3 were based on this test program.

### 2.4.4 Brazing Development

2.4.4.1 Brazing

Brazed assemblies processed during this phase are shown in Table II-31. As a result of the problems encountered with the first 603FTB035, a braze improvement program was initiated. This program consisted of a series of time-temperature laboratory tests and manufacturing tests to improve retort atmosphere and conditions of all components.

The "Braze Improvement Program" and observations of the first 603FTB035 FSIL Specimen Brazing Operation led to the following conclusions:

(1) Layup time from cleaning to braze needed to be reduced

(2) Glass cloth used as a stop off in the retort contributed to the contamination

(3) Silver braze alloy cleaning was not a major factor

(4) Improved purging was necessary

(5) Heat up rate to the brazing temperature needed to be improved

(6) Temperature reading near the braze line was necessary

Table II-31

BRAZED ASSEMBLIES

(Brazed Since 15 July 1973)

| PANEL NO. | BRAZE TIME (MIN) | TEMP (°F) | VAC ("Hg) | ARGON (CFH) | BZ ALLOY THICKNESS (in) | BUTTONS | BZ DATE | REMARKS |
|---|---|---|---|---|---|---|---|---|
| 603FTB035 #1 Pre Braze Cycle | -- | 1540 1580 | 15 | 10 | None | No | 8/7/73 | |
| 603FTB035 #1 | 10 | 1540 1585 | 15 | 10 | .005 | .002 x .125 | 8/20/73 | No BZ |
| 603FTB053 #1 | 10 | 1580 | 15 | 10 | .005 | .002 x .125 | 8/23/73 | Excellent BZ Good Fillets |
| 603FTB053 #2 | 10 | 1580 | 15 | 10 | .005 | .002 x .125 | 8/29/73 | Excellent BZ Good Fillets |
| 603FTB035 #1 ½ Panel ReBZ | 20 | 1605 1620 | 15 | 10 | .005 | .002 x .125 | 9/22/73 | Marginal BZ |
| 603FTB035 #2 | 7 | 1598 | 15 | 10 | .005 | .002 x .125 | 10/4/73 | Excellent BZ 100% Fillets |

Layup time can be reduced by organization and planning, such as, pre-cutting and pre-cleaning the braze alloy. Glass cloth was removed from the retort and was replaced by stop off. The stop off was baked at 700°F after application to tools to remove moisture and the carrier vehicle. Silver braze alloy cleaning was proven to be a minor factor but to insure consistency, all braze alloy foil is sanded and degreased.

Improved purging was obviously necessary due to atmosphere entrapment in the pocket areas of 603FTB035#1. On the -035 #1 argon was introduced through a 1/4" tube inside the barrier. The bottom pockets showed more discoloration than the top pockets. In order to insure purging, a tube with holes was placed in a groove in the base plate (See Figures 2-94, 2-95, 2-96 and 2-97). The holes provide argon in the center of the pocket areas to remove the atmosphere with a continuous flow. To improve the top pocket purging a tube with small holes was placed at the side of the titanium laminate so argon would flow through the slots on the other side (See Figures 2-98 and 2-99). This system was implemented for the rebraze operation of half of the 603FTB035#1 panel.

The strength of the Ag-Al-Mn brazements was shown to be dependent on the heating rate during brazing. At the lower brazing temperatures, slow heating rates produced low strength brazements. These brazements appeared spongy or grainy. Their microstructures revealed large void areas and incomplete melting along the central braze line.

A study of the experimental results in conjunction with the silver-aluminum and titanium-aluminum phase diagrams offered a metallurgical explanation to this heating rate dependence. The Ag-Al phase diagram shows that the liquidus temperature for this alloy system rises very rapidly from 1500°F to 1675°F with variations in the aluminum content from 5.5% to 2.0%. Microstructural and electron microprobe analyses of braze joints showed that a heterogeneous reaction takes place between the base titanium and the aluminum-rich molten portion of the braze alloy while heating through the liquid and solid region (1400-1600°F). This causes a wide compositional gradient to develop within the braze line. Given sufficient time, the aluminum content along the titanium interface region (gamma layer) rises to 36-44% with a corresponding drop in the central braze line

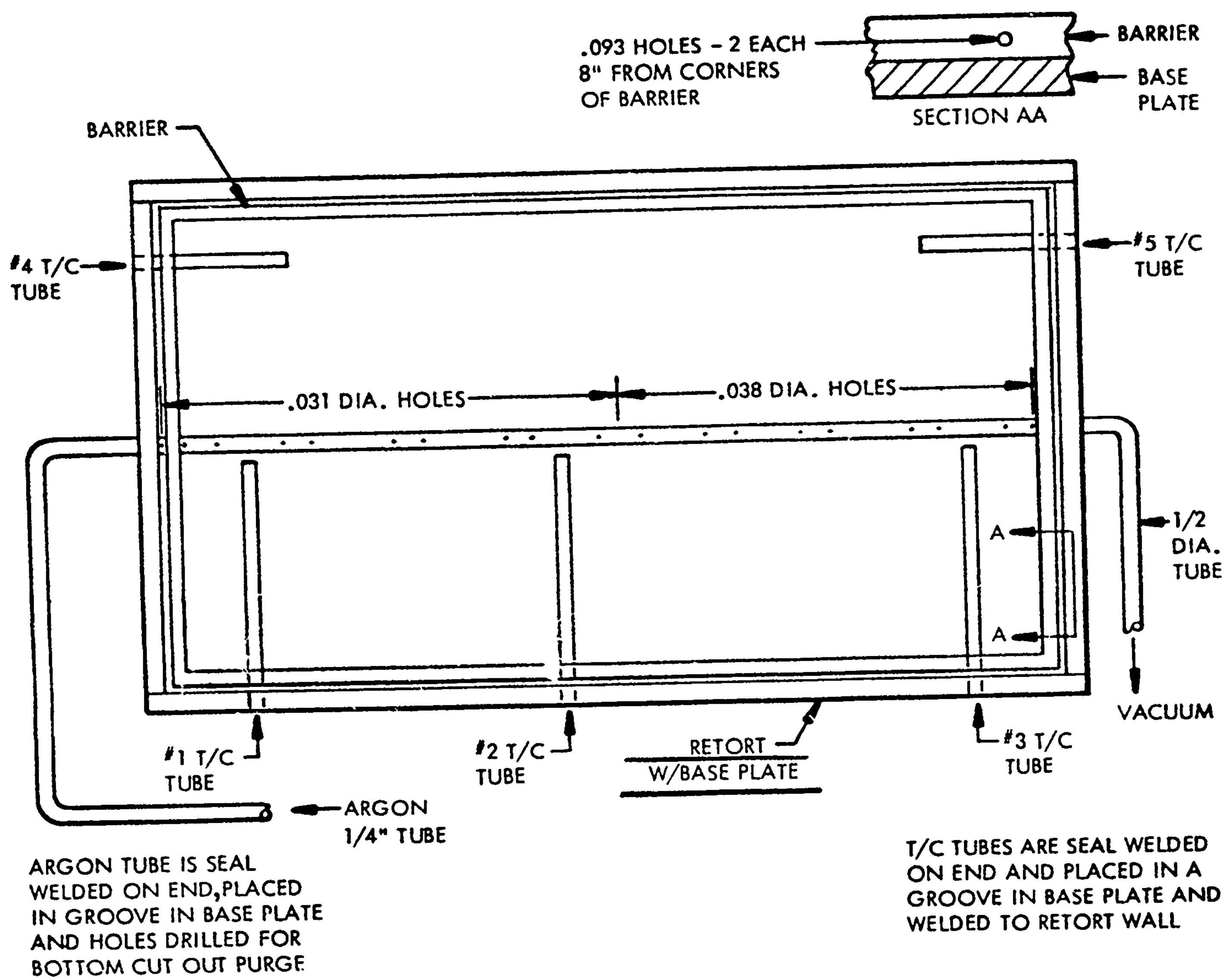


Figure 2-94 603FTB035 RE-BRAZE

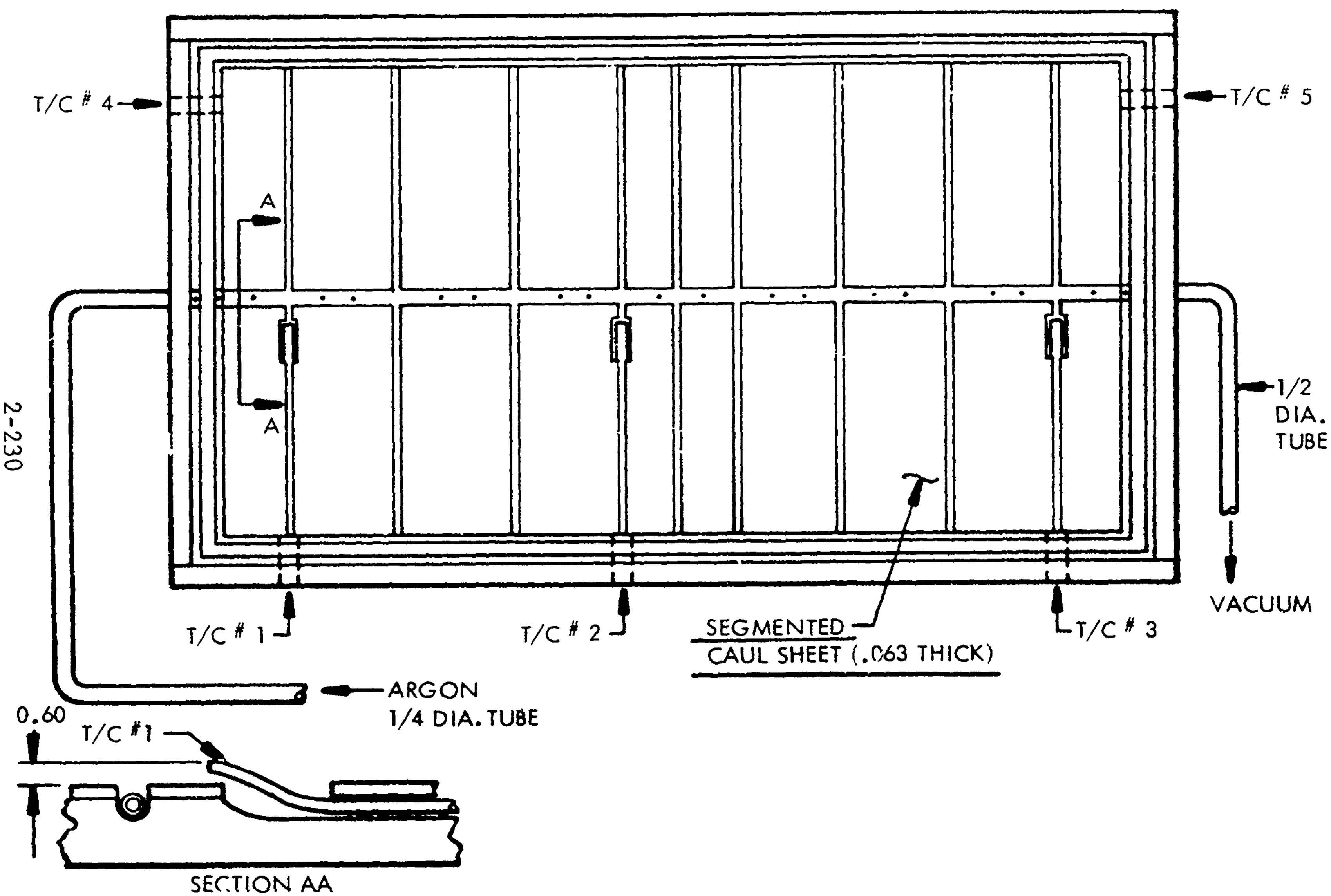


Figure 2-95 603FTB035 RE-BRAZE

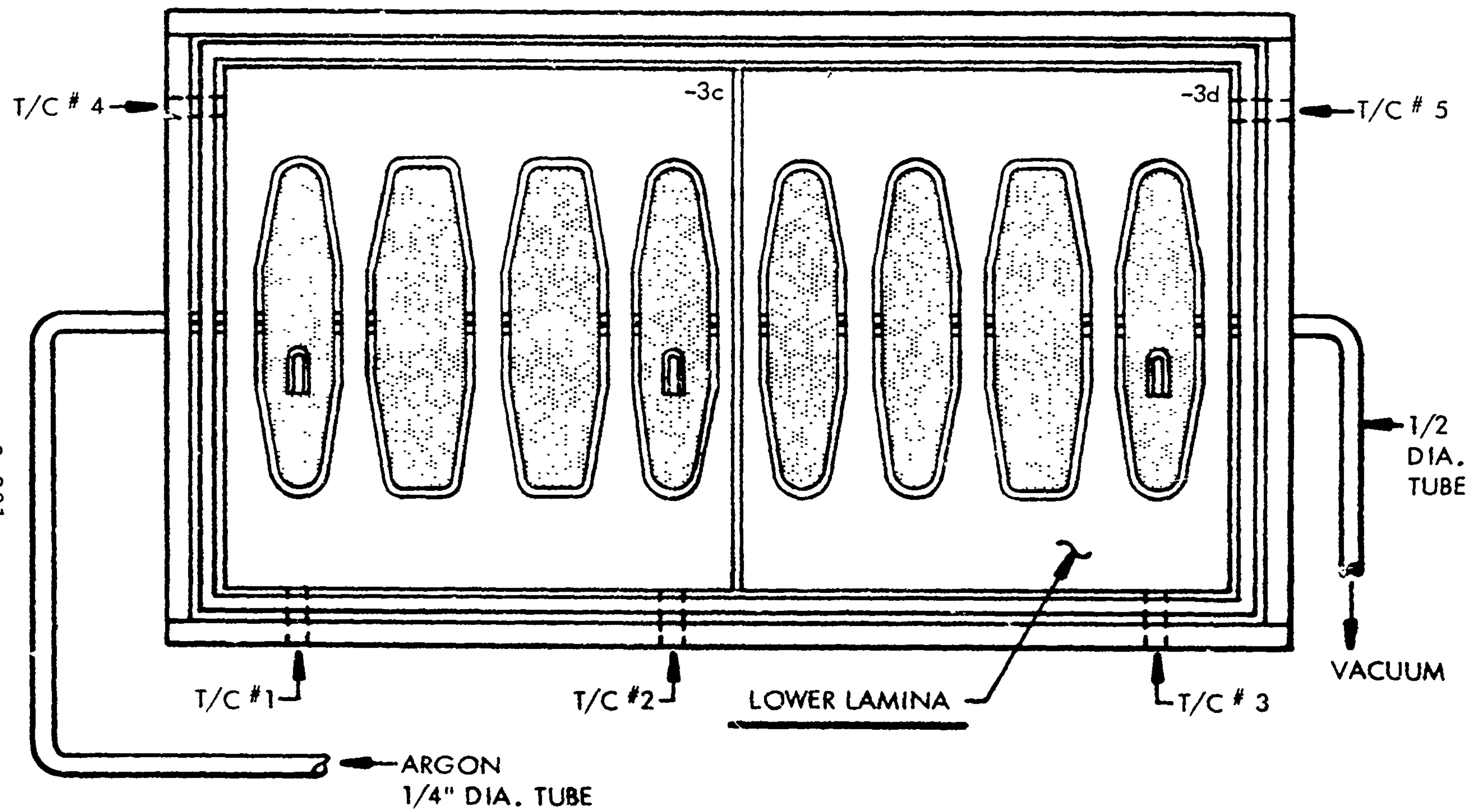


Figure 2-96 603FTB035 RE-BRAZE

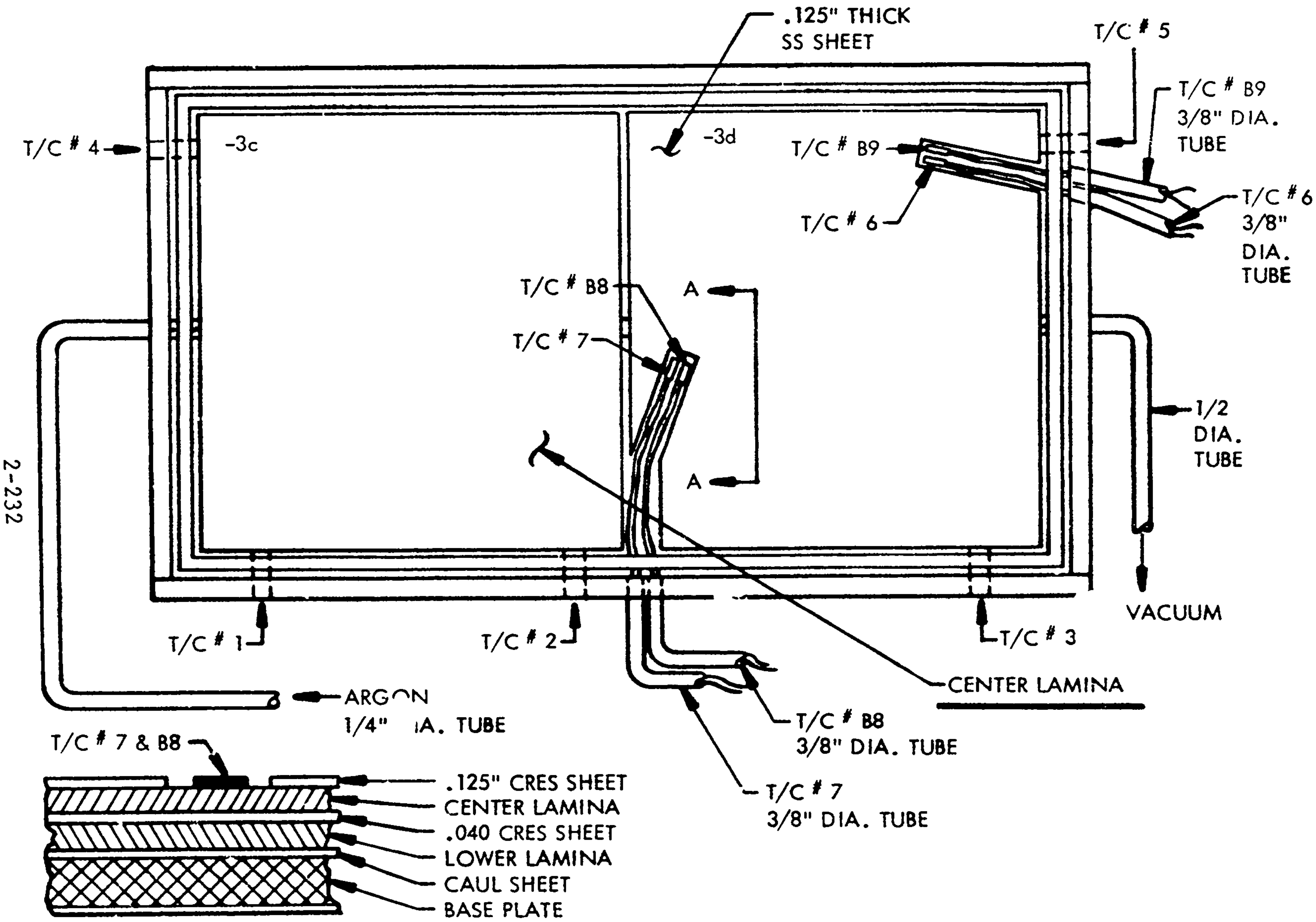


Figure 2-97 603FTB035 RE-BRAZE

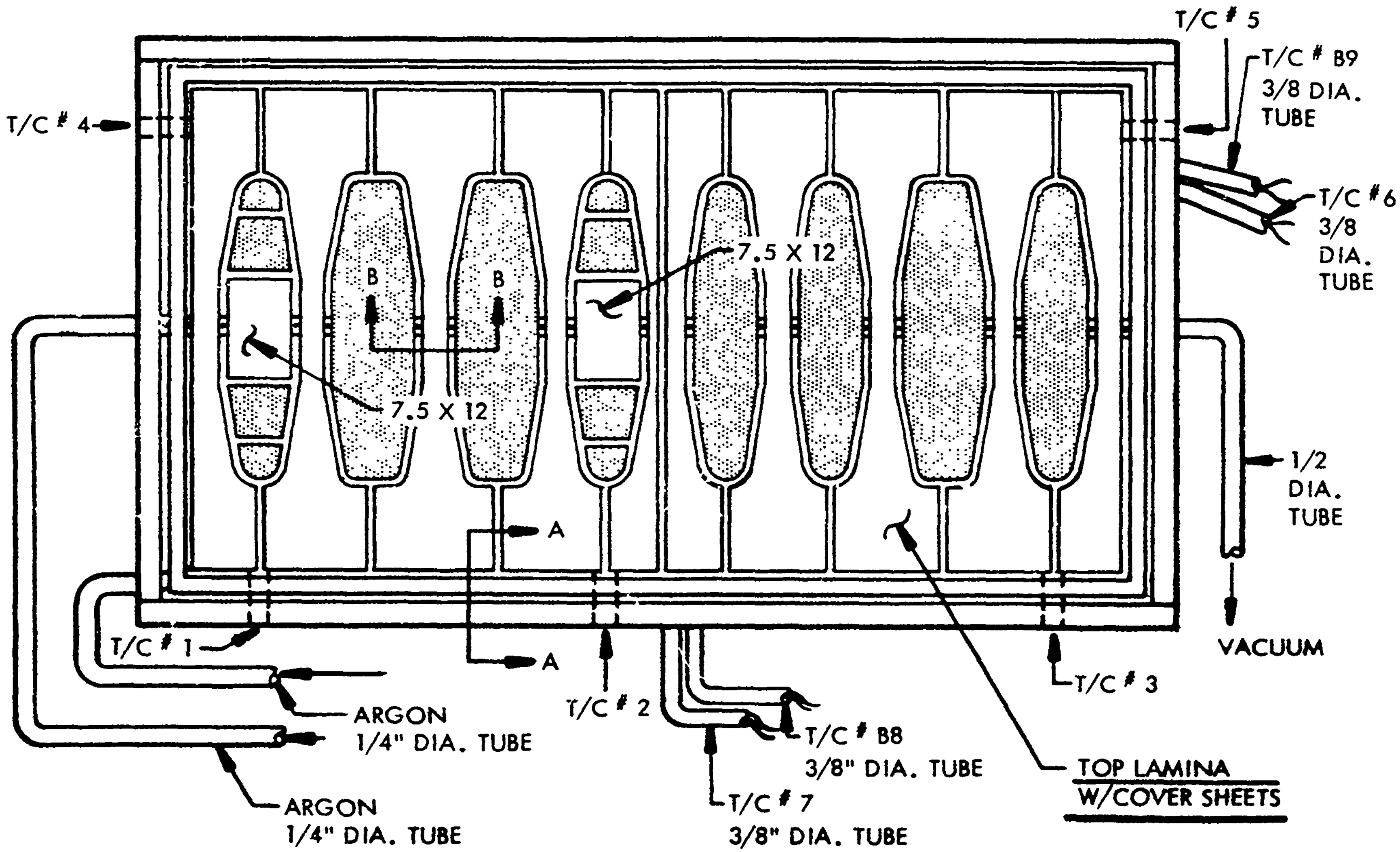


T/C # 10 IN STEEL
BLOCK ON TOP OF
VACUUM SHEET

2 EACH .250/250 X 7.5 X 12 NEW
Ti ASSEMBLIES WITH Ag
BRAZE ALLOY

Figure 2-98 603FTB035 RE-BRAZE

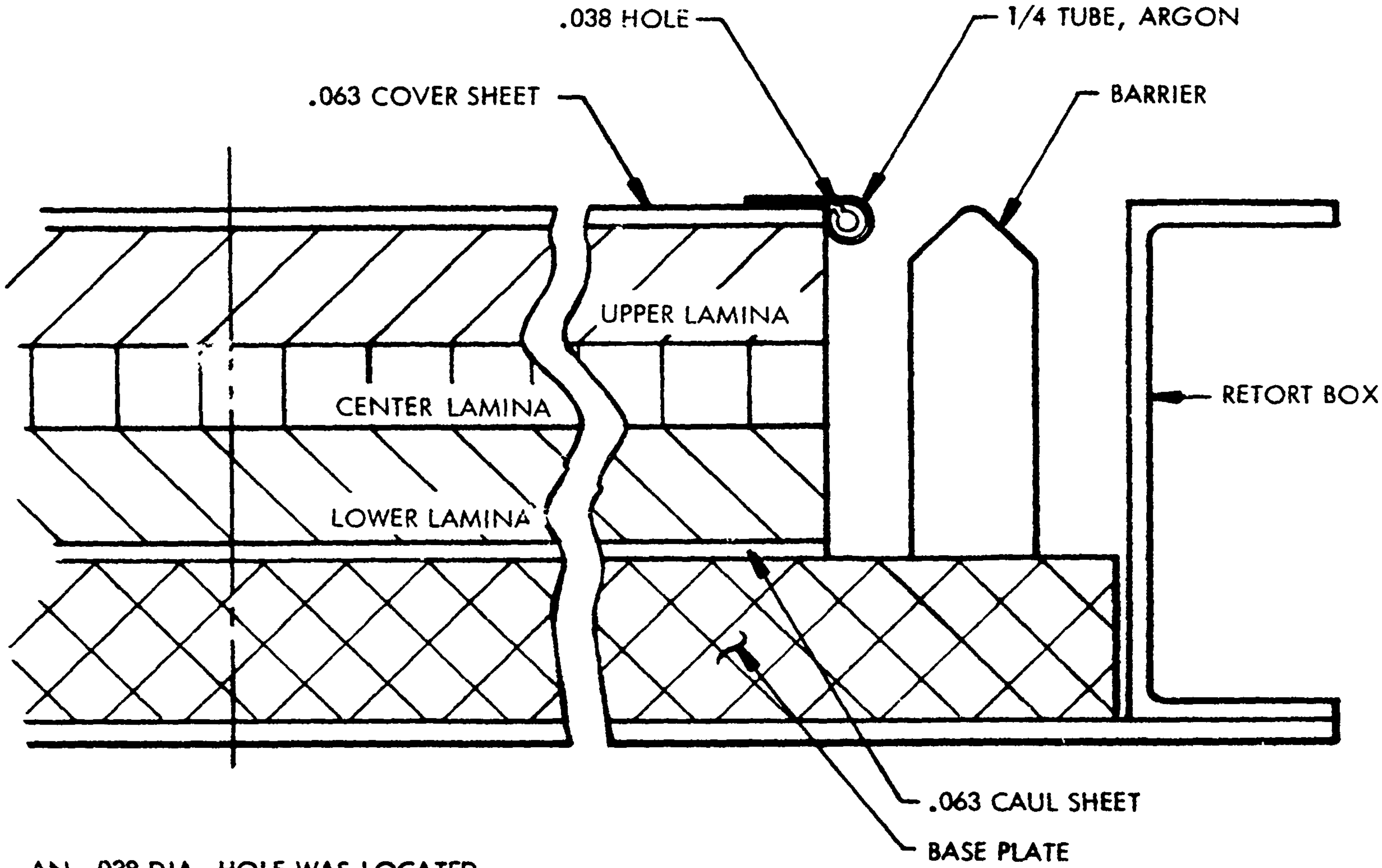


AN .038 DIA. HOLE WAS LOCATED AT EACH GAP (.250) BETWEEN THE SEGMENTS OF THE COVER SHEET. THE HOLE WILL BE POINTED UP AT 45°∠ TOWARD THE VACUUM SHEET.

SECTION AA

Figure 2-99 603FTB035 RE-BRAZE

to 2%. The phase diagram shows that an alloy with this low aluminum content will require a braze temperature of 1675°F to go fully liquid. If the chosen braze temperature is below this value the central braze line with its low aluminum content will not go fully liquid. A spongy, low-strength braze will be produced. The experimental results showed that with heating times of 60 minutes or more in the 1400-1600°F range, this condition was produced. It could be minimized by either reducing the heating time (less aluminum depletion) or increasing the maximum brazing temperature (to exceed the new liquidus temperature).

The furnace was raised to 1200°F prior to insertion for re-brazing the -035#1 half panel. Insulation was left on the top of the panel to insure uniform heating. Uniform heating was thought to be necessary to prevent warpage in the braze assembly. The furnace control was set at 1625°F and the re-braze package heated to the braze temperature faster than the initial -035 braze package. From room temperature the initial -035 took five hours - 40 minutes to reach a braze temperature of 1550°F. The re-braze package heating time from room temperature to 1600°F was four hours - 10 minutes. The time to heat from 1400°F to the top braze temperature was 80 minutes for the re-braze package compared to 70 minutes for the initial effort. The quality of the re-braze was better than the original though still marginal. The void content of the braze line was high and the flow was practically non-existent since the braze alloy did not change form. The braze joint was in excess of 0.005 inch thick and fillets did not exist. Microscopic examination of the braze joint indicated spongy appearance related to the high void count.

Temperature readings were suspect on the initial -035 braze operation since the thermocouples (T/C) were placed in the base plate. One T/C was embedded in a steel block on top of the vacuum sheet with the insulation removed in that area. The T/C's placed in the base plate were placed in CRES steel tubes seal welded on the end and welded to the retort wall. This allowed the sheathed T/C to be readily placed in position and removed. Also this arrangement minimized the number of tubes to be handled and mechanically sealed around the T/C. For the 603FTB053 #1 and #2 brazed assemblies the T/C CRES steel tube was formed up through a cut in the caul sheet and placed adjacent to the center Titanium lamina in a pocket. See Figure 2-95.

The #1 and #2 603FTB053 braze assemblies were of excellent quality with the braze alloy changing form - going from a foil sheet to a liquid. Wetting was excellent and fillets were consistently formed.

For the -035 rebraze half panel the T/C arrangement was modified. (See Figures 2-95, 2-96, 2-97, 2-98 and 2-100). T/C's #1, 2 and 3 were placed in tubes formed to end adjacent to the lower surface of the center lamina. T/C #4 and 5 were left in the base plate. Since only half of the -035 #1 was to be rebrazed the other half was used to dummy load the retort. In place of silver braze foil, CRES steel sheet was used to interleave the titanium lamina. (See Figure 2-97). By using 1/8 CRES steel sheet at the top braze line, it was possible to cut out slots and place sheathed T/C #6 and 7 geometrically opposite T/C 5 and 2. (See Figure 2-97).

To check sheathed T/C readings, unsheathed glass cloth coated T/C #B8 and #B9 were routed through exterior tubes to adjacent locations with T/C #7 and #6, respectively. The fragile nature of the glass cloth and routing through the holes and slots necessary to reach the T/C #7 and 6 location shorted out T/C #B8 and #B9. T/C #5 was lost due to a leak in the tube and had to be seal welded at the retort wall. Correlation between the remainder of the T/C's was very good. The T/C #6 and #7 indicated a slower heating rate than #4 and #2 which led to the conclusion that the Ti braze assembly was being heated primarily from the bottom. The insulation blanket is very efficient.

The rebraze half of -035 #1, as noted above, was not of desirable braze quality but the rebraze operation produced information on the heating rate and purging system.

Prior to the rebraze operation of -035 #1, a wood mock up of half of the -035 panel was fabricated. Using plexiglas as a cover sheet and smoke in place of argon, the flow from the tube purging system could be observed. Smoke was injected into the tube system after a partial vacuum was pulled on the mockup retort. The smoke flow indicated the desired flow of the argon.

After the rebraze of -035 #1 it was observed that the argon tube in the base plate injecting argon into the center of the pocket slots was much more effective than the tube at the side of the titanium laminate.

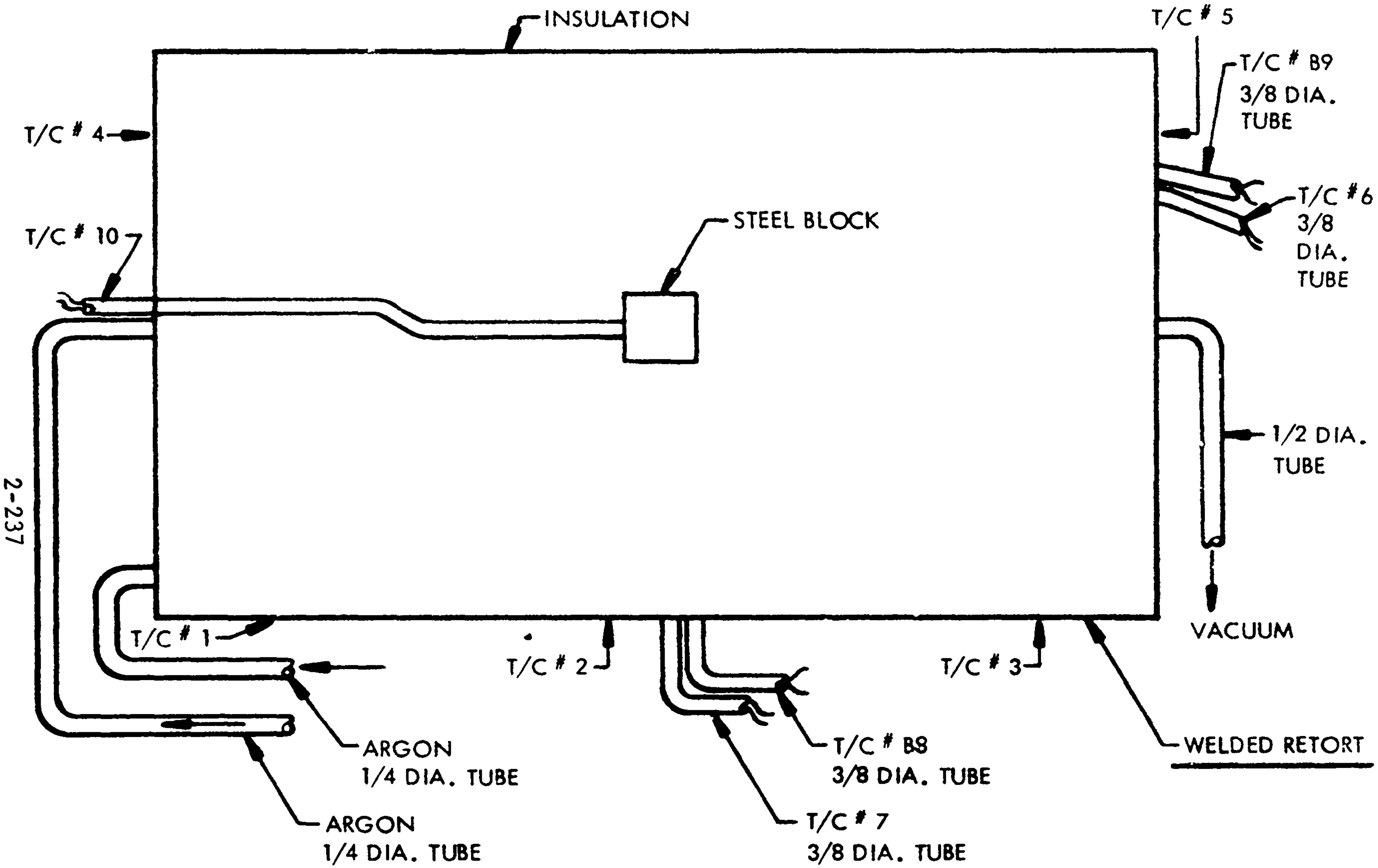


Figure 2-100 603FTB035 RE-BRAZE

Another observation was the discoloration of an area adjacent to the first two holes in the lower argon tube indicating improper cleaning of the argon tubing. All tubing is now degreased with 150°F trichloroethylene.

Two .250/.250 X 7.5 X 12 Ti panels were placed in the first and fourth slot, from the argon input end of the -035 rebraze panel. (See Figure 2-98). The titanium material in these panels was new. Some runout of the silver braze alloy was observed and the lap shear strength was 20 to 24 ksi. The microscopic examination indicated a general spongy appearance and fairly wide braze joint although not as spongy as the -035 rebraze panel. Small compression type shear specimens from the corners of the rebraze panel indicated a shear strength of 4 to 24 ksi. With small specimens, a wide variation can be expected. NDI results indicate greatly improved quality compared to the -035 #1 braze. The lower braze joint had estimated 45% void in the upper braze joint.

The analysis of the -035 #1 braze operation, the -035 #1 rebraze operation and the Braze Improvement Program Specimen Testing indicated the following changes for the -035 #2 braze operation.

(1) Minimize the penetrations of the retort

(2) Improve cleaning procedures

(3) Improve the Argon Purging System

(4) Increase the heat up rate (Target heat up rate 4°F/min)

The use of only five internal T/C's and one on top in a steel block reduced the penetrations of the retort and improved the handling of the retort considerably. (See Figures 2-100, 2-101, 2-102 and 2-103). Improved cleaning procedures were initiated as noted above.

The Argon System was changed primarily by shifting the top argon tube to the center of the retort. (See Figures 2-100, 2-101, 2-102, 2-103, 2-104, 2-105 and 2-106).

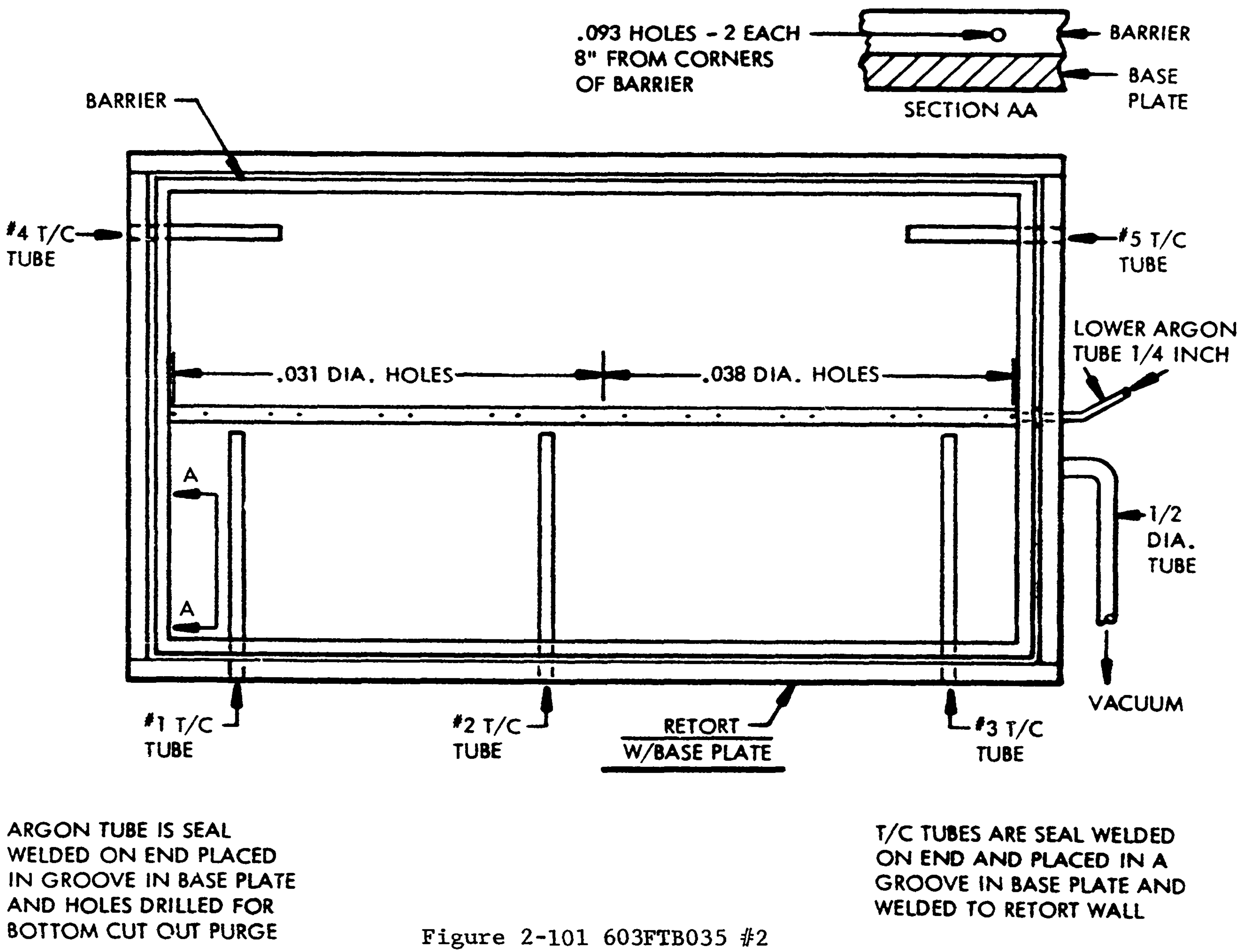


Figure 2-101 603FTB035 #2

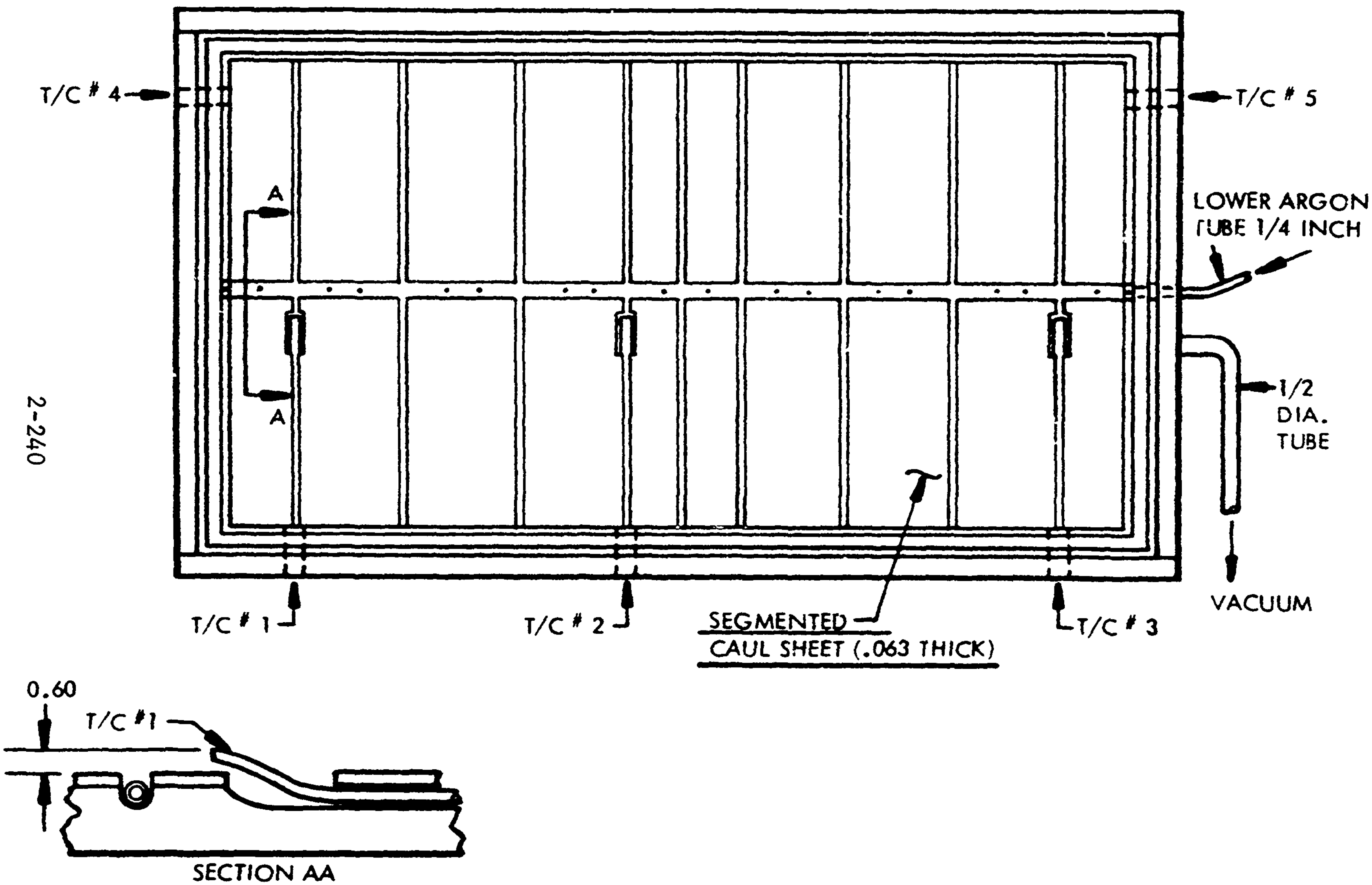


Figure 2-102 603FTB035 #2

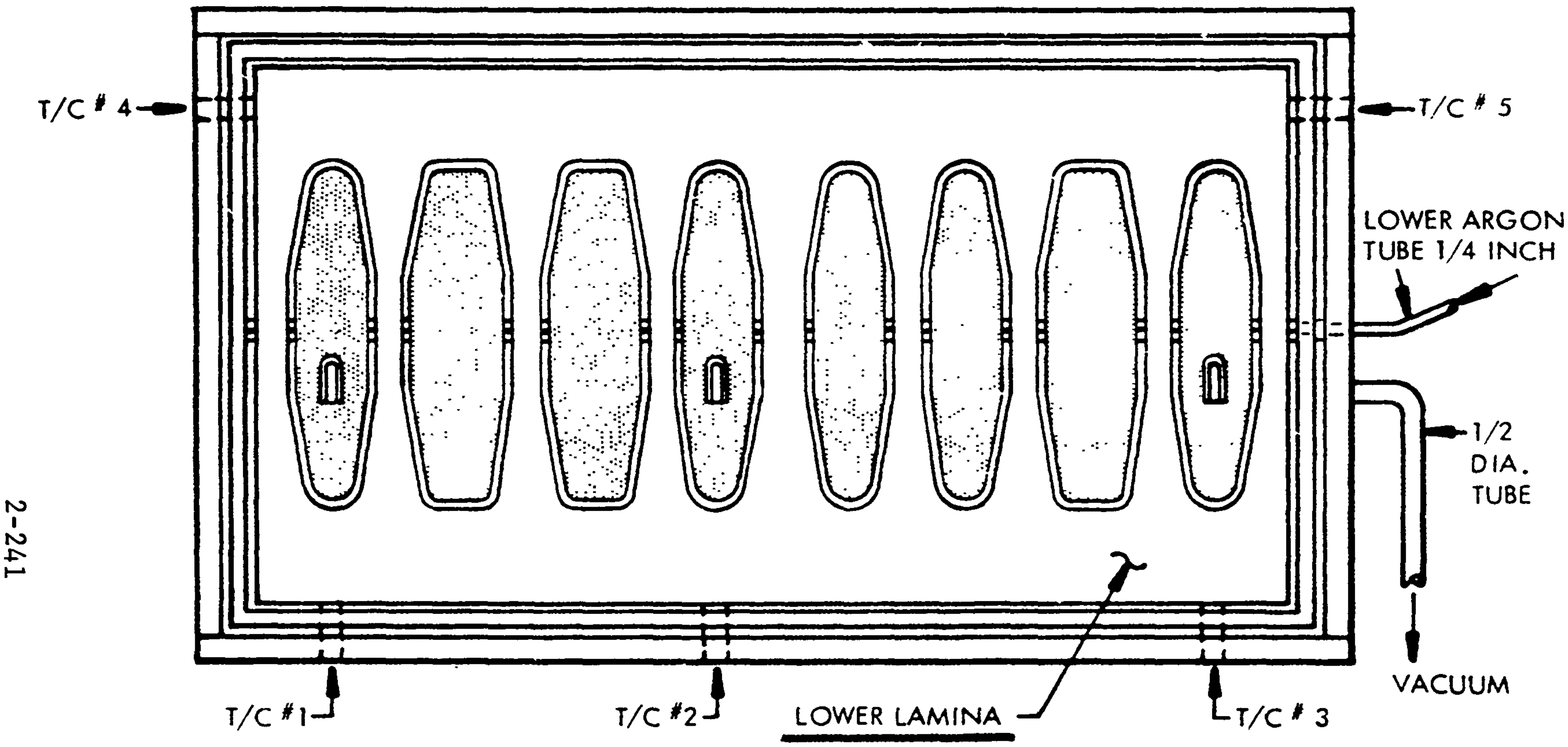


Figure 2-103 603FTB035 #2

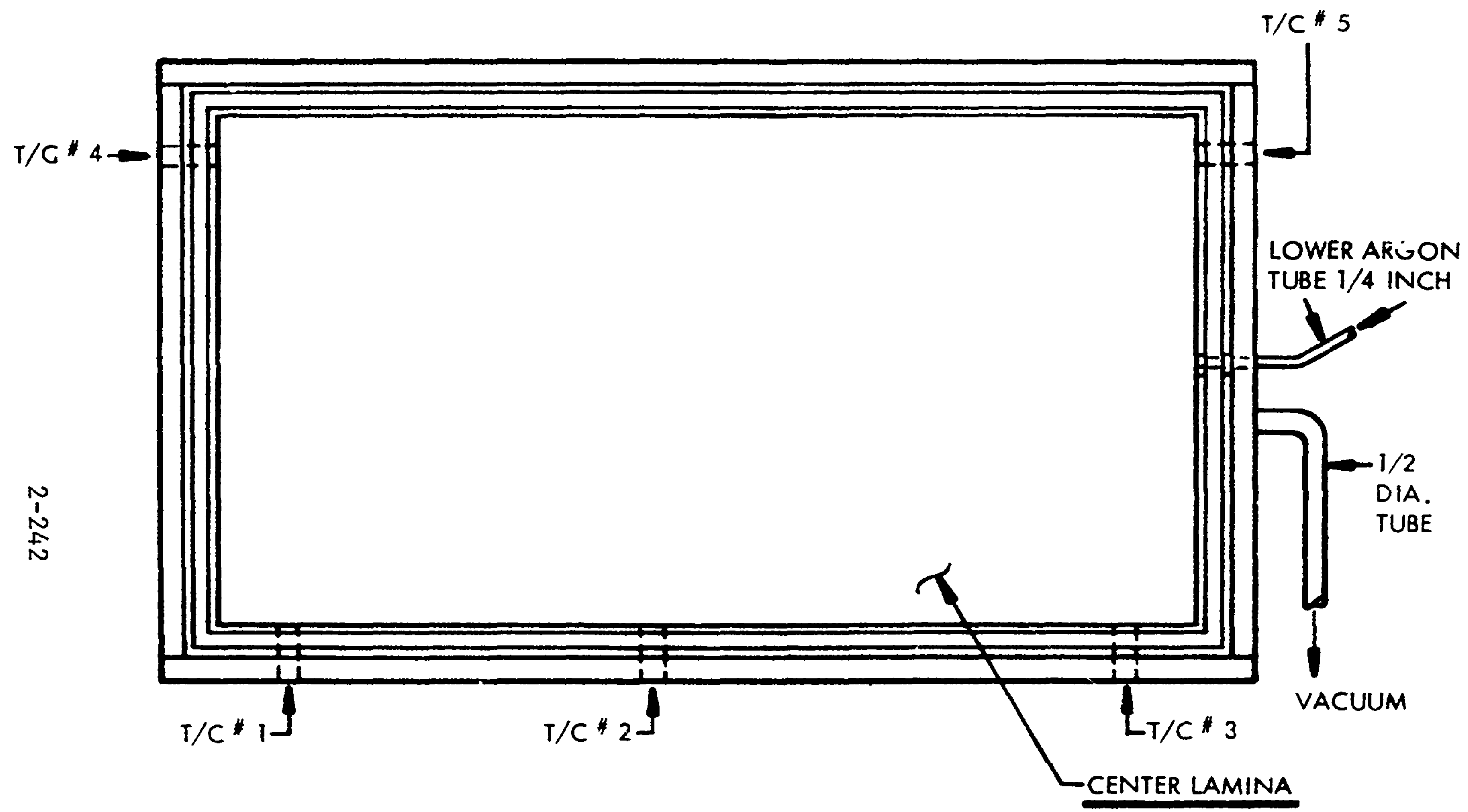


Figure 2-104 603FTB035 #2

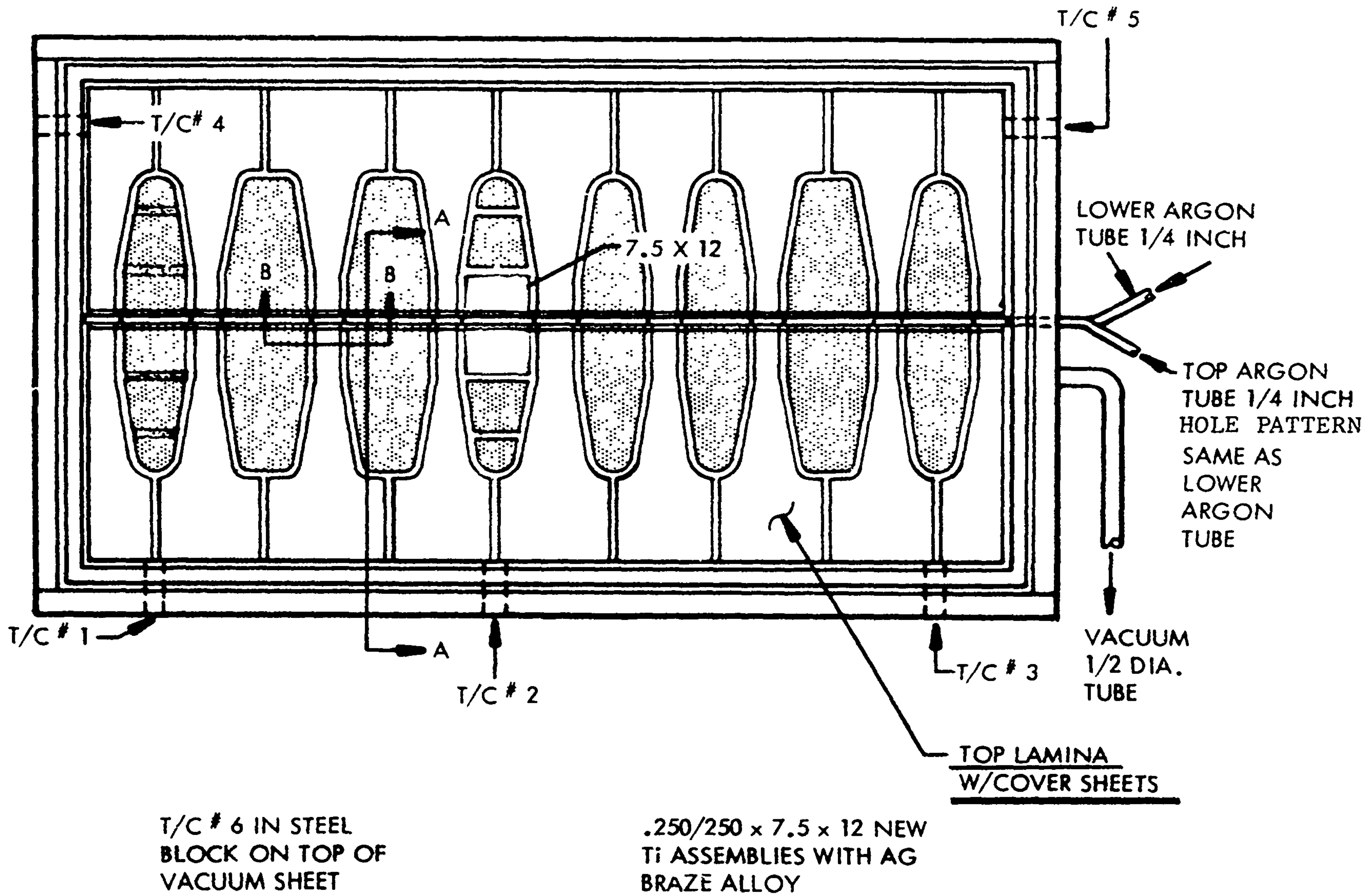


Figure 2-105 603FTB035 #2

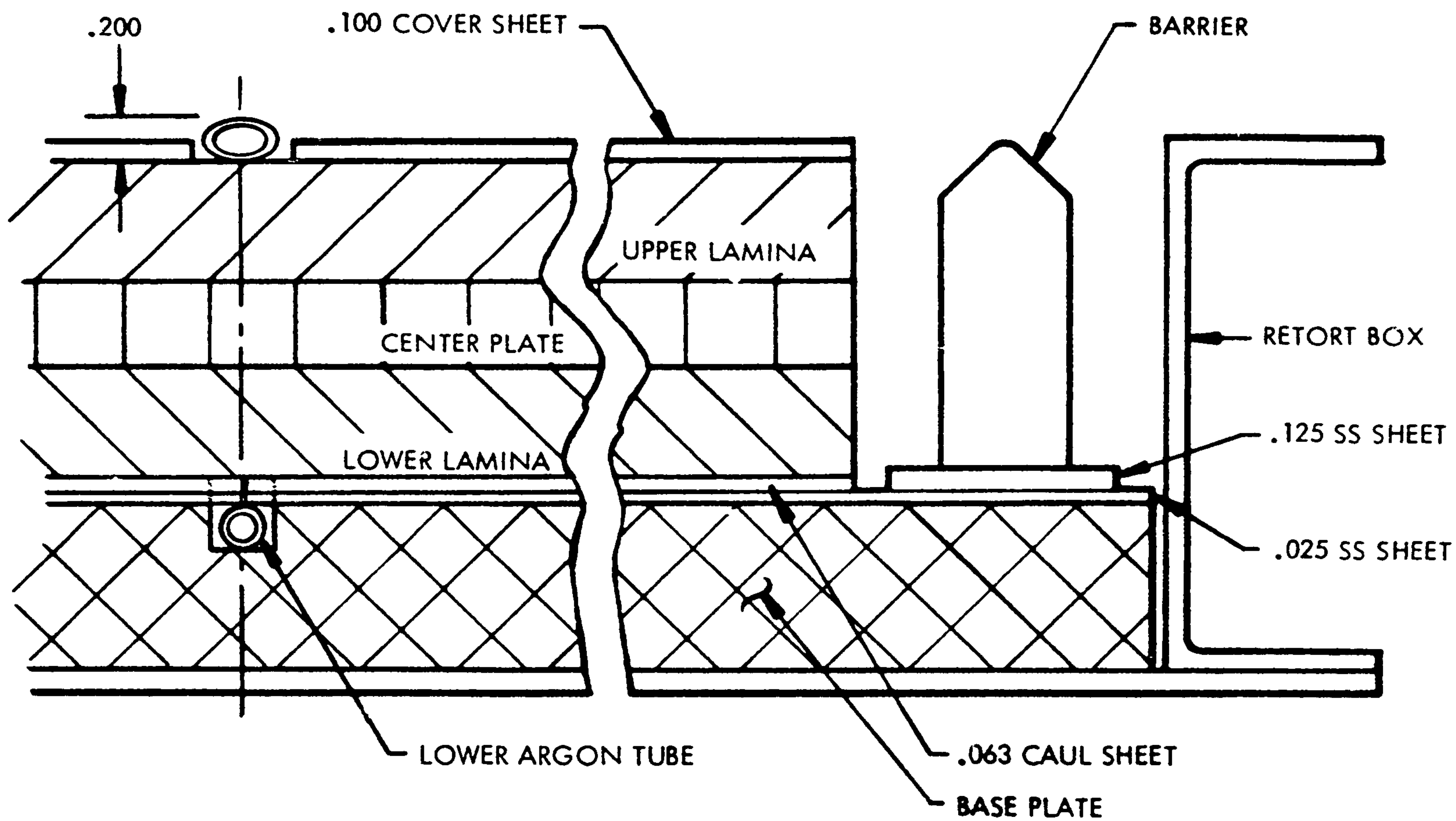


HOLES WILL BE LOCATED
AT EACH SLOT, (SHOWN IN
SKETCH 1, 2 & 3) IN
LOWER AND UPPER
ARGON TUBES

SECTION AA

Figure 2-106 603FTB035 #2

The concern over the effect of the argon tube on the vacuum sheet was minimized by flattening the 1/4" tube to an oval shape which enhanced the formability at the ends of the -035 panel. Introduction of Argon at the center of each center slot position produced an argon flushing action to the purging system. The majority of the Argon gas is introduced into the inside of the barrier. The holes in the barrier for the argon to flow from the inside to the outside were placed in the opposite end of the retort from the vacuum tube. The argon tubes were placed on the same end as the vacuum tube to minimize the length and handling. (See Figures 2-104 and 2-107). The changes improve the purging action. These changes were checked out with the wood mockup prior to brazing -035 #2.

To increase the heatup rate the insulation blanket was removed from the top of the retort. The insulation is used primarily to prevent warpage of the Ti braze assembly due to the rapid cooling of the CRES steel retort edges and rapid cooling of the top Ti lamina. The insulation was left off during the braze operation and two layers were placed on the retort after removal from the furnace (1350°F). Only one layer was necessary, however, since the panel cooled from the bottom due to the efficiency of the insulation and a slight bow was noticed in the -035 #2 braze assembly. With the removal of the insulation preheating of the furnace to 1400°F and setting the controls on 1650°F (maximum on this furnace) the package heated rapidly. For a time-temperature plot of 603FTB035#2, see Figure 2-108.

From the braze improvement program specimens and review of previous successful braze packages (603FTB053, etc.) it was evident a heat up rate from 1400°F to the braze temperature would need to be near 4°F/min.

The actual time from 1400°F to 1598°F (#2 T/C) was 53 minutes or approximately 3.8°F/min. This heat up rate was approximately 5°F/min. through the solidus to liquidus range of the braze alloy. The results were that the braze alloy changed form completely going from a foil sheet (.005 thick) to a liquid and produced excellent wetting. Fillets were found in the pockets (100% top and bottom). For wetting of this nature to occur, very good cleaning was obvious and purging was the best obtained to date.

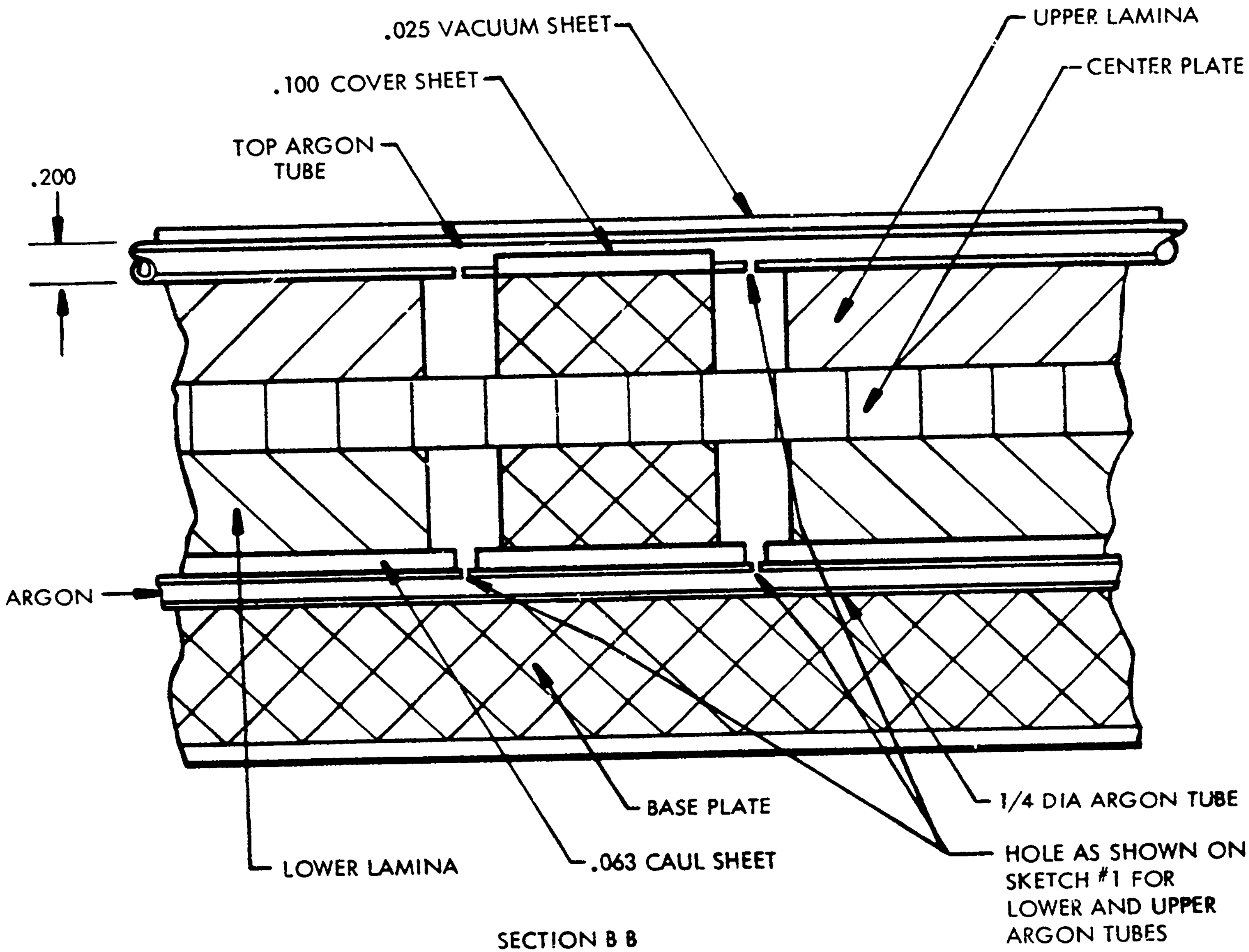


SECTION B B

Figure 2-107 603FTB035 #2

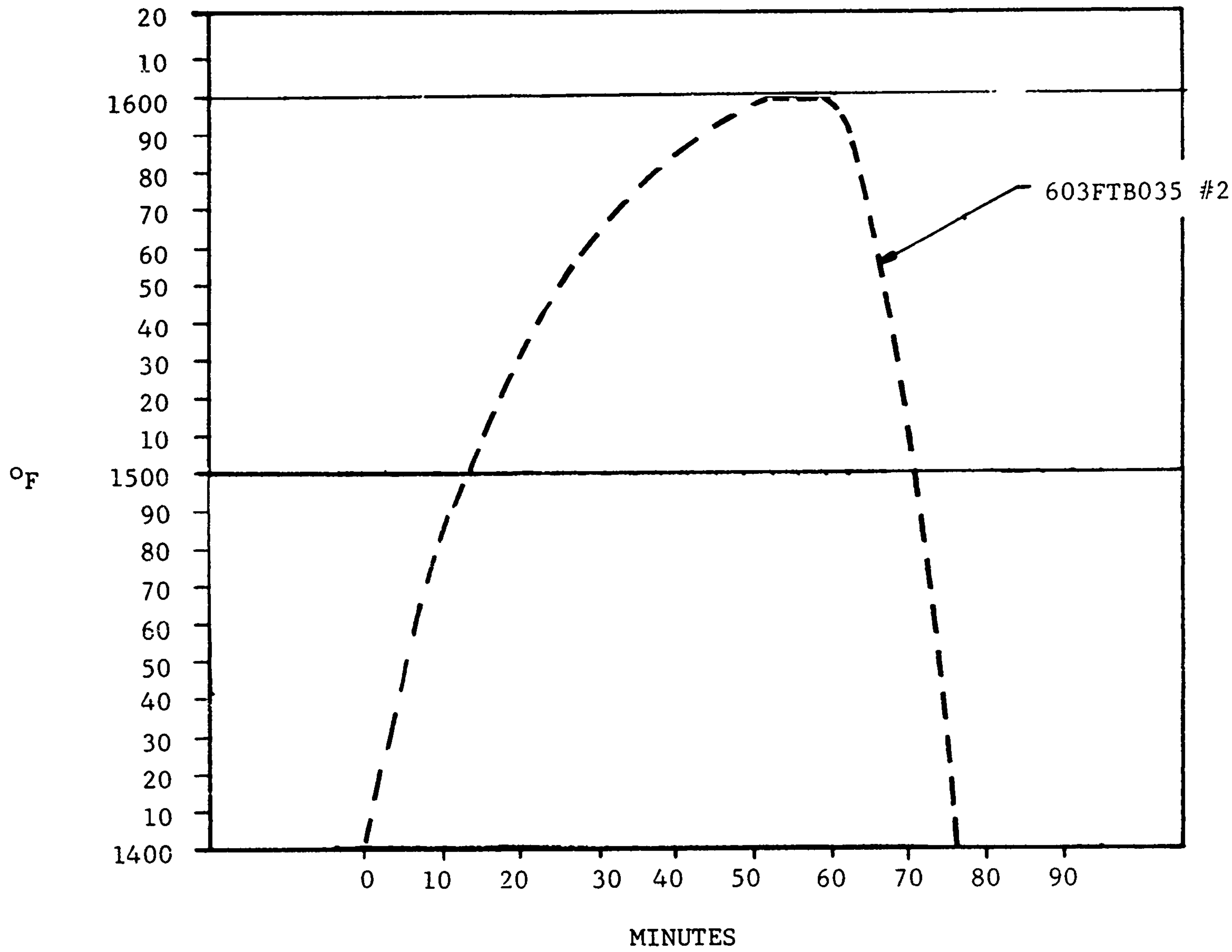


Figure 2-108 AMAVS BRAZING CYCLE FOR 603FTB035 #2

Lap shear specimen from the .250/.250 X 7.5 X 12 panel placed in the cutout produced an average of 20 KSI plus. Compression shear strength from a corner of the actual panel was 24 KSI plus. The microanalysis indicated a .003 to .004" thick braze joint and a minimum of voids and an excellent reaction area between the silver and titanium. NDI results indicate 90% minimum braze on both top and bottom braze joints.

### 2.4.4.2 Brazing Alloy

The Ag-Al-Mn brazing alloy used to braze all titanium laminates and assemblies was procured from Western Gold and Platinum Company, 525 Harbor Blvd., Belmont, California, 94002. The silver alloy foil was produced in approximately 100 troy ounce lots supervised by their laboratory personnel using extra care to control the manganese content. The quality of the foil was generally good except for a small percentage of the first foil produced which had oxide scale rolled into the surface. The producer eliminated this problem as soon as it was brought to his attention.

During the lay-up of the first 603FTB035 assembly, a feature of the braze foil was noticed that had escaped attention previously. Due to the size, 4 foot x 10 foot, of each braze joint, the .005" X 3.00" X random length foil was layed in strips in the 10 foot length. It was noticed that the strips of foil were not straight. If the strips were pulled straight parrallel to the 10 foot edge of the titanium, wrinkles resulted. To minimize the wrinkles the foil was cut in approximately 2 foot lengths. Discussion with the producer indicated the cause of the strips of foil being crooked was uneven tension on the roller that pulled the foil through the slitter. This problem is unique to large braze joint areas and has been corrected.

A compilation of pertinent data on the braze foil is found in Table II-32. Good uniformity in chemistry results in uniformity in solidus (1410 to 1440°F) and liquidus (1495 to 1525°F) melting temperature. Lot 19042 is excluded since the thickness was .002 and was never used in other than 3 inches X 3 inches specimens.

### 2.4.4.3 Stress Corrosion of Brazed Joints

Beta annealed 6Al-4V titanium brazed with Ag-Al-Mn alloy is subject to sustained load stress corrosion delamination in a sump tank water environment. Delamination occurs at the braze

Table II-32

BRAZE ALLOY

0.005 x 3 x Random Length Silver Alloy Foil

| *LOT NO. | QUANTITY (TROZ) | Analysis: Vendor Ag | Vendor AL | Vendor Mn | Convair Check Ag | Convair Check AL | Convair Check Mn | SOLIDUS (°F) | LIQUIDUS (°F) |
|---|---|---|---|---|---|---|---|---|---|
| 20608 | 166.135 | 93.67 | 5.62 | .71 | 94.00 | 5.48 | .52 | 1410 | 1495 |
| 20616 | 63.542 | 93.89 | 5.62 | .49 | 93.70 | 5.64 | .66 | 1430 | 1525 |
| 20682 | 222.148 | 93.95 | 5.51 | .54 | 94.00 | 5.48 | .52 | 1410 | 1515 |
| 20683 | | 93.56 | 5.57 | .67 | 94.00 | 5.49 | .51 | 1420 | 1510 |
| 20684 | | 93.71 | 5.61 | .68 | 93.75 | 5.76 | .49 | 1420 | 1505 |
| 20685 | | 93.55 | 5.79 | .66 | 94.10 | 5.39 | .51 | 1420 | 1500 |
| 20743 | 97.709 | 94.24 | 5.21 | .55 | 94.20 | 5.30 | .50 | 1425 | 1520 |
| 20811 | 295.104 | 94.14 | 5.27 | .59 | 93.80 | 5.73 | .47 | 1430 | 1520 |
| **19042 | 148.321 | 94.41 | 5.02 | .57 | 94.8 | 4.76 | .44 | 1415 | 1540 |
| 19455 | 71.260 | 93.87 | 5.33 | .55 | 93.80 | 5.55 | .65 | 1440 | 1515 |
| 18897 | 195.275 | 94.18 | 5.16 | .66 | 94.30 | 5.03 | .67 | 1425 | 1510 |
| 19577 | 312.281 | 94.09 | 5.34 | .57 | 94.10 | 5.20 | .70 | 1435 | 1495 |
| 19579 | | 93.81 | 5.49 | .70 | 93.60 | 5.60 | .80 | 1430 | 1510 |
| 19576 | | 94.07 | 5.34 | .59 | 93.60 | 5.80 | .60 | 1440 | 1500 |
| 19578 | | 93.78 | 5.63 | .59 | 93.70 | 5.70 | .60 | 1420 | 1500 |

*Western Gold and Platinum Lot Numbers

**.002"Thick Foil

Note: Convair check analysis was made on the Ag and Mn and Al obtained by mathematical deduction.

interface. No evidence of base metal cracking has been observed. Results from 51 single lap shear specimens brazed using a wide range of processing variables indicate that the stress corrosion threshold is at least 4 ksi as shown in Figure 2-109.

Metallurgical studies suggest that the threshold level may be a function of braze interface concentration (of Ag and Al) gradients. Minimum concentration gradients and the best stress corrosion delamination resistance occurred in panels with extensive reaction between the braze alloy and the base metal. Fast thermal cycles maximized susceptibility and vice versa.

Microsections of stress corrosion test (SCC) specimens from MR&D brazed panels #11 and #25A and 603FTB035 #1 and #2 brazed component test assemblies are shown in Figures 2-110 thru 2-113, respectively. The microsection from panel #11 (Figure 2-110) indicates a minimal reaction zone between the braze alloy and titanium showing some $\gamma$ phase with no apparent $\alpha$ zone. This panel was brazed at 1530°F and was above 1400°F only 28 minutes. The heating rate between 1400 and 1500°F was 10°F/min. Sustained load SCC testing (see Group I) at 12KSI in sump tank water failed 5 of the 6 specimens prior to 1000 hours. The microsections from panel #25A and 603FTB035#2 have a specific $\alpha$ and $\gamma$ zone and a wide reaction area between the braze alloy and titanium. Panel #25A was brazed at 1550°F with a total time above 1400°F of 55 minutes. The 603FTB035#2 panel was brazed at 1598°F with a total time above 1400°F of 75 minutes. The heating rate of #25A and -035#2 between 1400 and 1500°F was 3.8°F/min. and 7.15°F/min., average, respectively. SCC specimens from #25A and -035#2 endured for 1000 hours at 12 and 8KSI sustained load, respectively, Some evidence of SCC attack was found on the interface region of some of the brazed joints. The extent of actual stress corrosion attack was complicated by small void areas in some specimens.

The braze thermal cycle used to produce the -035#2 test component is close to the optimum thermal cycle. Specimens taken from the .250/.250 X 7.5 X 12 panel brazed with this component have satisfactory corrosion delamination resistance. Three specimens were tested at 8KSI for 1096 hours (as noted above). Upon completion of the test, the specimens were loaded statically to failure and examined for evidence of sub-critical stress corrosion delamination. The lap shear strengths were 22.9 KSI, 22.3 KSI and 14.3 KSI with the latter showing some evidence of corrosive attack at the braze joint.

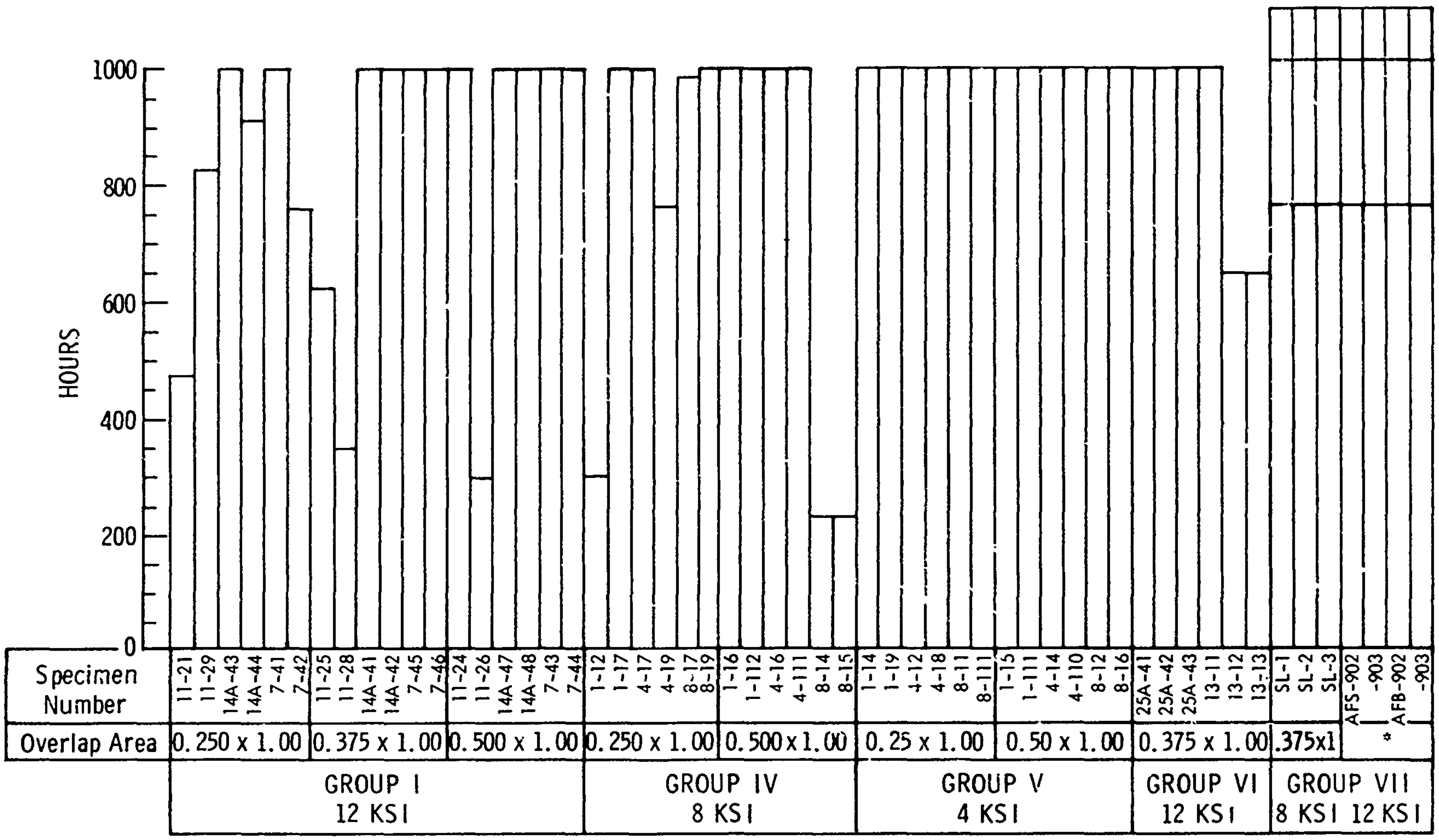


| | | | | | | |
|---|---|---|---|---|---|---|
| MR&D Panel Number and Test Condition | BZ 11 | Fast Heating Cycle | BZ 4 | Sanded Details (63 RMS) | | *Vac. Furnace |
| | BZ 14A | 30 Min. @ BZ Temp | BZ 8 | Low Pressure | | BZ - Small Spcm. |
| | BZ 7 | Good BZ | BZ 25A | Good BZ | | from AFML |
| | BZ 1 | No Buttons, 63 RMS | BZ 13 | Double Cycle Preform | | |

Figure 2-109 SUSTAINED LOAD STRESS CORROSION TESTS BRAZED SINGLE LAP SHEAR SPECIMENS

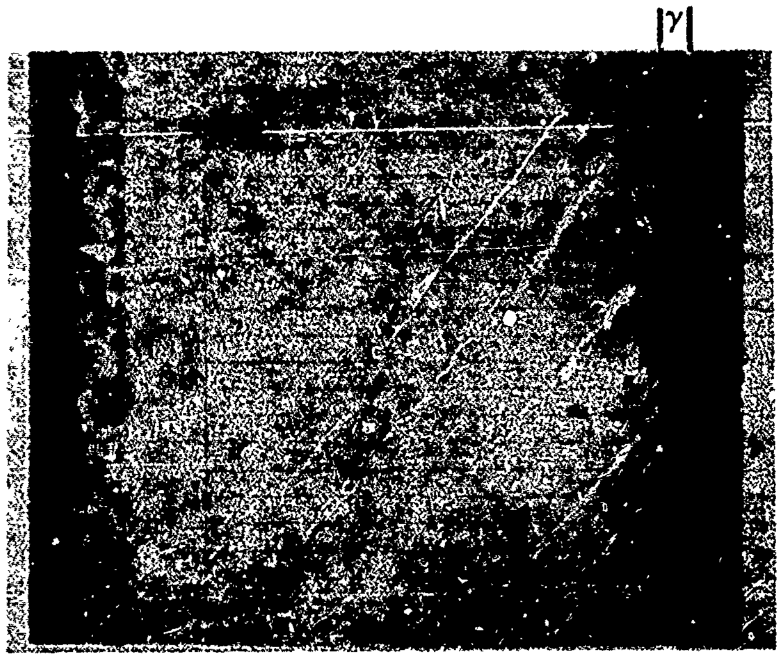


Figure 2-110 MICROSECTION OF BRAZE LINE OF STRESS CORROSION SPECIMEN 11-28 REMOVED FROM MR&D PANEL NO. 28, 750X

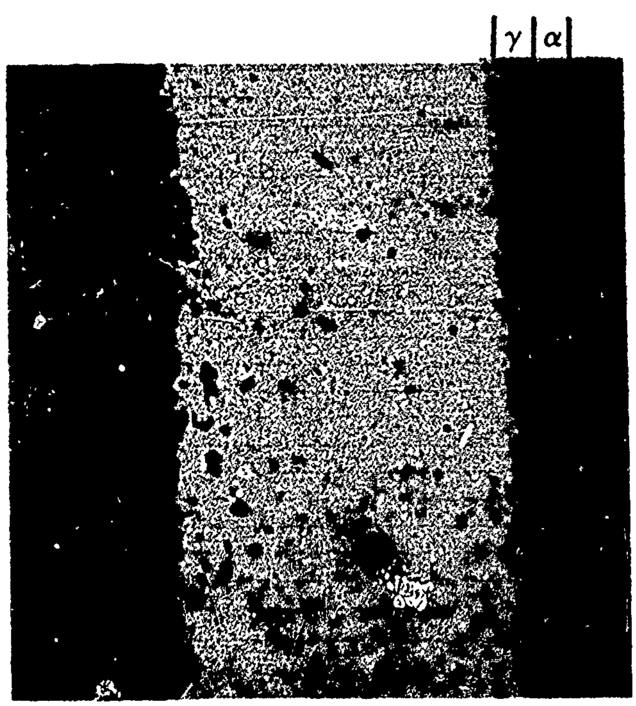


Figure 2-111 MICROSECTION OF BRAZE LINE REMOVED FROM MR&D PANEL NO. 25A, 750X

Figure 2-112 MICROSECTION OF BRAZE LINE REMOVED FROM 603FTB035 #1 PANEL, 750X

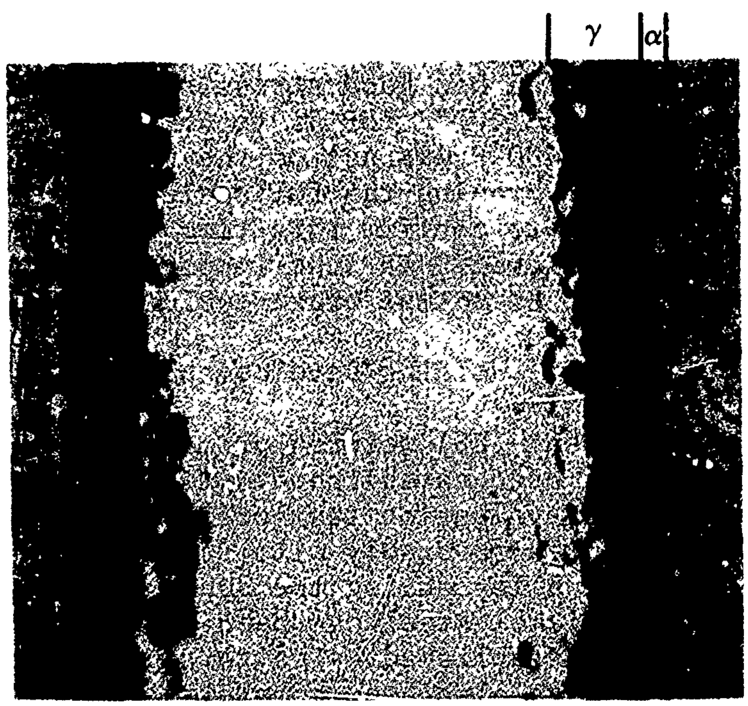


Figure 2-113 MICROSECTION OF BRAZE LINE REMOVED FROM 603FTB035 #2 PANEL, 750X

#### 2.4.4.4 Brazing Thermal Cycle

The braze thermal cycle required to consistently provide braze joints with excellent shear strength and stress corrosion delamination is shown in Figure 2-114. The boundaries in Figure 2-114 define acceptable heat rate, braze temperature, hold time and cooling rate. The heating rate up to 1400°F and the cooling rate below 1400°F are assumed to have little effect on the resulting braze joint.

To heat a large heavy retort package, preheating the furnace to the braze temperature is recommended to achieve a sufficient heating rate in the range of 1400°F to 1580°F. The time-temperature (T-T) boundaries shown in Figure 2-114 were established using the T-T curves from the brazed assemblies and the SCC test data. Faster heating rates than 8°F/minute produce wetting of the silver braze alloy on the titanium (See Figure 2-112) and adequate shear strength, however, the stress corrosion delamination resistance is very low. Heating rates slower than 3.8°F/minute between 1400°F and 1500°F do not produce a braze joint of acceptable quality and shear strength (See Figure 2-112). To ensure complete melting of the brazing alloy, the minimum temperature was set at 1580°F. As explained in Section V, the melting point of the alloy increases as the heating rate decreases. The total time above 1400°F was set at 55 minutes minimum because panels 25A, 14A, 4 and 7 which had good stress corrosion delamination resistance were above 1400°F for 55 to 65 minutes. The 90 minute maximum time above 1400°F was set on the basis of the anticipated cycle achievable for brazing the fullscale lower plate but no tests were conducted to confirm this time interval. The T-T braze curve for 603FTB035#2 is superimposed on Figure 2-114 to show the relation of an actual braze cycle to establish boundaries.

### 2.4.5 Welding Development

The electron beam (EB) welding process for beta annealed 6Al-4V titanium has been established. Test assemblies have been welded and the evaluation test program has been completed. The test data compares favorably with data generated by Boeing Company on the same alloy during the Supersonic Transport Program. GTA welding of 10 Nickel steel has been accomplished and a production process established. The test program for this process on 10 Nickel steel has also been completed. The data for both of EB welded titanium and the GTA weld 10 Nickel steel is being included in the Materials Property Data Report and static design

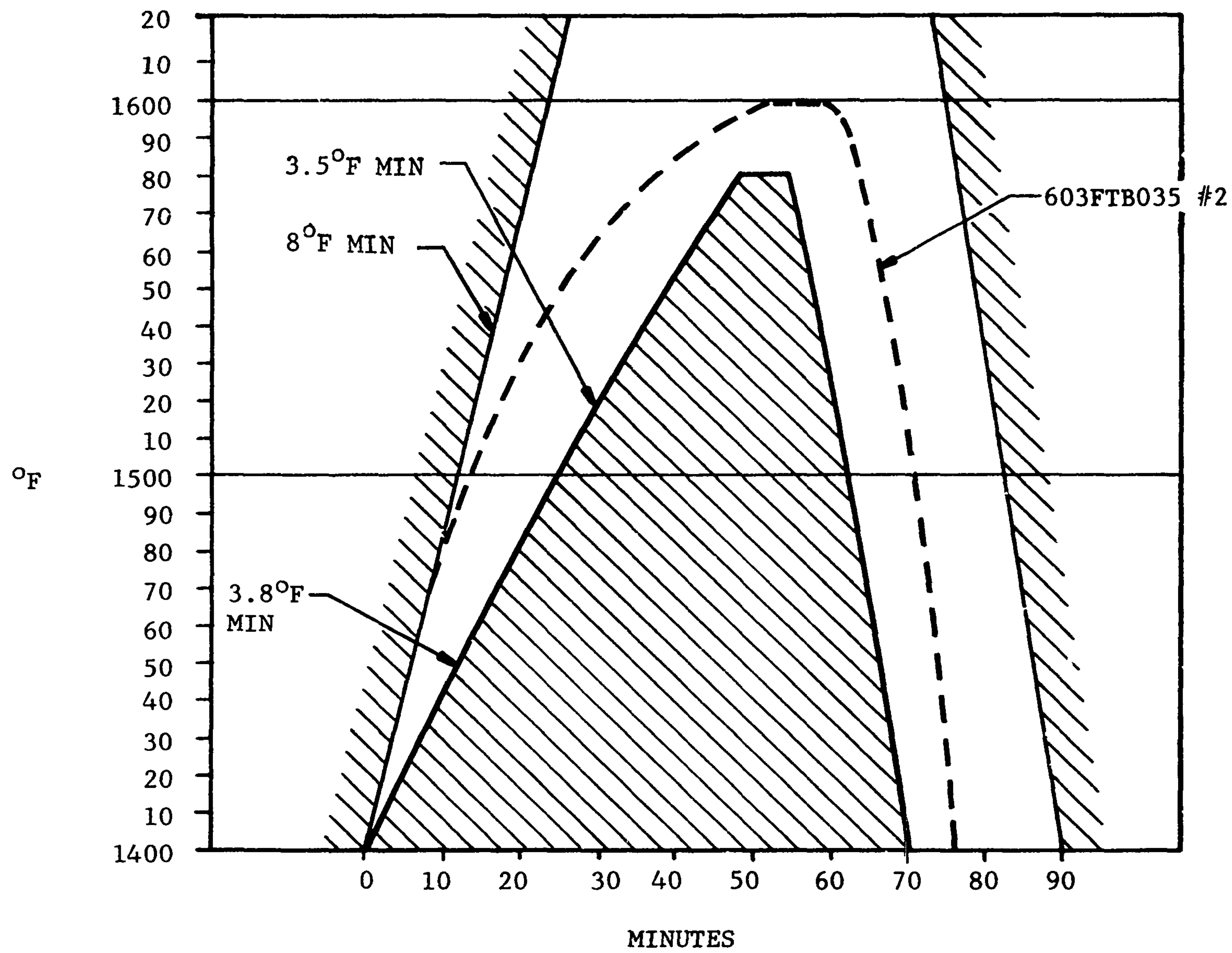


Figure 2-114 AMAVS BRAZING CYCLE TIME-TEMPERATURE BOUNDARIES

allowables and fracture mechanics properties based on this data is shown in Table II-33. The fatigue and crack growth data is included in subsection 2.3 of this report.

Election beam welding of 10 Nickel steel is also desirable for producing joints in thick sections. Welding of 1/2" and 1" thick section has not presented a problem and weld parameters are tentatively established. EB welding of 1.6-inch thick material using present procedures, however, has presented a cracking problem. The cracks are found in the center of the depth of the weld joint. A transverse cross-section of the weld joint shows the width of the center of the joint to be greater than the top or bottom. The heat transfer coefficient for 10 Nickel steel is different than that for D6ac steel which was used for establishing the parameters used to date. The high cobalt content of the 10 Nickel steel changes the heat transfer coefficient and therefore the parameters for heavy sections must be modified. Additional processing parameter studies are required.

### 2.4.6 Adhesive Bonding Development

Confirmation testing of aluminum adherends using the PL 717B adhesive and PL 718 corrosion inhibiting primer has been completed. Lapshear, peel, and flatwise tension tests were conducted. Data indicated no particular difference in strengths when using primer, and peel data was not sensitive to primer thickness. The peel strength was of interest because some corrosion inhibiting systems reduce peel strength. As noted, this is not the case with PL 717B adhesive and PL 718 primer. No processing problems are anticipated with the system during component fabrication. The test data will be included in the Materials Property Data Report.

### 2.4.7 Materials and Processes Specifications

A number of specifications are required to cover new materials and processes and speciality items required for the AMAVS program. A list of these which have been written for this program is shown in Table II-34. These documents will be released progressively as the drawings requiring their use are released, however, all but four have been completed.

Table II-33 DESIGN ALLOWABLES FOR WELD JOINTS

| | Beta Annealed 6Al-4V Ti | 10 Nickel Steel |
|---|---|---|
| Weld Joint Efficiency | 85% | 85% |
| $K_{IC}$ (KSI $\sqrt{\text{inch}}$) Typ. | 72 | N.A. |
| $K_{Iscc}$ (KSI $\sqrt{\text{inch}}$) Typ. | 60 | N.T.P. |

N.A. = Not Available

N.T.P. = No Test Planned

6Al-4V Ti EB Welded

10 Nickel Steel GTA Welded

TABLE II-34
AMAVS SPECIFICATIONS

| Number | Title |
|---|---|
| X7223990 | Exterior Finish |
| X7224194 | 7050 Aluminum Alloy Special Billet Procurement Specification |
| X7224195 | 7050 Aluminum Alloy Billet Special Process Treatment |
| X7224196 | Sealant Application |
| X7224197 | Adhesive Bonded Panel Detail Preparation |
| X7224198 | Identification of Parts |
| X7224199 | Material Traceability Procedures |
| FMS-1108 | Aluminum Alloy, 7050 Sheet and Plate |
| FMS-1109A | Titanium Alloy, 6Al-4V, Beta Annealed |
| FMS-1111 | Steel Alloy, 10Ni-2Cr-1Mo-8CO (10 Nickel) Bar, Forged Billet and Plate |
| FMS-1112 | Wire, Welding - Type 10 Nickel |
| FMS-1113 | Titanium Alloy, 3Al-8V-6Cr-4Mo-2Zr (Beta C) |
| FMS-1114 | Brazing Alloy, Silver-Aluminum-Manganese, Strip |
| FMS-1115 | Welding Wire, 6Al-4V Titanium Alloy, E.L.I. |
| FMS-1116 | Adhesive, 250°F Cure, 180° Service |
| FPS-1074 | Welding, Electron Beam, General Specification |
| FPS-1092 | Adhesive Bonding Process |
| FPS-1093 | Al-Mn Plating Process |
| FPS-1094 | Furnace Brazing Process |
| FPS-1095 | GTA Welding Process |
| FPS-1096 | Heat Treatment and Processing Requirements, 10 Nickel Steel |
| FPS-1097 | Inspection Processes and Acceptance Standards for Welded Joints |

### 2.4.8 Corrosion Prevention System

The corrosion prevention requirements for the AMAVS program are described in detail in FZM-6183, "Corrosion Prevention Requirements, AMAVS Program, Contract F33615-73-C-3001", dated 23 August 1973. The finishing procedures contained in FZM-6183 comply with the requirements of MIL-E-7179D and MIL-S-5002C and are compatible with those required by Rockwell International for the B-1.

A pilot scale aluminum-manganese alloy plating facility is in operation and has been used to plate approximately 400 high strength H-11 tapered shank fasteners for the AMAVS component test program. The aluminum manganese alloy plating will be used in lieu of cadmium on high strength H-11 fasteners installed in titanium alloy structures.

## 2.5 WEIGHTS

Weight estimates are shown for the FSIL and NBB configurations in Tables II-35 and II-36 by structural elements. The total weight of 12054.0 pounds for the FSIL is 12.4% less than the baseline. The total weight of 12508.4 pounds for the NBB is 9.1% less than the baseline. These estimated weights are also shown by material breakdown in Figures 2-115 and 2-116.

These reported weights include allowances to provide an aircraft compatible installation. Updated loads, conditions, and interfaces are included in this compatibility.

The impact of individual items on the FSIL configuration weight is shown below.

| | Pounds |
|---|---|
| Phase Ib - AFFDL TR-73-40 p. 2-434 (FSRL) | 11168 |
| 10% Gross Weight Increase | 500* |
| Update Loads | 284* |
| Fairing Support Ribs | 76* |
| Non-optimum allowance | 224 |
| Change to integral lug | -52 |
| Phase II Expected Weight for FSIL | 12200 |
| Current Status for FSIL (Fig. 1) | 12054 |
| *Remove task change from current status for comparison with Phase Ib target | -860 |
| Current status for comparison with Phase Ib target of 11168. | 11194 |

The current status of the NBB configuration is only 100 pounds above the Phase Ib estimate after incorporating the updated baseline data. However, significant configuration changes were incorporated simultaneously with the baseline update.

Table II-35



FAIL SAFE INTEGRAL LUG(FSIL)-ADV METALLIC WING CARRY THRU STRUCT
DESIGN GROUP 04 TOTAL

WEIGHT SUMMARY

| | 119 OUTBOARD | 84 -119 INTERMDTE | 0 - 84 CENTER | TOTAL STR |
|---|---|---|---|---|
| STRUCTURAL BOX | 1697.9 | 2494.0 | 3779.6 | 8171.5 |
| LOWER PLATE | 930.8 | 887.7 | 1179.2 | 2997.7 |
| COVER | 0.0 | 887.7 | 1179.2 | 2066.9 |
| LUGS | 930.8 | 0.0 | 0.0 | 930.8 |
| UPPER PLATE | 493.6 | 711.6 | 728.8 | 1933.9 |
| COVER | 0.0 | 711.6 | 728.8 | 1440.3 |
| LUGS | 493.6 | 0.0 | 0.0 | 493.6 |
| BULKHEADS | 39.4 | 6[illegible] | 1309.9 | 1953.9 |
| 932 BULKHEAD | 0.0 | 277.1 | 417.6 | 694.8 |
| 947 BULKHEAD | 0.0 | 28.0 | 269.9 | 297.9 |
| 962 BULKHEAD | 0.0 | 0.0 | 0.0 | 0.0 |
| 977 BULKHEAD | 0.0 | 38.1 | 79.3 | 117.3 |
| 992 BULKHEAD | 39.4 | 261.4 | 543.2 | 844.0 |
| RIBS | 309.8 | 240.1 | 301.2 | 931.1 |
| 0 BUTTLINE | 0.0 | 0.0 | 148.9 | 140.9 |
| 39 BUTTLINE | 0.0 | 0.0 | 232.3 | 232.3 |
| 84 BUTTLINE | 0.0 | 240.1 | 0.0 | 240.1 |
| 120 BUTTLINE | 309.8 | 0.0 | 0.0 | 309.8 |
| MISCELLANEOUS | 124.2 | 50.1 | 180.5 | 354.8 |
| MISCELLANEOUS | 124.2 | 51.1 | 180.5 | 354.8 |
| FITTINGS | 1967.4 | 505.9 | 978.3 | 3451.5 |
| XF72 TRUNNION | 0.0 | 0.0 | 169.9 | 169.9 |
| XF95 TRUNNION | 0.0 | 120.1 | 0.0 | 120.1 |
| 992 SIDE BRACE | 0.0 | 0.0 | 242.4 | 242.4 |
| MLG DRAG BRACE | 0.0 | 0.0 | 199.6 | 199.6 |
| WING SWEEP ACT | 113.4 | 386.0 | 0.0 | 499.4 |
| PIN/SHEAR/NAC | 1440.0 | 0.0 | 0.0 | 1440.0 |
| XF? LONGERON WF | 0.0 | 0.0 | 41.4 | 41.4 |
| LONGERON LOWER | 313.2 | 0.0 | 0.0 | 313.2 |
| LONGERON UPPER | 24.4 | -.3 | 0.0 | 24.1 |
| LONGERON 25 DEG | 0.0 | 0.0 | 140.0 | 140.0 |
| LONGERON DORSAL | 0.0 | 0.0 | 185.0 | 185.0 |
| LUG RIB | 76.4 | 0.0 | 0.0 | 76.4 |
| SUBTOTAL | 3865.3 | 2999.3 | 4757.9 | 11623.0 |
| MISCELLANEOUS | 2.5 | 15.3 | 413.2 | 431.0 |
| SUBTOTAL | 2.5 | 15.3 | 413.2 | 431.0 |
| UPPER FAIRING | 0.0 | 3.6 | 110.4 | 114.0 |
| LOWER FAIRING | 0.0 | 3.7 | 166.4 | 170.0 |
| EXTERIOR FINISH | 0.0 | 0.0 | 4.0 | 4.0 |
| FILLETS | 0.0 | 0.0 | 15.0 | 15.0 |
| PROVISIONS-FUEL | 2.5 | 8.0 | 77.5 | 88.0 |
| PROVISIONS-HYD | 0.0 | [illegible] | 2.0 | 2.0 |
| PROVISIONS-AUX G | 0.0 | 0.0 | 19.0 | 18.0 |
| PROVISIONS-ELEC | 0.0 | 0.0 | 20.0 | 23.0 |
| | 0.0 | 0.0 | 0.0 | 0.0 |
| TOTAL | 3867.8 | 3315.1 | 5171.1 | 12054.0 |

Table II-36

GENERAL DYNAMICS — CONVAIR AEROSPACE DIVISION — FORT WORTH OPERATION
6657 PROCEDURE RIK — PROBLEM 075405-06 — 11/12/73 PAGE 0042

NO-BOX BOX (N33)-ADVANCE METALLIC WING CARRY THRU STRUCTURE
DESIGN GROUP 04 TOTAL

WEIGHT SUMMARY

| | 119 OUTBOARD | 64 -119 INTERMDTE | 0 - 64 CENTER | TOTAL STR |
|---|---|---|---|---|
| STRUCTURAL BOX | 2423.2 | 3137.9 | 3346.1 | 8907.2 |
| LOWER PLATE | 1181.0 | 928.3 | 820.1 | 2929.4 |
| COVER | 0.0 | 928.3 | 820.1 | 1748.4 |
| LUGS | 1181.0 | 0.0 | 0.0 | 1181.0 |
| UPPER PLATE | 586.8 | 1113.2 | 431.7 | 2131.7 |
| COVER | 0.0 | 1113.2 | 431.7 | 1544.9 |
| LUGS | 586.8 | 0.0 | 0.0 | 586.8 |
| BULKHEADS | 0.0 | 893.3 | 1606.3 | 2499.7 |
| 932 BULKHEAD | 0.0 | 528.6 | 597.7 | 1126.3 |
| 947 BULKHEAD | 0.0 | 0.0 | 182.1 | 182.1 |
| 962 BULKHEAD | 0.0 | 0.0 | 0.0 | 0.0 |
| 977 BULKHEAD | 0.0 | 0.0 | 0.0 | 0.0 |
| 992 BULKHEAD | 0.0 | 364.7 | 826.5 | 1191.3 |
| RIBS | 493.5 | 171.5 | 347.1 | 1012.2 |
| 0 BUTTLINE | 0.0 | 0.0 | 149.2 | 149.2 |
| 39 BUTTLINE | 0.0 | 0.0 | 197.9 | 197.9 |
| 84 BUTTLINE | 0.0 | 171.5 | 0.0 | 171.5 |
| 120 BUTTLINE | 493.5 | 0.0 | 0.0 | 493.5 |
| MISCELLANEOUS | 161.8 | 31.6 | 140.9 | 334.3 |
| MISCELLANEOUS | 161.8 | 31.6 | 140.9 | 334.3 |
| FITTINGS | 1701.5 | 511.0 | 957.7 | 3170.2 |
| XF72 TRUNNION | 0.0 | 0.0 | 169.9 | 169.9 |
| XF95 TRUNNION | 0.0 | 120.1 | 0.0 | 120.1 |
| 992 SIDE BRACE | 0.0 | 0.0 | 225.3 | 225.3 |
| MLG DRAG BRACE | 0.0 | 0.0 | 198.2 | 198.2 |
| WING SWEEP ACT | 105.6 | 390.9 | 0.0 | 496.5 |
| PIN/SHEAR/NAC | 1440.0 | 0.0 | 0.0 | 1440.0 |
| XF0 LONGERON WF | 0.0 | 0.0 | 39.4 | 39.4 |
| LONGERON LOWER | 55.1 | 0.0 | 0.0 | 55.1 |
| LONGERON UPPER | 24.4 | 0.0 | 0.0 | 24.4 |
| LONGERON 25 DEG | 0.0 | 0.0 | 140.0 | 140.0 |
| LONGERON DORSAL | 0.0 | 0.0 | 185.0 | 185.0 |
| LUG RIB | 76.4 | 0.0 | 0.0 | 76.4 |
| SUBTOTAL | 4124.7 | 3648.9 | 4303.8 | 12077.4 |
| MISCELLANEOUS | 2.5 | 118.0 | 310.5 | 431.0 |
| SUBTOTAL | 2.5 | 118.0 | 310.5 | 431.0 |
| UPPER FAIRING | 0.0 | 114.0 | 0.0 | 114.0 |
| LOWER FAIRING | 0.0 | 0.0 | 170.0 | 170.0 |
| EXTERIOR FINISH | 0.0 | 0.0 | 4.0 | 4.0 |
| FILLETS | 0.0 | 0.0 | 15.0 | 15.0 |
| PROVISIONS-FUEL | 2.5 | 4.0 | 81.5 | 88.0 |
| PROVISIONS-HYD | 0.0 | 0.0 | 2.0 | 2.0 |
| PROVISIONS-AUX G | 0.0 | 0.0 | 18.0 | 18.0 |
| PROVISIONS-ELEC | 0.0 | 0.0 | 20.0 | 20.0 |
| | 0.0 | 0.0 | 0.0 | 0.0 |
| TOTAL | 4127.2 | 3766.9 | 4614.3 | 12508.4 |

FAIL SAFE INTEGRAL LUG(FSIL)-ADV METALLIC WING CARRY THRU STRUCT
DESIGN GROUP 04 TOTAL

MATERIAL BREAKDOWN

| MATERIAL | FORM | WEIGHT | PERCENT |
|---|---|---|---|
| 2024 ALUMINUM | | ( 445.4) | ( 3.69) |
| | SHEET | 171.4 | 1.41 |
| | PLATE | 275.0 | 2.28 |
| 5052 ALUMINUM | | ( 81.4) | ( .68) |
| | CORE | 81.4 | .68 |
| 7050 ALUMINUM | | ( 1685.2) | ( 13.98) |
| | SHEET | 217.3 | 1.80 |
| | PLATE | 1467.9 | 12.18 |
| OTHER ALUMINUM | | ( 66.5) | ( .55) |
| | PLATE | 63.5 | .53 |
| | FASTENERS | .8 | .01 |
| | SHIM STOCK | 2.2 | .02 |
| 6-4 BA TITANIUM | | ( 6624.3) | ( 54.95) |
| | PLATE | 6624.3 | 54.95 |
| COMPURE TITANIUM | | ( 32.6) | ( .27) |
| | SHEET | 32.6 | .27 |
| OTHERTITANIUM | | ( 21.9) | ( .18) |
| | PLATE | 13.4 | .11 |
| | FASTENERS | 8.5 | .07 |
| 662 TITANIUM | | ( 83.7) | ( .69) |
| | PLATE | 83.7 | .69 |
| 10 NI STEEL | | ( 214.2) | ( 1.78) |
| | PLATE | 214.2 | 1.78 |
| AMS 5629 STEEL | | ( 10.7) | ( .09) |
| | PLATE | 10.7 | .09 |
| OTHER STEEL | | ( 561.8) | ( 4.66) |
| | FASTENERS | 561.8 | 4.66 |
| ADHESIVES | | ( 93.5) | ( .78) |
| | FMS-1116 TYPE I | 42.5 | .35 |
| | FMS-1116 TYPEIII | 11.4 | .09 |
| | FMS-1116 TYPE II | .0 | .00 |
| | BRAZING ALLOY | 39.6 | .33 |
| RUBBERS | | ( 1.0) | ( .01) |
| | SILICONE | 1.0 | .01 |
| SEALANTS | | ( 28.0) | ( .23) |
| | FMS 1043 GENERAL | 28.0 | .23 |
| PURCHASED PARTS | | ( 2104.3) | ( 17.46) |
| | WING | 2104.3 | 17.46 |
| | TOTAL | (12054.0) | (100.00) |

Figure 2-115 CONVAIR AEROSPACE DIVISION PROBLEM 005485-05

NO-BOX BOX (N3B)-ADVANCE METALLIC WING CARRY THRU STRUCTURE
DESIGN GROUP 64 TOTAL

MATERIAL BREAKDOWN

| MATERIAL | FORM | WEIGHT | PERCENT |
|---|---|---|---|
| 2024 ALUMINUM | | ( 780.0) | ( 6.24) |
| | SHEET | 242.1 | 1.94 |
| | PLATE | 538.5 | 4.31 |
| 5052 ALUMINUM | | ( 136.1) | ( 1.09) |
| | CORE | 136.1 | 1.09 |
| 7050 ALUMINUM | | ( 344.2) | ( 2.75) |
| | SHEET | 14.9 | .12 |
| | PLATE | 329.3 | 2.63 |
| OTHER ALUMINUM | | ( 1.2) | ( .01) |
| | FASTENERS | .3 | .00 |
| | SHIM STOCK | .9 | .01 |
| 6-4 BA TITANIUM | | ( 1660.4) | ( 13.27) |
| | SHEET | 127.6 | 1.02 |
| | PLATE | 1532.9 | 12.25 |
| COMPURE TITANIUM | | ( 142.5) | ( 1.14) |
| | SHEET | 21.6 | .17 |
| | PLATE | 120.9 | .97 |
| OTHERTITANIUM | | ( 2.1) | ( .02) |
| | FASTENERS | 2.1 | .02 |
| 10 NI STEEL | | ( 6773.3) | ( 54.15) |
| | SHEET | 300.4 | 2.40 |
| | PLATE | 6049.9 | 48.37 |
| | FORGING | 423.0 | 3.38 |
| AMS 5629 STEEL | | ( 10.7) | ( .09) |
| | PLATE | 10.7 | .09 |
| OTHER STEEL | | ( 448.0) | ( 3.58) |
| | FASTENERS | 448.0 | 3.58 |
| PAINT + FINISHES | | ( 1.2) | ( .01) |
| | EPOXY PRIMER | 1.2 | .01 |
| ADHESIVES | | ( 53.0) | ( .42) |
| | FMS-1116 TYPE I | 44.6 | .36 |
| | FMS-1116 TYPEIII | 8.3 | .07 |
| | FMS-1116 TYPE II | .0 | .00 |
| RUBBERS | | ( 1.0) | ( .01) |
| | SILICONE | 1.0 | .01 |
| SEALANTS | | ( 20.7) | ( .17) |
| | FMS 1043 GENERAL | 20.7 | .17 |
| PURCHASED PARTS | | ( 2133.4) | ( 17.06) |
| | WING | 2133.4 | 17.06 |
| | TOTAL | (12508.4) | (100.00) |

Figure 2-116 CONVAIR AEROSPACE DIVISION PROBLEM 005485-06

## 2.6 CONFIGURATION RATINGS

The merit rating equation and the grading system developed in Section II, Volume II, of AFFDL-TR-73-40 were applied to the two WCTS configurations. Grades for each major category, with the exception of Technology Advancement, are shown in Tables II-37 through II-40. Technology Advancement was rated equal for the configurations and a grade of 6.0 was assigned for this category.

Table II-37 EFFICIENCY GRADE

| CONFIGURATION | % WEIGHT REDUCTION | $N_{WT}$ | % COST REDUCTION | $N_{COST}$ | $N_{EFF.}$ |
|---|---|---|---|---|---|
| FSIL | 12.42 | 5.97 | 33.15 | 7.63 | 6.97 |
| NBB | 9.11 | 4.64 | 35.0 | 8.00 | 6.66 |

Table II-38 INTEGRITY AND RELIABILITY GRADE

| SUB-CATEGORY GRADES | CONFIGURATION | |
|---|---|---|
| | FSIL | NBB |
| STATIC STRENGTH RESERVE | 0 | 0 |
| $N_{STATIC}$ | 1.0 | 1.0 |
| % FASTENER REDUCTION | 69.7 | 70.8 |
| $N_{FATIGUE}$ | 7.97 | 8.08 |
| DAMAGE TOLERANCE SCORES | | |
| MULTIPLE LOAD PATHS | 1.5 | 0.0 |
| PLANE STRESS FRACTURE | 2.0 | 2.0 |
| PLANE STRESS FRACTURE | 1.5 | 2.0 |
| SAFE CRACK GROWTH | 2.0 | 1.2 |
| LEAK BEFORE BREAK | 1.0 | 0.0 |
| FAIL SAFE | 1.0 | 0.0 |
| $N_{SCG} = N_{DAM.\ TOL.}$ | 8.0 | 5.2 |
| $N_{INTEG}$ | 6.59 | 5.22 |

Table II-39 ILITIES GRADE

| SUB-CATEGORY GRADES | CONFIGURATION | |
|---|---|---|
| | FSIL | NBB |
| INSPECTABILITY | | |
| MATERIAL | .3 | .6 |
| JOINING PROCESSES | .5 | .8 |
| DETAIL PART CONFIG. | .6 | .9 |
| SUB-ASSEMBLY CONFIG. | 1.3 | 1.7 |
| EQUIP. & TECHNIQUES | .8 | .8 |
| ACCESSIBILITY | 1.7 | 1.7 |
| FIELD INSPEC. CAP. | 1.4 | 1.1 |
| $N_{INSPECT}$ | 6.6 | 7.6 |
| MANUFACTURABILITY | | |
| BASIC MFG. | 1.968 | 1.527 |
| SECONDARY MFG. | 2.748 | 2.835 |
| SUB-ASSEMBLY | 1.886 | 1.28 |
| FINAL ASSEMBLY | 1.008 | 1.364 |
| $N_{MFT}$ | 7.61 | 7.01 |
| MAINTAINABILITY | | |
| ACCESSIBILITY | 0.3 | 0.9 |
| FUEL PURGING | 2.2 | 2.5 |
| MECH. JOINTS-COMPLEXITY | 2.2 | 2.5 |
| RESIST. TO GRD. DAMAGE | 0.8 | 0.9 |
| COMPLEXITY OF REPAIR | 1.5 | 2.0 |
| $N_{MAINT}$ | 6.4 | 8.2 |
| REPAIRABILITY | | |
| LUGS | 1.2 | 1.8 |
| LOWER PLATE/RAILS | 2.7 | 1.5 |
| UPPER COVER/RAILS | 1.5 | 1.8 |
| EXTERIOR PANELS | 0.7 | 0.8 |
| INTERNAL STRUCTURE | 0.8 | 0.8 |
| $N_{REPAIR}$ | 6.9 | 6.7 |
| PREDICTABILITY | | |
| PROCESS | 2.5 | 3.5 |
| MATERIAL | 2.8 | 2.6 |
| ANALYSIS | 2.5 | 2.5 |
| $N_{PREDICT}$ | 7.8 | 8.6 |

Table II - 40 CONFIGURATION RATINGS

| | CONFIGURATION | | | |
|---|---|---|---|---|
| | FSIL | | "NO-BOX" BOX | |
| CATEGORY | Detail Item Grades | Category Grade | Detail Item Grades | Category Grade |
| EFFICIENCY | $N_{WT} = 5.97$<br>$N_{COST} = 7.63$ | $N_{EFF.} = 6.97$ | $N_{WT} = 4.64$<br>$N_{COST} = 8.00$ | $N_{EFF.} = 6.66$ |
| TECHNOLOGY ADVANCEMENT | | $N_{TECH\ ADV} = 6.0$ | | $N_{TECH\ ADV} = 6.0$ |
| INTEGRITY AND RELIABILITY | $N_{STATIC} = 1.0$<br>$N_{FATIGUE} = 7.97$<br>$N_{SCG} = 8.0$<br>$N_{DAM.TOL.} = 8.0$ | $N_{INTEG.} = 6.59$ | $N_{STATIC} = 1.0$<br>$N_{FATIGUE} = 8.08$<br>$N_{SCG} = 5.2$<br>$N_{DAM.TOL.} = 5.2$ | $N_{INTEG.} = 5.22$ |
| ILITIES | $N_{INSPECT.} = 6.6$<br>$N_{MFT} = 7.61$<br>$N_{MAINT} = 6.4$<br>$N_{REPAIR} = 6.9$<br>$N_{PREDICT} = 7.8$ | $N_{ILITIES} = 7.03$ | $N_{INSPECT.} = 7.6$<br>$N_{MFT} = 7.01$<br>$N_{MAINT} = 8.2$<br>$N_{REPAIR} = 6.7$<br>$N_{PREDICT} = 8.6$ | $N_{ILITIES} = 7.49$ |
| Merit Rating | M.R. = | 6.57 | M.R. = | 6.11 |

## 2.7 CONFIGURATION SELECTION

Based on the configuration ratings of subsection 2.6, the FSIL configuration was recommended as the configuration to be manufactured in Phase III of the AMAVS Program. A Phase II Design Review, attended by AFFDL, AFML, ASD and contractor personnel, was held to review the two designs and select the configuration to be manufactured. After this review, the NBB was selected for Phase III.

Selection of the NBB configuration was based on the following major points:

1. The two designs were rated equal by AFFDL, AFML, and ASD personnel. Both were considered to be good designs which met the program objectives.

2. There are fewer manufacturing problems anticipated for the NBB configuration. The risk in the development of the brazing process was considered to be high in comparison to the expected pay-off.

3. It was also felt that the stresses induced in the braze line were not sufficiently high to prove the worth of the braze in this application. This concern was the result of the basic design philosophy of using mechanical fasteners at all points of load transfer in the FSIL configuration.

# SECTION 3

# TESTING

## 3.1 MATERIALS TESTING

Materials testing as required to support the detail design and analysis effort was started in Phase Ib and was essentially complete at the end of Phase II. This testing is defined in AFFDL-TR-73-40 and AFFDL-TR-73-77. Significant test results are presented in Section 2.4 of this report. The complete results of this testing are being reported to the Air Force Flight Dynamics Laboratory in General Dynamics Report No. FZM-6148.

## 3.2 COMPONENT TESTING

During Phase II a follow-on component test program was established. This series of tests, called Group II Tests, was established to verify the structural integrity of typical proposed hardware for the two configurations of WCTS, the "No-Box" Box, and the FSIL. A summary of the Group II Component Test Program is shown below.

Group II Tests

| Test | Config. | Dwg. No. | No. of Specs. | Type of Test |
|---|---|---|---|---|
| Crack Growth Test Lower Plate | FSIL | 603FTB033 | 6 | Crack Growth |
| Damage Tolerance Lower Surface | FSIL | 603FTB035 | 1 | Damage Tolerance |
| Upper Surface Compression | FSIL | ɔ3FTB034 | 1 | Static |
| Lower Aft Centerline Splice | "No-Box" | 603FTB052 | 2 | Fatigue |
| Lower Centerline Splice | FSIL | 603FTB053 | 2 | Fatigue-Static |

### 3.2.1 Test Results

3.2.1.1 <u>Crack Growth Test Lower Plate</u> (Dwg. No. 603FTB033)

The braze assembly shown on this drawing was cut up to produce several test specimens (Figure 3-1). The purpose of the test was to provide information for the type of flaw to create on the damage tolerance test (603FTB035) and to prove that a crack in the center plate would not cross the braze lines into the reinforcing bars. Specimen A-1 was edge saw-cut as shown in Figure 3-2. The specimen was constant amplitude cycled at a load which caused stress equal to $F_{tu}$ on the edge of the reinforcing bar. After 14 cycles of this loading a crack had initiated at the edge of the saw cut and progressed to the edge of the bar. At this point, constant amplitude cycling was stopped and spectrum cycling was started. Cycling was continued until one service life had been accomplished. The specimen was then static tested to failure. Failing load was 244,000 pounds. This load exceeds the predicted load, based on nominal specimen geometry and a fully plastic bending stress distribution, by about 40%. The larger than predicted failing load was the result of inelastic deformation of the specimen which caused the net section of the specimen to be more nearly in line with the load points.

Examination of the failed specimen showed that the crack in the center plate had progressed approximately two-thirds of the way under the bar, but the crack had not crossed the braze lines into the reinforcing bars.

Specimens B-1 and B-2 contained semi-circular surface cracks in the center plate. Cracks were created by eloxing and flexure of the center plate prior to brazing the assembly. Both specimens were spectrum fatigue tested identically using a 48.22 cycle per flight spectrum.

Specimen B-1 was tested for one service life, after which fatigue cracks were discovered in the load pin hole. The hole was bored out and the width of the center plate was reduced. Testing was resumed with the applied fatigue stresses increased by a factor of 1.33. The specimen failed through the loading hole after 549 flights of this loading.

Specimen B-2 was also reworked after one service life. Testing was resumed with the applied fatigue stresses increased by a factor of 1.33. Failure occurred in the test section after 1031 flights of this loading. Failure was due to independent fatigue of each of the three layers.

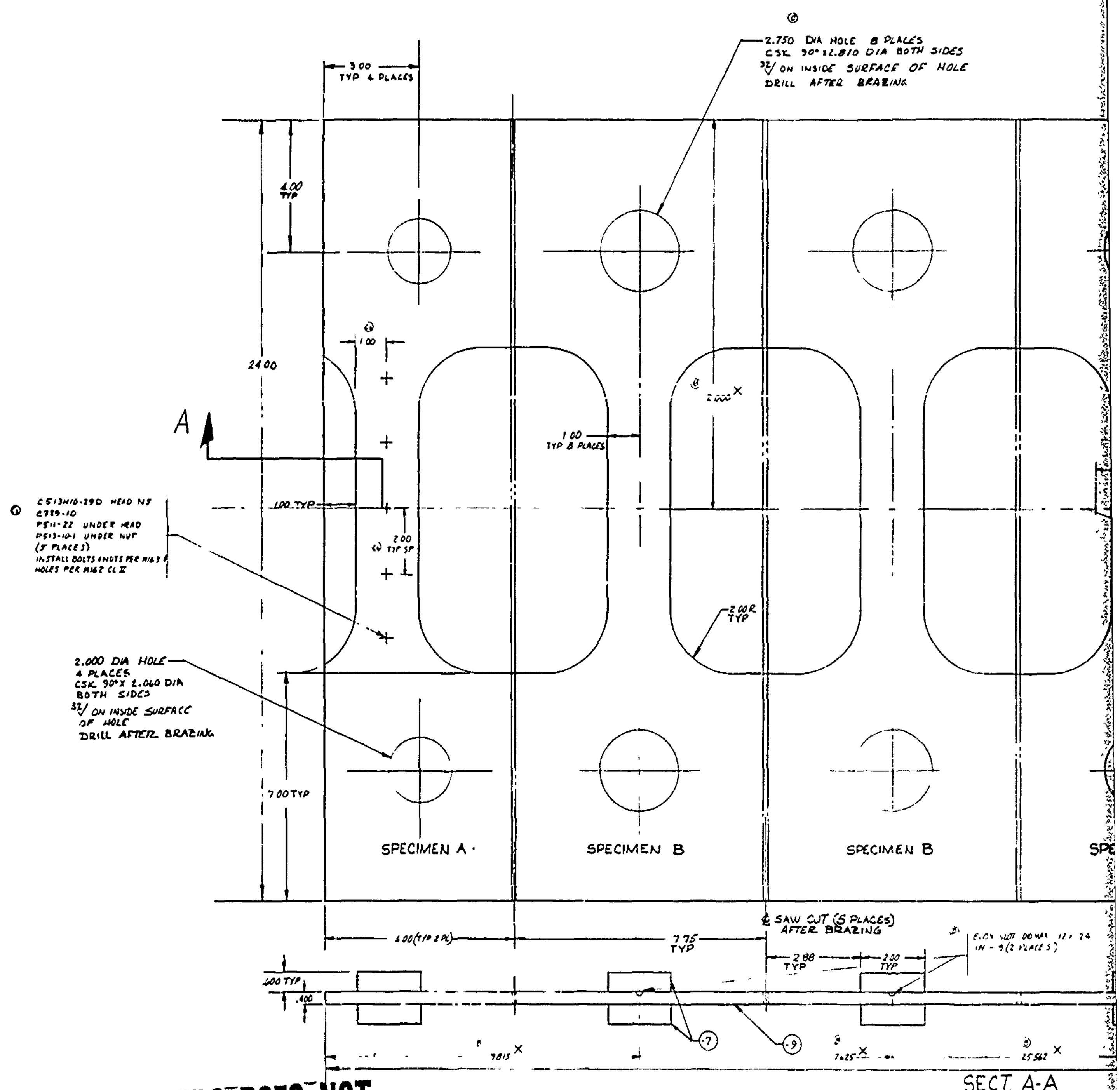




Figure 3-1 TEST SPECIMEN - DAMAGE TOLERANCE,

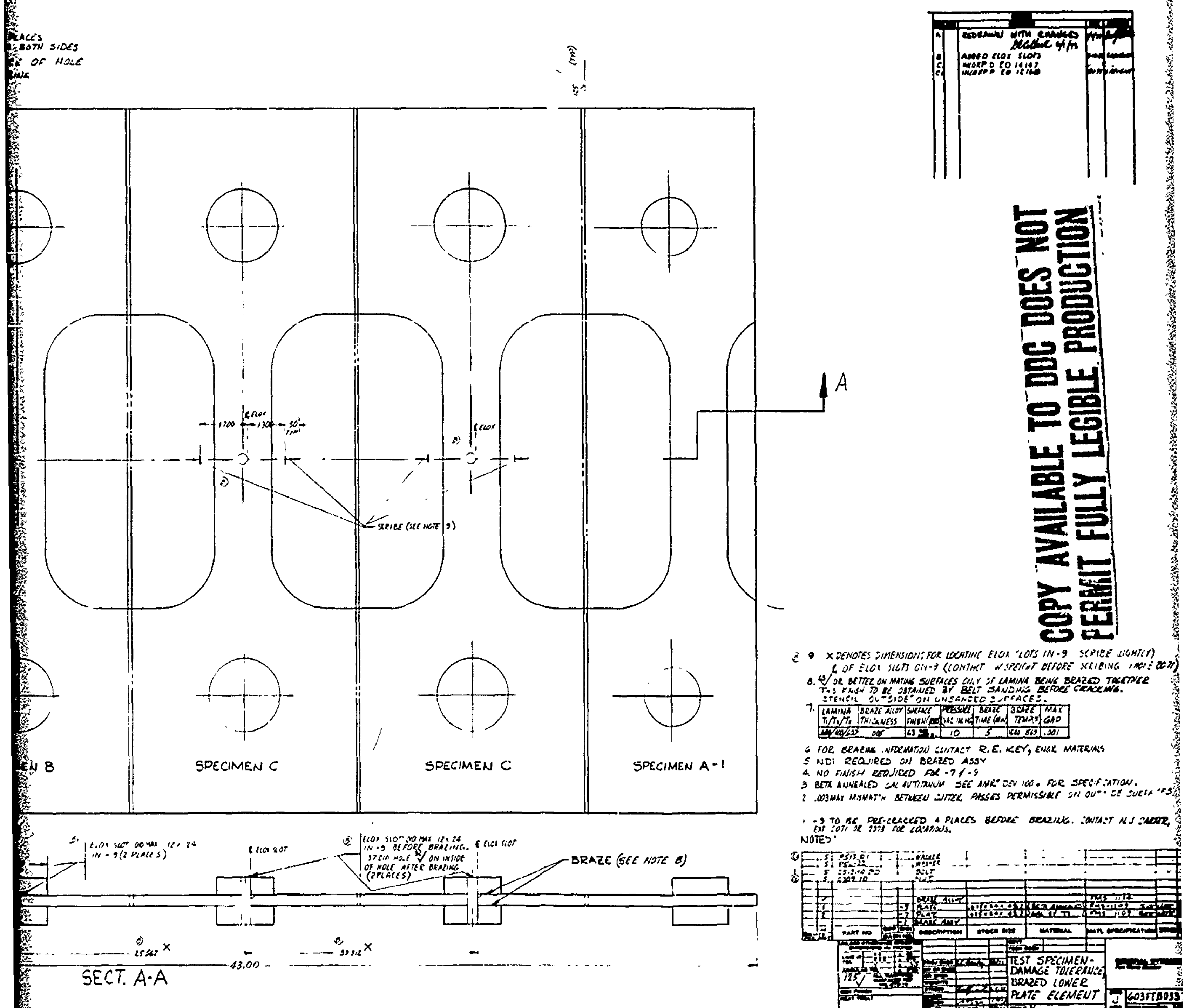




DAMAGE TOLERANCE, BRAZED LOWER PLATE ELEMENT

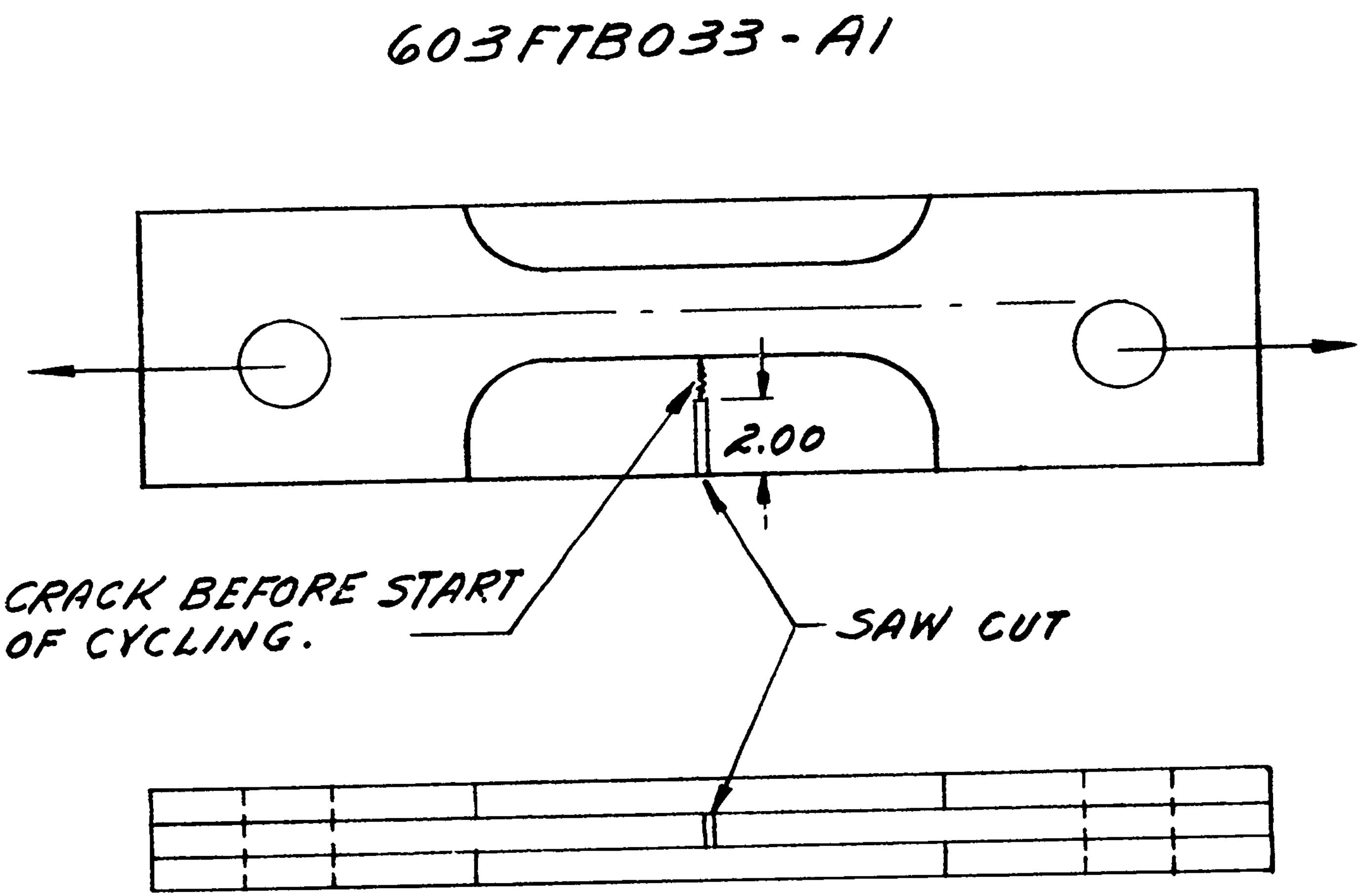


Figure 3-2 EDGE CRACKED CRACK GROWTH TEST

The Type C specimens each contained a corner crack in the center plate in a hole which was drilled through all three thickness. The crack was created by eloxing and flexure of the center plate prior to brazing and drilling the specimen.

The two specimens were tested identically using a 48.22 cycle per flight fatigue spectrum. Specimen C-1 failed through the load pin hole after one service life, plus 1166 flights. Specimen C-2 failed in the test section after one service life, plus 600 flights. Failure was due to independent fatigue of each of the three layers.

3.2.1.2 <u>FSIL - Lower Surface, Damage Tolerance Test</u> (Dwg. No. 603FTB035)

This specimen represented a cross section of the lower surface of the FSIL configuration in the region between $X_f = 84$, and the closure rib. Actual production material thicknesses were used. Because the magnitude of the loads required to test the specimen exceeded the capacity of the General Dynamics testing equipment, the specimen was tested at Southwest Research Institute in San Antonio, Texas. Figure 3-3 shows the specimen installed in the test rig.

The specimen had a 5-inch long elox slot through the web of one of the interior bays. The specimen was cycled 63 times from 0 to 110% of limit load, which resulted in the growth of cracks from the ends of the elox slot to almost the full width of the bay.

The specimen was then cycled to one quarter of a service life, using an accelerated spectrum of 3.22 cycles per flight. This did not result in any further extension of the cracks.

Following the fatigue cycling, the specimen was loaded to limit load. No additional crack growth was observed. Finally, the specimen was loaded to ultimate load, $3 \times 10^6$ pounds. During this loading the cracks extended under the bars.

An X-ray inspection following the test showed that the crack had progressed to about 2/3 of the way under the forward bar and about 1/2 of the way under the aft bar. Ultra-sonic inspection also revealed very local delamination of the braze lines in the region of the crack extensions.

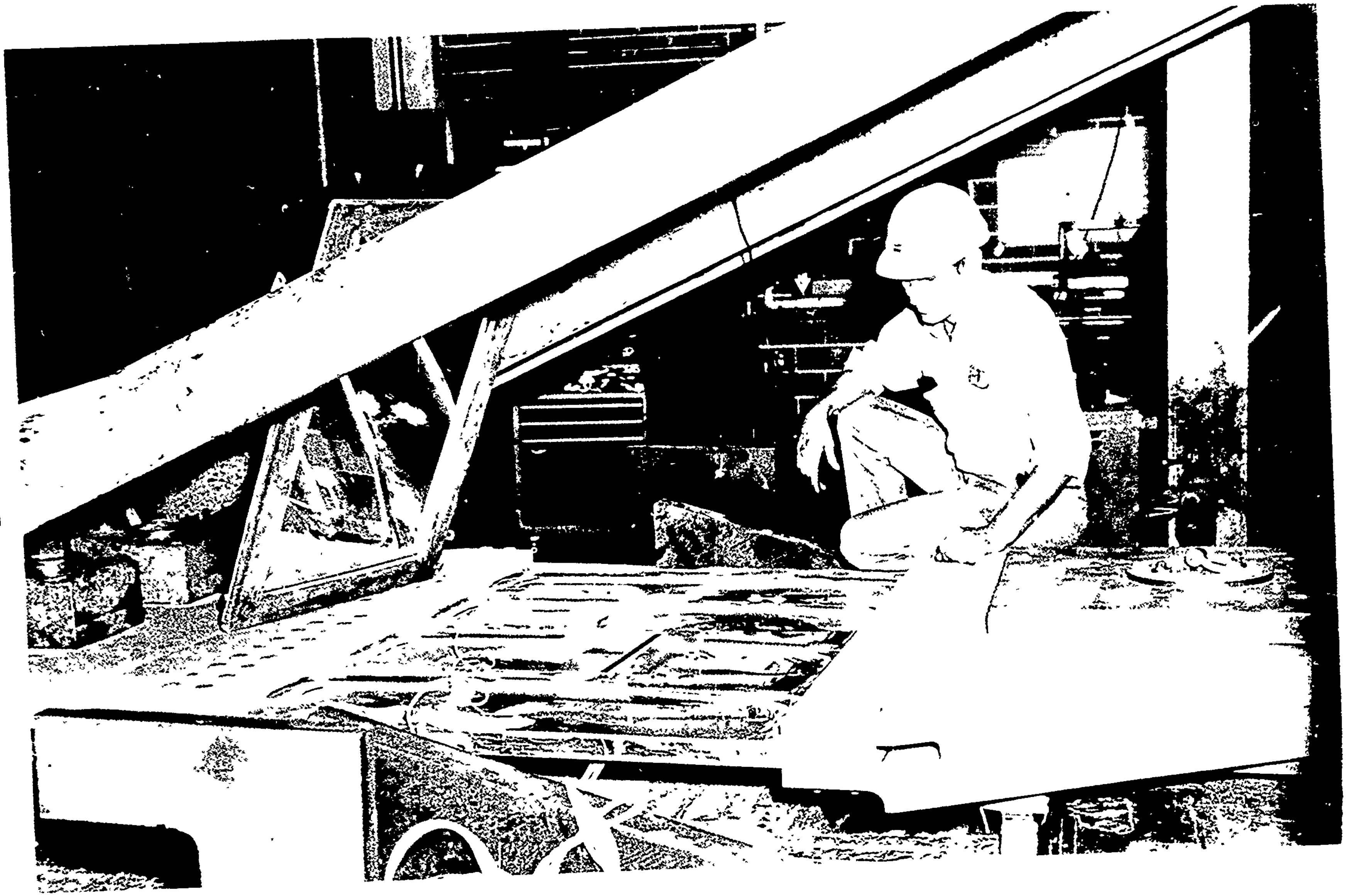

Figure 3-3 603FTB035 TEST SPECIMEN IN TEST FIXTURE

3.2.1.2 Upper Surface Compression Test FSIL (Dwg. No. 603FTB043)

The specimen was designed to represent the area of the upper surface of the FSIL between the closure rib and bulkhead 84, and between the front spar and $Y_f$ = 947. In order to simulate the normal support given to the upper surface by the spars and bulkheads of the WCTS, a fixture was designed that gives this support, but does not absorb any of the applied axial load. This fixture is shown in Dwg. No. 603FTB034. Figure 3-4 shows the specimen installed in the 1,000,000 pound test machine at General Dynamics

It was estimated that 800,000 to 1,000,000 pounds of applied load would be required to satisfy the requirements of the design. The specimen was loaded to the 1,000,000-pound capacity of the machine with no failure, and with no apparent permanent deformation.

3.2.1.3 Lower Aft Rail, Centerline Splice, "No-Box" Box (Dwg. No. 603FTB052)

This specimen design represented the splice at the centerline of the lower aft rail of an earlier configuration of the "No-Box" Box. Both specimens were tested to four service lives using a 48.22 cycle per flight fatigue spectrum. Figure 3-5 shows the specimen installed in the test fixture.

Following completion of the four lives of testing, the loading was changed on specimen No. 2 to an accelerated spectrum consisting of 3.22 cycles per flight. Testing was continued on this specimen until failure occurred at the equivalent of 9.6 lives.

3.2.1.4 Centerline Splice, Fuel Pump Holes, FSIL (Dwg. No. 603FTB053)

This specimen design represented the centerline splice of the lower surface of the FSIL in the second bay forward of the rear spar in the region of the cutouts for the fuel pump holes. Both specimens were tested to six service lives using a 48.22 cycle per flight spectrum. Figure 3-6 shows one of the specimens installed in the test fixture.

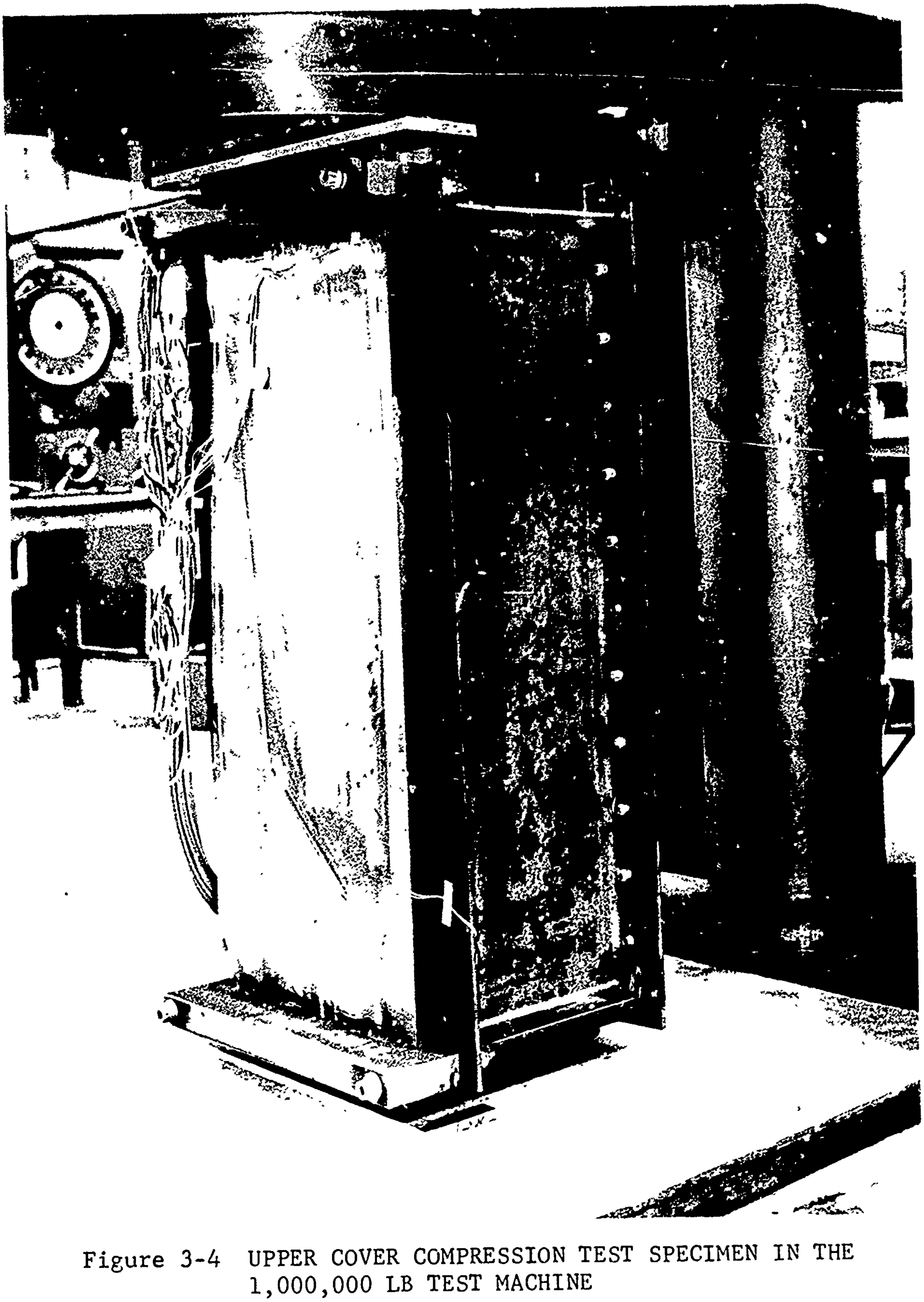

Figure 3-4 UPPER COVER COMPRESSION TEST SPECIMEN IN THE 1,000,000 LB TEST MACHINE

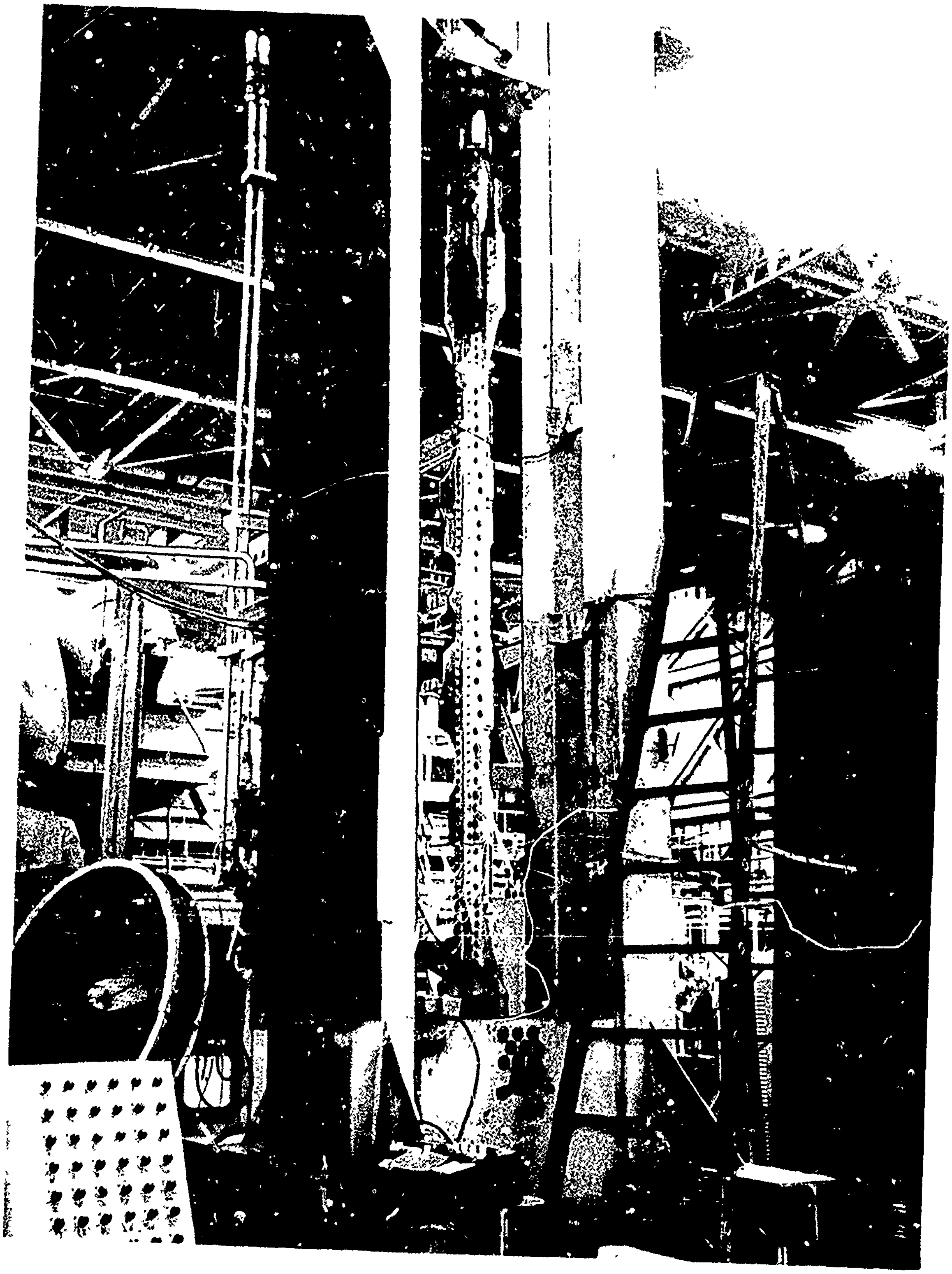

Figure 3-5 TEST SPECIMEN IN TEST FIXTURE (052)

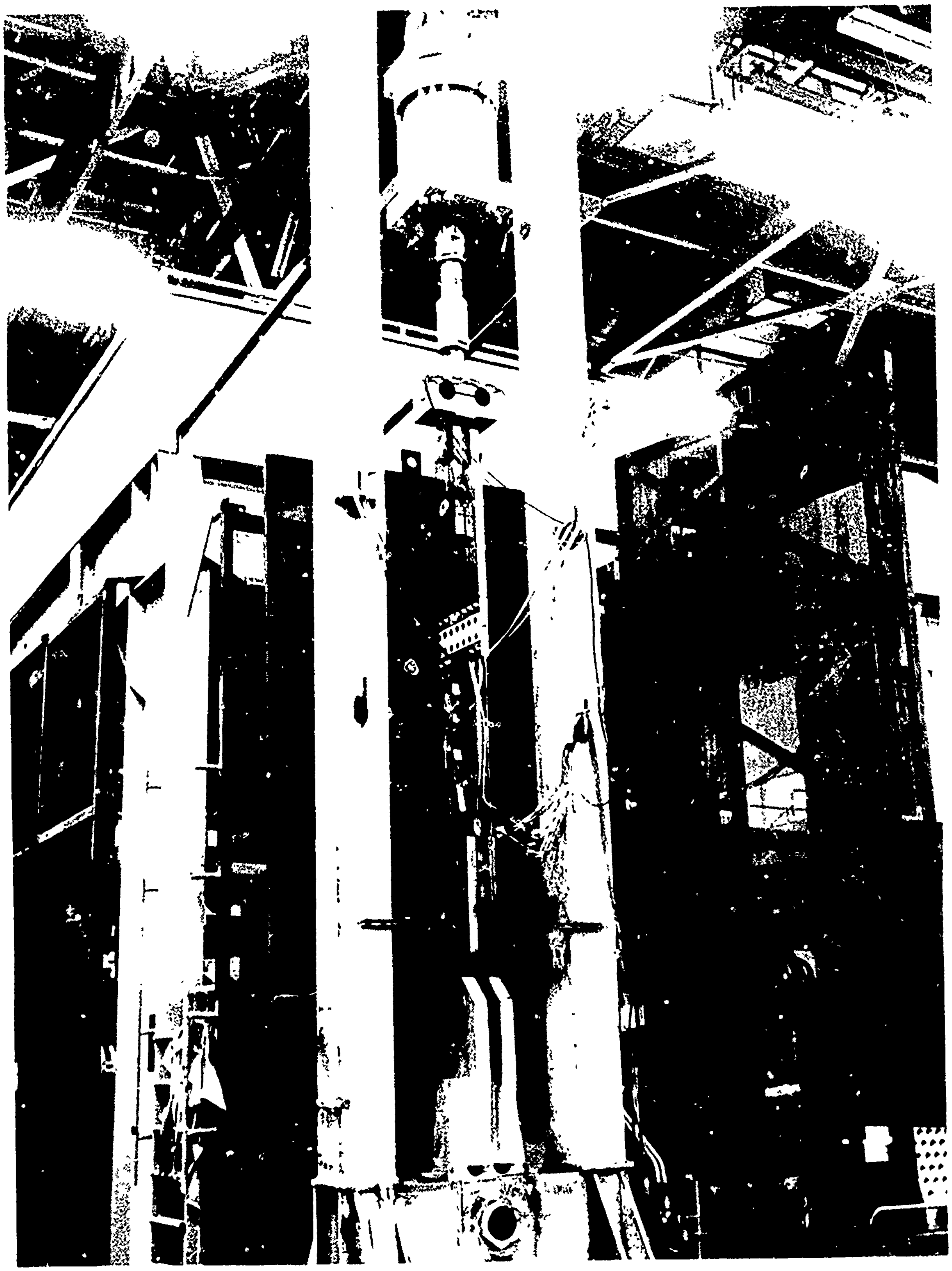

Figure 3-6 FSIL CENTERLINE SPLICE SPECIMEN IN FATIGUE FIXTURE

Specimen No. 2 was then continued in test using an accelerated spectrum of 3.22 cycles per flight for an additional 2.03 service lives at which time a fixture failure stopped the test. The specimen was then installed in the 1,000,000 Lb. test machine for static loading. The required static load capability of the specimen is 750,000 Lbs. The specimen was loaded three times to the 1,000,000 Lb. capability of the test machine. No failure occurred, and no permanent deformation was noted.

## 3.3 FULL SCALE TESTING

Testing is to be accomplished on a full-scale WCTS of the configuration chosen at the end of Phase II. This testing will be accomplished at AFFDL in the test setup shown in Figure 3-7. General Dynamics will provide test planning, test fixtures, and the test article, and AFFDL will provide test equipment and perform the testing. A definition of the planned testing is presented in AFFDL-TR-73-40 along with a description of the physical setup to be used for this testing.

### 3.3.1 Progress During Phase II

A plan was developed for manufacturing the full-scale test fixture, shipping it to AFFDL, and reassembling it. This plan involves three shipments of hardware as shown in Figures 3-8, 3-9, and 3-10. The initial shipment will allow early installation and checkout of loading systems and of some data systems elements. The second shipment will allow full preparation for final mating, while the test article is still in manufacture. The final shipment will complete the setup and will facilitate final checkout and testing. Design of the test fixture is nearing completion, as is the procurement of fixture materials and hardware. Manufacture of the test fixture is progressing satisfactorily. Status at the end of the reporting period is shown in Table III-1 for the main elements of the test fixture.

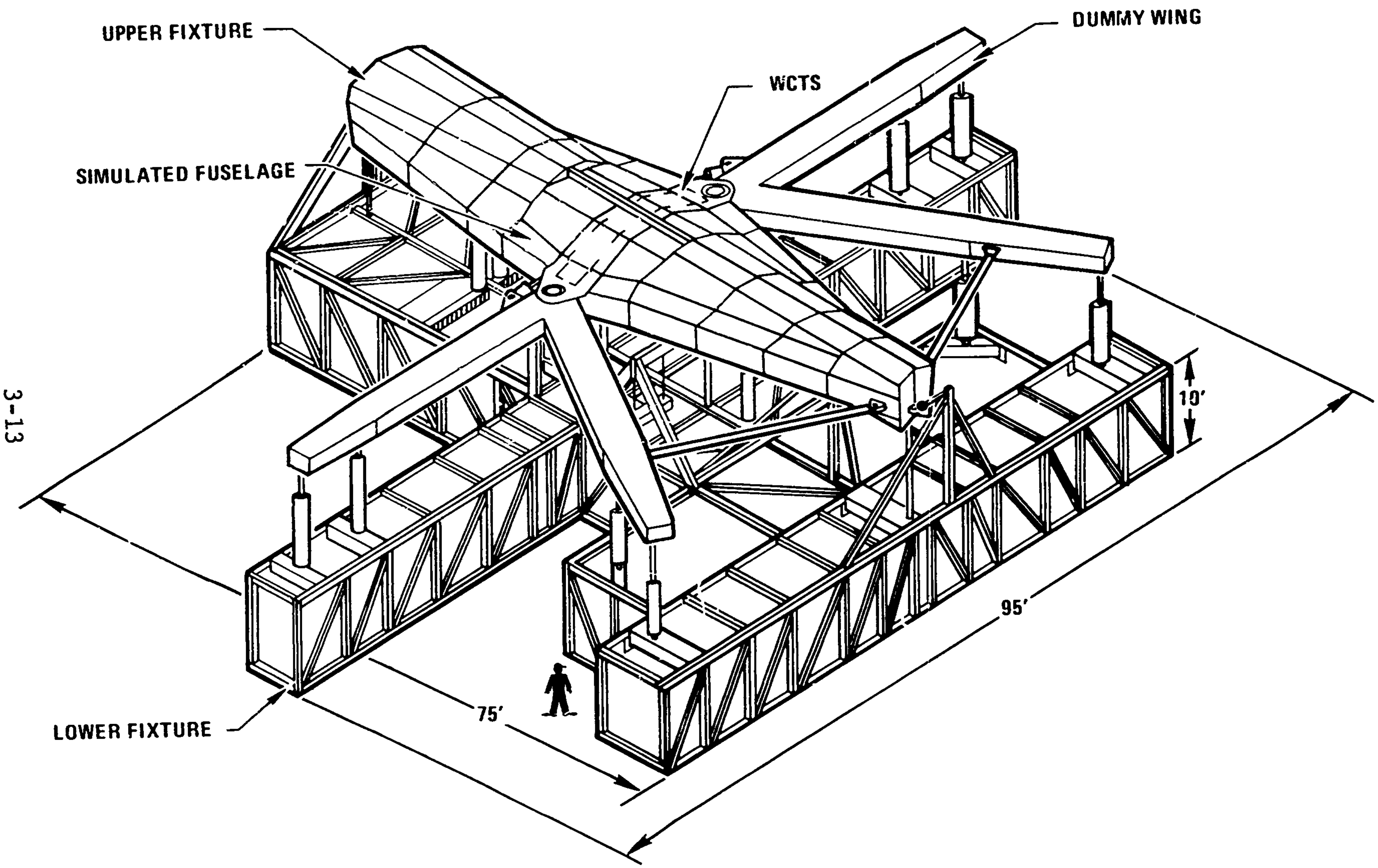


Figure 3-7 AMAVS FULL SCALE TEST

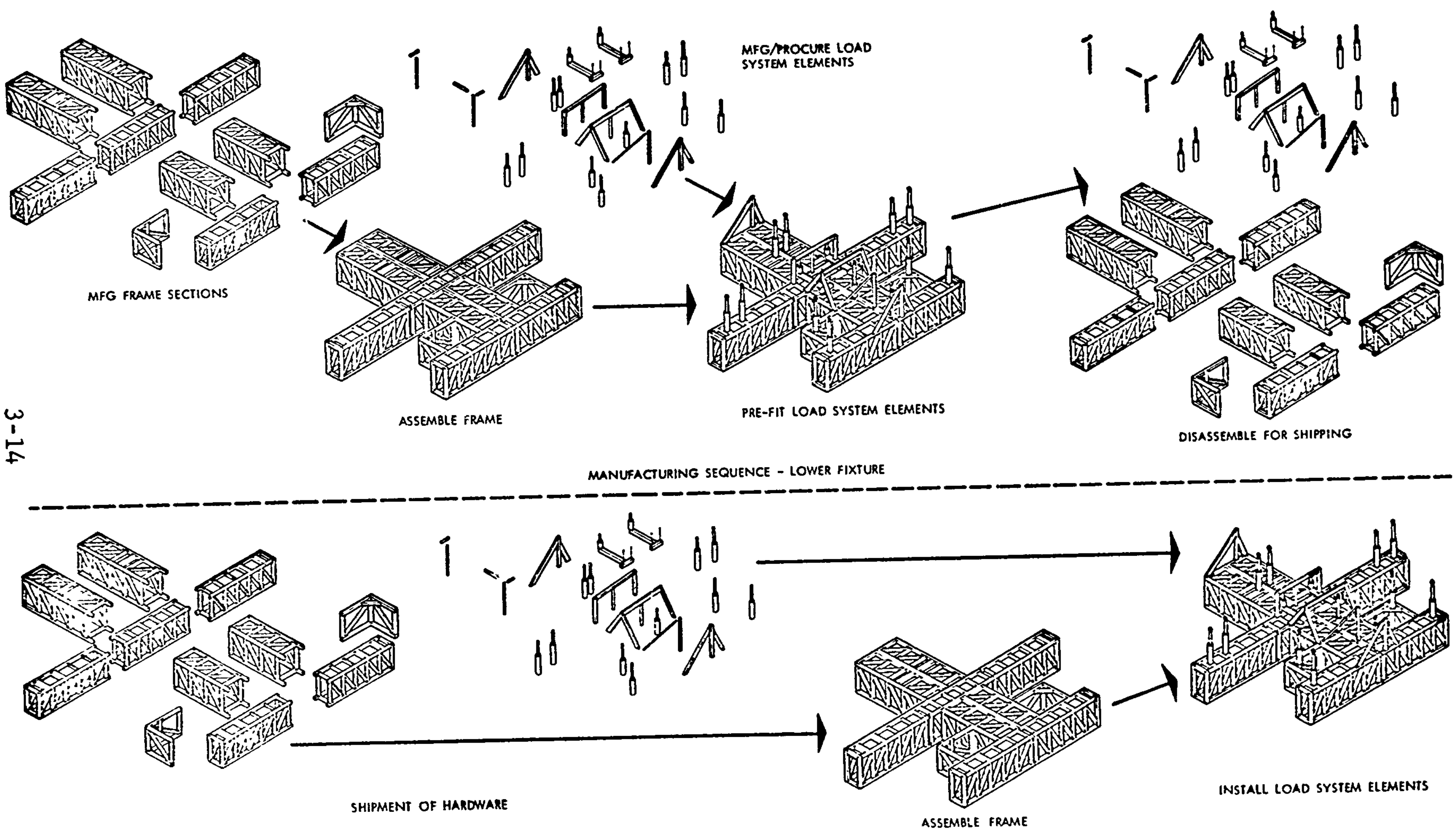


Figure 3-8 REASSEMBLY SEQUENCE - LOWER FIXTURE

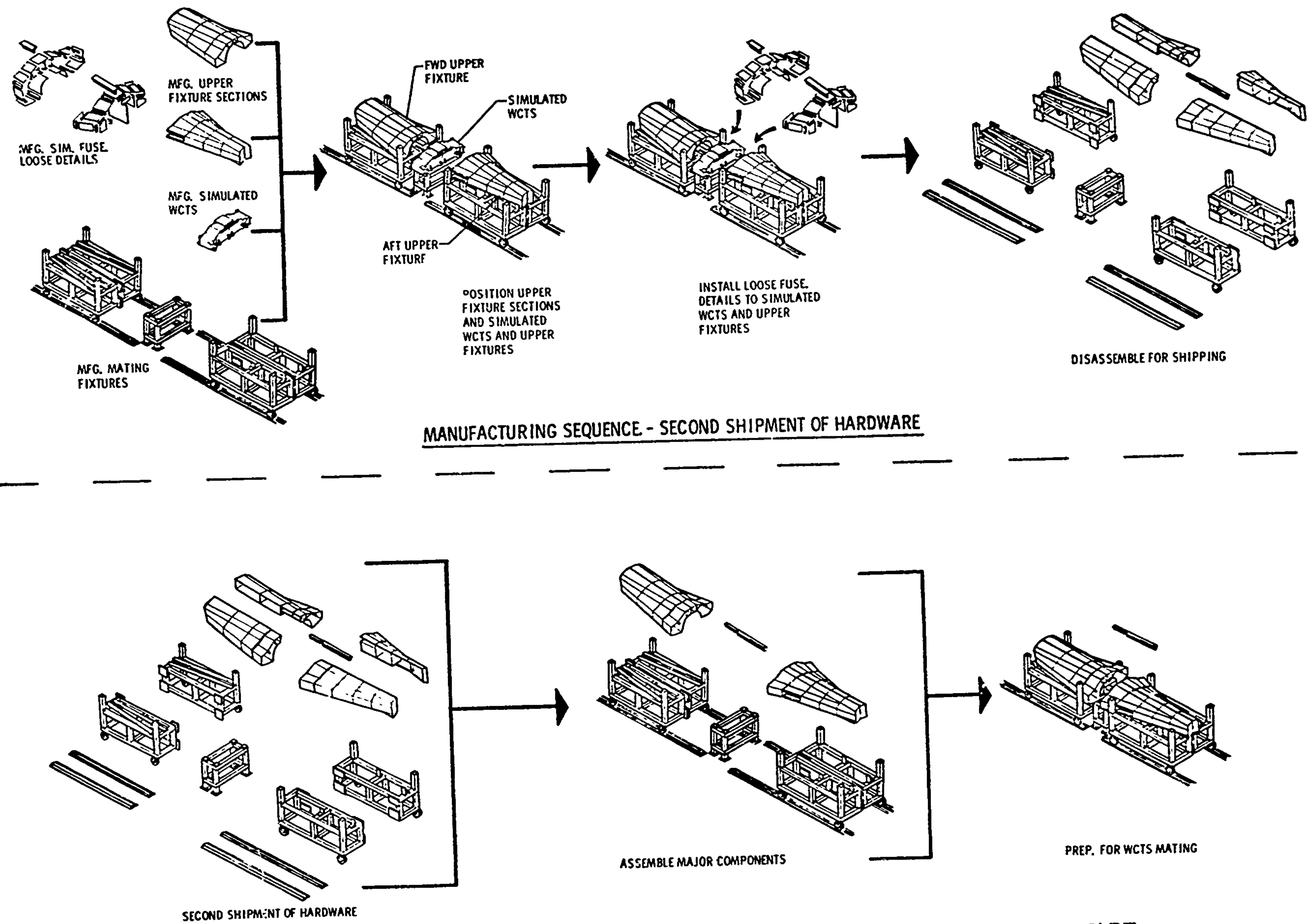


Figure 3-9 REASSEMBLY SEQUENCE - SECOND SHIPMENT OF HARDWARE

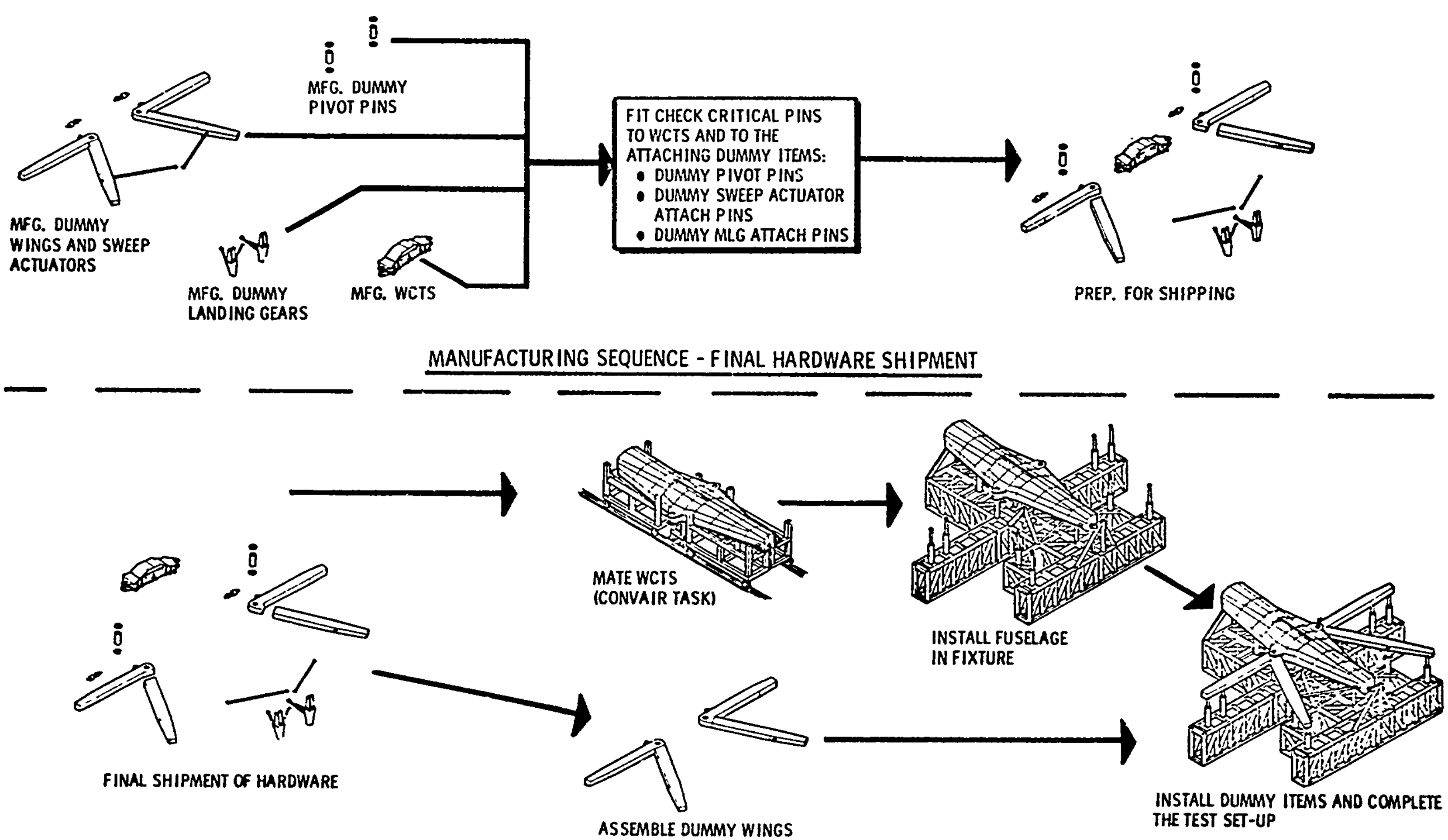


Figure 3-10 REASSEMBLY SEQUENCE - FINAL HARDWARE SHIPMENT

Table III-1 FULL-SCALE TEST FIXTURE STATUS

ITEM

INITIAL SHIPMENT OF HARDWARE

Load Systems Hardware
Flat Trusses for Base Frame
Assembly of Flat Trusses into Box Section
Assembly of Box Sections into Base Frame
Prefit Load Systems Hdw. on Base Frame
Disassemble for Shipping

SECOND SHIPMENT OF HARDWARE

Simulated Fuselage Loose Details
Upper Fixture Sections
Simulated WCTS
Mating Fixtures
Final Assembly & Mating
Disassemble for Shipping

FINAL SHIPMENT OF HARDWARE

Dummy Wings
Dummy Pivot Pin System
Dummy Sweep Actuators
Dummy Main Landing Gears
Mating
Prefit Dummy Hardware
Disassemble for Shipping

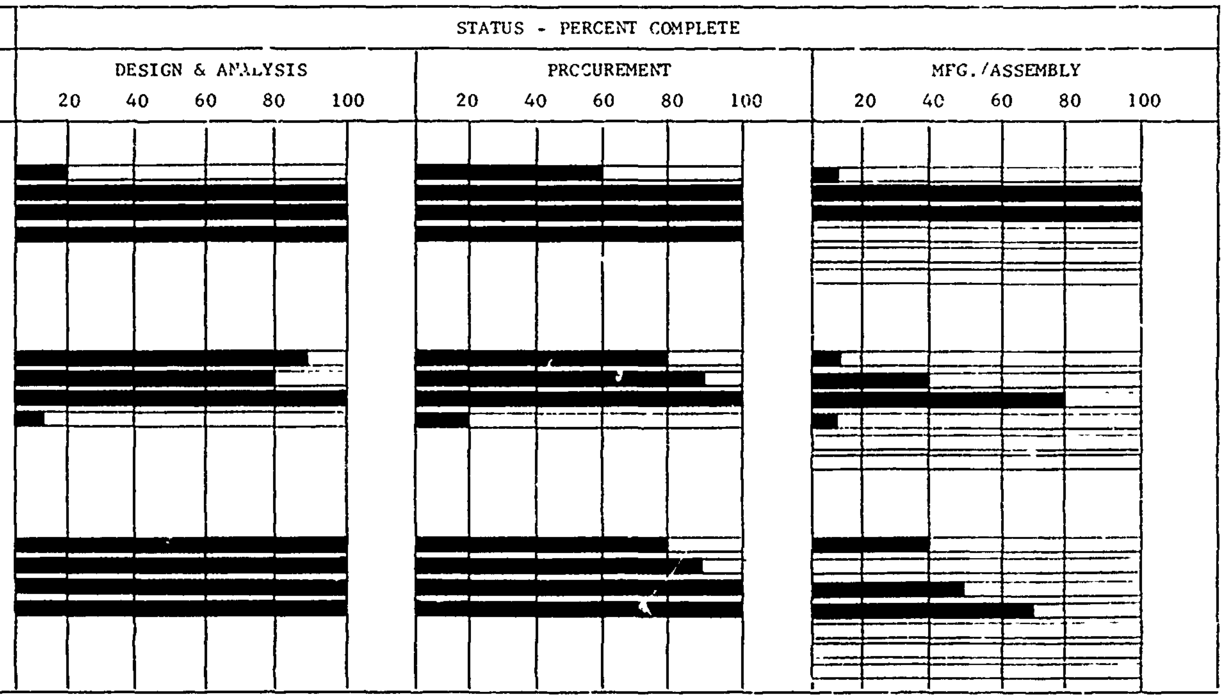

### 3.4 ALUMINUM-MANGANESE COATING FOR STEEL BOLTS

The use of cadmium plated steel bolts in titanium structure has been prohibited by USAF because of the possibility of inducing cadmium embrittlement in the titanium. For this reason Convair is investigating the use of Aluminum-Manganese coating for steel bolts in lieu of the cadmium plating for bolts installed in titanium structure.

For the initial investigation of this coating, 10 high strength steel bolts were given the Aluminum-Manganese coating and sent to Mr. Richard Stewart of ASD/ENFSS for stress corrosion investigation. In addition, 12 high strength steel bolts supplied by Omark Industries were coated and returned to Omark for static and fatigue testing.

Results of Testing

The results of four fasteners tested by Mr. Stewart are reported in his paper entitled "Preliminary Results of Stress Corrosion Test of Cadmium and Aluminum-Manganese Coated Taper-Loks in Titanium." While the test results are admittedly preliminary, the report is favorable and states that: "The Aluminum-Manganese Taper-Loks showed no signs of corrosion. There was no visible sign of cracking of the titanium specimen." Testing duration was 1000 hours. Bolts were 260-290,000 PSI heat treated. Figures 3-11 and 3-12 show Taper-Loks installed in the titanium specimens, parallel to each of the three major axis of the material. Note that the two specimens in Figure 3-12 are not joined together, but are merely in close proximity.

Omark Industries conducted three fatigue tests on both 1/2-inch-diameter and 5/8-inch-diameter bolts. The bolts were 220,000 minimum heat-treat.

The bolts tested in fatigue were cycled in axial tension from 3.5% to 35% of the rated axial strength. All bolts withstood 130,000 cycles of loading with no failures.

After completion of the fatigue tests, the bolts were failed statically. All static failing loads exceeded the minimum rated allowables.

Omark is also in the process of conducting alternate immersion salt-spray corrosion testing of Aluminum-Manganese fasteners.

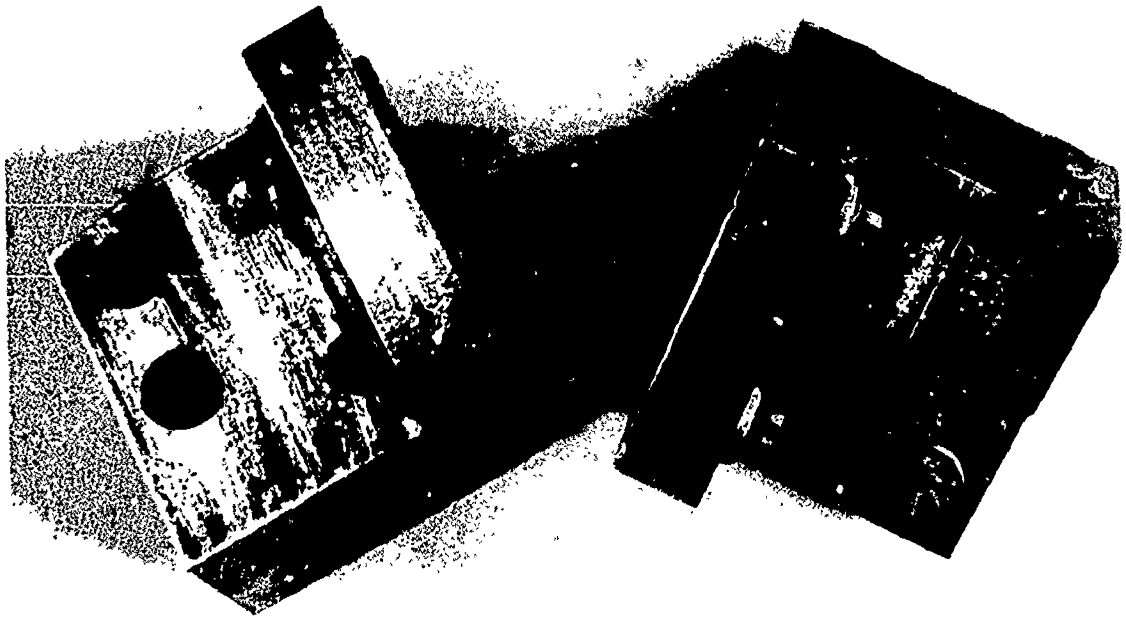

Figure 3-11 TAPER-LOKS, FASTENERS INSTALLED IN TITANIUM SPECIMENS

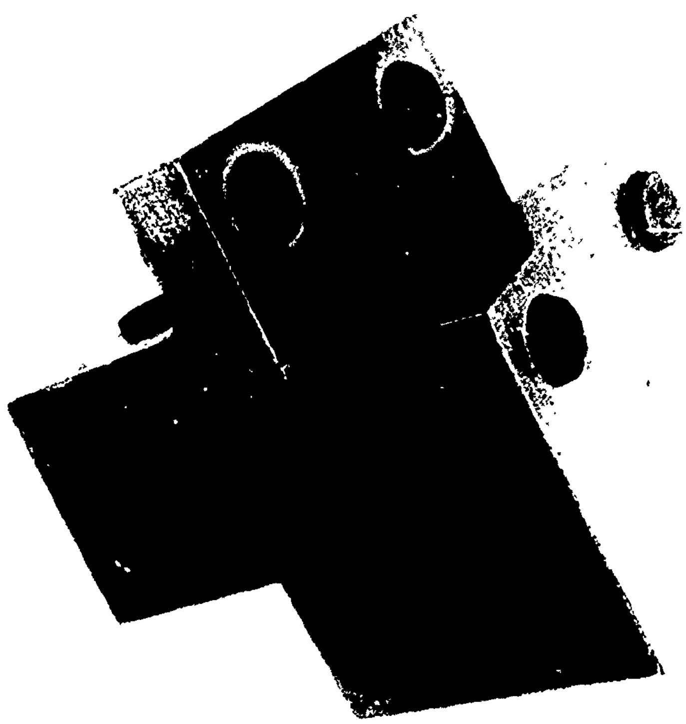

Figure 3-12 TAPER-LOK FASTENERS INSTALLED IN TITANIUM SPECIMENS

# SECTION 4

# QUALITY ASSURANCE AND NDI

Quality Assurance and NDI participated in the detail design phase to a large degree. Adhesive bonding, brazing and welding were evaluated as material joining techniques. The results of the activity are covered in the following paragraphs.

## 4.1 BONDING EVALUATIONS

A total of forty-eight bonded specimens were fabricated to be used in developing NDI techniques. As indicated in Table IV-1, forty-two specimens were titanium and aluminum sandwich structure while six panels (Table IV-2) were of a titanium multilayer laminate construction. These panels were designed to simulate various structures in the preliminary Fail Safe Integral Lug (FSIL) and "No-Box Box" (NBB) configurations. Each panel was bonded with the PL717 adhesive and contained intentional defects. The defects were a combination of the teflon tape insert type and, in some sandwich panels, a local crushed core type.

A through transmission ultrasonic C-scan recording (Figure 4-1) was made for each specimen. The through transmission evaluation was used as a baseline inspection to detect gross deficiencies in the specimens. This system was not considered as a candidate inspection system. The through transmission system detected only about 75% of the intentional defects. Also, extraneous indications were observed on some of the recordings.

Eight laminate-to-laminate type specimens consisting of different skin thicknesses were evaluated using several techniques. The Slik Bond Tester (Energy Summing Ultrasonic System) and Fokker Bond Tester (Resonance System) were evaluated using transducers of various sizes, types and frequencies. Results similar to the through transmission tests were obtained in detecting the induced flaws, but numerous additional areas were also detected with same response as the induced flaws. The destructive examinations provided a very close correlation of induced versus detected flaws. However, the cause of the additional indications were not determined.

Table IV-1

BONDED NDI SANDWICH PANELS

| Specimen No. | Material Skin | Skin Thickness $T_1$ | Core | Skin Thickness $T_2$ | Quantity Fabricated |
|---|---|---|---|---|---|
| MD3266 | 2024 Alum. | .200 | 1" Thk | .075 | 2 |
| MD3256 | " | .125 | " | .025 | 2 |
| MD3267 | " | .080 | " | .025 | 2 |
| MD3258 | " | .035 | " | .025 | 2 |
| MD3268 | " | .125 | " | .040 | 2 |
| MD3260 | " | .190 | " | .032 | 2 |
| MD3272 | " | .130 | " | .032 | 2 |
| MD3269 | " | .050 | " | .032 | 2 |
| MD3262 | " | .300 | " | .050 | 2 |
| MD3271 | " | .250 | " | .050 | 2 |
| MD3270 | " | .150 | " | .050 | 2 |
| MD3264 | " | .090 | " | .050 | 2 |
| MD3259 | " | .300 | 2" Thk | .063 | 2 |
| MD3261 | " | .213 | " | .063 | 2 |
| MD3263 | " | .125 | " | .063 | 2 |
| MD3257 | Ti 6AL-4V Mill | .250 | 1" Thk | .030 | 2 |
| MD3265 | Annealed | .135 | " | .030 | 2 |
| MD3278 | " | .060 | " | .030 | 2 |
| MD3279 | " | .135 | " | .060 | 2 |
| MD3280 | " | .185 | " | .060 | 2 |
| MD3281 | " | .300 | " | .060 | 2 |

Table IV-2

BONDED NDI LAMINATE SPECIMENS

| Specimen No. | Material | Laminate Thickness $T_1$ | $T_2$ | $T_3$ | $T_4$ | Quantity Fabricated |
|---|---|---|---|---|---|---|
| MD3204 | Beta C | .125 | .125 | .125 | .125 | 1 |
| MD3203 | Beta C | .062 | .125 | .125 | .062 | 1 |
| MD3253 | Beta C | .100 | .100 | .100 | .100 | 1 |
| MD3255 | Beta C | .100 | .100 | | | 1 |
| MD3254 | Beta C | .06 | .06 | | | 1 |
| MD3251 | Beta C | .125 | .125 | .05 | .100 | 1 |

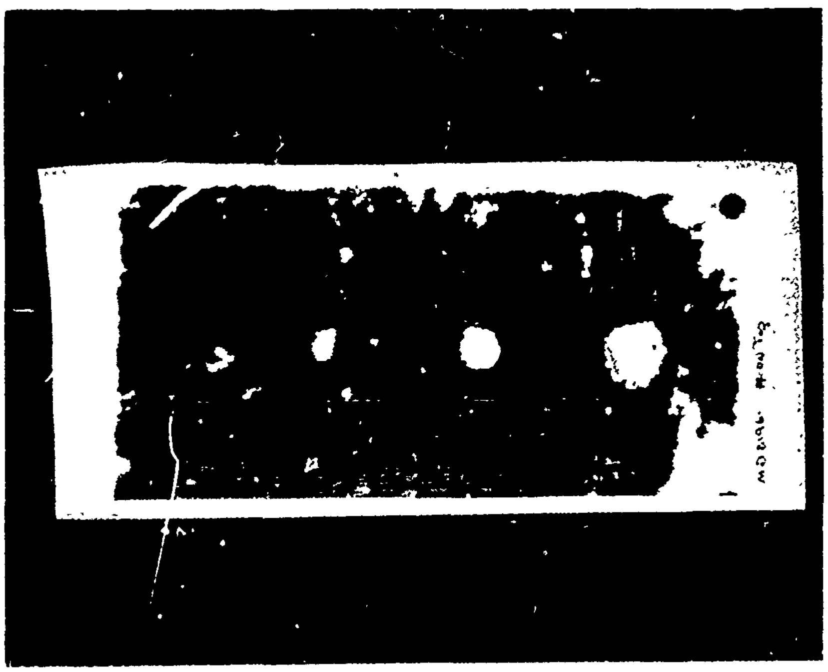

Figure 4-1 Typical Through Transmission C-Scan Recording of an NDI Sandwich Panel

Evaluation of laminate-to-laminate specimens was stopped due to engineering design changes of the FSIL and "No-Box Box" configurations and the cancellation of the titanium laminate configuration. However, the preliminary studies indicate the possibility of using the Energy Summing Ultrasonic System (Slik Bond Tester) to inspect titanium laminates but additional work would be required for production applications.

The sandwich specimens are currently being evaluated using the UM-721 Reflectoscope and Slik Bond Tester. Two different techniques are being considered with the UM-721 Reflectoscope, ring pattern for thick skin specimen and back surface reflection for thin skin specimens.

Each of the three different techniques has produced some favorable results. The Slik Bond Tester using a dual "pitch-catch" type transducer system will detect most of the induced flaws in skin thickness of .125" and greater. However, numerous additional indications have been recorded in some specimens. In most cases these indications are confirmed by the through transmission recordings.

The ring pattern and the energy summing technique results correlate very closely in the detection of both artificial and natural flaws in the thick skinned panels. This lends credit to the preliminary selection of one of these techniques. Final technique selection will depend on flaw configuration in the disassembly of selected panels and the final design of various AMAVS structures.

For the thin skinned panels (skin thickness of .124" and less) a back surface reflection technique application was recently developed. This technique monitors the inside surface of the opposite skin of the sandwich structures. The other standard technique applications have been ineffective in detecting flaws in the thin skinned panels due to the high porosity content in the PL-717 adhesive system.

The preliminary techniques indicated are necessarily tentative. The lack of a specific final design configuration (i.e. skin gage, core thickness, etc.) have delayed the technique selection. As the final production designs are completed, specimens will be fabricated that simulate these designs. The tentative techniques will be verified on the new specimens and production inspection procedures will be prepared.

## 4.2 BRAZED JOINT EVALUATIONS

### 4.2.1 NDI Development

NDI development has consisted of the selection and development of both flaw induction technique and a nondestructive inspection technique. Technique selection was made based on NDI data obtained from a series of specimens brazed with the existing optimum manufacturing techniques.

Initially the reference specimens were made using .25 thick 6AL-4V Beta Annealed laminates. These specimens were satisfactory for establishing flaw induction techniques. Specimens having .40 to .60 inch thick laminates were used to develop the NDI inspection technique.

A summary of the flaw induction results is shown in Table IV-3. The overall quality of the brazed specimens was not good, but was satisfactory for the flaw induction program. In addition to the flaw induction media shown in the above table, flat bottom holes were drilled and slots eloxed in a section of panel MD3211 (See Figure 4-2).

Stainless steel spacers, flat bottom holes and stop-off have provided the most uniform, dimensionally controllable flow induction media. Stop-off is a high temperature material used to prevent adherence of the braze alloy to a laminate and is used as a control in the brazing operation.

The size of flaws induced using spacers and stop-off is more difficult to control because of migration of both braze alloy and induction media during the braze operation. Diameters of flat bottom holes are easily controlled, but locating the depth of the braze line exactly is difficult. The time domain responses from each of the flaw types are the same.

Several ultrasonic techniques were evaluated for use in inspecting the brazed specimens. Of the techniques evaluated, five were effective in detecting defective conditions. The most effective technique was pulse echo. It is easy to set up and can be used with a wide variety of transducers. Both flat and focused transducers with frequencies of 5, 10 and 15 MHz were evaluated. The technique was employed strictly in an immersion mode, but can also be applied in the contact mode. Permanent recordings (C-Scan) can be made using existing equipment. Access to only one side of the part is required.

Table IV-3

NDI BRAZED JOINT SPECIMEN

| SPECIMEN NO. | FLAW INDICATION MEDIA | OVERALL PANEL QUALITY | REMARKS |
|---|---|---|---|
| MD3188-1-1 | Volatiles (corrosives, stop-off) | Fair | Good flaws |
| MD3187-1-2 | Inserts | Poor | Large void area. |
| MD3189-1 | Everlube T-50<br>Tungsten disulfide | Fair | Fairly good flaws. Used for techniques development. |
| MD3189-2 | Sulfuric acid<br>Nitric-hydrofluoric acids | Poor | Sulfuric flaws - present but large, $HF-HNO_3$ - absent. |
| MD3208 | Sulfuric acid, nitric acid | Poor | Large void area, poor induced flaw quality. |
| MD3209 | Stop-off material<br>Tungsten Disulfide | Poor | Naturally occurring flaws. |
| MD3210 | Kerosene Cutting Oil | Poor | Large void areas poor induced flaw quality. |
| MD3211 | Lube Oil<br>$HF-HNO_3$ acid | Fair | Poor flaw quality.<br>Excessive areas of naturally occurring flaws. |
| MD3222 | Inserts, stop-off | Poor | Large areas of naturally occurring voids (retort leak) |
| MD3223 | Inserts, stop-off | Poor | Same as MD3222. |

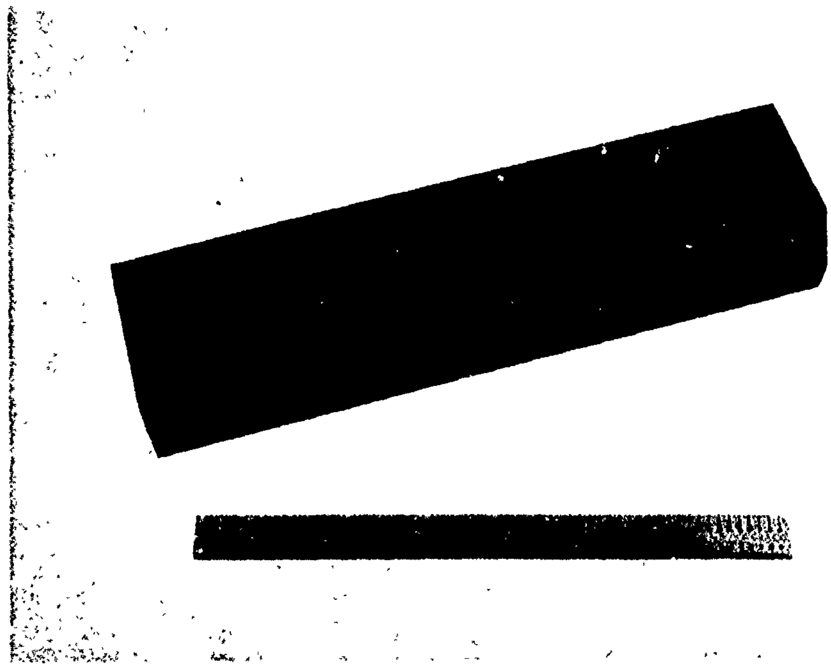

Figure 4-2 Flat Bottom Holes and an Elox Slot Evaluated as Flaw Induction Methods

Through transmission is also effective. It likewise has recording capabilities and is easy to set up. However, because access to both sides of the part is required, it is impractical for large-area brazed panels.

A pitch-catch technique proved effective, but hard to set up. Likewise, the ring pattern technique proved to be very difficult to apply. The Slik Bond Tester (energy summing ultrasonic technique) was only marginally effective and lacked recording capabilities.

The procedure selected to inspect the brazed structures employs a focused 10 MHz transducer. Basically, the procedure is as follows:

- o The transducer is normalized (made perpendicular) to the front surface of the test part.
- o The sound beam is focused on the brazeline under evaluation.
- o An electronic gate is placed on the signal from the brazeline.
- o Gain and accept/reject levels are determined from setting up on a reference part. Figures 4-3 and 4-4 show typical "good" and "bad" signals.
- o The entire part is scanned and a recording (C-scan) made of both the acceptable and unacceptable areas.

The primary problem that has been experienced with the focused transducer method is that the inspection is very dependent on normality and to a lesser degree on the water travel distance (distance between transducer and part). Frequent set-up adjustments are necessary to inspect the large area brazed parts.

A Schlieren study was undertaken to determine if the normality problem was caused by a malfunction in the transducer. Schlieren imaging is a process in which the sound beam emanating from a transducer is made visible. The process is helpful in determining transducer characteristics such as beam strength and beam pattern of the transducer. The Convair imaging equipment allows the operator to rotate the transducer and observe different cross-sections of the soundbeam. A marked difference in the intensity of the soundbeam of the transducer used in the

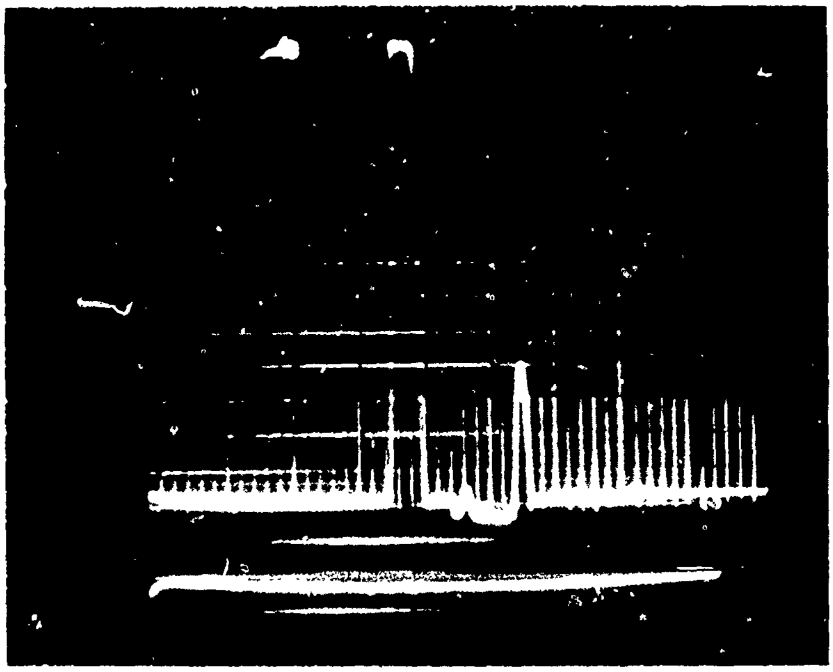

Figure 4-3 A "Good" Area Showed a Relatively Low Signal in the Gate

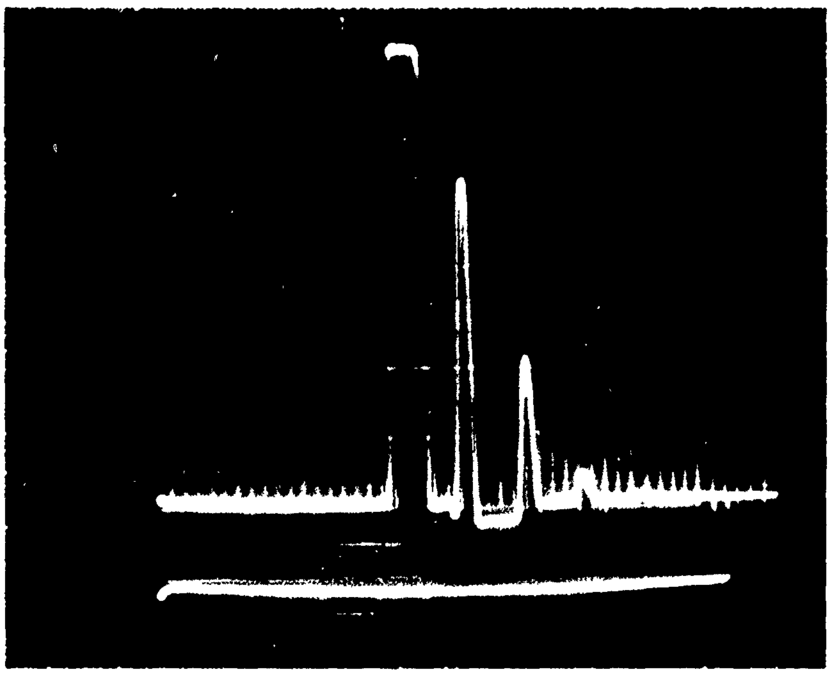

Figure 4-4 A Defective Area Was Indicated by a Relatively High Signal in the Gate

inspection was noted as shown in Figures 4-5 and 4-6. These two photographs depict the effect of a 45° of rotation of the transducer. They show that the normality problem is due to abnormalities in the beam pattern of the transducer. Because the transducer used was the only one of its type on hand at Convair, a new long-focus transducer of the same type would have been purchased to accomplish the inspection of the test part had the FSIL design been selected.

### 4.2.2 Engineering Specimen Evaluation

All the Group Engineering specimens were inspected using Radiography and the ultrasonic techniques. These specimens were used by manufacturing and engineering to establish manufacturing variables and allowables. They were also used to develop and improve the ultrasonic NDI technique. This preliminary technique was finalized at the end of the Group II portion of the program.

Part 603FTB033 was inspected before test and after two stages of testing. Scattered void areas were found in the panel before test, but did not propagate during test or appear to affect the crack stopping capabilities of the brazeline.

The ultrasonic response from the brazeline of the first 603FTB035 panel (-1, -2) was considerably different from previous brazed parts in that a large signal was present in the assumed "good" areas. Metallographic examinations showed the entire brazeline to be porous and to have a substandard strength. Half of the 603FTB035-1, -2 was rebrazed and tested ultrasonically. The part was found to contain enough defect areas to warrant cancellation of the structural testing of the panel.

The third large specimen, 603FTB035-2, showed to have a very good quality braze. Shown in Figure 4-7 is a photograph of the ultrasonic recording (C-scan) of one side of one end of the part. Subsequent physical testing of the part was successful. The part will be re-inspected when physical testing is completed.

Panel 603FTB053-21 was inspected a total of three times; before test, after four lifetimes, and after six lifetimes of testing. Figure 4-8 shows a photograph of the ultrasonic recordings (C-scan). No void propagation was observed. It should be noted that most of the defective areas present in the specimen before test, shown at the left of Figure 4-8, were machined away in the manufacture of the test specimen.

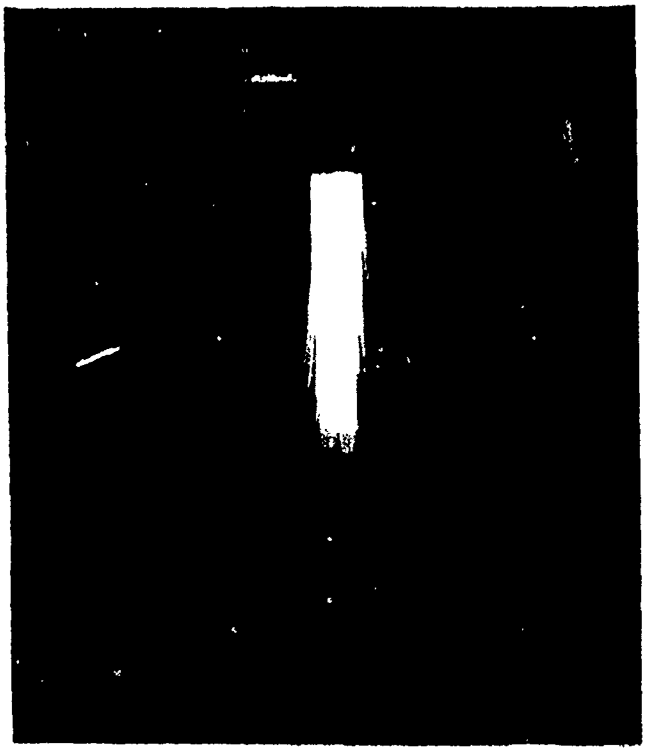

Figure 4-5 The Schlieren System Indicates One Cross Section of the Soundbeam to be Strong

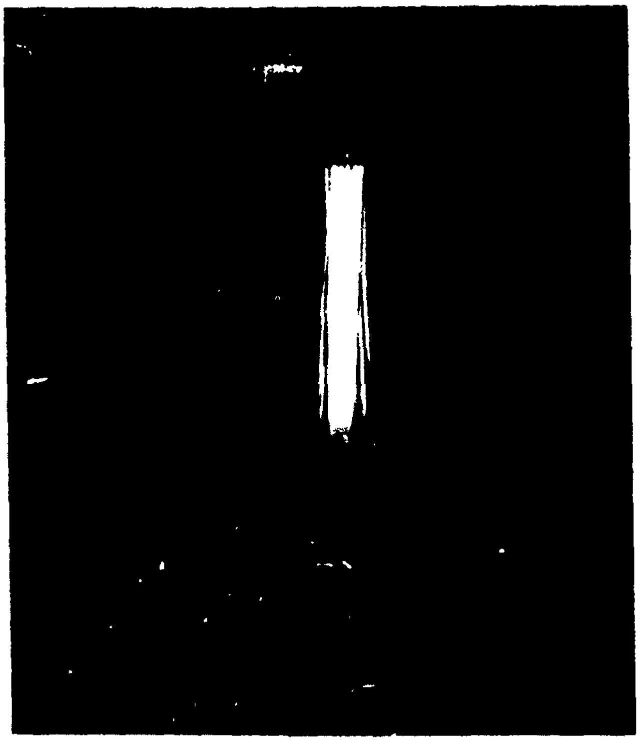

Figure 4-6 Because of a Malfunction in the Transducer, Part of the Soundbeam is Missing.

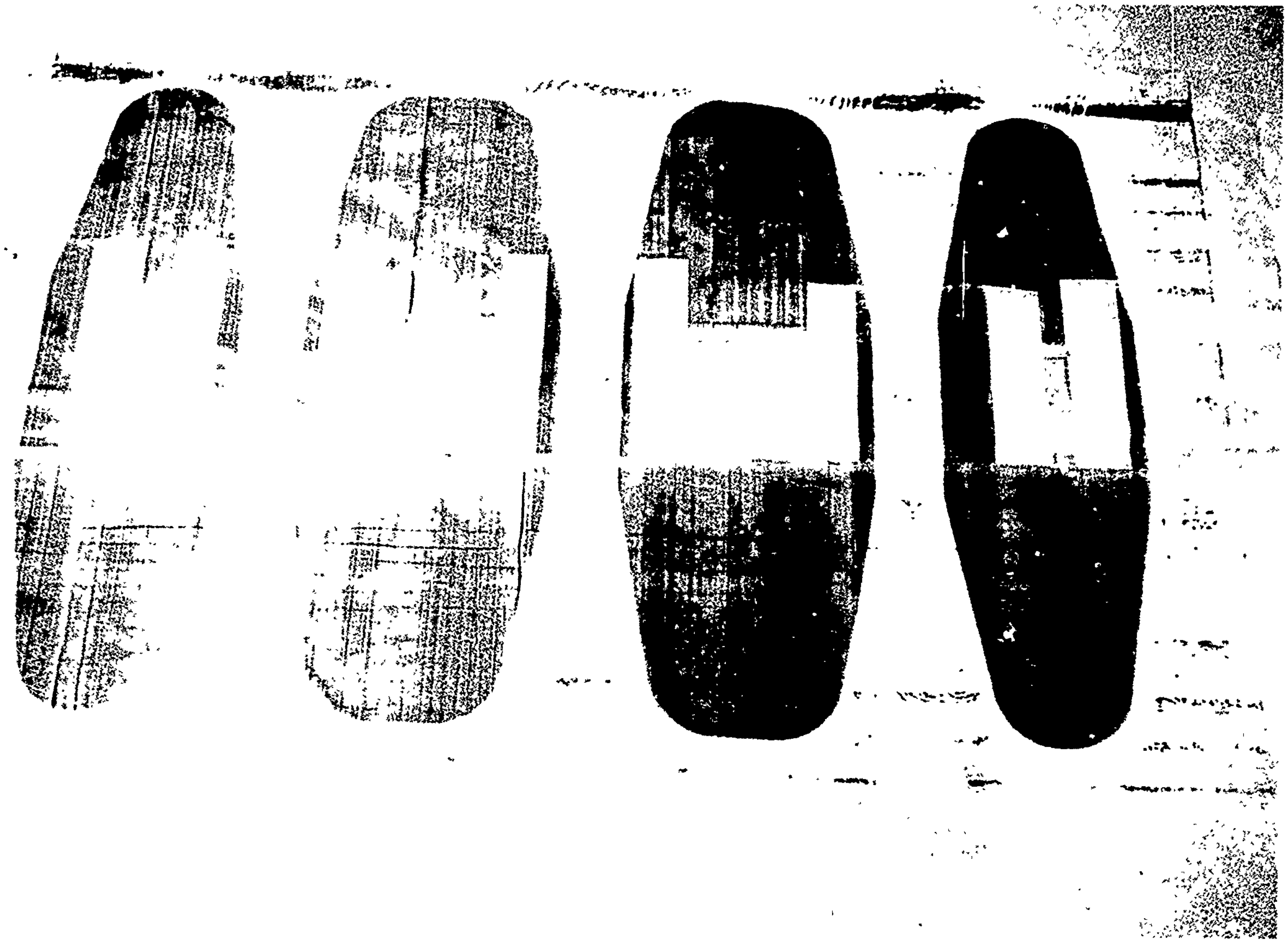

Figure 4-7 The Ultrasonic Inspection of 603FTB035-2 Recorded in a C-Scan Mode

Figure 4-8 Ultrasonic Recording of 603FTB053-21
A) Before Testing (Left),
B) After Four Lifetimes of Testing (Center), and
C) After Six Lifetimes of Testing (Right)

## 4.3 WELDED JOINT EVALUATIONS

### 4.3.1 NDI Specimen Design & Fabrication

Under this program provisions were made for the design and fabrication of 6AL-4V Beta Annealed Titanium and 10 Nickel (HY180) steel specimens necessary to provide adequate data to evaluate transducers and techniques for the NDI of weldments made from these alloys.

Configurations MD3190, MD3191 and MD3202 (Figure 4-9) were constructed to provide a titanium thickness range of weld from 0.5 to 1.5 inches. Configurations MD3232 and MD3233 (Figure 4-9) were fabricated with a similar weld thickness range for 10Ni.

### 4.3.2 Transducer Evaluation

Available transducers in the 5, 10 and 15 MHz range were evaluated. Response profiles were plotted for those transducers demonstrating best sensitivity and resolution for both Ti and 10Ni flat bottom hole (FBH) references. Transducers SIL (15 MHz), 1/2 inch OD, focused, immersion, and transducer A311, (15 MHz), 1/2 inch OD, focused, immersion, manufactured by Automation Industries and Panametrics respectively, were selected on the basis of their response profiles. Further experimentation confirmed their efficiency. Evaluation was performed on the basis of their response to 2/64 flat bottom holes (FBH) drilled at various depths in fabricated reference specimens. (See Figure 4-10).

### 4.3.3 Engineering Specimen Inspection

Most of the specimens manufactured for engineering testing purposes underwent a "best effort" ultrasonic inspection on a routine basis. Data was recorded and filed for further evaluation. These inspections included both 10Ni and 6AL-4V Ti specimens.

In addition, some of the 10 nickel specimens with natural defects were used to acquire preliminary ultrasonic information on this alloy, since the scheduled receipt of the formal NDI specimens was delayed. Preliminary references were constructed with some of these specimens. (See Figure 4-11).

Figure 4-9  NDI Welded Specimens

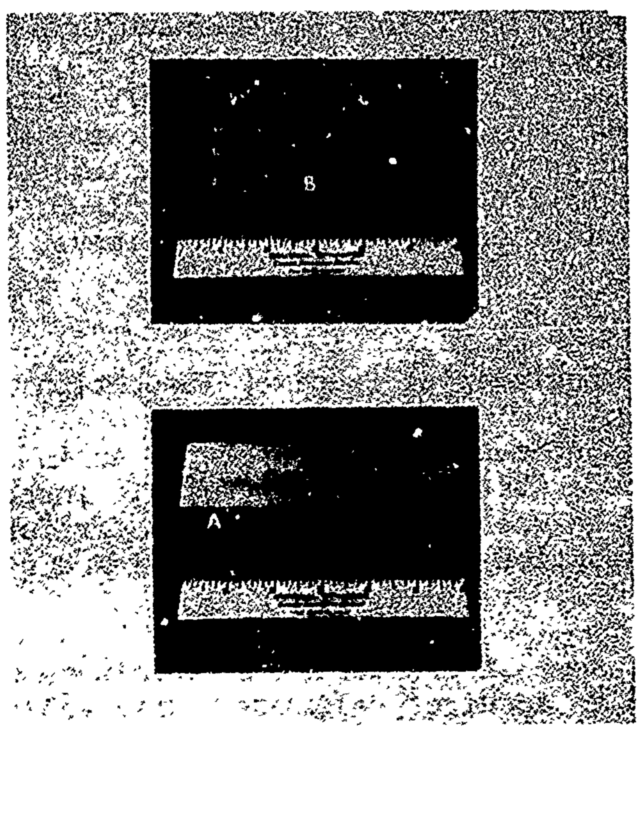


Figure 4-10  6AL-4V(A) and 10 Ni(B) Flat Bottomed Hole References

4.3.4 Shear Ultrasonic Techniques, 6AL-4V Titanium

Evaluation of shear techniques, at 45° and 30° with 2.5, 5 and 10 MHz shear contact transducers was discontinued almost immediately due to unsatisfactory results. At thicknesses from 0.5 to 0.900 inch, #3 electric discharge machined slot responses were detectable. For bottom and top surface slots for 1.5 inch thick materials only bottom surface responses were detectable. It was also noted that natural flaws easily detected with longitudinal techniques were not detectable with the shear transducers evaluated.

4.3.5 Delta Ultrasonic Techniques, 6AL-4V Titanium

Evaluation of ultrasonic delta techniques was completed for Ti 6AL-4V specimens with negative results. Available delta probes, GD/QC 148, 149 and 124 were tested and found unsuitable. Either top or bottom eloxed slots produced satisfactory responses, but not both. Some of the radiographicdetected flaws could not be detected or the response amplitudes were less than or equal to the weld structural or surface noise. Attempts were made to produce a working delta probe by using 5, 10 and 15 MHz transducers in various combinations of frequencies, angles and transducer spacing with unsatisfactory results. One of the variable depth and spacing fixtures used is shown in Figure 4-12. A dual 15 MHz transducer combination (focused) produced usable eloxed slot responses for 0.370, 0.425 and 0.620 inch thick weldments; but it also produced spurious responses where metalographic sectioning failed to produce any flaws. In addition, extreme sensitivity to surface conditions was noted.

4.3.6 Pulse Echo Longitudinal Evaluation, 6AL-4V Titanium

Scans of NDI specimens MD3202, MD3191 and MD3190 using 2/64 FBH reference specimens were performed in a series of tests to provide suitable weld responses (Figure 4-13). All radiographic detected flaws in these specimens were detected ultrasonically with additional responses in adjacent areas. This indicates that ultrasonic sensitivity is of an improved degree to that of radiography. Full confidence in the ability to detect flaws in this type of weld is based not only in the correlation of radiograph to ultrasonic responses for the specimens listed above; but also in results obtained in prior company programs.

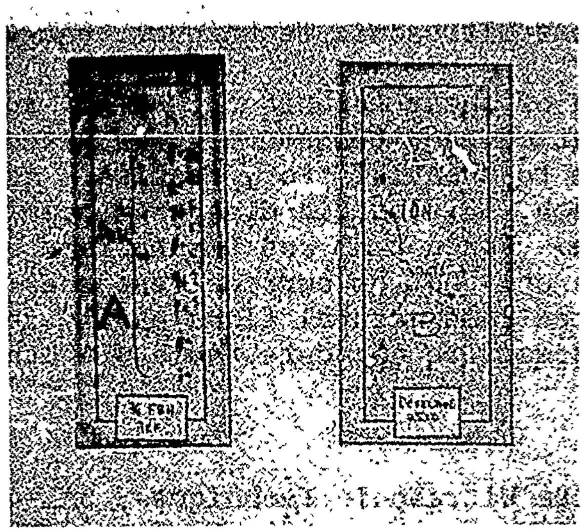

Figure 4-11  Typical Pulse-Echo Recordings of 10 Ni Weld and Preliminary Reference Specimen

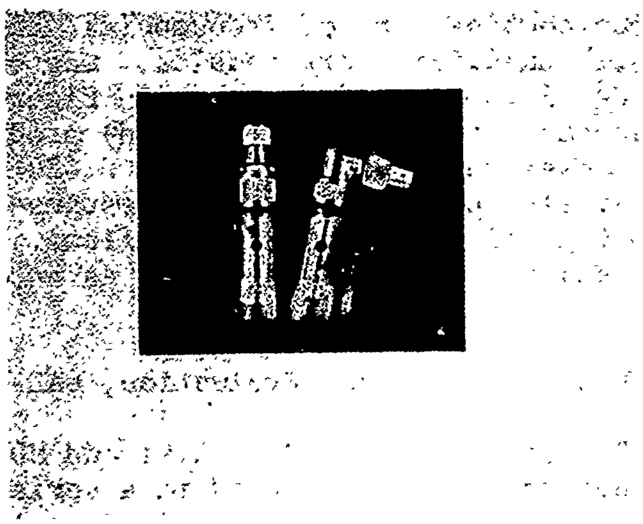

Figure 4-12  Variable Depth/Angle Delta Probe Fixture

### 4.3.7 Pulse Echo-Longitudinal Evaluation, 10 Nickel Specimens

Late arrival of 10 Nickel material and manufacture of 10 Nickel NDI specimens has precluded any ultrasonic evaluation other than pulse echo-longitudinal techniques. This has been possible only through the availability and use of some defective engineering 10 Nickel weld specimens.

Scans were performed on engineering weld specimens H9 and H27 using a 10 Nickel reference specimen with 2/64 FBH. Sectioning of H9 specimens verified that good ultrasonic response to flaw correlation was obtained. A microsection of a defective portion of engineering specimen H27 supplemented these findings where an equally effective ultrasonic response to flaw correlations was found. (Figure 4-14).

Radiography to ultrasonic response correlations on engineering specimen H9 can be seen in Figure 4-15. This correlation shows the improved sensitivity of ultrasonics over radiography detection.

### 4.3.8 Evaluation Summary

The following summary is preliminary and subject to re-evaluation as additional work is performed on Weld NDI specimens.

a. EB welds of 6AL-4V Titanium and 10 Nickel alloys may be ultrasonically inspected using pulse echo-longitudinal methods with water immersion or bubbler techniques.

b. The thickness range of inspection meets the requirement of the program: 0.5 - 1.6 inch (Ti and 10Ni).

c. Within the scope of these tests and materials, minimum detectable anomalies are estimated to be between 0.015 to 0.050 in. for 10Ni. No estimate can be made at this time for titanium since insufficient destructive analyses have been performed at this point in the program.

d. Ultrasonic longitudinal pulse echo and radiography "flaw" detection provide complementary NDI data. Inspection of 10Nickel and 6AL-4V Titanium will require the use of both techniques for the following reasons:

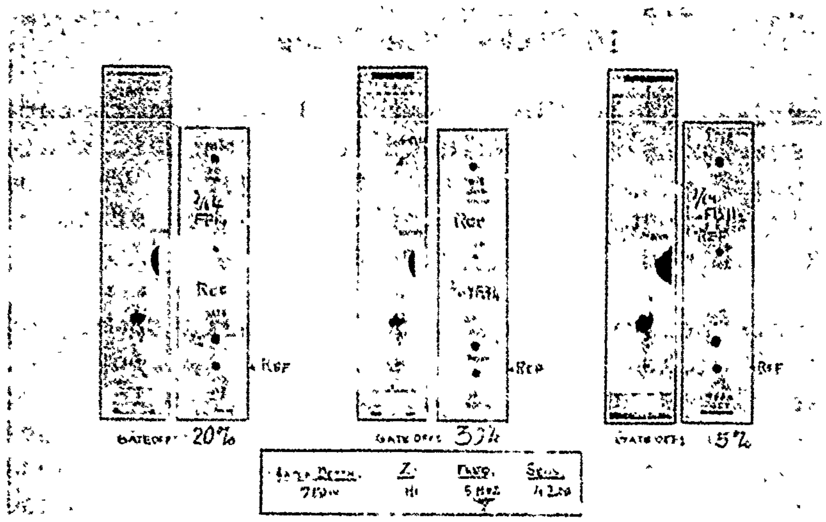

Figure 4-13 Typical 6AL-4V B Weld Responses Using Pulse Echo Longitudinal Technique

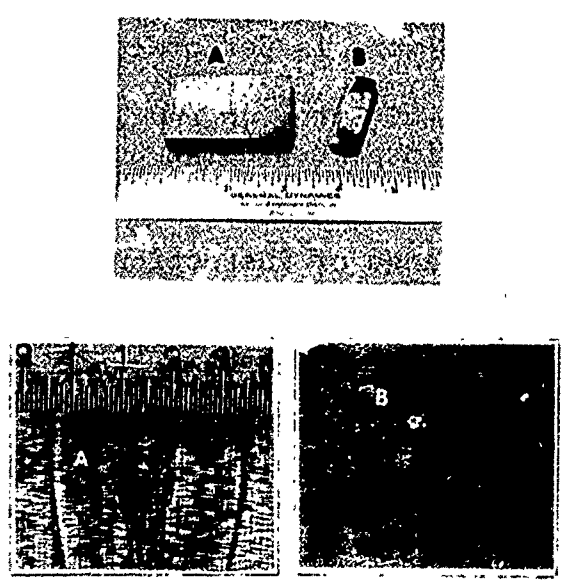

Figure 4-14 Metalographic Sections of Flaws in Specimen H27(A) and H9(B)

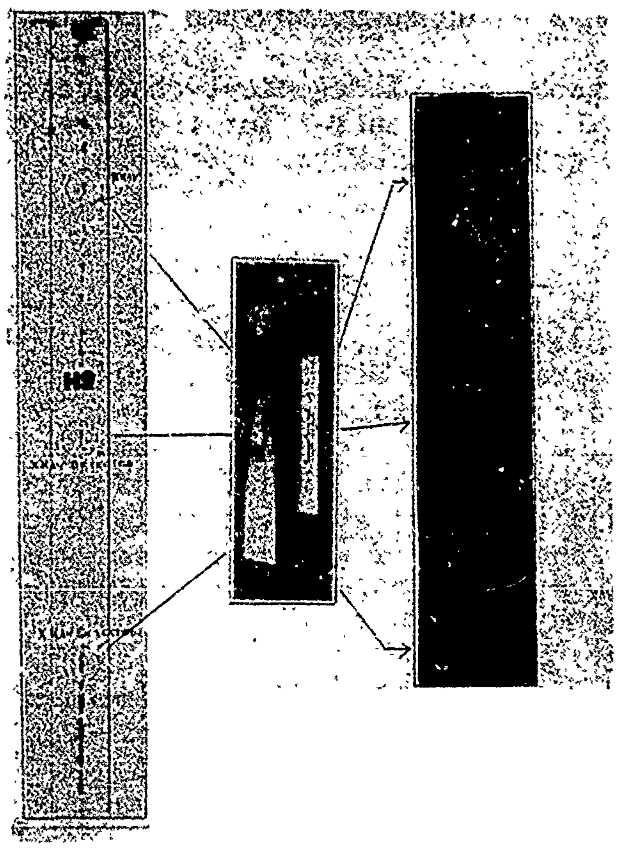

Figure 4-15 Radiographic/Ultrasonic Comparisons for the Inspections of 10Ni Specimen H9

- Some ultrasonically detected "indications" cannot be detected radiographically. (Figure 4-15).

- All pulse echo-longitudinal techniques are ultrasonically blind at the near front surface (front surface resolution). Radiography techniques minimize this 0.100 to 0.150 inch deficiency.

- Radiography and ultrasonic techniques have different accessibility potential for the inspection of different geometries of the specimens.

## 4.4 NDI PLANS

Drawings 603R234, 603R231, and 603R232 were developed to outline an NDI program on welded, bonded, and brazed specimens. These drawings are shown as Figures 4-16, 4-17, and 4-18, respectively. All of the NDI specimens shown in Figure 4-16 were completed during Phase II. The welded NDI specimens for both 6AL-4V titanium and 10 Nickel steel shown in Figure 4-17 were also completed. Fourty-two of the bonded sandwich panel NDI specimens shown in Figure 4-18 were evaluated during the Detail Design Phase.

Additional bonded and welded NDI specimens will be evaluated to assure inspectability of the "No-Box" Box configuration selected for manufacturing during Phase III.

## RAW MATERIAL SPECIMENS

| PART NO. | MATERIAL | QUANTITY REQD |
|---|---|---|
| MD3201 | 6AL-4V Ti | 1 |
| MD3220 | 10 Ni STEEL | 1 |
| MD3206 | BETA C | 1 |

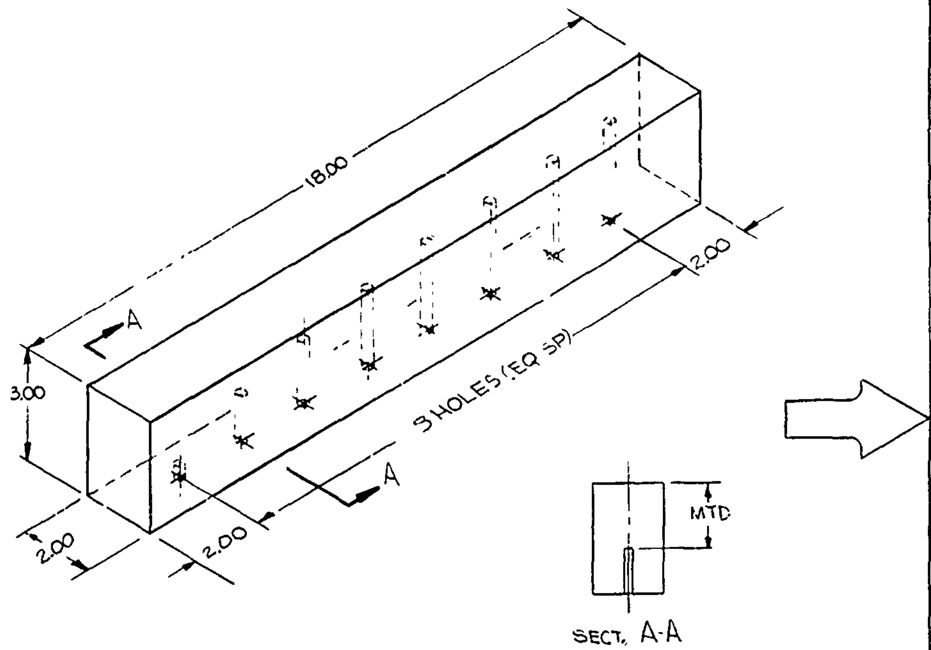


ESTABLISH NEED FOR REFERENCE BLOCKS; SPECIFY DESIGN REQUIREMENTS FOR ADDITIONAL BLOCKS

2. HOLES TO BE FLAT BOTTOMED # 5/64 DIA
1. PARTS TO HAVE MTD (METAL TRAVEL DISTANCE) OF: 2.275, 1.750, 1.250, 0.875, 0.625, 0.500, 0.375 & 0.250

NOTES (EXCEPT AS SHOWN)

Figure 4-16 RAW MATERIAL AND BRAZED N

| NO. | MATERIAL | QUANTITY REQD |
|---|---|---|
| 01 | 6AL-4V Ti | 1 |
| 0 | 10 111 STEEL | 1 |
| 06 | BETA C | 1 |

STABLISH NEED FOR
EFERENCE BLOCKS;
PECIFY DESIGN
REQUIREMENTS FOR
ADDITIONAL BLOCKS

## BRAZED SPECIMENS

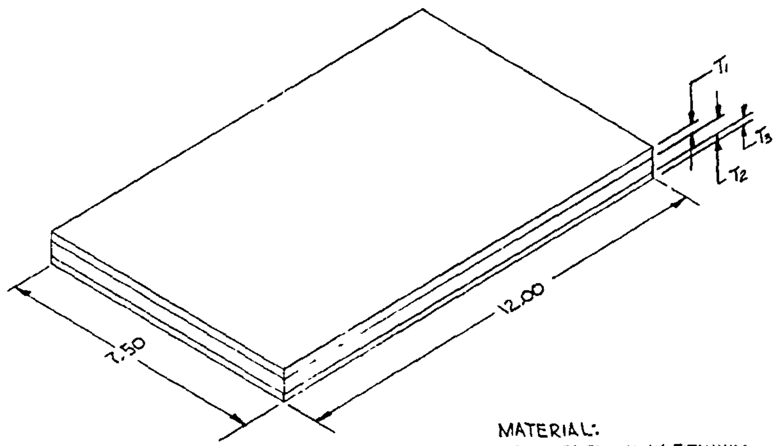


MATERIAL:
BETA ANNEALED 6AL-4V TITANIUM

| PART NO. | LAMINA T1 | T2 | T3 | TYPE FLAW | QTY REQD |
|---|---|---|---|---|---|
| MD3187-1-1 | .250 | .250 | | CORROSIVE | 1 |
| MD3187-1-2 | .250 | .250 | | INCLUSION | 1 |
| MD3189-1-1 | .250 | .250 | | CORROSIVE | 1 |
| MD3189-1-2 | .250 | .250 | | INCLUSION | 1 |
| MD3188-1 | .250 | .250 | | CORROSIVE | 1 |
| MD3188-2 | .250 | .250 | | CORROSIVE | 1 |
| MD3208 | .250 | .250 | | CORROSIVE | 1 |
| MD3209 | .250 | .250 | | INCLUSION | 1 |
| MD3210 | .400 | .600 | | CORROSIVE | 1 |
| MD3211 | .400 | .600 | | CORROSIVE | 1 |
| MD3212-1 | .250 | .250 | | SEE NOTE 1 | 1 |
| MD3213-1 | .250 | .250 | | | 1 |
| MD3215 | .400 | .600 | | | 1 |
| MD 3222 | .600 | .400 | .600 | | 1 |
| MD 3223 | .600 | .400 | .400 | SEE NOTE 1 | 1 |

1. FLAW TYPE WILL BE DEFINED AS A RESULT OF PRELIMINARY STUDIES

NOTES (EXCEPT AS SHOWN)

PRELIMINARY DESIGN DRAWING

RAW MATERIAL AND BRAZED NDI SPECIMENS

BY L. Bradie | APPROVED [signature] | SCALE | DATE 5-29-73

GENERAL DYNAMICS
Convair Aerospace Division
Fort Worth Operation

603R234

SHEET 1 OF 1

RAW MATERIAL AND BRAZED NDI SPECIMENS

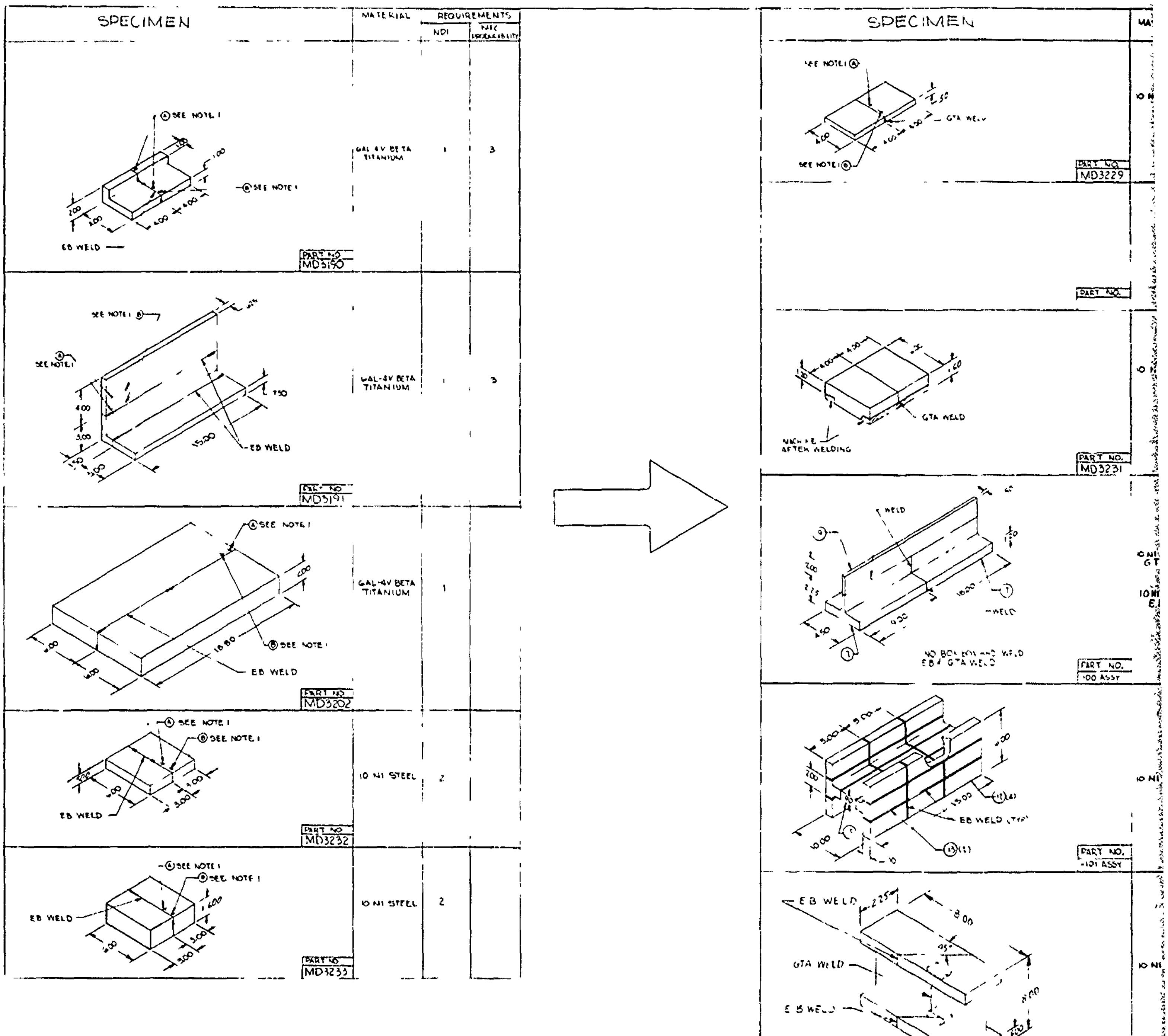


Figure 4-17 EB AND GTA WELDING NDI SPECIM

| ...IMEN | MATERIAL | REQUIREMENTS NDI | REQUIREMENTS MFG PRODUCABILITY |
|---|---|---|---|
| GTA WE... PART NO. MD3229 | 10 NI STEEL | 2 | |
| PART NO. | | | |
| GTA WELD PART NO MD3231 | 10 NI STEEL | | 2 |
| ...WELD NO BOX ... WELD EB / GTA WELD PART NO 100 ASSY | 10 NI STEEL GTA WELD<br>10 NI STEEL EB WELD | | 2<br>2 |
| EB WELD (TYP) PART NO. -101 ASSY | 10 NI STEEL | | 1 SEE NOTE 3 |
| PART NO -102 ASSY | 10 NI STEEL | | 2 SEE NOTE 2 |

SELECTED REF PARTS

3. MFG PRODUCABILITY SPECIMEN WILL BECOME NDI SPECIMEN UPON COMPLETION

2. MFG PRODUCABILITY SPECIMEN MAY BECOME NDI SPECIMEN UPON COMPLETION

1. INDUCED FLAWS

| HOLE | TYPE | SIZE |
|---|---|---|
| A | FBH | 1/64 DIA |
| B | FBH | 2/64 DIA |

NOTES (EXCEPT AS SHOWN)

PRELIMINARY DESIGN DRAWING

EB AND GTA WELDING NDI SPECIMENS

GENERAL DYNAMICS Convair Aerospace Division

603R231

WELDING NDI SPECIMENS

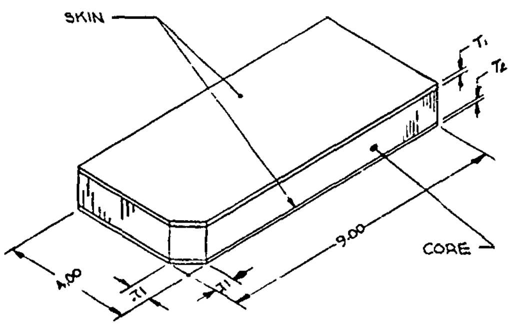


| SPECIMEN | PART NO. | MATERIAL: SKIN | MATERIAL: CORE | GAGE: $T_1$ | GAGE: CORE | GAGE: $T_2$ | QUANTITY REQUIRED |
|---|---|---|---|---|---|---|---|
| | MD3196 | 6AL-4V MILL ANNEALED | | .063 | | .063 | 1 |
| | MD3195 | 6AL-4V MILL ANNEALED | | .090 | | .032 | 1 |
| | MD3249 | BETA C | | .125 | | .040 | 3 |
| | MD3266 | 2024 ALUMINUM | | .200 | 1" THK | 075 | 3 |
| | MD3256 | | | .125 | | .025 | 2 |
| | MD3267 | | | .080 | | .025 | 3 |
| | MD3258 | | | .035 | | .025 | 2 |
| | MD3268 | | | .125 | | .040 | 3 |
| | MD3260 | | | .190 | | .032 | 2 |
| | MD3272 | | | .130 | | .032 | 3 |
| | MD3269 | | | .050 | | .032 | 2 |
| | MD3262 | | | .300 | | .050 | 3 |
| | MD3271 | | | .250 | | 050 | 2 |
| | MD3270 | | | .150 | | .050 | 3 |
| | MD3264 | | | .090 | 1" THK | .050 | 2 |
| | MD3259 | | | .300 | 2" THK | 063 | 3 |
| | MD3261 | | | .213 | | .063 | 2 |
| | MD3263 | 2024 ALUMINUM | | .125 | 2" THK | .063 | 3 |
| | MD3257 | 6AL-4V MIL ANNEALED | | .25 | 1" THK | .030 | 2 |
| | MD3265 | | | .135 | | .030 | 3 |
| | MD3278 | | | .060 | | .030 | 2 |
| | MD3279 | | | 135 | | 060 | 3 |
| | MD3280 | | | .185 | | .060 | 2 |
| | MD3281 | 6AL-4V MIL ANNEALED | | .300 | 1" THK | 060 | 3 |

PRELINARY TECHNIQUE SELECTION

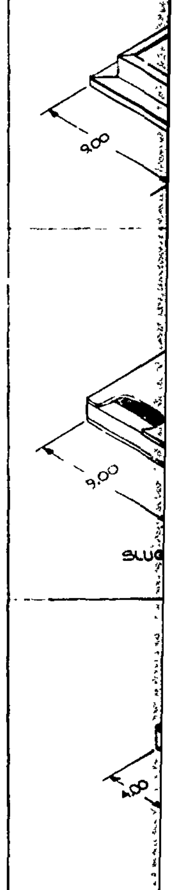


Figure 4-18 BONDED SANDWICH NDI SPECIM

TITY
UIRED

PRELIMINARY TECHNIQUE SELECTION

| SPECIMEN | PART NO. | MATERIAL | QUANTITY REQUIRED |
|---|---|---|---|
| 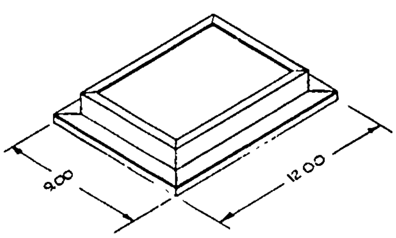  | | 2024 ALUMINUM | 30 |
| | | 6AL-4V MILL ANNEALED TI | 10 |
| 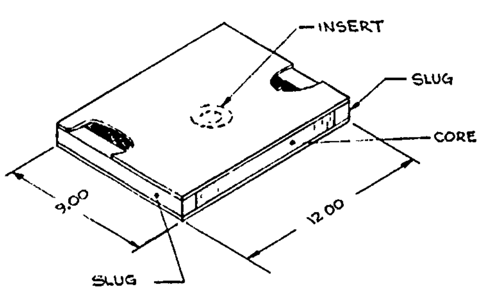  | | 2024 ALUMINUM | 10 |
| 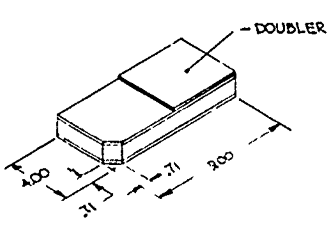  | | TITANIUM AND ALUMINUM AS REQUIRED TO EXTEND PRELIMINARY DEVELOPMENT | 15 |

SELECTED PANELS FOR INSPECT REF PARTS

3. DETAILED CONSTRUCTION AND QUANTITY DETERMINED BY PRELIMINARY RESULTS, DESIGN ITERATION AND INSPECTION CRITERIA

2. FLAW TYPES - TEFLON TAPE INSERTS, OTHER TYPES AS REQUIRED

1. USE PL717 ADHESIVE FOR ALL PANELS

NOTES (EXCEPT AS SHOWN)

PRELIMINARY DESIGN DRAWING

BONDED SANDWICH NDI SPECIMENS

GENERAL DYNAMICS
Convair Aerospace Division
Fort Worth Operation

603R232

Figure 4-18 BONDED SANDWICH NDI SPECIMENS

# SECTION 5

# MANUFACTURING DEVELOPMENT

The manufacturing development effort during Phase II was primarily concerned with manufacturing methods development, fabrication of engineering and production verification test specimens, and design support consultation. Phase II tasks accomplished through 15 March 1973 were reported in AFFDL-TR-73-70 and accomplishments through 15 July 1973 were reported in AFFDL-TR-73-77.

## 5.1 LAMINATED BRAZING PROCESS DEVELOPMENT

Work accomplished since the second interim report, 15 July 1973, includes brazing one 603FTB033 damage tolerance, braze lower plate element test specimen, two 603FTB053 center line splice lower plate brazed test specimens, and two 603FTB035 brazed lower plate damage tolerance test specimens. Also, special brazing parameter tests were run to resolve problems encountered in brazing the large area 603FTB035 parts.

### 5.1.1 603FTB033 Test Specimen, Damage Tolerance, Braze Lower Plate Element

The engineering test part consistedof three titanium details brazed with Ag-Al-Mn braze alloy. The upper and lower detailswere 0.600-inch thick with five equally spaced hog-outs and the center detailwas a solid plate 0.400-inch thick. Titanium details are shown in the photograph in Figure 5-1. The braze surface of the details were initially machined by face milling, then finished to final dimension by dry belt sanding. The complete detail lay-up in the braze box tooling is shown in Figure 5-2. Brazing was accomplished using standard procedures except a pre-braze cycle was run to flatten the titanium details. The pre-braze cycle and braze cycle are shown in the graphs in Figures 5-3 and 5-4. The part, after brazing is shown in Figure 5-5. Visual inspection of the part showed good alloy wetting and flow and the part relatively free of surface discoloration. X-ray and ultrasonic inspection was made and the part was sent to the engineering test lab for further testing.

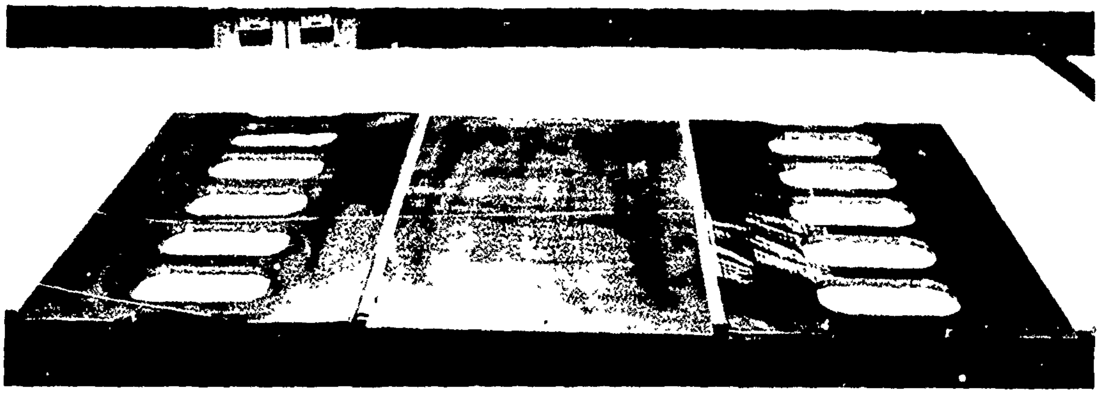

Figure 5-1 TITANIUM DETAILS FOR 603FTB033 BRAZE TEST SPECIMEN

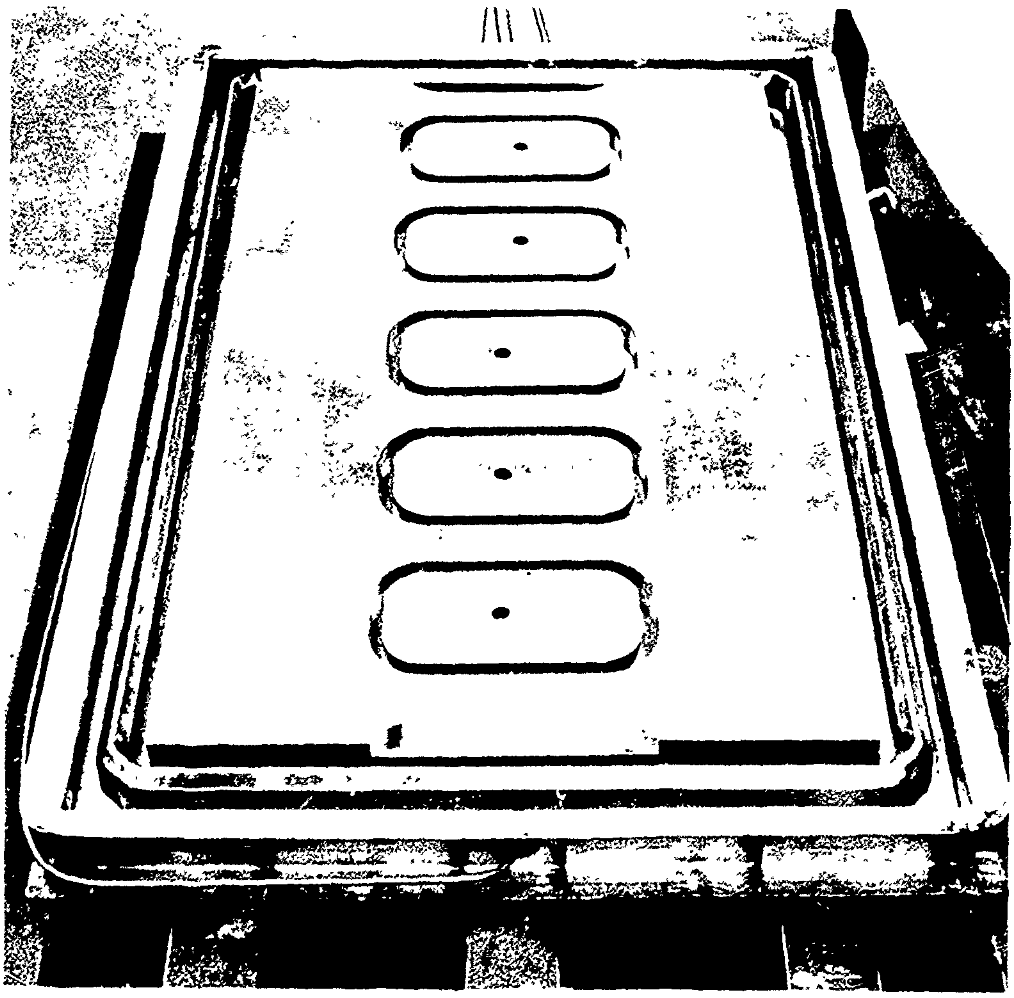

Figure 5-2 TITANIUM DETAILS FOR 603FTB033 BRAZE TEST SPECIMEN ASSEMBLED IN BRAZE BOX

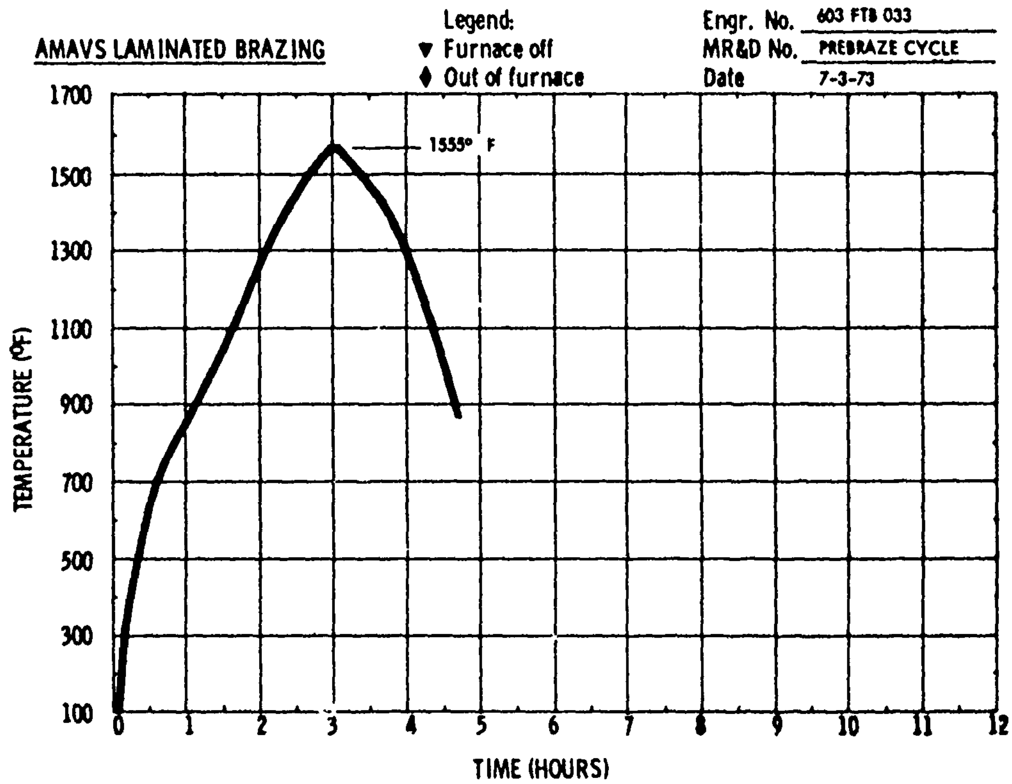


Figure 5-3 PREBRAZE CYCLE FOR 603FTB033 TEST SPECIMEN

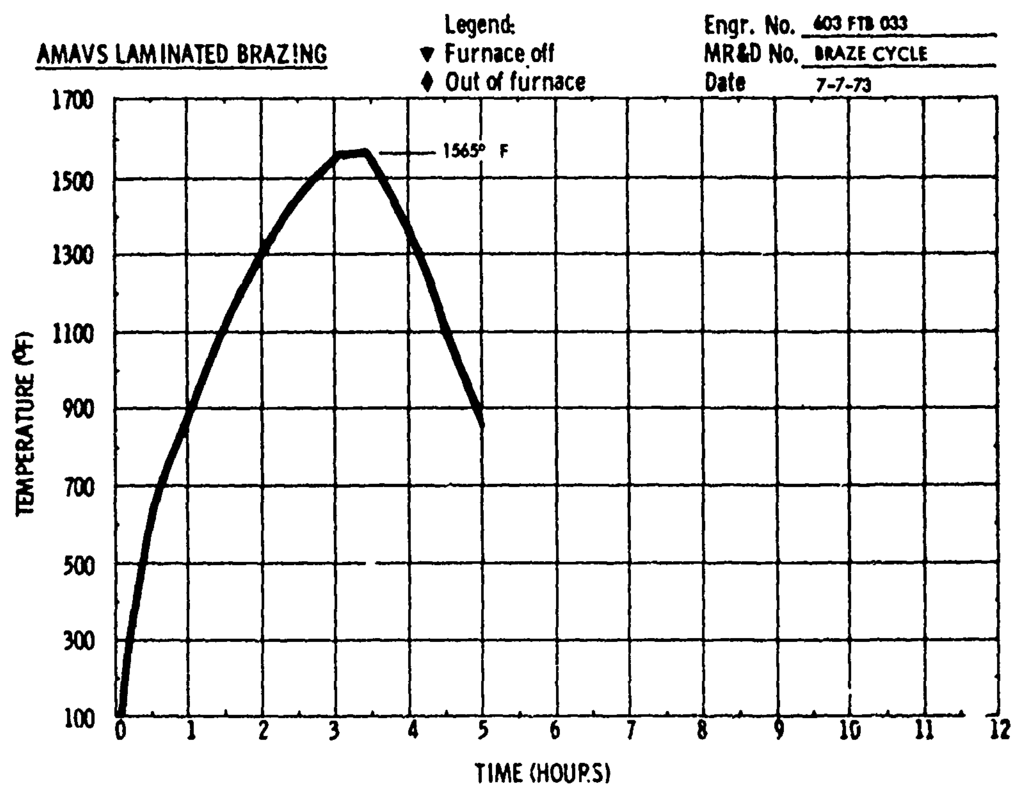


Figure 5-4 BRAZE CYCLE FOR 603FTB033 TEST SPECIMEN

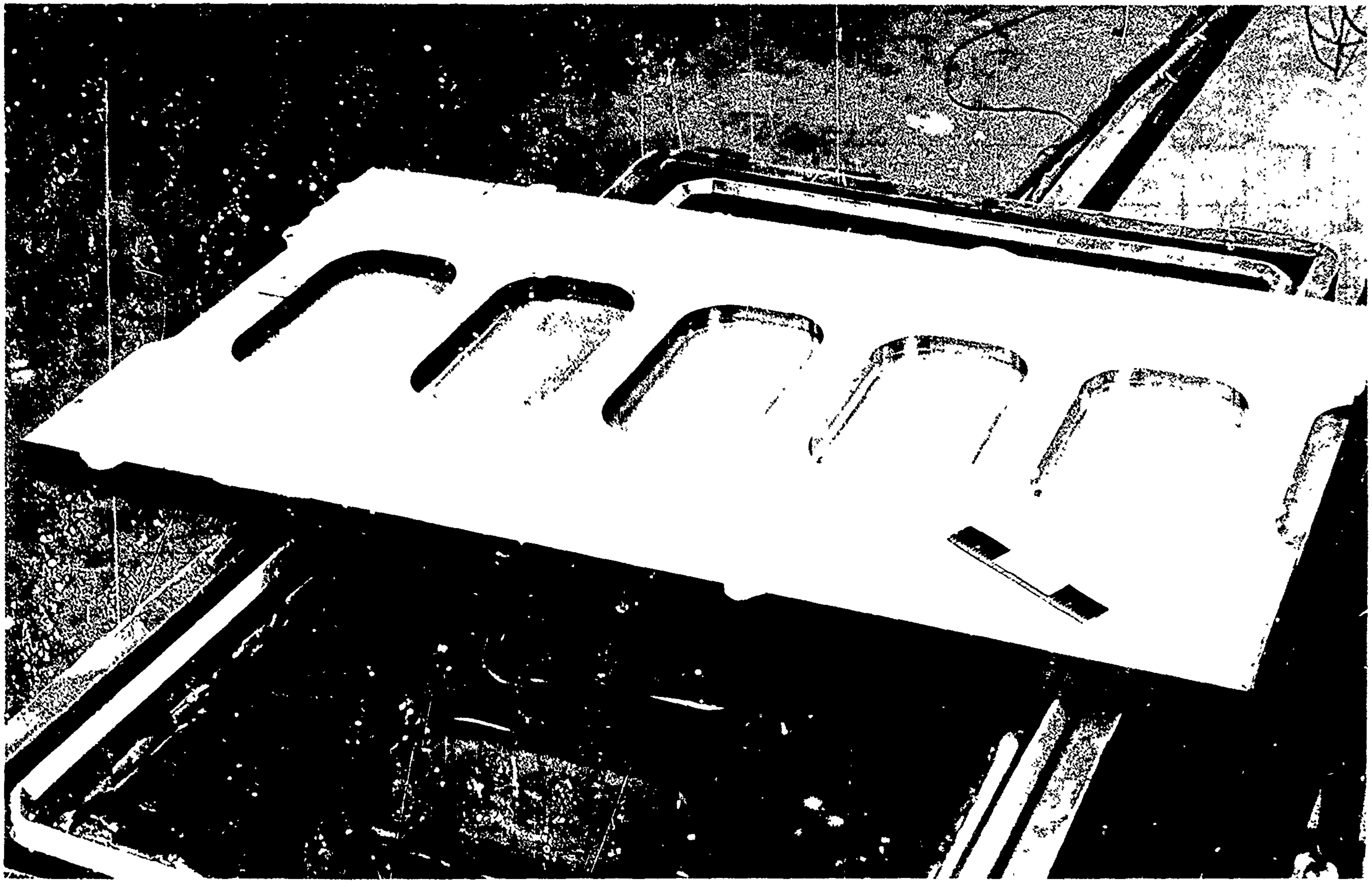

Figure 5-5 603FTB033 BRAZED TEST SPECIMEN AFTER REMOVAL FROM BRAZE BOX

4-53542

### 5.1.2 603FTB053 Braze Test Specimen Centerline Splice Lower Plate

Two 603FTB053 test parts were brazed using titanium details that were machined to thickness dimension by face milling followed by dry belt grinding. The part was a two-braze line component consisting of an upper and lower plate of 0.600-inch thick titanium and a center plate of 0.400-inch titanium. Standard cleaning and lay-up procedures were used and no difficulty was experienced throughout the braze operation. The photograph in Figure 5-6 shows the lower plate detail with 0.005-inch thick Ag-Al-Mn braze alloy tack welded in place. The braze cycle time/temperature curves for the two parts are shown in Figures 5-7 and 5-8. A part, after brazing, is shown in the photograp in Figure 5-9. Visual inspection of the parts showed good alloy wetting and flow with little surface discoloration. X-ray and ultrasonic inspection was made and the parts were sent to the engineering test lab for further evaluation.

### 5.1.3 603FTB035 Brazed Lower Plate Damage Tolerance Test Specimen

The brazed lower plate damage tolerance test specimen (603FTB035) is a double braze line component with dimensions of 1.60 inches x 48.0 inches x 114.3 inches. The part was several times larger in surface area than preceding brazed structures. The increased size and weight of the panel and braze tooling required additional development of both handling and brazing procedures. A pre-braze run and three braze runs established the necessary procedures for the production of a satisfactory brazed part. Each braze run is discussed separately below.

#### 5.1.3.1 Pre-braze Run for 603FTB035

A pre-braze cycle, simulating actual production, was run except that braze alloy was not used in the detail lay-up of the panel. The test was run to determine the effect of scale up on either tooling or the braze cycle. This test and all subsequent braze tests with 603FTB035 parts were run in the gas fired Holden-Pacific furnace shown in the photograph in Figure 5-10. Four .250/.250 x 7.5 x 12 inch test panels were brazed in the retort during the pre-braze cycle. The test panels were inserted in the hog-outs in the upper (-9) detail of the part. Six thermocouples were used in the test and locations are shown in the sketch in Figure 5-11. Time/temperature curves for the pre-braze cycle are shown in Figures 5-12 and 5-13. Components for the pre-braze cycle are shown in Figure 5-14 and the complete pre-braze procedure is shown below:

Figure 5-6 LOWER PLATE TITANIUM DETAIL OF 603FTB033 TEST SPECIMEN WITH BRAZE ALLOY TACK WELDED IN PLACE

4-53831

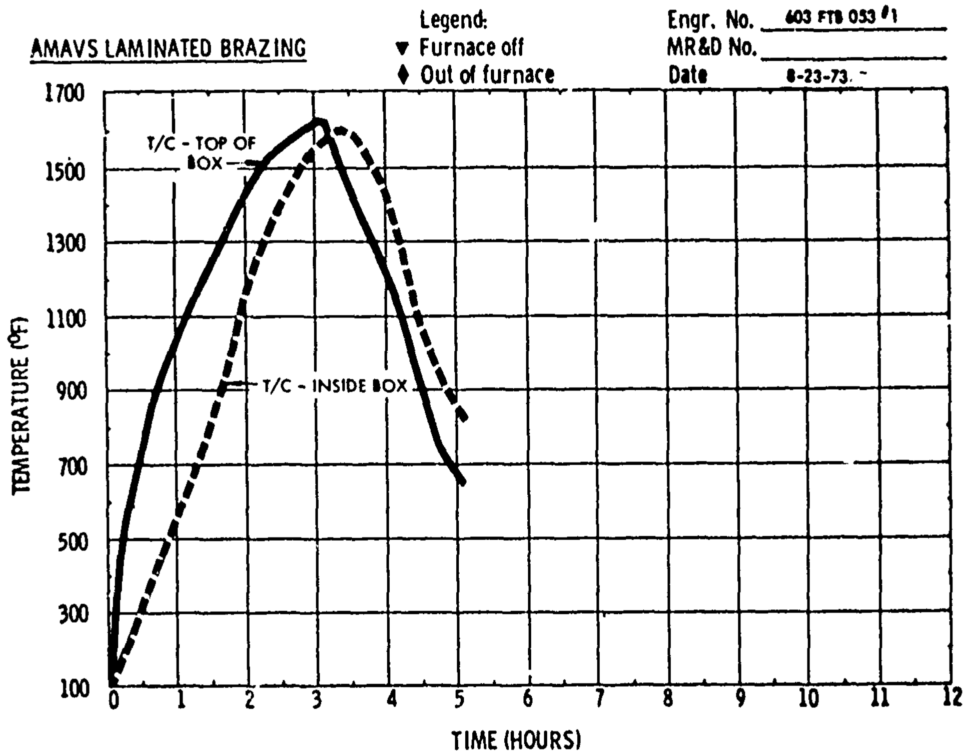


Figure 5-7 BRAZE CYCLE FOR 603FTB053 RUN #1

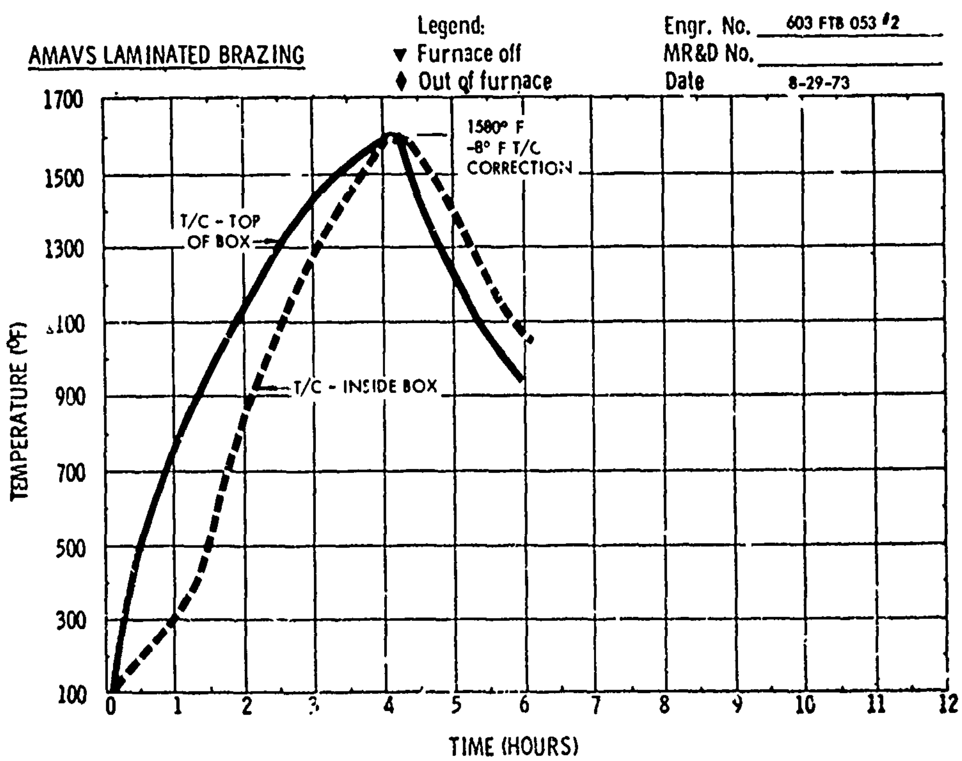


Figure 5-8 BRAZE CYCLE FOR 603FTB053 RUN #2

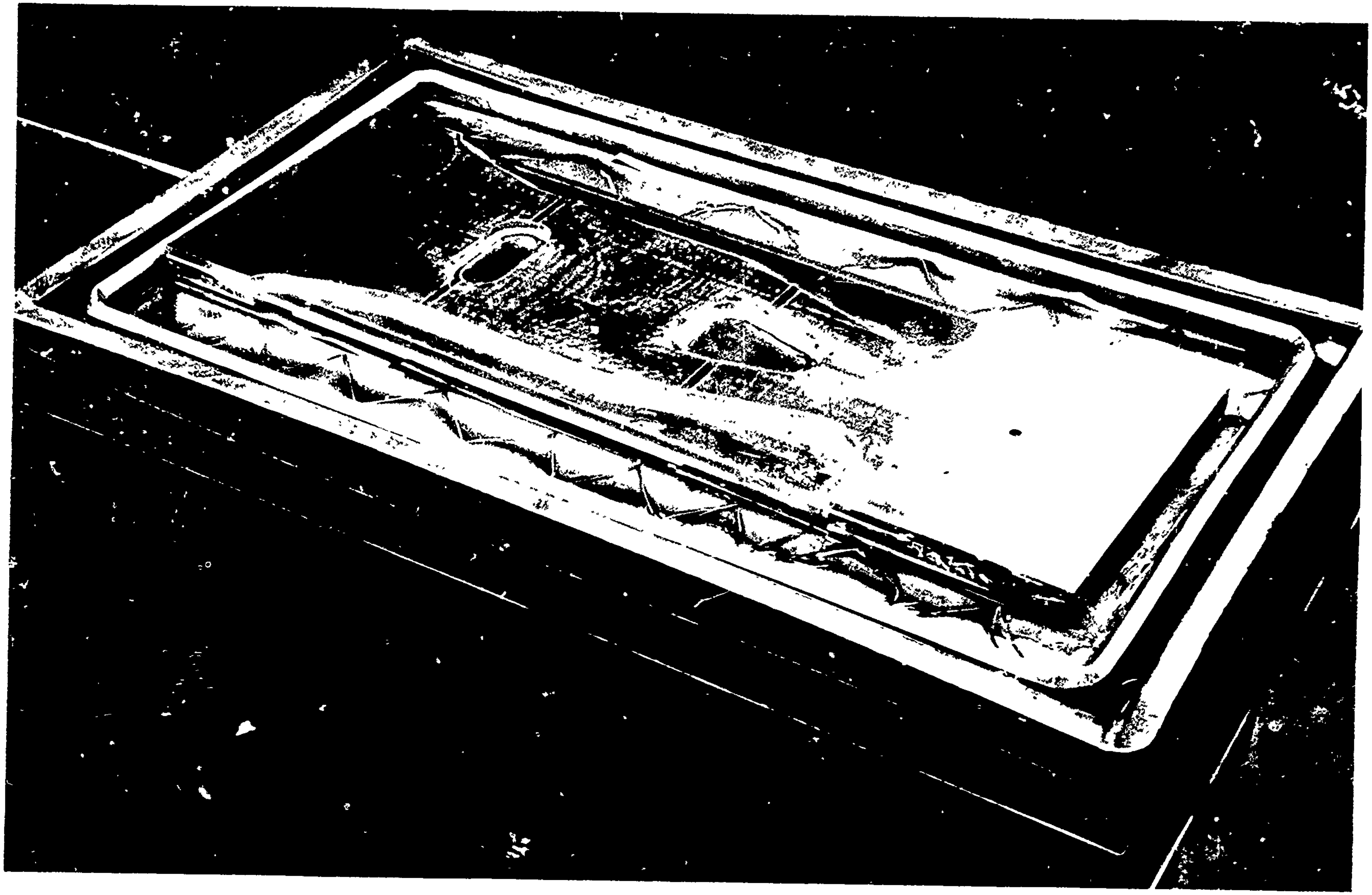

Figure 5-9 BRAZED TEST SPECIMEN 603FTB053 IN BRAZE BOX TOOLING

4-54075

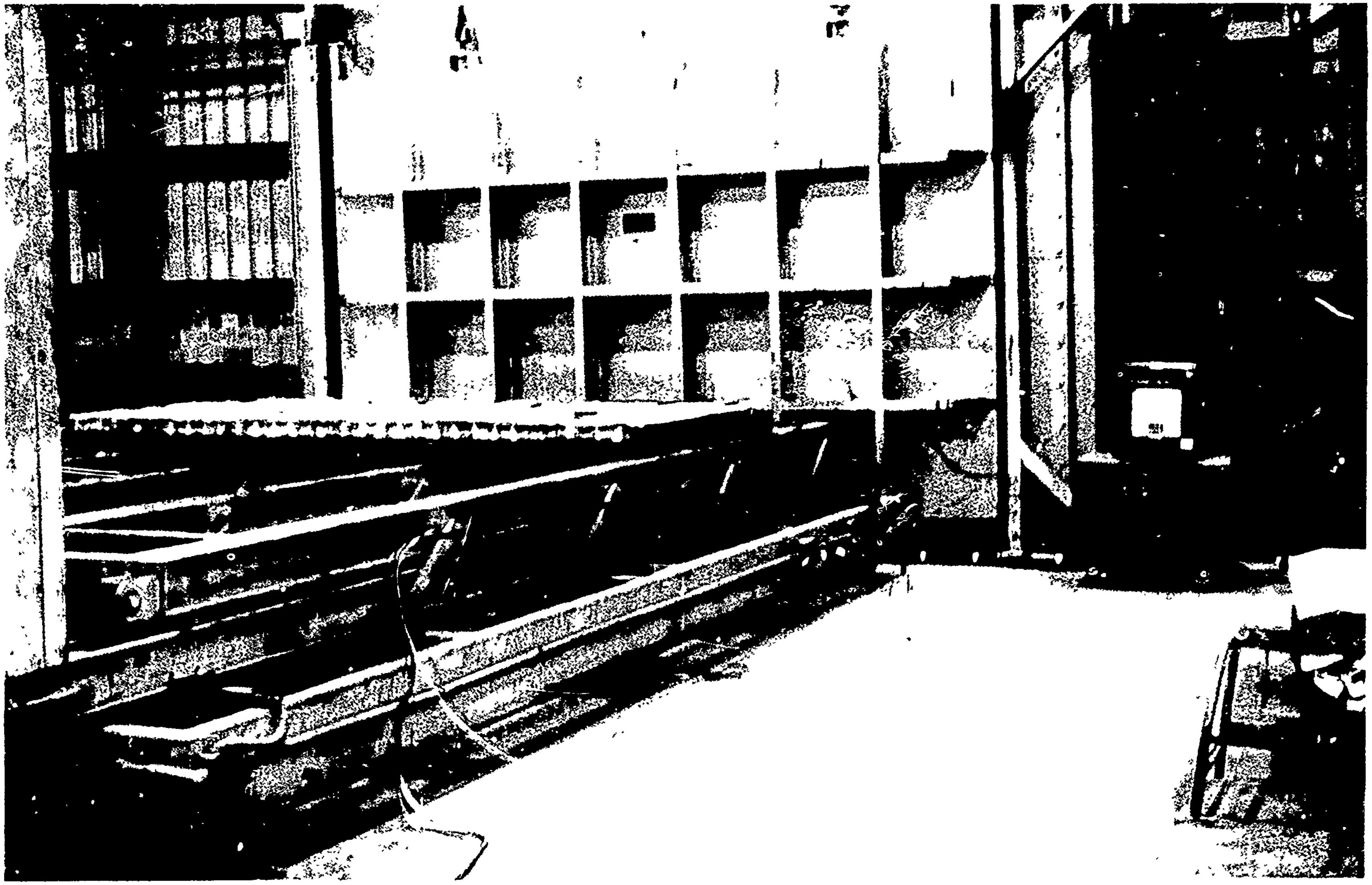

Figure 5-10 GAS FIRED HOLDEN PACIFIC FURNACE FOR BRAZING 603FTB035 TEST SPECIMENS

4-53792

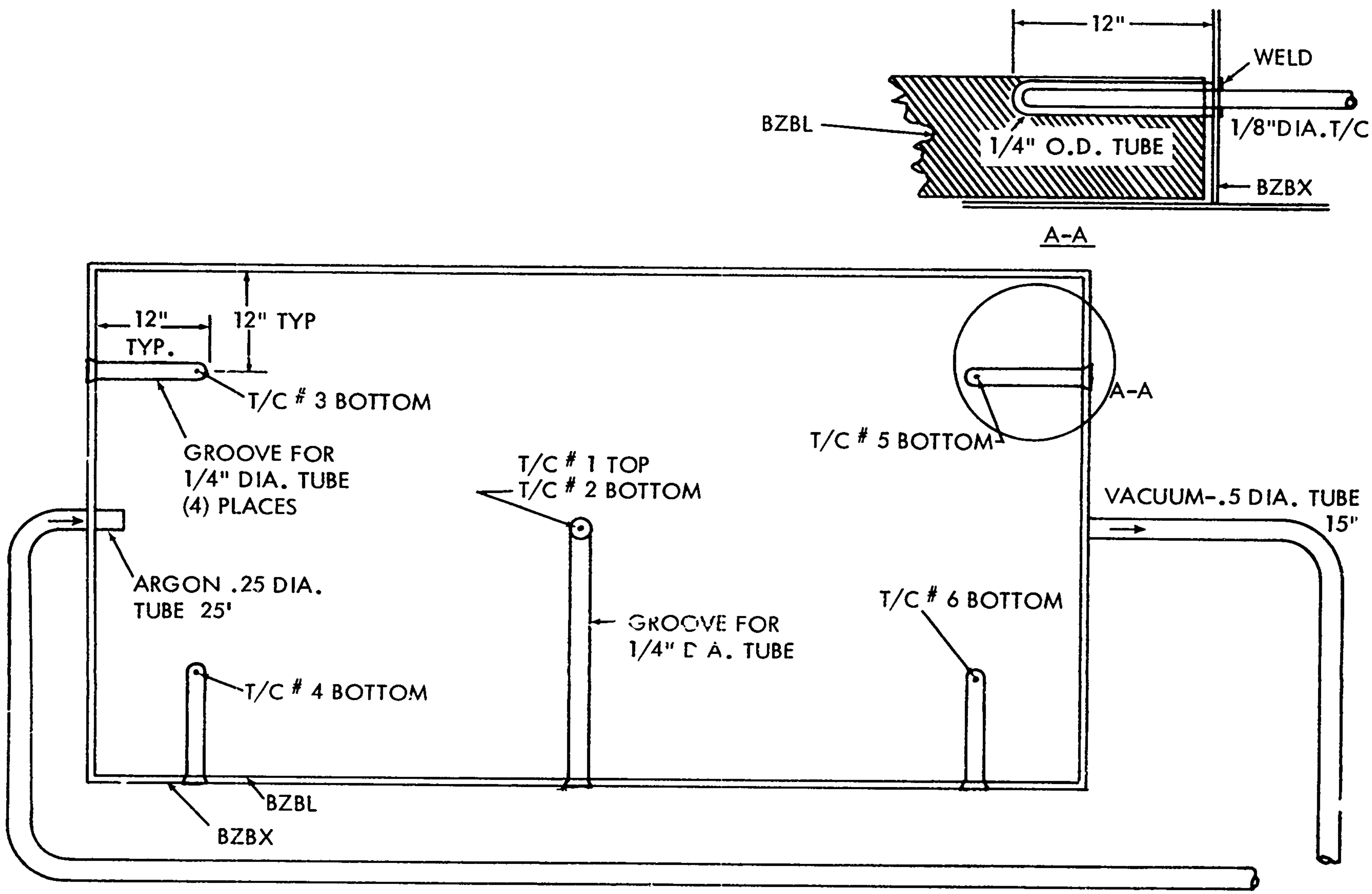


Figure 5-11 THERMOCOUPLE LOCATIONS FOR 603FTB035
TEST PART PREBRAZE CYCLE

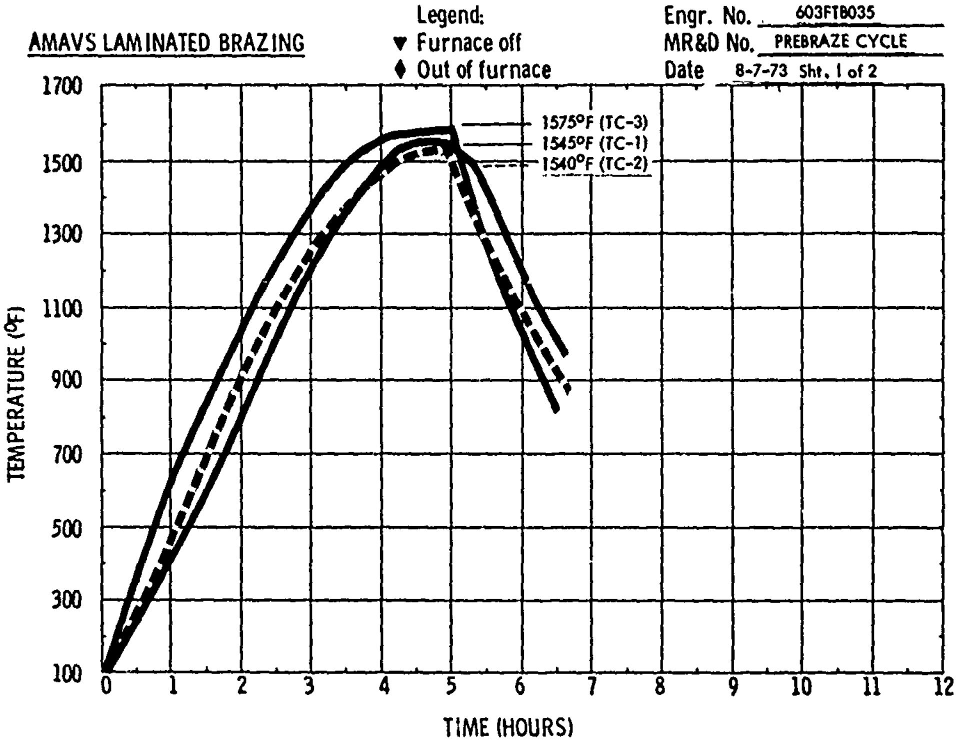


Figure 5-12 PREBRAZE CYCLE FOR 603FTB035 TEST SPECIMEN
THERMOCOUPLES 1, 2, AND 3

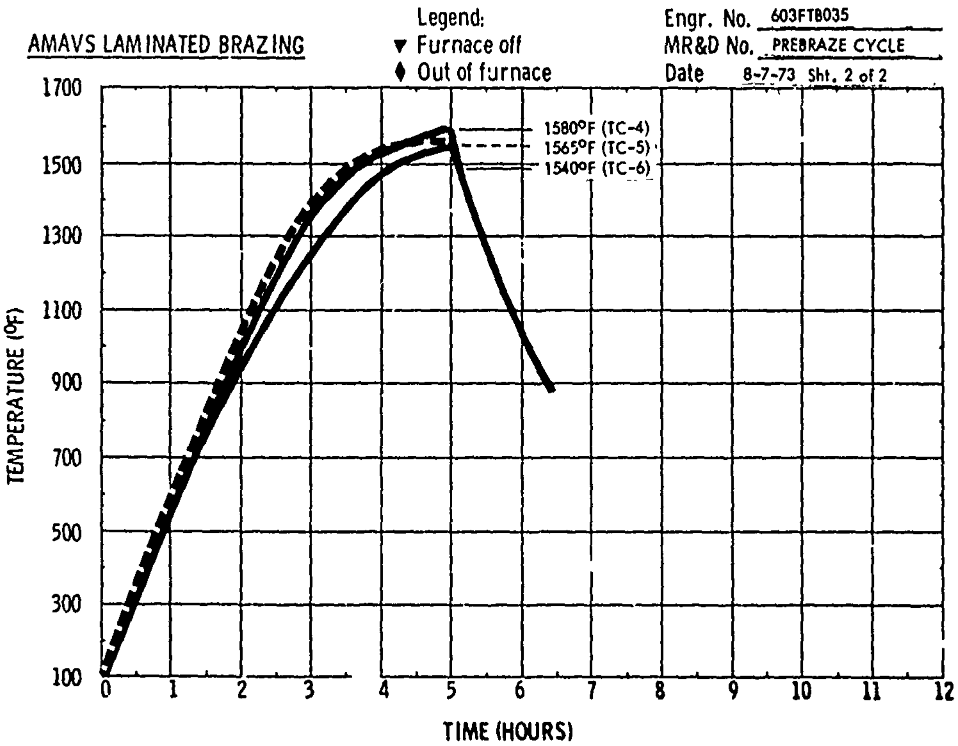


Figure 5-13 PREBRAZE CYCLE FOR 603FTB035 TEST SPECIMEN
THERMOCOUPLES 4, 5, AND 6

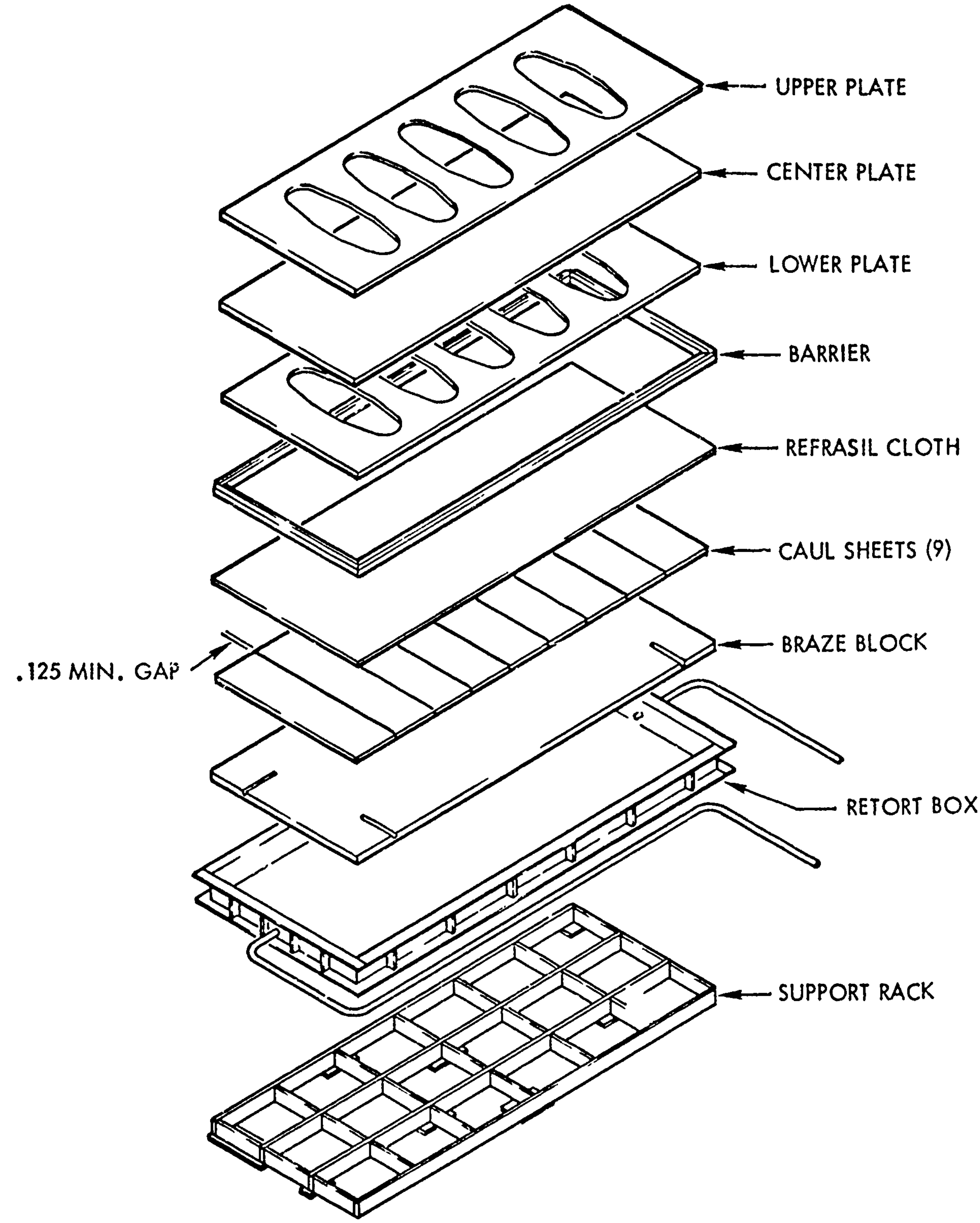


Figure 5-14 TOOLING AND TEST SPECIMEN COMPONENTS OF 603FTB035 PREBRAZE CYCLE

1. Preclean braze box and braze block using cheesecloth and acetone or distilled isopropyl alcohol.

2. Locate braze block in braze box. Use the required thickness shims around the perimeter of the block to prevent slipping.

3. Locate (5) 1/4 inch O.D. tubes in slots of braze block and weld to box.

4. Clean surface of block with cheesecloth and acetone. Use clean cotton gloves.

5. Clean (9) pieces of 0.062-inch thick caul sheets. Use Cheese-cloth and acetone. Paint bottom surface of sheets with stop-off.

6. Locate caul sheets on braze block with a minimum of 1/8 inch gap between each sheet. Tack weld sheets together with 0.002 x 0.5-inch stainless steel strips.

7. Place refrasil cloth over caul sheets and braze block.
   Note: Refrasil to be the same size as the braze block. This sheet of refrasil cloth does not require prebaking.

8. Clean atmosphere barrier with acetone and cheesecloth. Locate in braze box.

9. Clean 603FTB035-9 detail with acetone or distilled isopropyl alcohol. Locate the -9 plate in box equally spaced inside the atmosphere barrier.

10. Fabricate spacers to fit between the barrier and the -9 plate. Make spacers from 0.100-inch 321 stainless steel.

11. Clean spacers with acetone and cheesecloth. Locate spacers laying flat around the perimeter of the -9 part.
    Note: These spacers are to prevent the barrier from warping and pulling in toward the panel.

12. Remove the refrasil cloth from each cutout in -9 detail part.

13. Clean (8) filler blocks with acetone and cheesecloth. Locate filler block in hog-outs in the -9 detail.

14. Locate refrasil cloth over the -9 detail.
    Note: This refrasil cloth must be baked out at 1550°F for 5 minutes prior to lay-up.

15. Clean the -11 detail with acetone or alcohol and cheesecloth. Locate on top of the -9 detail.

16. Locate refrasil cloth over the -11 detail.
Note: This refrasil cloth must be baked out at 1550°F for 5 minutes prior to lay-up.

17. Clean the top -9 detail with acetone or distilled isoprophyl alcohol and cheesecloth. Locate on top of the -11 detail.

18. Clean (12) filler blocks with acetone and cheesecloth. Locate in slots per following sketch. Place 0.002-inch thick stainless steel foil under each 7.5 x 12 inch panel and crimp up the corners to trap any excess alloy run out.

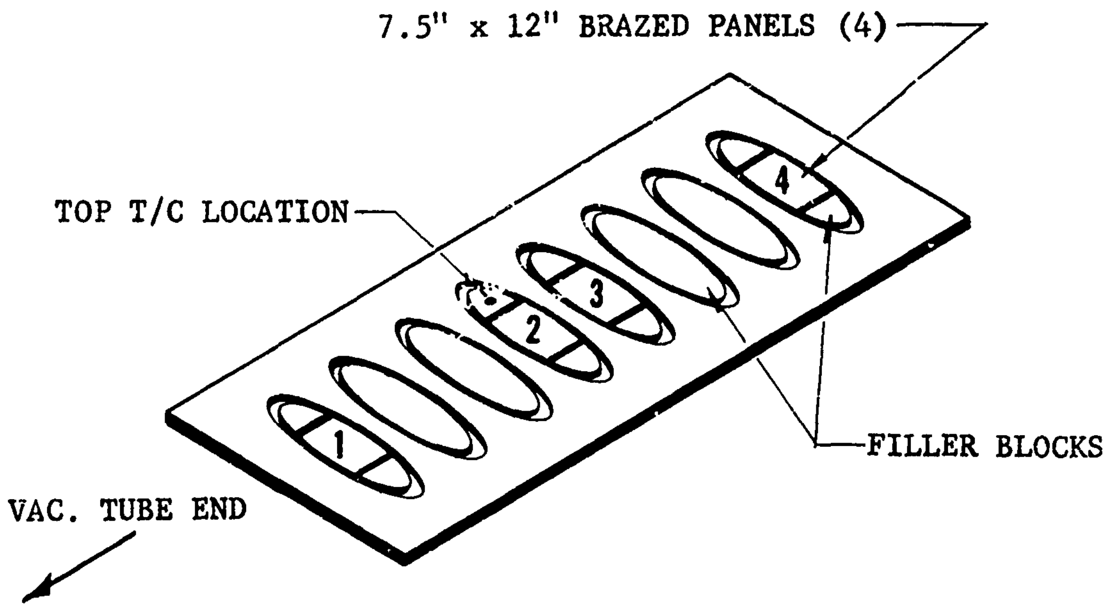


19. Clean (8) detail parts 0.250 x 7.5 x 12 inch 6Al-4V titanium with acetone and cheesecloth. Acid clean details per cleaning procedure for brazing.

20. Prefit alloy and punch 5/32 diameter holes on 3 inch centers for spacers.

21. Clean alloy to remove any oxides. Use steel wool or silicon carbide 320 grit sand paper. Note: When using steel wool, accomplish cleaning on table away from titanium details.

22. Clean alloy with acetone and cheesecloth.

23. Lay-up alloy and locate spacer buttons in four panels 7.5 x 12 inch. Tack weld a 0.002 x 0.375-inch stainless steel strip around the perimeter of each panel. Vibro etch number each panel No. 1-2-3-4-.

24. Locate panels in the hog outs of the -9 plate per above sketch. Place 1-inch sine wave strips of titanium inside and outside of the atmosphere barrier.

25. Locate refrasil cloth on top of panel. Cut the refrasil cloth into strips to match the steel caul sheets under the panel, leave a minimum of 1/8-inch gap between the strip. Note: Refrasil cloth to be the same size as the panel. This sheet of refrasil does not require prebaking.

26. Locate vacuum sheet and trim to size.

27. Weld vacuum sheet to braze box.

28. Check for leaks.

29. Argon purge braze box 15 cycles (hold maximum vacuum 3 minutes each cycle, then back fill with argon) and then maintain maximum vacuum.

30. Locate (5) 1/8-inch diameter Inco sheath chromel-alumel thermocouples 25 feet long into tubes in sides of braze box. Wedge thermocouples into the 1/4-inch diameter tubes. Locate and secure a 25-foot thermocouple in the 1/4-inch diameter x 0.400-inch tube on top of the box.

31. Place (2) layers of 1/4-inch fiberfrax on top of vacuum sheet. Secure by placing several pieces of 1/4 or 3/8-inch steel on top of fiberfrax. Note: Wind turbulence is fairly strong inside the furnace.

32. Furnace should be leveled out at 1000°F to 1200°F. Place retort in furnace and increase furnace controls to 1600°F. Make individual recordings on each thermocouple.

33. Preheat at 1550°F for 5 minutes. Note: When lowest thermocouple reaches 1545°F turn furnace control back to 1000°F. When lowest thermocouple reaches 1550°F open furnace door. Maintain a vacuum of 15 in. HG and 5 C.F.H. argon. Turn argon off at 800°F.

34. Furnace cool to 1400°F.

35. Remove from furnace and cool to room temperature.

36. Remove assembly from retort box.

37. Save the refrasil cloth for use in the braze cycle. Remove all filler blocks f om hog-outs and clean for use in the braze cycle.

38. Do not remove the 0.100-inch thick caul sheets, the bottom layer of refrasil cloth, or the atmosphere barrier.

39. Remove all thermocouples and forward to the cal. lab for calibration.

40. Grind flanges of the braze box. Make a new vacuum sheet for use on the braze cycle.

Braze Surface Preparation for 603FTB035 and 603FTB053

The braze surfaces of titanium details for 603FTB035 were prepared by face milling to within 0.060 + .030 -.000 inch of nominal blueprint dimension and finished to final dimension by wet precision belt sanding. Sanding was done at Mill Polish Corp., Del Air, N. J. Final detail thickness was within +.008 -.000 of nominal blueprint dimension. Surface finish was measured at 38 to 50 RMS.

Details for 603FTB053 were also face milled, then finished to final dimension by dry belt sanding using 80 to 180 grit belts. Parts were face milled to +.010 -.000 inch of nominal blueprint dimension and about .002 inch removed from each surface by dry sanding.

The pre-braze cycle test demonstrated that the tooling, furnace, and support equipment functioned properly and indicated that there would be no serious problems in brazing a 603FTB035 part.

5.1.3.2 First Braze Run - 603FTB035

The braze surfaces of the three titanium details for 603FTB035 were prepared by face milling to within 0.060 + 0.030 - 0.000 inch of nominal blueprint dimension and finished to final dimension by wet precision belt grinding. Grinding was done at Mill Polish Corp., Del Air, N. J. Final detail thickness w.. within + 0.008

-0.00 of nominal blueprint dimension. Surface finish was measured at 38 to 50 RMS. The remaining procedure and braze cycle was accomplished as follows:

Procedure and Braze Cycle for First 603FTB035 Braze

1. Remove all oxides from surfaces of the -9 and -11 details. Use vibro sander with 320 grit paper.

2. Acetone clean details - use clean cheesecloth.

3. Acid clean details, reference P.S. 40.01-25 section 2, using the following cleaning procedure.

   a. Wipe with clean cheesecloth and acetone to remove light oils and fingerprints. Handle parts with clean cotton gloves after this operation until brazing has been completed.

   b. Attach parts to cleaning rack then complete the following operations:

      o Alkaline soak* -180 $\pm$ 10$^{o}$F, 15 minutes.

      o Hot rinse -180 $\pm$ 10$^{o}$F, 5 minutes.

      o Nitric-hydrofluoric pickle** - Room temperature, 1 minute.

      o Cold rinse - Room temperature, 45 seconds.

      o Repeat the pickling and rinsing operations until a total of 5 cycles have been completed.

      o Nitric acid desmut*** - Room temperature, 5 minutes.

      o Deionized water rinse - Room temperature, 5 minutes.

      o Allow parts to drip dry. Clean cheesecloth may be used, as a wick, to remove water from depressions that will not drain easily.

      o Remove wires from parts. Wrap in clean brown paper, and forward to lay-up area.

* Sodium hydroxide 32-48 oz./gal.

** Nitric acid (29-31% by wt.) + hydrofluoric acid (2.4-3.2% by wt.)

Note: The hydrofluoric content stated above is contained in the initial tank charge. A periodic test of the active fluroides is made by etching titanium test coupons. Weight loss from the etched coupons is converted to thickness. The solution is maintained in a range that removes titanium at the rate of .022 to .028 mils/side/minute.

*** Nitric acid 35-64% by wt.

4. Check braze box to see that the caul sheets and refrasil cloth are in the correct location.

5. Prefit and trim the brazing alloy to fit the lower -9 plate. Punch 5/32-inch diameter holes on three-inch centers in the brazing alloy for the 1/8-inch diameter 0.002-inch thick stainless steel spacers.

6. Locate and tack the braze alloy and spacers to the -9 plate. Reference the following sketch for layout of the alloy. Do not overlap the alloy joints.

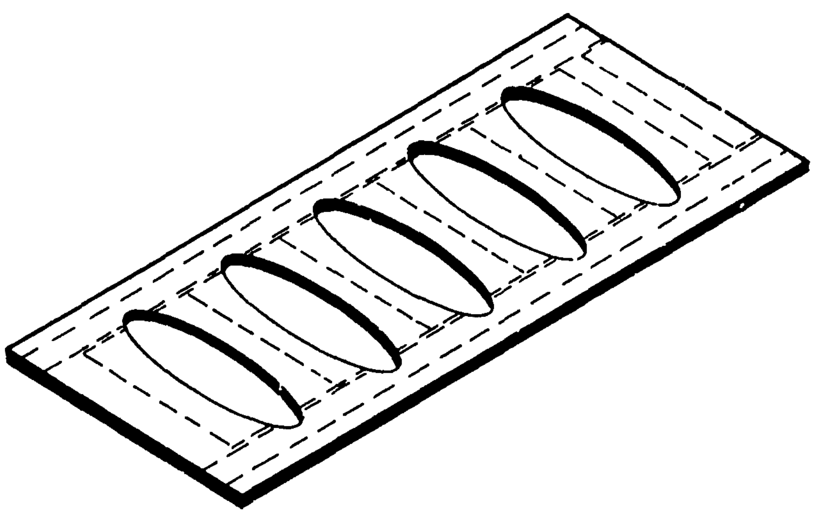

7. Locate the -9 plate in braze box. Equally space the plate inside the atmosphere barrier.

8. Locate the 0.100-inch thick shims around the perimeter of the -9 plate to prevent the atmosphere barrier from warping in toward the panel.

9. Locate filler blocks in hog-outs of -9 plate. Place refrasil cloth on top of each filler block.
   Note: All refrasil cloth used in the braze cycle must be baked before using in braze box. Do not use stainless steel retainer strips around the perimeter of the hog-outs.

10. Inspect the -11 plate for water marks or other contamination. Remove any contamination with distilled isopropyl alcohol and clean cheesecloth.

11. Locate the -11 plate on top of the -9 lower plate.

12. Punch 5/32-inch holes in the alloy. Tack alloy to the surface of -11 plate. Locate and tack 0.002-inch thick x 1/8 inch dia. stainless steel spacers in each hole in the alloy.

13. Locate the -9 upper plate on top of the -11 center plate. Scribe the braze alloy around the perimeter of each hog-out in -9 plate. Remove -9 plate and trim out alloy to the scribe lines.

14. Relocate the -9 upper plate in the braze box.

15. Tack weld a 0.002 x 1-inch stainless steel strip over the braze joints around the perimeter of the parts.

16. Place prebaked refrasil cloth in the bottom of each hog-out. Do not use 0.002-inch stainless steel retainer strips around the inside of the hog-outs.

17. Acetone clean the filler blocks and locate in the center of the hog-outs.

18. Preform a 1 inch wide titanium ribbon into a sinewave configuration and place in braze box. Ribbon is required both inside and outside of the atmosphere barrier.

19. Locate refrasil cloth on top of panel. Cut the refrasil cloth into strips to match the steel caul sheets under the panel; leave a minimum of 1/8-inch gap between the strips. This refrasil cloth must be prebaked.

20. Locate vacuum sheet and trim to size.

21. Weld vacuum sheet to braze box.

22. Check for leaks.

23. Argon purge braze box 15 cycles. Hold maximum vacuum 3 minutes each cycle, then back fill with argon. Hold at maximum vacuum.

24. Locate (5) 1/8"-diameter Inco sheath chromel-alumel thermocouples 25 feet long into tubes in sides of braze box. Wedge thermocouples into the 1/4-inch diameter tubes. Locate and secure a 25 foot thermocouple in the 1" x 8" x 8" steel block on top of box.

25. Place (2) layers of 1/4 inch fiberfrax on top of vacuum sheet. Secure by placing several pieces of 1/4 or 3/8-inch steel on top of fiberfrax.
Note: Wind turbulence is fairly strong inside the furnace. Place one layer of fiberfrax inside the "C" channels of the braze box.

26. Furnace should be leveled out at 900°F. Place retort in furnace and increase furnace controls to 1600°F. Make individual recordings on each thermocouple.

27. Preheat at 1550°F for 5 minutes.
Note: When lowest thermocouple reaches 1545°F turn furnace control back to 1000°F. When lowest thermocouple reaches 1550°F open furnace door. Maintain a vacuum of 15 in. Hg and 5 C.F.H. argon. Turn argon off at 800°F.

28. Furnace cool to 1400°F.

29. Remove from furnace and cool to room temperature.

30. Remove assembly from retort box.

The entire brazing procedure was completed with little difficulty and no apparent problems; however, tests of the part showed an inadequate braze. X-ray and NDI inspection indicated a heavy concentration of braze line irregularities, especially between the middle and lower details in the area of the hog-outs. Destructive testing showed what appeared to be a "cold braze" with a lack of alloy flow and insufficient melt. The braze surface of the titanium details also appeared to be contaminated. All thermocouples indicated sufficient temperature for brazing based on results of previous tests. Thermocouple locations are shown in the sketch in Figure 2. Braze cycle time/temperature graphs are shown in Figures 5-15 through 5-20.

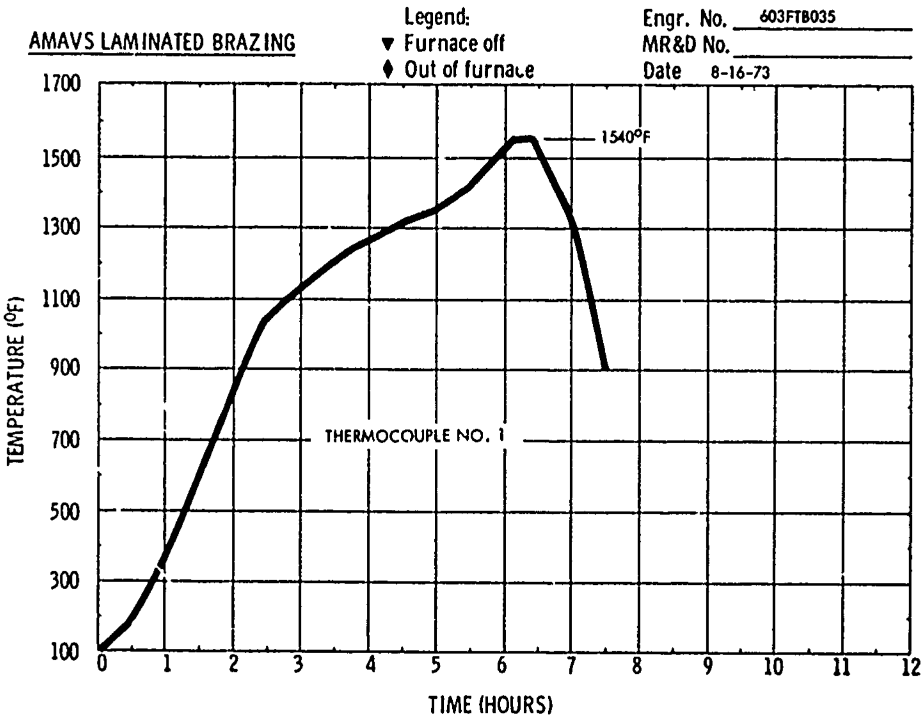


Figure 5-15 BRAZE CYCLE FOR 603FTB035 TEST SPECIMEN
RUN #1 THERMOCOUPLE NO. 1

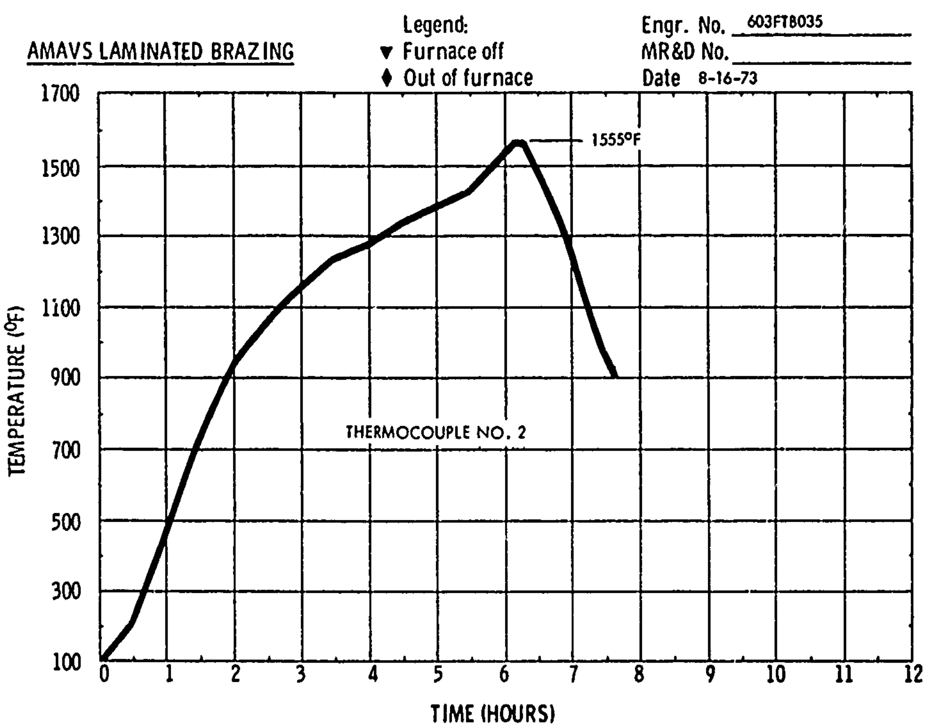


Figure 5-16 BRAZE CYCLE FOR 603FTB035 TEST SPECIMEN
RUN #1 THERMOCOUPLE NO. 2

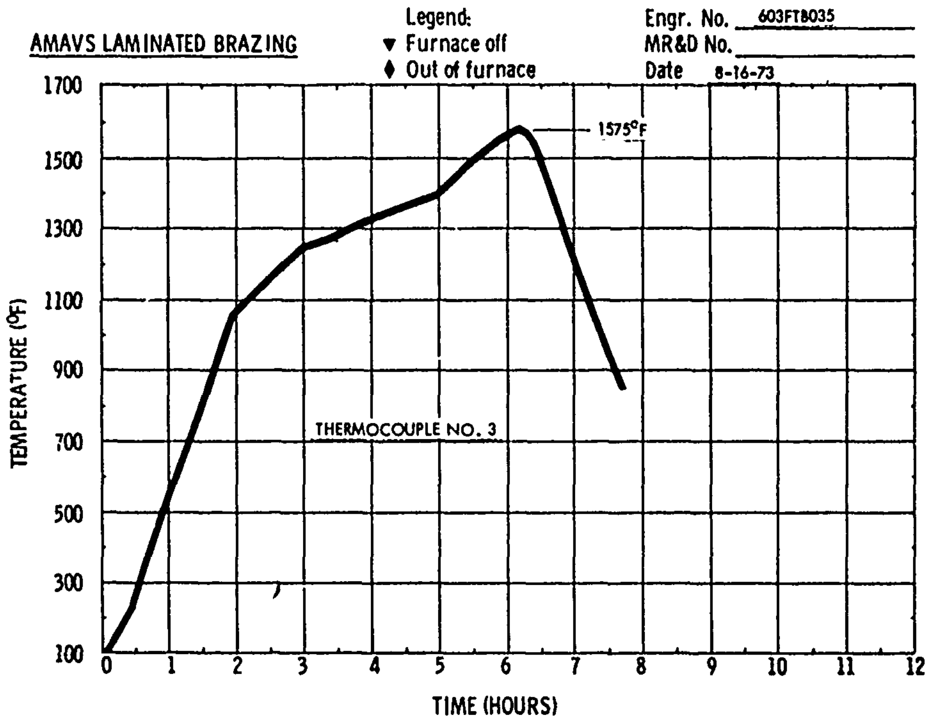


Figure 5-17 BRAZE CYCLE FOR 603FTB035 TEST SPECIMEN RUN #1 THERMOCOUPLE NO. 3

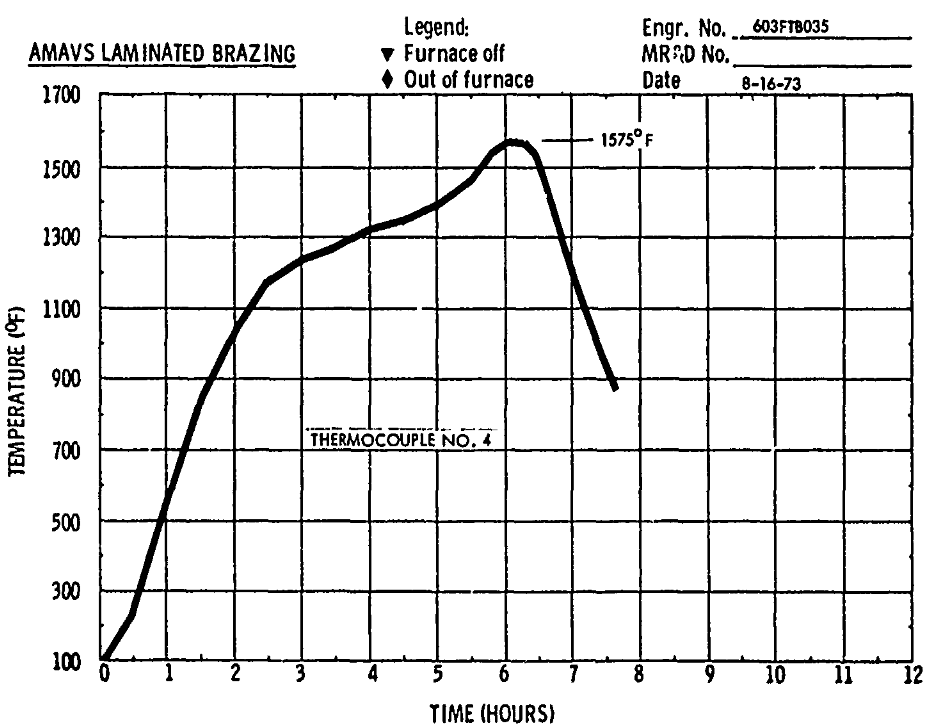


Figure 5-18 BRAZE CYCLE FOR 603FTB035 TEST SPECIMEN RUN #1 THERMOCOUPLE NO. 4

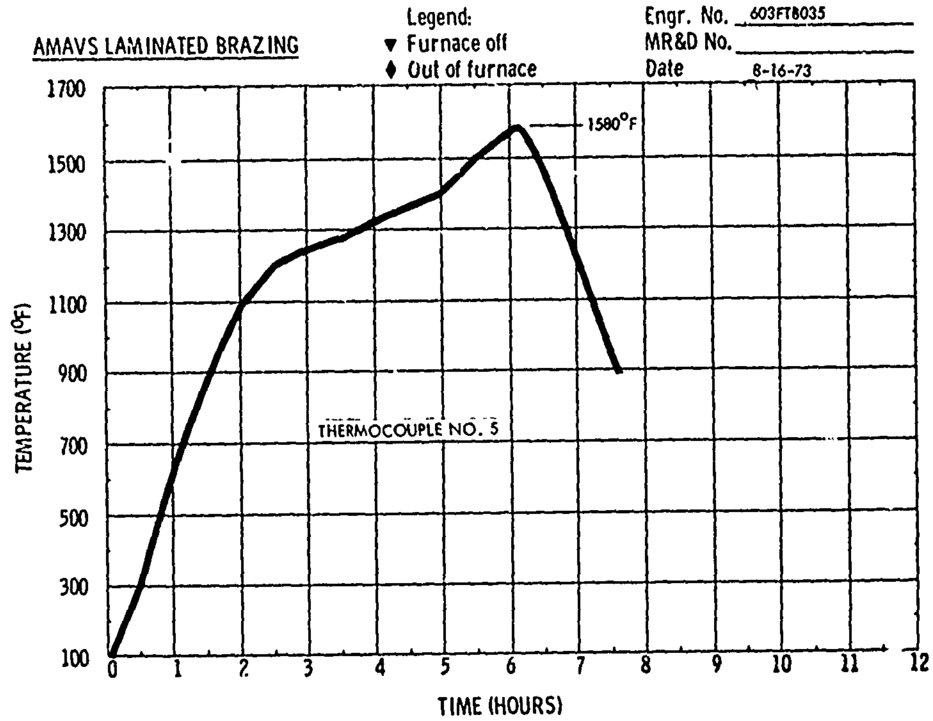


Figure 5-19 BRAZE CYCLE FOR 603FTB035 TEST SPECIMEN RUN #1 THERMOCOUPLE NO. 5

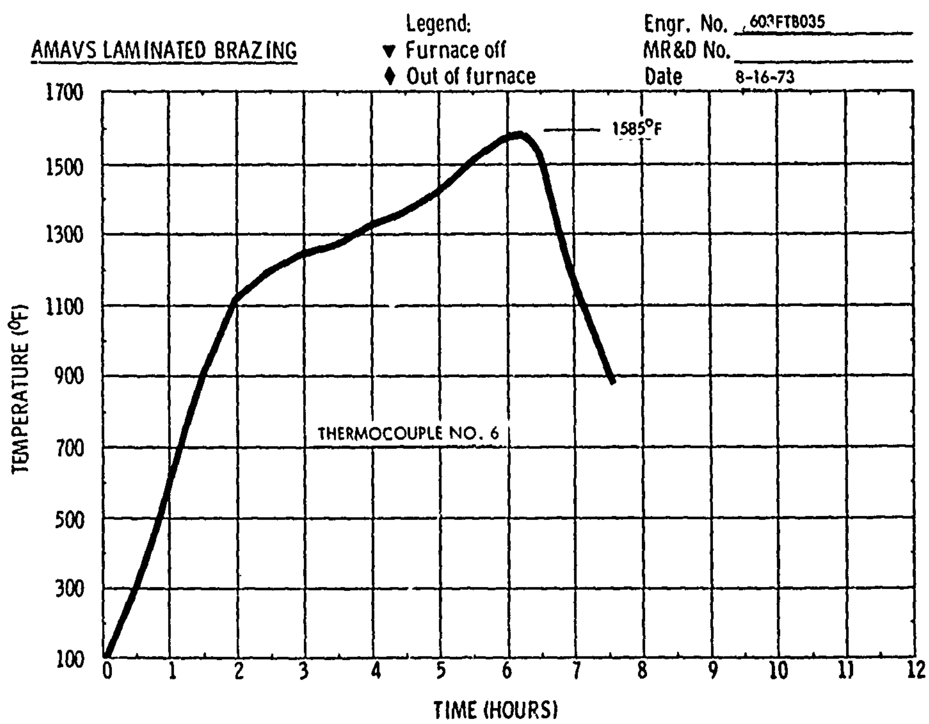


Figure 5-20 BRAZE CYCLE FOR 603FTB035 TEST SPECIMEN RUN #1 THERMOCOUPLE NO. 6

5.1.3.3 Rebraze of the First 603FTB035 Test Specimen (603FTB035-3C)

The first 603FTB035 brazed test specimen was sawed in half in the transverse direction, disassembled at each braze line, and prepared for a second braze operation. Disassembly was relatively easy because of an inadequate braze. The braze alloy was chemically stripped from the details prior to the standard pre-braze cleaning operation.

The second braze operation (603FTB035-3C) was run to refine the braze cycle, to further determine temperature distribution within the panel, to determine the requirements for an increased heat-up rate in the braze cycle, and to establish potential of rebrazing salvaged details.

After the braze alloy from the first braze operation was stripped, the titanium details were vibro sanded to provide a smooth surface and remove intermetallics that may have been present. Chemical cleaning the details was by standard procedure. Only one-half of the part (about 4' x 5') was prepared for brazing. The remaining half of the panel was installed in the braze box, without braze alloy, to provide a uniform load. Two 1/4" x 1/4" x 7 1/2" x 12" braze test panels were placed in the hog-out areas as illustrated in Figure 5-21. A total of ten thermocouple locations were planned for this test run. During the braze box leak detection test a leak was found in thermocouple tube No. 5. Attempts to repair the leak failed; therefore, the tube entry was welded and the thermocouple omitted. Complete tooling, detail layup and thermocouple entry locations are shown in Figure 5-22.

The braze time/temperature cycle for 603FTB035-3C is shown in the graphsin Figures 5-23 through 5-31. It is believed that thermocouples 8 and 9 (Figures 5-29 and 5-30) showed faulty readings due to shorting out on the braze box. Both of these thermocouples were insulated with a soft material and it is possible that the insulation was scraped off in localized areas in initial installation.

After brazing, visual inspection of the part showed only a small amount of alloy flow at the panel edges. Also, discoloration was evident around the periphery of the part and in the hog-out areas. The part was inspected by NDI and sent to the engineering test lab for further evaluation.

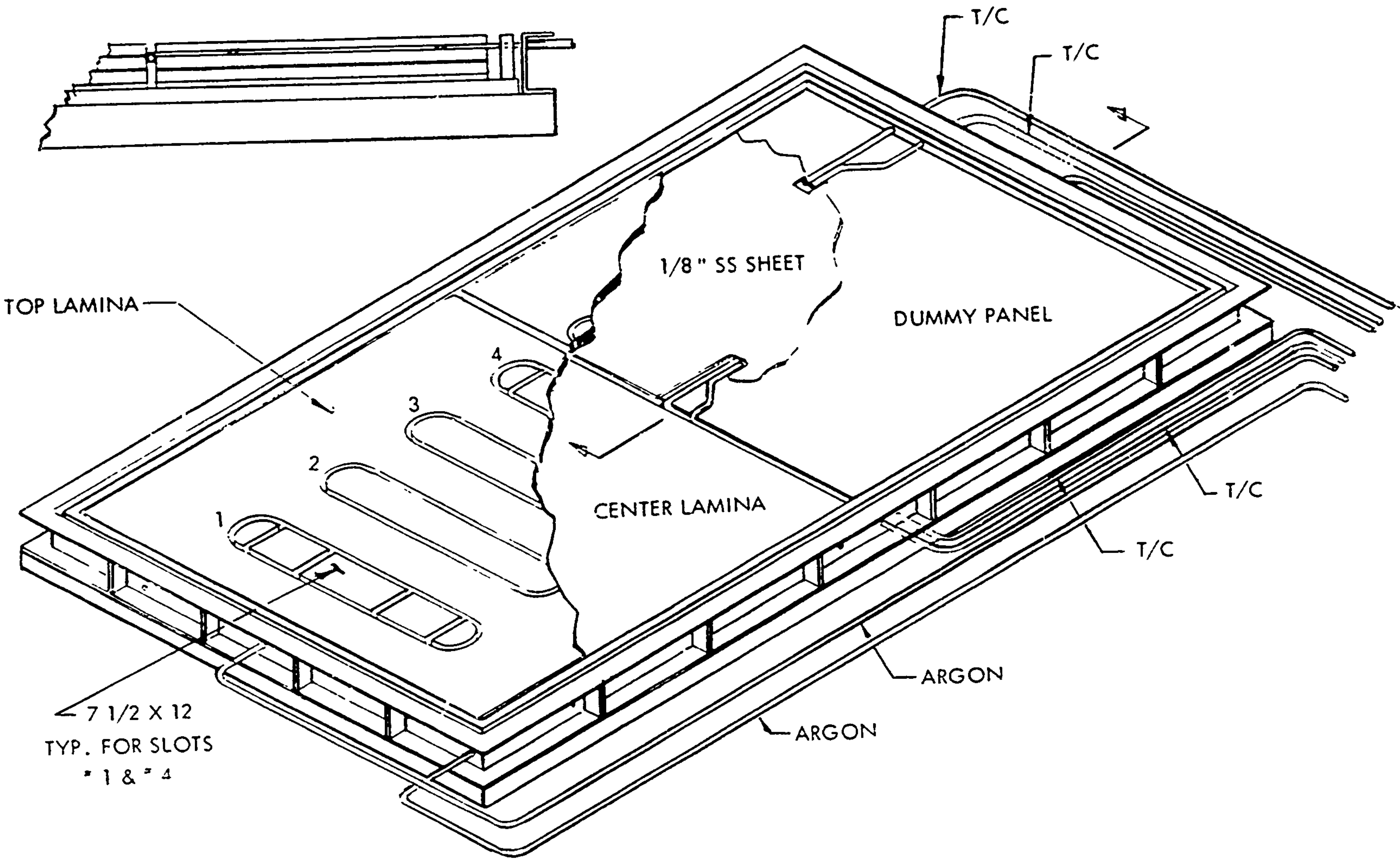


Figure 5-21 LAY-UP OF 603FTB035-3C ILLUSTRATING DUMMY PANEL, CENTER LAMINA AND 7 1/2 X 12" TEST SPECIMEN LOCATIONS

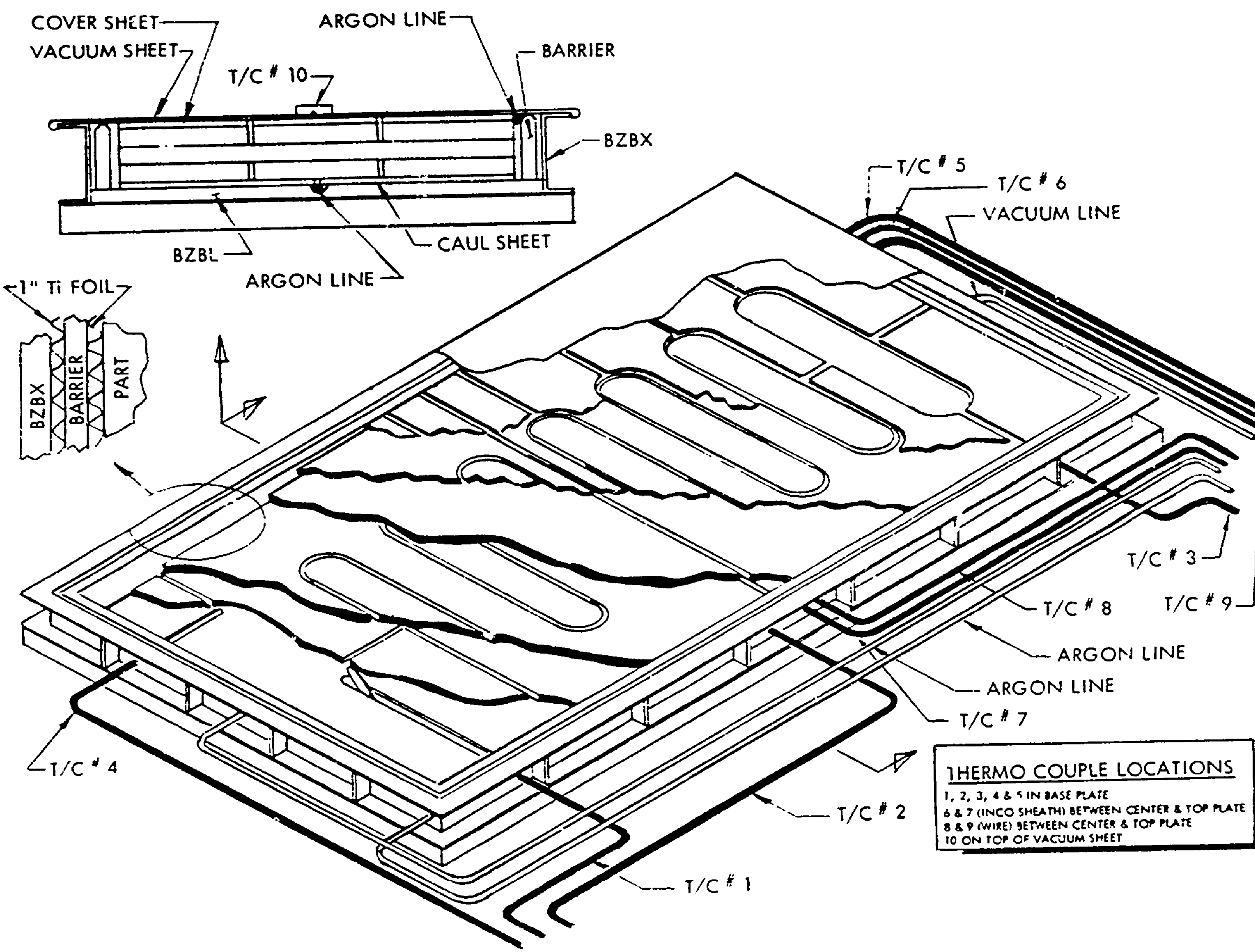


Figure 5-22 TOOLING, LAY-UP AND THERMOCOUPLE ENTRIES FOR 603FTB035-3C

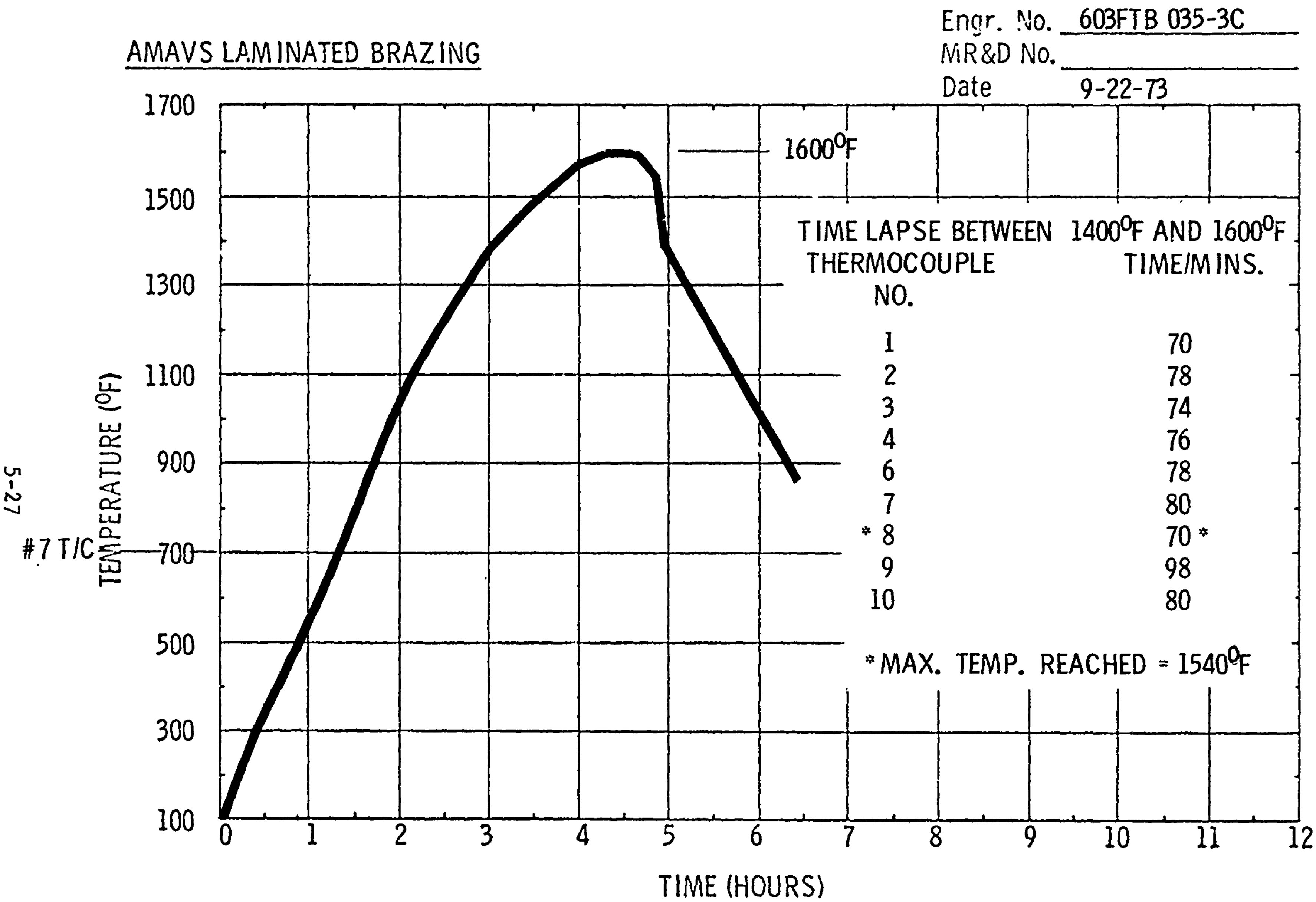


Figure 5-23 BRAZE CYCLE FOR 603FTB035-3C THERMOCOUPLE NO. 7

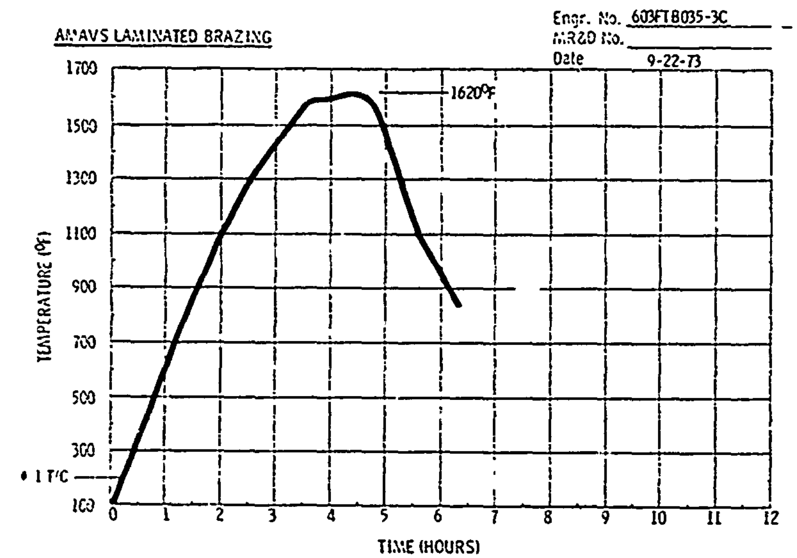


Figure 5-24 BRAZE CYCLE FOR 603FTB035-3C THERMOCOUPLE NO. 1

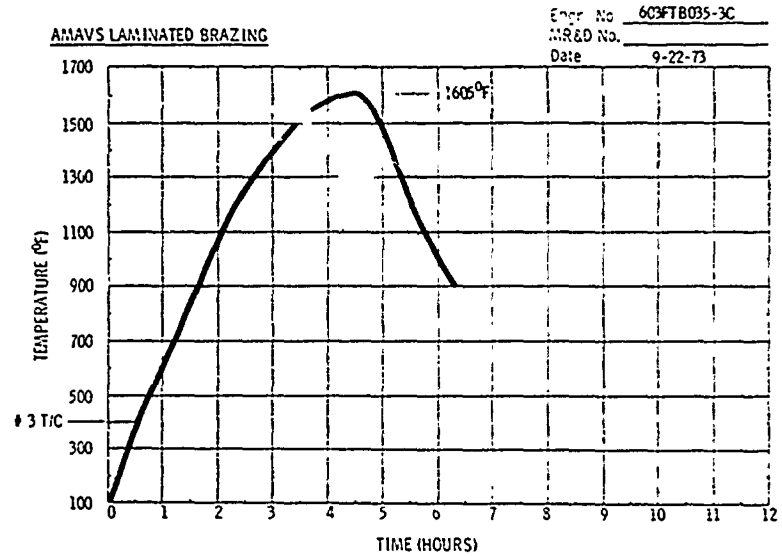


Figure 5-26 BRAZE CYCLE FOR 603FTB035-3C THERMOCOUPLE NO. 3

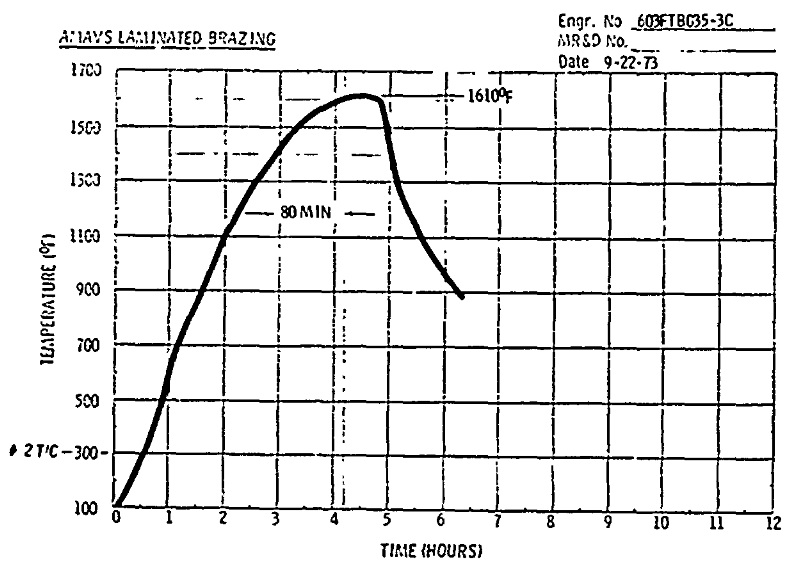


Figure 5-25 BRAZE CYCLE FOR 603FTB035-3C THERMOCOUPLE NO. 2

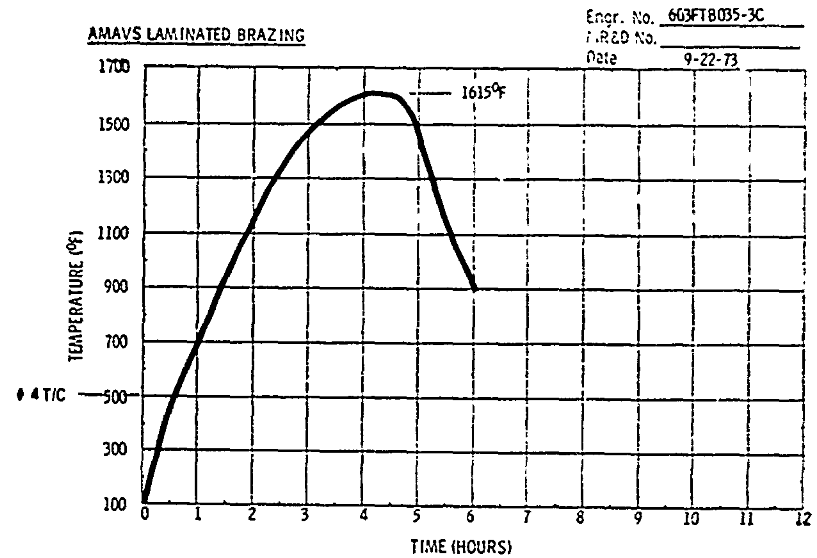


Figure 5-27 BRAZE CYCLE FOR 603FTB035-3C THERMOCOUPLE NO. 4

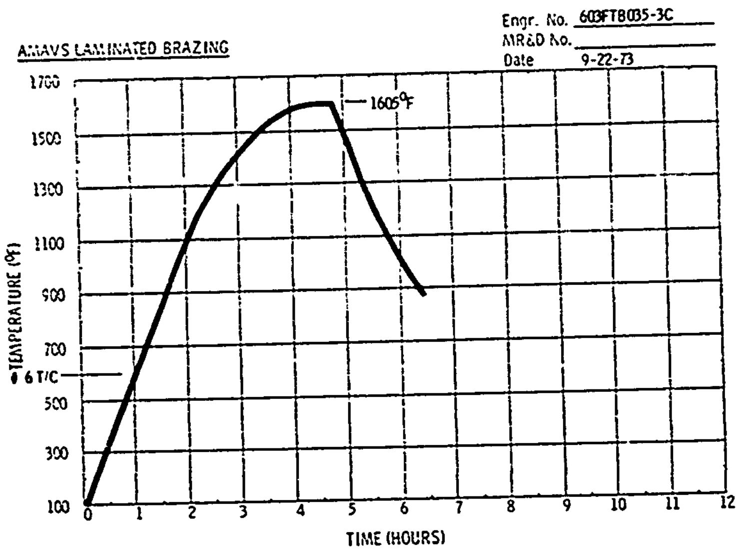


Figure 5-28 BRAZE CYCLE FOR 603FTB035-3C THERMOCOUPLE NO. 6

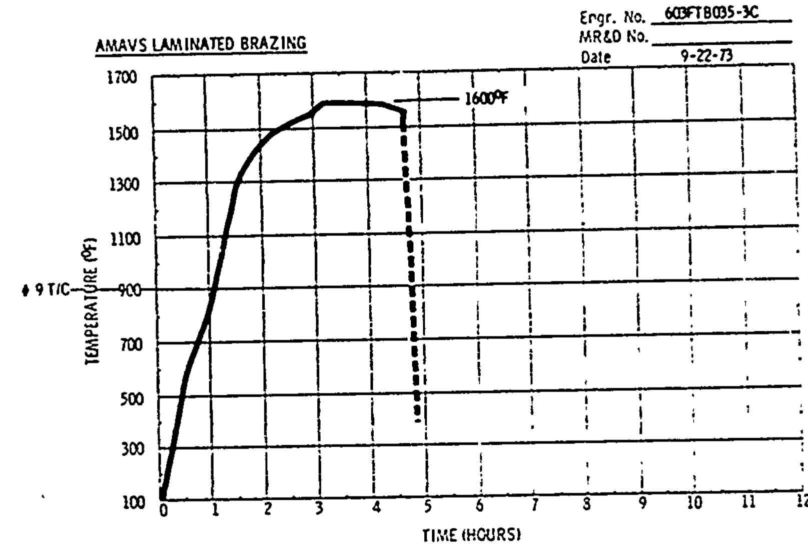


Figure 5-30 BRAZE CYCLE FOR 603FTB035-3C THERMOCOUPLE NO. 9

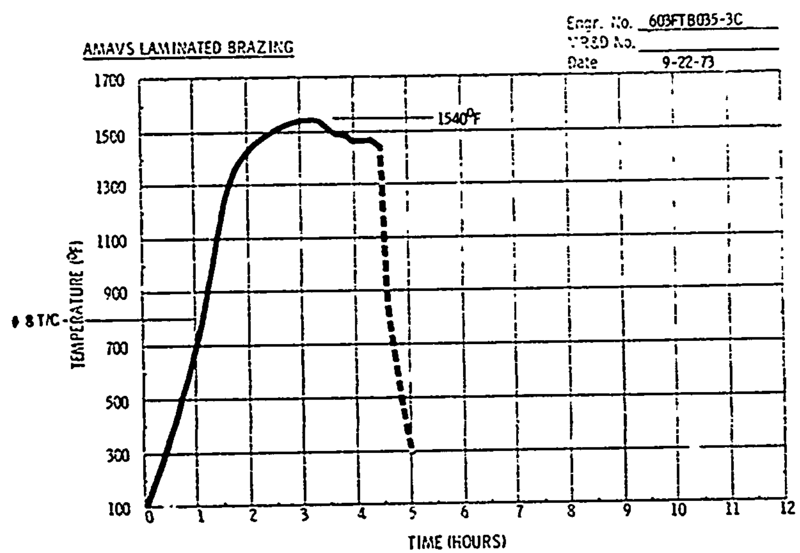


Figure 5-29 BRAZE CYCLE FOR 603FTB035-3C THERMOCOUPLE NO. 8

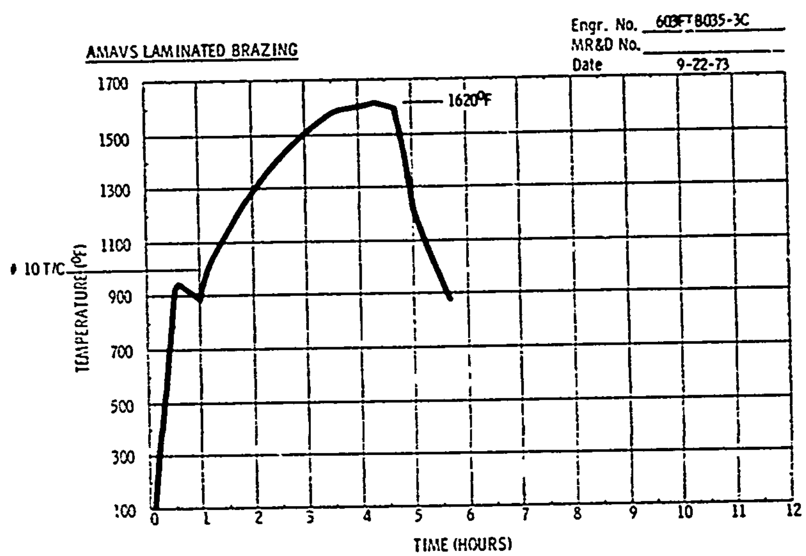


Figure 5-31 BRAZE CYCLE FOR 603FTB035-3C THERMOCOUPLE NO. 10

## 5.1.3.4 Brazing of the Second Lower Plate Damage Tolerance Test Specimen 603FTB035-7A

Before brazing the 603FTB035-7A test specimen, special braze tests were run using 1/4" x 1/4" x 6" x 6" test parts. These specimens were run to refine brazing parameters. Specifically, the variables investigated were effect of time delay between cleaning and brazing, the effect of sanded braze alloy vs. as-received alloy, heating rate, and the effect of using titanium plate previously subjected to a braze cycle.

Based on results of the previously brazed 603FTB035 parts and results of special tests several tooling and process changes were incorporated into the procedure for brazing the 603FTB035-7A test specimen. The major changes include:

(1) Central location of argon supply tubes to improve purging in upper and lower hog-out areas. (Figure 5-37)

(2) Elimination of insulation on top of braze box during braze heat cycle (to increase heating rate).

(3) Higher furnace temperature in initial stage of braze cycle (to increase heating rate).

(4) Increased energy input into furnace during braze cycle (to increase heating rate).

Tooling, thermocouple inlet locations, and lay-up procedure are illustrated in Figures 5-32 through 5-37 and a complete tooling, layup and braze check off list for 603FTB035-7A is shown below:

1. Clean braze block with isopropyl alcohol and clean cheesecloth.

2. Bake braze block at 1600$^{o}$F for 15 minutes.

3. Clean braze box

   a. Vacuum

   b. Isopropyl alcohol and clean cheesecloth.

4. Insert braze block in braze box.

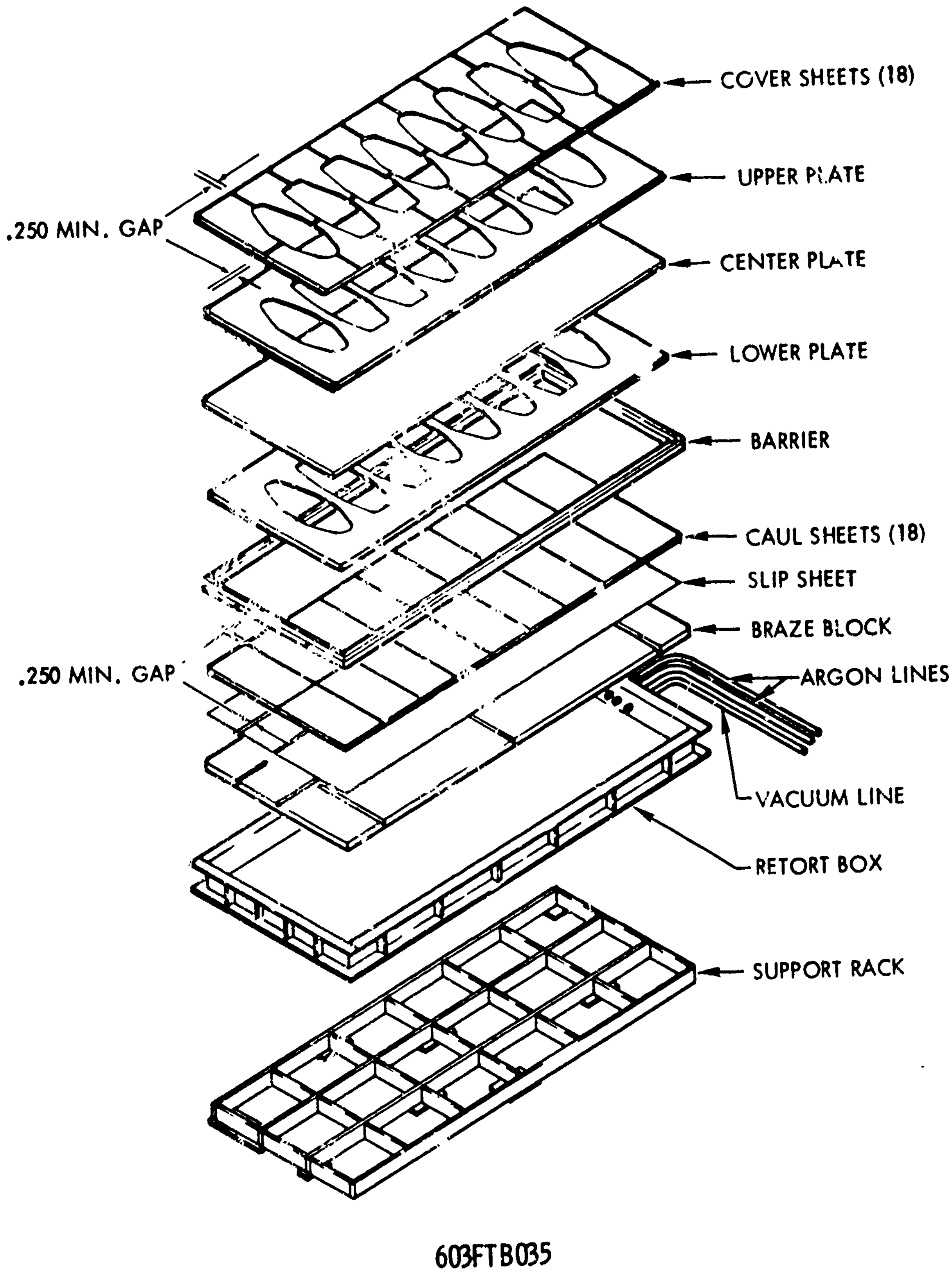


Figure 5-32 BRAZE COMPONENTS FOR 603FTB035-7A

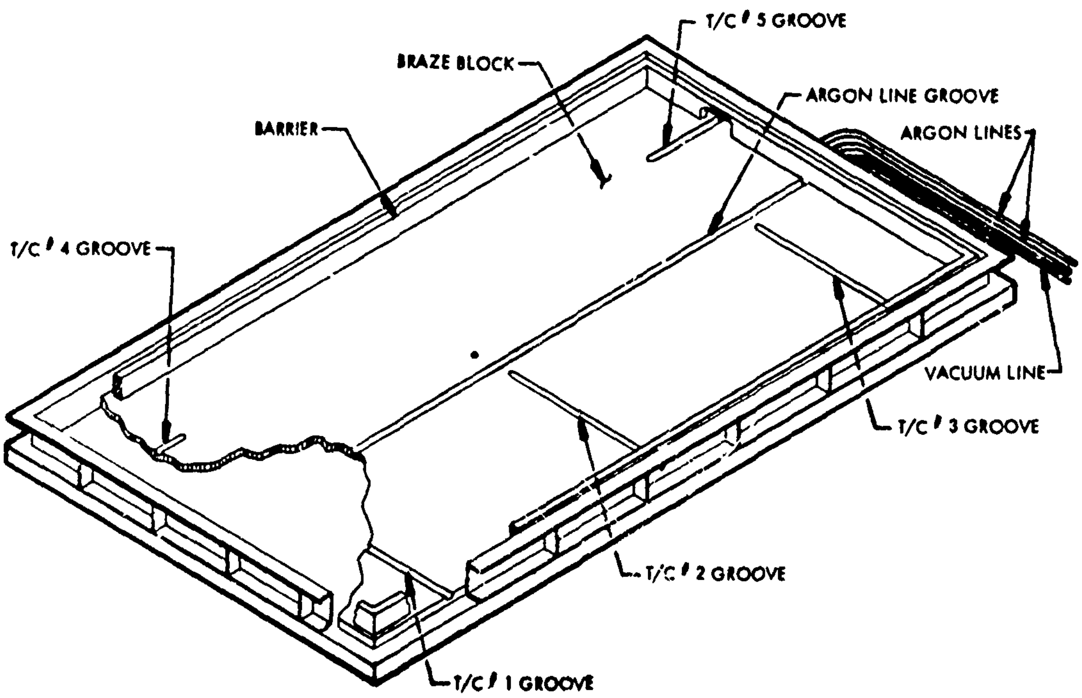


Figure 5-33 BRAZE BOX TOOLING ILLUSTRATING THERMOCOUPLE LOCATIONS

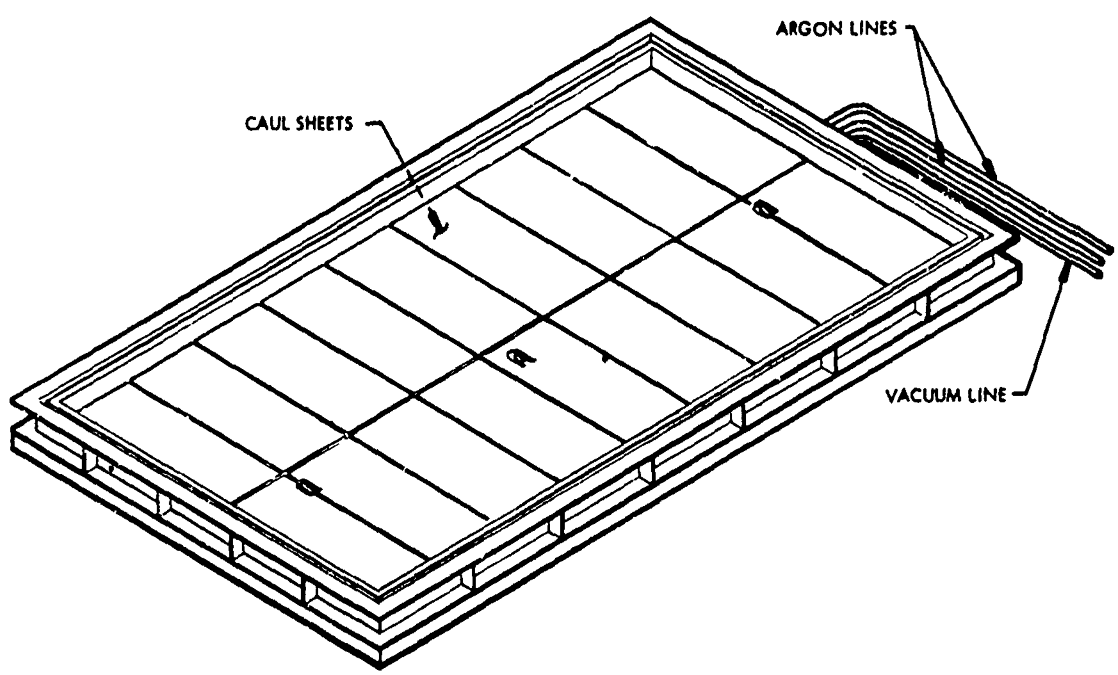


Figure 5-34 BRAZE BOX TOOLING ILLUSTRATING CAUL SHEETS, ARGON LINES AND VACUUM LINE

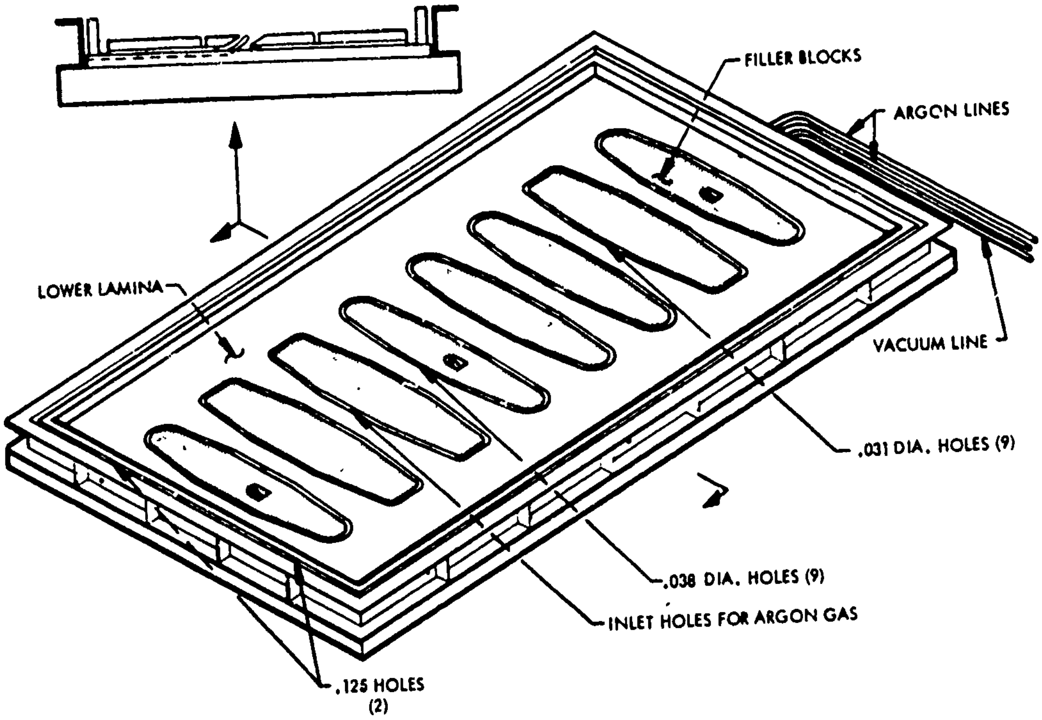


Figure 5-35 BRAZE BOX ILLUSTRATING ARGON GAS LINES FOR PURGING LOWER LAMINA HOG-OUTS

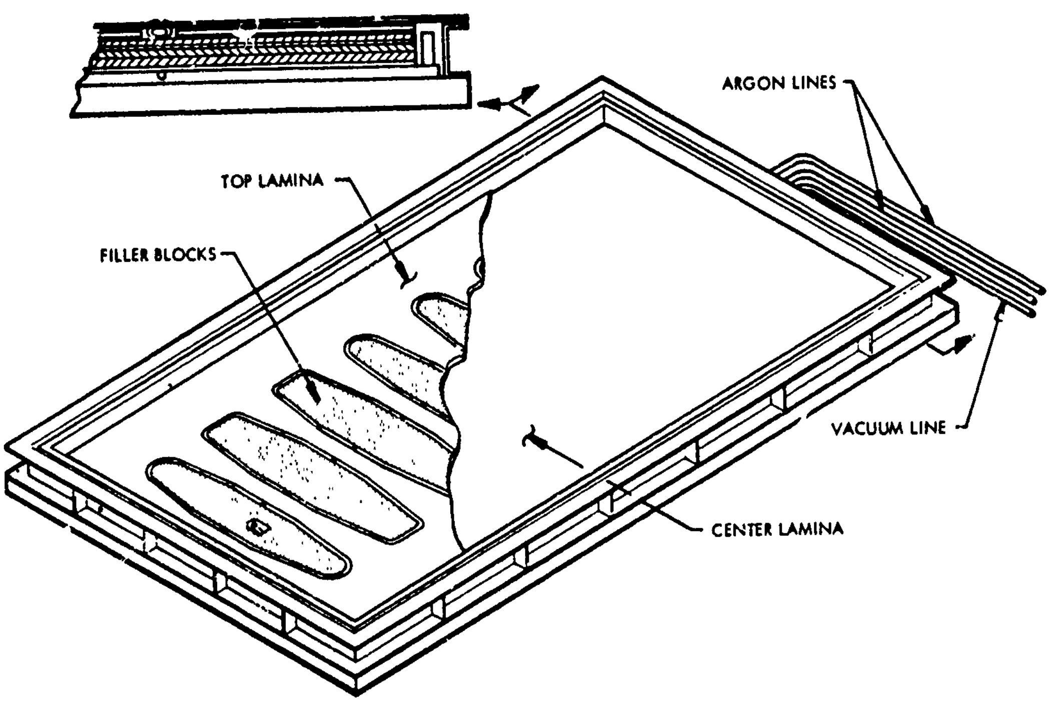


Figure 5-36 BRAZE BOX ILLUSTRATING TITANIUM LAMINA AND FILLER BLOCKS

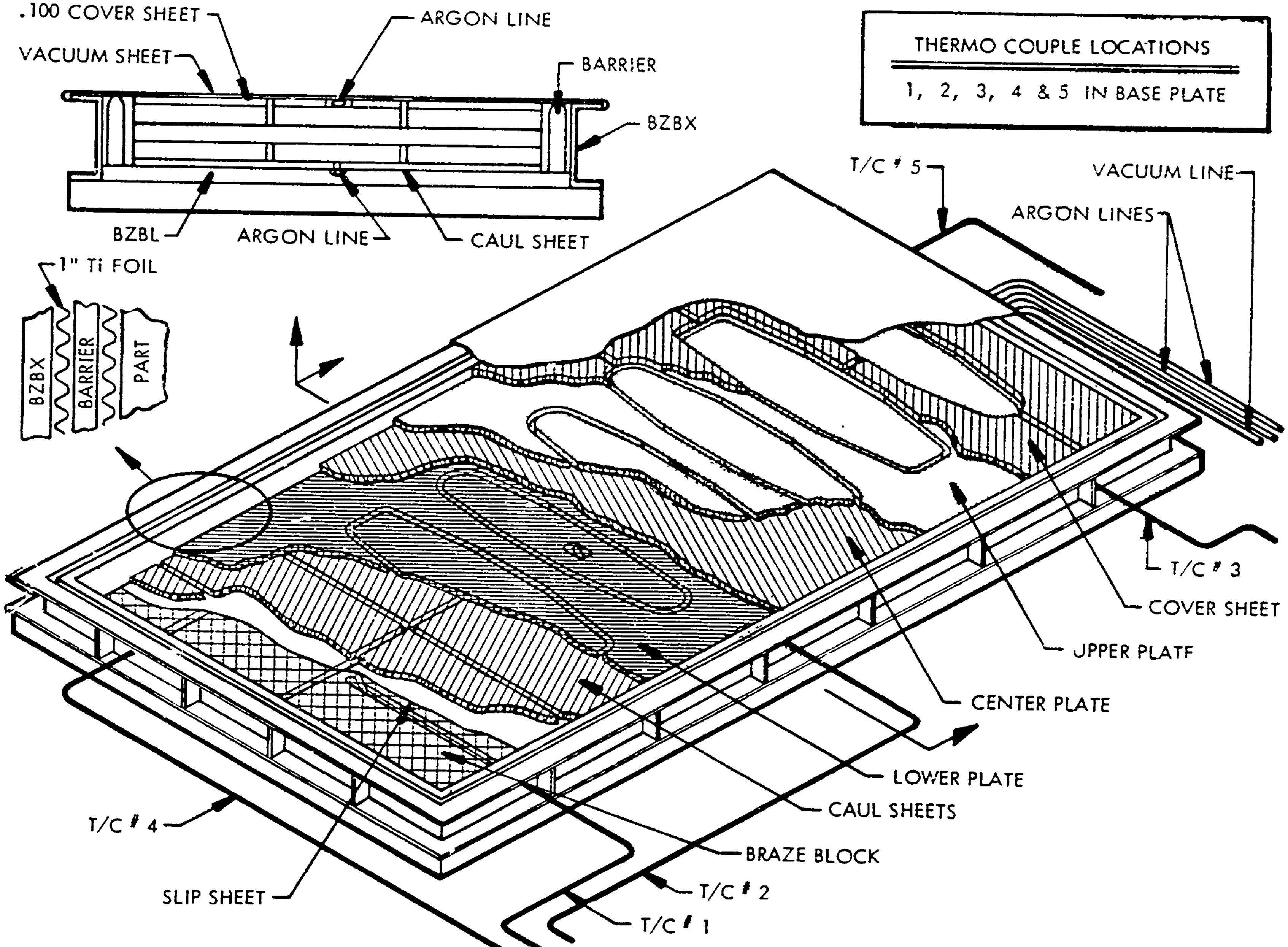


Figure 5-37 COMPLETE LAY-UP FOR 603FTB035-7A

5. Fabricate thermocouple tubes.

6. Leak check thermocouple tubes.

7. Clean thermocouple tubes - vapor degrease (150$^{\circ}$F tank).

8. Weld thermocouple tubes in braze box.

9. Fabricate caul sheets.

10. Disc grind surface of caul sheets to remove oxides and manufacturer's identification (ink stencil).

11. Clean both surfaces of caul sheets with alcohol and clean cheesecloth.

12. Paint upper surface of caul sheets with stop-off (Stopyt), air dry, bake at 800$^{\circ}$F for 10 minutes.

13. Fabricate lower argon line of 0.250-inch diameter, 0.020" wall, 321 stainless steel tube.

    a. Drill (9) 0.038-inch holes and (9) 0.031-inch holes in tube using prepared template for hole spacing. Smaller holes will be at argon entry end.

    b. Deburr holes and flare one end.

    c. Clean argon supply line using vapor degrease (150$^{\circ}$F tank).

    d. Plug weld end of argon line.

    e. Drill 1/4-inch hole in braze box to receive lower argon line.

    f. Locate and weld tube to braze box. Holes to be normal to top surface of braze plate.

14. Seal weld the argon and (5) T/C tubes directly beneath the atmosphere barrier. Grind welds flush with top of base plate.

15. Locate slip sheets (2) on top of braze block.

16. Locate caul sheets in braze box on top of slip sheets. Maintain 1/4 inch minimum gap between each caul sheet. Tack weld one place, each sheet on end near argon line.

17. Drill (1) hole for upper argon line in the vacuum end of barrier.

18. Drill (2) 1/8" vent holes in the opposite end of atmosphere barrier located 8" in from the corners.

19. Fabricate picture frame type spacer (0.100-inch thick 321 stainless steel) and locate in braze box.

20. Place atmosphere barrier in braze box (on top of picture frame).

21. Mill T/C slot in (3) filler blocks. Paint one surface and all edges of 16 filler blocks with (Stopyt) and bake off at 800°F for 30 minutes.

22. Prepare upper argon supply line.

    a. Flatten 1/4-inch diameter 321 stainless steel tube to 0.200-inch height.

    b. Drill argon exit holes with size, location, and pattern as described in 13a. Flare one end of tube.

    c. Clean argon line using vapor degrease (150°F tank).

    d. Crimp end of upper argon line and seal weld.

Reference Material

| | | |
|---|---|---|
| CSA 760-8-6-1 | 603FTB035-9 | Plate |
| CSA 760-8-7-1 | 603FTB035-9 | Plate |
| CSA 760-8-8-1 | 603FTB035-11 | Plate (center plate) |

23. Inspect and log test tag.

24. Prefit details and rough trim braze alloy to details.

25. Remove all oxides from surfaces of the -9 and -11 details. Use vibro sander with 320 grit paper.

26. Acid clean details (P.S. 40.01-25 section 2) Reference the following cleaning procedure.

    a. Wipe with clean cheesecloth and acetone to remove light oils and fingerprints. Handle parts with clean cotton gloves after this operation until brazing has been completed.

b. Attach parts to cleaning rack then complete the following operations.

- o Alkaline soak at 180 ± 10°F, 15 minutes, tank 650.
- o Hot rinse at 180 ± 10°F, 5 minutes, tank 651.
- o Nitric-hydrofluoric pickle at room temperature, 1 minute, tank 652.
- o Cold rinse at room temperature, 45 seconds, tank 653.
- o Repeat the pickling and rinsing operations until a total of 5 cycles have been completed.
- o Nitric acid desmut at room temperature, 5 minutes, tank 721.
- o Deionized water rinse at room temperature, 5 minutes, tank 722.
- o Allow parts to drip dry. Clean cheesecloth may be used, as a wick, to remove water from depressions that will not drain easily.

27. Inspect

28. Remove wires from parts and wrap in clean brown paper. Handle parts with clean cotton gloves.

29. Forward parts to lay-up area, Col. 41 C-D.

    Note: All succeeding operations shall be accomplished per instructions from L. I. Burnett, extension 4461 and will be monitored by the assigned MR&D brazing engineer.

30. Check braze box to see that the caul sheets are in correct location.
    Note: Paint top sides of caul sheets with stop-off and bake at 800°F 10 minutes prior to location.

31. Prefit and trim the brazing alloy to fit the lower -9 plate. Punch 9/32-inch holes on four inch centers in the brazing alloy for the 0.250 x 0.002-inch thick stainless steel spacers.

32. Sand braze alloy with 240 grit paper.

33. Wipe braze alloy and -9 plate with distilled isopropyl alcohol and clean cheesecloth to remove fingerprints or other contamination. Handle parts only with white cotton gloves.

34. Locate and tack the braze alloy and spacers to the -9 plate. Do not overlap the alloy joints.

35. Locate the -9 plate in braze box. Equally space the plate inside the atmosphere barrier.

36. Locate filler blocks in hog-outs of -9 plate. Paint all surfaces with stop-off and bake at 800°F 30 minutes prior to locations. Do not use stainless steel retainer strips around the perimeter of the hog-outs.

37. Inspect the -11 plate for water marks or other contamination. Remove any contamination with distilled isopropyl alcohol and clean cheesecloth. Use cotton gloves for handling part.

38. Locate the -11 plate on top of the -9 lower plate.

39. Punch 5/32-inch holes in the alloy. Remove contamination with distilled alcohol and clean cheesecloth. Handle parts only with cotton gloves. Tack alloy to the surface of -11 plate. Locate and tack 0.002 thick x 1/8 inch dia. stainless steel spacers in each hole in the alloy(holes to be 4" centers).

40. Remove contamination with distilled alcohol and clean cheesecloth. Handle parts only with cotton gloves. Locate the -9 upper plate on top of the -11 center plate. Scribe the braze alloy around the perimeter of each hog-out in -9 plate. Remove -9 plate and trim out alloy to the scribe lines.

41. Relocate the -9 upper plate in the braze box.

42. Tack weld a 0.002 x 1 inch stainless steel strip over the braze joints around the perimeter of the parts.

43. Locate the filler blocks in the center of the hog-outs.
    Note: Paint surfaces with stop-off and bake at 800°F 30 minutes prior to location.

44. Preform a 1 inch wide titanium ribbon into a sinewave configuration and place in braze box. Ribbon is required both

inside and outside of the atmosphere barrier.

45. Locate 0.100-inch thick cover sheets on top of panel.
Note: Paint lower surfaces with stop-off and bake at 800°F 10 minutes prior to location. Locate and weld upper argon line in braze box.

46. Locate vacuum sheet and trim to size.

47. Weld vacuum sheet to braze box.

48. Check for leaks.

49. Argon purge braze box 15 cycles, hold maximum vacuum 3 min. (accomplish at furnace with liquid argon).

50. Locate (5) 1/8" diameter Inco sheath chromel-alumel thermocouples 25 feet long into tubes in sides of braze box. One (1) T/C on top of box in 1 x 8 x 8-inch steel block.

51. Place one layer of fiberfrax inside the "C" channels of the braze box. Purge box 5 minutes at 17" Hg vacuum and 10 CFH argon.

52. Set furnace temperature at 1400°F prior to locating panel in furnace. Place panel in furnace and turn furnace heat controls to 1650°F. Allow low T/C to reach 1600°F and adjust controls to hold for 15 minutes.
Note: Turn argon off at 900°F on heat up. Adjust vacuum to 17" Hg vacuum.

53. Turn furnace control off and cool until T/C #2 reads 1200°F.

54. Remove retort from furnace and place two layers of fiberfrax on top of box. Cool to room temperature.

55. Forward to pilot shop, Col. 47J on mezz.

56. Open retort - remove brazed assembly and remove all oxides and alloy from surfaces.

57. Identify with assembly part number.

58. X-ray inspect.

59. Ultrasonic inspect (Attention: D. L. Duncan) (Col. 47J Mezz.)

60. Record all data.

61. Forward to stock room No. 1000.

5.1.3.5 Lay-up of Details for 603FTB035-7A Test Specimen

To avoid excessive contamination of the clean titanium details and braze alloy effort was made to minimize the time between acid cleaning and brazing. Also, handling of details was kept to a minimum and clean white cotton gloves were used at all times. In periods of inactivity during the lay-up procedure, all details were covered with brown kraft paper. A pictorial history of lay-up through sealing the braze box is shown in the photographs in Figures 5-38 through 5-45.

Other precaution taken in lay-up procedure included an increased cure cycle for the stop-off material (Stopyt) used on caul sheets, cover sheets, and filler blocks and an elimination of the use of refrasil cloth in the braze box. Smoke originating in the braze box in previous runs was traced, by tests, to uncured stop-off material. Tests also demonstrated that a thermal treatment of 800°F for 10 minutes was sufficient to eliminate the smoke. It was also believed that refrasil cloth contributed to contamination, therefore its use was discontinued.

The braze box containing 603FTB035-7A was placed in a furnace operating at 1400°F. After placement in the furnace the temperature controller was raised to 1650°F. At about 1500°F (furnace temperature) input was automatically reduced to 95 to 98%. As furnace temperature increased the furnace automatic controller decreased BTU input. To avoid a slowing down in the heat-up rate of the braze panel, BTU input was controlled manually to maintain 100%. Manual control was continued until the furnace reached 1645°F. At this temperature BTU input was cut to zero for three minutes then gradually increased to maintain 1650°F. The manual input control, coupled with the effect of the omitted insulation on top of the braze box, increased heat-up rate considerably as compared to previous braze runs with similar panels. (See Figure 5-46.)The braze time/temperature cycle for 603FTB035-7A is shown in the graphs in Figures 5-47 through 5-51. Thermocouple locations are the same as shown previously in Figures 5-11 and 5-37. The planned heating rate for 603FTB035-7A was 4°F per minute in the range between 1400°F and maximum braze temperature. A heating rate 3.8°F per minute was attained.

4-53802

Figure 5-38  UPPER TITANIUM DETAIL FOR 603FTB035-7A BRAZE TEST SPECIMEN IMMEDIATELY AFTER ACID CLEAN

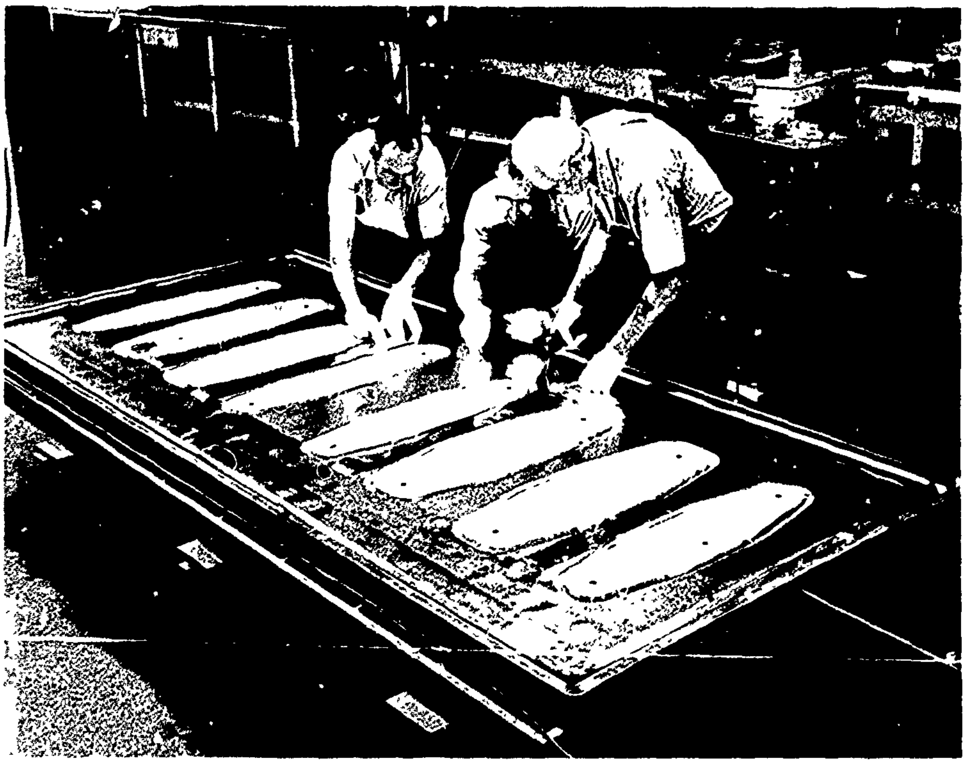

4-53794

Figure 5-39  LAY-UP OF BRAZE ALLOY ON LOWER PLATE OF 603FTB035-7A TEST SPECIMEN

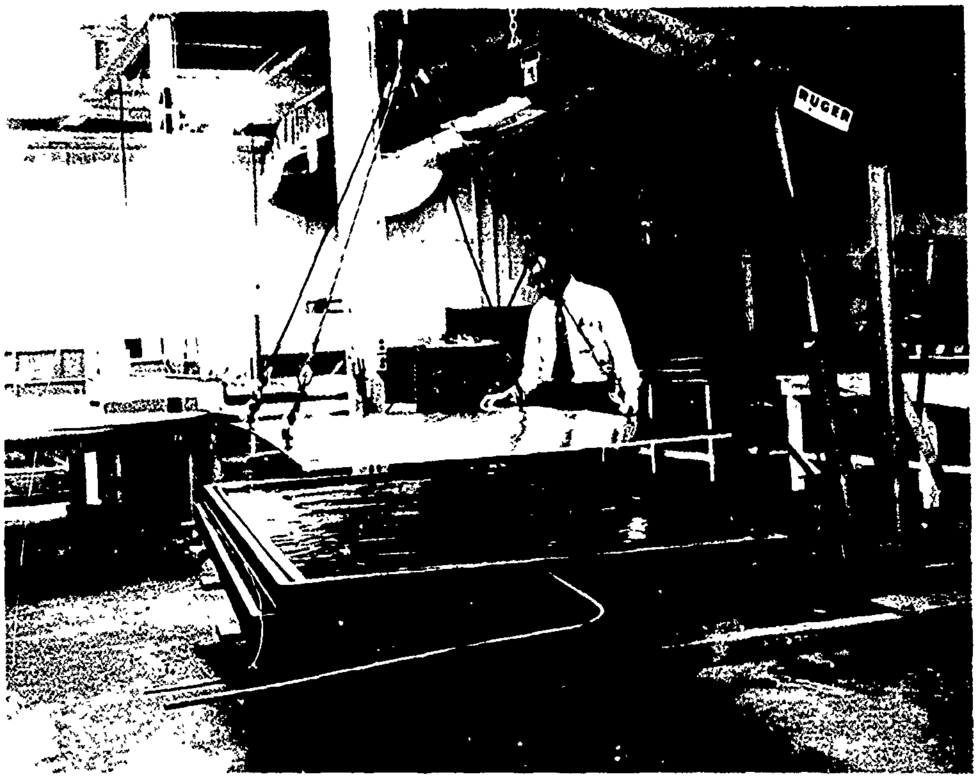

4-53793

Figure 5-40 PLACEMENT OF CENTER TITANIUM DETAIL AFTER LAY-UP OF BRAZE ALLOY ON LOWER TITANIUM DETAIL -603FTB035-7A

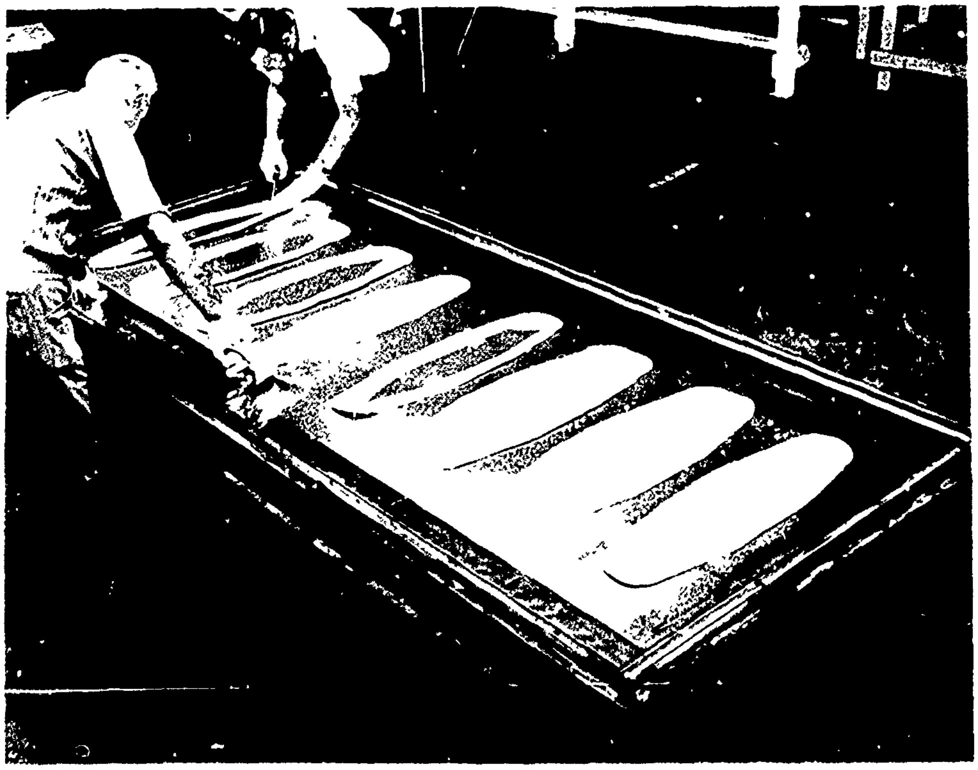

4-53807

Figure 5-41 LAY-UP OF BRAZE ALLOY ON UPPER SURFACE OF CENTER TITANIUM PLATE (TOP BRAZE LINE) FOR 603FTB035-7A

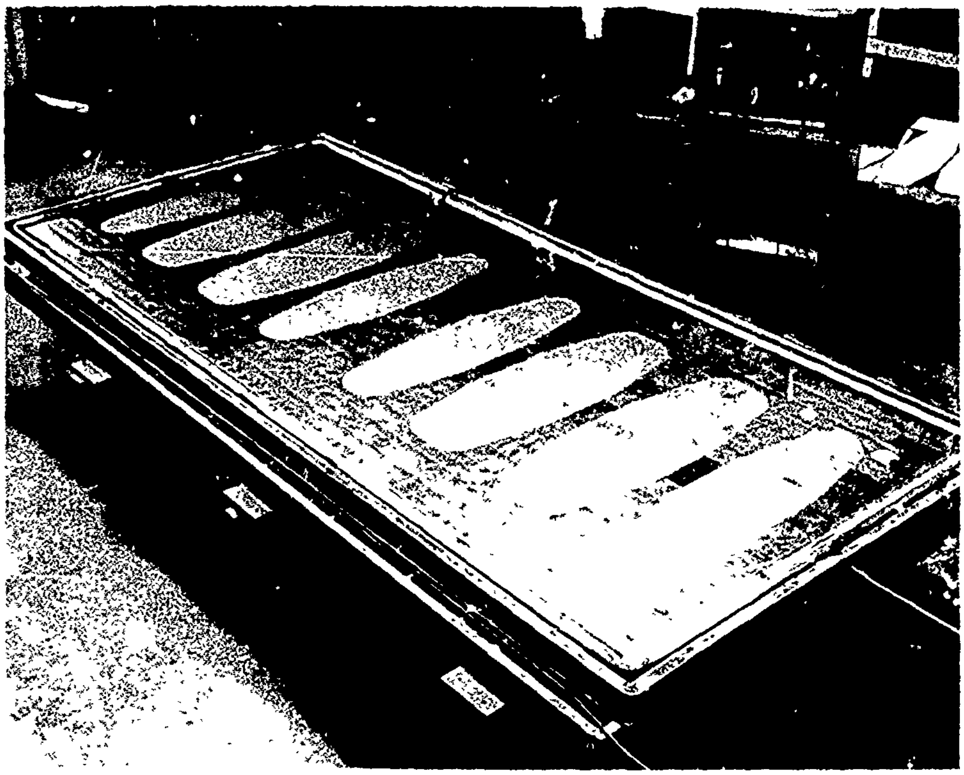

4-53805

Figure 5-42 FINAL ALLOY LAY-UP ON CENTER TITANIUM DETAIL OF 603FTB035-7A

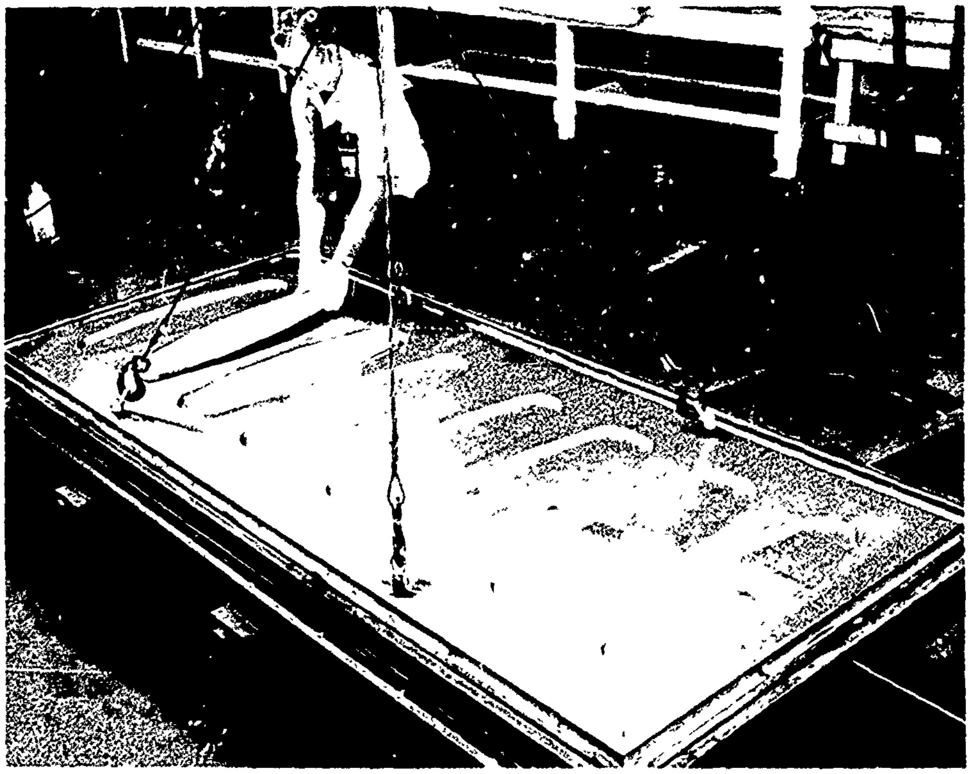

4-53806

Figure 5-43 INSERTION OF FILLER BLOCKS IN HOG-OUTS OF UPPER TITANIUM DETAIL OF 603FTB035-7A

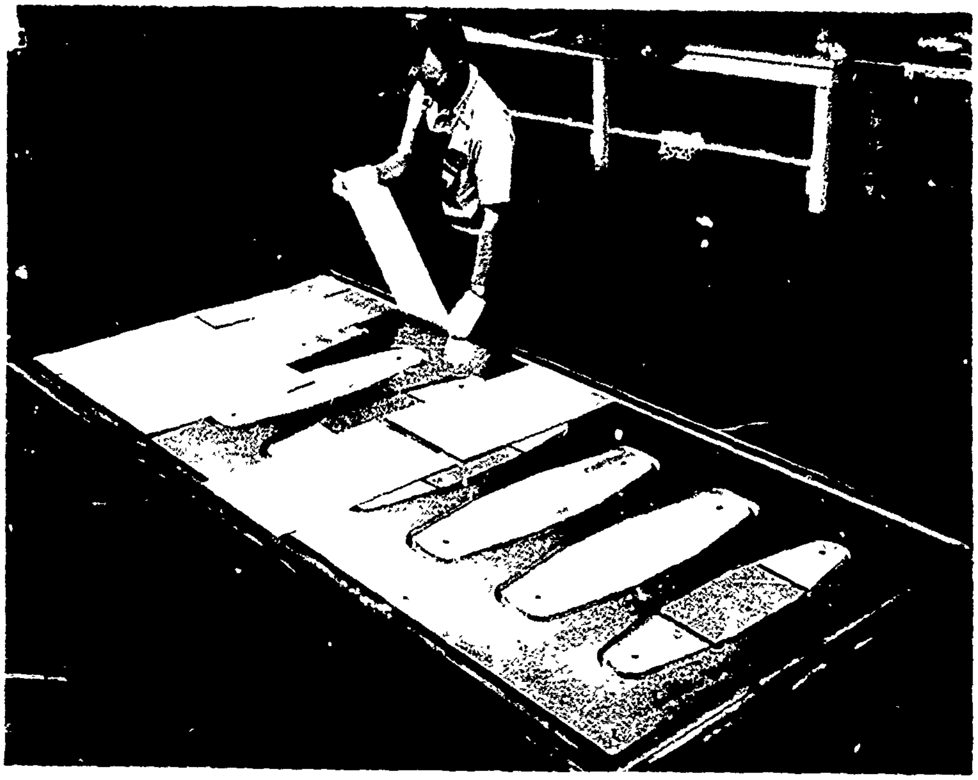

4-53804

Figure 5-44 PLACEMENT OF COVER SHEETS ON TOP OF LAID-UP ASSEMBLY OF 603FTB035-7A

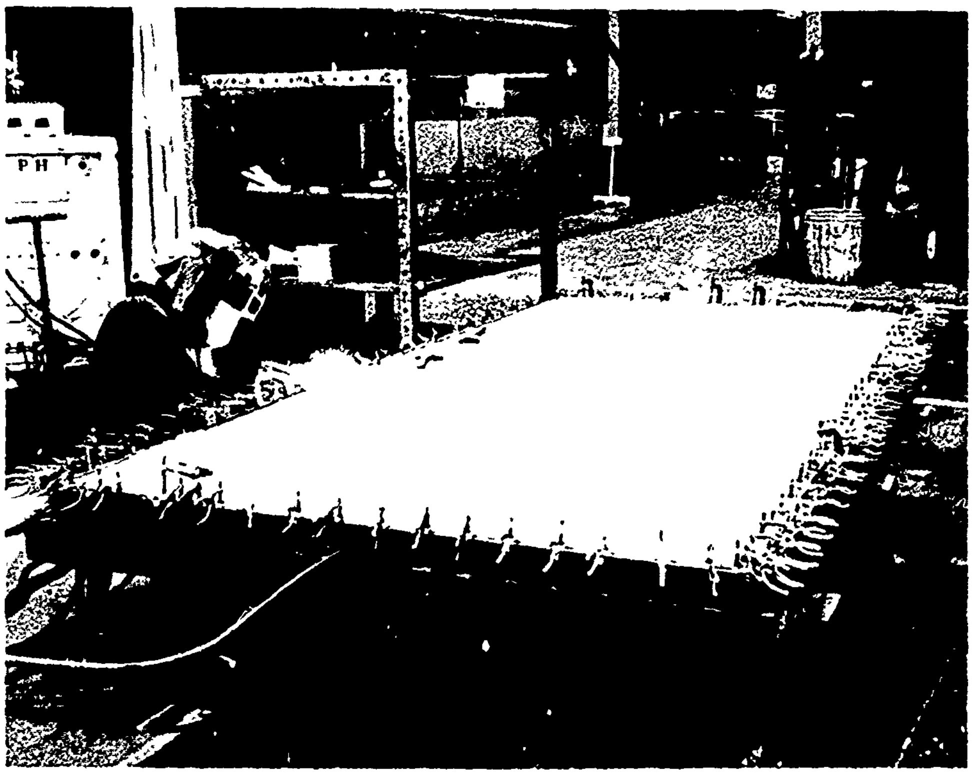


4-53799

Figure 5-45 WELDING VACUUM SHEET ON BRAZE BOX RETORT FOR 603FTB035-7A

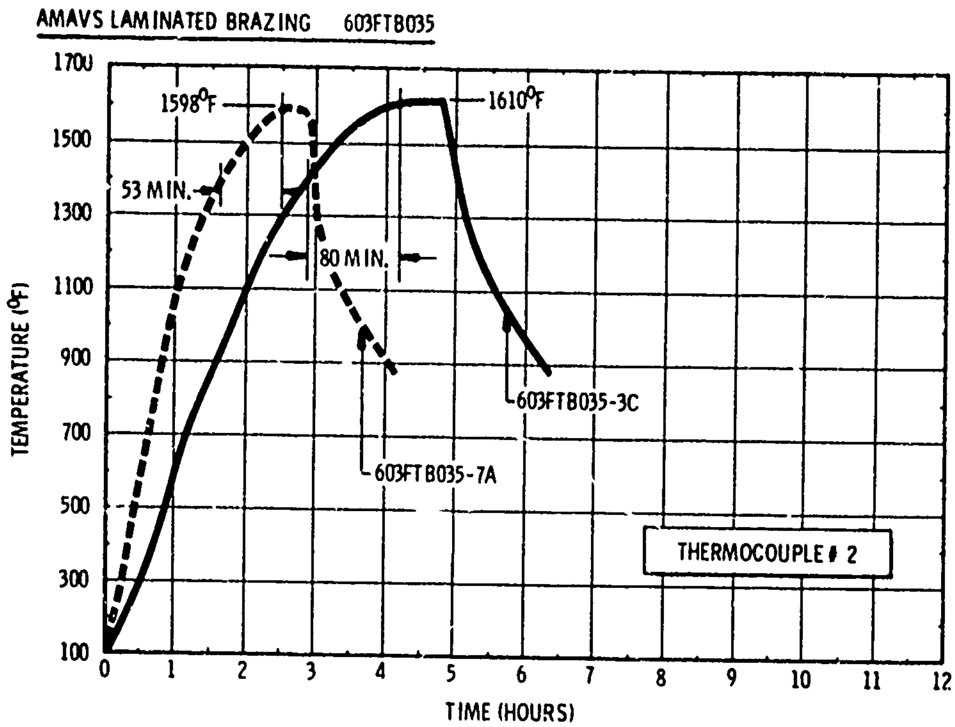


Figure 5-46 HEAT-UP RATE COMPARISON OF 603FTB035-3C AND -7A

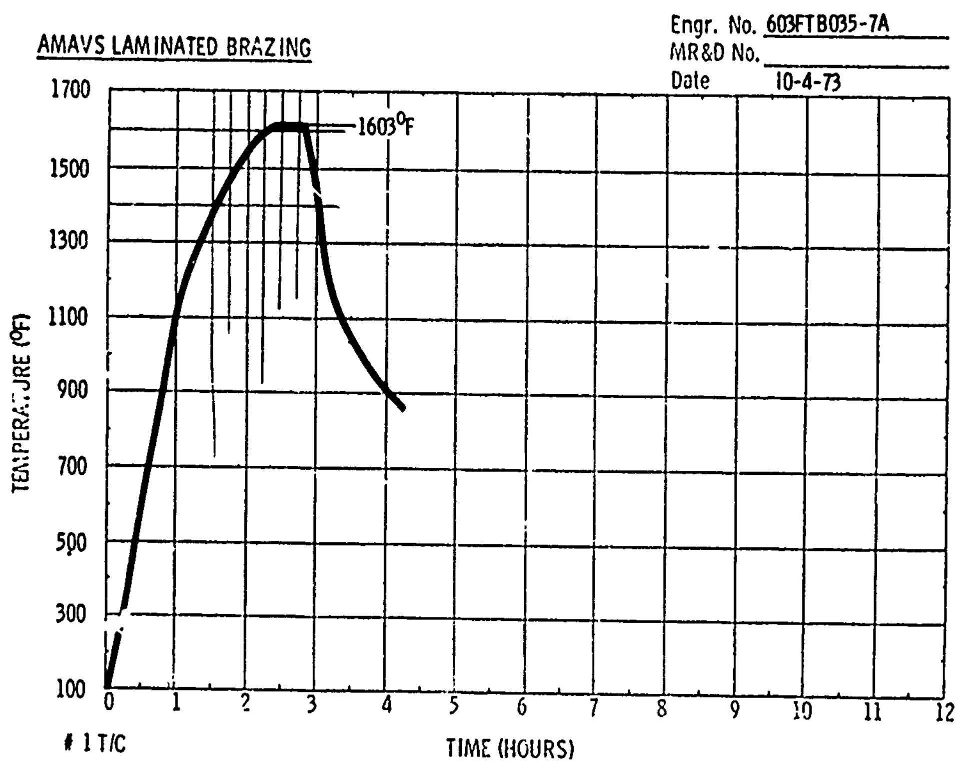


Figure 5-47 BRAZE CYCLE FOR 603FTB035-7A THERMOCOUPLE NO. 1

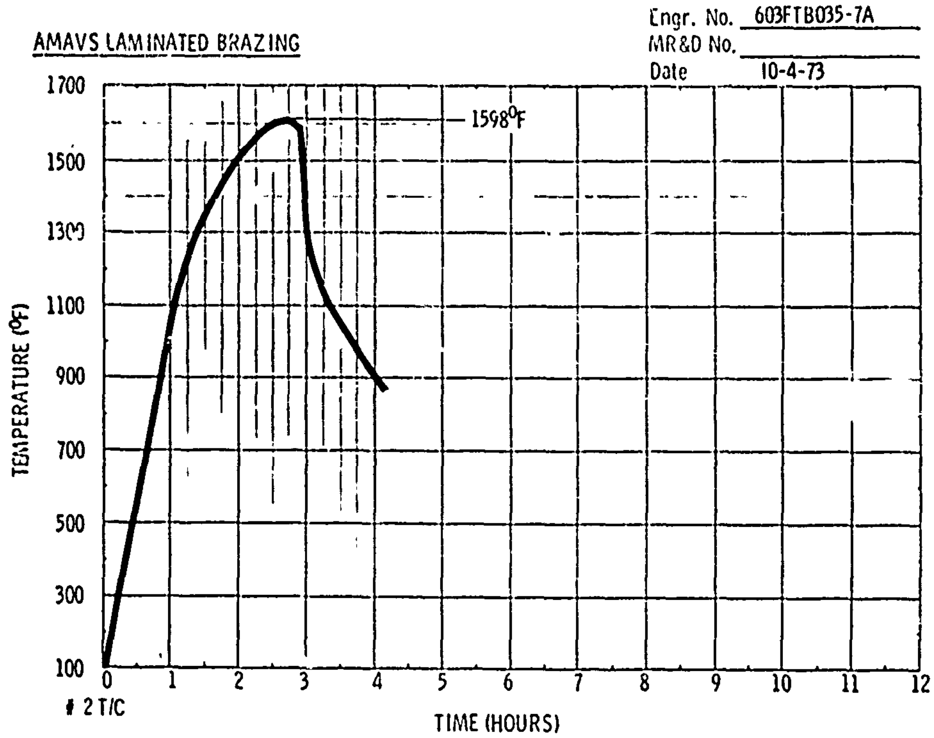


Figure 5-48 BRAZE CYCLE FOR 603FTB035-7A THERMOCOUPLE NO. 2

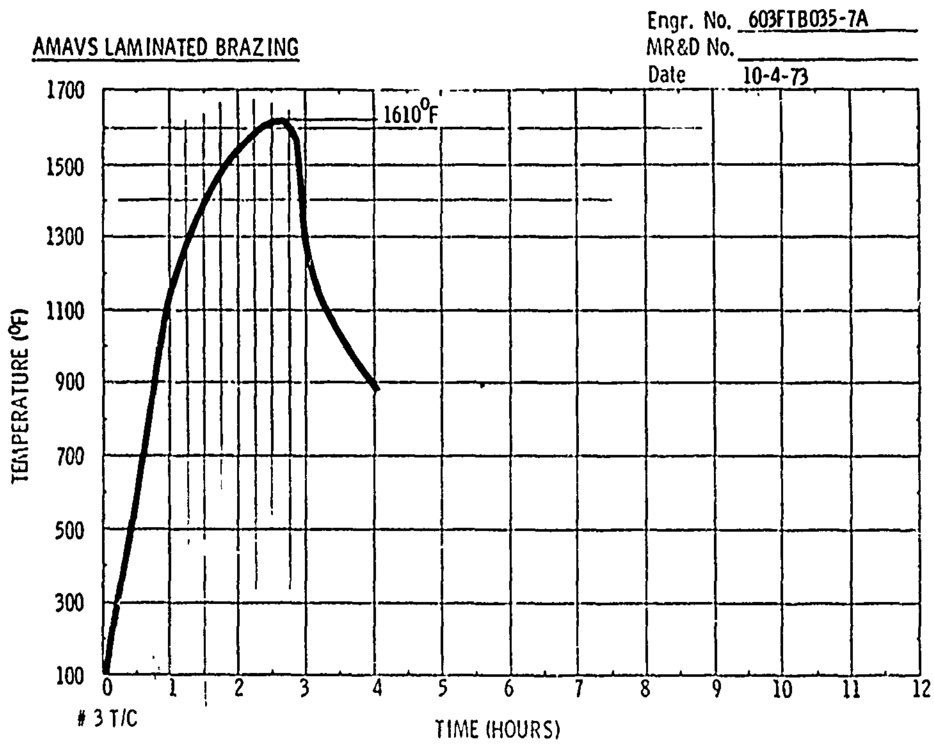


Figure 5-49 BRAZE CYCLE FOR 603FTB035-7A THERMOCOUPLE NO. 3

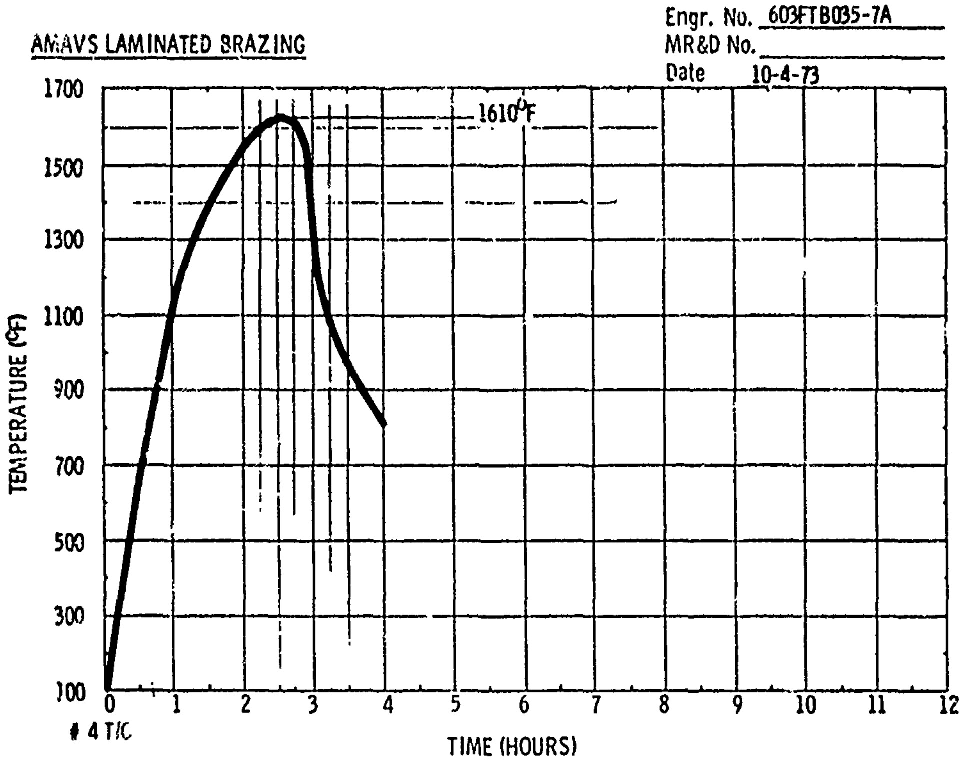


Figure 5-50 BRAZE CYCLE FOR 603FTB035-7A THERMOCOUPLE NO. 4

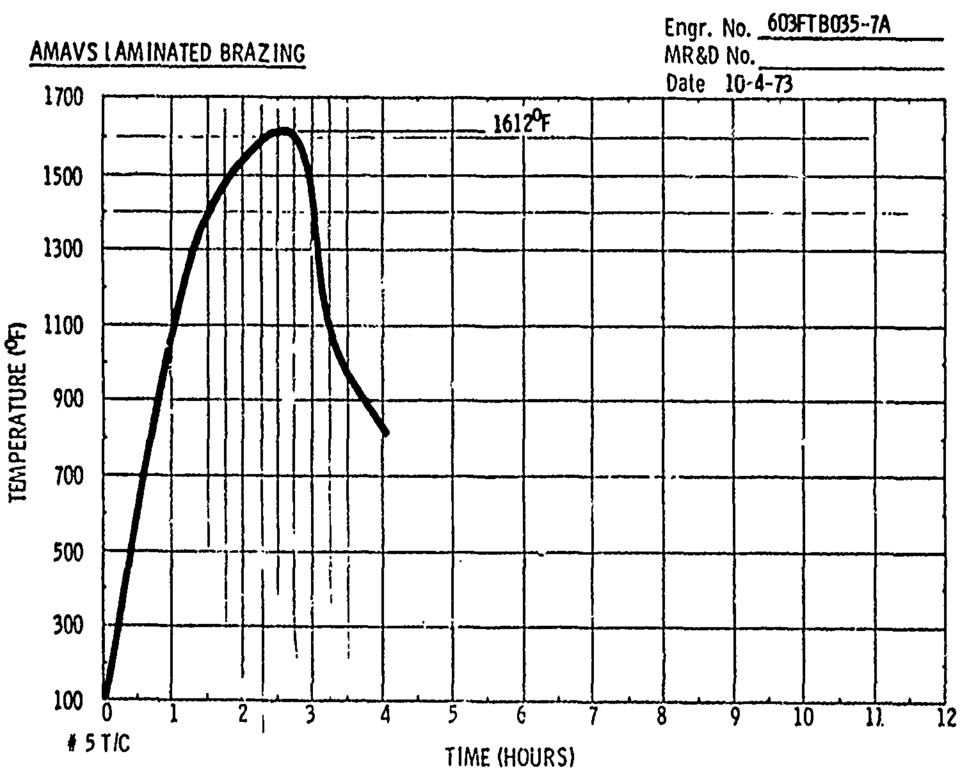


Figure 5-51 BRAZE CYCLE FOR 603FTB035-7A THERMOCOUPLE NO. 5

Visual inspection of the brazed part showed good filleting, alloy wetting, and flow in both braze lines around all exposed edges. There was little discoloration on the titanium details. Examples of alloy filleting and flow are shown in the photographs in Figures 5-52 and 5-53. The upper and lower surfaces of the brazed part are shown in the photographs in Figures 5-54 and 5-55.

Ultrasonic inspection showed narrow, intermittent light voids extending in the longitudinal direction the entire length of the part. It is believed that these voids resulted from longitudinal depressions in the braze surface of the titanium details. The titanium braze details for this part were finished for brazing by wet precision belt grinding after rough machining both surfaces. Previous inspection of the details after grinding had detected longitudinal depressions running the length of the part (see Figure 5-56). The most severe depressions had a maximum depth of 0.001-inch over a width of 1.5-inches. This condition was apparent in varying degrees in all three titanium details.

Braze Alloy Used in 603FTB035-3C and -7A

The braze alloy used in test parts 603FTB035-3C and -7A was an Ag-Al-Mn alloy supplied by Western Gold and Platinum Co. of Belmont, California. After receipt of the alloy liquidus-solidus tests were run to verify the compatibility of the alloy with the projected brazing temperature. Curves from which liquidus-solidus determinations were made are shown in Figures 5-57 and 5-58.

## 5.2 WIDE-AREA ADHESIVE BONDING

Large Beta C titanium adhesive bonded, metal laminate (3 and 4 ply) bulkhead panels were required for both the FSRL and "No Box" box designs.

Details for a typical bulkhead panel (Figure 5-59) were prepared to determine if machining cutouts, pockets and "finger strips" would cause distortion detrimental to bonding. In addition, a 1/8 x 36 x 40 inch sheet of Beta C titanium was chemically etched to evaluate this method of metal removal as an alternate to machining.

4-54298

Figure 5-52 UPPER PLATE SURFACE OF BRAZED 603FTB035-7A-
NOTE ALLOY FILLETING IN HOG-OUT AREA

4-54299

Figure 5-53 LOWER PLATE SURFACE OF BRAZED 603FTB035-7A-
NOTE ALLOY FILLETING IN HOG-OUT AREA

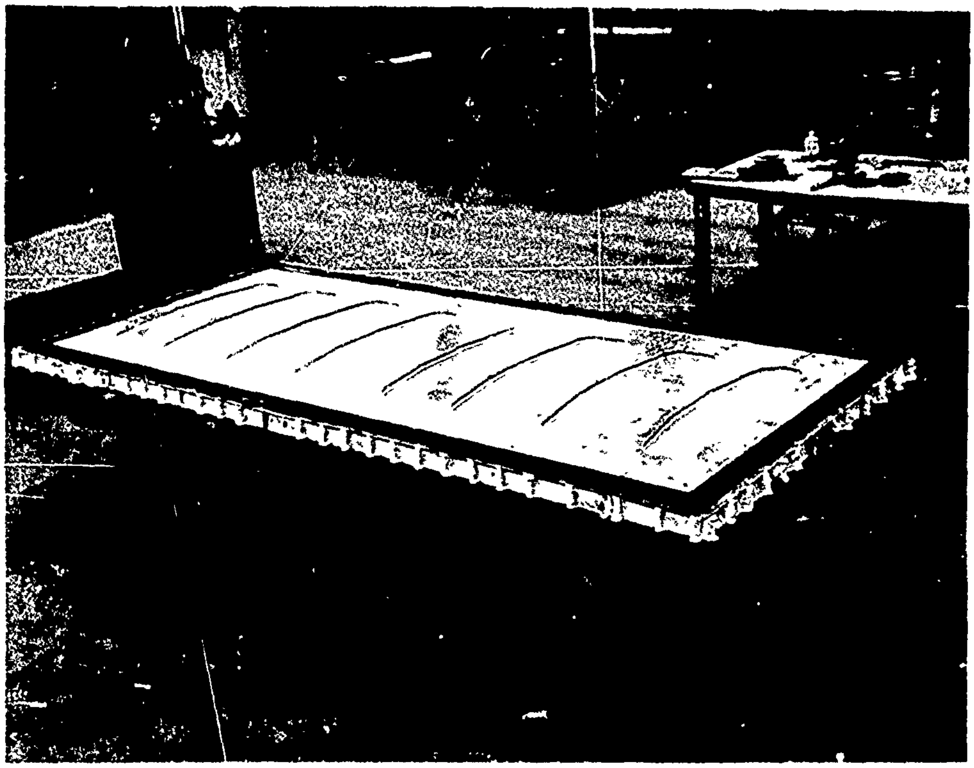

4-54302

Figure 5-54 BRAZED TEST SPECIMEN 603FTB035-7A READY FOR REMOVAL FROM BRAZE BOX (UPPER SURFACE)

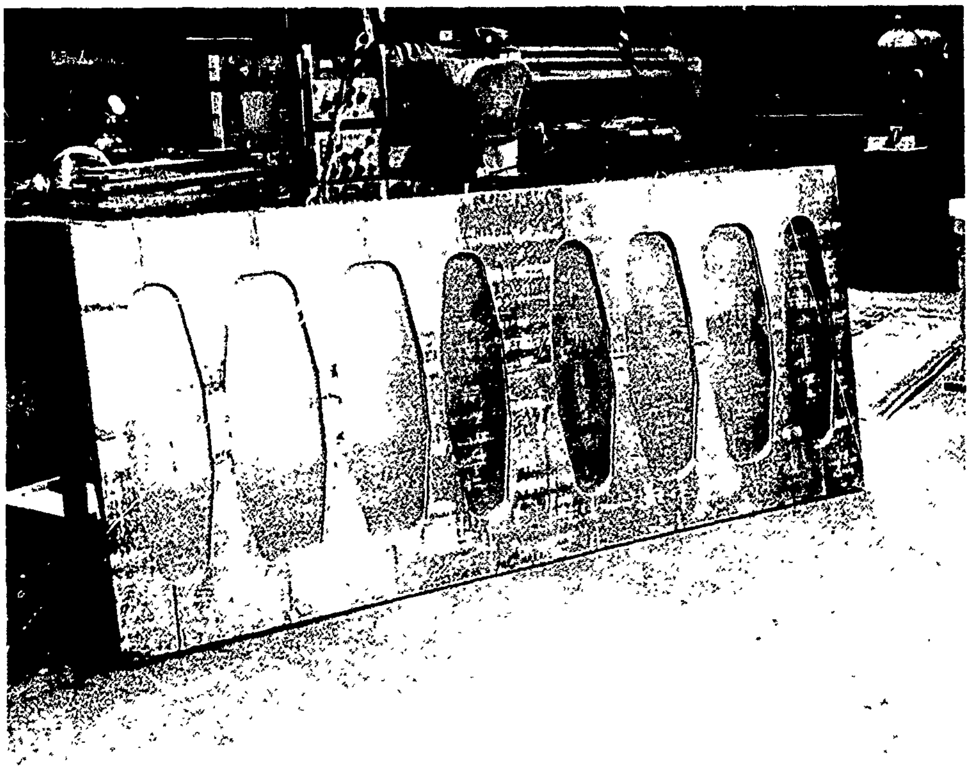

4-54300

Figure 5-55 LOWER SURFACE OF BRAZE TEST SPECIMEN 603FTB035-7A

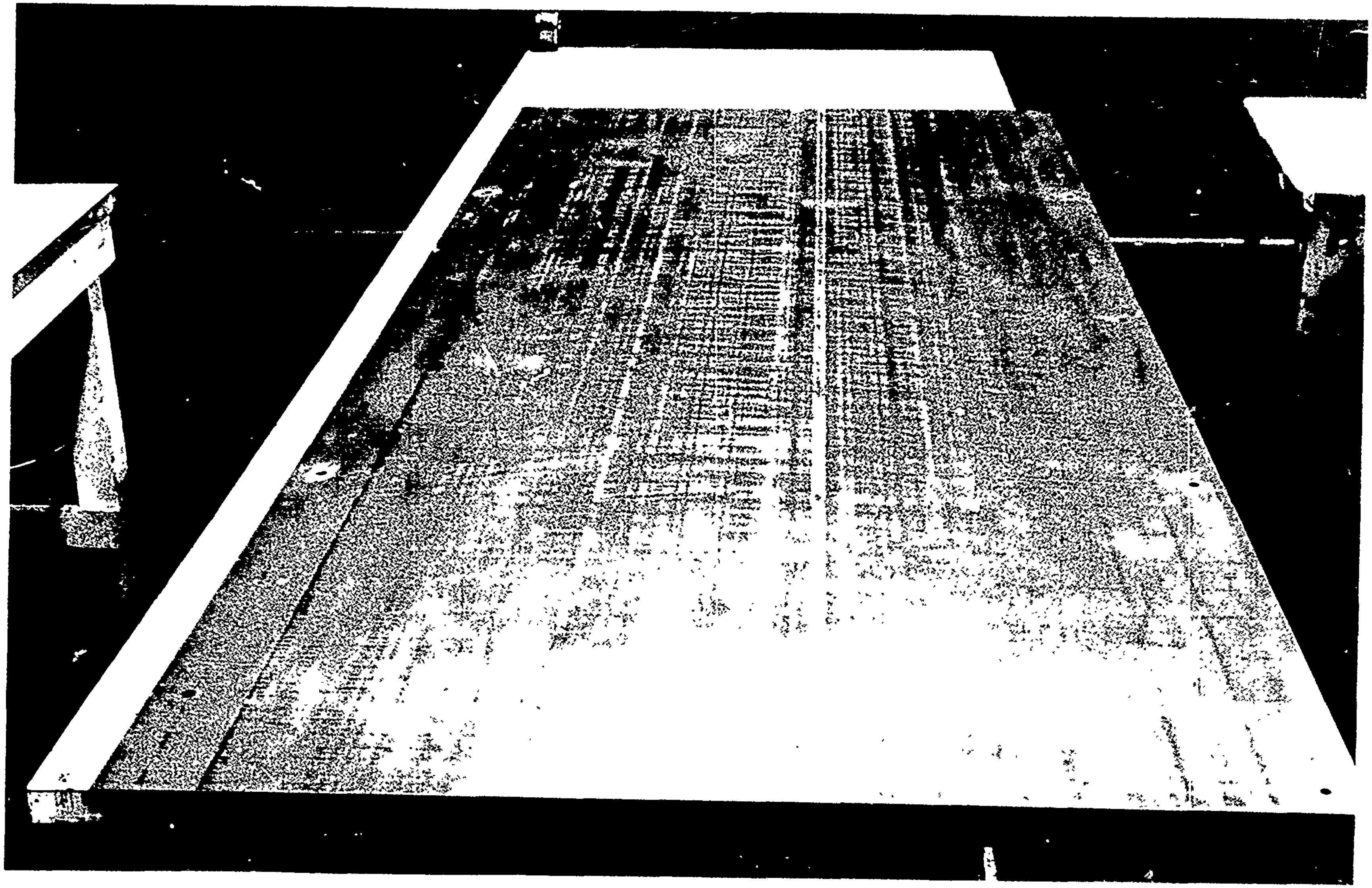

Figure 5-56 BRAZE SURFACE OF CENTER TITANIUM PLATE FOR 603FTB035-7A

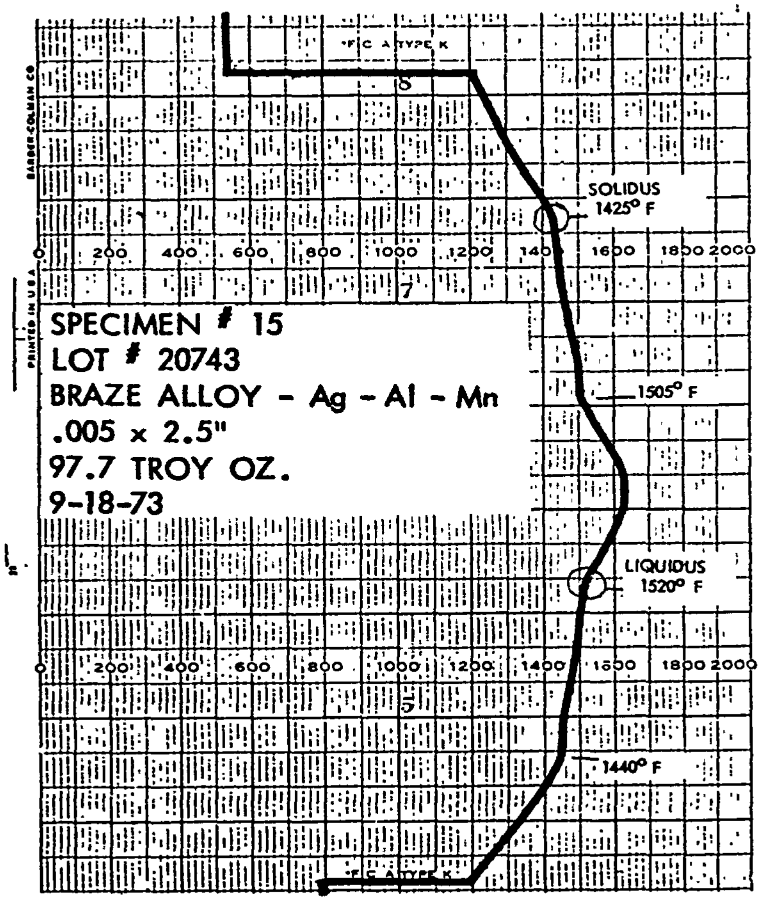


Figure 5-57 LIQUIDUS/SOLIDUS CURVE FOR BRAZE ALLOY USED IN 603FTB035-3C

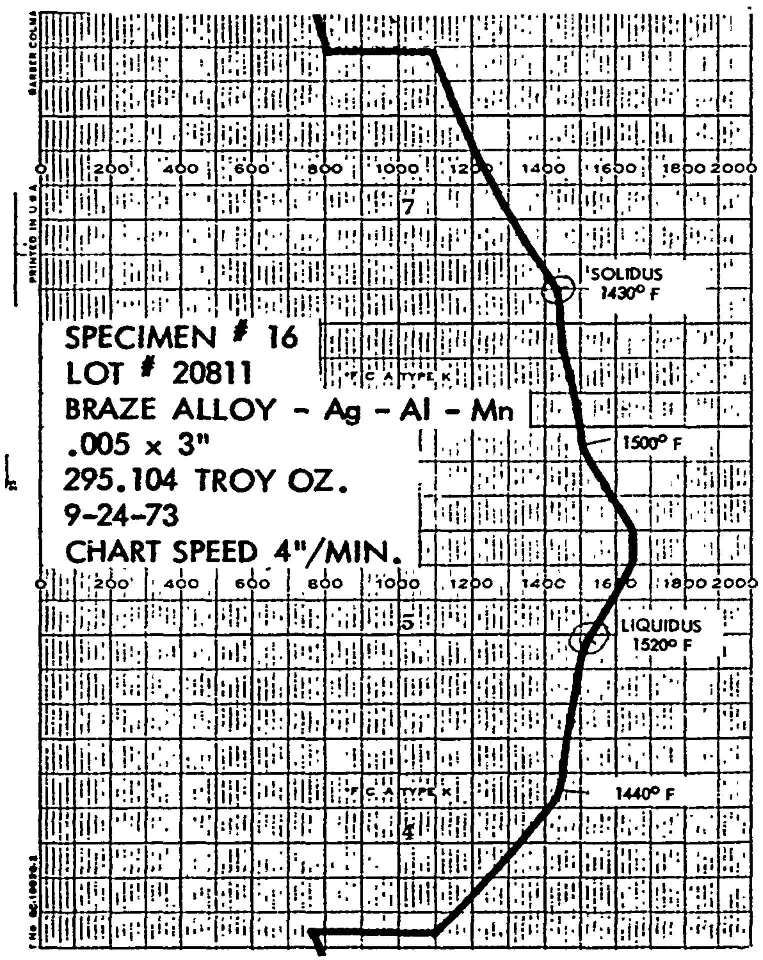


Figure 5-58 LIQUIDUS/SOLIDUS CURVE FOR BRAZE ALLOY USED IN 603FTB-35-7A

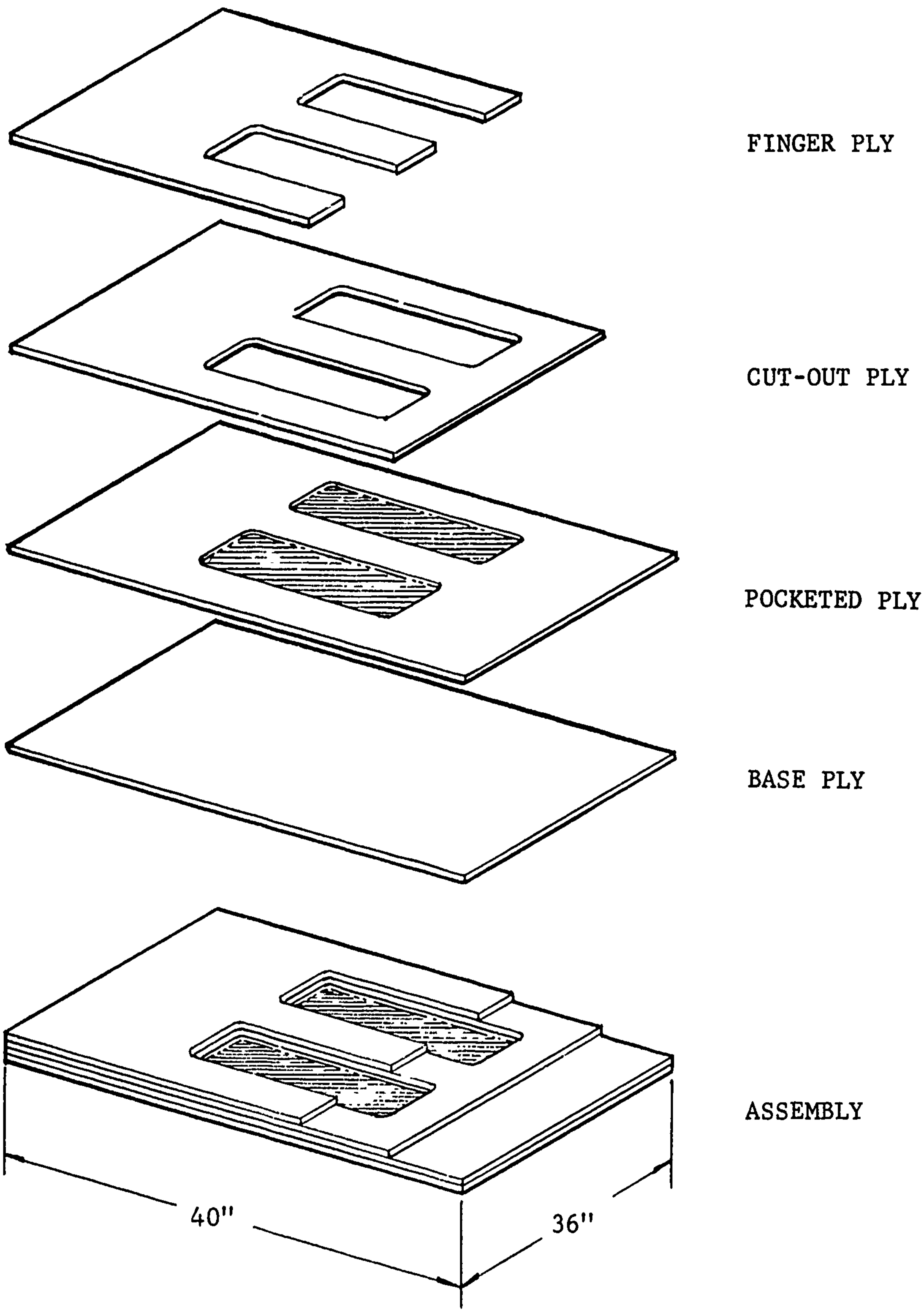


Figure 5-59 SIMULATED 4 PLY BULKHEAD PANEL (ADHESIVE BONDED BETA C TITANIUM)

Machining and bonding tests were not completed. Failure of the Beta C titanium to meet critical engineering requirements deleted the material from the carry-through structure design and the machining and bonding tests were terminated. However, the chemical etching test was completed and significant data obtained.

Pockets and cutouts were etched from the 1/8 inch Beta C titanium alloy sheet as shown in Figure 5-60. The pockets were approximately 0.060-in. deep. Etching operations drastically changed the sheet contour, making it unsuitable for bonding. Curvature greater than one inch occurred along the 40 inch sheet length as shown in Figure 5-61. In addition, the etched pocket areas "canned" 0.100 inch or greater, away from area where the material was removed. Figure 5-62 shows this distortion on the material side opposite of the etched pockets (areas that contact the straight edge).

Analysis of specimens taken from selected areas in the panel showed extremely high hydrogen pickup by the Beta C alloy from chemical etching.

| Area | $H_2$ (PPM) |
| --- | --- |
| No chemical etch | 78 |
| Edge etched | 150 |
| Bottom of pocket 1 | 534 |
| Bottom of pocket 2 | 573 |

Chem etching thickness results are shown in Figure 5-63.

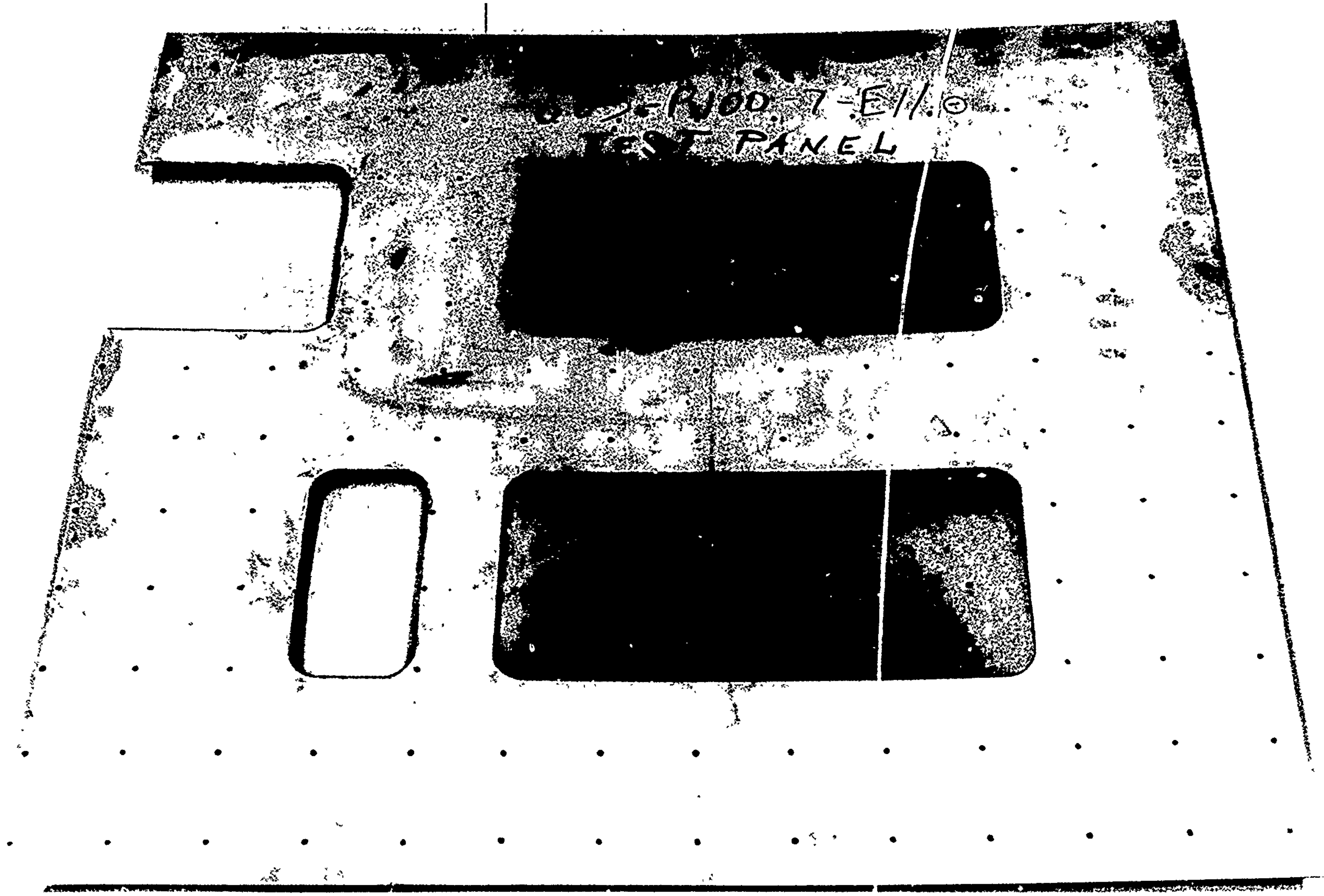

Figure 5-60 CHEMICALLY ETCHED TEST PANEL (1/8 X 36 X 40 INC
BETA C TITANIUM)

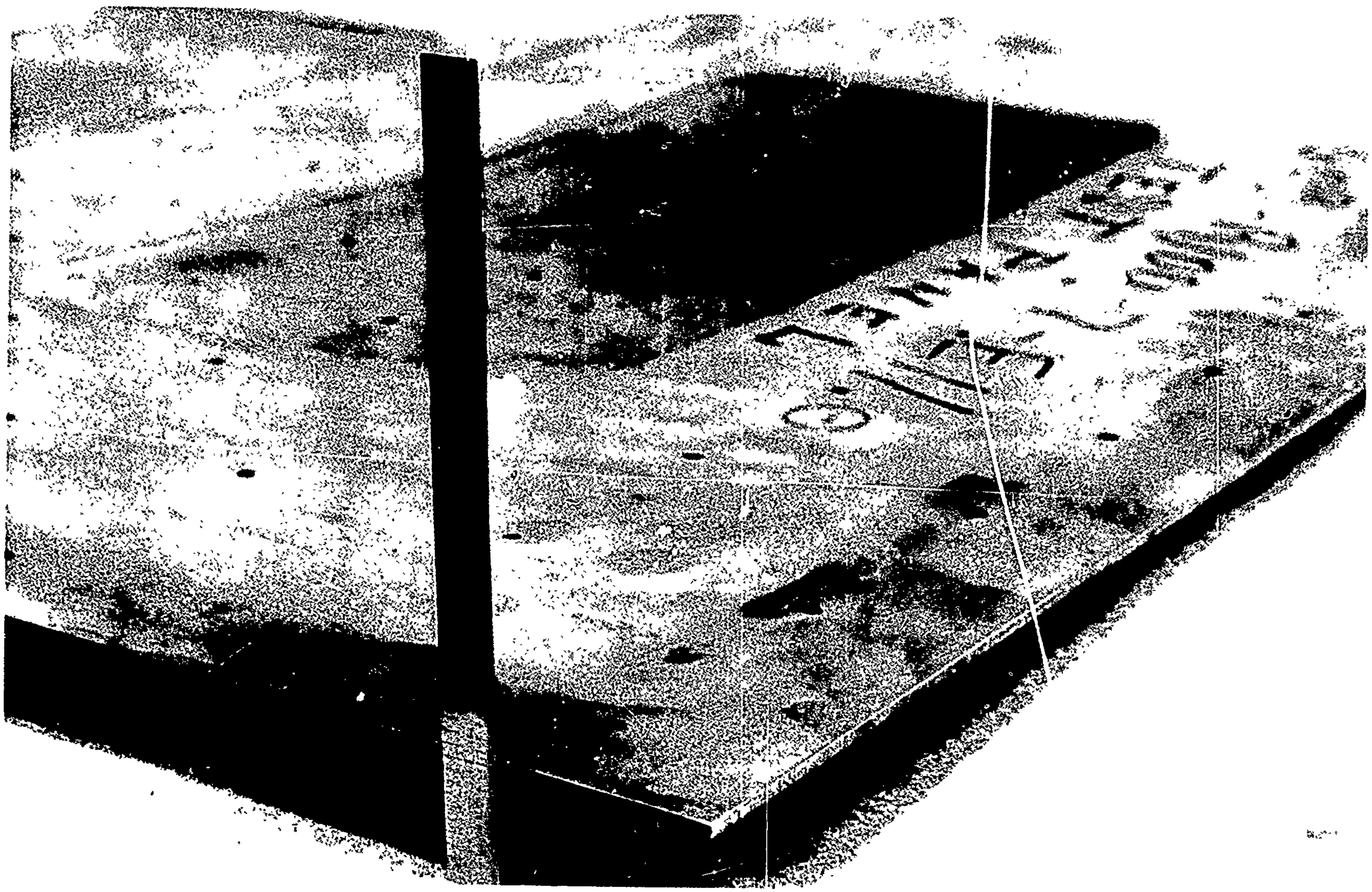

4-53037

Figure 5-61 OVERALL WARPAGE OF 1/8 INCH BETA C TEST PANEL FROM CHEMICAL ETCHING

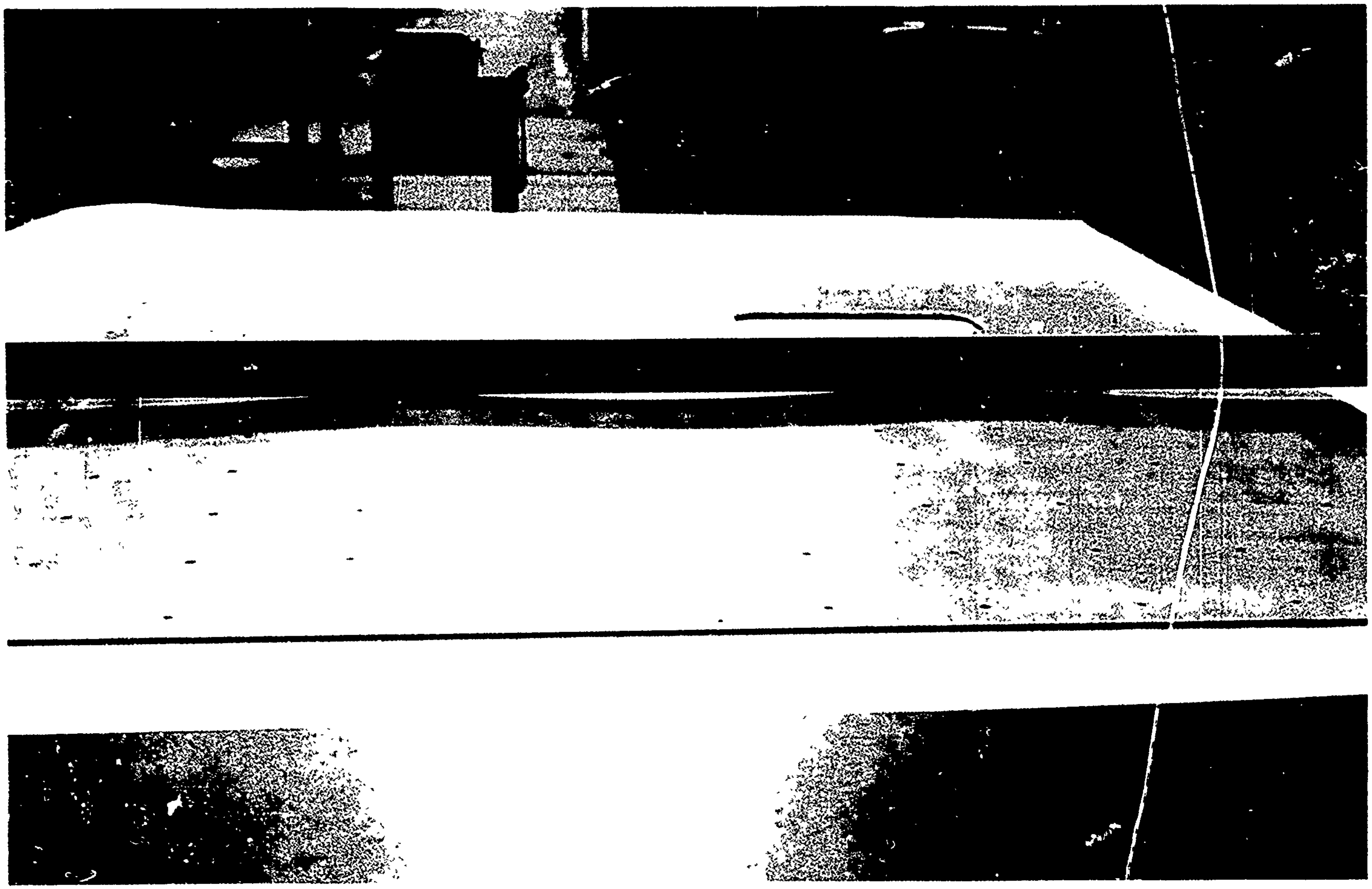

Figure 5-62 WARPAGE RESULTING FROM CHEMICAL ETCHING .060 INCH DEEP POCKETS IN 1/8 INCH BETA C TITANIUM

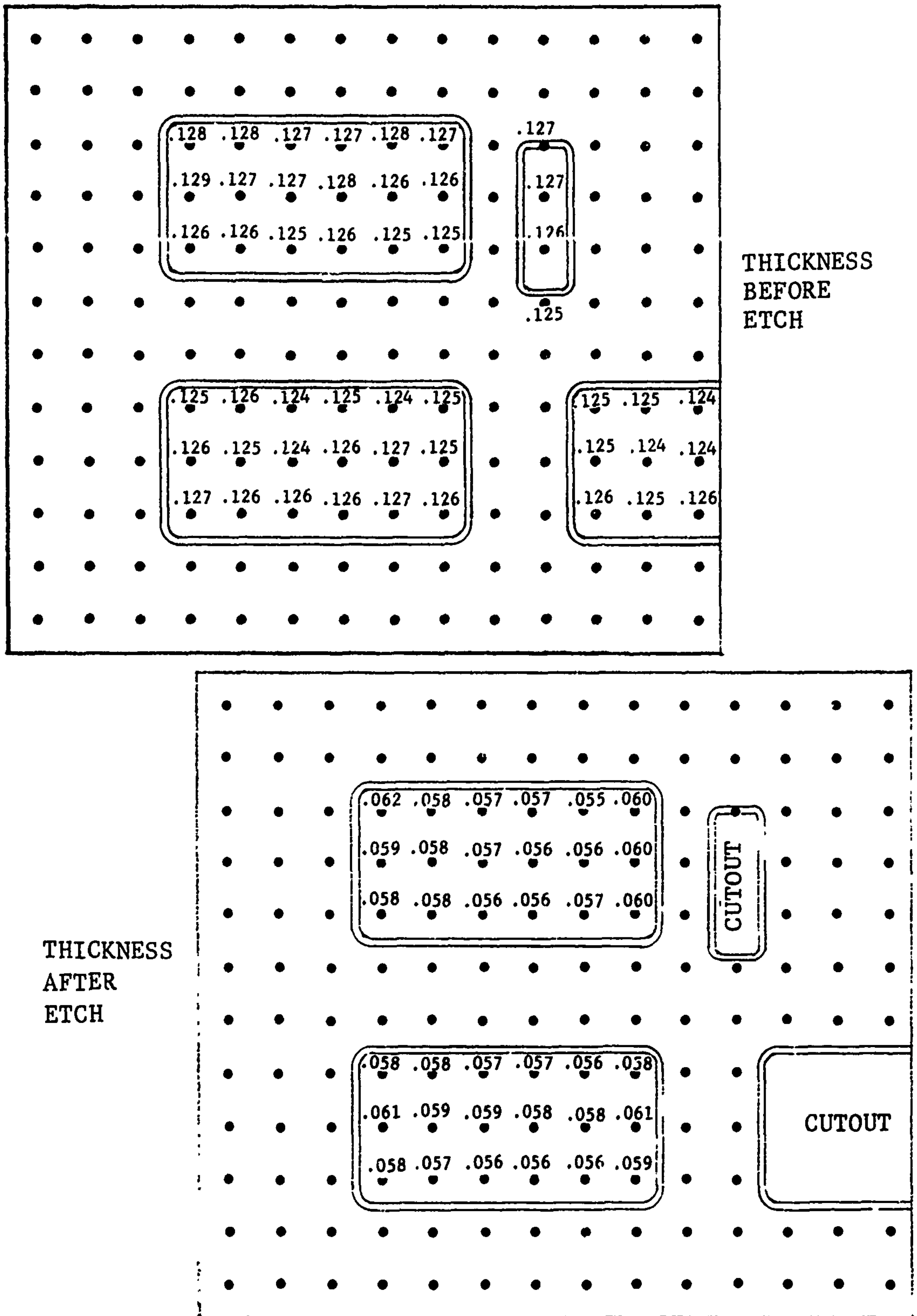


Figure 5-63 THICKNESS MEASUREMENTS BEFORE AND AFTER CHEMICAL ETCHING OF BETA C TITANIUM SHEET

## 5.3 WELDING 10 NI STEEL

The NBB configuration includes several 10 Ni steel welded joints in relatively thick material. An industry survey disclosed very limited information on gas tungsten arc (GTA) welding of 10 Ni steel, and no data on electron beam (EB) welding. Development programs were initiated to provide the necessary data on both processes.

### 5.3.1 Electron Beam Welding

The objectives of the EB weld program were to establish capability and process limitations for joining various thicknesses of 10 Ni (HY-180) steel.

Requirements for EB butt welds in the NBP design were originally in 0.375, 0.90 and 2.10-inch thick 10 Ni steel. Subsequent design refinements changed the maximum section thickness to 1.6 inches. EB weld parameters were successfully developed for 0.50-inch thick 10 Ni steel and consistently good welds produced. Efforts to EB weld 1.6-inch thick 10 Ni were unsuccessful. Defect free welds could not be consistently made with the limited available material. This does not mean that thick sections of 10 Ni steel cannot be EB welded, however, considerable time and material will be required to achieve consistent, good quality welds on 1.0-inch and thicker material.

#### 5.3.1.1 Development of Weld Parameters for Thick 10 Ni Material (1.0 and 1.6 inch)

Based on previous EB welding experience with other materials, the ideal EB weld nugget is parallel-sided with a uniform crown on the face of the weld. Full (100%) penetration welds should have a uniform root, the width of which is dependent on the welding parameters and material heat transfer characteristics.

In EB welding thick sections of material, the face and root surface condition is dependent upon surface tension supporting the column of molten metal as the weld is being made. Insufficient surface allowed the 10 Ni material to flow and form an extremely heavy globular underbead (Figure 5-64) when welding speed was decreased or beam power increased to get full penetration. The sag of these globules caused a severe underfill on the face of the weld and even with added filler metal, produced gross internal voids as shown by the longitudinal X-ray in Figure 5-65.

Weld parameter adjustments to eliminate this condition consisted of a careful increase in speed to reduce the time at melting temperature or a reduction of beam current density. Balance of the welding parameters became more sensitive as the material thickness increased. The effect of small changes is illustrated in Figure 5-64 where a change of 2 inches per minute weld speed drastically altered the weld root shape.


Figure 5-64 EB WELD ROOT OF 1.6 INCH THICK 10 Ni STEEL SHOWING GLOBULAR AND UNIFORM PENETRATION 4-54719

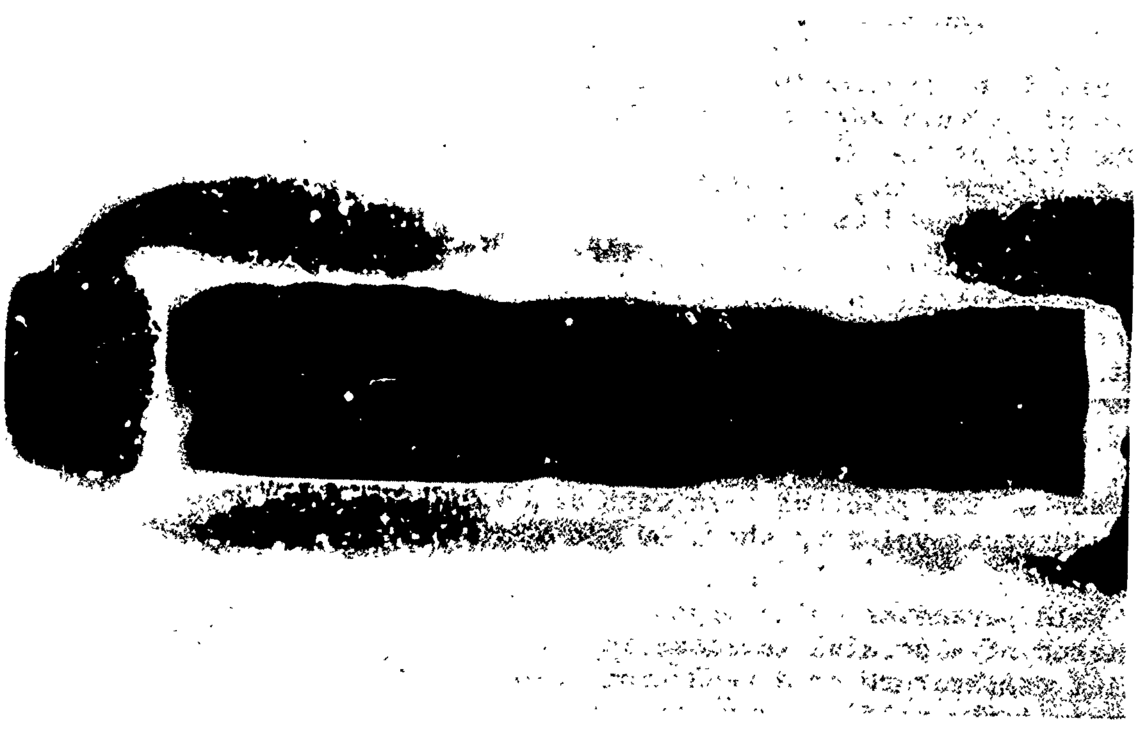

Figure 5-65 X-RAY OF WELD SPECIMEN FROM FIGURE 5-64 SHOWING VOIDS AND MICROFISSURES

The longitudinal X ray (Ref. Figure 5-65) of this particular weld shows voids above the globules and micro fissures above the uniform root. The microfissures shown are typical for thick section EB welds on low alloy steels. In many cases, they are impossible to detect by conventional X-ray techniques because of the small size and location. However, ultrasonics was successfully used to inspect EB welds on 10 Ni in the "as welded" condition after the weld reinforcement was removed. Ultrasonic inspection results were verified by macro section and longitudinal section X ray.

## Beam Focus

Heat input for electron beam welding is controlled by four basic parameters; voltage, beam current, weld travel speed and the diameter of the beam at the surface or within the workpiece. This beam crossover point location is usually referred to as face, midpoint or root focus and simply indicates the point of maximum beam current density. The work accomplished to date indicates that very close control of the beam focal point and its resulting weld profile is extremely important in obtaining sound EB welds in 10 Ni steel.

Initial bead-on-plate studies on 2.0-inch thick 10 Ni consisted of determining the effect of the focal point on the weld geometry. Midpoint focus resulted in the best weld cross section geometry. However, the parallel side weld geometry obtained with 0.500-inch thick material (Figure 5-66), was not obtained on the thicker sections. Macro sections of 1.6-inch thick welds shown in Figure 5-67 (A, B and C) are typical examples of microfissures that occurred in the center of non-parallel sided welds. This indicates that solidification occurred last in that area, forming a crack when the relatively weak hot metal attempted to contract and pull the adjacent strong cold metal with it. Figure 5-67 (D) shows a defect free macrosection.

## Beam Oscillation

Beam oscillation is sufficient to produce parallel-sided weld geometry on thinner sections, such as the 0.500-inch thick weld shown in Figure-5-68. Attempts to spread the weld with beam oscillation in the thicker sections were unsuccessful.

## Multipass Welding

Welds were made using both single and multipass techniques, but no appreciable difference could be noted on the weld quality.

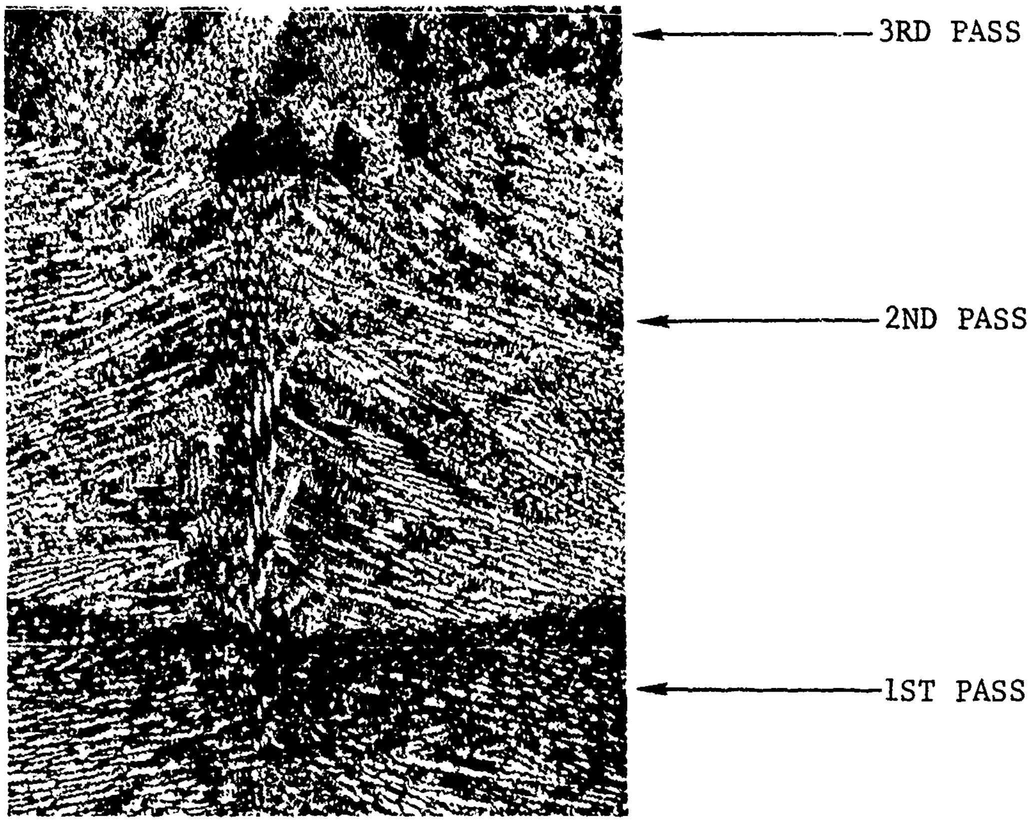


100X

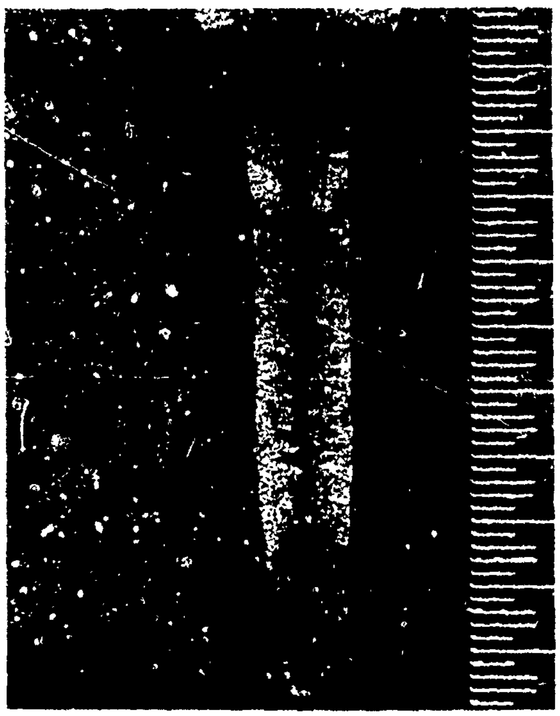

10X

Figure 5-66 MACRO AND MICRO STRUCTURE OF EB WELDED .500 INCH THICK 10 Ni STEEL (WELD NO. H10)

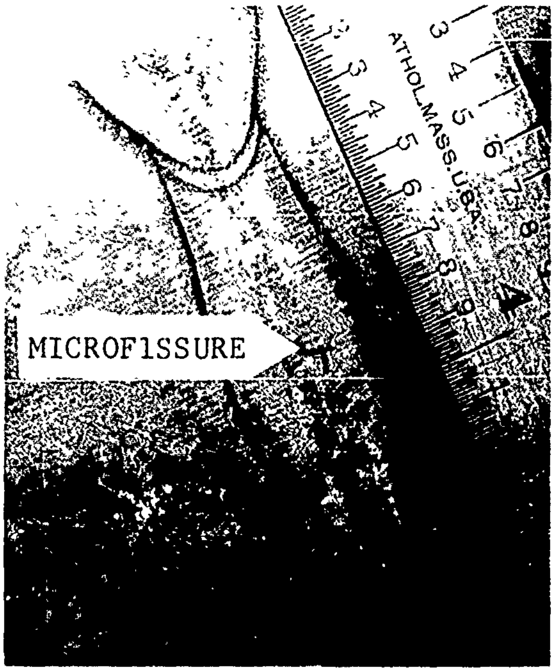


A - DEFECTIVE WELD

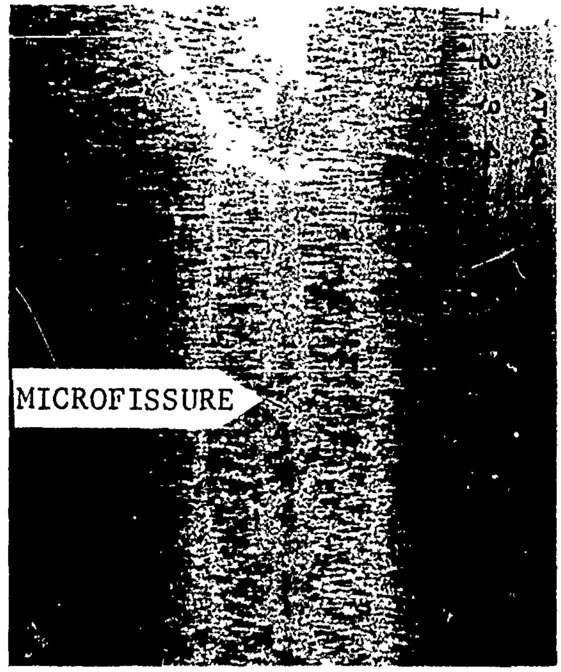


B - DEFECTIVE WELD

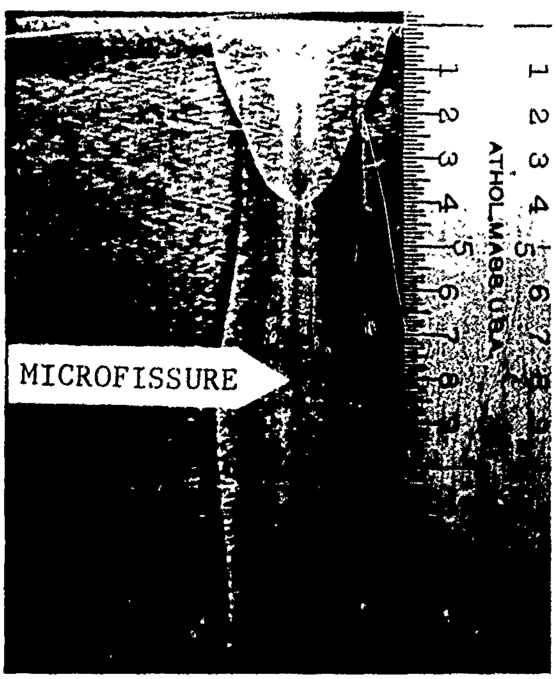


C - DEFECTIVE WELD

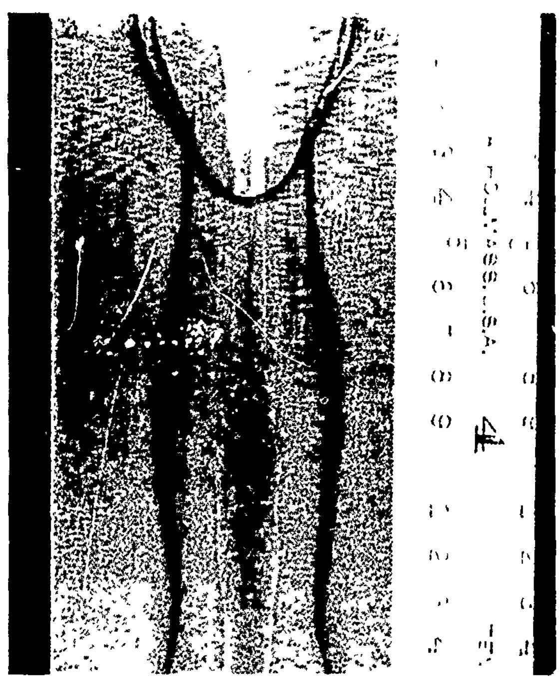

D - GOOD WELD

Figure 5-67 MACROS OF EB WELDS ON 1.61 INCH THICK 10 Ni STEEL SHOWING TYPICAL MICROFISSURES AND GOOD WELD

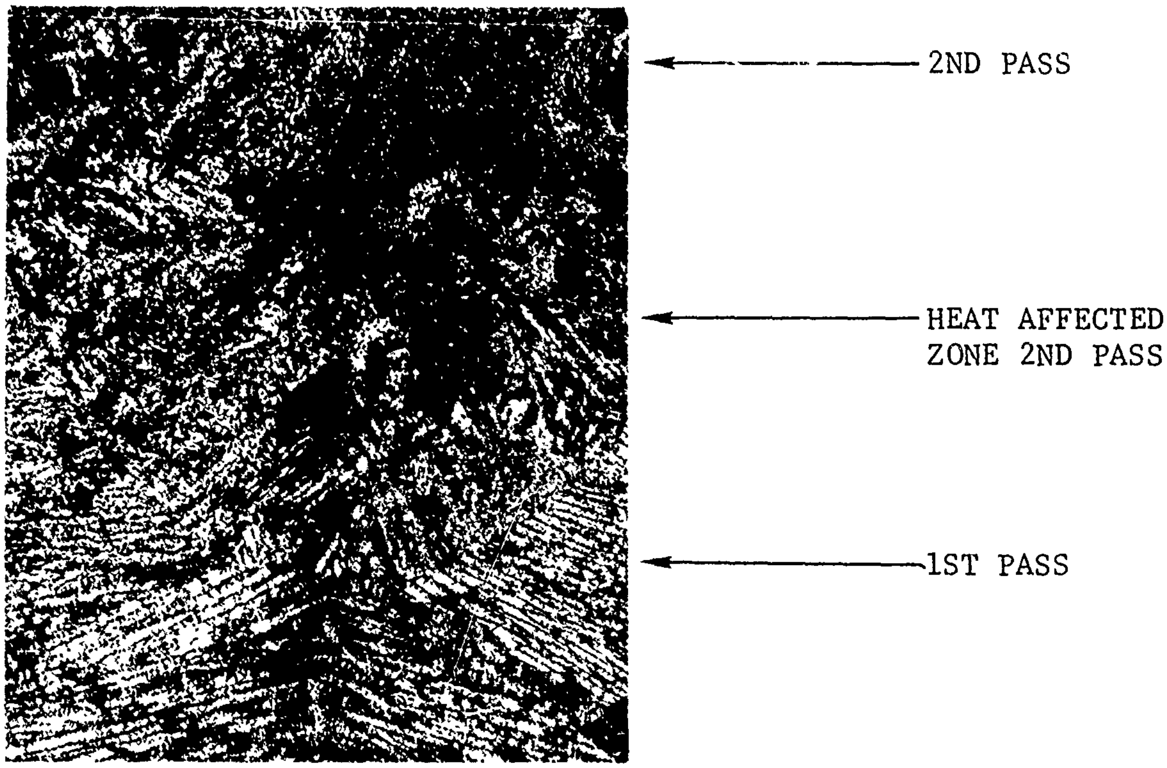


100X

10X

Figure 5-68 MACRO AND MICRO STRUCTURE OF EB WELDED .500 INCH THICK 10 Ni STEEL (WELD NO. H11)

It is significant that defects found in the cross-section macros could not be attributed to the multipass technique since defects are not near the root of the filler pass.

Filler Wire

Welds were made with and without filler wire to study the effects of added filler metal. The results of several bead-on-plate welds with added filler did not solve the cracking problems but did increase the gap allowance from ± 0.005 inch to ± 0.020 inch. Machine cleanup of both face and root beads was also reduced from 0.090 inch per surface to less than 0.030 inch per surface by using filler wire.

Weld Shrinkage

Transverse shrinkage measurements were made across two 1.6-inch thick welds and are shown in Table V-1. These measurements were made on 15-inch long welds to represent conditions that would be found in full scale parts. The shrinkage was small and uniform, indicating very little movement in the transverse plane.

Backup Plates

A backup plate of the same material is used for EB welding thick sections when the root geometry cannot be controlled by adjusting weld parameters. Backup plates have been used successfully on materials that are not producers of high vapor pressures. In the case of 10 Ni steel, the backup plates acted as a thermal barrier and vapor trap instead of supporting the molten metal column. This condition caused the molten steel to boil and form an uncontrollable weld puddle. Metal expulsion, in the form of splatter and a heavily ionized vapor column back streaming into the EB gun, caused high voltage discharges or arc outs. Weld root porosity resulted from the use of backup plates and no satisfactory welds could be made.

5.3.1.2 EB Welding of 0.500-Inch Thick 10 Ni Steel

Engineering design on the main landing gear drag fitting (common to both WCT designs) requires EB welds on 0.375, 0.400 and 0.500-inch thick 10 Ni steel.

A limited number of 0.500-thick welds were made to determine joint efficiency, weld shrinkage and inspection methods. Weld shrinkage on 0.500-inch thick welds is shown in Table V-2

Table V-1 TRANSVERSE SHRINKAGE OF ELECTRON BEAM WELDS WITH 1.6 INCH THICK 10 Ni STEEL

| Location | SPECIMEN WIDTH (INCHES) Before Welding | After Welding | Transverse Shrinkage | |
|---|---|---|---|---|
| 1 | 5.970 | 5.956 | .014" | |
| 2 | 5.970 | 5.956 | .014 | |
| 3 | 5.970 | 5.955 | .015 | |
| 4 | 5.970 | 5.955 | .015 | |
| 5 | 5.970 | 5.955 | .015 | |
| 6 | 5.970 | 5.955 | .015 | |
| 7 | 5.970 | 5.955 | .015 | Weld No. H-28 |
| 8 | 5.970 | 5.955 | .015 | |
| 9 | 5.971 | 5.955 | .016 | Average weld |
| 10 | 5.970 | 5.955 | .015 | shrinkage |
| 11 | 5.971 | 5.955 | .016 | .0015" |
| 12 | 5.971 | 5.955 | .016 | |
| 13 | 5.971 | 5.915 | .016 | |
| 14 | 5.971 | 5.955 | .016 | |
| 15 | 5.970 | 5.956 | .014 | |
| 16 | 5.971 | 5.957 | .014 | |
| 1 | 5.998" | 5.982" | .016" | |
| 2 | 5.998 | 5.591 | .017 | |
| 3 | 5.997 | 5.980 | .017 | |
| 4 | 5.997 | 5.979 | .018 | |
| 5 | 5.998 | 5.980 | .018 | |
| 6 | 5.998 | 5.980 | .018 | |
| 7 | 5.998 | 5.980 | .018 | Weld No. H-29 |
| 8 | 5.998 | 5.980 | .018 | |
| 9 | 5.998 | 5.980 | .018 | Average weld |
| 10 | 5.998 | 5.981 | .017 | shrinkage |
| 11 | 5.998 | 5.981 | .017 | .0016" |
| 12 | 5.998 | 5.981 | .017 | |
| 13 | 5.998 | 5.982 | .016 | |
| 14 | 5.998 | 5.982 | .016 | |
| 15 | 5.998 | 5.983 | .015 | |
| 16 | 5.998 | 5.984 | .014 | |

All measurements taken at 1 inch spacing.

Table V-2 TRANSVERSE SHRINKAGE OF ELECTRON BEAM WELDS WITH .500 INCH THICK 10 Ni STEEL

SPECIMEN WIDTH (INCHES)

| Location | Before Welding | After Welding | Transverse Shrinkage | |
|---|---|---|---|---|
| 1 | 5.500 | 5.493 | .007 | |
| 2 | 5.501 | 5.494 | .007 | |
| 3 | 5.501 | 5.493 | .008 | |
| 4 | 5.501 | 5.493 | .008 | |
| 5 | 5.501 | 5.493 | .008 | |
| 6 | 5.501 | 5.493 | .008 | |
| 7 | 5.502 | 5.493 | .009 | Weld No. H-11 |
| 8 | 5.502 | 5.493 | .009 | |
| 9 | 5.502 | 5.493 | .009 | Average weld |
| 10 | 5.502 | 5.493 | .009 | shrinkage |
| 11 | 5.502 | 5.493 | .009 | .0082" |
| 12 | 5.502 | 5.494 | .008 | |
| 13 | 5.502 | 5.494 | .008 | |

| | | | | |
|---|---|---|---|---|
| 1 | 5.820 | 5.817 | .003 | |
| 2 | 5.820 | 5.816 | .004 | |
| 3 | 5.821 | 5.816 | .005 | |
| 4 | 5.822 | 5.816 | .006 | |
| 5 | 5.822 | 5.816 | .006 | |
| 6 | 5.823 | 5.816 | .007 | |
| 7 | 5.823 | 5.816 | .007 | Weld No. H-10 |
| 8 | 5.824 | 5.817 | .007 | |
| 9 | 5.824 | 5.816 | .008 | Average weld |
| 10 | 5.825 | 5.817 | .008 | shrinkage |
| 11 | 5.826 | 5.818 | .008 | .0064" |
| 12 | 5.826 | 5.818 | .008 | |

All measurements taken at 1 inch spacing.

with an average of 0.0064 inch for weld No. H-10 and 0.0082 inch for weld No. H-11.

The two welded plates were machined into tensile specimens and tested to determine weld integrity. The mechanical properties of the two welds are shown in Table V-3. All failures were in the base metal except weld No. H-11-4 which had a termination crack caused by a missed joint. It is significant that this specimen pulled 174 KSI before failure. Both welds were made with the same parameters (see weld schedules in Appendix A ) except that the face pass was oscillated on weld No. H-11 and the beam defocused on weld No. H-10. X-ray inspection of both plates shows only termination flaws.

Figure 5-69 shows the tensile specimens after they had been tested. Note that all failures are in the base metal. The elongation averaged 16.2 percent and 17 percent for the two welds. The type of fracture surfaces of these specimens are typical for 10 Ni steel.

Welding schedules and beam current traces of parameter development welds are included in the appendix.

5.3.1.3 Conclusions from EB Weld Tests

1. Satisfactory EB welds can be made on 0.375, 0.500, 0.625-inch thick 10 Ni to Class I quality standards.

2. One-inch thick 10 Ni steel can be EB welded, but further work is required to achieve reproducibility and maintain quality.

3. EB welding thicknesses greater than 1.0 inch will require extensive additional development including both welding and metallurgical considerations.

4. Transverse weld shrinkage is consistent and can be predicted on both thick and thin sections.

5. Added filler wire can be used to minimize the amount of post weld machining requirements and to increase the gap tolerance from $\pm$ 0.005 inch without wire to + 0.020 inch with filler wire.

6. 10 Ni steel details must be thoroughly demagnetized just prior to welding. Any magnetized areas, with a field strength in excess of 1 gauss on a field strength meter, can cause

Table V-3 MECHANICAL PROPERTIES OF EB WELDED .500 INCH THICK 10 Ni STEEL TENSILE TEST SPECIMEN

| 10 Ni STEEL (HY-180) ELECTRON BEAM WELD | | | | | | |
|---|---|---|---|---|---|---|
| IDENT. | YIELD STRENGTH | ULTIMATE | ELONGATION | HARDNESS | | IMPACT |
| S/N | Fty at 0.2 Offset | Ftu KSI | % of 2 Inches | Rc | KSI | Ft/Lbs |
| H-10-1 (2,3) | 183.2 KSI | 186.2 | 16 | 41.8 | 193 | |
| -2 | 183.7 | 186.9 | 16 | 42.0 | 194 | |
| -3 | 183.5 | 186.0 | 16 | 42.8 | 198 | 84 (5) |
| -4 | 184.1 | 186.9 | 16 | 43.0 | 200 | |
| -5 | 182.3 | 185.6 | 16 | 42.2 | 195 | |
| -6 | 183.2 | 186.2 | 17 | 41.5 | 191 | |
| AVG. | 183.3 | 186.3 | 16.2 | 42.2 | 195.2 | (5) |
| H-11-1 (4) | 185.9 | 195.3 | 17 | 42.8 | 198 | 54 (Weld) |
| -2 | 182.5 | 194.7 | 18 | 43.8 | 205 | (5) |
| -3 | - | 193.3 | 16 | 44.8 | 212 | 60 (Base) |
| -4 | | 174.8 (1) | | 44.2 | 208 | |
| AVG. | 183.9 | 193.4 | 17.0 | 43.9 | 205.7 | (5) |

1. Approximately 0.100 inch weld joint at root was not fusion welded.
2. H-10, heat treatment was as follows: Austenitized: 1500°F for 2 hours, WQ, 950° Aged, 8 hours.
3. H-10, only initial weld pass plus cosmetic weld pass.
4. H-11, heat treatment was as follows: Austenitized: 1500°F for 2 hours, WQ, 950° Aged, 8 hours.
5. Impact tests were made in the Engineering Department Test Laboratory.

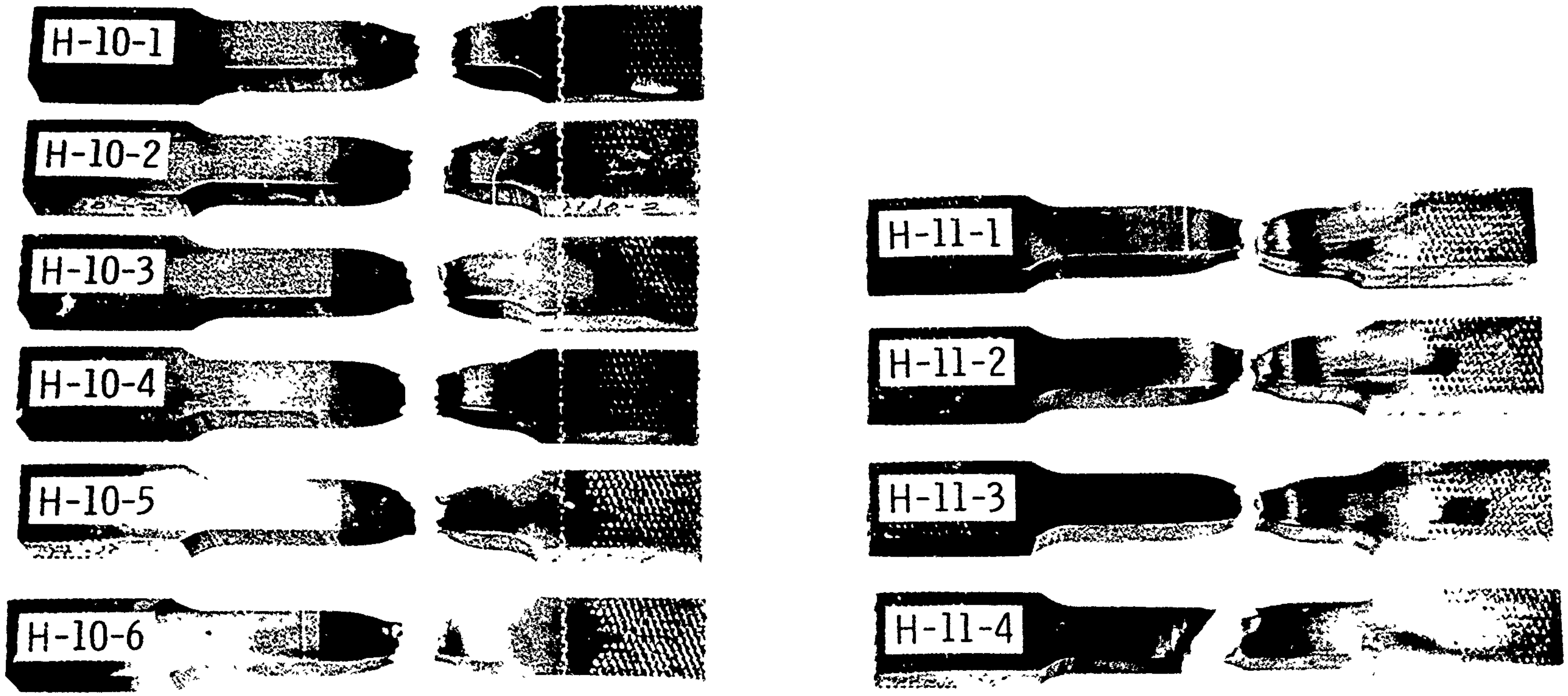


Figure 5-69 FAILED TENSILE SPECIMENS FROM EB WELDED .500 INCH THICK 10 Ni STEEL SHOWING FRACTURES

4-54718

serious beam deflection

7. The longitudinal cross-section method of EB weld inspection must be used for parameter development because of the small size of flaws in thick section welds.

#### 5.3.1.4 Recommendations for EB Welding of 10 Ni Steel

1. EB welding on 10 Ni steel should be restricted to joint thickness less than 1.0 inch until satisfactory procedures are developed for thicker sections.

2. Use of EB welding of 10 Ni steel on the wing carrythrough test structure should include the following procedures:

   - o Witness lines should be scribed on both face and root side of the weld joint and included on the engineering design.

   - o Beam current traces should be required on all EB welds to assure reproducibility and to provide a permanent record.

### 5.3.2 Gas Tungsten Arc Welding

#### 5.3.2.1 Weld Parameter Development

The first attempt at GTA welding 0.500-inch thick 10 Ni steel plate was accomplished using information supplied by Linde and U. S. Steel. The information indicated that the best fracture toughness resulted from very low heat input (KJ) values during welding. Weld test plates were machined with standard J-grooves as shown in Figure 5-70. The plates were set up and welded in the weld fixture shown in Figures 5-71 and 5-72. Recommended values did not achieve 100 percent root penetration and severe lack of fusion resulted. The weld current was incrementally increased 100 percent above the recommended level without adequate root penetration. To conserve material, the weld was cut out of the plate and the J-Grooves remachined. Weld travel speed was reduced from 6 ipm to 2.5 ipm and the plate was

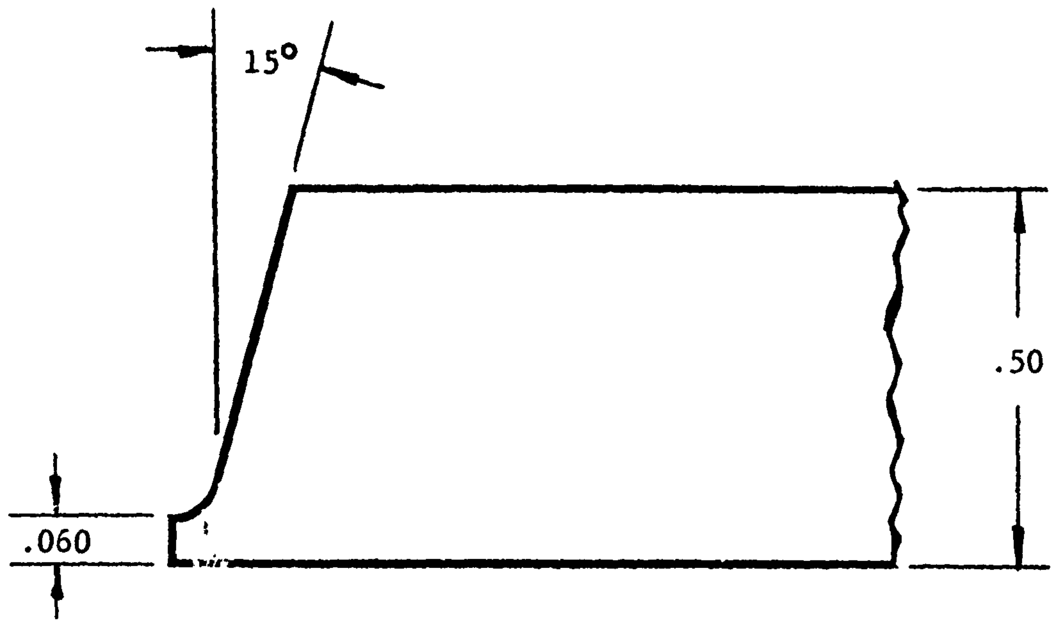


Figure 5-70 TEST PLATE J-GROOVE CONFIGURATION

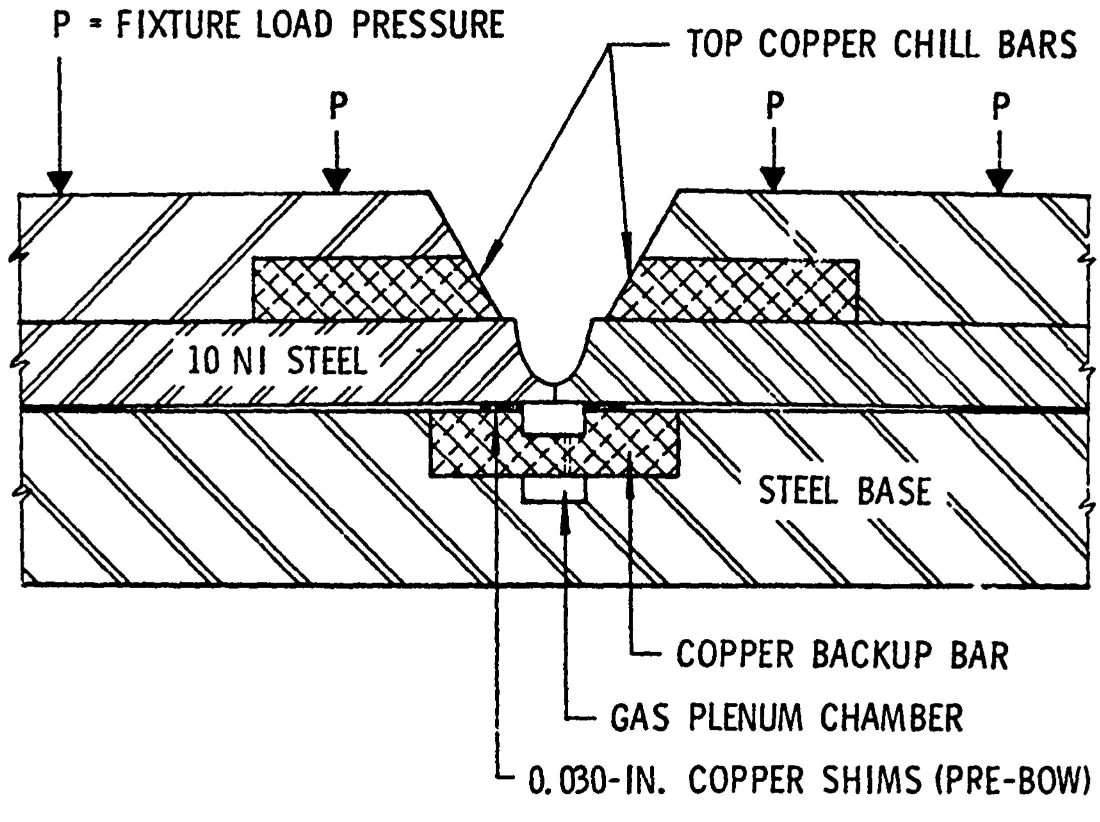


Figure 5-71 SECTION OF GTA WELD FIXTURE

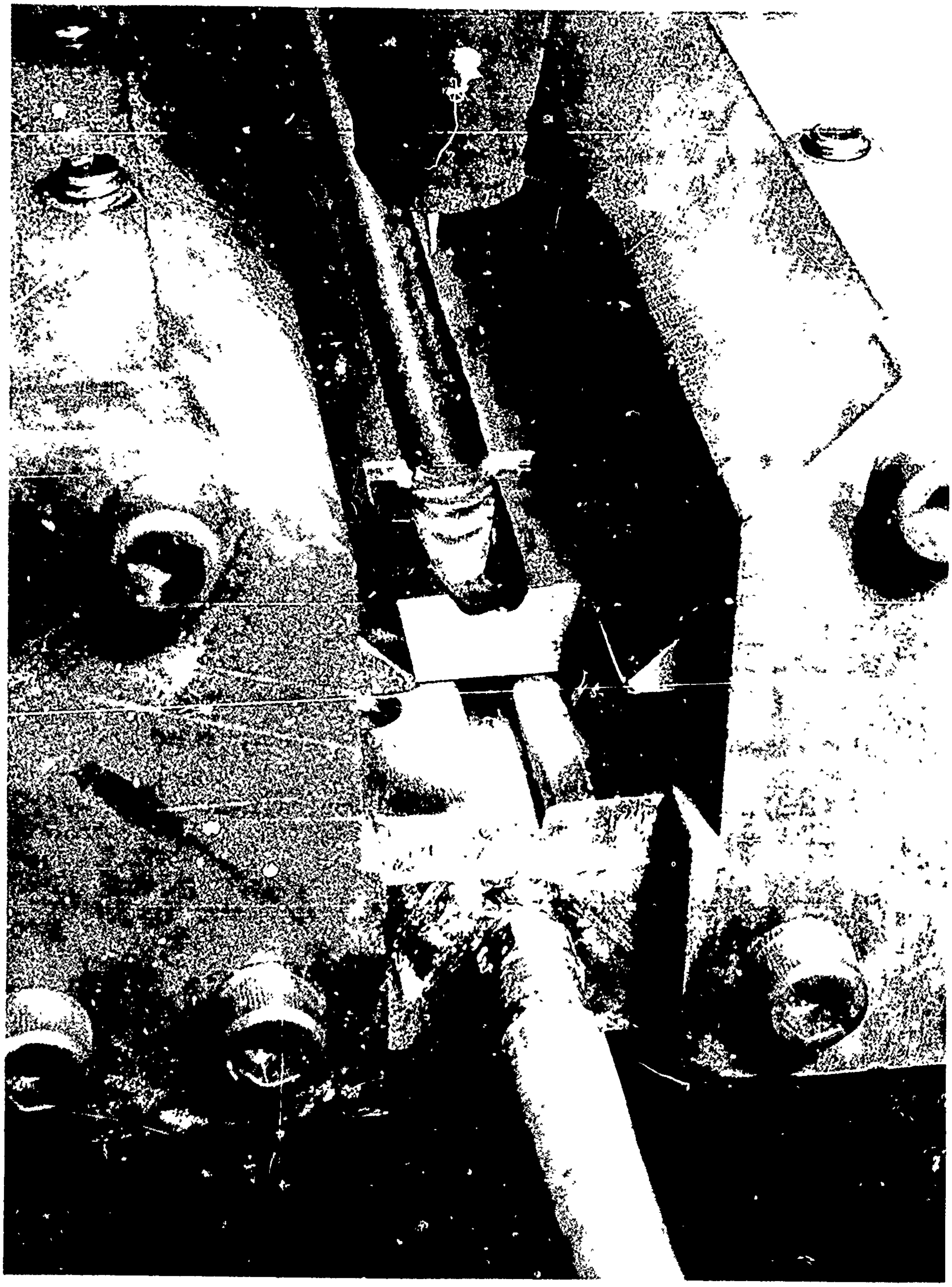

Figure 5-72 SETUP FOR USING WELD TABS

rewelded. Penetration was achieved. Further refinements were made in the weld parameters to obtain the weld schedule shown in Table V-4.

The root pass required higher heat input than the subsequent filler passes. The total joules/inch input was:

$$H = \frac{E \times I \times 60}{S}$$

H = Heat Input (Joules/inch)

E = Arc Voltage arc

I = Total pulsed current for level 1 and level 2

therefore:

$$H = \frac{13.0 \; \left(\frac{225 \times 10 + 180 \times 5}{15}\right)}{2.0} \times 60 = 75{,}600 \text{ Joules/inch}$$

The subsequent filler pass heat input is expressed as:

$$H = \frac{13 \; \left(\frac{160 \times 15 + 200 \times 5}{20}\right)}{4.0} \; 60 = 33{,}200 \text{ Joules/inch}$$

The capping pass which is used solely to refine the previous weld pass grain structure, is expressed as:

$$H = \frac{13.5 \; \left(\frac{120 \times 15 + 160 \times 5}{20}\right) 60}{4.0} = 26{,}300 \text{ Joules/inch}$$

As can be seen from the above data, it is very easy to alter the pulsed arc heat input by either varying the current level or the duration of current. However, the heat input values as expressed above can be used only as a reference. It does not take

Table V-4 GTA WELDING SCHEDULE FOR 10 Ni STEEL

WELDING SCHEDULE FOR MECHANIZED FUSION WELDING

PROGRAM AMAVS DATE 4-4-73

MATERIAL 10 NI STEEL THICKNESS 0.500 IN. CONDITION AUST. QUENCH & AGE

EQUIPMENT NO. 36911 PART NO. 603 R 100-2

PREHEAT TEMP. 100°F INTERPASS TEMP. 150-180°F

PRECLEANING MACHINED EDGE, WIRE BRUSH, MEK-WIPED

NOZZLE SIZE NO. 10 TUNGSTEN: Type 2% TH Diameter 0.125 IN.

TUNGSTEN: Extension 0.500 IN. Shape 15° ANGLE

FILLER WIRE: Type 10 NI Diameter 0.045 IN.

TORCH GAS: Type HE Flow 90 cfh; BACKUP GAS: Type HE Flow 15 cfh

| Weld Pass No. | 1 | 2 | 3 | 4 | 5 | 6 | 7 | 8 | 9 | 10 | 11 | 12 |
|---|---|---|---|---|---|---|---|---|---|---|---|---|
| Voltage | 13 | 13 | 13 | 13 | 13 | 13 | 13 | 13 | 13 | 13.5 | 13.5 | 13.5 |
| Weld current (amperage) | | | | | | | | | | | | |
| Level 1 | 225 | 160 | 160 | 160 | 160 | 160 | 160 | 160 | 160 | 160 | 160 | 120 |
| Level 2 | 180 | 200 | 200 | 200 | 200 | 200 | 200 | 200 | 200 | 200 | 200 | 160 |
| Number of cycles | | | | | | | | | | | | |
| Level 1 | 10 | 15 | 15 | 15 | 15 | 15 | 15 | 15 | 15 | 15 | 15 | 15 |
| Level 2 | 5 | 5 | 5 | 5 | 5 | 5 | 5 | 5 | 5 | 5 | 5 | 5 |
| Wire speed (ipm) | 32 | 32 | 32 | 32 | 32 | 32 | 32 | 32 | 32 | 32 | 32 | 16 |
| Weld speed (ipm) | 2 | 4 | 4 | 4 | 4 | 4 | 4 | 4 | 4 | 4 | 4 | 4 |

into consideration variations of preheat or the unit volume of filler wire additions. Also, if transverse arc oscillation is used, another dimensional factor must be considered. Therefore, data reported as heat input alone is totally inadequate. Another important consideration in the documentation of welding variables is that of the basic tooling configuration. It was later found that some of the recommended welding parameters were used to weld 10 Ni steel on a flat metal table using a solid copper backup plate. Hence, no penetration was expected or achieved. Back grinding or chipping was used to clean the back side root area. A weld bead was then applied to the back side. The preferred method is to use backup bars for inert gas shielding whenever possible, thus eliminating the back grinding or chipping operation. This, however, may be necessary on thicknesses in excess of 1/2 inch.

#### 5.3.2.2 Weld Set-Up Procedure

The test plates were positioned in the weld fixture (Ref. Figure 5-71). A 0.030 x 0.375-inch copper strip was used for shims to provide prebow to compensate for weld distortion. Weld run off tabs (Ref. Figure 5-72) were installed so that arc initiations and terminations would not be included in the weld plate test zones. The test plates were stainless steel wire brushed and MEK wiped. An oxy-acetylene torch was used to preheat the test plates to approximately 100°F. Weld passes were then made keeping the interpass temperature between 150 - 180°F.

#### 5.3.2.3 Weld Shrinkage

Transverse weld shrinkage was measured after the weld parameters were established. A ground gage block was placed on top of the unwelded plates, and lines were scribed along the edges of the gage block at each end of the plate. The distance between the scribe lines was measured and recorded. The test plates were welded and the scribe lines were remeasured. The net difference is the actual transverse weld shrinkage. As shown in Table V-5, the average shrinkage for the starting end of the weld was 0.019 inch and the finished end of the weld was 0.027 inch. The average weld shrinkage was 0.023 inch. The shrinkage experienced is approximately half that of most other high strength materials welded in the same manner. The low shrinkage most likely resulted from the pulsed arc welding mode. Further work should be pursued to define the benefits from using the pulsed arc welding technique.

Table V-5 TRANSVERSE GTA WELD SHRINKAGE DATA
1/2" THICK 10 Ni STEEL

| TEST PLATE | S/N | START END SHRINKAGE | FINISH END SHRINKAGE | AVG START | AVG FINISH | TOTAL AVG |
|---|---|---|---|---|---|---|
| W-6 | F467195 | -.015 | -.035 | | | |
| W-7 | F528036 | -.010 | -.015 | | | |
| W-8 | F528033 | -.015 | -.020 | | | |
| W-9 | F467193 | -.025 | -.030 | | | |
| W-10 | F528032 | -.010 | -.020 | | | |
| W-11 | F528031 | -.030 | -.030 | | | |
| W-12 | F528034 | -.020 | -.040 | | | |
| W-13 | F467196 | -.015 | -.025 | | | |
| W-14 | F528030 | -.025 | -.030 | | | |
| W-15 | F528035 | -.020 | -.025 | | | |
| W-16 | F467197 | -.025 | -.025 | | | |
| | | | | -.019" | -.027" | -.023" |

5.3.2.4 Weld Producibility Test Specimen

The NBB designs were reviewed and evaluated with Engineering Design on the usage of GTA welding. Because of the thicknesses involved in the bulkhead T-members, it was decided these members would best be electron beam welded. GTA welds were thus limited to the bulkhead web areas. The weld joints were designed to make the final welds by GTA because the assembly was too large for available electron beam weld chambers.

A simulated test detail was designed to represent the web to T-member joint. The weld fixture design is shown in Figure 5-73. This fixture provides side load pressure to assure tight fit up of the details. Downward pressure for alignment is also provided. Copper chill bars are provided to control bead shape and heat buildup. A copper gas backup bar is also used to control root penetration and provide inert gas shielding.

The weld fixture was designed for both the GTA and electron beam welding tests. The GTA backup bar and support block (details -4 and -8) are removable and replacement bars can be added to facilitate electron beam welding.

Two sets of test details were machined but were not welded. These specimens are representative of both the Yf 992 and Yf 932 outboard bulkheads (Ref. X7224071 and X7224091 respectively).

## 5.4 METALLURGICAL EVALUATION OF 10 NI STEEL

Data on heat treatment was generated as a result of the EB/GTA welding and machining programs. Weldments produced in establishing GTA/EB weld parameters were cross sectioned after X-ray inspection. Defects that were picked up by X ray were evaluated by metallographic examination. Macro and microphotographs were made for records.

### 5.4.1 Thermal Treatment

Several pieces of 10 Ni steel were austenitized at 1500°, 1550°, 1650°F and double austenitized at 1650° and 1550°F and water quenched. Aging was accomplished at 950°F for 3, 4, 5 or 8 hours with air cool. Aging was also accomplished at 950°F for 4 or 5 hours and water quenched. Other age temperatures were 1050° and 1150°F. Hardness tests were conducted on welded and base metal specimens after welding and the various thermal treatments. GTA and EB weldments plus base metal specimens were thermally pro-

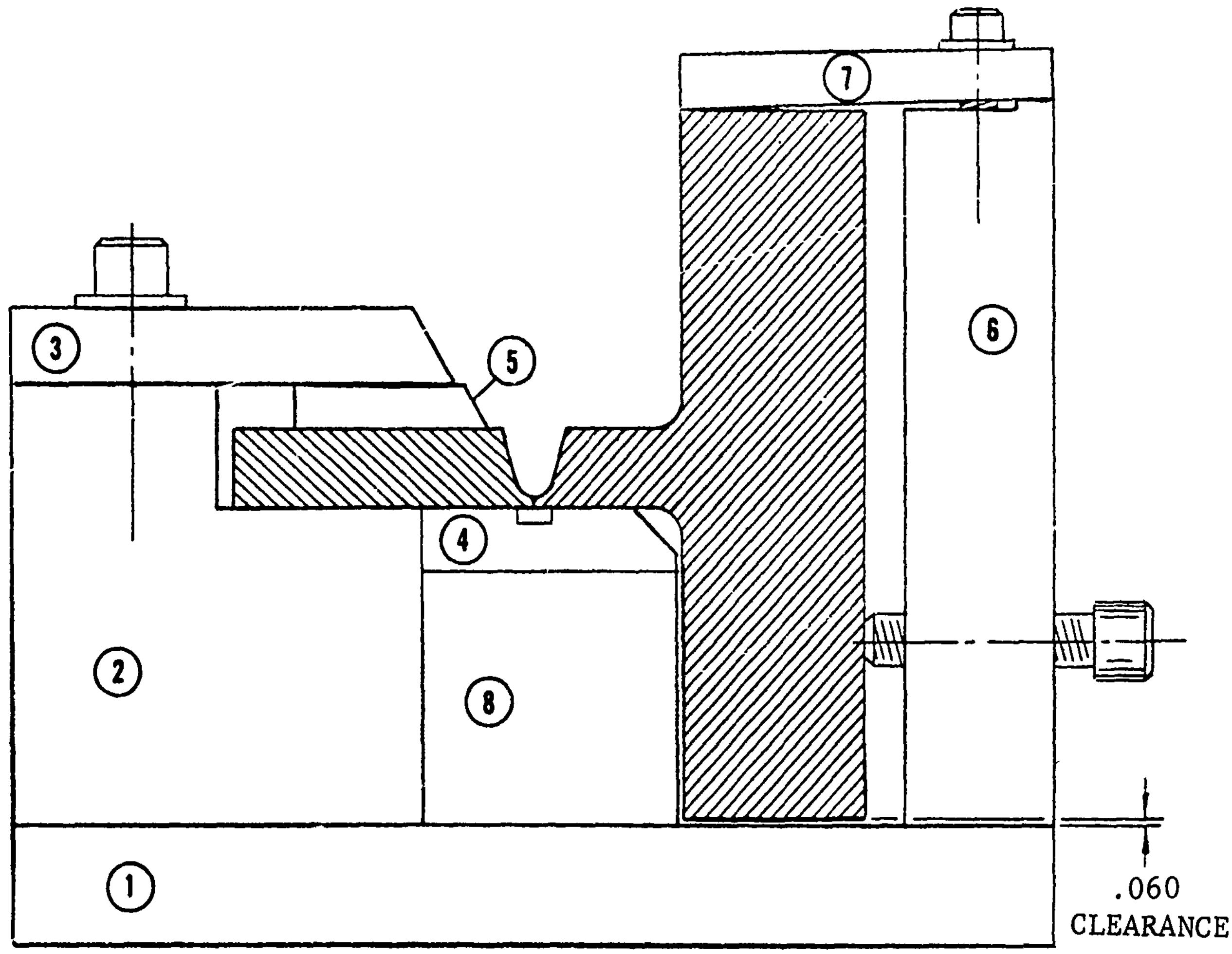


Figure 5-73 COMBINATION GTA AND EB WELD FIXTURE FOR WELDING BULKHEAD TEST SPECIMENS

cessed. Several small plates were austenitized and water quenched for machining tests.

Plate stock in the as-received, "austenitized and aged" condition and "reaustenitized plus water-quenched" condition were utilized in the machining tests previously reported.

### 5.4.2 Microstructure Evaluation

Metallographic examination of the 10 Ni steel base metal and GTA/EB weldments, involved five different etchants. U. S. Steel Corp. and Linde recommended a three-step etch procedure. Etchant (I) - Use 25% $HNO_3$ + ethanol for 10 to 30 seconds to reveal solidification structure, etchant (II) - use 40% sodium bisulfite in water for 30 to 120 seconds to reveal the transformation structure, etchant (III) - use 1% picric + 5% HCl in ethanol for 10 to 30 seconds to reveal grain boundary contrast. These etchants were evaluated separately and jointly. Microstructure obtained is shown in Figure 5-74. It was found that the 40 percent sodium bisulfite reaction was too severe. A 10 percent sodium bisulfite etchant for 30 to 120 seconds developed a better surface. Also, Nital etchant (either 2 or 10 percent solution) may be utilized to show the grain structure.

The 1650° and the 1650 + 1550°F solution treated (ST) and water quenched specimens showed a banded structure after polish and etch, but this type structure disappeared after the aging operations. (Figure 5-75 A and B). The 950°F age for 5 hours plus water-quenched versus the 950°F age for 8 hours and air-cooled to room temperature shows that the grain size varies. The water-quenched specimen had a grain size of 6 to 8 and the air-cooled specimens had a grain size of 8 or finer. There was a drastic difference in the microstructure after the 1500°F solution treated (Figure 5-75 B and C). There was no banding in the 1500°F austenitized specimens. Double solution treated (ST) and aged (STA) microstructure is shown in Figure 5-75D.

### 5.4.3 Microhardness Tests

Test specimens taken from GTA weldments, that utilized 10 Ni steel purchased in the solution treated and aged condition, were evaluated for microhardness and microstructure. A traverse microhardness was made on specimens from the center of the final GTA weld pass, through the multipass welds, heat affected zones, and the base metal. Weldments were aged at 950°, 1050° and 1150°F for four hours and air-cooled. The Knoop hardness was converted to R"c". The 950°F reaged test specimens had a minimum hardness

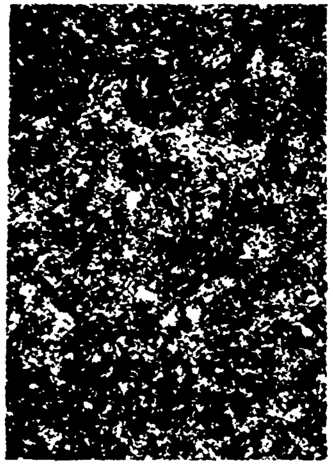

BASE METAL

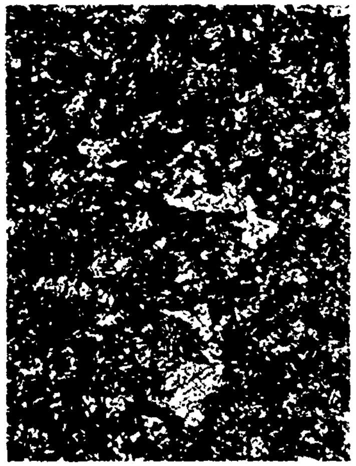

BASE METAL

BASE METAL

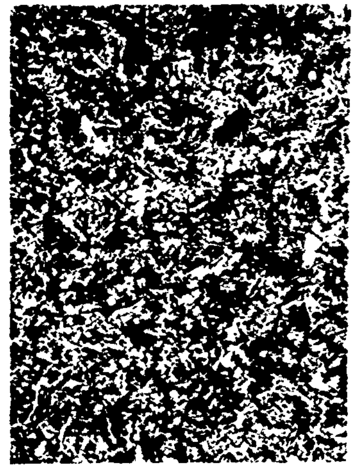

BASE METAL

WELD METAL
(2ND WELD PASS)

ETCHANT NO. I

WELD METAL
(2ND WELD PASS)

ETCHANT NO. II
OVER ETCHANT NO. I

WELD METAL
(2ND WELD PASS)

ETCHANT NO. III
OVER ETCHANT I & II

WELD METAL
(2ND WELD PASS)

ETCHANT NO. III

Figure 5-74 COMPARISON OF MICROSTRUCTURE OF 10 Ni STEEL USING VARIOUS ETCHANTS ON BASE AND GTA WELD METAL (200X)

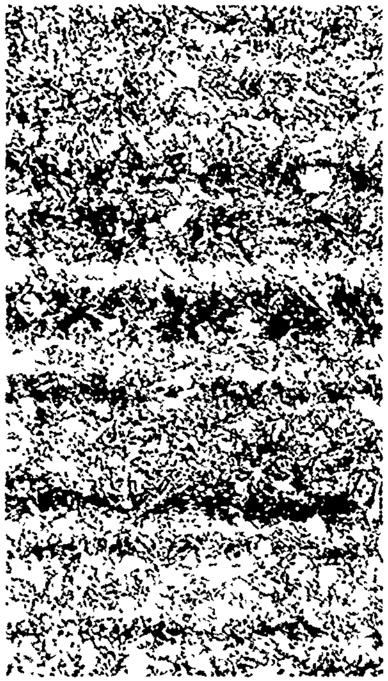

A -
1650 $\pm$ 25°F SOLUTION TREATMENT ($1\frac{1}{2}$ HRS) AND WATER QUENCH

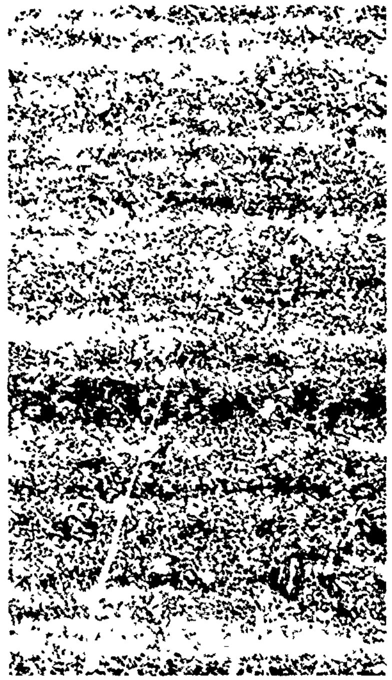

B -
1650°F + 1550 $\pm$ 25°F SOLUTION TREATMENT ($1\frac{1}{2}$ HRS) AND WATER QUENCH

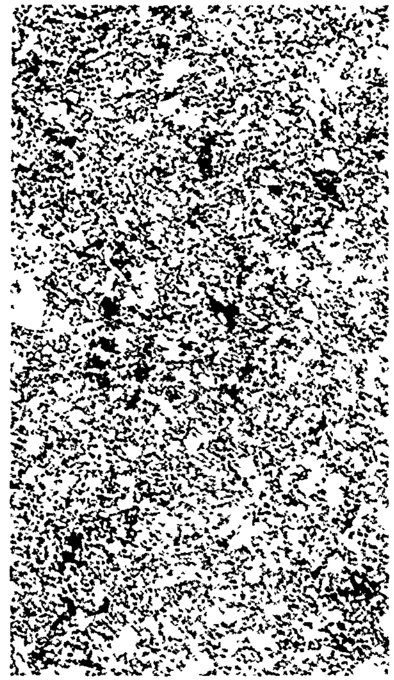

C -
1500 $\pm$ 25°F SOLUTION TREATMENT ($1\frac{1}{2}$ HRS) AND WATER QUENCH

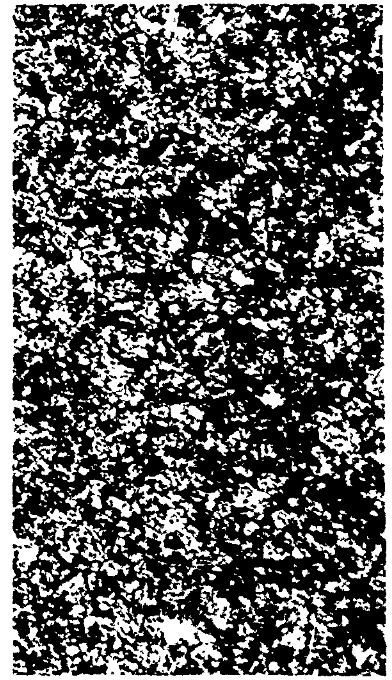

D -
SOLUTION TREATMENT A + B + 950 $\pm$ 10°F AGE (8 HRS) AND AIR COOLED

Figure 5-75 MICROSTRUCTURE OF SOLUTION TREATED AND SOLUTION TREATED AND AGED 10 Ni STEEL - 2% NITAL ETCHANT (200X) of R"c" 37.9 in the center of the final GTA weld pass to a maximum hardness of R"c" 44.9 in the primary heat affected zone. The secondary heat affected zone had a hardness of R"c" 40 to 42. The base metal hardness ranged from R"c" 39 to 41. Hardness values for the third through fifteenth weld passes are shown in Table V-6. Macrostructure of the multipass weld is shown in Figure 5-76 B. Microstructure of the base and weld metal is shown in Figure 5-76 A and C.

## 5.5 MACHINING

### 5.5.1 Machinability Evaluation of 10 Ni Steel

Machinability tests conducted during Phase II encompass the basic metal removal operations anticipated for fabricating the wing carrythrough test structure. The machinability test data is segregated into the following categories of machine operations.

1. Band sawing and cut-off sawing
2. Turning and boring
3. Machine drilling and reaming
4. End milling
5. Skin milling

#### 5.5.1.1 Band Sawing

Band sawing tests were conducted on 10 Ni steel plate specimens, 1.0-inch thick x 4.8-inches wide x 17.5-inches long. Based on the 1.0-inch plate thickness a 6 pitch (tooth) blade was selected. A standard 1 inch x 6P Simonds "Weld Edge" premium HSS blade was used for the test. A band speed of 90 surface feet/minute (SFM) was initially used and failed after 0.5 square inch of cut.

A new blade was installed and adjusted to maximum recommended band tension. A band speed of 55 SFM produced good cuts at an average sawing rate of 0.5 sq. in./min. A DoAll variable speed contourmatic power feed band saw was used for all tests to simulate the sawing speeds and feed rates of other sawing operations All sawing test cuts were accomplished without coolant.

Table V-6 HARDNESS VALUES OF GTA WELDED AND AGED 10 Ni STEEL 1/2 INCH PLATE

| STA. FUSION WELD (2) | AGED @ 950°F (3) | | | AGED @ 1050°F (3) | | | AGED @ 1150°F (3) | | |
|---|---|---|---|---|---|---|---|---|---|
| LOCATION OF TEST | RC (1) | | | RC (1) | | | RC (1) | | |
| Center of 14th Weld Pass | 42.0 | 37.9 | 40.0 | 36.9 | 35.5 | 36.2 | 28.0 | 26.0 | 27.0 |
| Bottom of 14th Weld Pass | 41.8 | 41.6 | 41.7 | 36.9 | 36.8 | 36.8 | 26.0 | 26.0 | 26.0 |
| Center of 13th Weld Pass | 44.9 | 44.7 | 44.8 | 38.9 | 39.7 | 39.3 | 28.8 | 28.3 | 28.5 |
| WM 12th Weld Pass | 41.9 | 44.2 | 43.0 | 36.9 | 39.2 | 38.0 | 28.3 | 29.5 | 28.9 |
| WM 11th Weld Pass | 43.8 | 44.2 | 44.0 | 38.8 | 39.2 | 39.0 | 28.3 | 28.8 | 28.6 |
| WM 10th Weld Pass | 41.8 | 42.6 | 42.2 | 36.8 | 37.6 | 37.2 | 28.8 | 28.8 | 28.8 |
| FZ 9th Weld Pass | 44.2 | 44.9 | 44.5 | 39.2 | 39.2 | 39.2 | 28.8 | 28.8 | 28.8 |
| HAZ-FZ 8th Weld Pass | 42.6 | 42.6 | 42.6 | 37.6 | 37.6 | 37.6 | 30.0 | 29.5 | 29.7 |
| HAZ- 7th Weld Pass | 44.7 | 44.2 | 44.2 | 39.2 | 39.4 | 39.3 | 28.8 | 28.8 | 28.8 |
| HAZ- 6th Weld Pass | 44.2 | 43.8 | 44.0 | 39.2 | 38.8 | 39.0 | 30.3 | 30.3 | 30.3 |
| HAZ- 5th Weld Pass | 40.0 | 40.0 | 40.0 | 35.0 | 35.0 | 35.0 | 30.3 | 30.0 | 30.0 |
| BM/HAZ 4th Weld Pass | 41.9 | 41.9 | 41.9 | 36.9 | 36.9 | 36.9 | 29.1 | 30.0 | 30.1 |
| BM/HAZ 3rd Weld Pass | 41.8 | 41.6 | 41.7 | 38.8 | 36.6 | 37.7 | 30.0 | 29.1 | 29.5 |

(1) Microhardness (KNOOP) Values Converted to Rockwell "C"
(2) 10 Ni Steel Condition STA Prior to GTA Fusion Welding
(3) Material Was Aged for 4 Hours After Welding at 950°, 1050°, or 1150°F


(200X)

A - BASE METAL
(REAGED)

(6X)

B - GTA MULTIPASS WELD OF SOLUTION TREATED AND AGED MATERIAL (REAGED AT 950°F FOR 4 HOURS)


(200X)

C - WELD METAL
(REAGED)

Figure 5-76 MACRO AND MICRO STRUCTURE OF MULTIPASS GTA WELDED AND REAGED 10 Ni STEEL (ETCHANT - 25% $HNO_3$ + ETHANOL)

5.5.1.2 Boring and Turning

A series of single tool boring tests were conducted on a Monarch engine lathe in the MR&D machining test center. The lathe is equipped with an infinitely variable spindle speed selector with visual readout of spindle speeds. Availability of 10 Ni steel for this test was limited to (2) pieces 1.0 inch thick x 5 inches wide x 10 inches long. Tests were conducted by boring a series of holes, starting with a 1.5-inch hole in 1.0-inch plate material. Figure 5-77 shows one of the 1.0-inch thick machined specimens after boring tests. The plate was also used for drilling and reaming tests discussed in the next section. Table V-7 presents the boring test results conducted on the two test plates. The data developed during the boring test is representative and adequate for turning, as both operations employ the same cutting principle.

The boring test results reveal that 100 SFM for roughing and 150 SFM for finishing is adequate. Feed rates of 0.0075 inch per revolution (IPR) for rough boring and 0.005 IPR for finishing were best when using C-6 grade carbide throwaway inserts with positive rake angles.

5.5.1.3 Machine Drilling and Reaming

Drilling and reaming tests were conducted on 1.0-inch thick, aged 10 Ni steel plate material. The tests were performed on a power feed drill press in the MR&D machining center using Gulf HD51 water soluble coolant. The drills tested were 0.4846 diameter oil hole types of HSS and cobalt. The C15002-4844 test drill shown in Figure 5-78 is a 20 degree helix type cobalt normally used for drilling high strength steel. The C15013-4844 test drill in Figure 5-79 is a 30 degree helix high speed steel type normally used for aluminum and mild steel.

Test results presented in Table V-8 reveal that the C15013-4844 30 degree helix HSS drill performed better than the C15002-4844 20 degree helix cobalt drill, except for tolerance control. It is assumed that the resulting tolerance is adequate to allow for subsequent reaming operations. The reaming tests proved that the C15481 (GD/FW specification) carbide tipped reamer (Figure 5-80) performed better than the C15014 (GD/FW specification) cobalt reamer (Figure 5-81) for producing finished holes in 10 Ni steel.

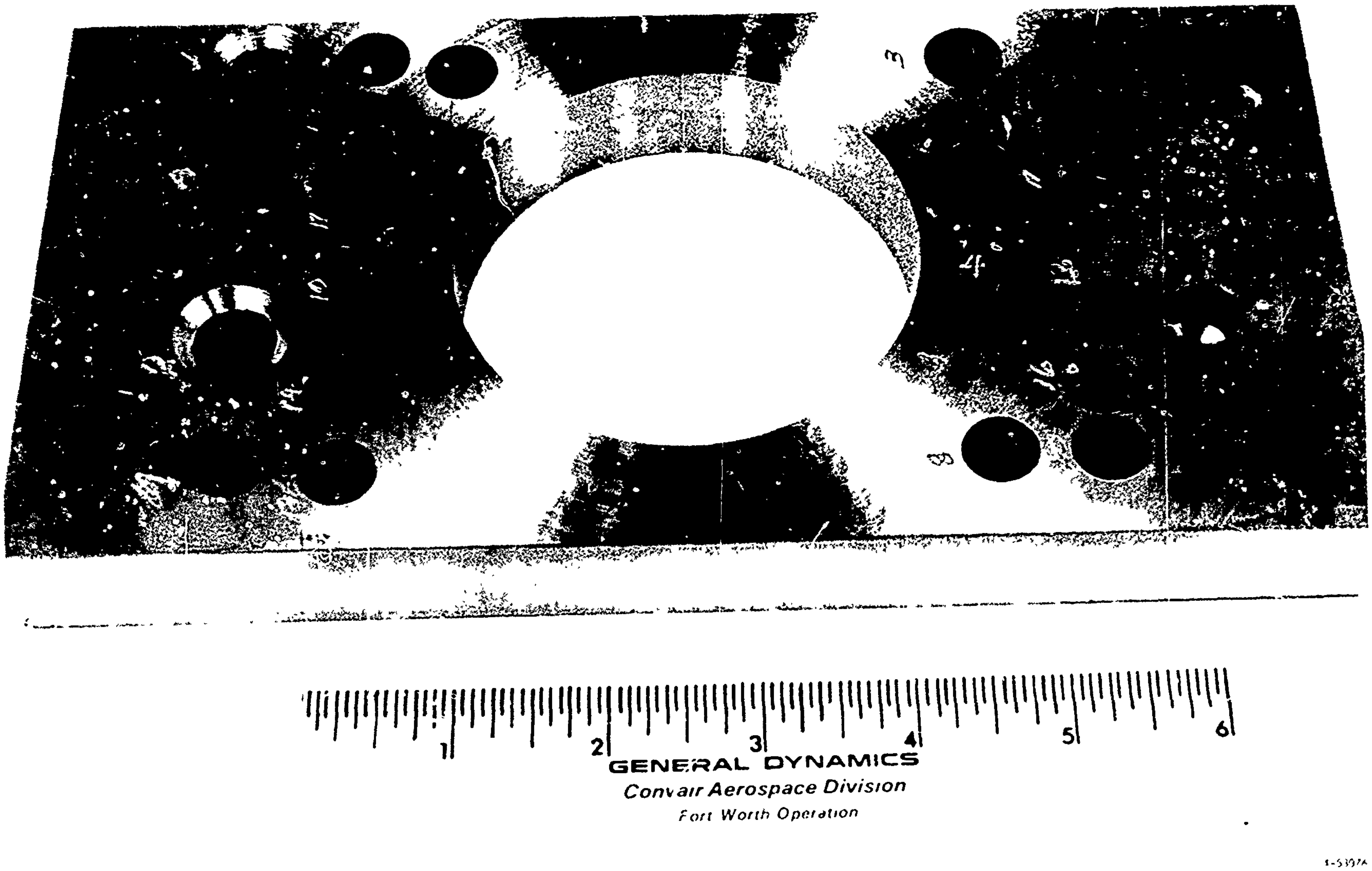


Figure 5-77 10 Ni STEEL PLATE USED FOR BORING, DRILLING AND REAMING TESTS

Table V-7 BORING TEST DATA - 1 INCH THICK 10 Ni STEEL

| MATERIAL | HEAT TREAT CONDITION | HARDNESS | DEPTH OF CUT | FPM SPEED | IPR. FEED | TOOL MAT'L. | REMARKS |
|---|---|---|---|---|---|---|---|
| HY180 (10 Ni) | Solution treated and aged (S.T.A.) | 200-205 KSI | .062 | 100 | .0075 | C-5 Carbide | Poor finish 140-160 micro inches chip blue |
| HY180 (10 Ni) | S.T.A. | 200-205 | .062 | 150 | .0050 | C-5 Carbide intent | Fair finish tool chipped |
| HY180 (10 Ni) | S.T.A. | 200-205 | .125 | 100 | .0050 | C-5 Carbide | Excessive chatter tool chipped |
| HY180 (10 Ni) | S.T.A. | 200-205 | .062 | 100 | .0040 | C-5 Carbide | Good finish 125 micro inches chip bronze |
| HY180 | S.T.A. | 200-205 | .032 | 100 | .0040 | C-6 Carbide | Good finish 60-80 micro inches slight tool wear |
| HY180 | S.T.A. | 200-205 | .032 | 75 | .0045 | C-6 Carbide | Good finish 60-80 micro inches negligible tool wear |
| HY180 (10 Ni) | Solution treated only | 186 KSI | .062 | 100 | .0075 | C-6 Carbide | Chip blue 140 micro inch finish |
| HY180 (10 Ni) | Solution treated only | 186 KSI | .125 | 100 | .0075 | C-6 Carbide | Chip blue excessive chatter tool chipped |
| HY180 (10 Ni) | Solution treated only | 186 KSI | .062 | 150 | .0045 | C-6 Carbide | Chip bronze 125 finish slight tool wear |
| HY180 (10 Ni) | Solution treated only | 186 KSI | .032 | 150 | .0045 | C-6 Carbide | Chip bronze 60-80 micro inch finish min. tool wear |

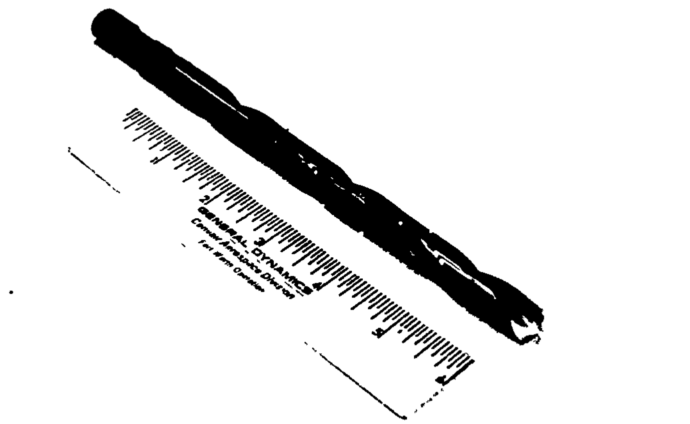

Figure 5-78 C15002 - 4844 COBALT, 20° HELIX DRILL (NORMALLY USED FOR HIGH STRENGTH STEEL)

4-53073

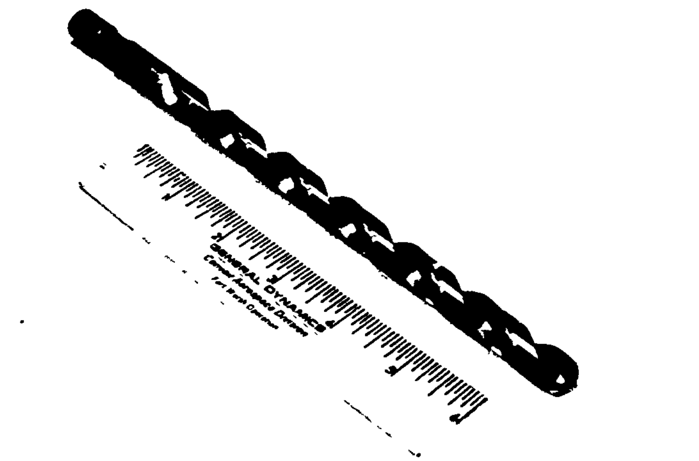

Figure 5-79 C15013 - 4844 HSS, 30° HELIX DRILL (NORMALLY USED FOR ALUMINUM AND MILD STEEL)

4-53072

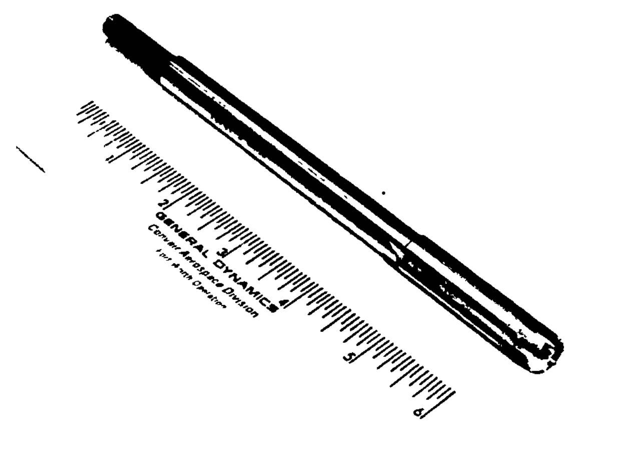

Figure 5-80 C15481 CARBIDE TIPPED REAMER

4-53074

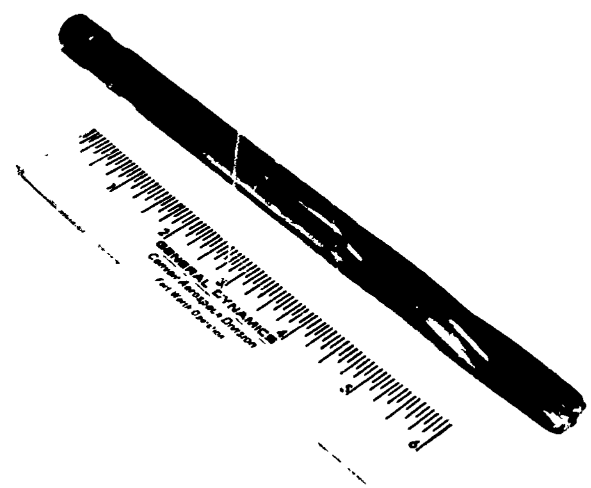

Figure 5-81 C15014 COBALT REAMER

4-53075

Table V-8 DRILL TEST DATA - 1 INCH THICK 10 Ni STEEL

MATERIAL = 10 Ni - AGED @ 205 KSI (1" THICK)

| DRILL | RPM | FEED | HOLE NO | HOLE SIZE | FINISH RMS | COMMENT |
|---|---|---|---|---|---|---|
| C15002-4844 | 250 | .001 | 1 | .4846 | 50-80 | TOO SLOW |
| COBALT | 250 | .001 | 2 | .4846 | 50-80 | |
| $20^{\circ}$ HELIX | 250 | .002 | 3 | .4856 | 50-80 | |
| | 250 | .002 | 4 | .4857 | 50-80 | BURR ON FAR SIDE |
| | 250 | .002 | 5 | .4851 | 50-80 | LARGE BURR ON FAR SIDE - LIP WORN CHIP BUILD UP ON CUTTING EDGE VISIBLE |
| C15013-4844 | 250 | .002 | 6 | .4884 | 50-80 | |
| HSS | 250 | .002 | 7 | .4882 | 50-80 | |
| $30^{\circ}$ HELIX | 250 | .002 | 8 | .4883 | 50-80 | |
| | 250 | .002 | 9 | .4885 | 50-80 | |
| | 250 | .002 | 10 | .4884 | 50-80 | |
| | 250 | .002 | 11 | .4885 | 50-80 | |
| | 250 | .002 | 12 | .4882 | 50-80 | DRILLS SMOOTH WITH NO CHIP |
| | 250 | .002 | 13 | .4883 | 50-80 | REMOVAL PROBLEM |
| | 250 | .002 | 14 | .4888 | 50-80 | |
| | 250 | .002 | 15 | .4885 | 50-80 | DRILL SHARP AFTER 15 HOURS |
| | 250 | .002 | 16 | .4884 | 50-80 | |
| | 250 | .002 | 17 | .4886 | 50-80 | |
| | 250 | .002 | 18 | .4885 | 50-80 | |
| | 250 | .002 | 19 | .4884 | 50-80 | |
| | 250 | .002 | 20 | .4886 | 50-80 | |
| | | | | | | |
| C15013-4844 | 250 | .004 | 21 | .4849 | | |
| | 250 | .004 | 22 | .4849 | | GALLED AND BRCKE IN HOLE #23 |
| | 250 | .004 | 23 | - | | FEED TOO GREAT |

5.5.1.4 End Milling

Preliminary end milling tests were performed on a small test block of 10 Ni steel material using 1 1/2-inch diameter 8 flute HSS end mill cutters. (See Figure 5-82.) The test consisted of multipasses at various feeds and speeds to determine the cutting rate for milling Group II detail parts. A 1 1/2-inch diameter 8 flute 30 degree helix end mill performed best using 75 SFM speed and 0.002 inch per tooth (IPT) feed at 0.21 inch depth of cut. Test cuts at 0.35 inch and 0.50-inch depth of cut exceeded the 125 microinch surface finish requirement. The preliminary end milling data was used to establish machine shop milling procedures for the fabrication of the large detail parts for Group II production verification test components. Figure 5-83 is a profile milling operation on a 10 Ni steel part of thin flange design. Figure 5-84 is an end milling operation on a thick 10 Ni steel splice plate using an 8-flute 2-inch diameter end mill cutter.

5.5.1.5 Skin Milling

Skin milling 10 Ni steel represents one of the more difficult metal removal operations. The difficulty is associated with the rapid breakdown of the cutter edges causing high machining stresses and the subsequent warpage of large plate material. Initial face milling tests were conducted using negative rake carbide inserted face milling cutters. The negative rake cutters produced rapid buildup of the 10 Ni steel on the cutter edges causing premature cutter failure and rough surface finishes. Positive shear angle cutters were then tested. Initial test data using positive rake carbide inserted face mills (Table V-9), proved that positive shear angle cutters perform satisfactorily. A round throwaway carbide insert (7 degrees axial, 2 degrees radial) face milling cutter (Figure 5-85), produced best results at 100 SFM and .004 feed per tooth. This cutter was used for skin milling 10 Ni plate stock in the production machine shop during fabrication of Group II production verification test specimens.

5.5.1.6 Flame Cutting 10 Ni Steel

A 2 3/8 x 60 x 135 inches 10 Ni steel plate was flame cut using oxygen and Mapp gas. Fifty-eight details were removed from the plate using the Airco automatic tracing flame cutting machine. The plate was in the austenitized and quenched condition before flame cutting. After solution treating, the plate

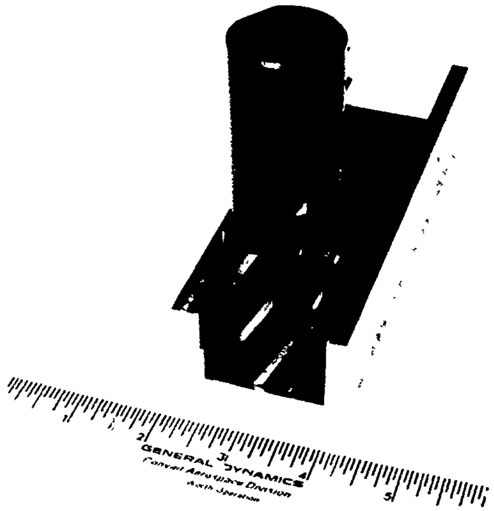


4-53071

Figure 5-82 PRELIMINARY END MILLING TEST ON 10 Ni STEEL - 1 1/2 INCH DIAMETER, 8 FLUTE, HSS CUTTER

4-53788

Figure 5-83 PROFILE MILLING 10 Ni STEEL, THIN FLANGE, PRODUCTION VERIFICATION TEST PART (603FTB052)

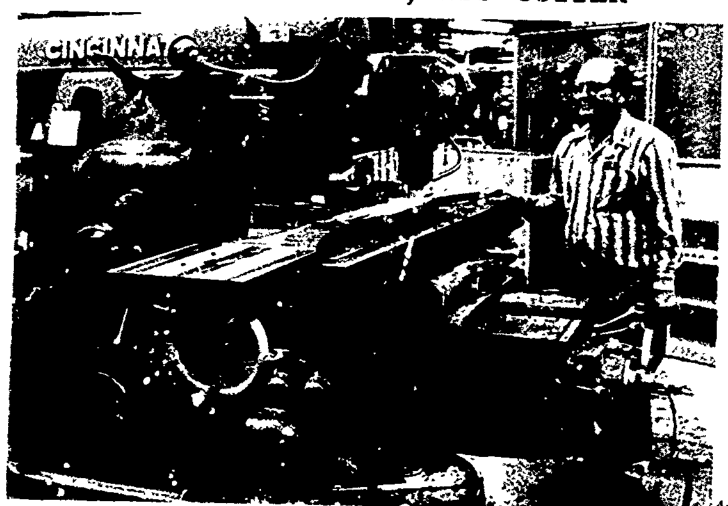

4-53787

Figure 5-84 END MILLING 10 Ni STEEL SPLICE PLATE (603FTB052 PRODUCTION VERIFICATION TEST SPECIMEN)

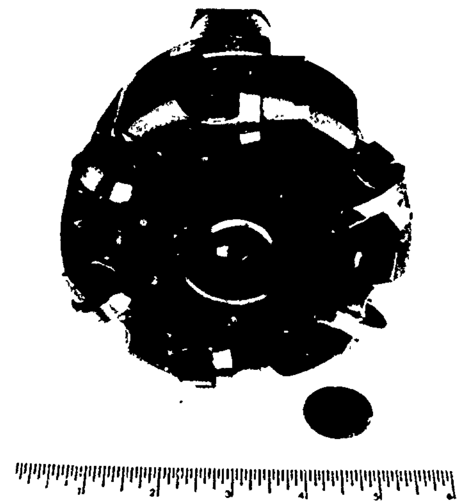

4-53070

Figure 5-85 FACE MILLING CUTTER WITH ROUND CARBIDE INSERTS

## Table V-9 FACE MILLING TESTS ON 10 Ni STEEL

| MATERIAL | SURFACE FT/MIN. | CHIP/TOOTH | CUT | RPM | FEED MIN. | CUTTER | # TEETH | TOOTH CONFIG. | FINISH | TOOTH CONDITION | CHIPS |
|---|---|---|---|---|---|---|---|---|---|---|---|
| 1. 10 Ni @ 200-205 KSI (AGED) | 60 | .003 | .10 x 2.5 x 12 | 28 | 1.0 | 8" DIA. @ 25° POS. | 12 | .12 x 45° @ 30° POS. | GOOD | 2 CHIPPED | SMOOTH, BRIGHT, COOL |
| 2. " | 60 | .003 | .12 x 2.5 x 12 | 45 | 1.0 | 5" DIA. @ 7° POS. | 6 | 1/2" RAD. @ 15° RELIEF | GOOD | GOOD | SMOOTH, BRIGHT, COOL |
| 3. " | 100 | .003 | .12 x 2.5 x 12 | 71 | 1.4 | 5" DIA. @ 7° POS. | 6 | 1/2" RAD. @ 15° RELIEF | GOOD | GOOD | SMOOTH, BRIGHT, COOL |
| 4. " | 130 | .003 | .12 x 2.5 x 12 | 90 | 1.6 | 5" DIA. @ 7° POS. | 6 | 1/2" RAD. @ 15° RELIEF | GOOD | GOOD | SMOOTH, BRIGHT, COOL |
| 5. " | 130 | .003 | .25 x 2.5 x 12 | 90 | 1.6 | 5" DIA. @ 7° POS. | 6 | 1/2" RAD. @ 15° RELIEF | FAIR | GOOD | STARTING TO TURN BROWN |
| 6. " | 100 | .008 | .31 x 2.5 x 12 | 71 | 3.5 | 5" DIA. @ 7° POS. | 6 | 1/2" RAD. @ 15° RELIEF | FAIR | CHIPPING | SOME BROWN AND PURPLE |
| 7. " | 100 | .008 | .25 X 2.5 x 12 | 71 | 3.5 | 5" DIA. @ 7° POS. | 6 | 1/2" RAD. @ 15° RELIEF | FAIR | CHIPPING | SOME LIGHT BROWN |
| 8. " | 100 | .006 | .25 x 2.2 x 12 | 71 | 2.56 | 5" DIA. @ 7° POS. | 6 | 1/2" RAD. @ 15° RELIEF | GOOD | GOOD | SMOOTH, BRIGHT, WARM |
| 9. " | 100 | .006 | .31 x 2.5 x 12 | 71 | 2.56 | 5" DIA. @ 7° POS. | 6 | 1/2" RAD. @ 15° RELIEF | FAIR | CHIPPING | SOME BROWN |
| 10. 10 Ni @ 186-202 KSI (NON-AGED) | 100 | .006 | .25 x 1.0 x 9.0 | 71 | 2.56 | 5" DIA. @ 7° POS. | 6 | 1/2" RAD. @ 15° RELIEF | GOOD | FAIR | SOME LIGHT BROWN |
| 11. 10 Ni @ 186-202 KSI (WITH SCALE) | 100 | .006 | .25 x 4.5 x 9.0 | 71 | 2.56 | 5" DIA. @ 7° POS. | 6 | 1/2" RAD. @ 15° RELIEF | GOOD | CHIPPING SOME | SOME PURPLE |
| 12. 10 Ni @ 186-202 KSI (SCALE REMOVED) | 100 | .006 | .25 x 4.5 | 71 | 2.56 | 5" DIA. | 6 | 1/2" RAD. | FAIR | CHIPPING SOME | SOME PURPLE |
| 13. 10 Ni @ 200-205 KSI (AGED) | 95 | .006 | .25 x 2.5 x 12 | 45 | 2.15 | 8" DIA. RADIAL POS. 4° NORMAL POS. 5½° | 8 | .12 x 45° | FAIR | CHIPPING | CHIPPING BAD AFTER ONLY 1" OF TRAVEL - BROWN CHIPS - |
| 14. 10Ni @ 200-205 KSI (AGED) | 105 | .006 | .25 x 2.5 x 12 | 45 | 3.25 | 9" DIA. | 12 | .12 x 45° #10 | FAIR | CHIPPING | HEAVY CHIPPING ALL DARK BLUE CHIPS |
| 15. 10 Ni @ 200-205 KSI (AGED) | 100 | .006 | .25 x 2.5 x 6.0 | 71 | .4 | 5" DIA. @ 7° POS | 1 | ½" RAD. CHIP-BREAK @ 15°REL | FAIR | CHIPPED | WRINKLED-BROWN-BLUE CHIPBREAKER CHIPPED OUT |
| 16. 10 Ni @ 200-205 KSI (AGED) | 100 | .006 | .25 x 2.5 x 6.0 | 71 | .4 | 5" DIA. @ 7° POS | 1 | ½" Rad. CHIP-BREAK @ 12° REL. | | | WRINKLED-BROWN-BLUE CHIPBREAKER CHIPPED OUT SLIGHTLY CHIPPED |
| 17. 10 Ni @ 200-205 KSI (AGED) | 100 | .005 | .25 x 2.5 x 6.0 | 71 | .35 | 5" DIA. @ 7° POS | 1 | ½" RAD. @ 15° REL. | FINE | LIGHT WEAR | SMOOTH, BRIGHT, COOL |
| 18. 10 Ni @ 200-205 KSI (AGED) | 100 | .004 | .25 x 2.5 x 6.0 | 71 | .29 | 5" DIA. @ 7° POS | 1 | ½" RAD. @ 15° REL. | FINE | LIGHT WEAR | SMOOTH, BRIGHT, COOL |
| 19. 10 Ni @ 190-200 KSI (AGED) | 95 | .005 | .12 x 2.5 x 12 | 90 | .44 | 4" DIA. 6°POS NOR 1°POS RAD | 1 | SQUARE .03R 10°REL T-15 | FINE | GOOD | SMOOTH, BRIGHT, COOL |
| 20. 10 Ni @ 190-200 KSI (AGED) | 95 | .004 | .25 x 2.5 x 10 | 90 | .36 | 4" DIA. 6°POS NOR 1° POS RAD | 1 | SQUARE .03R 10°REL T-15 | FINE | GOOD | SMOOTH, BRIGHT, COOL NO CHIPPING OF INSERT BUT SHOWS SLIGHT WEAR |
| 21. 10 Ni @ 190-200 KSI (AGED) | 95 | .005 | .25 x 2.5 x 10 | 71 | .35 | 5" DIA. @ 7°POS. | 1 | ½" RAD. @ 10° RELIEF | POOR | GOOD | BROWN AND BLUE - NOT ENOUGH RELIEF HEEL DRAGGING |
| 22. 10 Ni @ 190-200 KSI (AGED) | 120 | .004 | .25 x 2.5 x 10 | 90 | .36 | 5" DIA. @ 7° POS. | 1 | ½" RAD. @ 15° RELIEF | FINE | GOOD | SOME BROWN/BLUE SLIGHT CHIPPING |

was machined on both sides; therefore, all flame cutting was accomplished on clean machine cut surfaces.

Difficulty was encountered in the initiation of the cut. A preheat temperature of approximately 150°F was used. This was accomplished by allowing the cutting torch to follow the cutting pattern four times before turning on the cutting oxygen. Occasional blowout at the cut initiation was experienced. The flame would cut through two-thirds of the plate and then expel the molten metal at 90° as shown in Figure 5-86A. It was found that by preheating the lower edge of the plate with a manual torch (Figure 5-86 B), successful cutting starts were consistently achieved without blowouts. When good cutting starts were made no problems were encountered in maintaining the cut.

Manual edge preheating was used on long, thin details at the edge of the plate to eliminate warpage from cutting. Two details were 4 inches wide by 80 inches long. Because of material limitation, a waster strip could not be removed to equalize cutting stresses. The preheating technique is depicted in Figure 5-86C.

The heat affected zone obtained on the 2-3/8-inch thick plate is shown in Figure 5-86D. The allowance for heat affected zones was established at 0.100-inch per inch of thickness. However, other plate thicknesses should be checked in the same manner, if a significantly different cutting speed is used.

This was the first thick plate that was torch cut on this program. It is felt that further improvements can be made in the area of flame cutting. This plate was cut at 7 inches per minute. Satisfactory cuts were achieved at this speed, therefore, no other speeds were evaluated. The 1/2-inch per side cut allowance proved to be adequate and assured stock clean up around 90° corners and profiled shapes.

It is recommended that plasma arc cutting be investigated for use on thick plates. The higher velocity of the cutting gases may overcome the edge starting problem and eliminate the requirement for manual preheating.

5.5.1.7 Stress Relief Test on Machined 10 Ni Steel

A preliminary stress relief test was conducted on a machined 10 Ni steel part. The purpose of this test was twofold; to determine if appreciable machining stresses were retained in the part and to determine if the part would warp when subjected to

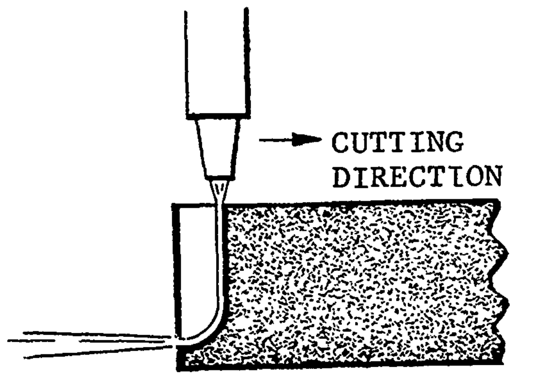


A. TYPICAL BLOW-OUT CONDITION

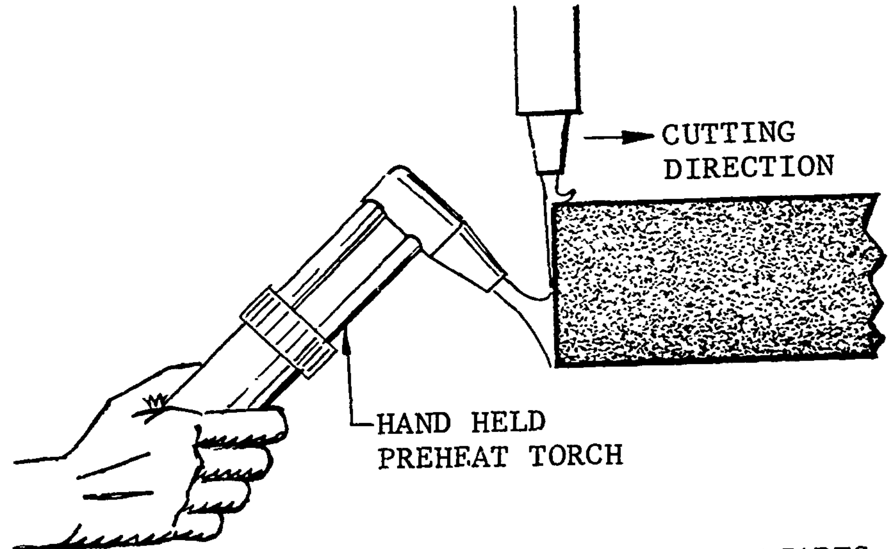


B. PREHEATING TECHNIQUE FOR EDGE STARTS

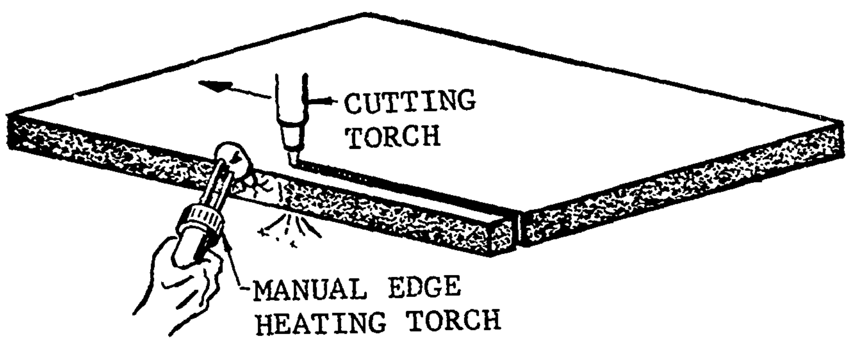


C. EDGE HEATING TO MINIMIZE WARPAGE

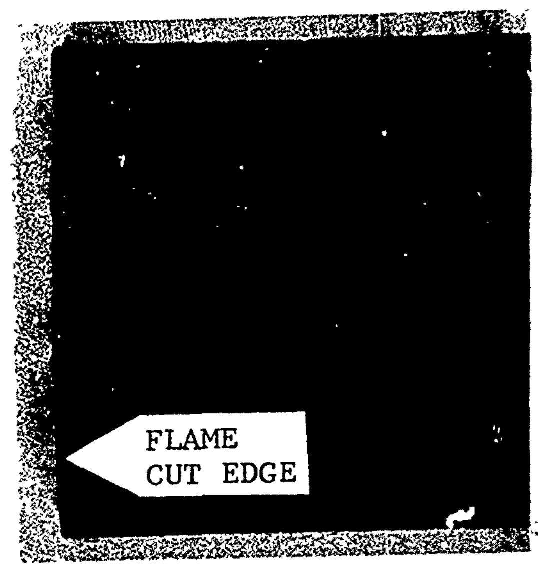


D. MACRO OF HEAT AFFECTED ZONE

Figure 5-86 FLAME CUTTING TECHNIQUES FOR 2 3/8 INCH THICK 10 Ni STEEL stress relief temperatures. The part shown in Figure 5-87 was free-state stress relieved at 950°F for one hour and dimensional changes noted. A second 950 F stress relief was accomplished for four hours. The dimensional changes per side are shown. These readings were dial indicated and the net change by location is given. It should be noted that although only 0.002 inch movement was detected on this part, it may not be representative of large machined wide flanged or deep pocketed configurations. Subsequent to the above tests an engineering specification is being published. Since the age temperature was established at 950 ± 10°F for 8 hours, the post stress relieve treatment must heat at least 50°F below the age temperature to prevent over-aging; therefore, stress relieve at 900°F maximum. The producer indicates that such a stress relief will not affect material properties.

## 5.6 ASSEMBLY OF GROUP II PRODUCTION VERIFICATION TEST SPECIMENS

### 5.6.1 603FTB052 Lower Lug to Rail Splice Assembly

A combination assembly and drill fixture was designed and fabricated to accurately locate and secure all detail parts for drill and ream operations. Two fixtures were necessary, one for the -A10 subassembly (consisting of details -31, -15, and -21) and another for the -A1 assembly (consisting of the -A10 subassembly and the remaining six detail parts). Prior to design of the fixtures, portable tooling kit accessories were selected from available stock to eliminate manufacture of special bushing, nosepieces, etc. The portable equipment power kits were altered using present motor kits to increase torque and reduce spindle speed.

The 603FTB052-A10 subassembly fixture is shown in Figure 5-88. Forty-nine 0.375 + 0.002/-0.000-inch diameter holes were drilled and reamed using the subassembly fixture. The detail parts were removed from the fixture, cleaned and deburred. FMS1043 sealant was applied to the faying surfaces of the parts and the Hi-lok fasteners were installed. After the sealant had cured, the Hi-lok fasteners were removed in areas of interference with other bolts and for fixture clearance.

The 603FTB052-A1 assembly fixture was loaded with the detail parts shown in Figure 5-89 plus the -A10 subassembly. Before any holes were drilled, detail part locations and hole edge distances were checked and detail parts were securely clamped. The first holes drilled were selected for threaded

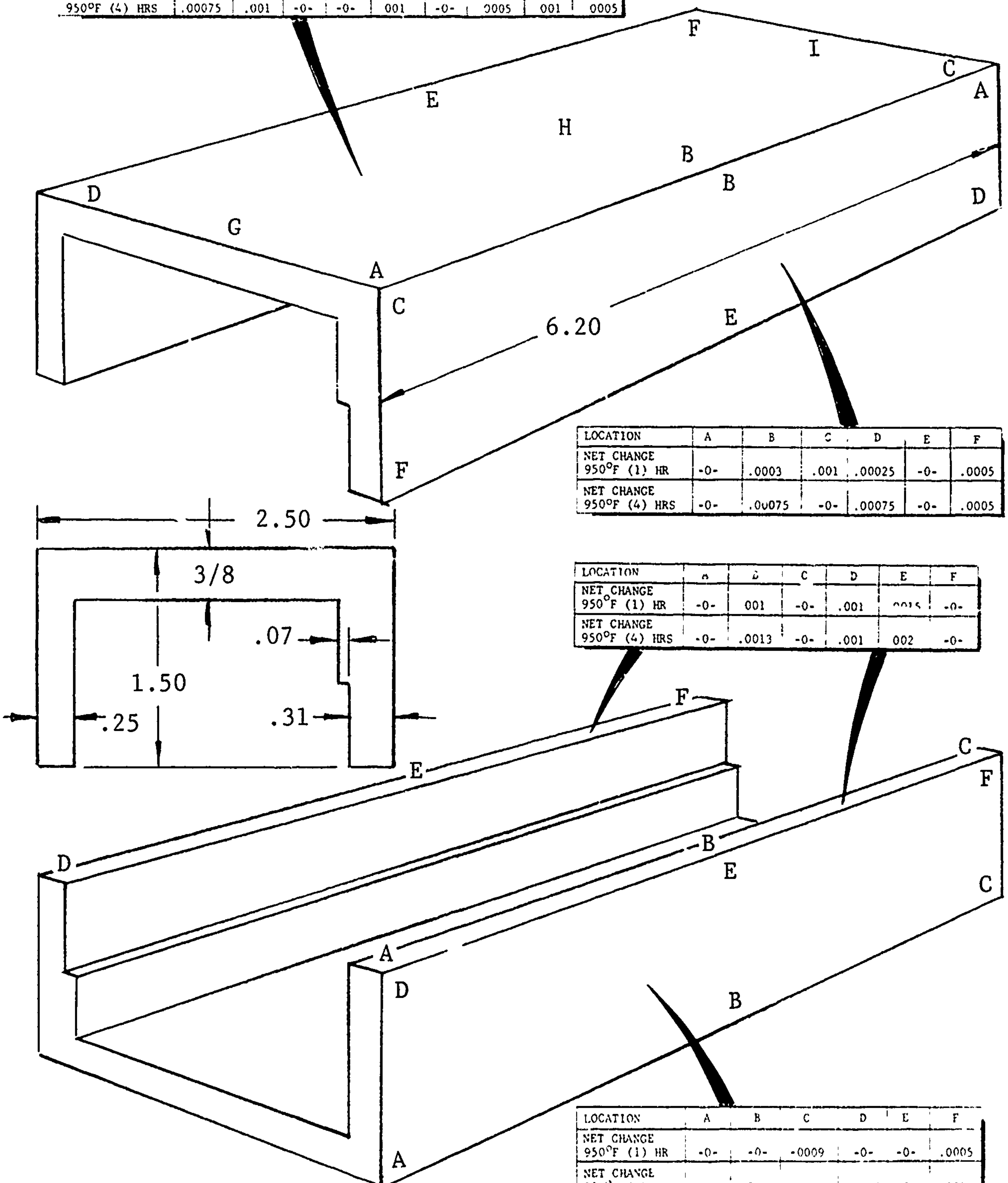


| LOCATION | A | B | C | D | E | F | G | H | I |
|---|---|---|---|---|---|---|---|---|---|
| NET CHANGE 950°F (1) HR | 0005 | .001 | -0- | -0- | -0005 | -0- | 0015 | .001 | -0- |
| NET CHANGE 950°F (4) HRS | .00075 | .001 | -0- | -0- | 001 | -0- | 0005 | 001 | 0005 |

| LOCATION | A | B | C | D | E | F |
|---|---|---|---|---|---|---|
| NET CHANGE 950°F (1) HR | -0- | .0003 | .001 | .00025 | -0- | .0005 |
| NET CHANGE 950°F (4) HRS | -0- | .00075 | -0- | .00075 | -0- | .0005 |

| LOCATION | A | B | C | D | E | F |
|---|---|---|---|---|---|---|
| NET CHANGE 950°F (1) HR | -0- | 001 | -0- | .001 | 0015 | -0- |
| NET CHANGE 950°F (4) HRS | -0- | .0013 | -0- | .001 | 002 | -0- |

| LOCATION | A | B | C | D | E | F |
|---|---|---|---|---|---|---|
| NET CHANGE 950°F (1) HR | -0- | -0- | -0009 | -0- | -0- | .0005 |
| NET CHANGE 950°F (4) HRS | -0- | .001 | -0002 | .0005 | -0- | .001 |

Figure 5-87 POST STRESS RELIEF DIMENSIONAL SURVEY

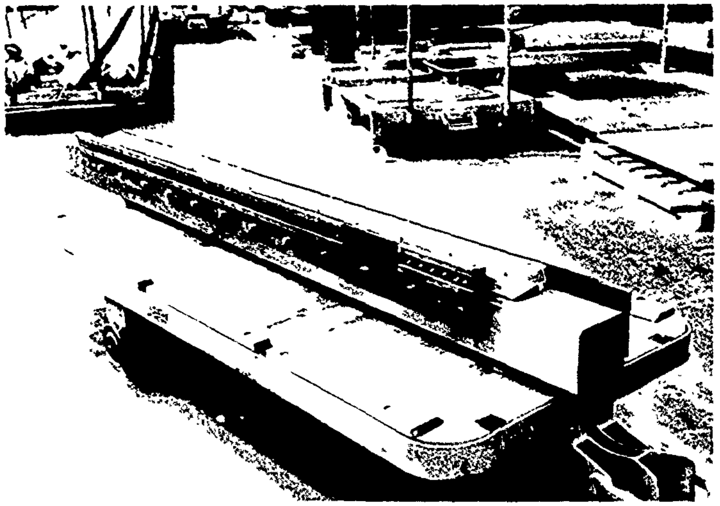

4-51110

Figure 5-88 -A10 SUBASSEMBLY FIXTURE FOR 603FTB052 TEST COMPONENT

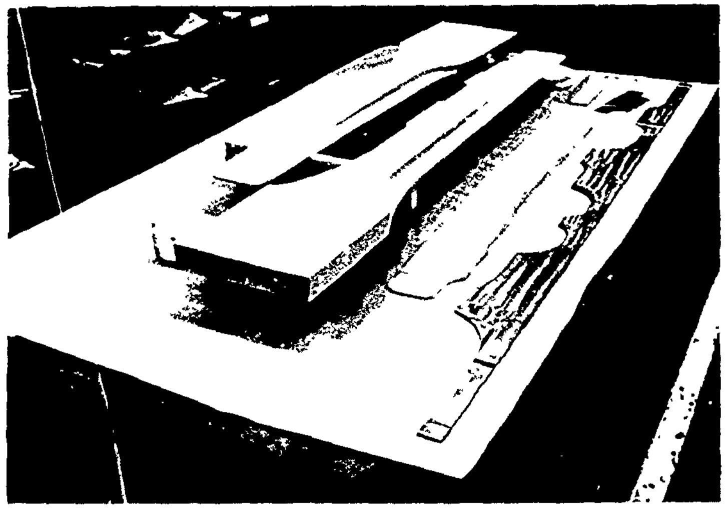

4-51124

Figure 5-89 603FTB052 10 Ni STEEL DETAILS (UNPAINTED PART IS 6AL-4V TITANIUM)

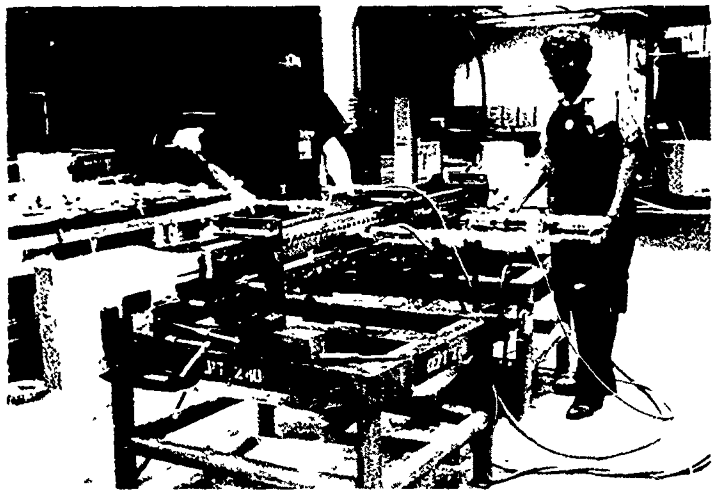

4-51138

Figure 5-90 FIXTURE FOR INSTALLING BOLTS IN 603FTB052-A1 ASSEMBLY (-A10 ASSEMBLY SIDE)

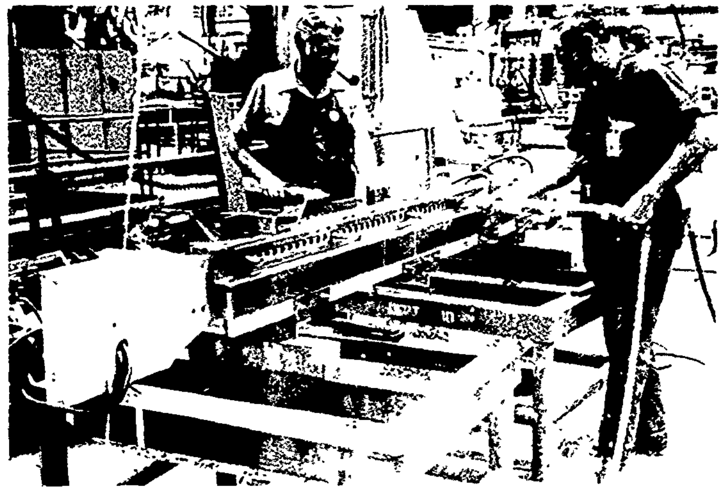

4-51139

Figure 5-91 FIXTURE FOR INSTALLING BOLTS IN 603FTB052-A1 ASSEMBLY (OPPOSITE SIDE) tooling pin locations. The tooling pins clamped the fixture to the assembly in all splice and end locations. Undersize holes were drilled for Taper-lok bolts in 128 places in the assembly. All holes were drilled in accordance with Process Standard PS-22.02-6. Figures 5-90 and 5-91 show the drilling operation in the 603FTB052-A1 assembly fixture. The undersize holes drilled in the -A1 assembly included (58) 0.3594-inch diameter, (20) 0.4844-inch diameter and (50) 0.6094-inch diameter for piloted Taper-lok rough reamer operations.

The -A1 assembly fixture was disassembled and all detail parts were removed for cleaning and deburr operations. Figures 5-92 and 5-93 show the complete assembly after undersize holes were drilled and the fixture removed. After final deburr and cleaning operations were complete, FMS1043 sealant was applied to all faying surfaces in a reassembly sequence. Close tolerance tooling pins and setup bolts were installed in all even number holes. All setup bolts were torqued, the sealant allowed to cold flow, and all bolts were then retorqued.

After final sealant cure, the assembly was reloaded in the assembly fixture for Phase I taper-ream operation. Alignment was maintained using tapered tooling pins in the rough taper reamed holes before removing the undersize tooling pins. All odd numbered holes were rough taper reamed with depth controlled pre-set portable tool kits.

The drill and assembly fixture was removed from the assembly and final hole preparation was made on all open holes. This included multiflute reaming for proper hole finish, maintaining the correct head protrusion. After final inspection on the Phase 1 holes, the taper-lok bolts were installed. Prior to bolt installation, all bolts were cetyl alcohol coated. All of the bolts were torqued to maintain M263 Engineering Standard.

Phase 2 hole preparation and bolt installation was made identical to the Phase 1 operation sequence. Figures 5-94 and 5-95 show the 603FTB052 final assembly ready for instrumentation and test.

### 5.6.2 603FTB053 Lower Plate Centerline Splice Assembly

A drill plate was designed and fabricated for drilling and rough taper reaming twenty-five holes for 5/8-inch diameter taper-lok fasteners. The drill plat included locators for the splice plates and provisions to control the gap between the lower plates. Straight and taper tooling pins were also fur-

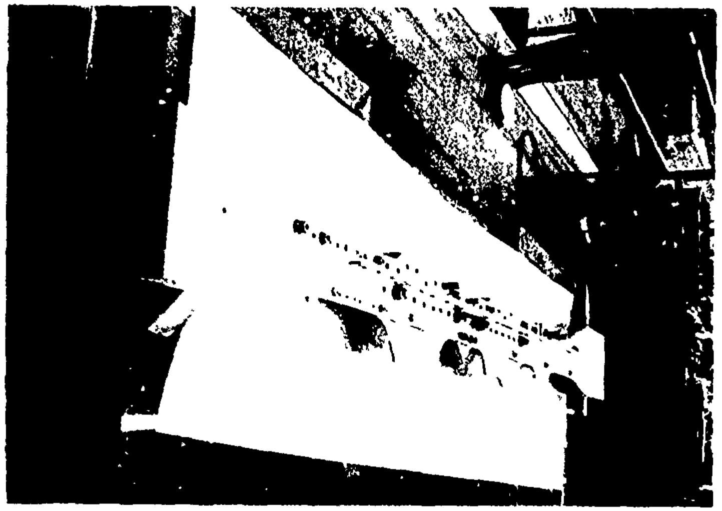

Figure 5-92 PARTIALLY ASSEMBLED 603FTB052 TEST COMPONENT (-A10 ASSEMBLY SIDE)

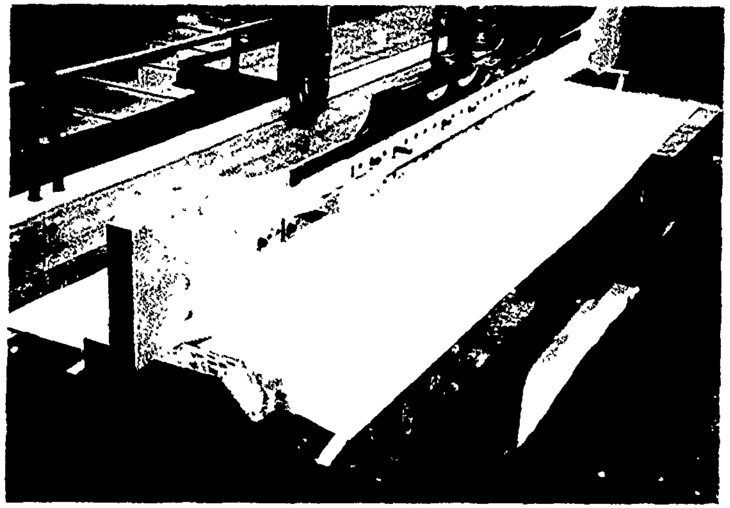

Figure 5-93 PARTIALLY ASSEMBLED 603FTB052 TEST COMPONENT (OPPOSITE SIDE)

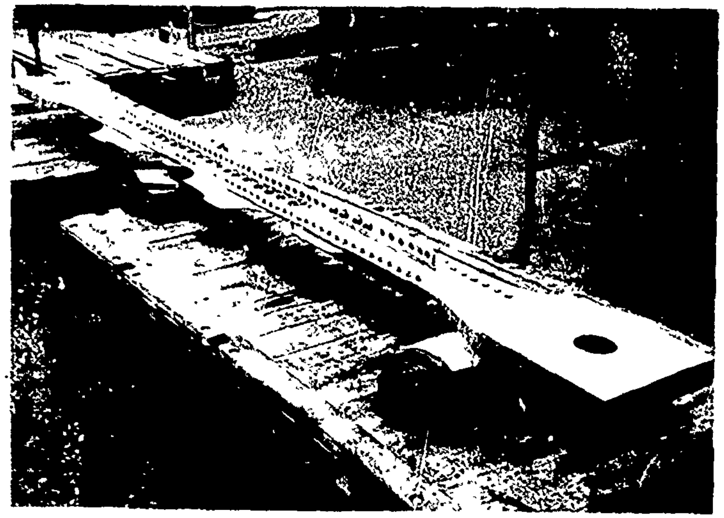

Figure 5-94 COMPLETED 603FTB052 TEST COMPONENT

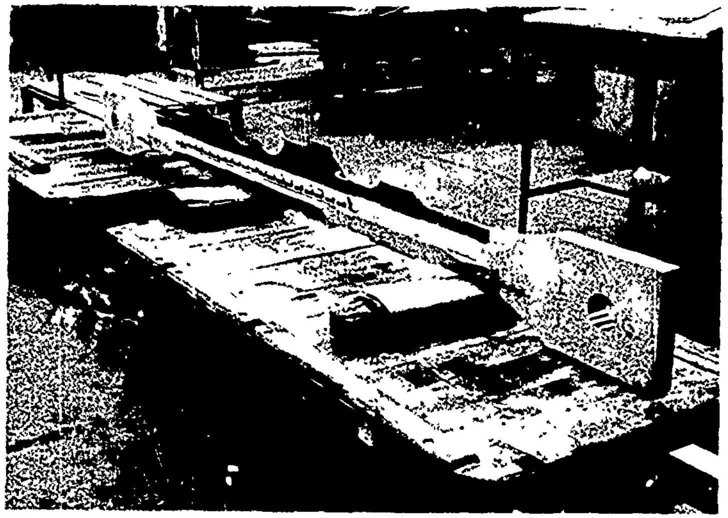

Figure 5-95 COMPLETED 603FTB052 TEST COMPONENT (OPPOSITE SIDE)

nished since the drill plate was moved from upper to lower surface several times during the drilling and reaming operations. The portable equipment kits and all accessories were identical to the ones used on the 603FTB052 assembly.

The drill plate was located on the assembled 603FTB053 details, rigidly secured, using large C-clamps. Inspection before any holes were drilled disclosed voids or gaps between the detail parts caused by accumulative tolerances in the lap splice design. FMS1048 liquid shim was applied to the splice plates to compensate for this mismatch. The four corner holes were then drilled. Threaded tooling pins were installed to secure the drill plate to the assembly and the remaining seven holes were drilled through the upper surface.

Close tolerance set-up bolts were installed in the assembly at four locations and the drill plate repositioned on the lower surface using tooling pins in the same holes to secure the drill plate. Fourteen holes were then drilled in the lower surface and all detail parts were marked to assure correct reassembly.

The drill plate was removed and the assembly was disassembled for cleaning and deburring. FMS1048 liquid shim was applied to the faying surfaces of the splice plates and parting agent applied to the lower plates at the splice areas. The reassembly sequence was made using twenty-five close tolerance set-up bolts torqued from center to outer edge to allow excess liquid shim to squeeze out. Final torque was made in one hour. After liquid shim cure, the parts were disassembled again for removal of the parting agent and final cleaning for FMS1043 sealant. Figure 5-96 shows detail parts ready for sealant application.

FMS1043 sealant was applied to all faying surfaces and final assembly of the 603FTB053 was made using set-up bolts in all odd numbered holes. The set-up bolts were retorqued and the sealant allowed to cure. All locators were removed from the drill plate for ease of locating and to reduce weight. Figure 5-97 shows the drill plate and the portable equipment kit used for Phase 1 rough taper reaming. All open holes were power reamed from the upper and lower surfaces and the drill plate removed. Phase 1 holes were final reamed and taper-lok bolts were installed.

Set-up bolts were removed from the even numbered holes and Phase 2 rough taper reaming, final carbide reaming and bolt installation was made in the same sequence as for Phase 1. Hole preparation and bolt installation was made in accordance with

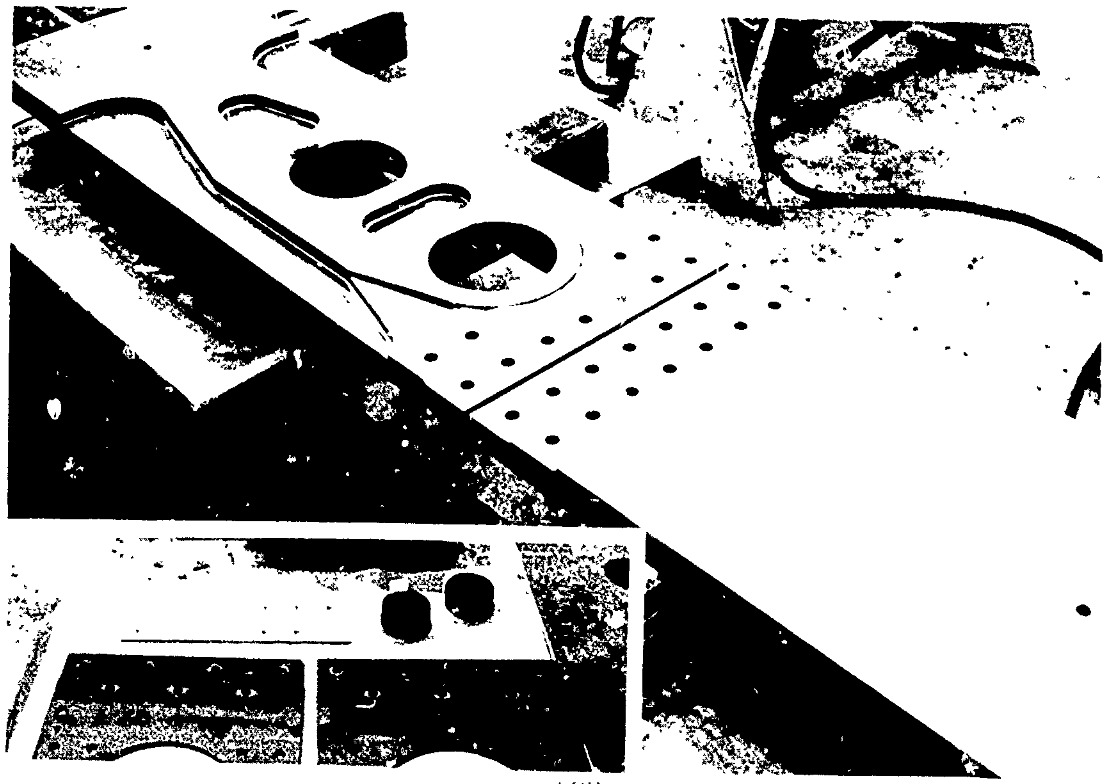

Figure 5-96 603FTB053 DETAIL PARTS READY FOR SEALING APPLICATION AND ASSEMBLY

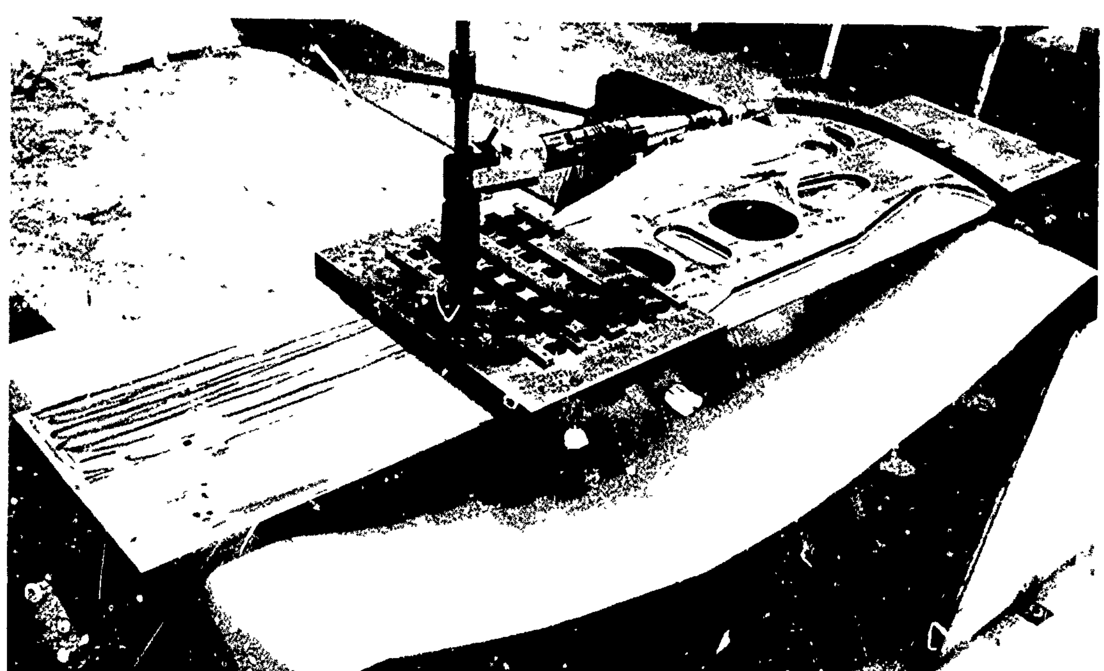

Figure 5-97 DRILL PLATE AND PORTABLE EQUIPMENT KIT USED TO POWER REAM TAPER-LOK HOLES IN 603FTB053

M263 Engineering specification. Figure 5-98 shows the completed 603FTB053-2 assembly.

### 5.6.3 603FTB035 Brazed Lower Plate Assembly

A one-piece picture frame drill plate was designed and fabricated for drilling and rough reaming the twelve 5/8-inch diameter taper holes in the brazed assembly. The fixture attached to four corner bolt holes used for mounting the support lugs. All twelve holes were drilled and power reamed complete, without removing the fixture, since no deburr or sealant operations were required. The drill plate was then removed and the final carbide reaming was completed in all twelve holes. The hole finish and protrusion was verified by Quality Control. The twelve taper-lok bolts were installed and torqued per M263 Engineering specification.

The end lugs were attached with straight shank bolts in matched hole patterns that were drilled in the detail parts using a N/C tape controlled American drill press. The assembled 603FTB035 is shown in Figure 5-99 prior to boring the test fixture attach holes.

## 5.7 MACHINING OF 603FTB043 UPPER COVER

## GROUP II TEST SPECIMEN

The 603FTB043 test specimen was numerically control (N/C) machined from a 6Al-4V beta annealed titanium billet. Excess material was face milled from all surfaces of the billet and starter holes drilled in the pocket areas prior to N/C machining. Figure 5-100 shows the part completely machined except for tooling tab removal.

Pocket milling starter holes (2.5-inch diameter by 3.170-inch depth) were N/C drilled on an American radial arm drill press. A 2.5-inch diameter spade drill was operated at 31 RPM and a feed rate of .004 inch per revolution.

Milling was accomplished on an Onsrud N/C milling machine. Surface material was removed using a 6-inch diameter face mill with 6 inserted carbide teeth. Feeds and speeds were 50 RPM (80 SFM) 2.0-IPM feed rate and 0.0065-inch feed per tooth. The pockets were profiled with 8-flute, 2-inch diameter end mills. Feeds and speeds were 100 RPM (52 SFM), 3.5-IPM feed, and 0.0044-inch feed per tooth.

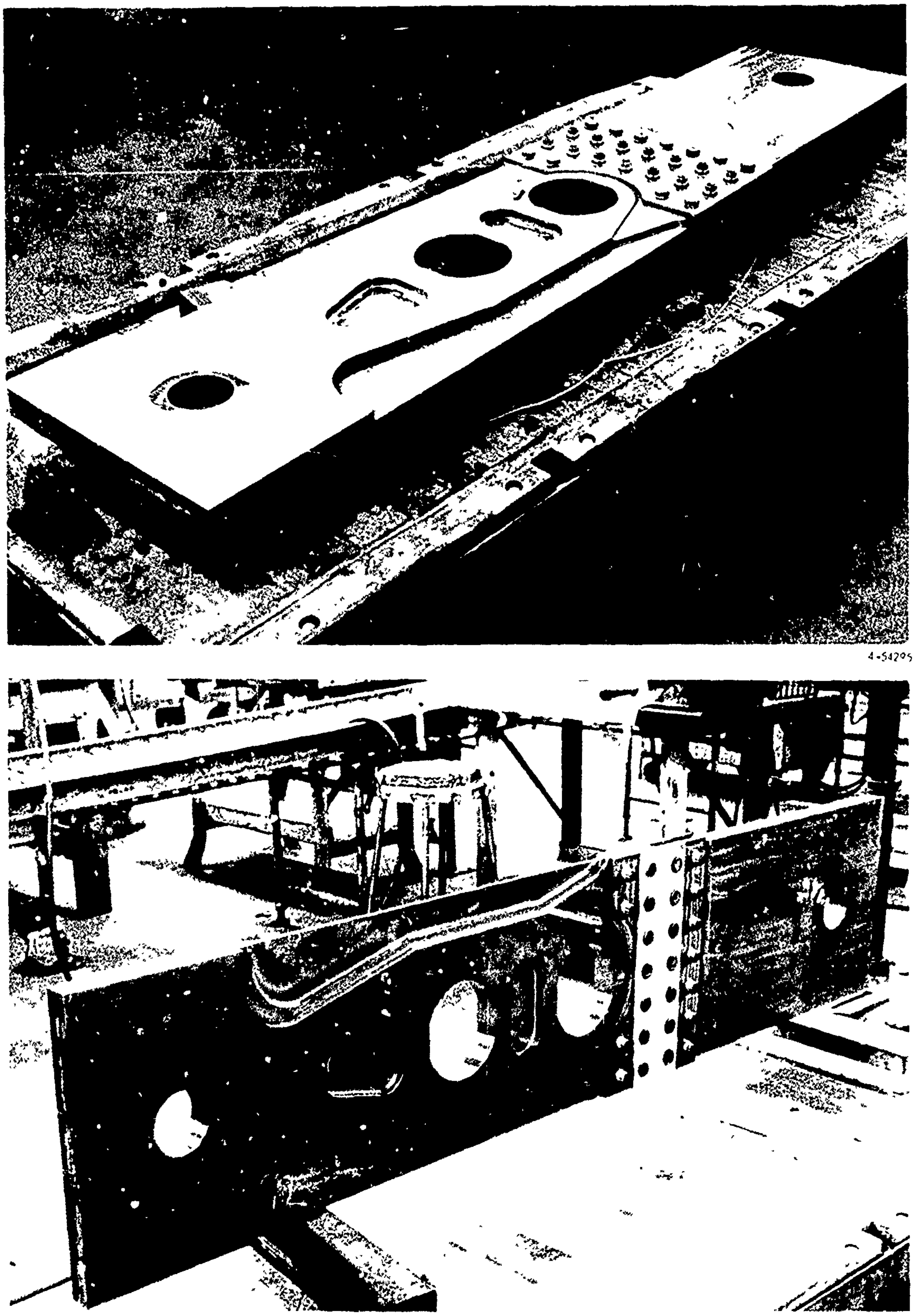

Figure 5-98 ASSEMBLED 603FTB053 (TOP SIDE AND BOTTOM SIDE)

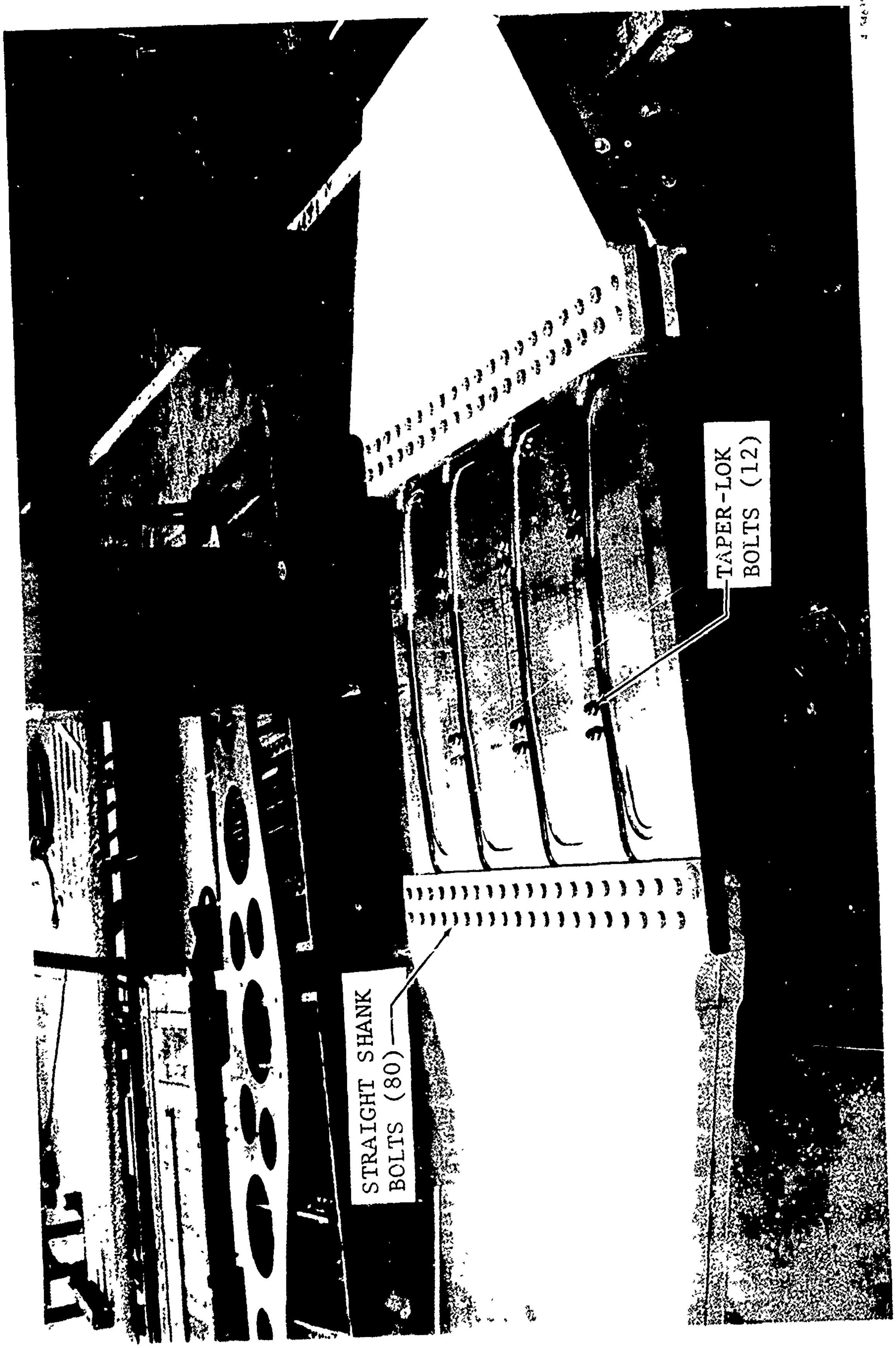


Figure 5-99 ASSEMBLED 603FTB035 TEST COMPONENT

(OUTER SURFACE)

(OPPOSITE SIDE)

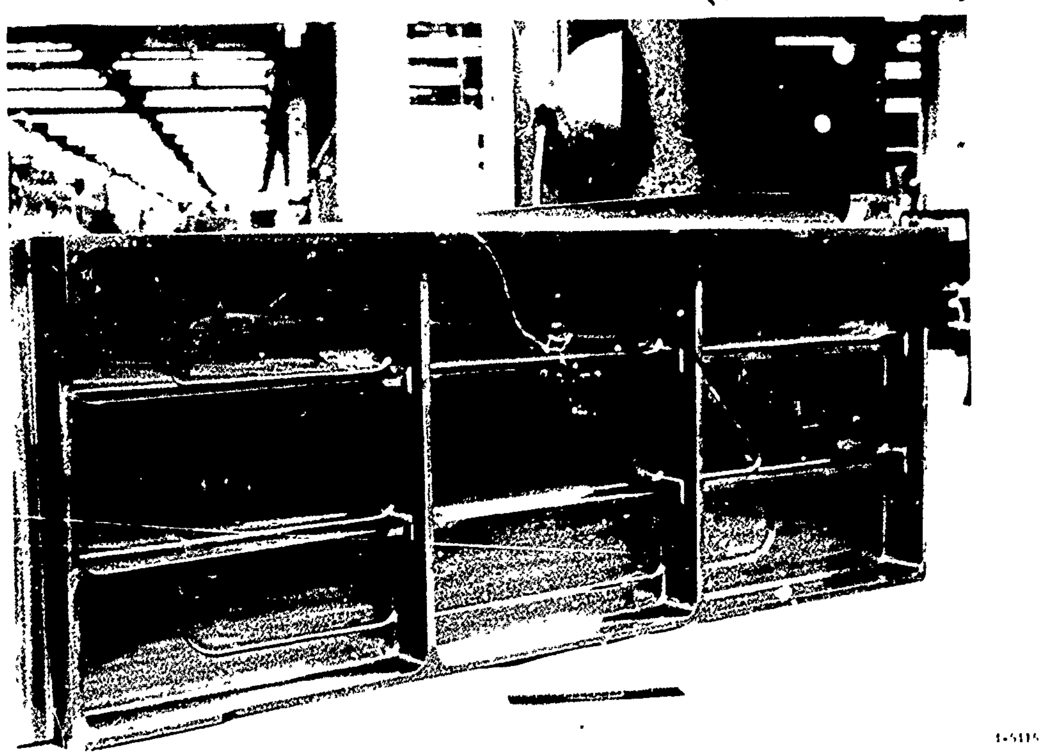

Figure 5-100 603FTB043 UPPER COVER GROUP II TEST SPECIMEN

Cutter life was reduced approximately 20 percent in machining the beta annealed 6Al-4V titanium as compared to conventionally annealed material.

# A P P E N D I X   A

- o ELECTRON BEAM WELD SCHEDULES
- o ELECTRON BEAM CURRENT TRACES

## ELECTRON BEAM SCHEDULES

Gun-to-Work Distance 3.5 Inches — Date 9-25-73

| Weld No. | Mat'l | Thickness inch | Weld Type | Wire Feed ipm | Weld Speed ipm | Weld Axis | Current ma | Voltage kv | Focus Pot. | Oscillator Freq. | Oscillator Atten. | Current Trace | Filament | Remarks |
|---|---|---|---|---|---|---|---|---|---|---|---|---|---|---|
| (1) | D6ac | 1.00 | BOP | 3[illegible] | 15 | X | 460 | 34.5 | 5.22 | 5Kc | -9 | ✓ | 66 amps. | |
| (2) | " | " | " | 30 | 15 | X | 180 | 18.0 | 5.22 | 5Kc | -7 | ✓ | " | |
| | | Parameter development weld - (good setting) | | | | | | | | | | | | |
| | | | | | | | | | | | | | | |
| (1) | 10Ni. | 1.00 | BOP | 30 | 15 ~~20~~ | X | 400 | 34.5 | 5.22 | 5Kc | -9 | ✓ | 66 amps. | |
| (2) | " | " | " | 30 | 12 ~~18~~ | X | 160 | 18.0 | 5.22 | 5Kc | -7 | ✓ | " | |
| | | Parameter development weld. | | | | | | | | | | | | |
| | | | | | | | | | | | | | | |
| (1) | 10Ni. | 1.00 | BOP | 30 | 18 ~~15~~ | X | 440 | 34.[illegible] | 5.22 | 5Kc | -9 | ✓ | [illegible] amps. | |
| (2) | " | " | " | 30 | 15 | X | 160 | 18.0 | 5.22 | 5Kc | -7 | ✓ | " | |
| | | Appearance Fair - | | | | | | | | | | | | |
| | | Parameter development weld. | | | | | | | | | | | | |
| | | | | | | | | | | | | | | |
| (1) | 10Ni. | 1.00 | BOP | 30 | 18 | X | 400 | 34.5 | 5.22 | 5Kc | -9 | ✓ | 66 amps. | |
| (2) | " | " | " | 30 | 18 | X | 160 | 18.0 | 5.22 | 5Kc | -7 | ✓ | " | |
| (3) | " | " | " | 30 | 15 | X | 160 | 16.0 | 5.22 | 5Kc | -7 | ✓ | " | |
| | | Root uniform, face underfilled, required 3 passes. | | | | | | | | | | | | |
| | | | | | | | | | | | | | | |

ELECTRON BEAM SCHEDULES

Gun-to-Work Distance 3.5 Inches Mid Point

Date 10-4-73

| Weld No. | Mat'l | Thickness inch | Weld Type | Wire Feed ipm | Weld Speed ipm | Weld Axis | Current ma | Voltage kv | Focus Pot. | Oscillator Freq. | Oscillator Atten. | Current Trace | Filament | Remarks |
|---|---|---|---|---|---|---|---|---|---|---|---|---|---|---|
| X-1(1) | 10Ni. | 1.00 | BOP | 30 | 18 | x | 460 | 34.5 | 5.22 | 5Kc | -9 | ✓ | 68 amps | |
| (2) | " | " | " | 30 | 15 | x | 180 | 18.0 | 5.22 | 5Kc | -8 | ✓ | " | |
| | | Root good, face underfilled. | | | | | | | | | | | | |
| | | | | | | | | | | | | | | |
| X-2(1) | 10Ni. | 1.00 | BOP | 30 | 18 | x | 460 | 34.5 | 5.22 | 5Kc | -9 | ✓ | 68 amps | |
| (2) | " | " | " | 30 | 18 | x | 180 | 18.0 | 5.22 | 5Kc | -7 | ✓ | " | |
| | | Root good, face fair. | | | | | | | | | | | | |
| | | | | | | | | | | | | | | |
| X-3(1) | 10Ni. | 1.00 | BOP | 30 | 18 | x | 420 | 34.5 | 5.22 | 5Kc | -9 | ✓ | 68 amps | |
| (2) | " | " | " | 35 | 18 | x | 160 | 18.0 | 5.22 | 5Kc | -9 | ✓ | " | |
| | | Root good, face irregular. | | | | | | | | | | | | |
| | | Parameter development welds. | | | | | | | | | | | | |
| | | | | | | | | | | | | | | |
| H-17(1) | 10Ni. | 1.6 | Butt | 30 | 12.8 | x | 680 | 47.5 | 5.22 | 5Kc | -7 | ✓ | 67 amps | |
| (2) | " | " | " | 30 | 15.8 | x | 200 | 20.0 | 5.22 | 5Kc | -7 | ✓ | " | |
| | | X-ray - porosity - cracks. | | | | | | | | | | | | |
| | | Weld cut out and inspection through the longitudinal plane. | | | | | | | | | | | | |
| | | | | | | | | | | | | | | |

ELECTRON BEAM SCHEDULES

Gun-to-Work Distance 3.5 Inches

Date 8-7-73

| Weld No. | Mat'l | Thickness inch | Weld Type | Wire Feed ipm | Weld Speed ipm | Weld Axis | Current ma | Voltage kv | Focus Pot. | Oscillator Freq. | Oscillator Atten. | Current Trace | Filament | Remarks |
|---|---|---|---|---|---|---|---|---|---|---|---|---|---|---|
| X-1(1) | 10Ni. | 2.00" | BOP | 30 | 28 | X | 700 | 47.5 | 5.22 | 8Kc | -9 | ✓ | 65 amps | |
| (2) | " | " | " | 30 | 26 | X | 200 | 20.0 | 5.22 | " | -6 | ✓ | " | |
| | | Appearance - Face good, root globular, cutout for inspection - X-ray shows | | | | | | | | | | | | |
| | | very fine cracks - 5/8 inch from face. | | | | | | | | | | | | |
| | | | | | | | | | | | | | | |
| X-2(1) | 10Ni. | 2.00" | BOP | 30 | 30 | X | 700 | 47.5 | 5.22 | 8Kc | -9 | ✓ | 65 amps | |
| (2) | " | " | " | 30 | 26 | X | 200 | 20.0 | " | " | -6 | ✓ | " | |
| | | Face underfilled because of heat buildup. | | | | | | | | | | | | |
| | | Root globular - cutout for NDI - X-ray - cracks. | | | | | | | | | | | | |
| | | | | | | | | | | | | | | |
| X-3(1) | 10Ni. | 2.00 | BOP | 30 | 30 | X | 630 | 46.0 | 5.22 | 8Kc | -9 | ✓ | 65 amps | |
| (2) | " | " | " | 30 | 26 | X | 200 | 20.0 | 5.22 | 8Kc | -6 | ✓ | " | |
| | | Face good - Root globular - | | | | | | | | | | | | |
| | | X-ray shows porosity and hairline cracks. | | | | | | | | | | | | |
| | | | | | | | | | | | | | | |
| X-4(1) | 10Ni. | 2.00 | BOP | OPP | 30 | X | 620 | 45.0 | 5.22 | 8Kc | -9 | ✓ | 65 amps | |
| (2) | " | " | " | 30 | 26 | X | 200 | 20.0 | " | 8Kc | -6 | ✓ | " | |
| | | BOP = Bead on plate. | | | | | X-ray cracks. | | | | | | | |

## ELECTRON BEAM SCHEDULES

Gun-to-Work Distance 3.5 Inches AMAVS Date 3-27-73

| Weld No. | Mat'l | Thickness inch | Weld Type | Wire Feed ipm | Weld Speed ipm | Weld Axis | Current ma | Voltage kv | Focus Pot. | Oscillator Freq. | Oscillator Atten. | Current Trace | Filament | Remarks |
|---|---|---|---|---|---|---|---|---|---|---|---|---|---|---|
| H-1(1) | Hy180 (10Ni) | 1.00 | Butt | 30 | 28 | X | 560 | 34.5 | 5.22 | 8Kc | -9 | ✓ | 65 amps | |
| (2) | " | 1.00 | Butt | 30 | 30 | X | 380 | 25.0 | " | " | -9 | ✓ | " | |
| (3) | " | 1.00 | Butt | 0 | 30 | X | 220 | 18.0 | " | " | " | ✓ | " | |
| (4) | " | 1.00 | Butt | 30 | 28 | X | 160 | 16.0 | " | " | -6 | ✓ | " | |
| | | 4th pass made to determine effects of tempering pass. | | | | | | | | | | | | |
| | | | | | | | | | | | | | | |
| H-2(1) | 10Ni. | .500 | Butt | 30 | 28 | X | 380 | 27.5 | 5.22 | 8Kc | -9 | ✓ | 65 amps | |
| (2) | " | .500 | Butt | 30 | 28 | X | 180 | 16.0 | " | " | -7 | ✓ | " | |
| (3) | " | .500 | Butt | 30 | 28 | X | 160 | 16.0 | " | " | -7 | ✓ | " | |
| | | | | (Good Setting) | | | | | | | | | | |
| | | | | | | | | | | | | | | |
| H-3(1) | 10Ni. | .500 | Butt | 30 | 28 | X | 340 | 27.5 | 5.22 | 8Kc | -9 | ✓ | 65 amps | |
| (2) | " | .500 | Butt | 30 | 28 | X | 160 | 16.0 | " | " | -7 | ✓ | " | |
| (3) | " | .500 | Butt | 30 | 27 | X | 160 | 16.0 | " | " | -6 | ✓ | " | |
| | | | | | | | | | | | | | | |
| H-4(1) | 10Ni. | .500 | Butt | 30 | 28 | X | 340 | 27.5 | 5.22 | 8Kc | -9 | ✓ | 65 amps | |
| (2) | " | .500 | Butt | 30 | 27 | X | 160 | 16.0 | " | " | -7 | ✓ | " | |
| | | | | | | | | | | | | | | |

ELECTRON BEAM SCHEDULES

Gun-to-Work Distance 3.5 Inches

Date 5-14-73

| Weld No. | Mat'l | Thickness inch | Weld Type | Wire Feed ipm | Weld Speed ipm | Weld Axis | Current ma | Voltage kv | Focus Pot. | Oscillator Freq. | Oscillator Atten. | Current Trace | Filament | Remarks |
|---|---|---|---|---|---|---|---|---|---|---|---|---|---|---|
| H-5(1) | 10Ni. | .500 | Butt | 30 | 30 | X | 350 | 27.5 | 5.22 | 8Kc | -9 | ✓ | 65 amps | |
| (2) | " | .500 | Butt | 30 | 25 | X | 140 | 16.0 | " | " | -6 | ✓ | " | |
| (3) | " | .500 | Butt | 30 | 25 | X | 140 | 15.0 | " | " | -6 | ✓ | " | |
| (4) | " | .500 | Butt | 30 | 25 | X | 150 | 16.0 | " | " | -4 | ✓ | " | |
| | | X-ray OK - Weld area cut out for NDI. | | | | | | | | | | | | |
| | | | | | | | | | | | | | | |
| H-10(1) | 10Ni. | .500 | Butt | 30 | 30 | X | 330 | 27.5 | 5.22 | 8Kc | -8 | ✓ | 65 amps | |
| (2) | " | .500 | Butt | 30 | 28 | X | 160 | 16.0 | 4.90 | OFF | | ✓ | " | (Defocused) pass. |
| | | (Weld Shrinkage measurements) | | | | | | | | | | | | |
| | | X-ray OK - Magnaflux OK | | | | | | | | | | | | |
| | | Will be used for impact and tensile test. | | | | | | | | | | | | |
| H-11(1) | 10Ni. | .500 | Butt | 30 | 30 | X | 340 | 27.5 | 5.60 | 8Kc | -9 | ✓ | 68 amps | |
| (2) | " | .500 | Butt | 30 | 28 | X | 160 | 16.0 | 5.60 | 8Kc | -6 | ✓ | " | |
| | | (Weld shrink measurements). | | | | | | | | | | | | |
| | | X-ray OK. Ultrasonics OK. - 2 defects | | | | | | | | | | | | |
| | | will be used for impact and tensile test. | | | | | | | | | | | | |

ELECTRON BEAM SCHEDULES

Gun-to-Work Distance 3.5 Inches

Date 8-22-73

| Weld No. | Mat'l | Thickness inch | Weld Type | Wire Feed ipm | Weld Speed ipm | Weld Axis | Current ma | Voltage kv | Focus Pot. | Oscillator Freq. | Oscillator Atten. | Current Trace | Filament | Remarks |
|---|---|---|---|---|---|---|---|---|---|---|---|---|---|---|
| H-12(1) | 10Ni. | .500 | Butt | 30 | 30 | X | 320 | 27.5 | 5.22 | 8Kc | -9 | ✓ | 66 amps. | |
| (2) | " | " | " | 30 | 28 | X | 140 | 16.0 | " | " | -7 | ✓ | " | |
| | | Appearance fair - root narrow. | | | | | | | | | | | | |
| | | Wire feed intermittant - 1st pass. | | | | | | | | | | | | |
| | | | | | | | | N.D.I. | Specimen | | MD-3232-1 | | | |
| H-13(1) | 10Ni. | .500 | Butt | 30 | 30 | X | 300 | 27.5 | 5.22 | 5Kc | -9 | ✓ | 67 amps. | |
| (2) | " | " | " | 30 | 26 | X | 160 | 18.0 | 5.22 | 5Kc | -6 | ✓ | " | |
| | | Appearance - face good, root narrow. | | | | | | | | | | | | |
| | | | | | | | | N.D.I. | Speciman | | MD-3232-2 | | | |
| | | | | | | | | | | | | | | |
| H-14(1) | 10Ni. | 2.00 | Butt | 30 | 28 | X | 680 | 47.5 | 5.22 | 5Kc | -8 | ✓ | 66 amps. | |
| (2) | " | " | " | 30 | 25 | X | 160 | 18.0 | 5.22 | 5Kc | -6 | ✓ | " | |
| | | Arc out first pass. Repaired - | | | | | | | | | | | | |
| | | Face good - root globular - | | | | | | | | | | | | |
| | | X-ray shows gross voids. | | | | | | | | | | | | |
| | | | | | | | | | | | | | | |
| | | | | | | | | | | | | | | |
| | | | | | | | | | | | | | | |
| | | | | | | | | | | | | | | |

ELECTRON BEAM SCHEDULES

Gun-to-Work Distance 3.5 Inches or noted. Date 8-21-73

| Weld No. | Mat'l | Thickness inch | Weld Type | Wire Feed ipm | Weld Speed ipm | Weld Axis | Current ma | Voltage kv | Focus Pot. | Oscillator Freq. | Oscillator Atten. | Current Trace | Filament | Remarks |
|---|---|---|---|---|---|---|---|---|---|---|---|---|---|---|
| Fatigue | 10Ni. | .900 | Butt | OFF | 26 | X | 440 | 34.5 | 5.22 | 5Kc | -8 | ✓ | 66 amps. | |
| Specimen | 10Ni. | .900 | Butt | 30 | 24 | X | 160 | 18.0 | 5.22 | 5Kc | -6 | ✓ | " | |
| E.T.L. | | Appearance - Face good, root good. | | | | | | | | | | | | |
| | | Bolt hole failure - new end welded on to complete | | | | | | | | | | | | |
| | | fatigue test. X-ray OK. | | | | | | | | | | | | |
| | | | | | | | | | | | | | | |
| | | 3.5 inch focal point - 3 inch gun to work distance | | | | | | | | | | | | |
| H-15(1) | 10Ni. | 1.6 | Butt | 30 | 13 | X | 660 | 47.5 | 5.22 | 5Kc | -7 | ✓ | 67 amps. | |
| (2) | " | " | " | 30 | 13 | X | 200 | 20.0 | 5.22 | 5Kc | -6 | ✓ | " | |
| | | Appearance face wide .375 inch. root uniform. | | | | | | | | | | | | |
| | | Weld cut out, - longitudinal X-ray shows porosity and cracks. | | | | | | | | | | | | |
| | | | | | | | | | | | | | | |
| H-15A(1) | 10Ni. | 1.6 | BOP | 30 | 13 | X | 660 | 47.5 | 5.22 | 5Kc | -7 | ✓ | 67 amps. | |
| (2) | " | " | " | 30 | 13 | X | 200 | 20.0 | 5.22 | Kc | -7 | ✓ | " | |
| | | Appearance - face good, root good. | | | | | | | | | | | | |
| | | X-ray scattered porosity, mid point cracks. | | | | | | | | | | | | |
| | | | | | | | | | | | | | | |
| | | | | | | | | | | | | | | |

ELECTRON BEAM SCHEDULES

Gun-to-Work Distance 3.5 Inches MP

Date 10-9-73

| Weld No. | Mat'l | Thickness inch | Weld Type | Wire Feed ipm | Weld Speed ipm | Weld Axis | Current ma | Voltage kv | Focus Pot. | Oscillator Freq. | Oscillator Atten. | Current Trace | Filament | Remarks |
|---|---|---|---|---|---|---|---|---|---|---|---|---|---|---|
| H-18(1) | 10Ni. | .900 | Butt | 30 | 18 | x | 440 | 34.5 | 5.22 | 5Kc | -9 | ✓ | 65 amps. | |
| (2) | " | " | " | 30 | 18 | x | 180 | 18.0 | 5.22 | 5Kc | -9 | ✓ | " | |
| (3) | " | " | " | 30 | 18 | x | 160 | 18.0 | 5.22 | 5Kc | -7 | ✓ | " | |
| | | Part No. 603R-100-11-5 -H-18 | | | | | | | | | | | | |
| | | Magnaflux shows root crack - | | | | | | | | | | | | |
| | | X-ray rejection, processing stopped. | | | | | | | | | | | | |
| | | | | | | | | | | | | | | |
| H-19(1) | 10Ni. | .900 | Butt | off | 18 | x | 440 | 34.5 | 5.22 | 5Kc | -9 | ✓ | 65 amps. | |
| (2) | " | " | " | 30 | 18 | x | 160 | 18.0 | 5.22 | 5Kc | -9 | ✓ | " | |
| (3) | " | " | " | 30 | 18 | x | 160 | 18.0 | 5.22 | 5Kc | -7 | ✓ | " | |
| | | Part No. 603R-100-11-5- H-19 | | | | | | | | | | | | |
| | | Appearance face-good, root - good. | | | | | | | | | | | | |
| | | Magnaflux shows indications on weld face of surface cracks but this | | | | | | | | | | | | |
| | | inspection is inconclusive because dye penetrant shows an acceptable weld. | | | | | | | | | | | | |
| | | X-ray shows starting and termination cracks-remainder of weld acceptable. | | | | | | | | | | | | |

ELECTRON BEAM SCHEDULES

Gun-to-Work Distance 3.5 Inches

Date 10-10-73

| Weld No. | Mat'l | Thickness inch | Weld Type | Wire Feed ipm | Weld Speed ipm | Weld Axis | Current ma | Voltage kv | Focus Pot. | Oscillator Freq. | Oscillator Atten. | Current Trace | Filament | Remarks |
|---|---|---|---|---|---|---|---|---|---|---|---|---|---|---|
| H-20(1) | 10Ni. | 1.6 | Butt | off | 13 | x | 700 | 47.5 | 5.22 | 5Kc | -8 | ✓ | 65 amps. | |
| (2) | " | " | " | 30 | 13 | x | 200 | 20.0 | 5.22 | 5Kc | -8 | ✓ | " | |
| | | Parameter development joint. | | | | | | | | | | | | |
| | | | | | | | | | | | | | | |
| H-21(1) | 10Ni. | 1.6 | BOP | 30 | 10/18 | x | 540 | 41.0 | 5.22 | 5Kc | -9 | ✓ | 65 amps. | |
| (2) | " | " | " | 30 | 18 | x | 200 | 20.0 | 5.22 | 5Kc | -7 | ✓ | " | |
| (3) | " | " | " | 30 | 15 | x | 200 | 20.0 | 5.22 | 5Kc | -6 | ✓ | " | |
| | | Weld bend cross section shows bulge and included cracks. | | | | | | | | | | | | |
| | | | | | | | | | | | | | | |
| | | Gun to work distance changed to 2.7 inches. | | | | | | | | | | | | |
| H-22(1) | 10Ni. | 1.6 | BOP | 30 | 10 | x | 540 | 41.0 | 5.22 | 5Kc | -9 | ✓ | 65 amps. | |
| (2) | " | " | " | 30 | 10 | x | 200 | 20.0 | 5.22 | 5Kc | -8 | ✓ | " | |
| (3) | " | " | " | 30 | 10 | x | 200 | 20.0 | 5.22 | 5Kc | -7 | ✓ | " | Osc. too wide. |
| | | | | | | | | | | | | | | |
| H-23(1) | 10Ni. | 1.6 | Butt | 30 | 10 | x | 560 | 41.0 | 5.22 | 5Kc | -9 | ✓ | 65 amps | Arc out |
| (2) | " | " | " | 30 | 10 | x | 200 | 20.0 | 5.22 | 5Kc | -9 | ✓ | " | |
| (3) | " | " | " | 30 | 10 | x | 200 | 20.0 | 5.22 | 5Kc | -8 | ✓ | " | |

ELECTRON BEAM SCHEDULES

Gun-to-Work Distance 3.5 Inches Fx

Date 10-12-73

| Weld No. | Mat'l | Thickness (inch) | Weld Type | Wire Feed (ipm) | Weld Speed (ipm) | Weld Axis | Current (ma) | Voltage (kv) | Focus Pot. | Oscillator Freq. | Oscillator Atten. | Current Trace | Filament | Remarks |
|---|---|---|---|---|---|---|---|---|---|---|---|---|---|---|
| H-24(1) | 10Ni. | 1.6 | Butt | 30 | 12 | x | 580 | 41.0 | 5.22 | 5Kc | -9 | ✓ | 65 amps. | |
| (2) | " | " | " | 30 | 12 | x | 200 | 20.0 | 5.22 | 5Kc | -10 | ✓ | " | |
| | | E.B. welded run in - run out tabs. | | | | | | | | | | | | |
| | | Appearance face good, root good. | | | | | | | | | | | | |
| | | X-ray, cracks - ultrasonics, cracks | | | | | | | | | | | | |
| | | NDI speciman - MD 3232 - H-24 | | | | | | | | | | | | |
| | | | | | | | | | | | | | | |
| H-25(1) | 10Ni. | 1.6 | Butt | 30 | 12 | x | 560 | 41.0 | 5.22 | 5Kc | -9 | ✓ | 65 amps. | |
| (2) | " | " | " | 30 | 12 | x | 200 | 20.0 | 5.22 | 5Kc | -10 | ✓ | " | |
| | | E.B. Welded tabs - Appearance, face good, root good. | | | | | | | | | | | | |
| | | X-ray, cracks - Ultrasonics, intermittent cracks. | | | | | | | | | | | | |
| | | NDI speciman - MD 3233 - H-25 | | | | | | | | | | | | |

ELECTRON BEAM SCHEDULES

Gun-to-Work Distance 3.5 Inches

Date 10-17-73

| Weld No. | Mat'l | Thickness inch | Weld Type | Wire Feed ipm | Weld Speed ipm | Weld Axis | Current ma | Voltage kv | Focus Pot. | Oscillator Freq. | Oscillator Atten. | Current Trace | Filament | Remarks |
|---|---|---|---|---|---|---|---|---|---|---|---|---|---|---|
| H-26(1) | 10Ni | 1.6 | Butt | 30 | 12 | x | 480 | 41.0 | 5.22 | 5Kc | -9 | ✓ | 65 amps | |
| (2) | " | " | " | 30 | 12 | x | 200 | 20.0 | 5.22 | 5Kc | -10 | ✓ | " | |
| (3) | " | " | " | 30 | 12 | x | 200 | 20.0 | 5.22 | 5Kc | -7 | ✓ | " | |
| | | Appearance face good, root good. | | | | | | | | | | | | |
| | | Macro of run out tab show cross section bulge | | | | | | | | | | | | |
| | | 5/8 inch from face surface. | | | | | | | | | | | | |
| | | Ultrasonic inspection - immersion, C scan recording | | | | | | | | | | | | |
| | | show cracks. | | | | | | | | | | | | |
| | | | | | | | | | | | | | | |
| H-27(1) | 10Ni | 1.6 | Butt | 30 | 12 | x | 460 | 41.0 | 5.22 | 5Kc | -9 | ✓ | 65 amps | |
| (2) | " | " | " | 30 | 12 | x | 200 | 20.0 | 5.22 | 5Kc | -9 | ✓ | " | Wire fouled |
| (3) | " | " | " | 30 | 12 | x | 200 | 20.0 | 5.22 | 5Kc | -8 | ✓ | " | |
| | | Macro of tab shows cross section bulge with micro-fissure in the | | | | | | | | | | | | |
| | | vertical plane. | | | | | | | | | | | | |
| | | Ultrasonic inspection - shows intermittent cracks. | | | | | | | | | | | | |

ELECTRON BEAM SCHEDULES

Gun-to-Work Distance 3.5 Inches

Date 10-7-73

| Weld No. | Mat'l | Thickness inch | Weld Type | Wire Feed ipm | Weld Speed ipm | Weld Axis | Current ma | Voltage kv | Focus Pot. | Oscillator Freq. | Oscillator Atten. | Current Trace | Filament | Remarks |
|---|---|---|---|---|---|---|---|---|---|---|---|---|---|---|
| M-1(1) | 10Ni. | .500 | Butt | 30 | 24 | x | 340 | 27.5 | 5.22 | 5Kc | -9 | ✓ | 65 amps. | |
| (2) | " | " | " | 30 | 24 | x | 180 | 18.0 | 5.22 | 5Kc | -8 | ✓ | " | |
| | Appearance - face good, root good. | | | | | | | | | | | | | |
| | X-ray OK, Send to ETL for fatigue test. | | | | | | | | | | | | | |
| | | | | | | | | | | | | | | |
| H-28(1) | 10Ni. | 1.6 | Butt | 30 | 14 | x | 560 | 41.0 | 5.22 | 5Kc | -9 | ✓ | 65 amps. | Wire fouled |
| (2) | " | " | " | 30 | 12 | x | 180 | 20.0 | 5.22 | 5Kc | -9 | ✓ | | because of |
| | Appearance, face under cut on high side. | | | | | | | | | | | | | mismatch |
| | Root good, Weld shrink measurements. | | | | | | | | | | | | | |
| | Mismatch of .050 inch. | | | | | | | | | | | | | |
| | Ultrasonics show intermittent cracks | | | | | | | | | | | | | |
| | verified by macrosection. | | | | | | | | | | | | | |
| H-29(1) | 10Ni. | 1.6 | Butt | 30 | 15 | x | 580 | 41.0 | 5.22 | 5Kc | -9 | ✓ | 65 amps. | |
| (2) | " | " | " | 30 | 15 | x | 200 | 20.0 | 5.22 | 5Kc | -9 | ✓ | " | |
| (3) | " | " | " | 30 | 12 | x | 200 | 20.0 | 5.22 | 5Kc | -8 | ✓ | " | |
| | Weld shrink measurements. | | | | | | | | | | | | | |
| | Ultrasonics shows intermittent cracks | | | | | | | | | | | | | |
| | verified by macrosection. | | | | | | | | | | | | | |

ELECTRON BEAM SCHEDULES

Gun-to-Work Distance 3.5 Inches

Date 10-22-73

| Weld No. | Mat'l | Thickness inch | Weld Type | Wire Feed ipm | Weld Speed ipm | Weld Axis | Current ma | Voltage kv | Focus Pot. | Oscillator Freq. | Oscillator Atten. | Current Trace | Filament | Remarks |
|---|---|---|---|---|---|---|---|---|---|---|---|---|---|---|
| H-30(1) | 10Ni. | 1.6 | Butt | 30 | 15 | x | 540 | 41.0 | 5.22 | 5Kc | -9 | ✓ | 65 amps. | |
| (2) | " | " | " | 30 | 15 | x | 180 | 20.0 | 5.22 | 5Kc | -9 | ✓ | " | |
| (3) | " | " | " | 30 | 12 | x | 180 | 20.0 | 5.22 | 5Kc | -8 | ✓ | " | |
| | | Push up tabs - Appearance face good. | | | | | | | | | | | | |
| | | Root good - Ultrasonics shows cracks. | | | | | | | | | | | | |
| | | Macrosection verifies hot cracking | | | | | | | | | | | | |
| | | | | | | | | | | | | | | |
| H-31(1) | 10NI. | 1.6 | Butt | 30 | 15 | x | 580 | 41.0 | 5.22 | 5Kc | -9 | ✓ | 65 amps. | |
| (2) | " | " | " | 30 | 15 | x | 200 | 20.0 | 5.22 | 5Kc | -9 | ✓ | " | |
| (3) | " | " | " | 30 | 12 | x | 200 | 20.0 | 5.22 | 5Kc | -8 | ✓ | " | |
| | | Welded tabs. | | | | | | | | | | | | |
| | | Appearance face good, root good. | | | | | | | | | | | | |
| | | Ultrasonics show cracks. | | | | | | | | | | | | |
| | | Macrosection show good geometry, and no defects. | | | | | | | | | | | | |
| H-32(1) | 10Ni. | 1.6 | Butt | 0 | 10 | x | 450 | 38.0 | 5.22 | 5Kc | -8 | ✓ | 65 amps. | |
| (2) | " | " | " | 0 | 10 | x | 380 | 30.0 | 5.22 | 5Kc | -7 | ✓ | " | |
| (3) | " | " | " | 30 | 10 | x | 200 | 20.0 | 5.22 | 5Kc | -6 | ✓ | " | |
| | | | | | | | | | | | | | | |

# ELECTRON BEAM WELDING SCHEDULE

Schedule Number ______ Date 10-12-73

Part Number MD 32.33 Part Name ______ Material Type 10Ni.(Hy 180)

Serial Number F 530647 -H-24 Tool Number ______ Mat'l. Thick 1.6"

Filler Wire Type Low alloy Hy180/220 (10Ni.Chr.-Mo. Co) Diameter .062

## UPPER CONTROL PANEL

| HV START Delay | MOTOR START Delay | HIGH VOLTAGE Initial KV | HIGH VOLTAGE Final | SPEED ADJUSTMENT Initial and Final |
|---|---|---|---|---|
| 0 0 2 | 0 0 2 | 4 0 0 | 0 5 9 | |
| Seconds: X 15 30 60 120 | Seconds: X 15 30 60 120 | Slope: 0 1 4 | Slope: 0 4 5 | Run: 0 0 4 |

## OSCILLATOR

AXIS X [X] Y [ ]

ATTENUATION, Db 0 0 0

FREQUENCY, KC 0 5 0

METER RANGE 2 0

RANGE X 1 0 0

METER READING -9

## CENTER CONTROL PANEL

| | BEAM CURRENT, MA | HIGH VOLTAGE, KV | TRAVEL, IPM |
|---|---|---|---|
| Pass 1 | 5 8 0 | 4 1. 0 | 1 2. 0 |
| Pass 2 | 2 0 0 | 2 0. 0 | 1 2. 0 |
| Pass 3 | | | |

FOCUS CURRENT METER 5.2 2 DC Amps.

GUN FILAMENT METER 0 6 5 AC Amps.

FILAMENT ADJUST POT. 0 7 6

## SKETCH OF JOINT

TYPE OF JOINT BUTT

## GUN ELEMENTS

| | | |
|---|---|---|
| GUN TYPE, | KV | 6 0 |
| FILAMENT, | MA | 5 0 0 |
| CATHODE, | MA | 7 5 0 |
| ANODE, | KV/MA | 7 5 0 |
| SPACER, | Inches | 0 0 0 |

BIAS On [ ] Off [2]

METER, AC VOLTS ______

VOLTAGE ADJUST. ______

Mid-point focus

GUN-TO-WORK DISTANCE, Inches 3 .5

## OPERATOR'S STATION CONTROL

X-AXIS On [X] Off [ ]

DIRECTION Fwd. [ ] Rev. [X]

TRAVEL SPEED, IPM 1 2. 0

Y-AXIS On [ ] Off [ ]

DIRECTION Fwd. [ ] Rev. [ ]

TRAVEL SPEED, IPM ______

WIRE FEED On [x] Off [ ]

BEAM ALIGNMENT NA

HIGH VOLTAGE ADJUST. NA

INCH PER MINUTE 3 0. 0

FOCUS ADJUST. 5 .2 2

AVR Lock [ ] Unlock [X]

X-Ray Serial Number ______

Mag. Inspection ______

Acceptance Standard ______

Metallurgical Exam. ______

Operator ______

MR&D Engineer J. C. Collins

Process Control ______

# ELECTRON BEAM WELDING SCHEDULE

Schedule Number FMR 60-2154 Date 8-7-73
Part Number ______ Part Name ______ Material Type 10Ni.(Hy 180)
Serial Number ______ Tool Number ______ Mat'l. Thick 2.00"
PARAMETER Filler Wire Type Low alloy Hy 180/220 Diameter 0.062"
Development (10Ni. - Chr., Mo., Co.)

## UPPER CONTROL PANEL

| HV START Delay | MOTOR START Delay | HIGH VOLTAGE Initial KV | HIGH VOLTAGE Final | SPEED ADJUSTMENT Initial and Final |
|---|---|---|---|---|
| 0 0 2 | 0 0 5 | 4 5. 0 | 0 5 9 | |
| Seconds | Seconds | Slope | Slope | Run |
| X 15 30 60 120 | X 15 30 60 120 | 0 0 2 | 0 4 5 | |

## OSCILLATOR

AXIS X [X] Y [ ]
ATTENUATION, Db 0 0 0
FREQUENCY, KC 0 8 0
METER RANGE 2 0
RANGE X 1 0 0
METER READING - 9

## CENTER CONTROL PANEL

| | BEAM CURRENT, MA | HIGH VOLTAGE, KV | TRAVEL, IPM |
|---|---|---|---|
| Pass 1 | 7 0 0 | 4 7. 5 | 3 0. 0 |
| Pass 2 | 2 0 0 | 2 0. 0 | 3 0. 0 |
| Pass 3 | | | |

FOCUS CURRENT METER 5 2 2 DC Amps.
GUN FILAMENT METER 0 6 6 AC Amps.
FILAMENT ADJUST POT. 0 7 6

SKETCH OF JOINT

TYPE OF JOINT BUTT

## GUN ELEMENTS

| | | |
|---|---|---|
| GUN TYPE, | KV | 6 0 |
| FILAMENT, | MA | 5 0 0 |
| CATHODE, | MA | 7 5 0 |
| ANODE, | KV/MA | 7 5 0 |
| SPACER, | Inches | 0 0 0 |

BIAS On [ ] Off [X]
METER, AC VOLTS
VOLTAGE ADJUST.
MID point, and as noted
GUN-TO-WORK DISTANCE, Inches 3 .5

## OPERATOR'S STATION CONTROL

X-AXIS On [X] Off [ ]
DIRECTION Fwd. [ ] Rev. [X]
TRAVEL SPEED, IPM 3 0. 0

Y-AXIS On [ ] Off [ ]
DIRECTION Fwd. [ ] Rev. [ ]
TRAVEL SPEED, IPM

WIRE FEED On [X] Off [ ]
INCH PER MINUTE 3 0. 0
BEAM ALIGNMENT
FOCUS ADJUST.
HIGH VOLTAGE ADJUST. N A
AVR Lock [ ] Unlock [X]

X-Ray Serial Number ______
Mag. Inspection ______
Acceptance Standard ______
Metallurgical Exam. ______
Operator ______
MR&D Engineer J. C. Collins
Process Control ______

# ELECTRON BEAM WELDING SCHEDULE

Schedule Number ______ Date 8-22-73
Part Number MD-3232-2 Part Name ______ Material Type 10Ni. Hy180
Serial Number H-13 Tool Number ______ Mat'l. Thick .500
Filler Wire Type Low alloy Hy180/220 Diameter .062
(10Ni.Cr. Mo-Co)
Heat No. 51361

## UPPER CONTROL PANEL

| HV START Delay | MOTOR START Delay | HIGH VOLTAGE Initial KV | HIGH VOLTAGE Final | SPEED ADJUSTMENT Initial and Final |
|---|---|---|---|---|
| 0 0 2 | 0 0 2 | 4 7.5 | 0 0 9 | |
| Seconds | Seconds | Slope | Slope | Run |
| X 15 30 60 120 | X 15 30 60 120 | 0 1 2 | 0 4 5 | 3 0.0 |

## OSCILLATOR

| | | | |
|---|---|---|---|
| AXIS X [ ] Y [X] | FREQUENCY, KC 0 0 5 | RANGE X 1 0 0 | |
| ATTENUATION, Db 0 0 0 | METER RANGE 2 0 | METER READING 0 0 9 | |

## CENTER CONTROL PANEL

| | BEAM CURRENT, MA | HIGH VOLTAGE, KV | TRAVEL, IPM |
|---|---|---|---|
| Pass 1 | 3 0 0 | 2 7.5 | 3 0.0 |
| Pass 2 | 1 6 0 | 1 8.0 | 2 6.0 |
| Pass 3 | | | |

FOCUS CURRENT METER 5.2 2 DC Amps. GUN FILAMENT METER 0 6 5 AC Amps. FILAMENT ADJUST POT. 0 7 7

**SKETCH OF JOINT**

TYPE OF JOINT BUTT

## GUN ELEMENTS

| | | | | |
|---|---|---|---|---|
| GUN TYPE, | KV | 6 0 | BIAS | On [ ] Off [X] |
| FILAMENT, | MA | 5 0 0 | METER, AC VOLTS | — |
| CATHODE, | MA | 7 5 0 | VOLTAGE ADJUST. | — |
| ANODE, | KV/MA | 7 5 0 | Mid-point focus | |
| SPACER, | Inches | 0 0 0 | GUN-TO-WORK DISTANCE, Inches | 3.5 |

## OPERATOR'S STATION CONTROL

| | | | |
|---|---|---|---|
| X-AXIS | On [X] Off [ ] | Y-AXIS | On [ ] Off [X] |
| DIRECTION | Fwd. [ ] Rev. [ ] | DIRECTION | Fwd. [ ] Rev. [ ] |
| TRAVEL SPEED, IPM | 3 0. 0 | TRAVEL SPEED, IPM | — |
| WIRE FEED | On [X] Off [ ] | INCH PER MINUTE | 3 0.0 |
| BEAM ALIGNMENT | NA | FOCUS ADJUST. | 5.2 2 |
| HIGH VOLTAGE ADJUST. | NOTED | AVR | Lock [ ] Unlock [X] |

X-Ray Serial Number ______
Mng. Inspection ______ Operator ______
Acceptance Standard ______ MR&D Engineer J. C. Collins
Metallurgical Exam. ______ Process Control ______

# ELECTRON BEAM WELDING SCHEDULE

Schedule Number FMR 60-2154 Date 10-9-73
Part Number 603R-100-11-5-H18 Part Name ______ Material Type 10Ni.(Hy180)
Serial Number 473943 Tool Number ______ Mat'l. Thick .900
CSC 1000-1-2-4 thru 7 Filler Wire Type ______ Diameter .062"

## UPPER CONTROL PANEL

| HV START Delay | MOTOR START Delay | HIGH VOLTAGE Initial KV | HIGH VOLTAGE Final | SPEED ADJUSTMENT Initial and Final |
|---|---|---|---|---|
| 0 0 5 | 0 0 3 | 4 4 0 | 0 5 9 | 004 |
| Seconds: ■ 15 30 60 120 | Seconds: X 15 30 60 120 | Slope: 0 0 7 | Slope: 0 4 5 | Run: 0 1 4 |

## OSCILLATOR

| | | |
|---|---|---|
| AXIS X [X] Y [ ] | FREQUENCY, KC 0 0 5 | RANGE X 1 0 0 |
| ATTENUATION, Db 0 0 0 | METER RANGE 2 0 | METER READING - 9 |

## CENTER CONTROL PANEL

| | BEAM CURRENT, MA | HIGH VOLTAGE, KV | TRAVEL, IPM |
|---|---|---|---|
| Pass 1 | 4 4 0 | 3 4. 5 | 1 8. 0 |
| Pass 2 | 1 8 0 | 1 8. 0 | 1 8. 0 |
| Pass 3 | 1 6 0 | 1 8. 0 | 1 8. 0 |

SKETCH OF JOINT

| FOCUS CURRENT METER | GUN FILAMENT METER | FILAMENT ADJUST POT. | TYPE OF JOINT |
|---|---|---|---|
| 5. 2 2 DC Amps. | 0 6 5 AC Amps. | 0 7 6 | BUTT |

## GUN ELEMENTS

| | | | | |
|---|---|---|---|---|
| GUN TYPE, KV | 6 0 | | BIAS | On [ ] Off [X] |
| FILAMENT, MA | 5 0 0 | | METER, AC VOLTS | |
| CATHODE, MA | 7 5 0 | | VOLTAGE ADJUST. | |
| ANODE, KV/MA | 7 5 0 | | Mid-point focus | |
| SPACER, Inches | 0 0 0 | | GUN-TO-WORK DISTANCE, Inches | 3. 5 |

## OPERATOR'S STATION CONTROL

| | | | |
|---|---|---|---|
| X-AXIS | On [X] Off [ ] | Y-AXIS | On [ ] Off [ ] |
| DIRECTION | Fwd. [ ] Rev. [X] | DIRECTION | Fwd. [ ] Rev. [ ] |
| TRAVEL SPEED, IPM | 1 8. 0 | TRAVEL SPEED, IPM | |
| WIRE FEED | On [X] Off [ ] | INCH PER MINUTE | 3 0. 0 |
| BEAM ALIGNMENT | | FOCUS ADJUST. | 5. 2 2 |
| HIGH VOLTAGE ADJUST. | NOTED | AVR | Lock [ ] Unlock [X] |

X-Ray Serial Number ______
Mag. Inspection ______ Operator ______
Acceptance Standard ______ MR&D Engineer J. C. Collins
Metallurgical Exam. ______ Process Control ______

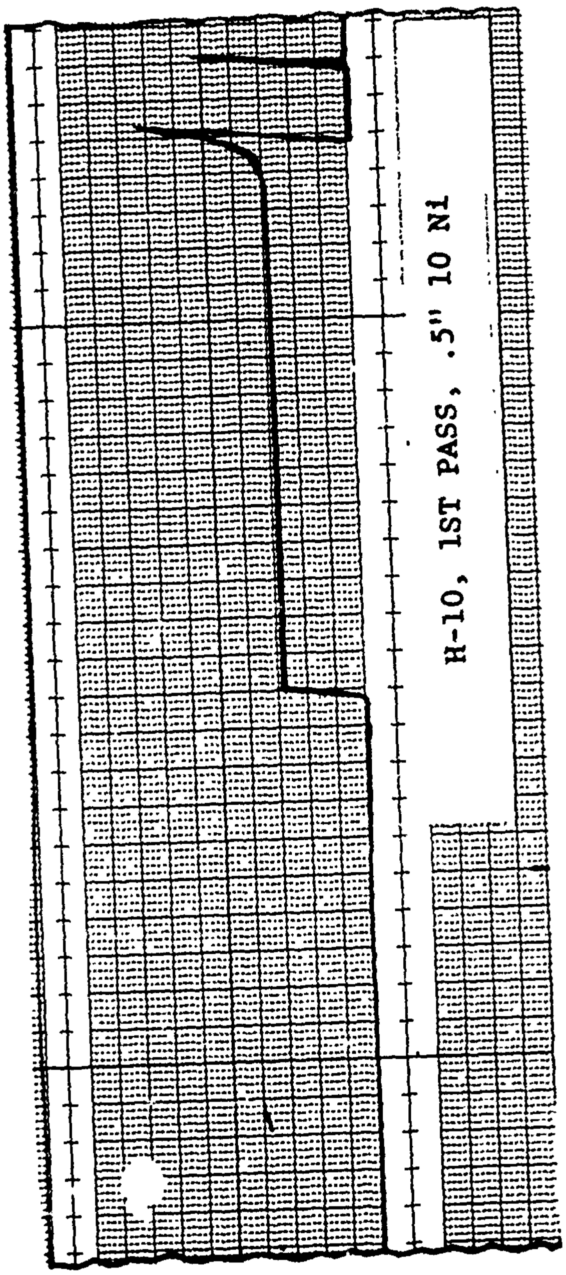
H-10, 1ST PASS, .5" 10 N1

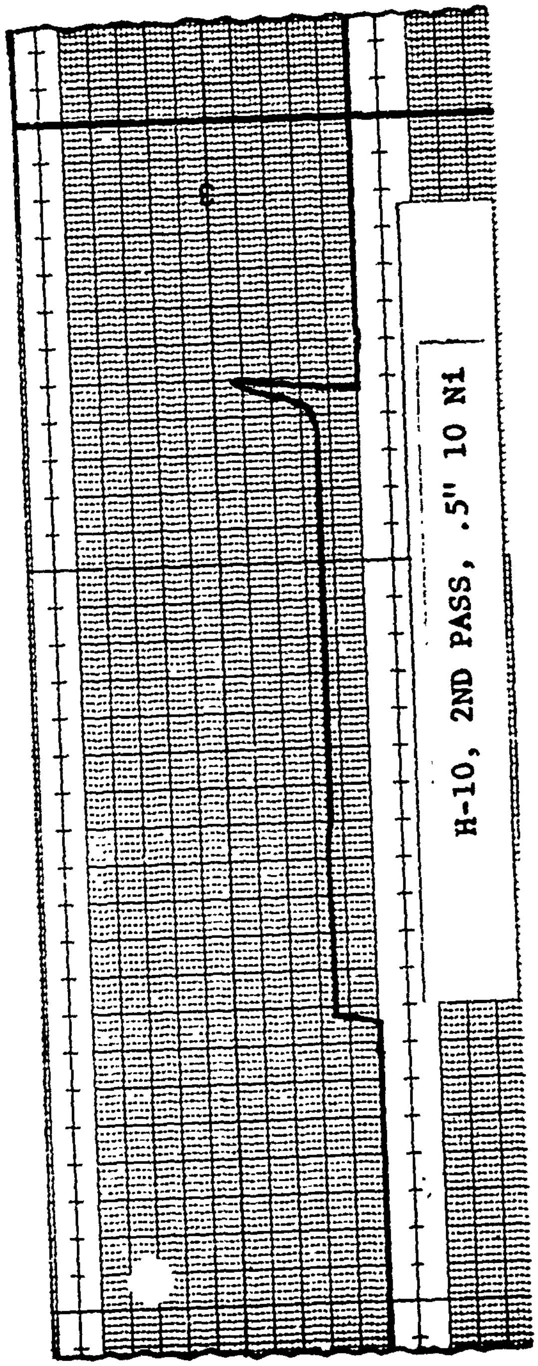
H-10, 2ND PASS, .5" 10 N1

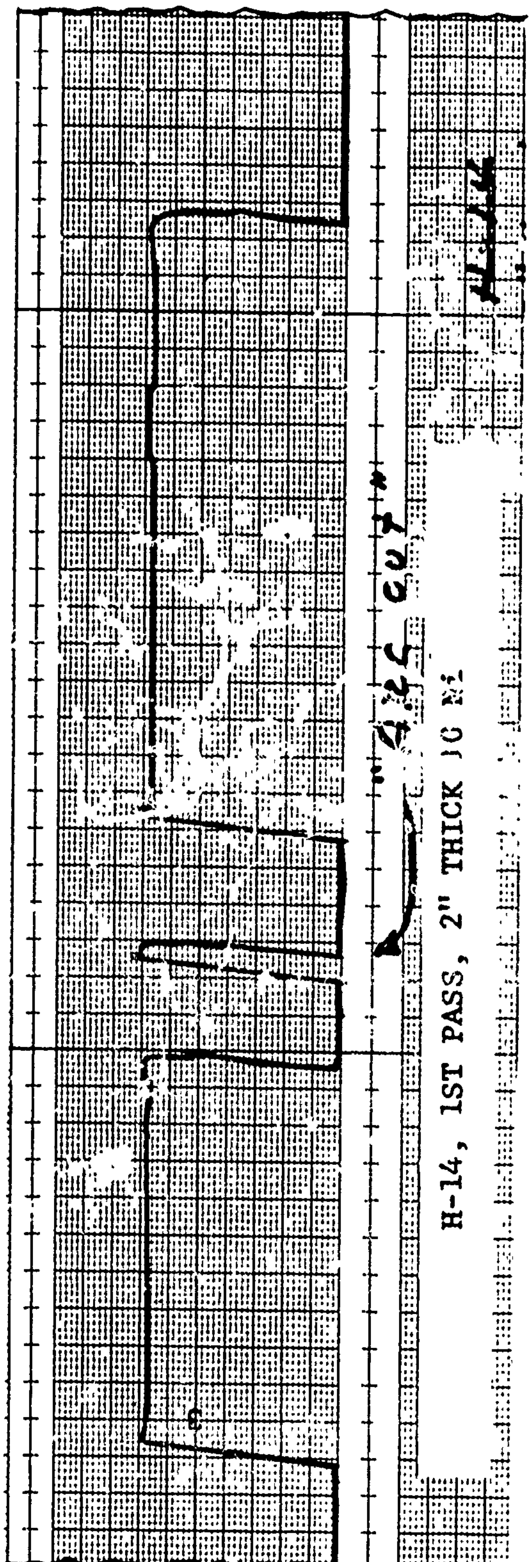
"ARC CUT"
H-14, 1ST PASS, 2" THICK 10 Ni

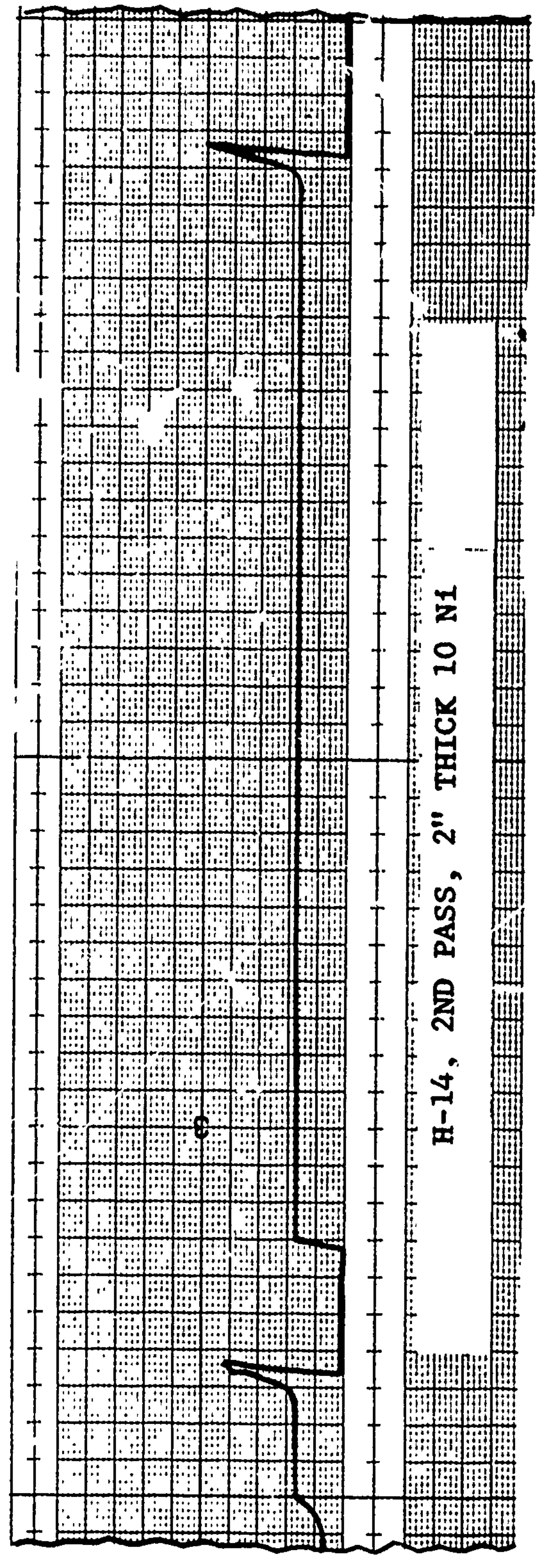
H-14, 2ND PASS, 2" THICK 10 Ni

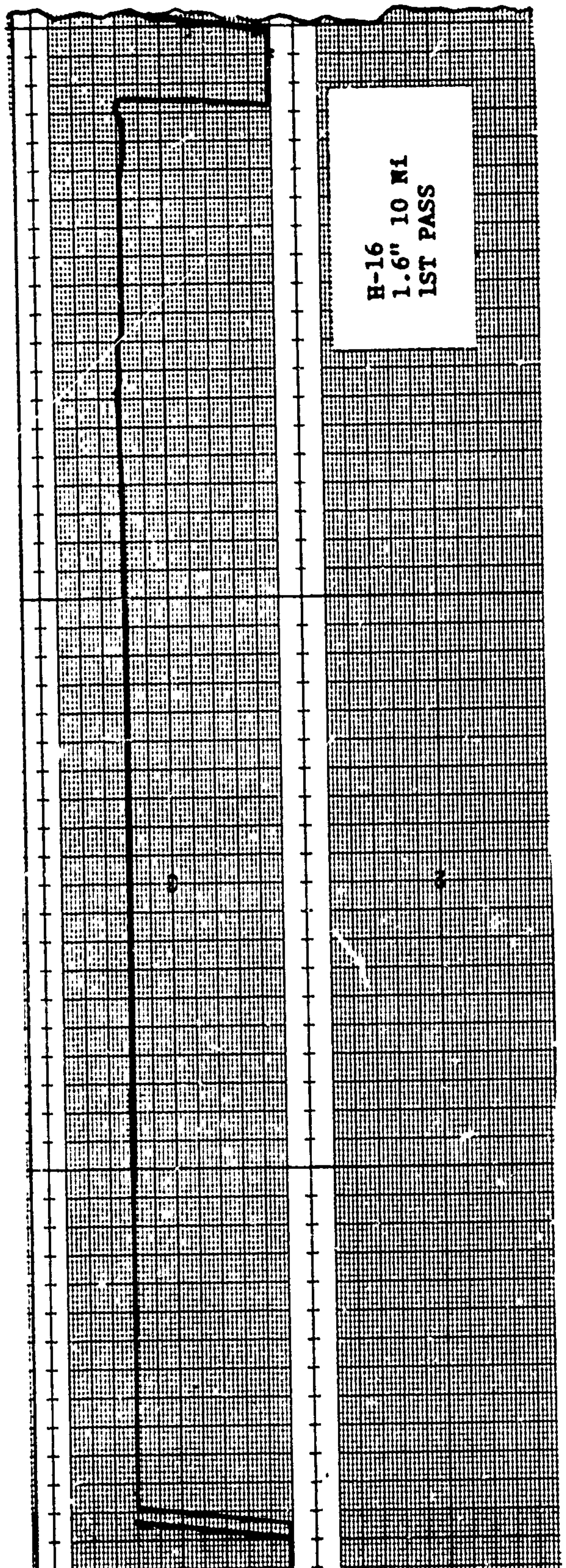
H-16
1.6" 10 Ni
1ST PASS

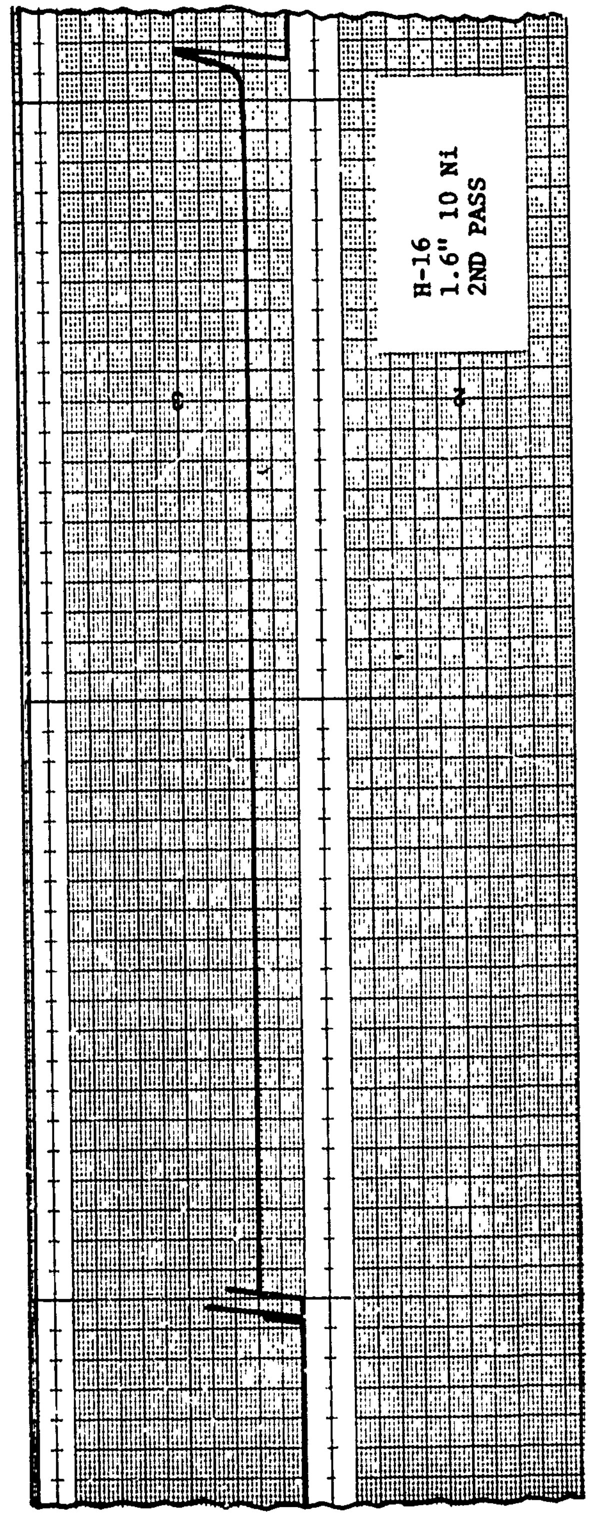
H-16
1.6" 10 Ni
2ND PASS

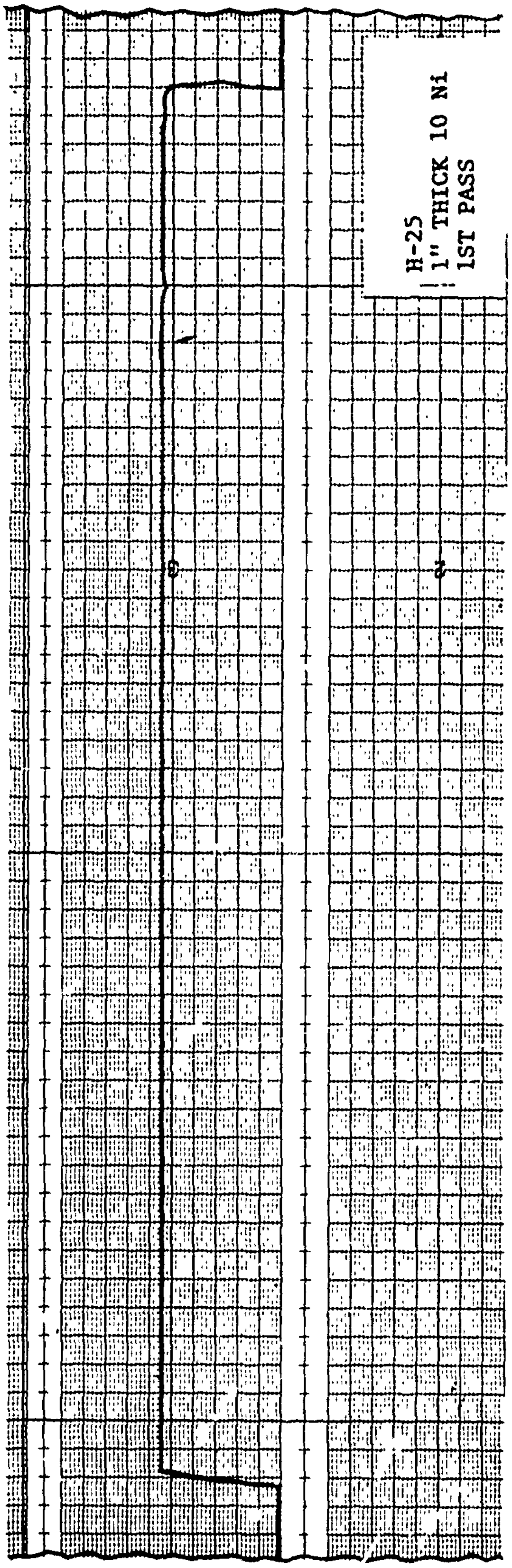
H-25
1" THICK 10 Ni
1ST PASS

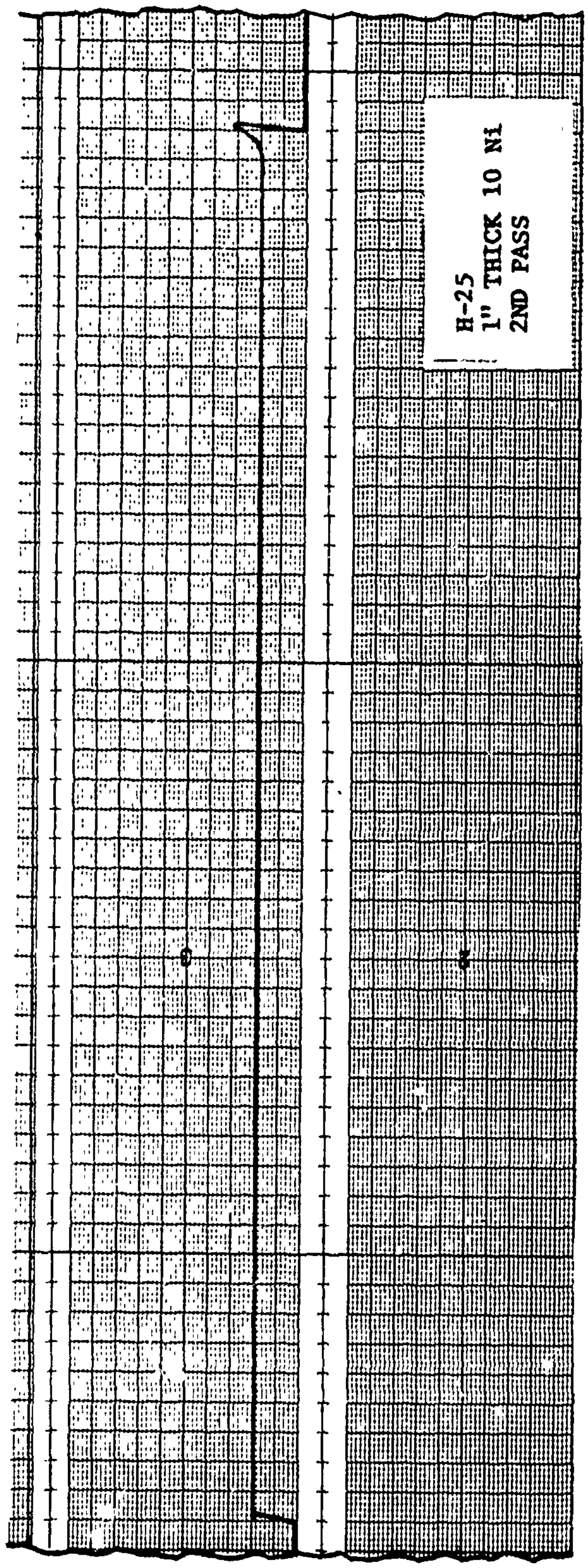
H-25
1" THICK 10 Ni
2ND PASS

Unclassified
Security Classification

**DOCUMENT CONTROL DATA - R & D**

*(Security classification of title, body of abstract and indexing annotation must be entered when the overall report is classified)*

1. ORIGINATING ACTIVITY (Corporate author)
Air Force Flight Dynamics Laboratory (FBA)
Air Force Systems Command
Wright-Patterson Air Force Base, Ohio 45433

2a. REPORT SECURITY CLASSIFICATION
Unclassified

2b. GROUP

3. REPORT TITLE
Advanced Metallic Air Vehicle Structure Program

4. DESCRIPTIVE NOTES (Type of report and inclusive dates)
Phase II - Detail Design and Analysis Summary Report - Technical

5. AUTHOR(S) (First name, middle initial, last name)
C. E. Hart, et al.

6. REPORT DATE

7a. TOTAL NO. OF PAGES
476

7b. NO. OF REFS

8a. CONTRACT OR GRANT NO
F33615-73-C-3001

b. PROJECT NO.
486U

c.

d.

9a. ORIGINATOR'S REPORT NUMBER(S)
AFFDL-TR-74-17

9b. OTHER REPORT NO(S) (Any other numbers that may be assigned this report)

26 AUG 1974

10. DISTRIBUTION STATEMENT
Distribution limited to U.S. Government Agencies only. Reason: Test and Evaluation. Other requests for this document must be referred to Air Force Flight Dynamics Laboratory/FBA, Wright-Patterson Air Force Base, Ohio 45433.

11. SUPPLEMENTARY NOTES

12. SPONSORING MILITARY ACTIVITY
Air Force Flight Dynamics Laboratory
Air Force Systems Command
Wright-Patterson AFB, Ohio 45433

13. ABSTRACT

This report covers the design, analysis, manufacturing and testing done during Phase II, Detail Design, of the Advanced Metallic Air Vehicle Structure (AMAVS) program. The objectives of Phase II were to complete the detail design work for two configurations of a wing carrythrough structure for a movable-wing aircraft, to complete materials and component testing in support of the two configurations, to select one of the configurations for manufacture in Phase III and to continue design and manufacture of a fixture for full-scale testing of the carrythrough structure.

Additional trade studies and design optimization studies were conducted in the early part of Phase II for the two configurations selected in Phase Ib: Fail Safe Integral Lug (FSIL) and "No-Box" Box (NBB). An updated baseline data package was received during Phase II and the configurations were revised to meet the modified baseline requirements.

Material testing and component testing were completed. Beta annealed 6Al-4V and Beta C titanium and 10Ni steel (HY180) were used in these tests.

Some detail design work remains on the full-scale test fixture but manufacturing has started. Manufacture of the simulated fuselage structure has also begun.

The NBB configuration which utilizes the outstanding fracture toughness and good crack growth characteristics of 10Ni steel has been selected for manufacture in Phase III.

DD FORM 1 NOV 65 1473

Unclassified
Security Classification

Unclassified
Security Classification

| 14 KEY WORDS | LINK A | | LINK B | | LINK C | |
|---|---|---|---|---|---|---|
| | ROLE | WT | ROLE | WT | ROLE | WT |
| Structural Design | | | | | | |
| Stress Analysis | | | | | | |
| Fracture Mechanics | | | | | | |
| Materials | | | | | | |
| Manufacturing Technology | | | | | | |
| Damage Tolerance | | | | | | |

Unclassified
Security Classification

☆U.S.Government Printing Office: 1974 — 758-436/719